

NATIONAL INSTITUTE FOR FUSION SCIENCE

**Comparison of Ionization Rate Coefficients of Ions
from Hydrogen through Nickel**

T. Kato, K. Masai and M. Arnaud

(Received — Aug. 2, 1991)

NIFS-DATA-14

Sep. 1991

RESEARCH REPORT
NIFS-DATA Series

This report was prepared as a preprint of compilation of evaluated atomic, molecular, plasma-wall interaction, or nuclear data for fusion research, performed as a collaboration research of the Data and Planning Center, the National Institute for Fusion Science (NIFS) of Japan. This document is intended for future publication in a journal or data book after some rearrangements of its contents.

Inquiries about copyright and reproduction should be addressed to the Research Information Center, National Institute for Fusion Science, Nagoya 464-01, Japan.

Comparison of ionization rate coefficients of ions
from Hydrogen through Nickel

Takako KATO, Kuniaki MASAI
National Institute for Fusion Science, Nagoya 464-01, Japan

Monique ARNAUD*
Harvard-Smithsonian Center for Astrophysics, 60 Garden Street,
Cambridge, MA 02138, USA

* present address : CEN Saclay, 91191 Gif sur Yvette, France

Abstract

Ionization rate coefficients based on several empirical formulae are compared with each other for ions from Hydrogen to Nickel. The coefficients are shown illustratively, and the differences are discussed.

Key words

ionization rate coefficients, plasma, ions, empirical formulae

1. Introduction

Ionization rate coefficients for various ions are important in understanding ionization balance in both laboratory and astrophysical plasmas. Several empirical formulae have been proposed to calculate ionization rate coefficients as well as cross sections. We compare in this report the ionization rate coefficients for ions from Hydrogen to Nickel reviewing the empirical formulae for them.

Recently, experimental technique of crossed beam method for ions has been developed and data for various ions have been compiled. The experimental results revealed that the excitation autoionization process is important for complex configuration such as Li-like, Na-like ions which have inner shell excitation processes. The ionization process from the metastable states is also important in the experiment.

2. Empirical formula

2.1 Lotz formula

As for empirical formula for ionization cross sections and rate coefficients, the formulae by Lotz[1, 2] have been widely used in fields related to plasma physics. Lotz deduced a cross section based on experimental data of low ionized ions with comparatively low Z elements.

$$\sigma = \sum_{j=1}^N a_j \zeta_j \frac{\ln u_j}{u_j I_j^2} \{1 - b_j \exp[-c_j (u_j - 1)]\}, \quad (1)$$

where $u_j = E / I_j$, E (eV) is the energy of the impact electron, I_j (eV) is the binding energy of an electron in j -th subshell ($j = 1$ means the outermost subshell), ζ_j is the number of equivalent electrons of j -th subshell, and a_j , b_j , c_j are the individual constants to be adjusted from the experimental data and some scaling. The coefficients a_j , b_j and c_j are given in Tables for certain ions from Hydrogen to Calcium in [1] and from Scandium to Zinc in [2]. For experimentally known cross sections, this formula gives values within the experimental errors. For the ions ionized more than four times, he assumed that $a_j = 4.5 \times 10^{-14} \text{ cm}^2 (\text{eV})^2$, $b_j = 0$ and $c_j = 0$. The number of subshell, N , is taken to be 2 for ions of H to Ca and to be 3 for Sc to Zn. The ionization rate coefficient is obtained by integrating the cross section in a form of eq.(1) over a Maxwellian distribution as follows,

$$C = 6.7 \times 10^7 \sum_{j=1}^N \frac{a_j \zeta_j}{T_e^{3/2}} \left\{ \frac{1}{I_j / T_e} \int_{I_j / T_e}^{\infty} \frac{\exp(-z)}{z} dz - \frac{b_j \exp C_j}{I_j / T_e + C_j} \int_{I_j / T_e + C_j}^{\infty} \frac{\exp(-y)}{y} dy \right\} \text{ cm}^3 \text{ s}^{-1} \quad (2)$$

where T_e is the electron temperature in eV.

2.2 Arnaud et al.

Arnaud and Rothenflug [3] evaluated the cross sections for ions of H, He, C, N, O, Ne, Na, Mg, Al, Si, S, Ar, Ca, Fe, Ni which are major species in astrophysical plasmas. Recently Arnaud and Raymond[5] updated the cross section for iron ions. They used the following parametric formula proposed originally by Younger[4] for the direct ionization cross section,

$$\sigma_{DI} = \sum_j \frac{1}{u_j I_j^2} \left[A_j \left(1 - \frac{1}{u_j} \right) + B_j \left(1 - \frac{1}{u_j} \right)^2 + C_j \ln(u_j) + D_j \frac{\ln(u_j)}{u_j} \right] \text{cm}^2 \quad (3)$$

with $u_j = \frac{E}{I_j}$.

The coefficients A_j , B_j , C_j and D_j are given in the Tables of their paper together with the values of I_j .

Then, the direct ionization (DI) rate coefficients are expressed as a function of electron temperature,

$$C_{DI} = \frac{6.69 \times 10^7}{T^{3/2}} \sum_j \frac{\exp(-x_j)}{x_j} F(x_j) \text{ cm}^3 \text{ s}^{-1}, \quad (4)$$

where

$$F(x) = A_j [1 - x_j f_1(x_j)] + B_j [1 + x_j - x_j (2 + x_j) f_1(x_j)] + C_j f_1(x_j) + D_j x_j f_2(x_j)$$

$$\text{with } x_j = \frac{I_j}{T_e}; \quad f_1(x) = e^x \int_1^{\infty} \frac{dt}{t} e^{-tx} \quad \text{and} \quad f_2(x) = e^x \int_1^{\infty} \frac{dt}{t} e^{-tx} \text{Ln}(t) .$$

For the excitation autoionization (EA) cross section, they adopted the following formula [5] which is a generalization of the formulae they used in [3],

$$\sigma_{EA} = \frac{1}{u I_{EA}} \left[A + B \left(1 - \frac{1}{u} \right) + C \left(1 - \frac{1}{u^2} \right) + D \left(1 - \frac{1}{u^3} \right) + E \ln(u) \right] \text{cm}^2$$

with $u = \frac{E}{I_{EA}}$ (5)

where I_{EA} is the excitation autoionization threshold (in eV). A, B, C, D and E are given in Tables of their paper. The EA ionization rate coefficient is then,

$$C_{EA} = \frac{6.69 \times 10^7 \exp(-x)}{\sqrt{T_e}} F(x) \text{ cm}^3 \text{ s}^{-1} \quad (6)$$

$$F(x) = A + B [1 - x f_1(x)] + C [1 - x (1 - x f_1(x))] + D [1 - 0.5 (x - x^2 + x^3 f_1(x))] + E f_1(x)$$

$$\text{with } x = \frac{I_{EA}}{T_e} \quad \text{and} \quad f_1(x) = e^x \int_1^{\infty} \frac{dt}{t} e^{-tx} .$$

The excitation autoionization process is taken into account only when the data are available experimentally or theoretically. Therefore EA process is not systematically considered. For all iron ions, EA process is considered.

2.3 Belfast group

Bell et al.[6] and Lennon et al.[7] in Belfast compiled ionization cross sections and gave the recommended data for atoms and ions of Hydrogen to Oxygen[6] and of Fluorine to Nickel[7], respectively. The recommended cross sections are fitted to the following formulae

$$\sigma = \frac{1}{uI^2} \left[A \ln u + \sum_{i=1}^N B_i \left(1 - \frac{1}{u}\right)^i \right] \quad (7)$$

The coefficients A and B_i obtained by least square fitting are given in the Tables for $N = 5$. The parameter A is the Bethe coefficient to represent the high energy behaviour of the cross section.

The rate coefficients for the temperature range $I / 10 \leq T \leq 10I$ are fitted to a following formulae,

$$C = \exp\left(-\frac{I}{T_e}\right) \left(\frac{T_e}{I}\right)^{1/2} \sum_{n=0}^5 a_n \left[\log_{10}\left(\frac{T_e}{I}\right)\right]^n \quad (8)$$

and for $T > 10I$ to

$$C = \left(\frac{T_e}{I}\right)^{1/2} \left[\alpha \ln\left(\frac{T_e}{I}\right) + \sum_{n=0}^2 \beta_n \left(\frac{I}{T_e}\right)^n \right] \quad (9)$$

The ionization potential I is given in Table 1, and the coefficients a_0, \dots, a_5 and α, β_0, β_1 and β_2 are given in Tables 2 and 3 in their paper.

2.4 Pinzola et al.

Pinzola et. al.[8] reviewed atomic data for the ionization cross sections for iron isonuclear sequence. They used the same formula as eq.(3) for the direct ionization cross sections and gave the coefficients A, B, C and D for the ground and excited configurations based on calculations by the average configuration statistical model. Rate coefficients are calculated from the theoretical and experimental cross section data. They recommended to use the experimental results for Fe^+ , Fe^{2+} , Fe^{5+} , Fe^{6+} , Fe^{9+*} , Fe^{11+} , Fe^{13+} and Fe^{15+} , while for Fe^{3+} , Fe^{4+} , Fe^{7+} , Fe^{8+*} , Fe^{10+*} , Fe^{12+} , Fe^{14+*} they recommended the theoretical results and the direct ionization results for Fe^{16+} through Fe^{25+} . Here Fe^{8+*} , Fe^{9+*} , Fe^{10+*} and Fe^{14+*} should be read as ionization from the excited states $3s^23p^53d$, $3s^23p^43d$, $3s^23p^33d$ and $2p^63s3p$, respectively. The populations of the excited states depend on the plasma conditions. It is not clear why they recommended data from the excited states for these ions. The calculated rate coefficients are fitted to a direct expansion of Chebychev polynomials of the first kind $T_n(x)$,

$$\ln C = A_0 / 2 + \sum A_n T_n(x) \quad (10)$$

where

$$x = \frac{[2 \ln(T_e) - \ln(E_{\max}) - \ln(E_{\min})]}{\ln(E_{\max}) - \ln(E_{\min})}, \quad T_e \text{ and } E_{\min} \text{ in (eV)}, \quad E_{\max} = 20000 \text{ eV}$$

The values E_{\min} and the parametric coefficients A_0, \dots, A_n are given in Tables of their paper[8].

3. Comparison of the rate coefficients

We have compared the rate coefficients proposed by the authors mentioned in the previous section and show the comparison illustratively for atoms and ions of H to Ni in Sec.5..

The rate coefficients by Arnaud and Raymond [5] and by Pindzola for Fe ions are in fairly good agreement with each other except for Fe^{8+} , Fe^{9+} and Fe^{10+} ions for which Pindzola recommended ionization from excited states. In that case the differences with ionization from ground state, used by AR, amount to about a factor of 2. For Fe^{14+} , Fe^{6+} and Fe^{7+} ions, the Arnaud's values are larger than Pindzola's at high temperatures. For Fe^{14+} , the rate coefficients for ionization from the excited state (Pindzola) and from the ground state (AR) are less drastically different. Arnaud's value are larger at high temperature (due to the different EA cross sections) by about 20%. For Fe^{6+} both rate coefficients are based on the same measurements. The differences of about 20% at very high temperatures is probably due to slightly different extrapolation of the data at high energies. For Fe^{7+} rates, based on the same theoretical computations, the differences at high temperatures amount to about 30% we did not understand the origin of this discrepancy.

We discuss here the rate coefficients according to the isoelectronic sequence, since the differences usually have a common origin in a given sequence. We mainly compare the values by [3, 5] (hereafter AR) and [6, 7] (hereafter Belfast).

3.1 H sequence (1s)

H - Ca^{19+}

Excellent agreement < 10 %.

Sources: Distorted Wave Born Exchange (DWBX) [9, 10, 11]

Fe^{25+}

The values by Belfast should be multiplied by 1.626 due to the misprint of table 2 of Younger [9] (The coefficients are given in $\pi a_0^2 \text{Ryd}^2$ and not in $10^{-14} \text{ cm}^2 \text{ eV}^2$ as stated).

The values given in Pindzola et al. [8] had also the same error but they distributed an erratum giving the corrected coefficients for eq.(10) afterwards. We used these corrected

values in this report.

Sc²⁰⁺-Ni²⁷⁺

Since Belfast scaled the values for Fe²⁵⁺, the values by Belfast should be multiplied by 1.626. The same error was apparently made by Belfast for Fe ions (and Sc - Ni ions) in the He to B sequences.

3.2 He sequence (1s²)

He

Excellent agreement.

Sources: Crossed beam measurement.

C⁴⁺, N⁵⁺, O⁶⁺, Si¹²⁺, S¹⁴⁺, Ar¹⁶⁺, Ca¹⁸⁺

The Belfast's values are lower than AR's by 30 - 50 % at low temperature ($T / I < 0.5$).

Sources: AR from DWBX [11]. Belfast adopted the scaled cross section ($uI^2\sigma$) from the measurements of B³⁺. The scaled cross sections are nearly independent of Z for $Z \geq 6$ but not for $Z \leq 6$. This explains the discrepancies.

Na⁹⁺

Excellent agreement.

Sources: DWBX [12]

Ne⁸⁺, Mg¹⁰⁺, Al¹¹⁺

The Belfast's values are lower than AR's by 30 - 50 % at low temperature ($T / I < 0.5$).

Sources: AR from DWBX [12], Belfast from plane wave Born (PWB) approximation [13]. PWB calculations give the lower cross sections near the threshold.

Sc¹⁹⁺ - Ni²⁶⁺

See Sc²⁰⁺ - Ni²⁷⁺ in sec.3.1

Lotz's values agree with AR's ones within 20 %.

3.3 Li sequence (1s²2s)

C³⁺, N⁴⁺, O⁵⁺

Excellent agreement between Belfast and AR. Only for C³⁺, Lotz's values are greater than AR's by more than factor of 2.

Sources: crossed beam measurements.

Ne⁷⁺

Good agreement.

Sources: Belfast from Coulomb Born [14] for DI and EA cross sections. AR from Younger

[10, 11] for DI and [15] for EA.

Al¹⁰⁺

Lennon's values is lower than AR's by 50 % at low temperature. See Ne⁸⁺, Mg¹⁰⁺ and Al¹¹⁺ in sec. 3.2.

Sources: Belfast from PWB [13], AR from DW [10].

Na⁸⁺, Mg⁹⁺, Si¹¹⁺ - Ca¹⁷⁺

AR's values are higher at high temperature than those by Belfast, whereas the agreement is almost perfect at low temperatures, because AR took into account the EA process.

Sources: Belfast scaled the O⁵⁺ curves without EA contribution. AR from Younger for DI [10, 11] and from [15] for EA.

Sc¹⁸⁺ - Ni²⁵⁺[15]

See Sc¹⁸⁺- Ni²⁵⁺ in sec.3.1.

3.4 Be sequence (1s²2s²)

No EA contribution is taken into account.

C²⁺ - O⁴⁺, Ne⁶⁺, Na⁷⁺, Mg⁹⁺, Si¹⁰⁺, Ar¹⁴⁺, Ca¹⁶⁺

The discrepancies are less than 10 % (usually less than 5 %).

Sources: AR from DWX [16], Belfast deduced by scaling the O⁴⁺ cross sections or from CBX computations [17].

Al⁹⁺, S¹²⁺

Belfast's values are lower than AR's by more than a factor of 2 at low temperatures.

Sources: Belfast from PBW approximation [13], AR from DW by Younger.

See Ne⁸⁺, Mg¹⁰⁺, Al¹¹⁺ in sec.3.2.

Sc¹⁷⁺ - Ni²⁴⁺

See Sc²⁰⁺ - Ni²⁷⁺ in sec.3.1.

3.5 B sequences (2s²2p)

C⁺, N²⁺, O³⁺

Excellent agreement between AR and Belfast.

Lotz's values are smaller than AR's by more than 50% at low temperatures for C⁺ and N²⁺.

Sources: Both values are based on measurement.

Al⁸⁺

Belfast 's values are lower than AR's at low temperatures. The differences are typically 50 % at $T / I \sim 0.5$ and reach a factor of 2 at $T / I \sim 0.1$.

Sources: Belfast from PBW and AR from DWBX, as Al⁹⁺.

Ne⁵⁺ - Mg⁷⁺, Si⁹⁺ - Ca¹⁵⁺

Belfast 's values are lower than AR's at low temperatures (30 - 50 % at $T / I \sim 0.1 - 0.2$) and slightly higher at high temperatures (5 - 20 %). This is a consequence of the variation with Z of the scaled cross section as discussed in sec.3.2 (C⁴⁺ - O⁶⁺).

Sources: Belfast scaled classically from O³⁺ values. AR interpolated the values between low Z ions and Fe ions for the scaled cross section. The scaled cross section increases with Z for a given reduced energy at low energies whereas the scaled cross section decreases with Z at very high energies (Bethe approximation).

Sc¹⁶⁺ - Ni²³⁺

See Sc²⁰⁺ - Ni²⁷⁺ in sec.3.1.

3.6 C sequence (2s²2p²)

C, N⁺, O²⁺

Excellent agreement with AR and Belfast. Lotz's are lower than AR about 50% at low temperatures for O²⁺.

Sources: Both values are based on measurements.

Al⁷⁺

Same as Al⁸⁺.

Ne⁴⁺, Na⁵⁺, Mg⁶⁺, Si⁸⁺ - Ca⁴⁺

Same as the discussion for Ne⁵⁺ - Ca¹⁵⁺.

Sources: Belfast scaled classically from O²⁺ values. AR from interpolated between low Z and Fe ions.

3.7 N sequences (2s²2p³)

N, O⁺

Same as C - O²⁺ in sec.3.6. Lotz's are lower than AR by more than factor of 2 at low temperatures for N.

Ne³⁺

The discrepancies at low temperature is due to the use of different ionization potential (97.1 eV in AR whereas 92.5 eV in Belfast).

Sources: measurements

Al⁶⁺

Same as Al⁸⁺.

Na⁴⁺ - Ca¹³⁺

Same as the discussion for Ne⁵⁺ - Ca¹⁵⁺ in sec.3.5.

Sources: Belfast scaled classically from Ne³⁺ values. AR from interpolation between low Z and Fe ions.

3.8 O sequences (2s²2p⁴)

O

Same as C - O²⁺ in sec.3.6.

Ne²⁺

AR's are lower than Belfast's about 40 %.

Sources: AR from the less reliable trapped ion measurements [18] and Belfast from the crossed beam measurements [19].

Al⁵⁺

Same as Al⁸⁺ in sec.3.5.

Na³⁺ - Ca¹²⁺

Scaled from Al⁵⁺, same as Al⁸⁺ in sec.3.5.

3.9 F sequence (2s²2p⁵)

Ne⁺

AR's are lower than Belfast about 20 % at high temperatures.

Sources: based on the measurements.

Na²⁺

Good agreement.

Al⁴⁺

Same as Al⁸⁺ in sec.3.5.

Mg³⁺ - Ca¹¹⁺

Same as Na⁵⁺ - Ca¹⁵⁺ in sec.3.5.

Source: Belfast scaled from Na²⁺.

3.10 Ne sequence ($2s^22p^6$)

Ne, Na⁺

Sources: Based on the same measurements. AR made an error in the fitting of Na⁺ (negative cross sections near threshold). Belfast probably did a fitting error for Ne (increasing cross sections for decreasing energies near threshold). This explains the important discrepancies (factor of 10) at very low temperatures.

Mg²⁺

Same as C - O²⁺ in sec.3.6.

Al³⁺, Si⁴⁺, S⁶⁺, Ca¹⁰⁺

AR's are larger than Belfast's at low temperatures.

Both rate coefficients are based on DWBX [20]. The discrepancies are due to an error made by AR in fitting the results. For Ca¹⁰⁺ we think that Belfast also made an error in fitting the results (too low rate coefficients).

3.11 Na sequence ($2p^63s$)

Na, Mg⁺, Al²⁺

Both rate coefficients based on the crossed beam measurements. Discrepancies are less than 15 % and usually smaller.

Si³⁺

Belfast's values at low temperature are much smaller than AR's (factor of 2 at 10 eV). It is due to the use of a wrong ionization potential (54 eV instead of 45 eV) by Belfast.

Sources: Based on the same crossed beam measurements.

S⁵⁺ - Ni¹⁷⁺

Belfast's values are smaller than AR's ones for S⁵⁺ (by 40 %) through Fe¹⁵⁺ (by factor of 2.7) at high temperature. The differences are mainly due to the contribution of EA process. The discrepancies at very low temperature by more than a factor of 2 is due to the choice of the scaled cross section by Belfast as discussed for Ne⁵⁺ - Ca¹⁵⁺ in sec.3.5.

Sources: Belfast scaled the cross section curve intermediate between the curves of Si³⁺ and Al²⁺. AR used the computations of Younger [21] for DI and those of Sampson [22] for EA process.

3.12 Mg sequence ($2p^63s^2$)

Mg

Lotz's are smaller than AR's by factor of 2 at low temperatures.

The differences more than factor of 2 are probably due to an fitting error by Belfast.

Sources: Based on the same measurement.

Al⁺

Lotz's are larger than AR's by more than factor of 2 at high temperatures.

Good agreement with AR and Belfast.

Based on the same measurements.

Si²⁺, S⁴⁺, Ar⁶⁺, Ca⁸⁺, Ti¹⁰⁺ - Ni¹⁶⁺

AR's are always smaller than Belfast at low temperatures (e.g., a factor of 2 for Si²⁺ and 50 % for S⁴⁺), the discrepancy decreases with increasing temperatures and for high Z ions.

AR's values even become larger than Belfast's at high temperatures. The scaled cross sections by Belfast ($3s^2$ only) are much higher than the results in Younger [23]. This is probably a mistake which explains the higher values compared to AR. The inclusion of EA and innershell ionization ($2p^6$) by AR compensate this overestimate for high Z ions and high temperatures.

Sources: Belfast scaled cross sections of Sc⁹⁺ and Fe¹⁴⁺ ($3s^2$ only). AR scaled the results of DWBX [23] for Fe¹⁴⁺ and add the contribution of the $2p^6$ shell by scaling the cross section of Na sequence. EA contribution is taken into account for Ar⁶⁺, Ca⁸⁺ by AR.

Fe¹⁴⁺

AR's values are higher than Belfast's by factor of 2 at high temperatures.

Sources: Belfast from DWBX [23], AR from DWBX and add the contribution of the $2p^6$ shell by scaling Na sequence as well as EA process.

3.13 Al sequence ($3s^23p$)

Al

AR's values are lower by a factor of 2 at $T/I \sim 0.1$ and 1.5 at $T/I \sim 10$ than Belfast's.

Sources: AR from PWB [13], Belfast scaled the Ar⁵⁺ cross section.

Si⁺, S³⁺

AR's are lower than Belfast by 20 % at $T/I = 1$ and 40 % at $T/I = 10$.

Sources: Both scaled the cross section of Ar ions (without EA contribution).

Belfast scaled the total cross section using only the first ionization potential whereas AR scaled the contribution of each individual shell.

Ar⁵⁺

Good agreement within 15 %.

Based on the measurement.

Ca⁷⁺

Belfast's values are lower than AR's at high temperature by 10 - 50 % due to the neglect of EA process.

Sources: AR and Belfast scaled the cross sections of Sc ions by DWBX [23] for DI process. AR adds an estimate of EA process.

Fe¹³⁺

Belfast's values are lower than AR's at high temperature due to the neglect EA process by Belfast.

Sources: DWBX [23] for DI process.

3.14 Si sequence (3s²3p²)

Si, S²⁺

Same as Si⁺, S³⁺.

Ca⁶⁺

Same as Ca⁷⁺.

Ar⁴⁺

Same as Ar⁵⁺.

Fe¹²⁺

Same as Fe¹³⁺.

3.15 P sequence (3s²3p³)

Ar³⁺

Large differences at low temperature.

Based on the measurement. Ionization potential of Belfast is 59.7 eV whereas 52.3 eV in AR.

S⁺

Belfast's values are larger than AR by 20 - 40 %.

Belfast scaled the measured cross section of Cl²⁺. AR scaled the Ar³⁺ results.

Ca⁵⁺

Same as Ca⁷⁺ in sec.3.13.

Fe¹¹⁺

Same as Fe¹³⁺.

3.16 S sequences (3s²3p⁴)

S

Good agreement.

Based on the measurement.

Ar²⁺

Same as Ar⁵⁺.

Ca⁴⁺

Belfast is higher than AR more than 25 % for T / I < 0.5.

Sources: Belfast scaled the measured cross section of Ar²⁺, AR scaled cross section of Sc ions by Younger [22].

Fe¹⁰⁺

Same as Fe¹³⁺.

3.17 Cl sequence (3s²3p⁵)

Ar⁺

There are discrepancies at high temperatures (20 - 40 %).

Sources : Measurement by Muller et al.[27] for AR and by Woodruff et al.[28] for Belfast.

Ca³⁺

Same as Ca⁴⁺.

Fe⁹⁺

Same as Fe¹³⁺.

3.18 Ar sequence (3s²3p⁶)

Ar

Good agreement within 10 - 20 %.

Sources : Measurements.

Ca²⁺

Good agreement within 10 - 20 %.

Sources : Belfast scaled the measurements of K⁺ and AR scaled the DW calculation of Sc³⁺.

3.19 K sequence (3s²3p⁶4s)

Ca⁺

Good agreement.

Sources : Based on the same measurement.

Fe⁷⁺

AR's values are smaller at high temperature and larger at low temperatures by 50 % at maximum than Belfast's.

Sources: AR from DW calculation [8], Belfast scaled the measured cross section of Ti³⁺.

3.20 Ca sequence (3s²3p⁶4s²)

Ca

Discrepancies of the order of 40 %.

Sources: AR adopted the measured cross section [24], Belfast the PWB computations [25]

Fe⁶⁺

Good agreement.

Based on the same measurement.

3.21 Other ions

Fe

Good agreement.

Sources : PWB

Fe⁺, Fe²⁺, Fe⁵⁺

Excellent agreement based on measurements.

Fe³⁺, Fe⁴⁺

AR's are larger than Belfast's typically by a factor of 2. Belfast and AR adopted Pindzola [26] for the DI process, AR included the EA process [8].

$N_i^+ - N_i^{6+}$

Discrepancies are more than factor of 2. Temperature dependence of Belfast is steeper than AR at low temperatures.

4. Discussions

Generally, the rate coefficients derived on the basis of experimental data of cross sections are in good agreement among the authors.

When no experimental data are available, AR included the EA process whereas Belfast did not. This choice is important especially for Na like ions and for ions of Li and Mg to Ar sequences (less and less important with increasing number of p electrons). This results in differences at high temperatures.

The rate coefficients at very low temperatures ($T/I < 0.5$) are very sensitive to the cross section behaviour near the threshold ($E/I < 1.5$). There exist significant discrepancies between various theoretical calculations and/or empirical scalings. The plane wave Born approximation is not valid at low energy and gives typically lower cross sections than DW computations near threshold by a factor 2.

The classical scaling law ($u^2I\sigma$) does not look valid for complex sequences or for low ionized ions even in rather simple sequences. When inner shell ionization cannot be ignored, scaled cross section for each shell should be taken into account. Therefore the rate coefficients depend on the procedure adopted (classical scaling, interpolation between reduced cross sections of different ions, theoretical methods) and also on the cross section of the ion chosen as a reference in the scaling process.

In the actual plasmas, we have to take into account the ionization from the excited states since the populations of excited states are not always negligible compared to the population of the ground states. In this report the rate coefficients are those from the ground states, except for the recommended data for iron ions by Pindzola [8].

The formulae for cross sections of Lotz, AR and Belfast are very similar to each other, as mentioned in sec.1. The fit with Chebychev polynomials of the rate coefficients given in Pindzola can not reproduce the real rate coefficients at very low temperatures. We found the same disagreements sometimes for Belfast's expression of eq.(8). This is because the values of the rate coefficients increase very rapidly at low temperature. To fit accurately the integrated cross section (rate coefficients) we should first rescale the rate coefficient so that to define an "effective" rate coefficient, similar to the "effective collision strength" used for excitation, which has no strong temperature dependence. It would be easier to fit the cross section in a form which gives a correct behavior at both low and high energies and which is easy to integrate with Maxwellian distribution

than to fit the rate coefficient. However in that case we have to find a reasonable expression for the autoionization. It is difficult to approximate accurately the cross section for Excitation Autoionization, especially nearby its onset, since this process involves many possible excited levels, resulting in a complex shape of the cross section.

We are now doing the data evaluations for ionization process.

5. Graphs

The ionization rate coefficients are compared by the element from H though Ni as a function of electron temperatures. The solid lines, dashed lines and dotted lines indicate the rate coefficients by Belfast, Lotz and Arnaud, respectively. The Pindzola's data for iron ions are shown by dot-dashed lines.

We have also shown the ratios of the rate coefficients to the values of Belfast namely; $C(\text{Lotz}) / C(\text{Belfast})$, $C(\text{AR}) / C(\text{Belfast})$ and $C(\text{Pinzola}) / C(\text{Belfast})$ are shown by dashed, dotted and dott-dashed lines, respectively. The scale for the ratio is indicated in the right side, whereas for the rate coefficients in the left side.

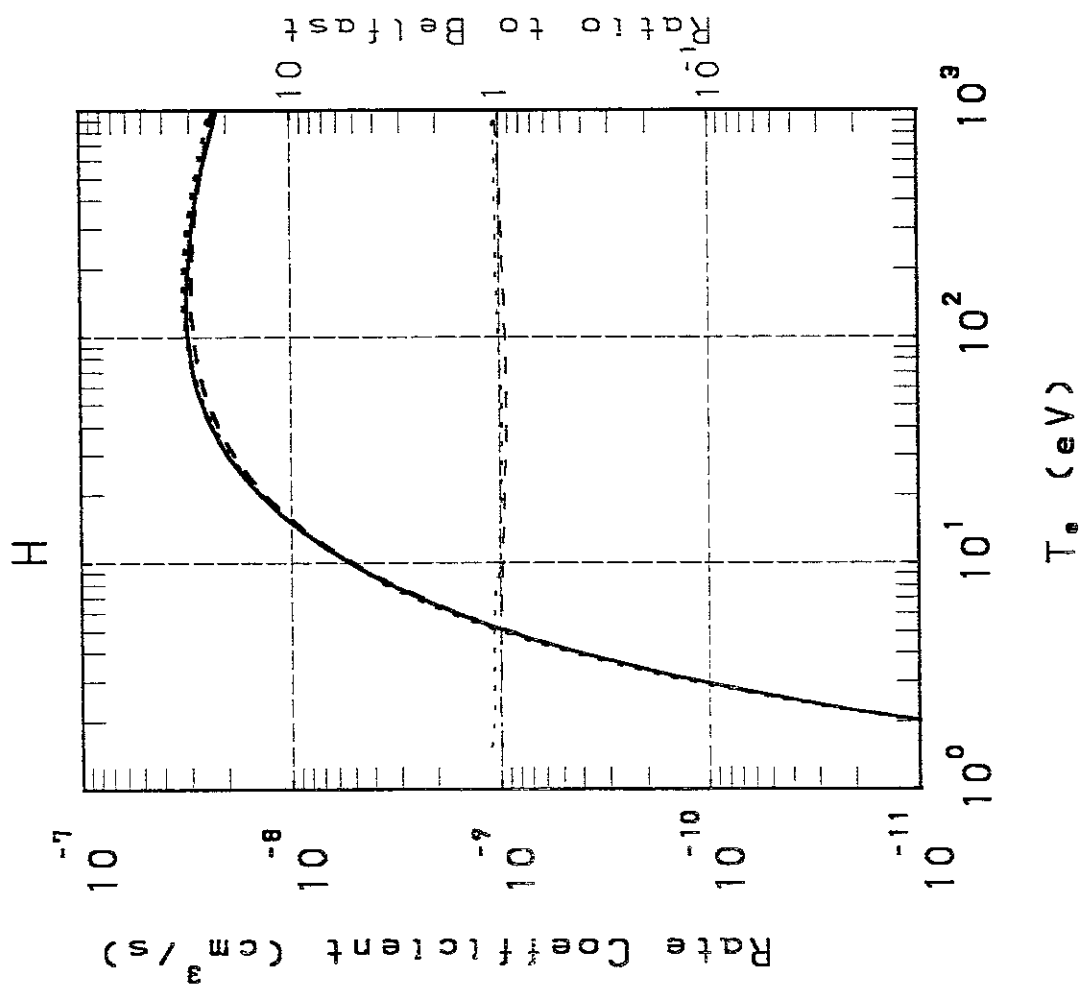
Aknowledgement

The authors would like to thank Mr. E. Asano for making graphs.

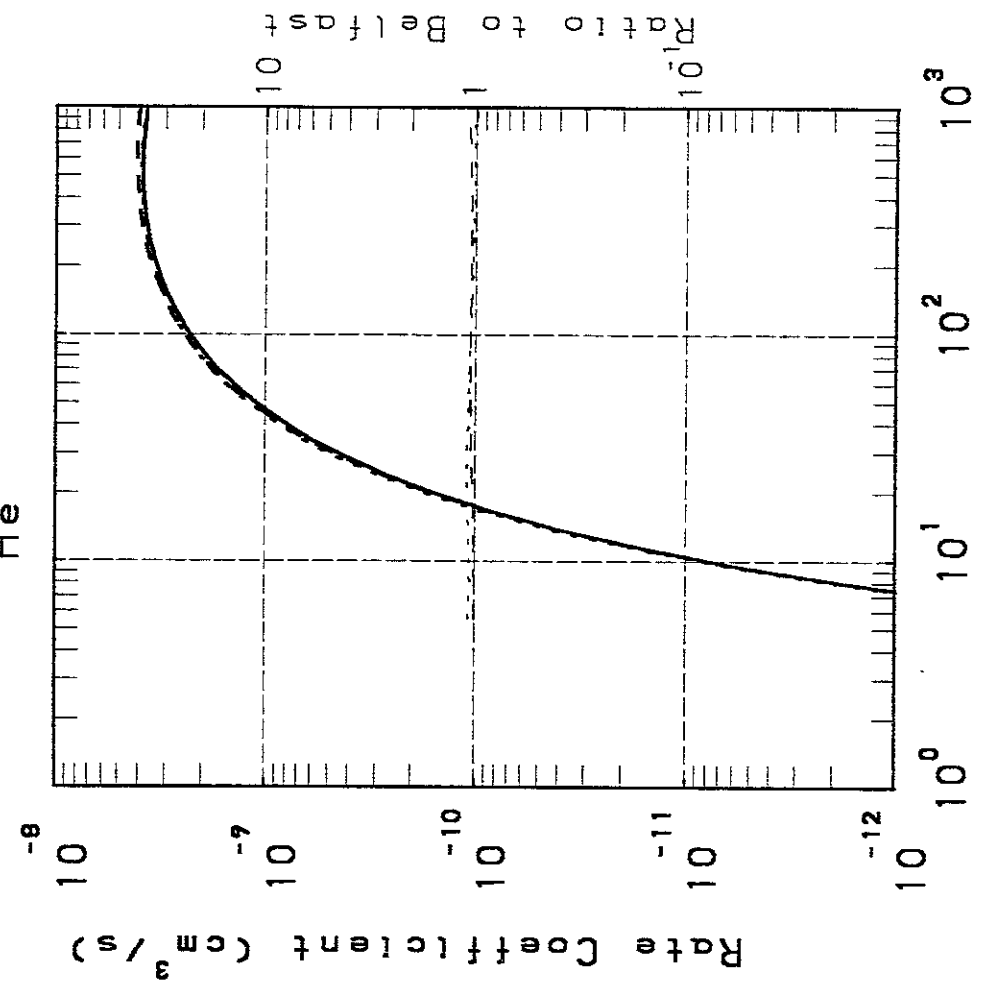
This work was supported in part by NASA Grant NAG 548(MA). MA thanks Dr. J. Raymond for very useful discussions.

References

- [1] Lotz, W., 1967, Report Institute fur Plasma physics, IPP 1/62
- [2] Lotz, W., 1968, Report Institute fur Plasma Physics, IPP 1/76
- [3] Arnaud, M., Rothenflug, R., 1985, *Astron. Astrophys. Supply. Series*, **60**, 425
- [4] Younger, S.M., 1981, *J. Quant. Spectrosc. Radiat. Transfer*, **26**, 329
- [5] Arnaud, M., Raymond, 1991, to be submitted to *Astrophysical Journal*
- [6] Bell, K.L., Gilbody, H.B., Hughes, J.G., Kingston, A.E., Smith, F.J., 1983, *J. Phys. Chem. Ref. Data* **12**, 891
- [7] Lennon, M.A., Bell, K.L., Gilbody, H.B., Hughes, J.G., Kingston, A.E., Murray, M.J., Smith, F.J., 1988, *J. Phys. Chem. Ref. Data* **17**, 1285
- [8] Pinzola, M.S., Griffin, D.C., Bottcher, C., Younger, S.M., Hunter, H.T., 1987, *Nuclear Fusion, Special Supplement*, 21
- [9] Younger, S. M., 1982, *J. Quant. Spectrosc. Radiat. Transfer*, **27**, 541
- [10] Younger, S.M., 1980a, *Phys. Rev. A.*, **22**, 111
- [11] Younger, S. M., 1981a, *J. Quant. Spectrosc. Radiat. Transfer*, **26**, 329
- [12] Younger, S. M., 1980b, *Phys. Rev. A.*, **22**, 1425
- [13] Mc Guire, E.J., 1982, *Phys. Rev. A.*, **26**, 125
- [14] Jakubowitz, H., Moores, D.L., 1981, *J. Phys. B.*, **14**, 3733
- [15] Sampson, D.H., Golden, L.B, 1981, *J. Phys. B.*, **14**, 903
- [16] Younger, S. M., 1981b, *Phys. Rev. A.*, **24**, 1278
- [17] Jakubowitz, H., 1980, Ph. D. Thesis, University of London
- [18] Hamdam, M., Birkinshaw, K., Hasted, J.B. 1978, *J. phys. B.*, **11** (1978) 331
- [19] Danjo, A., Matsumoto, A., Ohtani, S., Suzuki, H., Tawara, H., Wakita, K., Yoshino, M., 1984, *J. Phys. Soc. Jap.*, **53** 4091
- [20] Younger, S. M., 1981c, *Phys. Rev. A.*, **23**, 1138
- [21] Younger, S. M., 1981d, *Phys. Rev. A.*, **24**, 1272
- [22] Sampson, D.H., 1982, *J. Phys. B.*, **15**, 2087
- [23] Younger, S. M., 1983, *J. Quant. Spectrosc. Radiat. Transfer*, **29**, 61
- [24] Rakhovskii, V.I., Stefanov, A.M., 1969, *Teplofizika Vysokikh Temperatur*, **7**, 1071
- [25] Mc Guire, E.J., 1977, *Phys. Rev. A.*, **16**, 62
- [26] Pinzola, M.S., Griffin, D.C., Bottcher, C., Gregory, C., Howald, A.M., Phaneuf, R.A., Crandall, D.H., Dunn, G.H., Muller, D.W., Morgan, T.J., 1985, Oak Ridge National Laboratory report No ORNL/TM-9436 DIST. CATEGORY UC-20, UC-20F
- [27] Muller, D.w., Salzborn, E., Frodl, R., Becker, R., Klein, H., Winter, H., 1980, *J. Phys. B.*, **13**, 1877
- [28] Woodruff, P.R., Hublet, M.C., Harrison, M.F.A., 1978, *J. Phys. B.*, **11**. L305

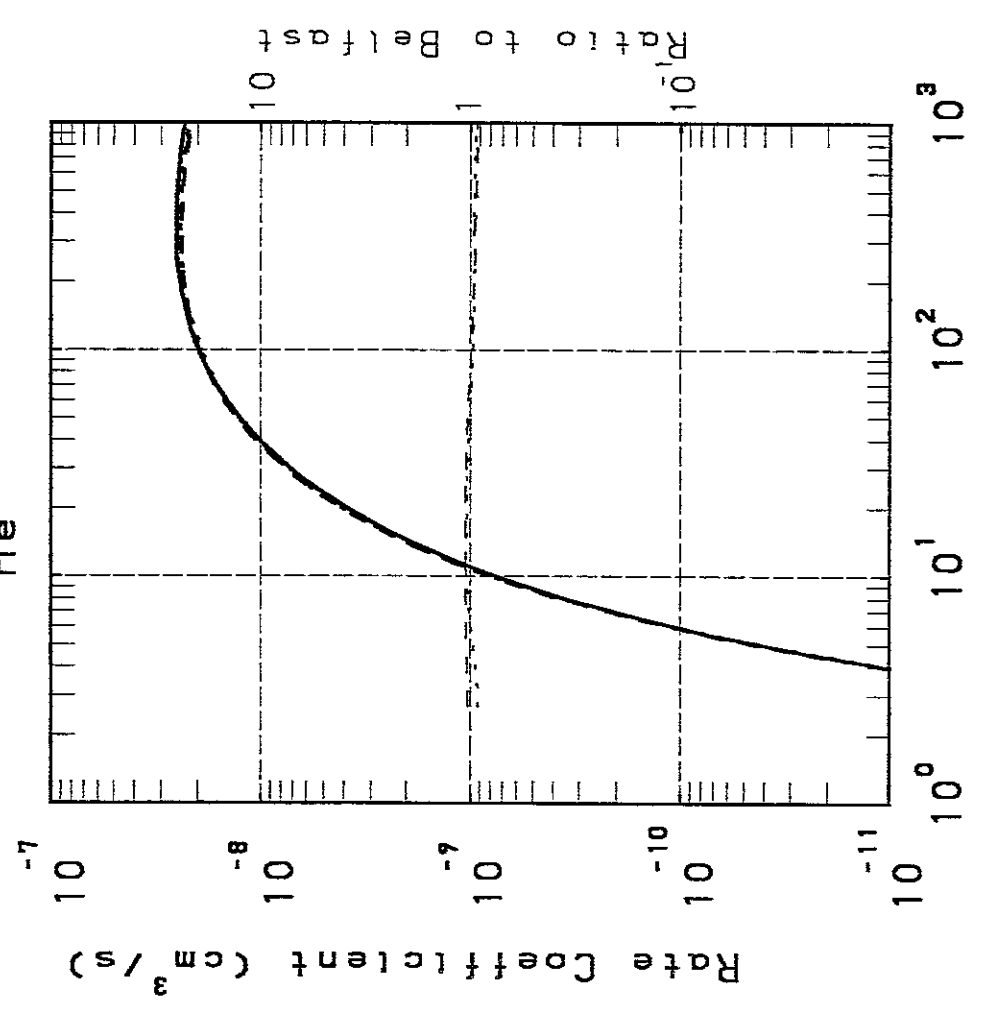


He¹⁺

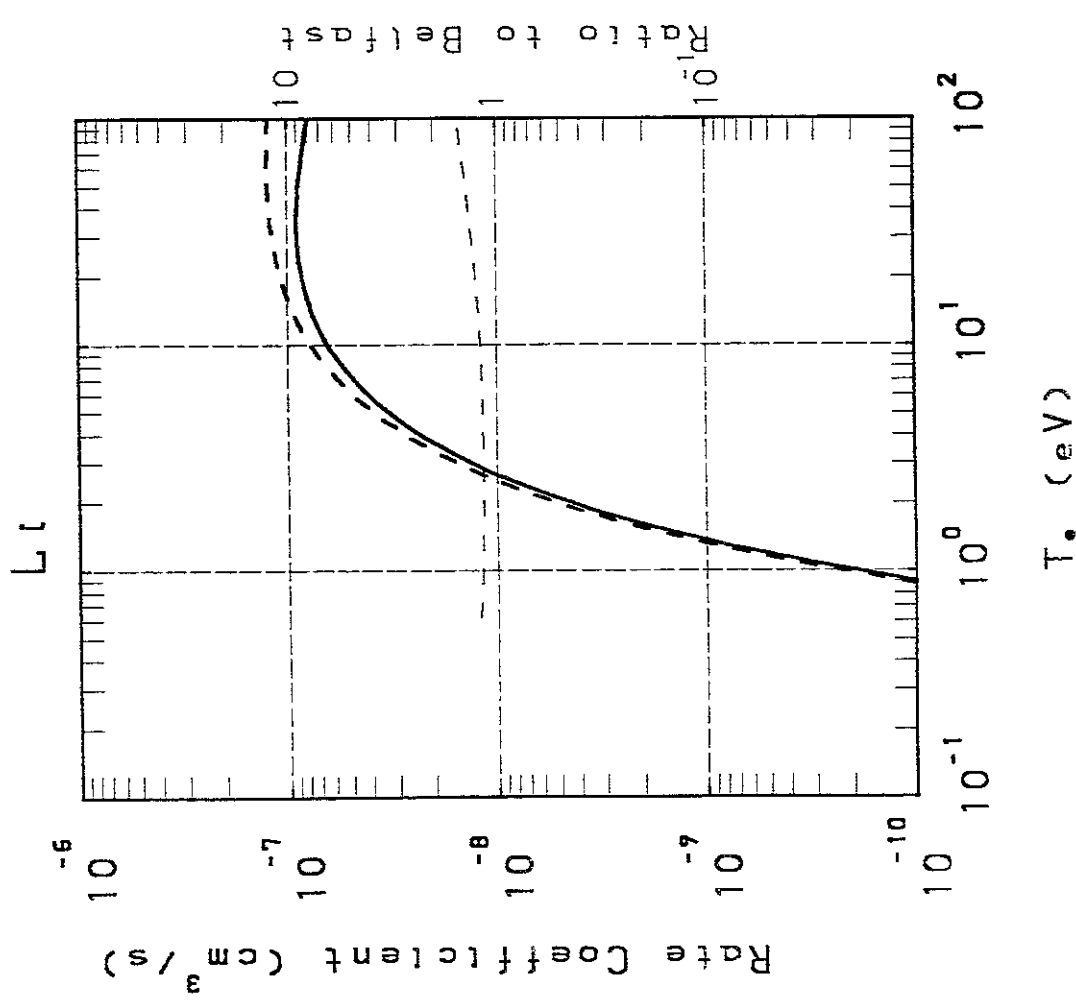
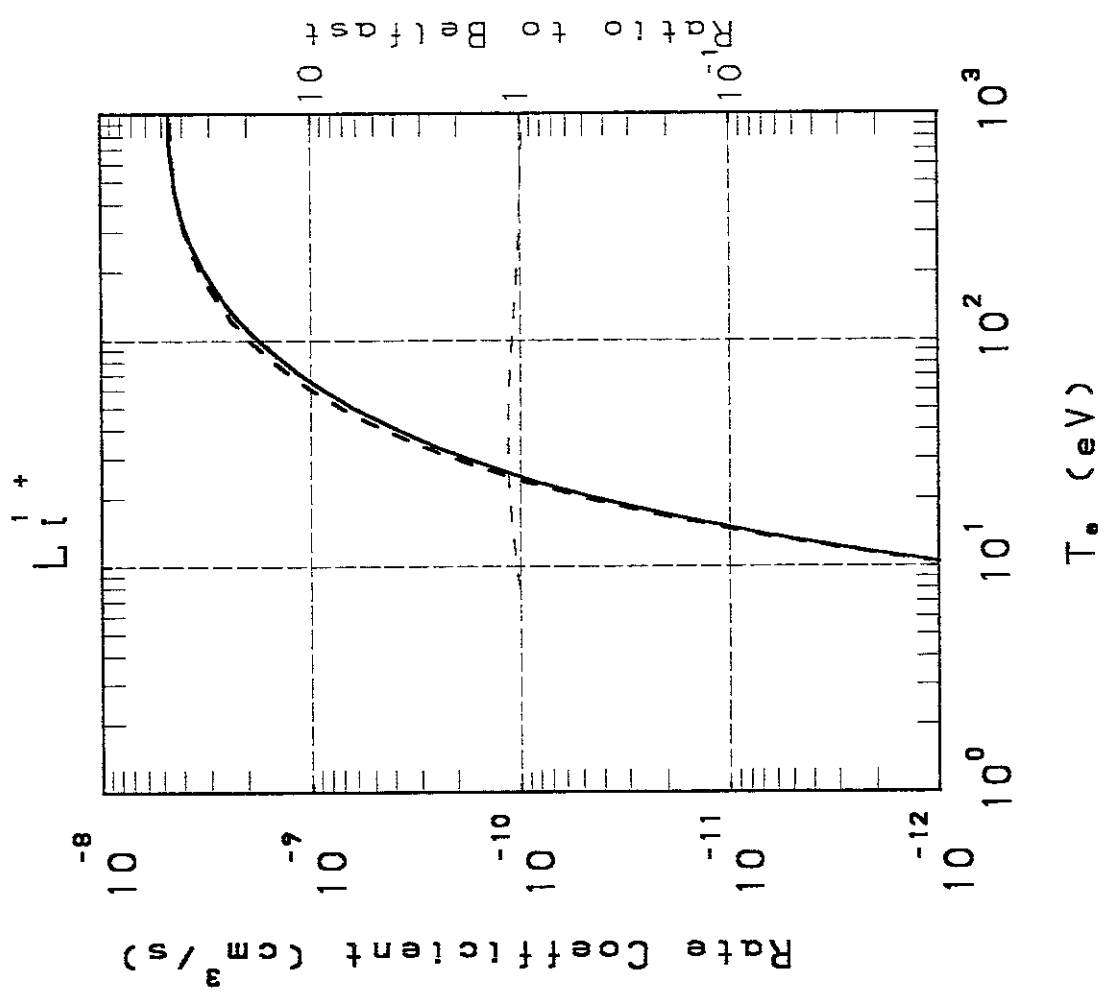


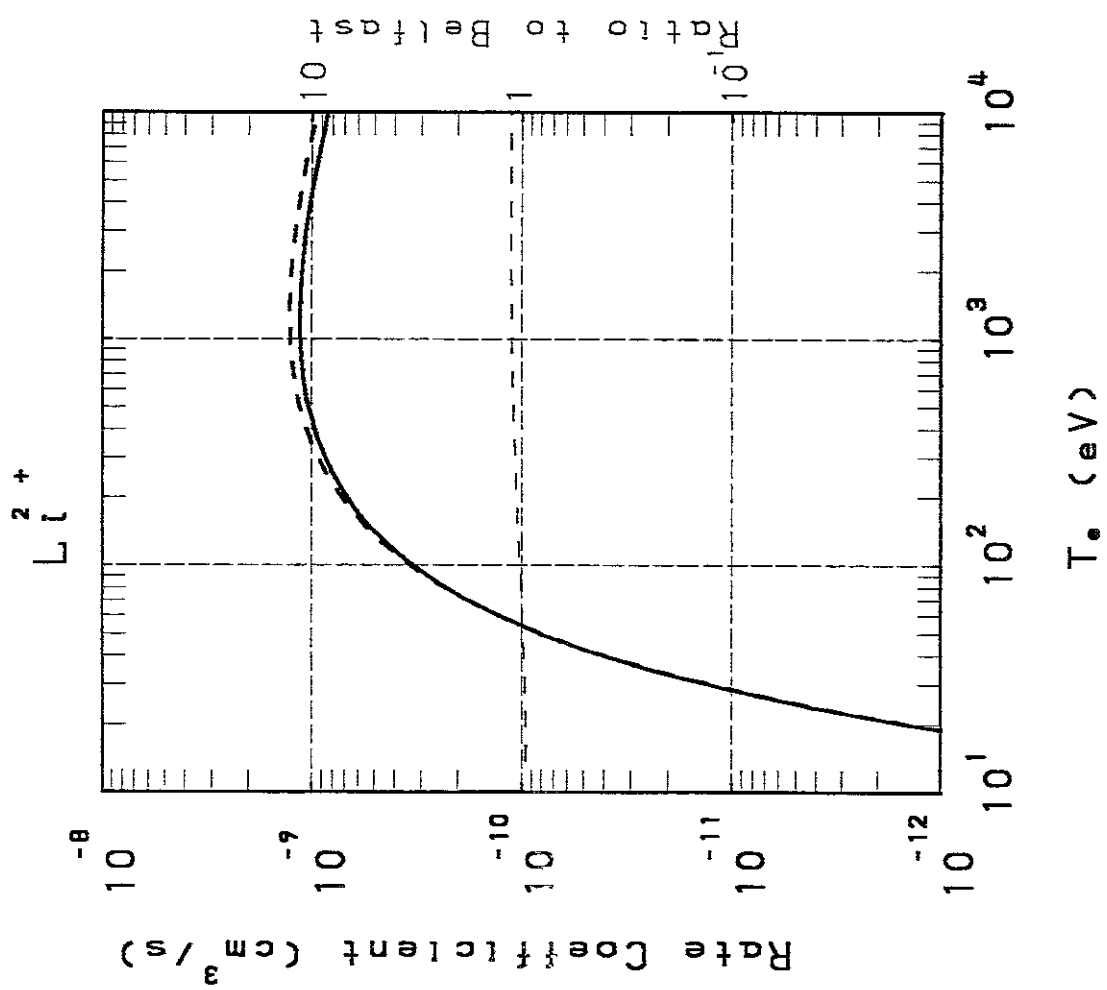
T_e (eV)

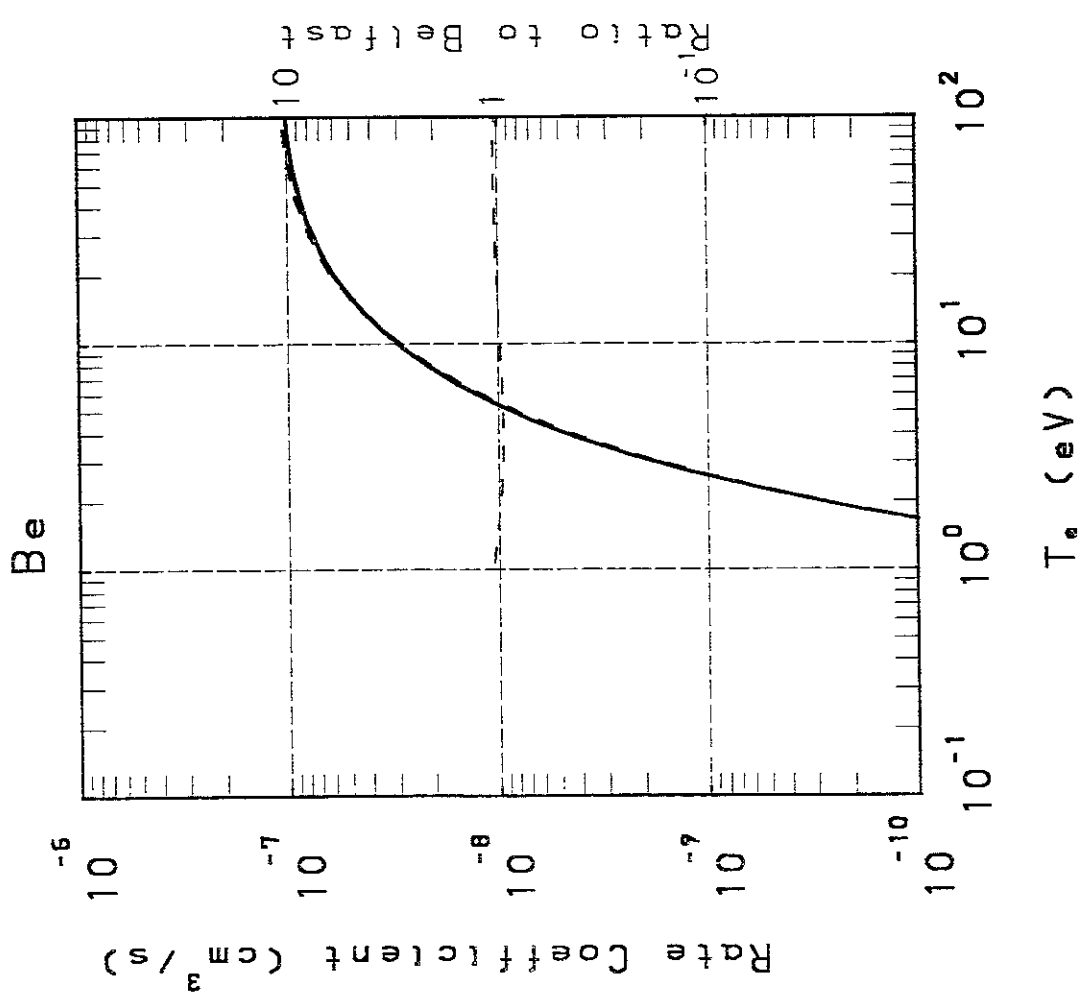
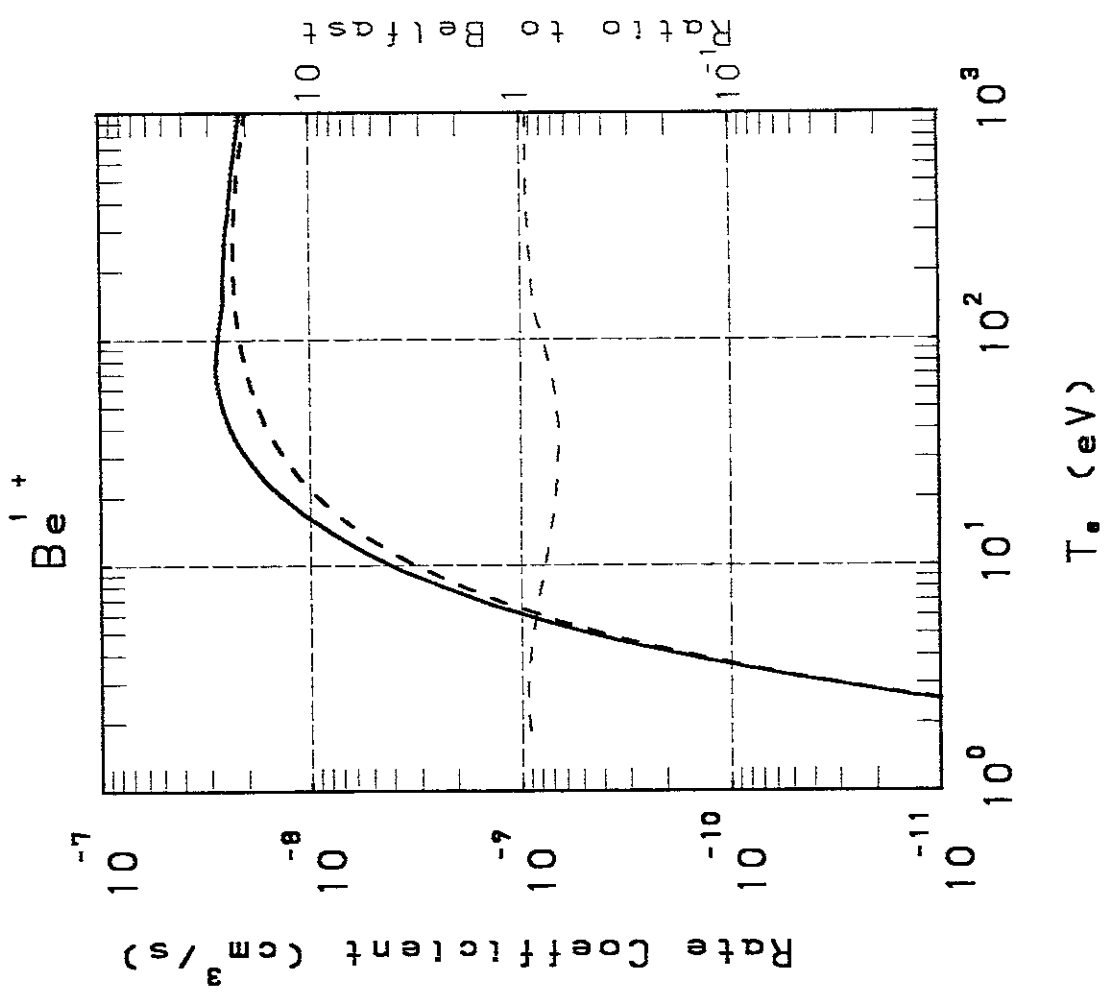
He

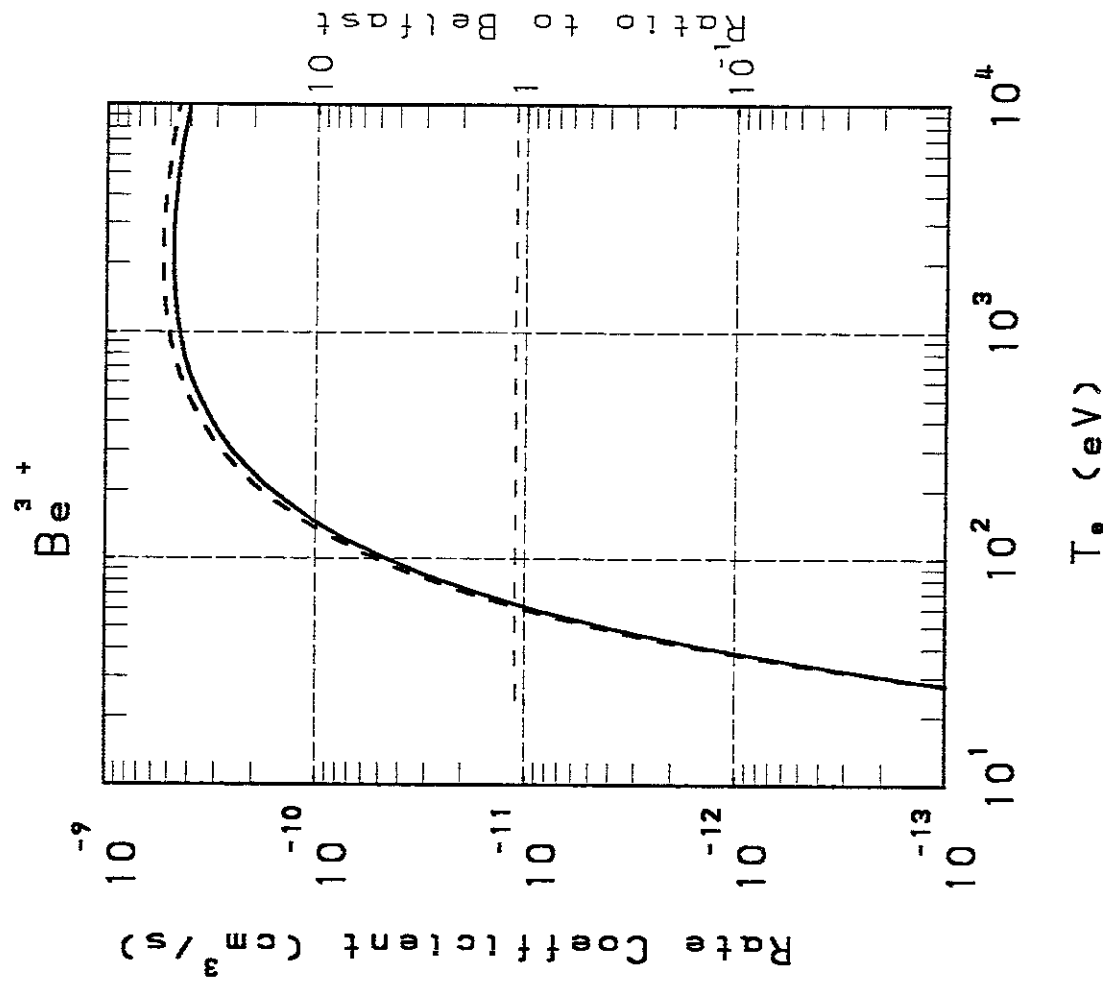
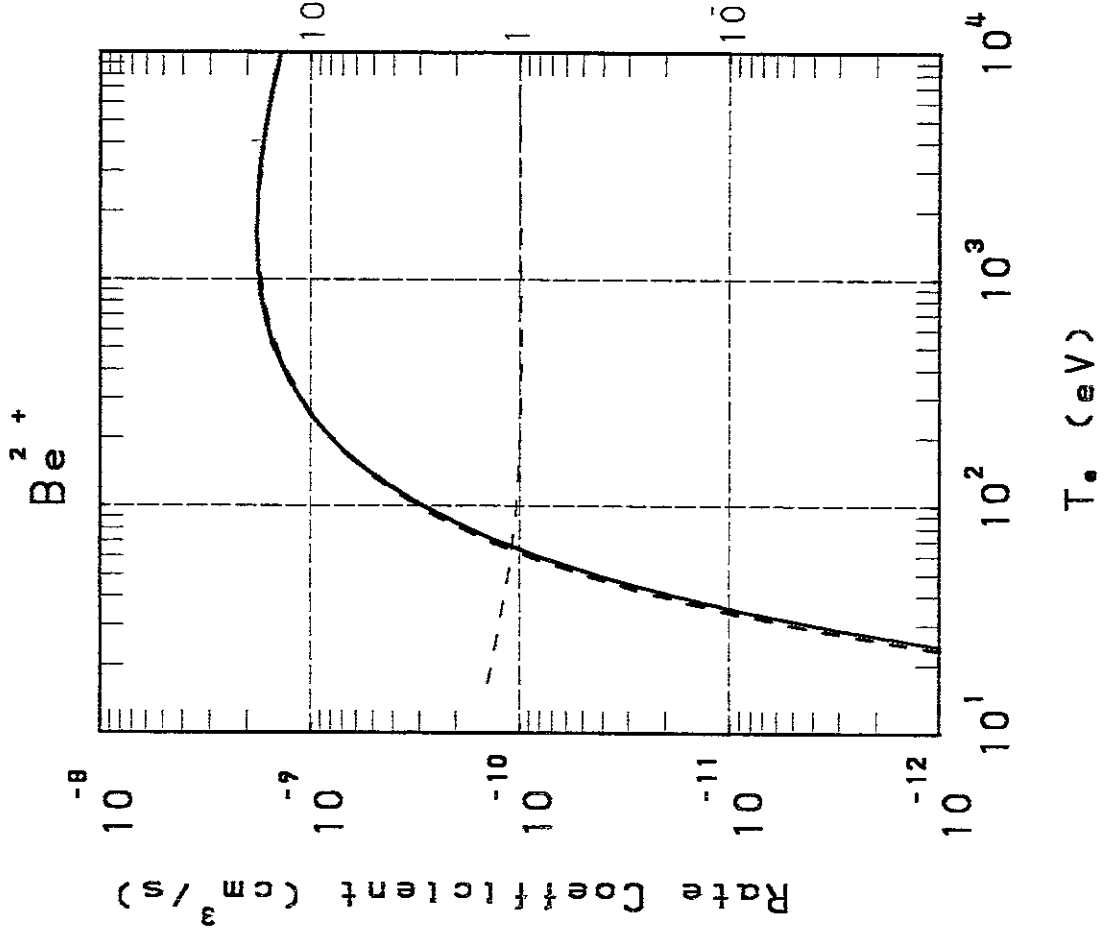


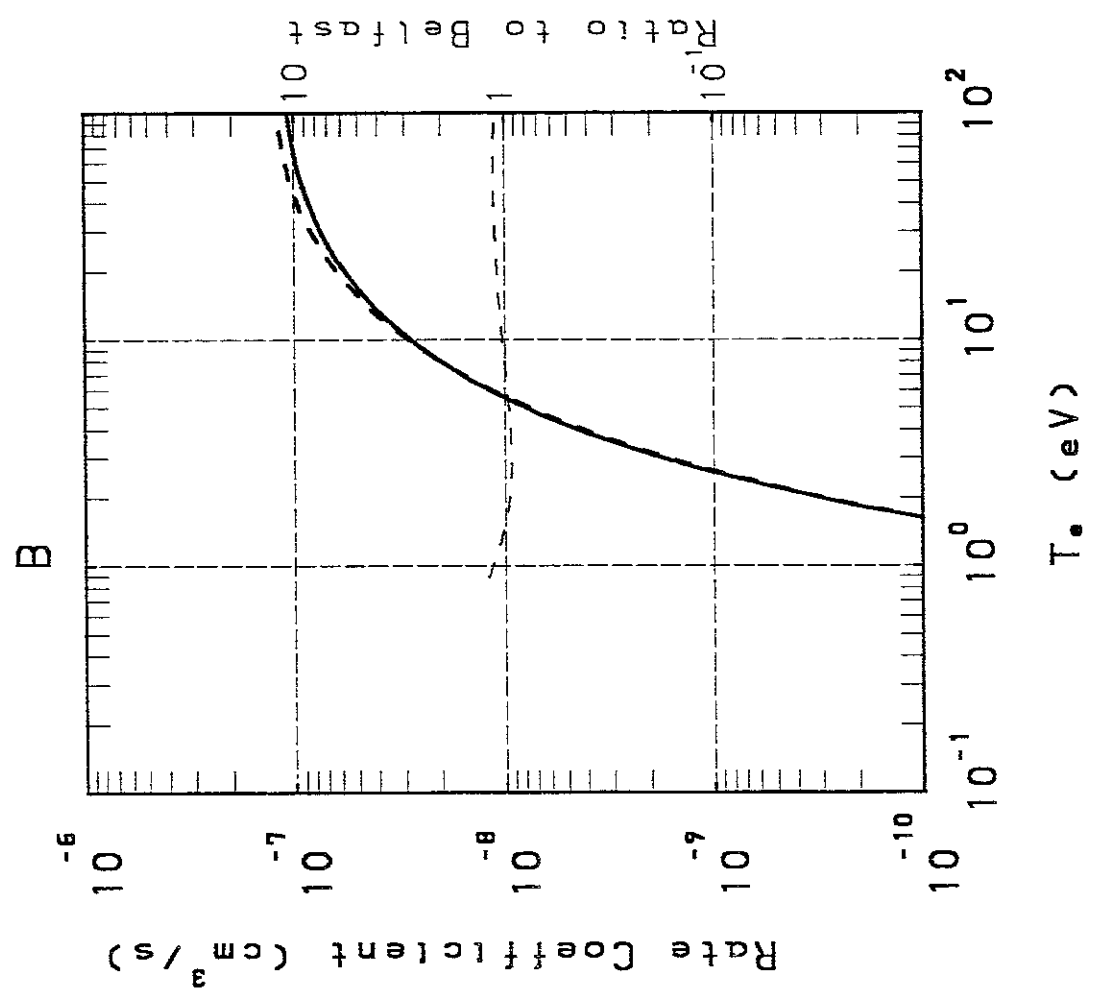
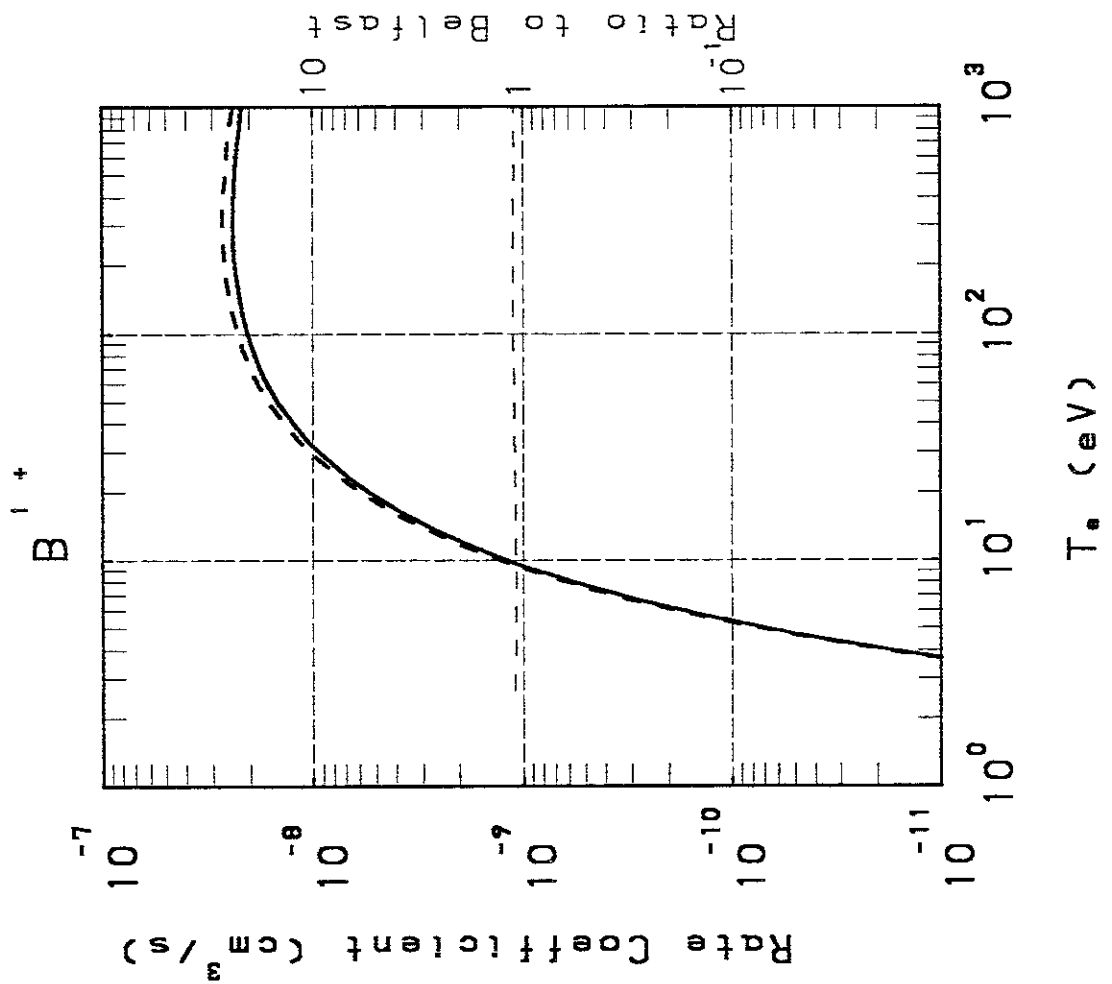
T_e (eV)

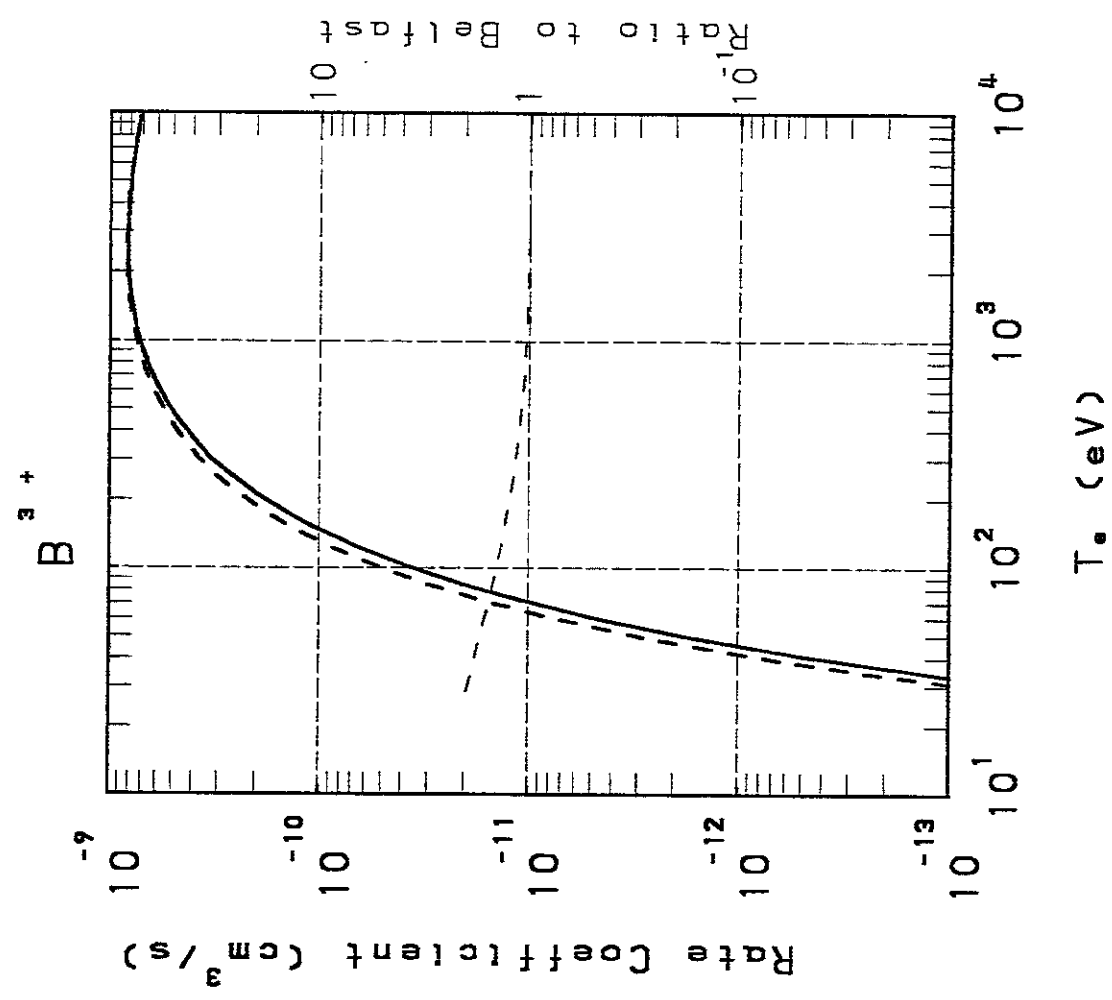
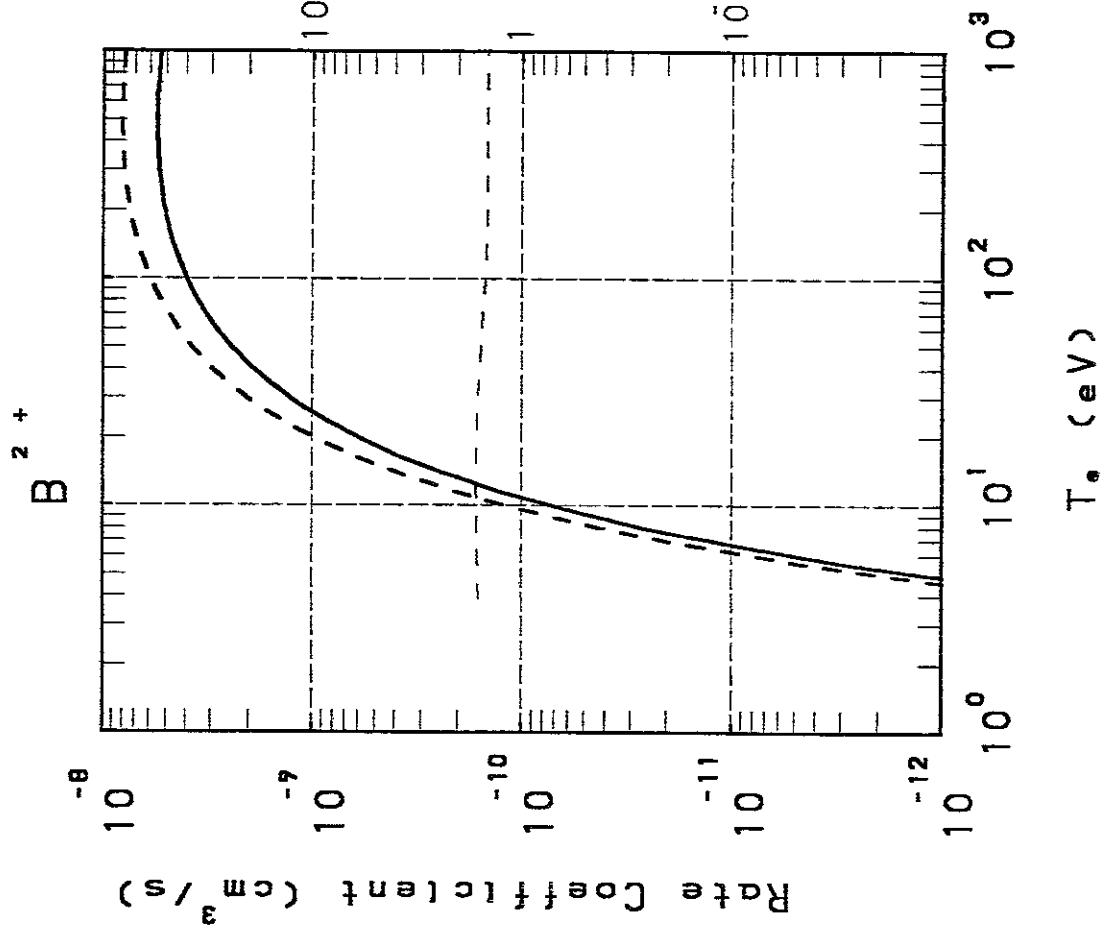


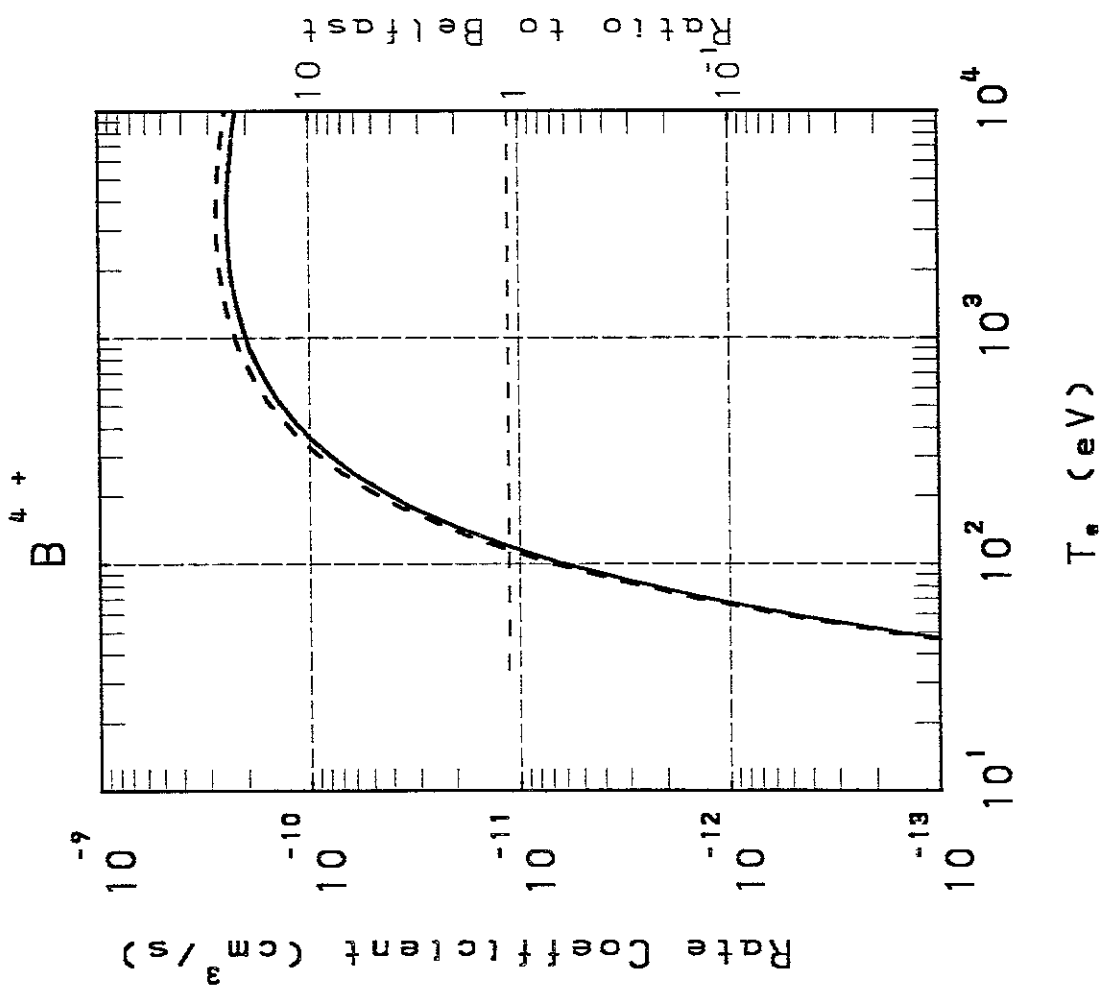


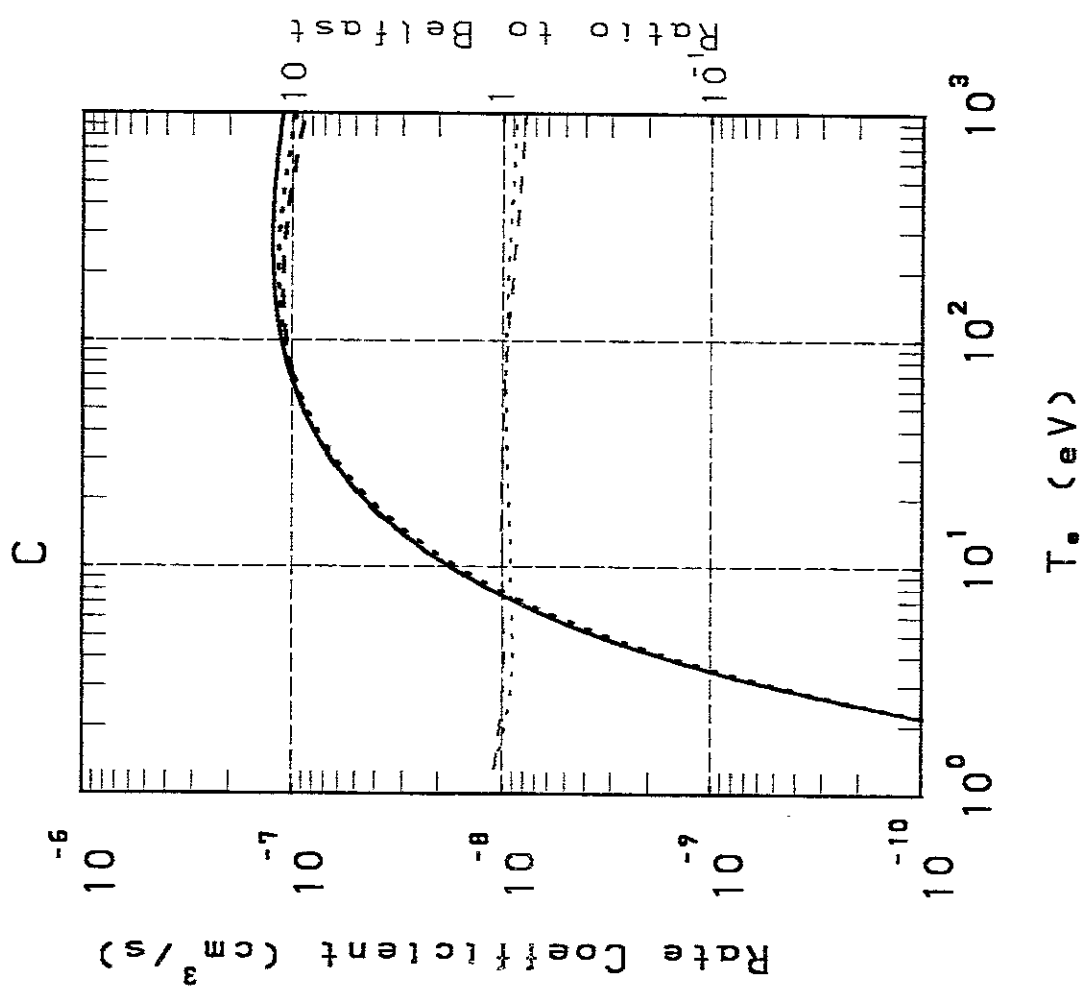
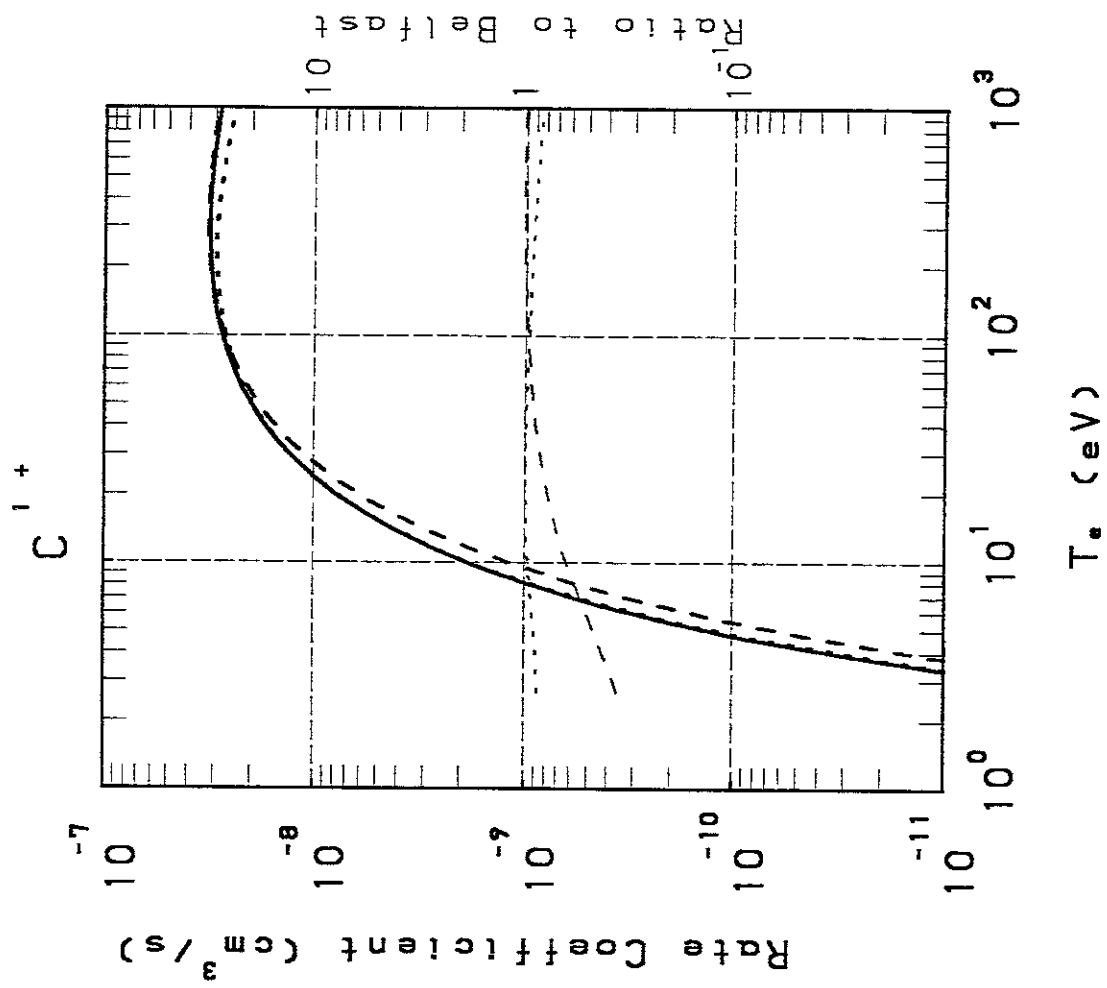


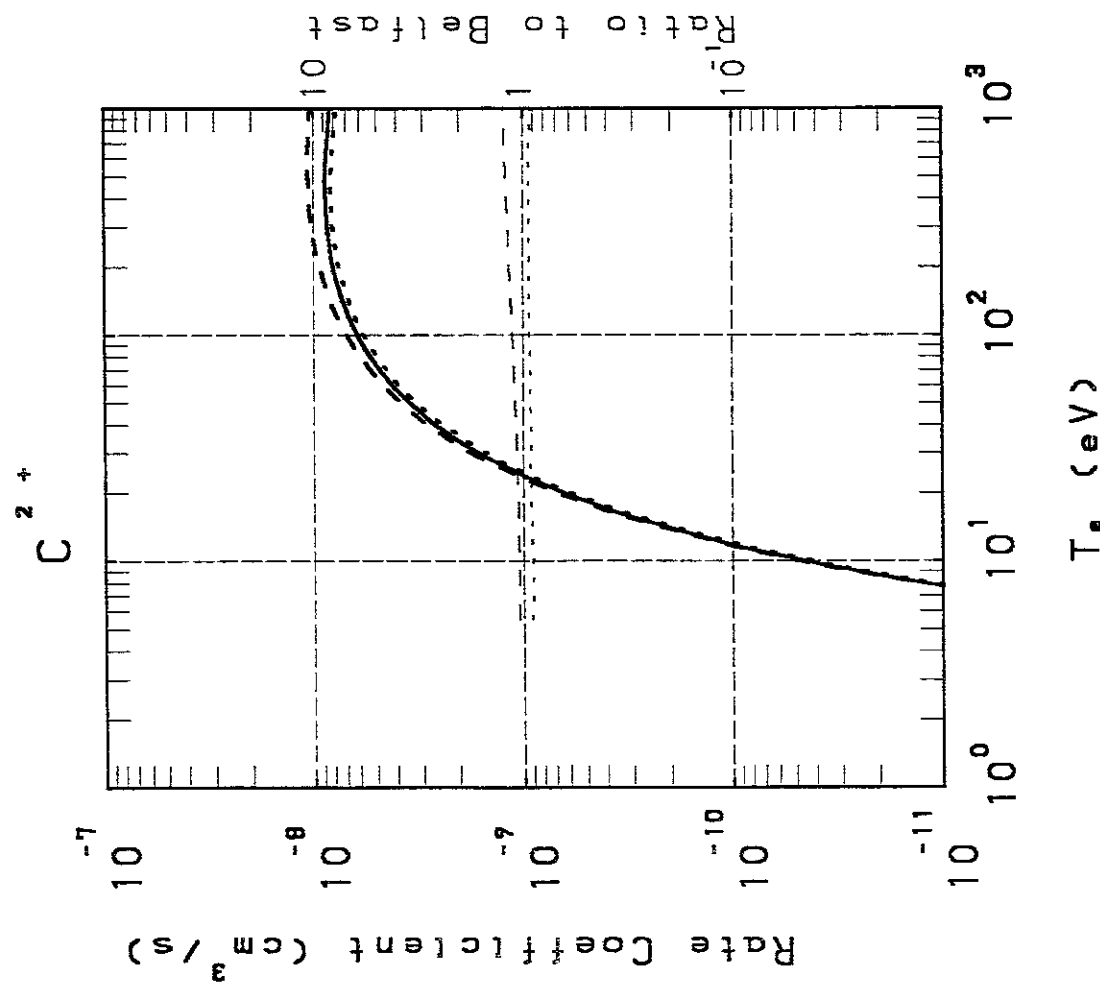
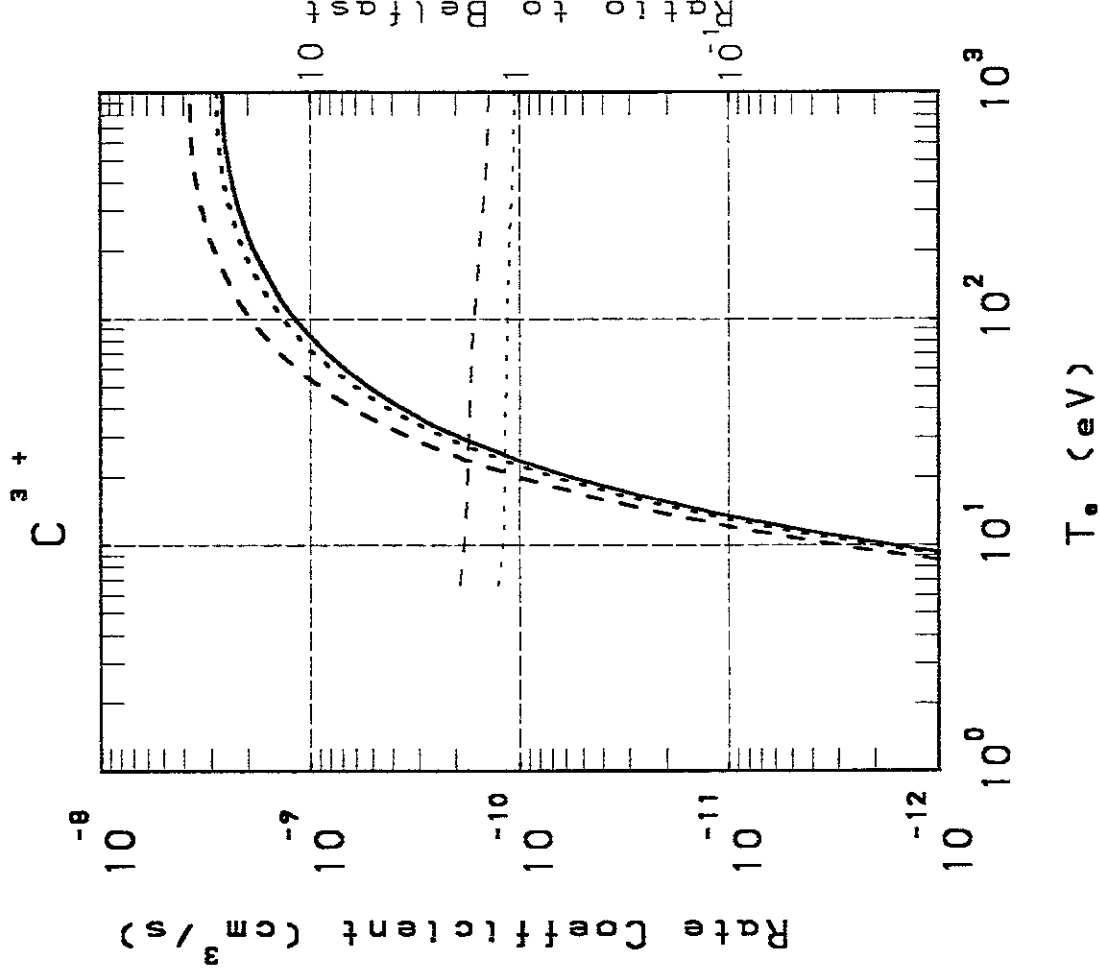


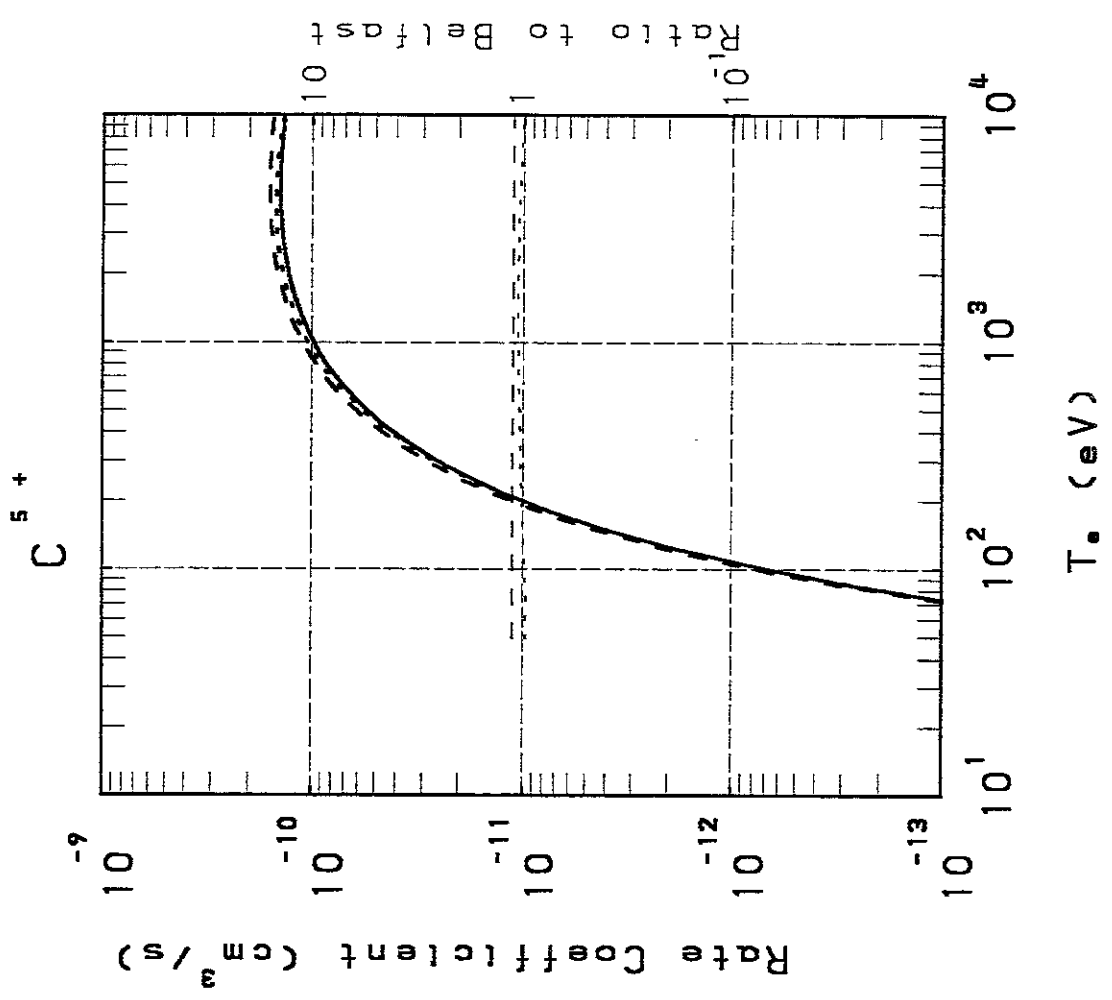
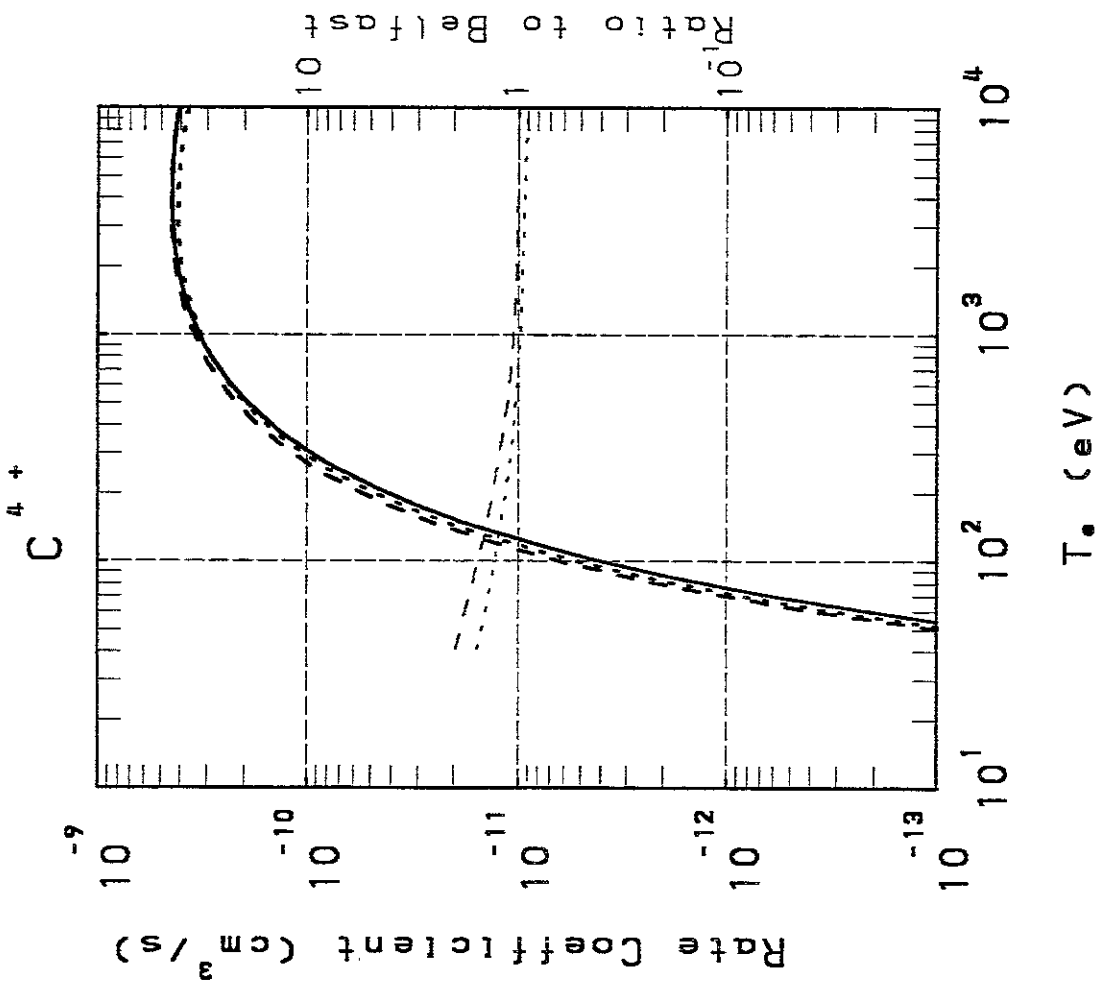


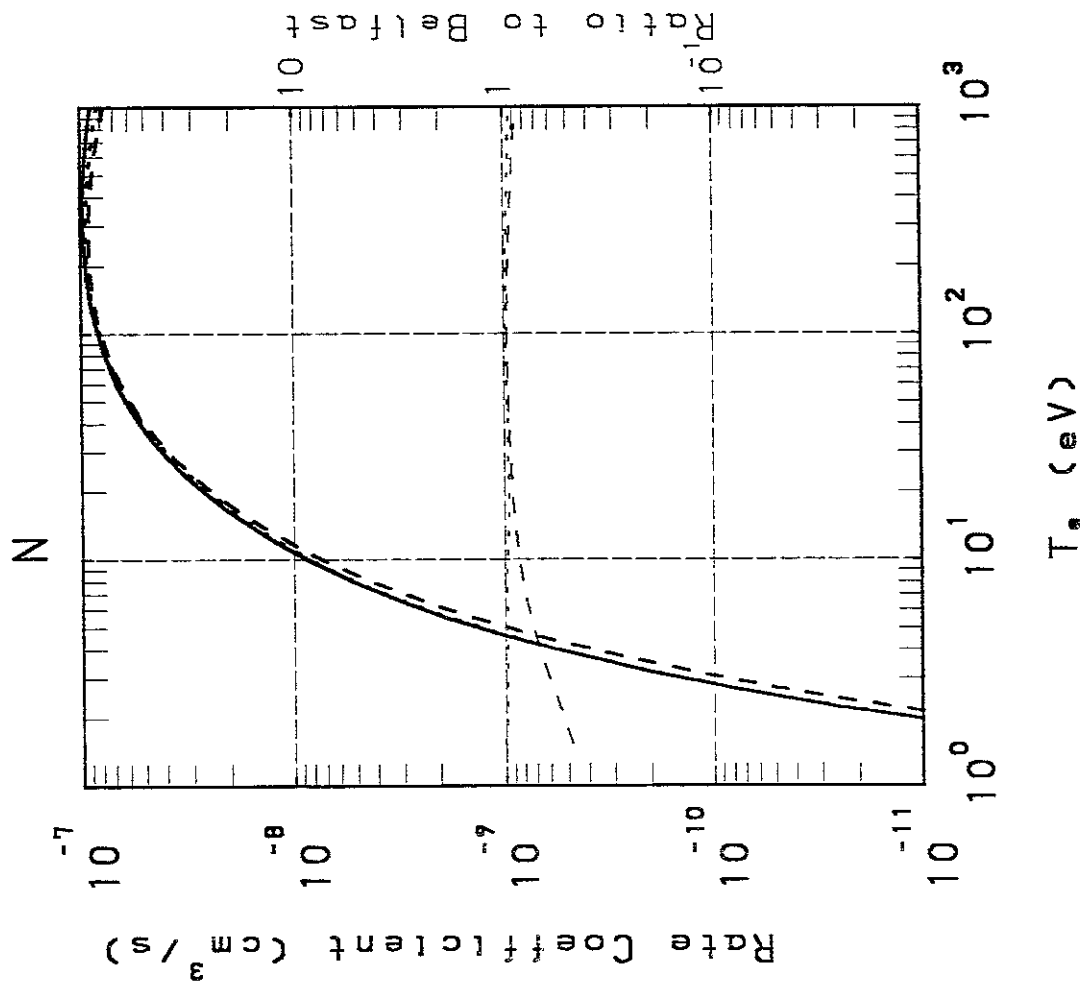
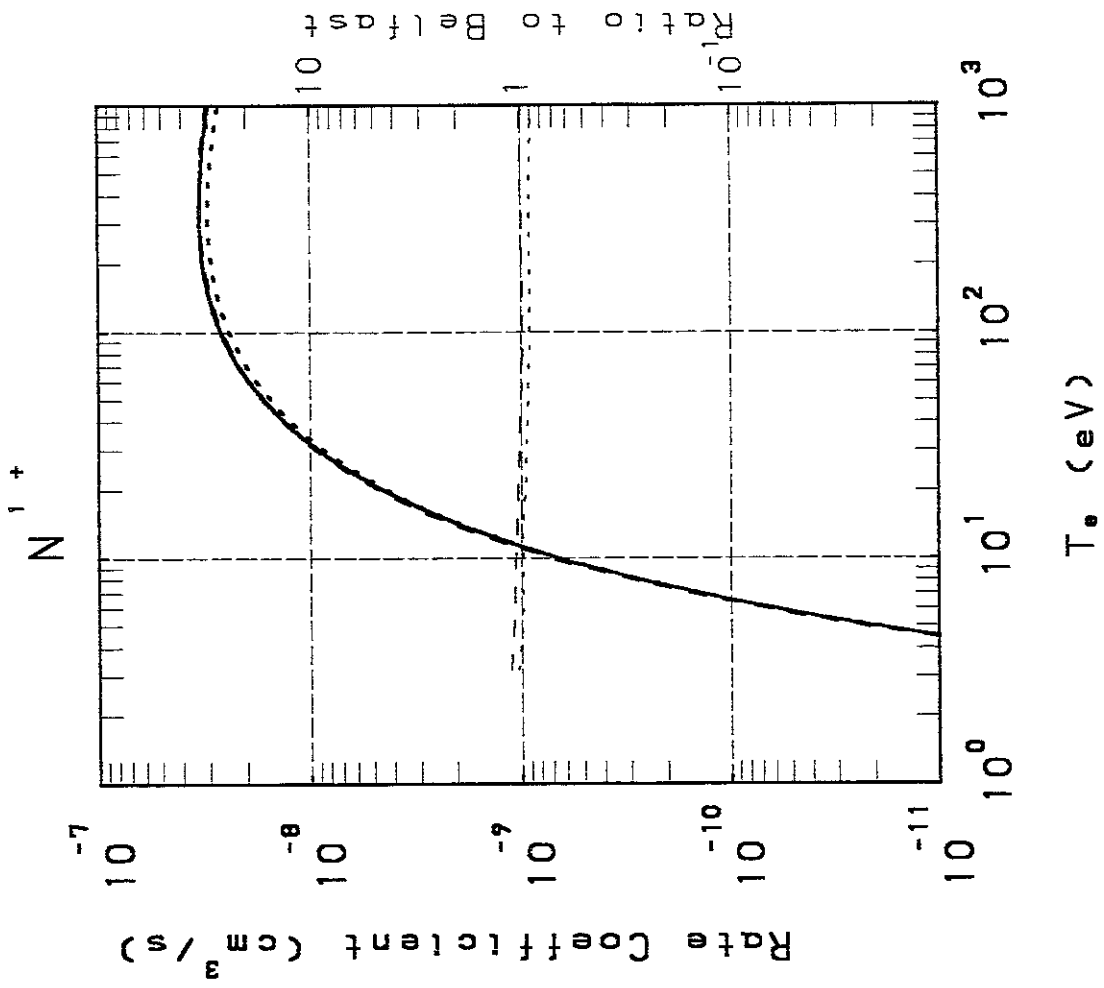




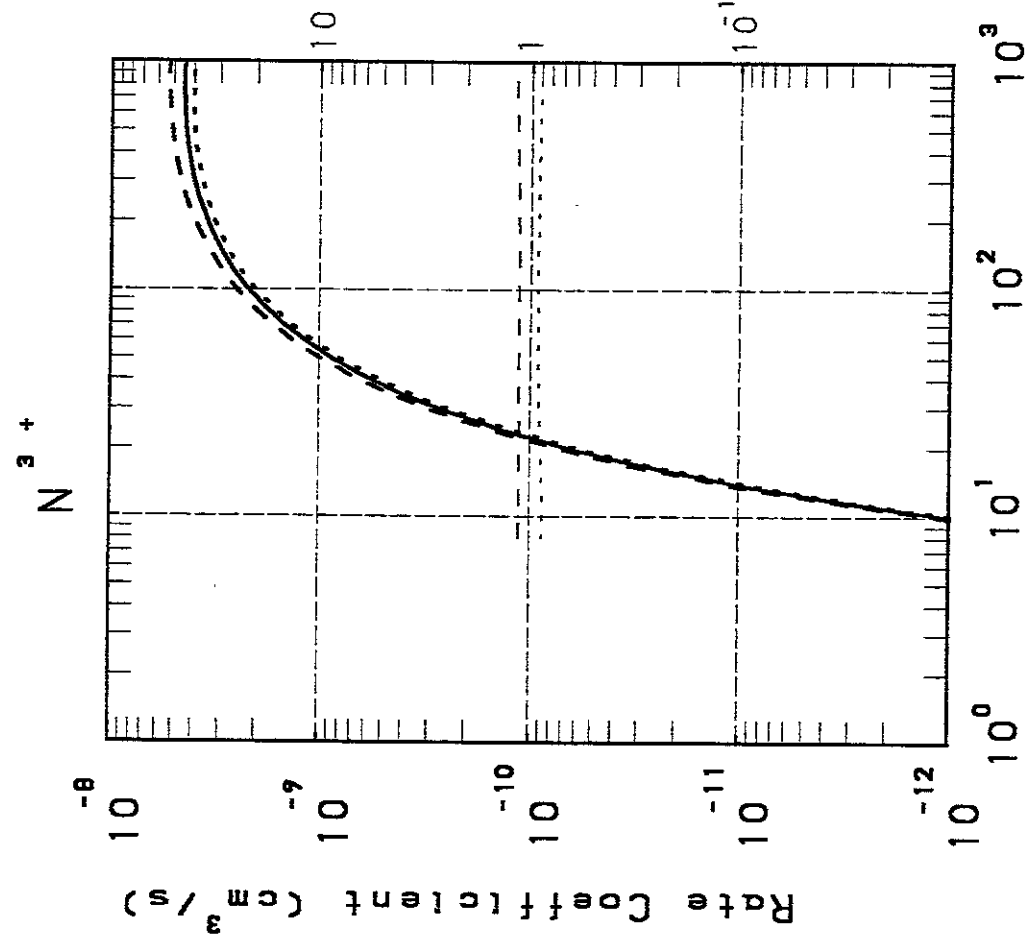




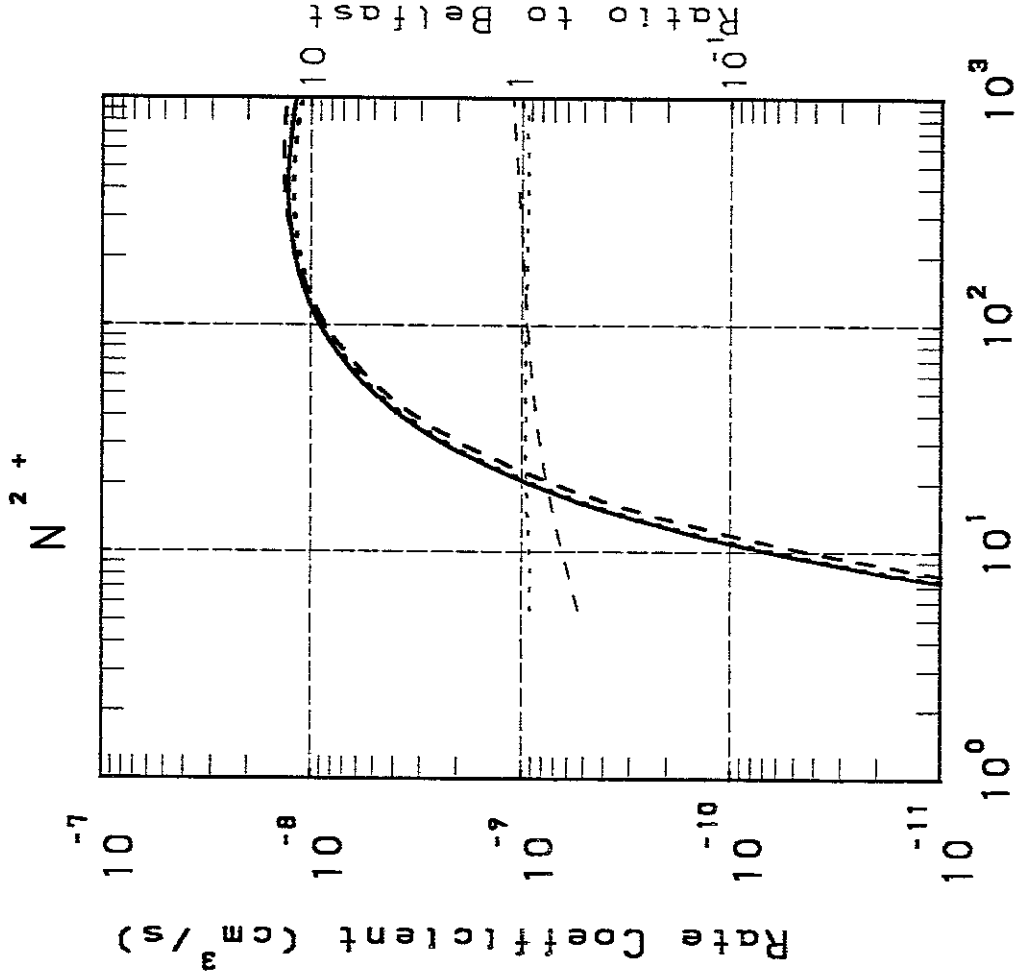


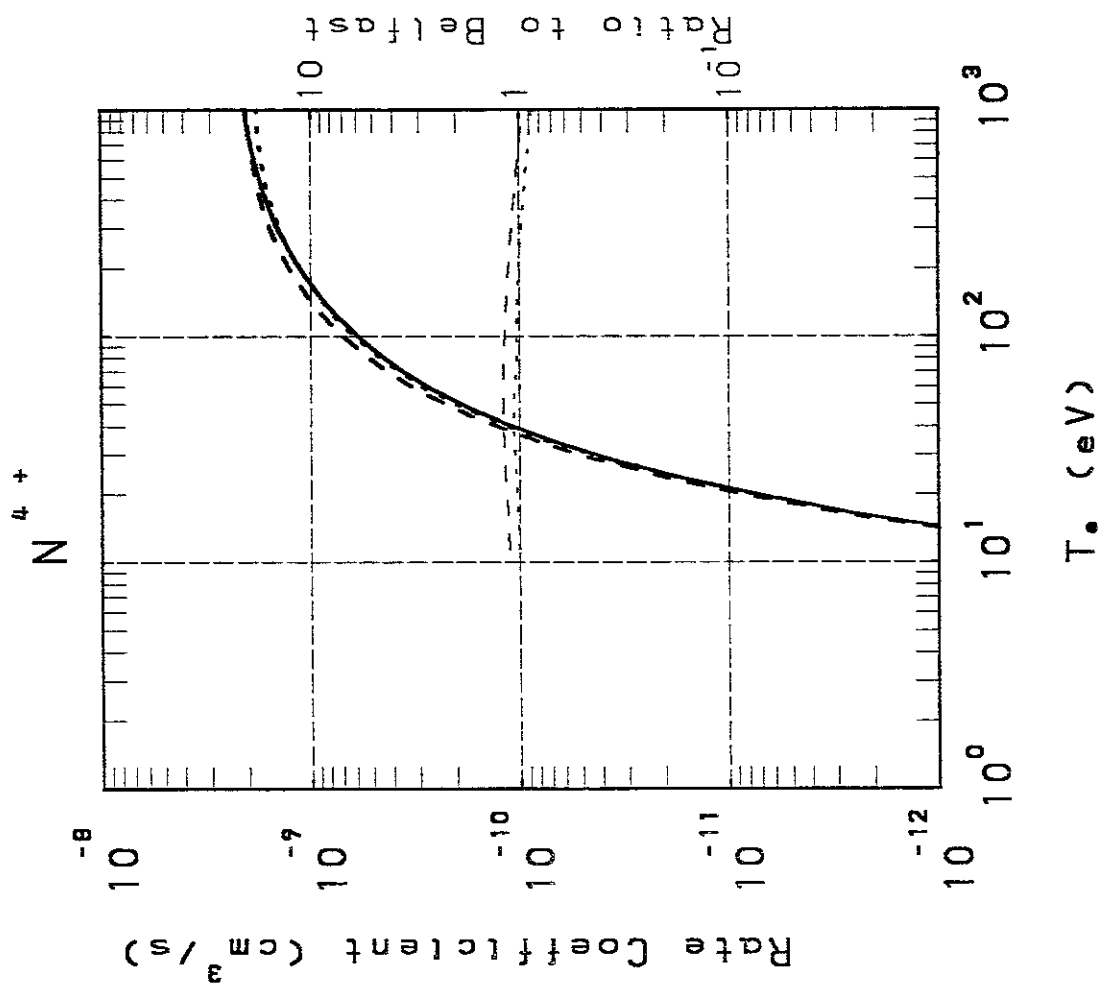
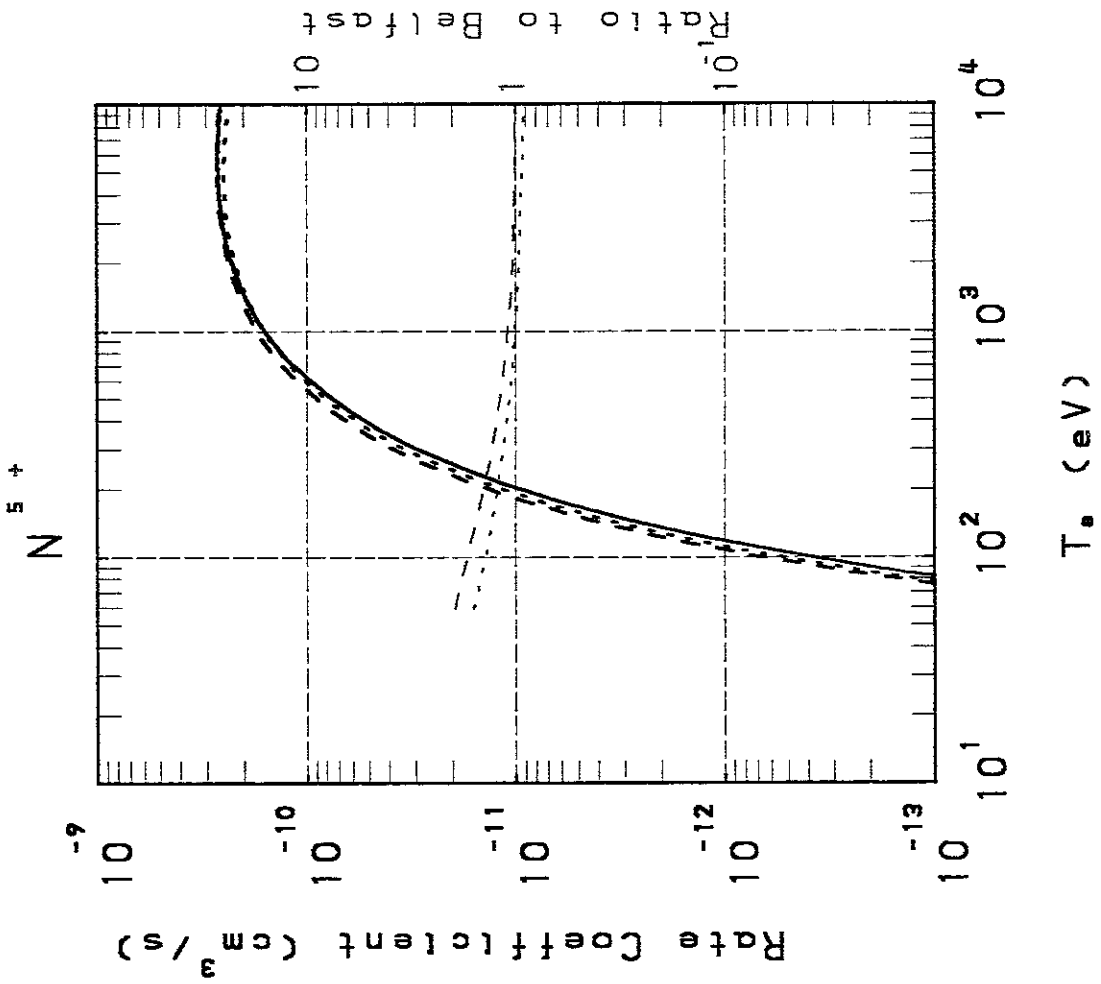


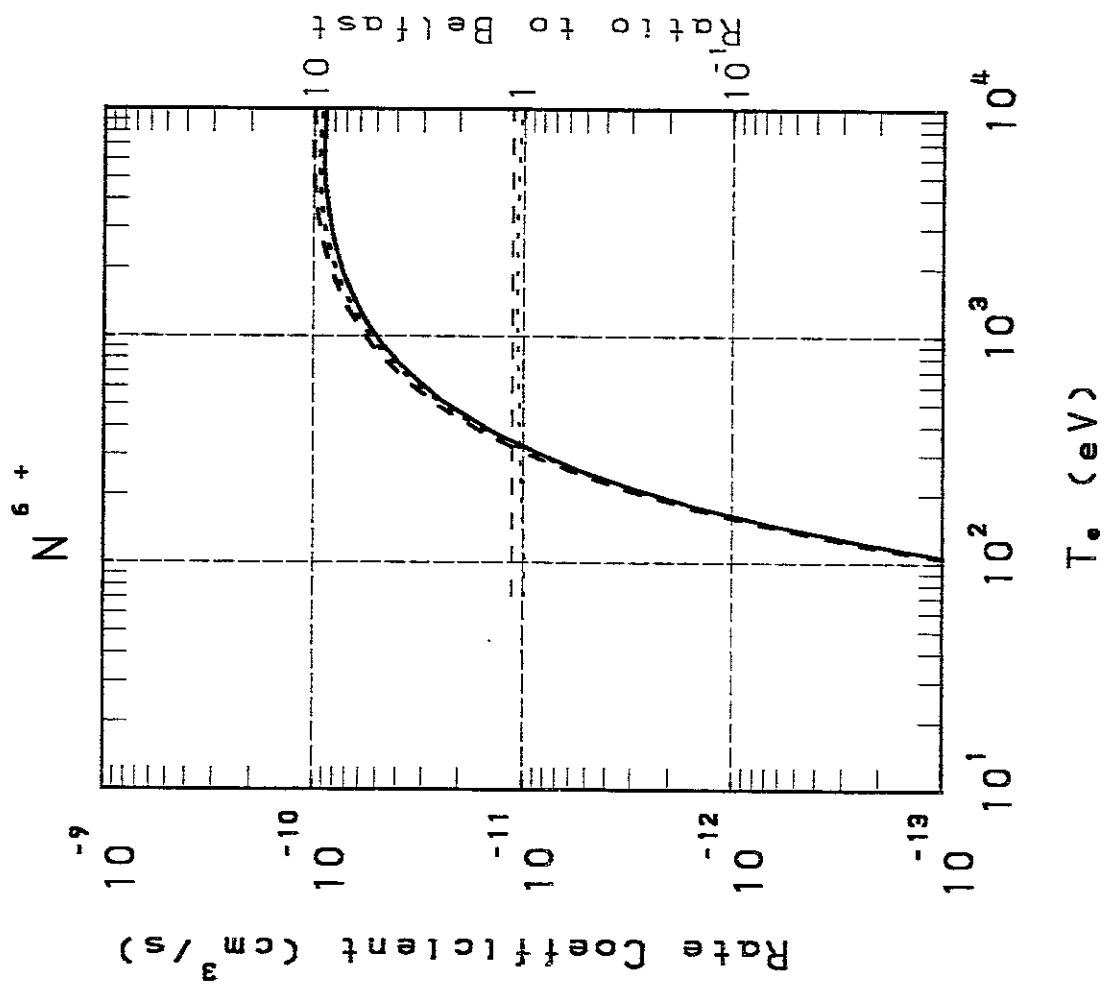
N^{3+}

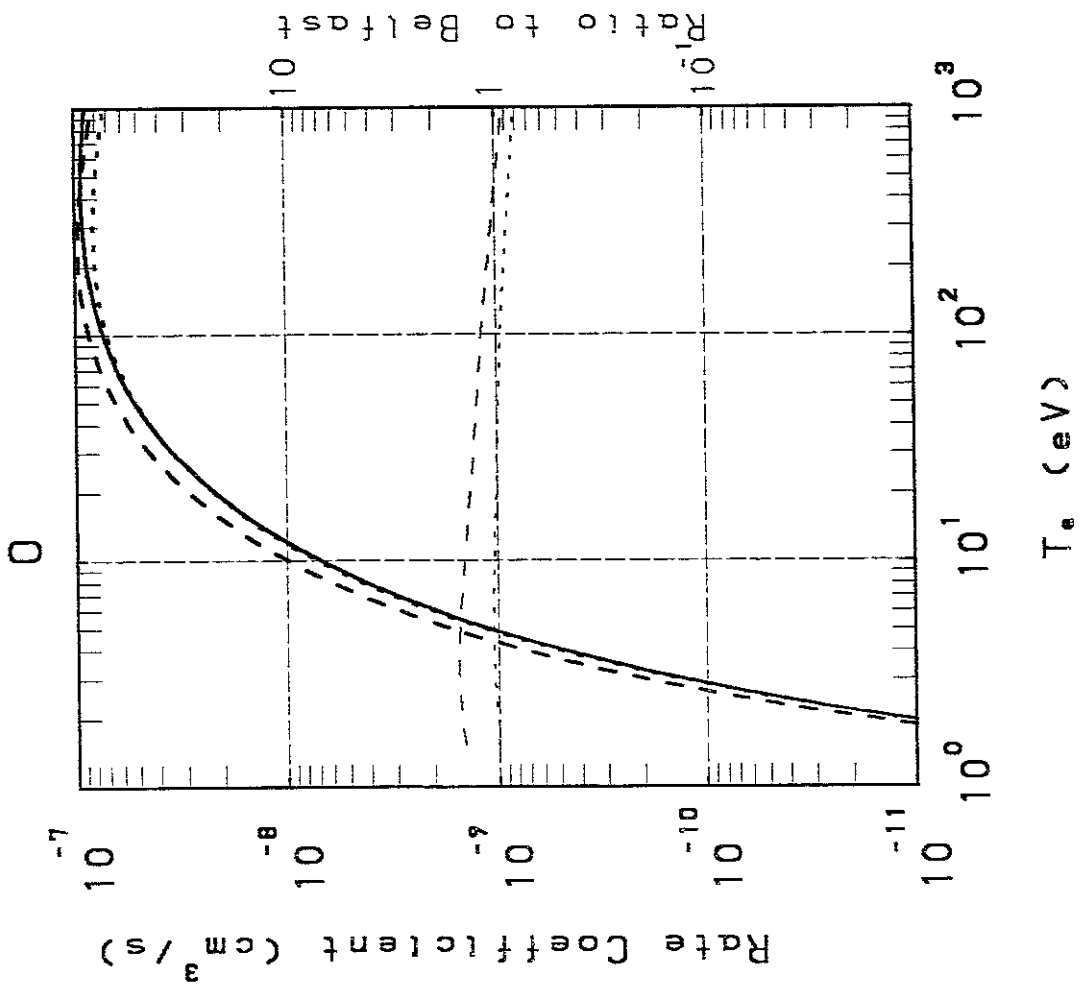
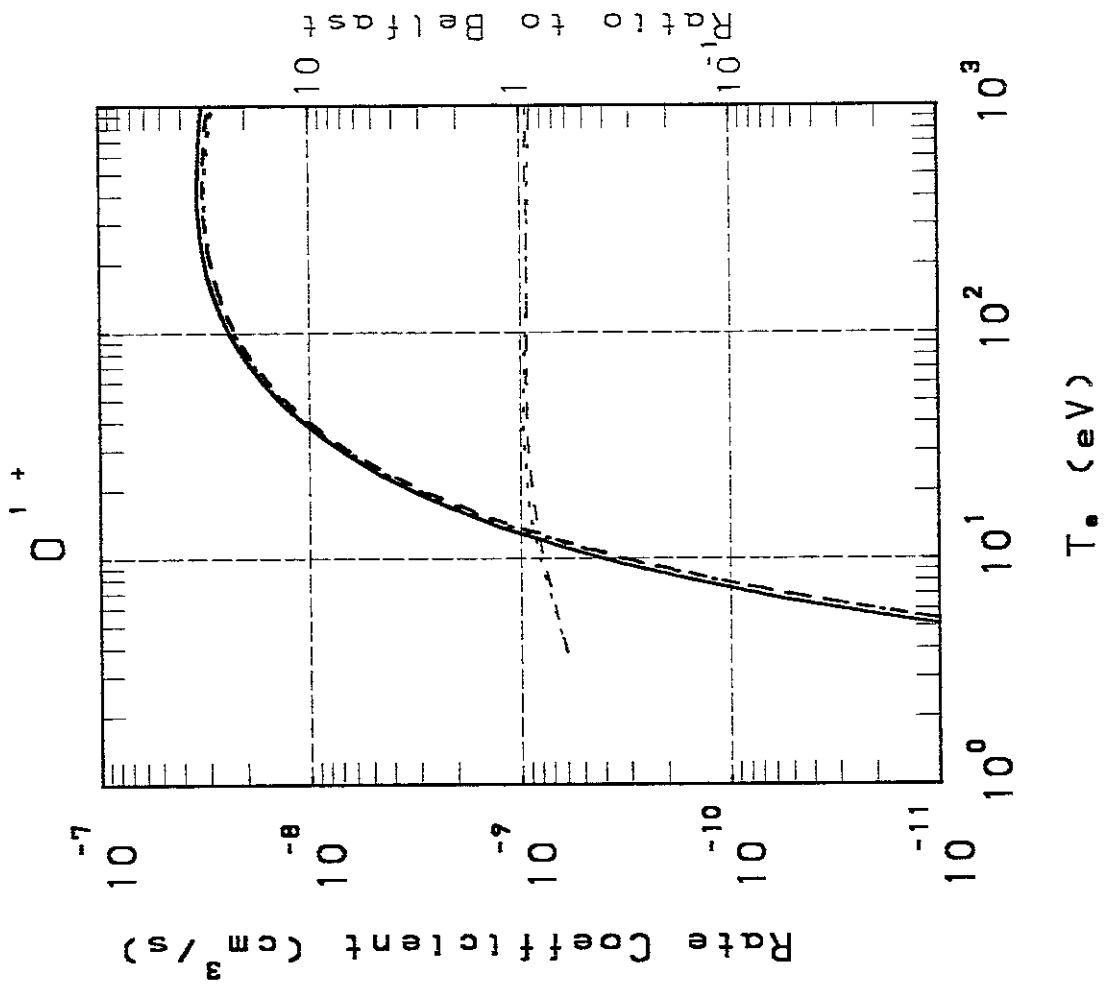


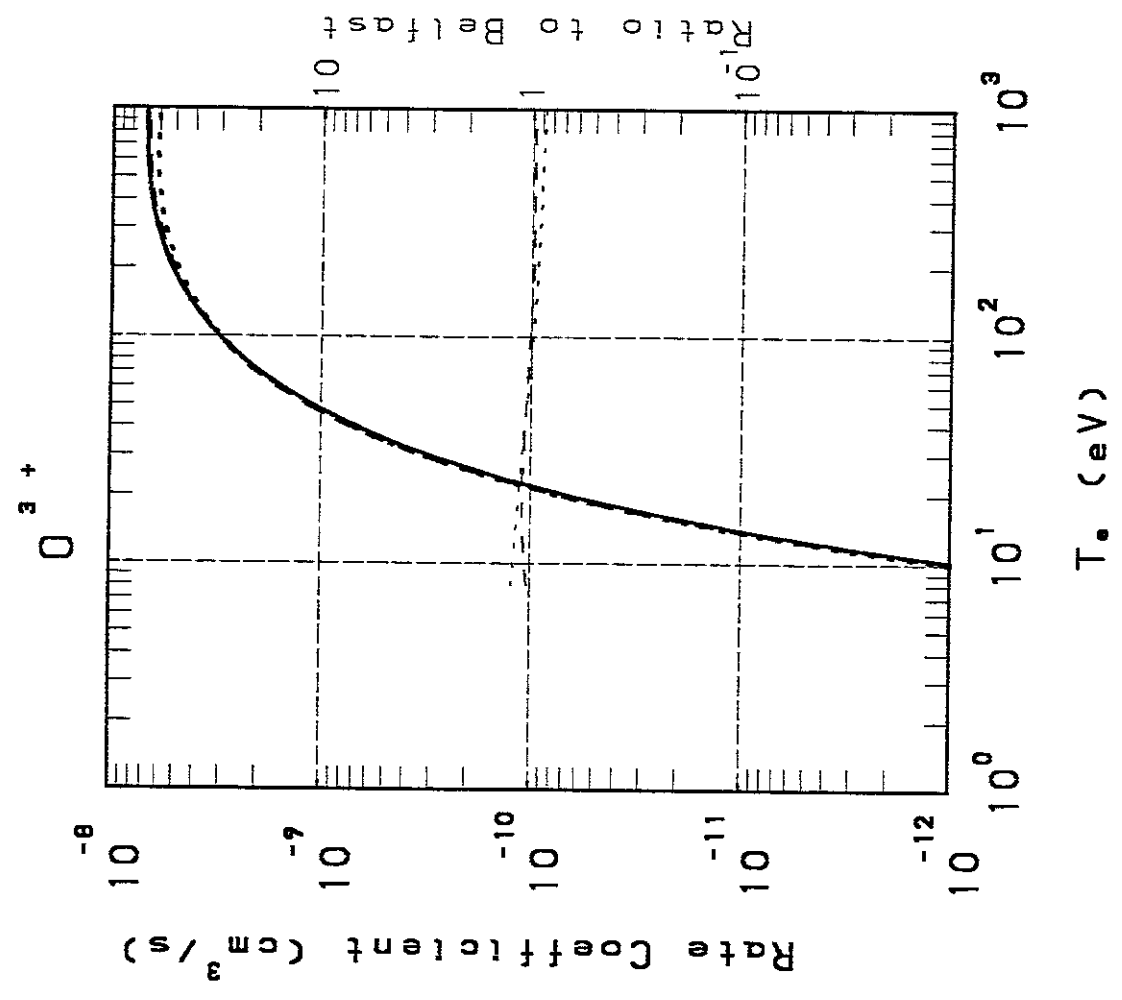
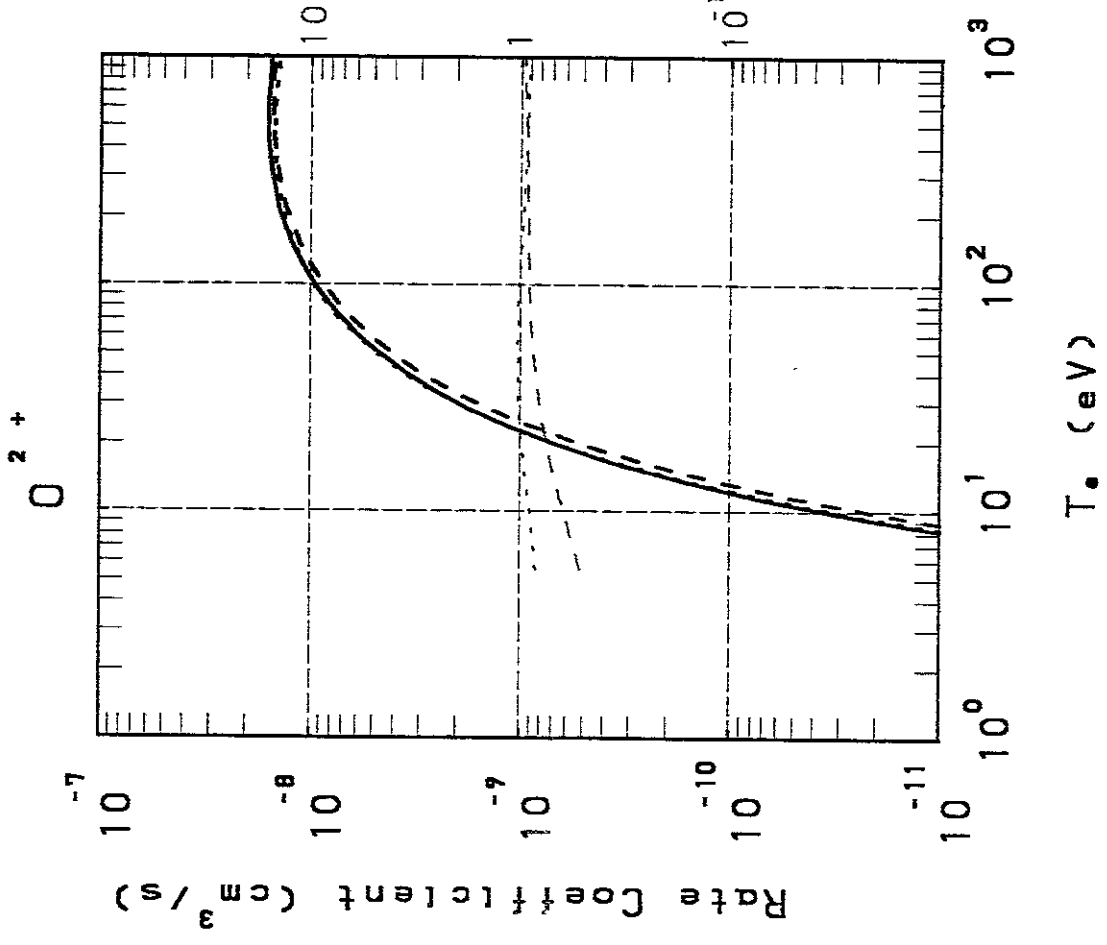
N^{2+}

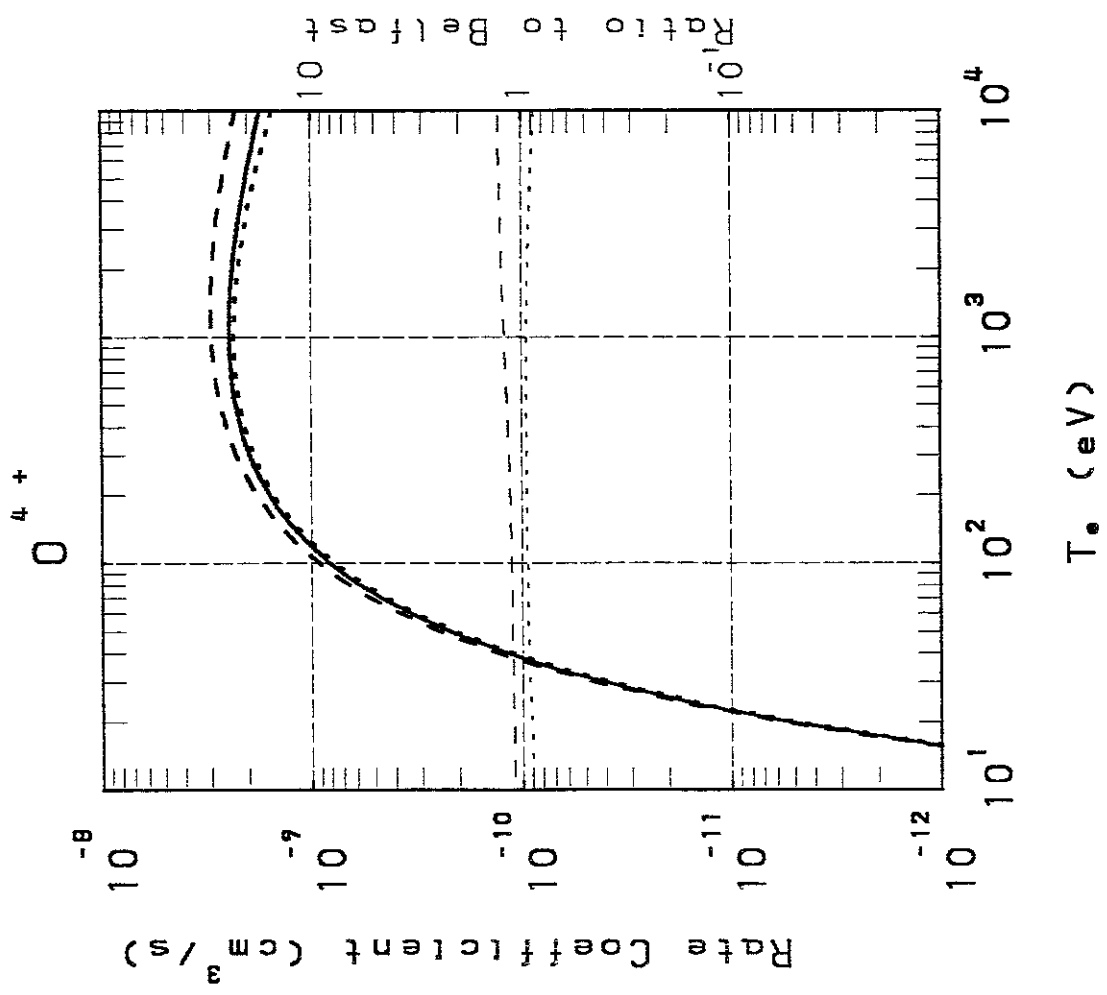
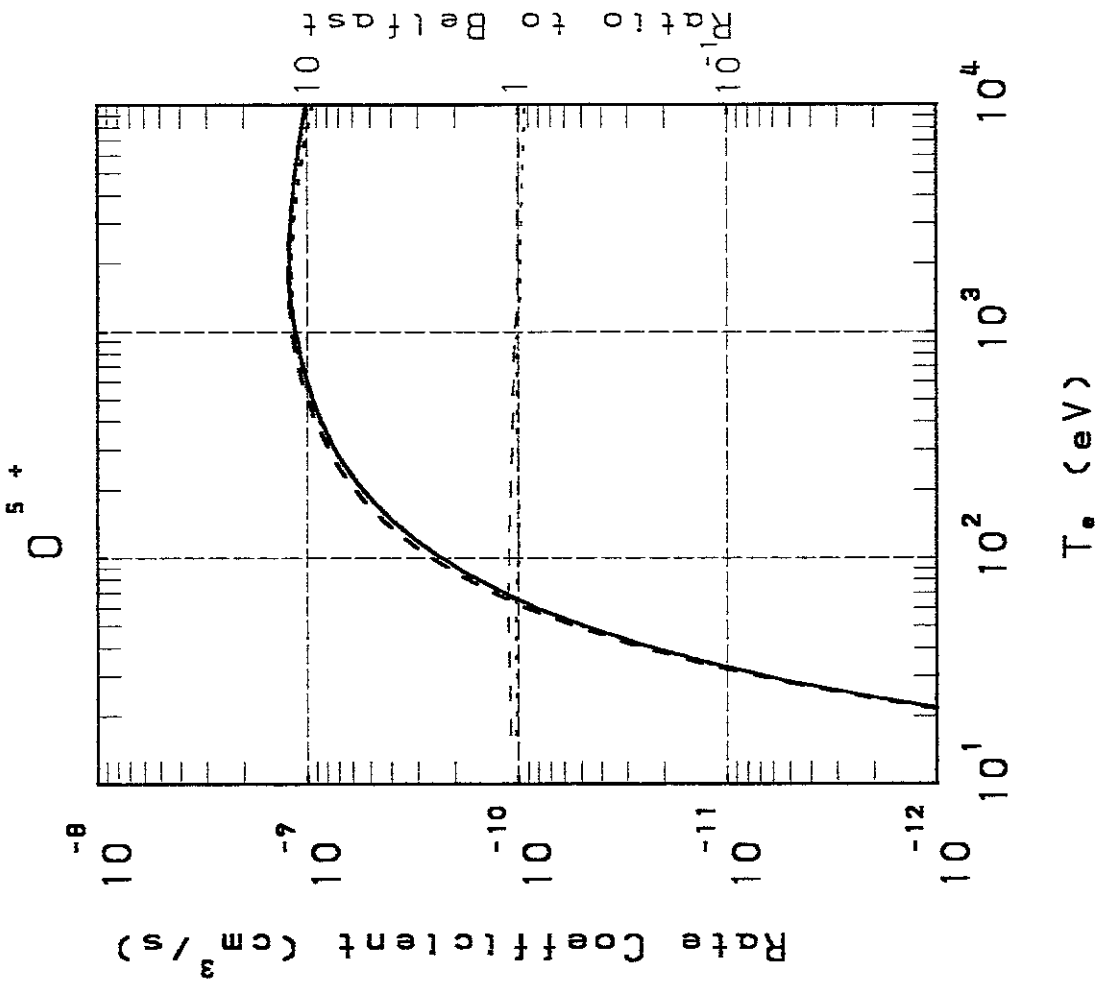






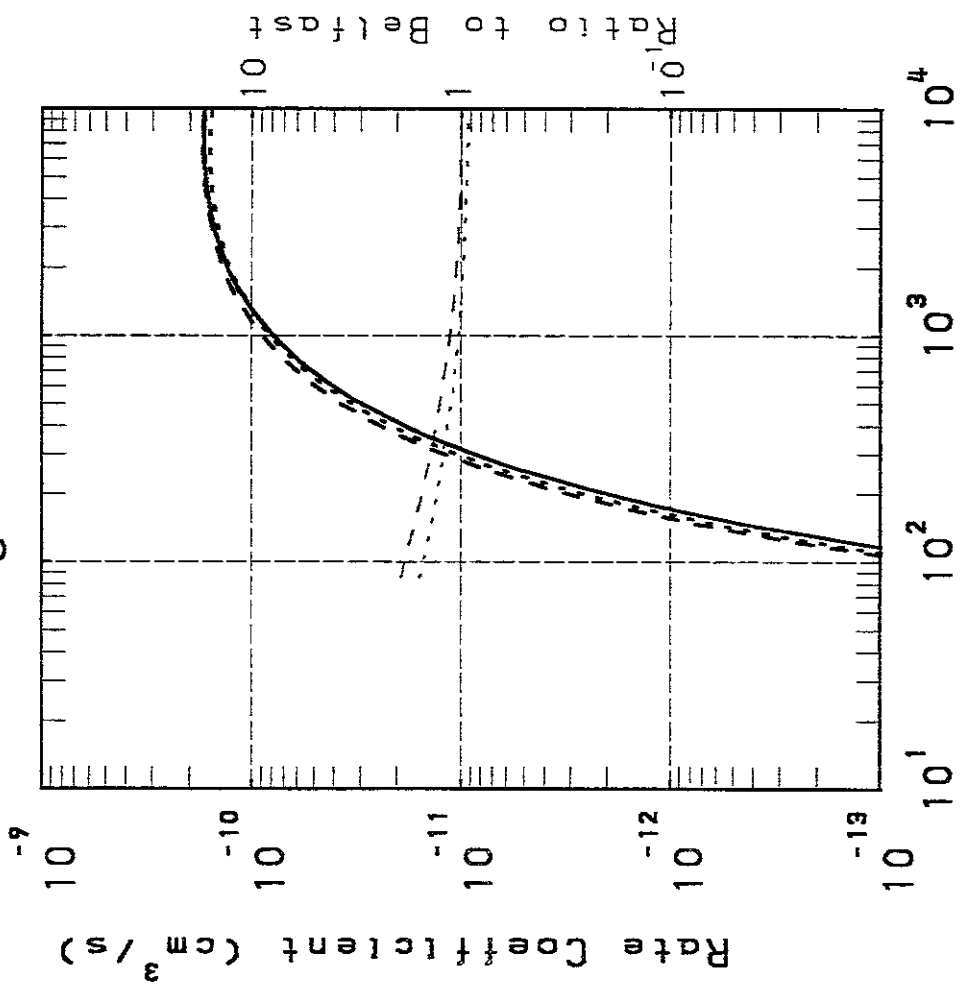
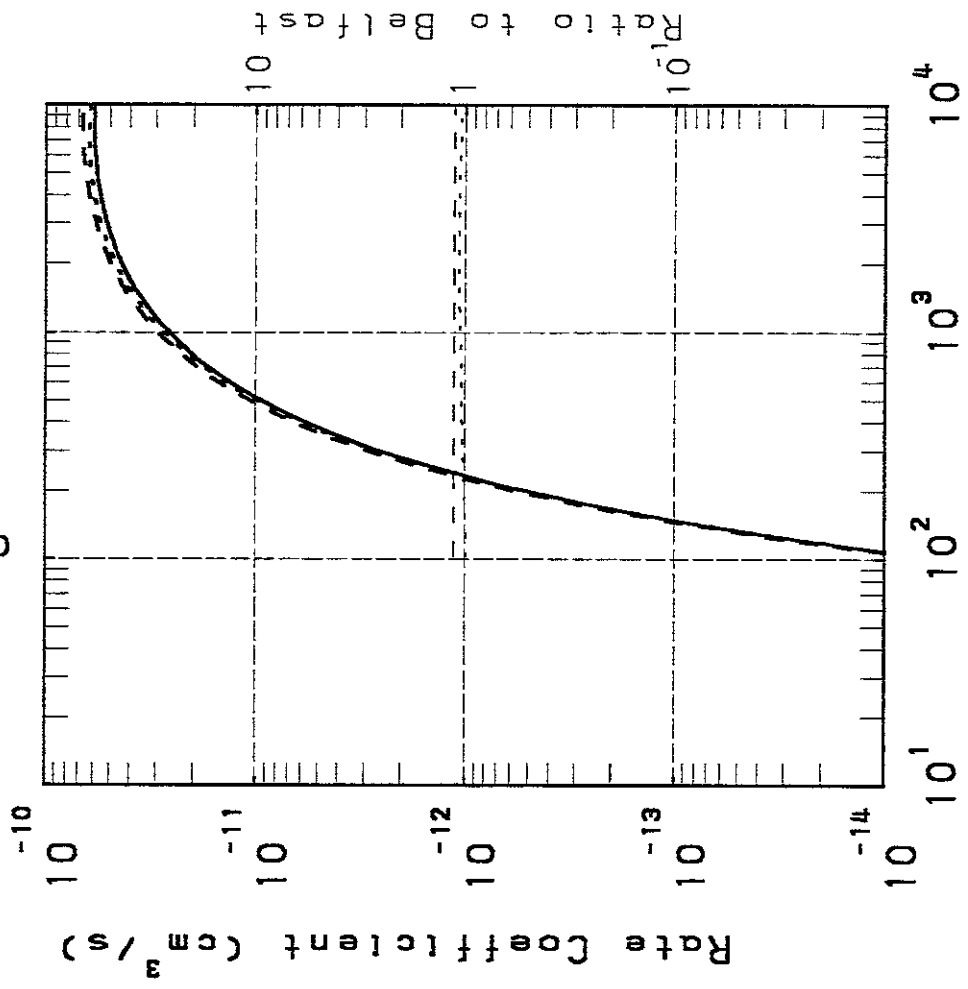






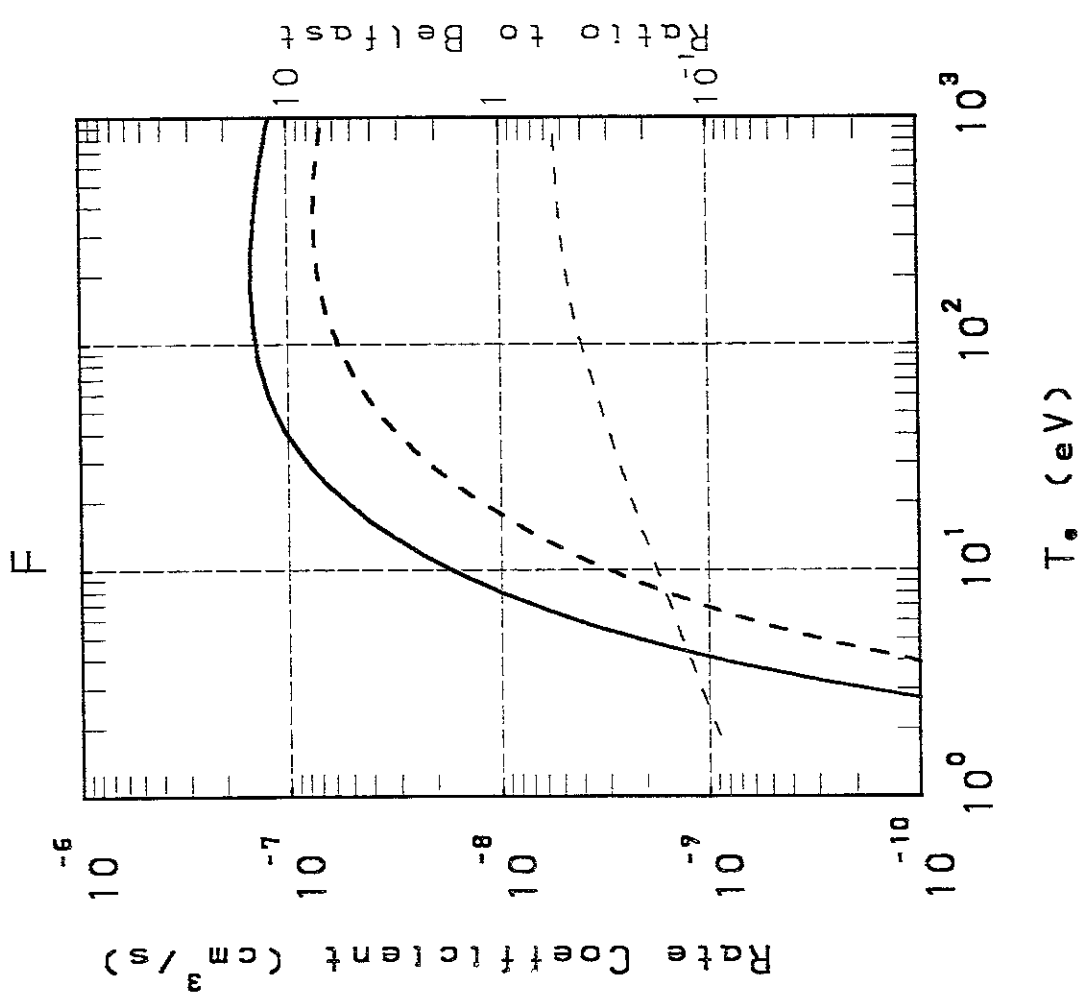
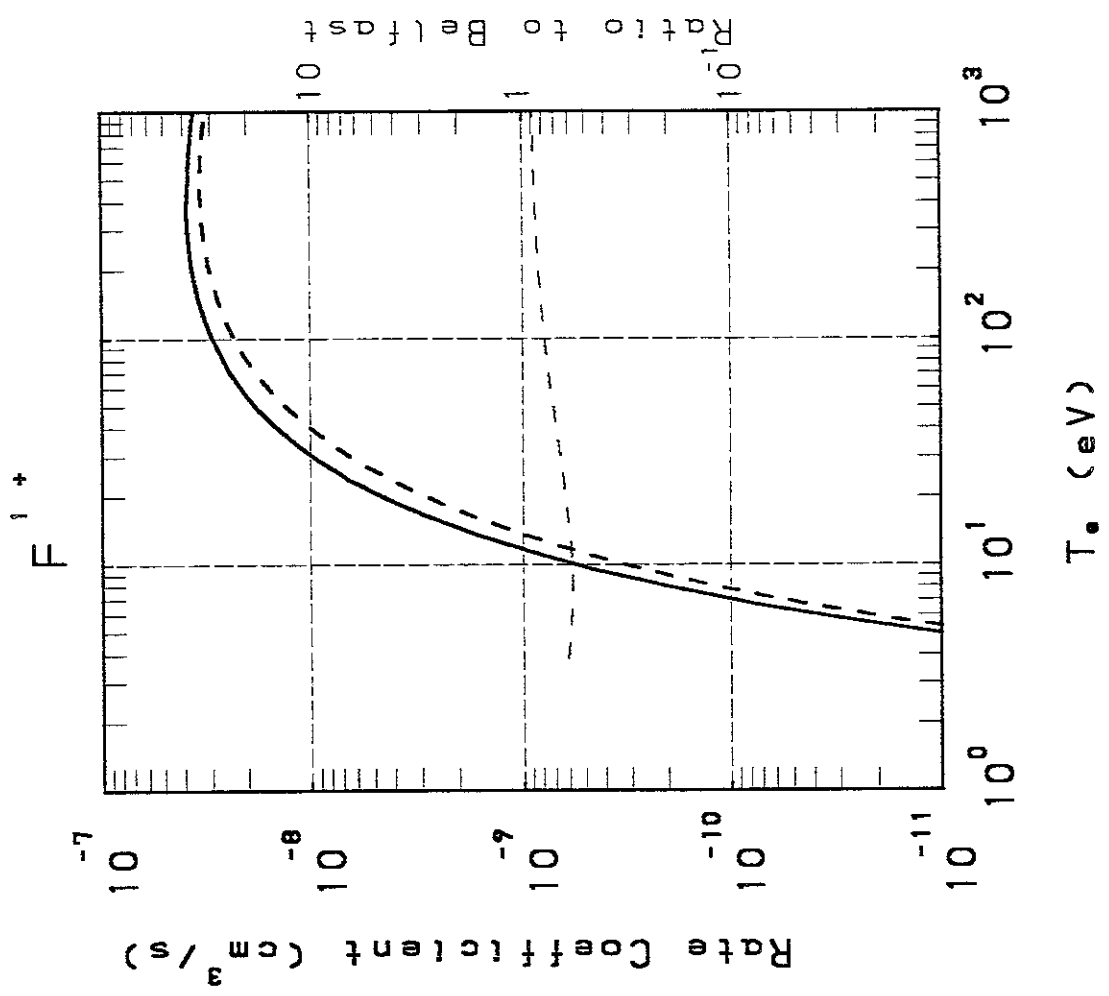
0 7 +

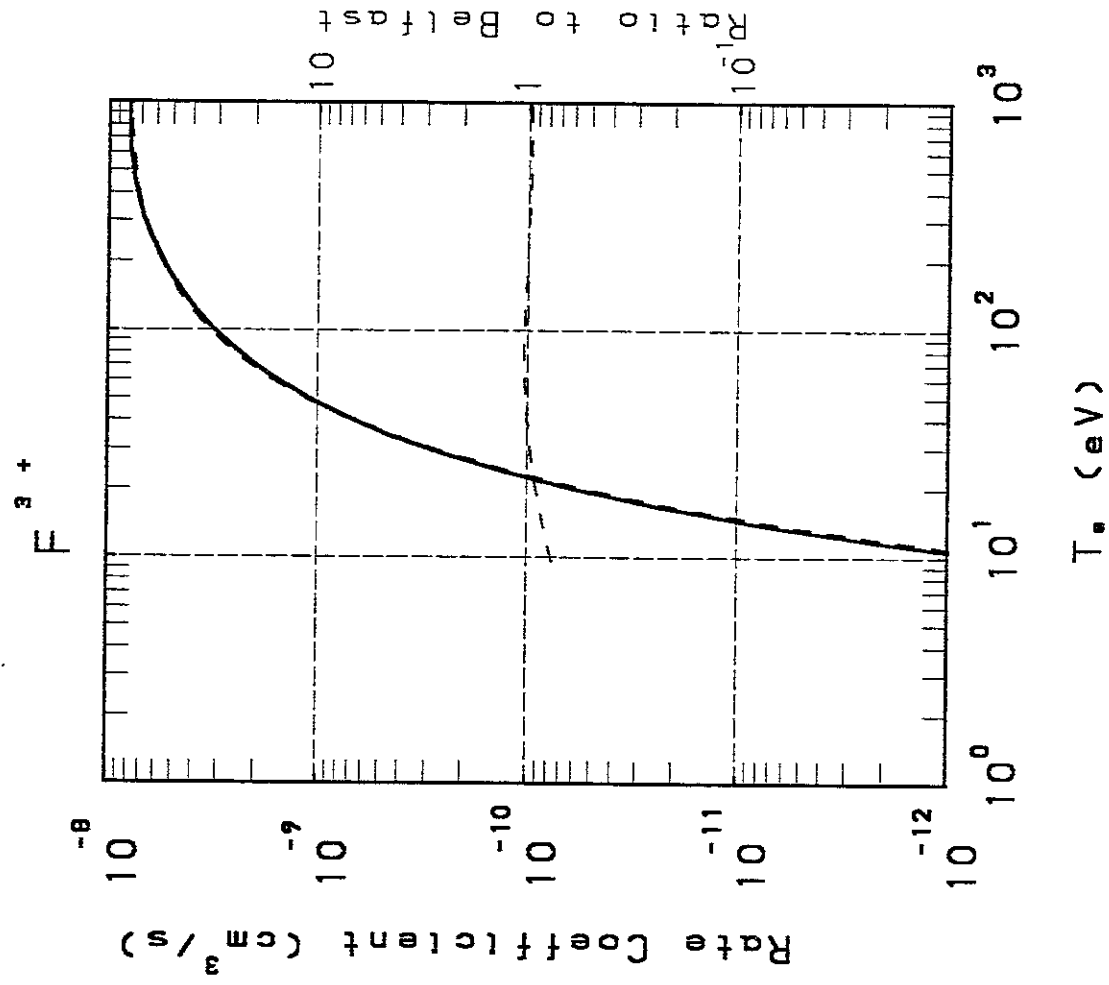
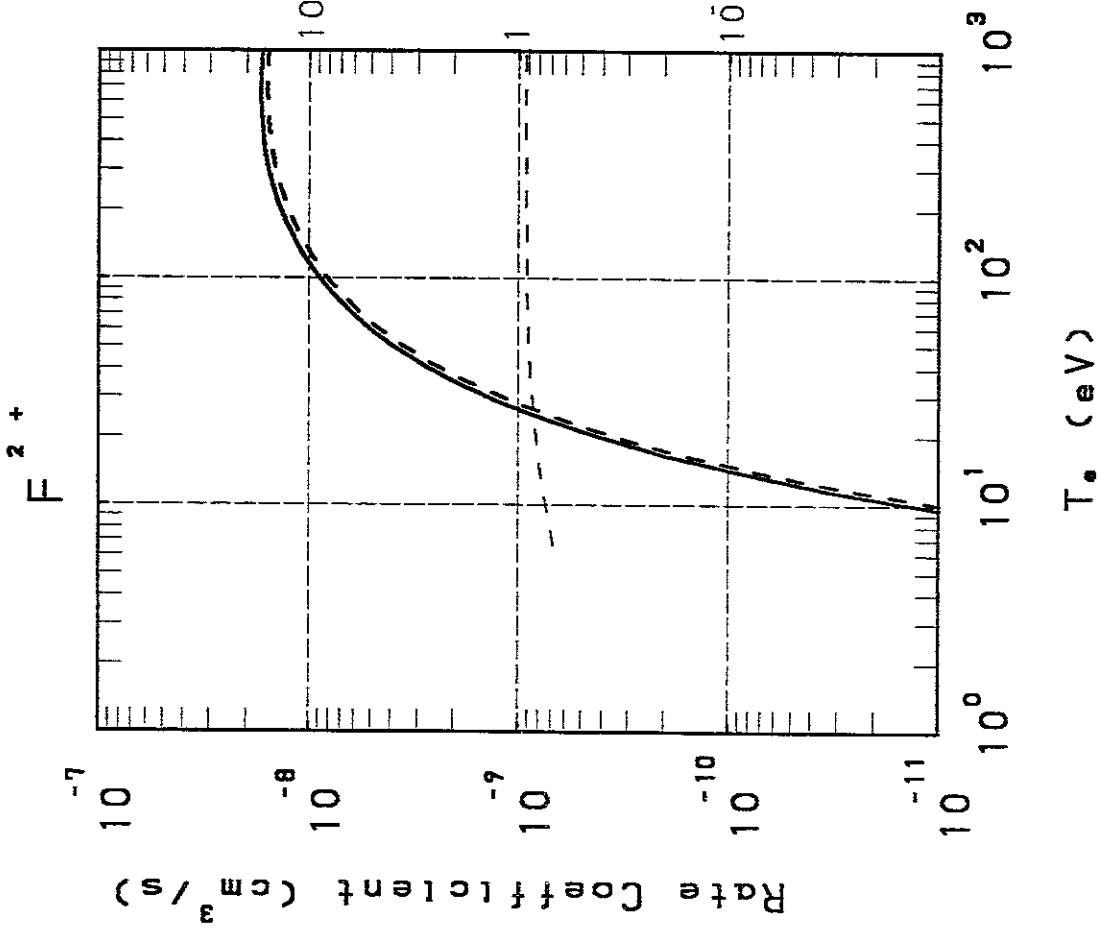
0 6 +

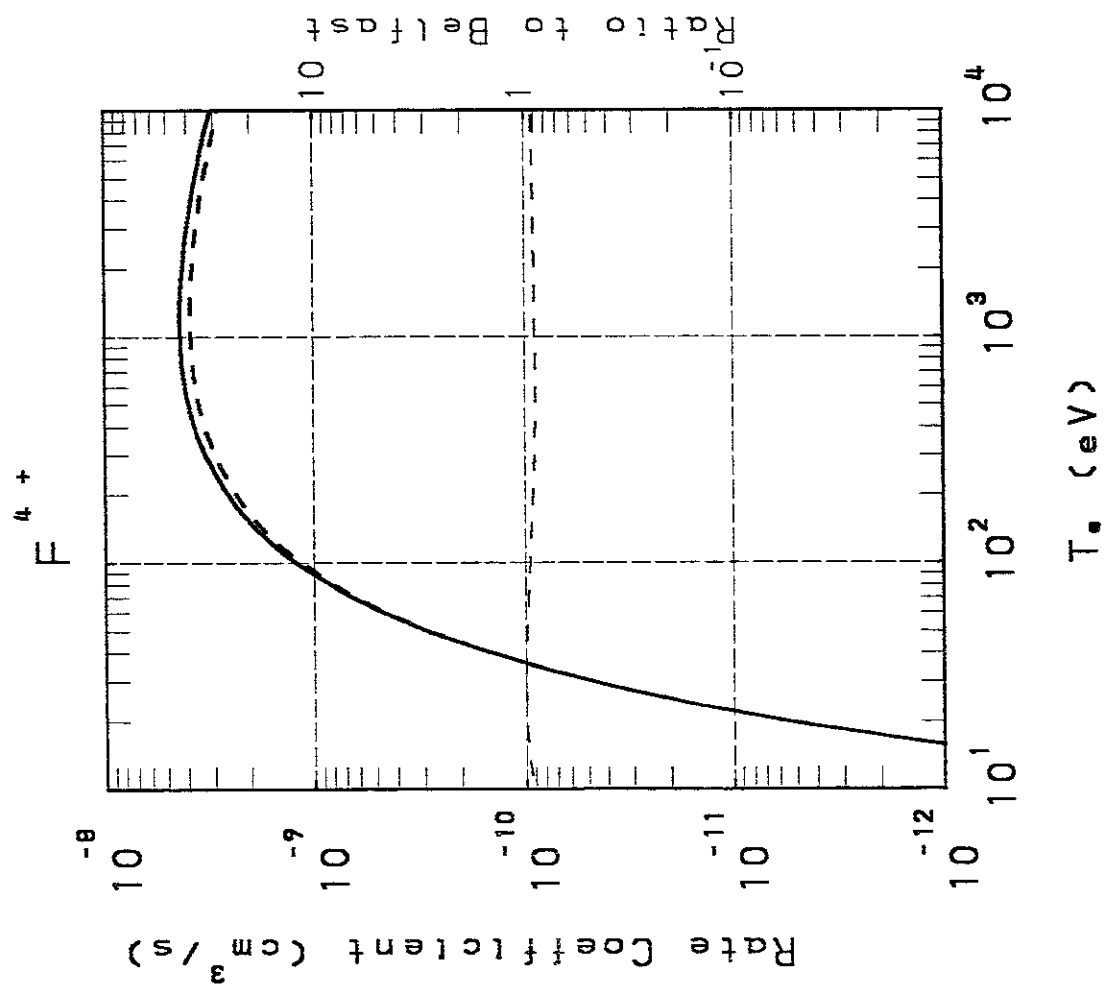
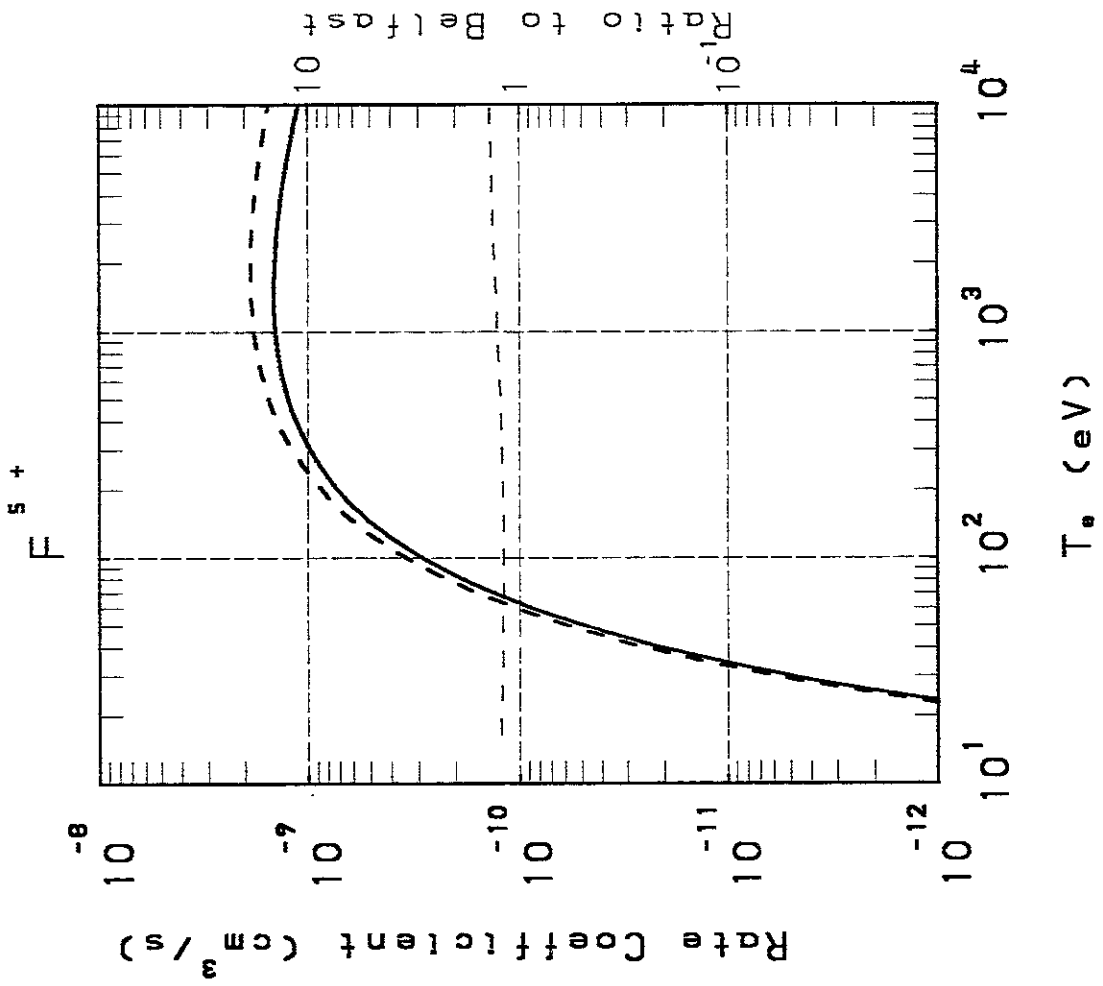


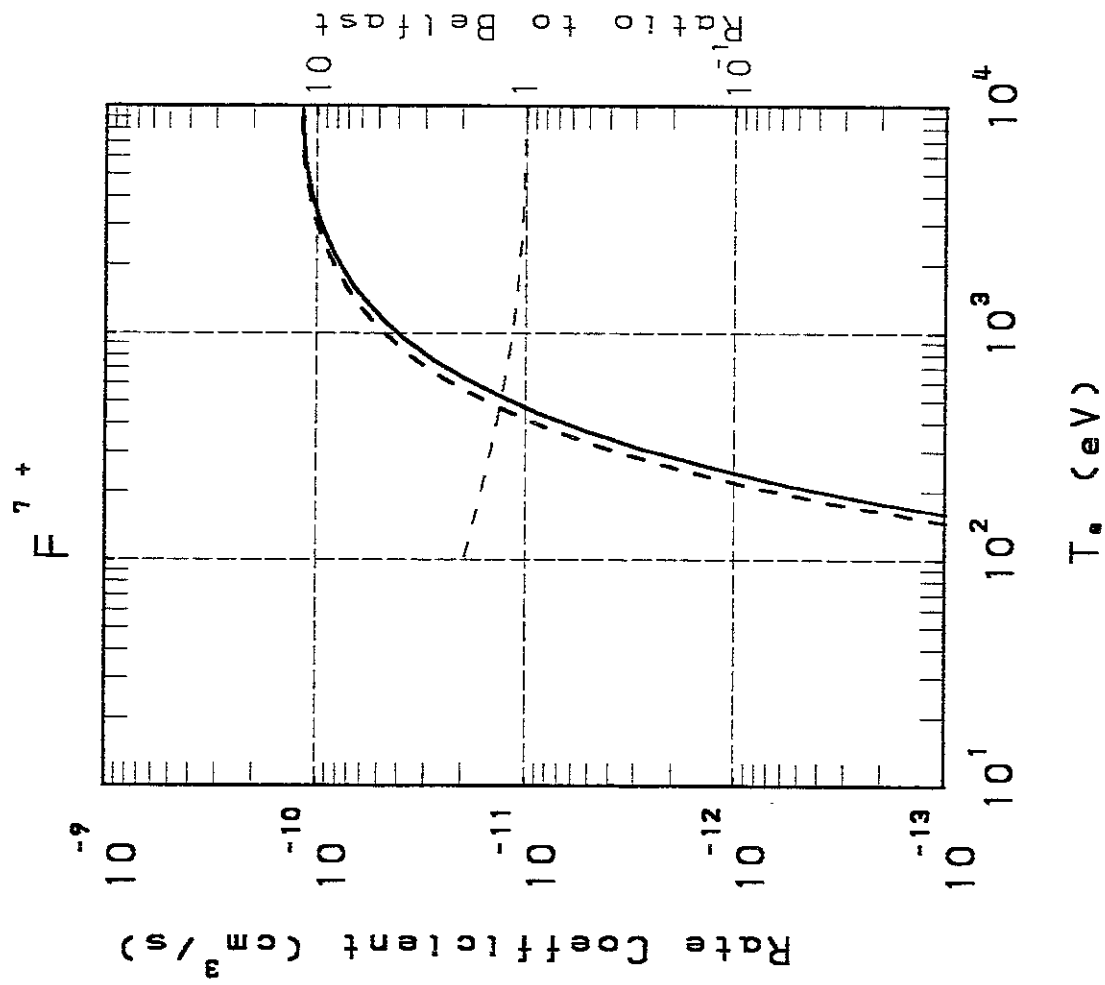
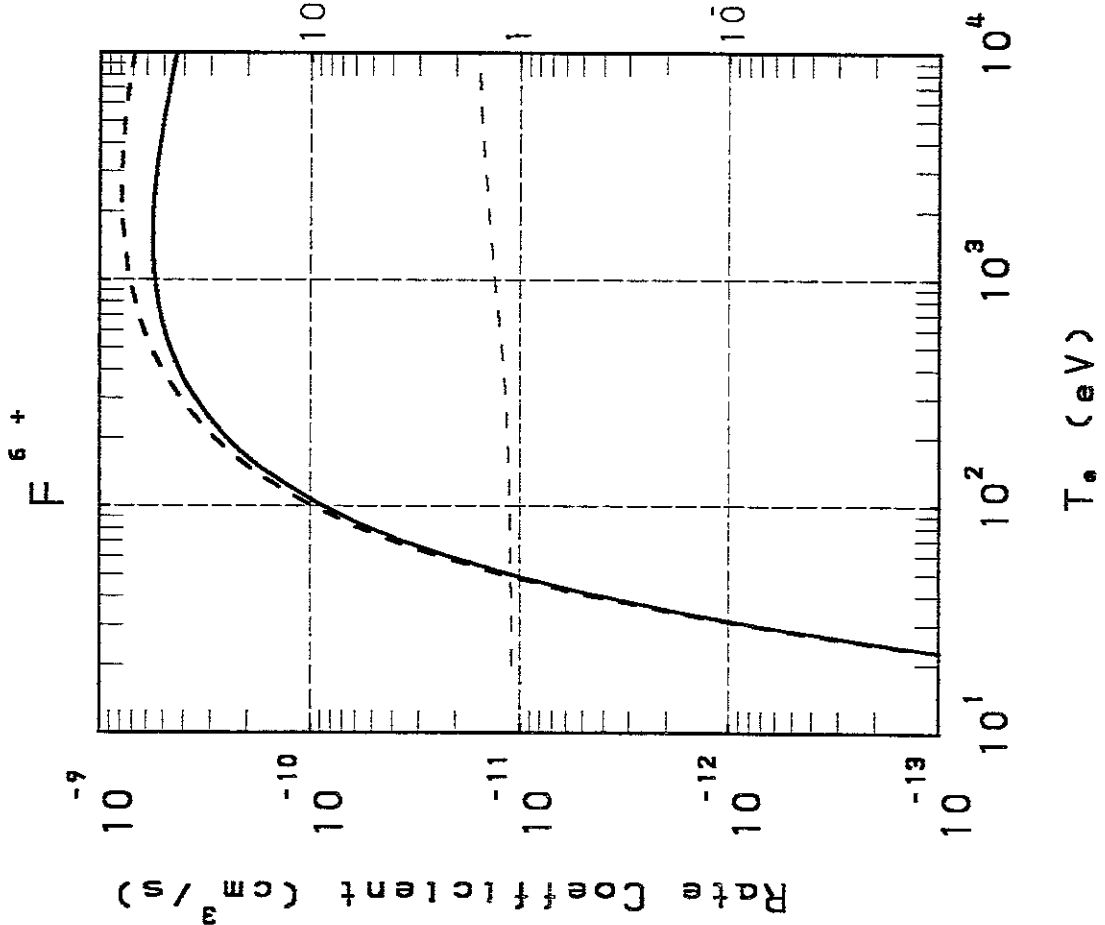
T_e (eV)

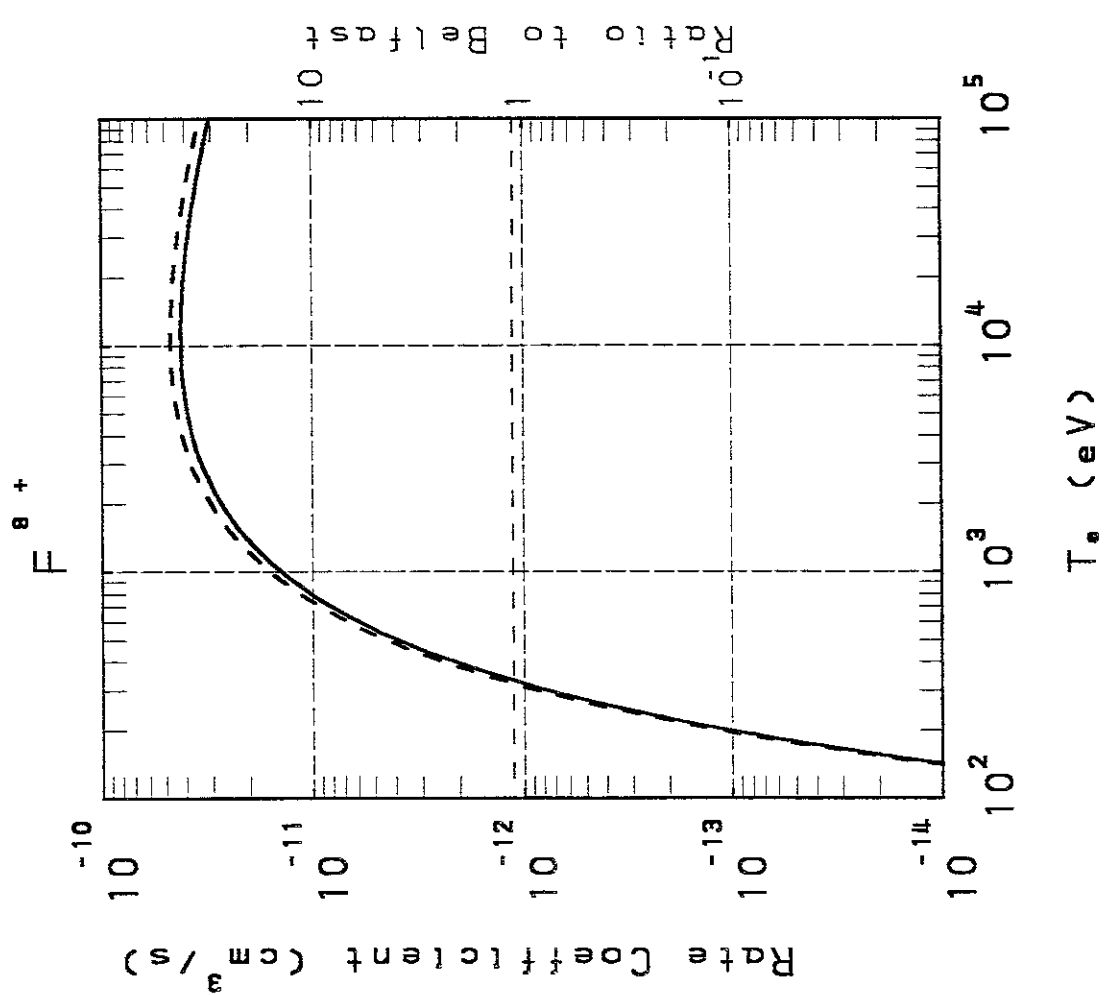
T_e (eV)



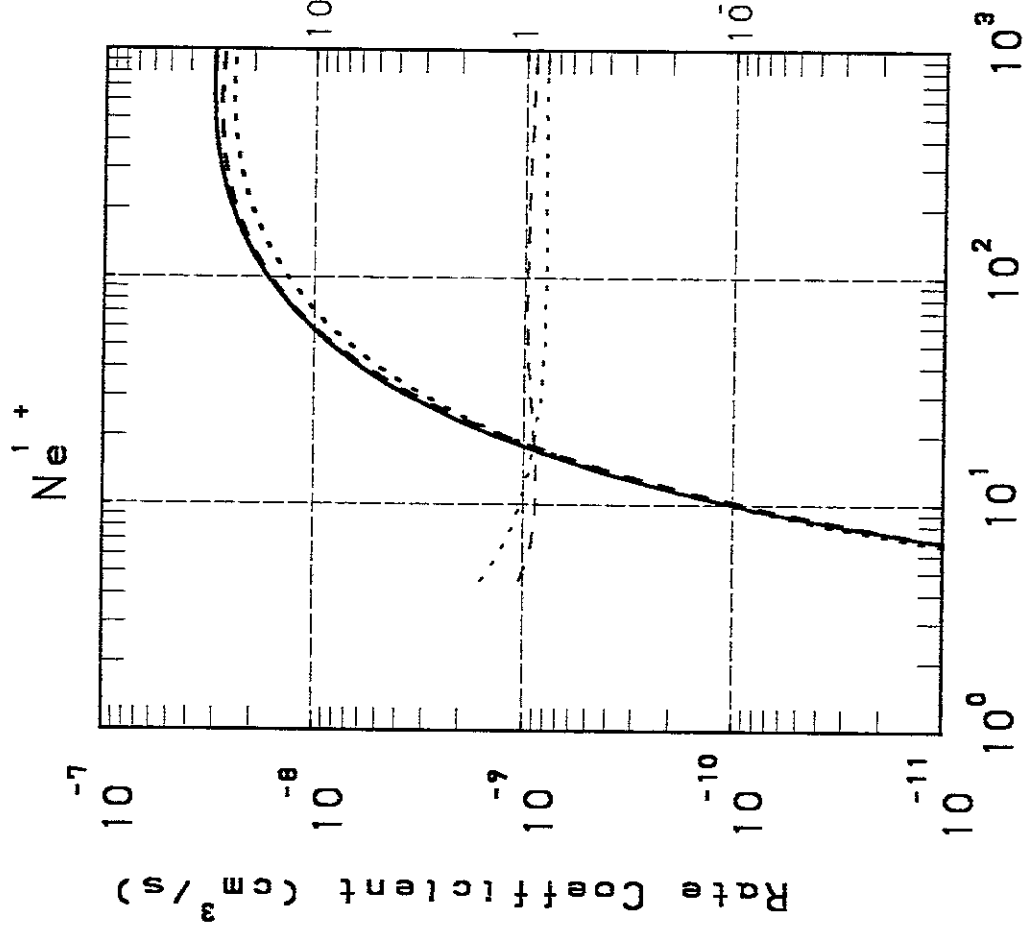




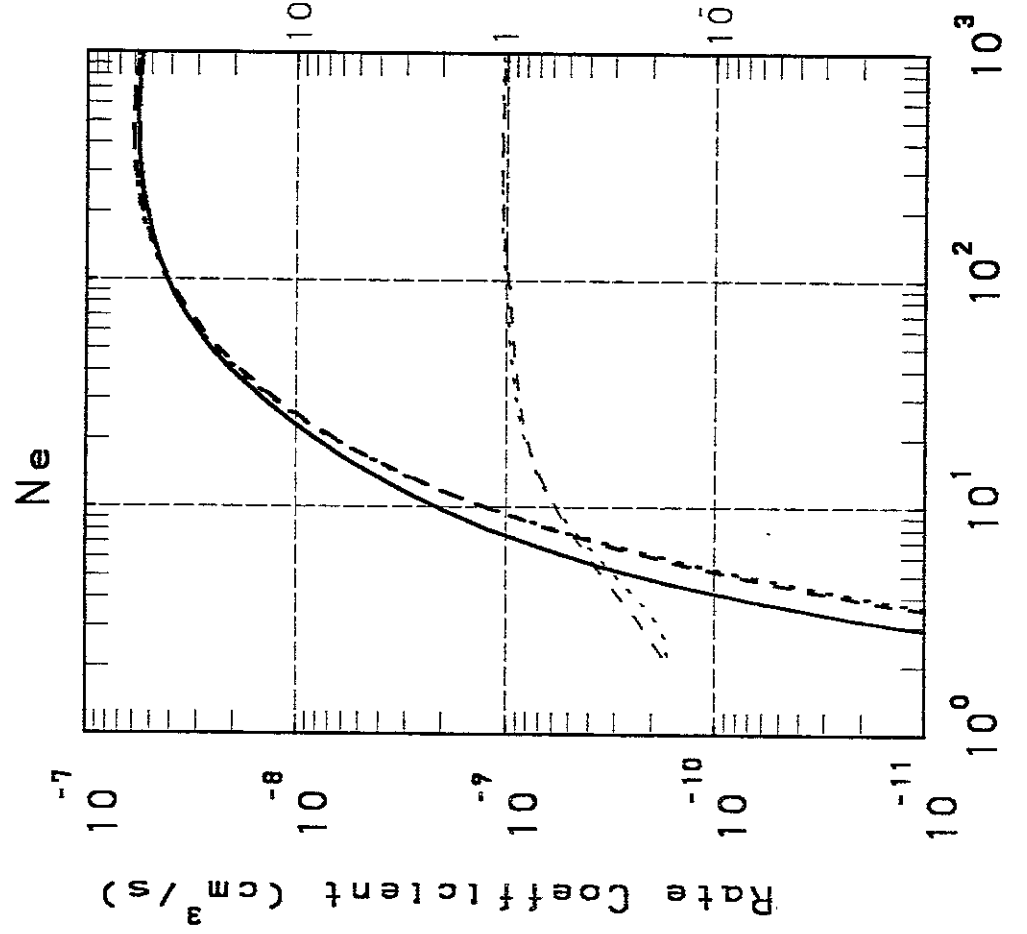


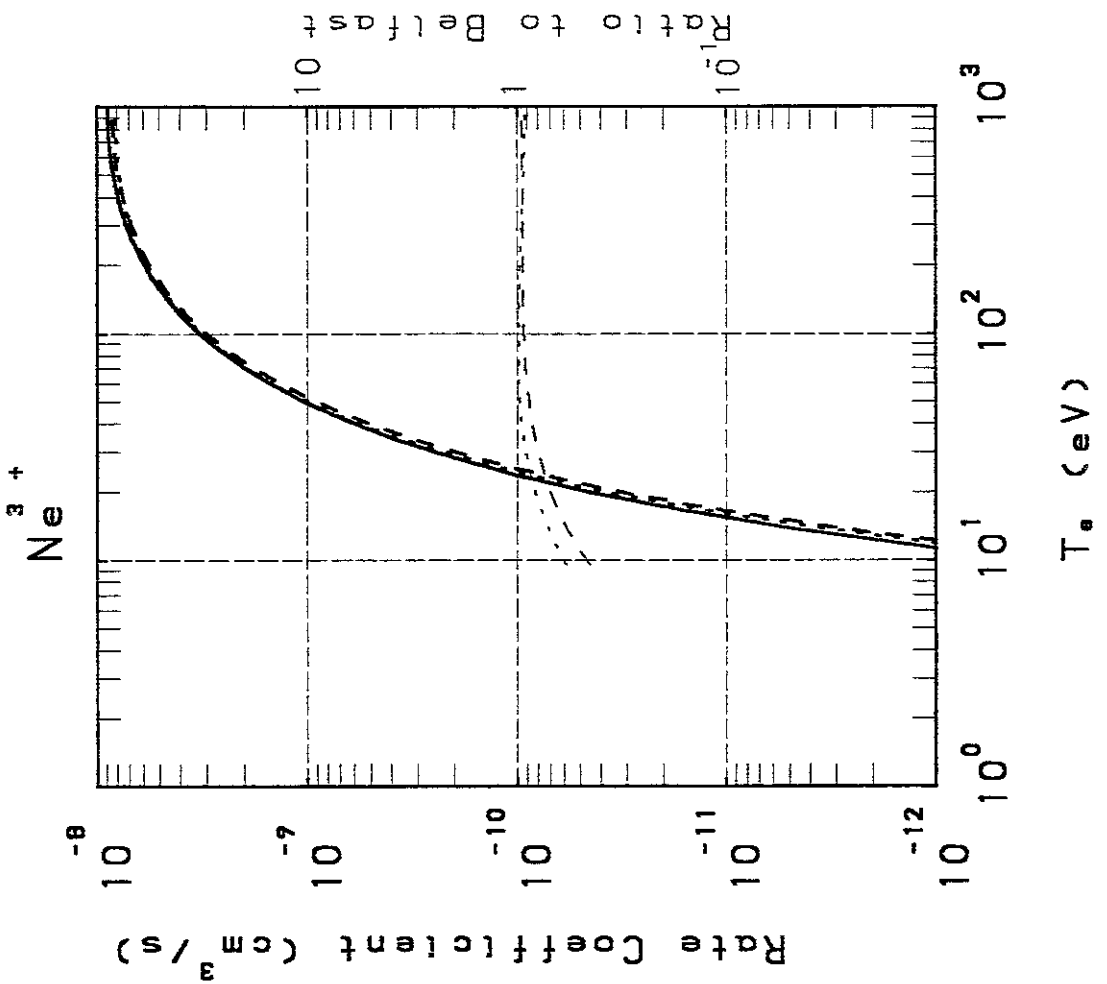
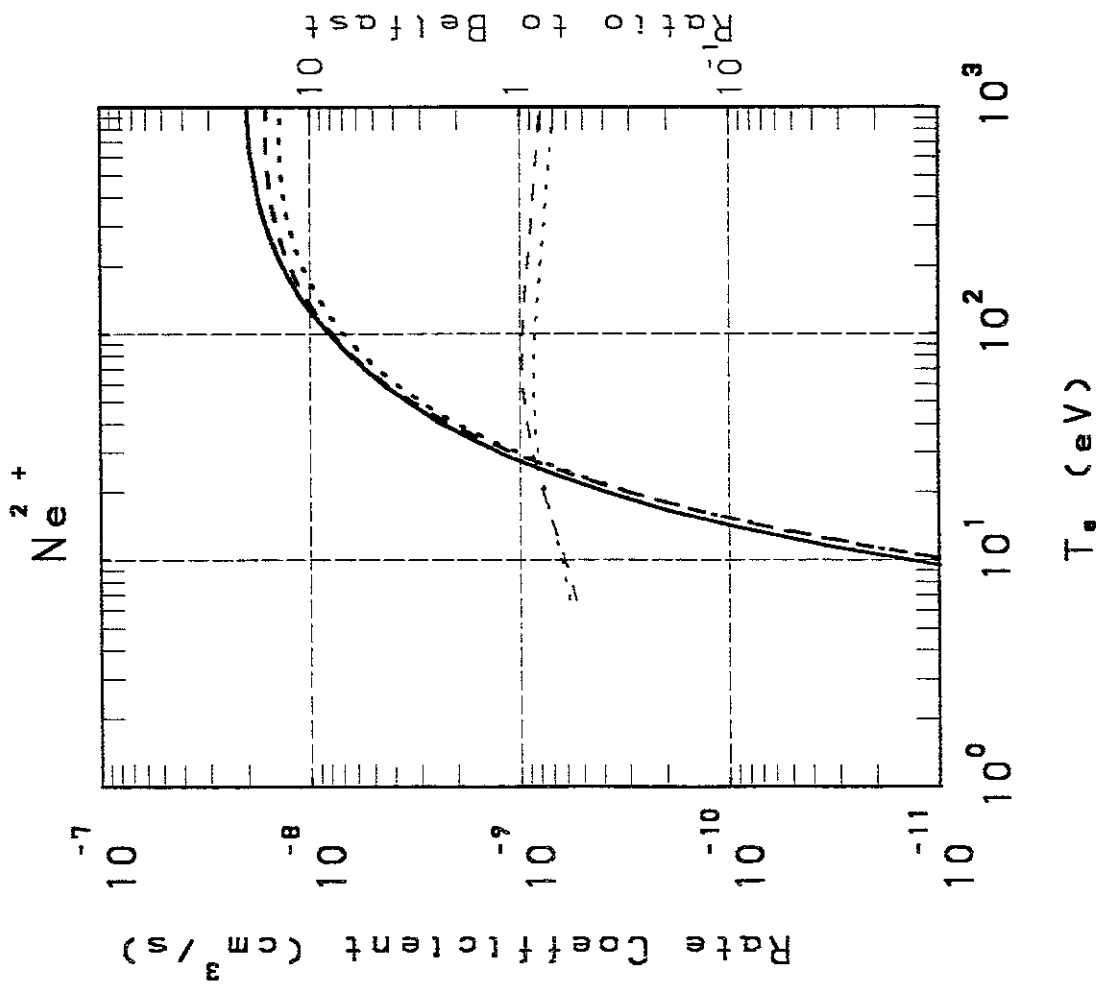


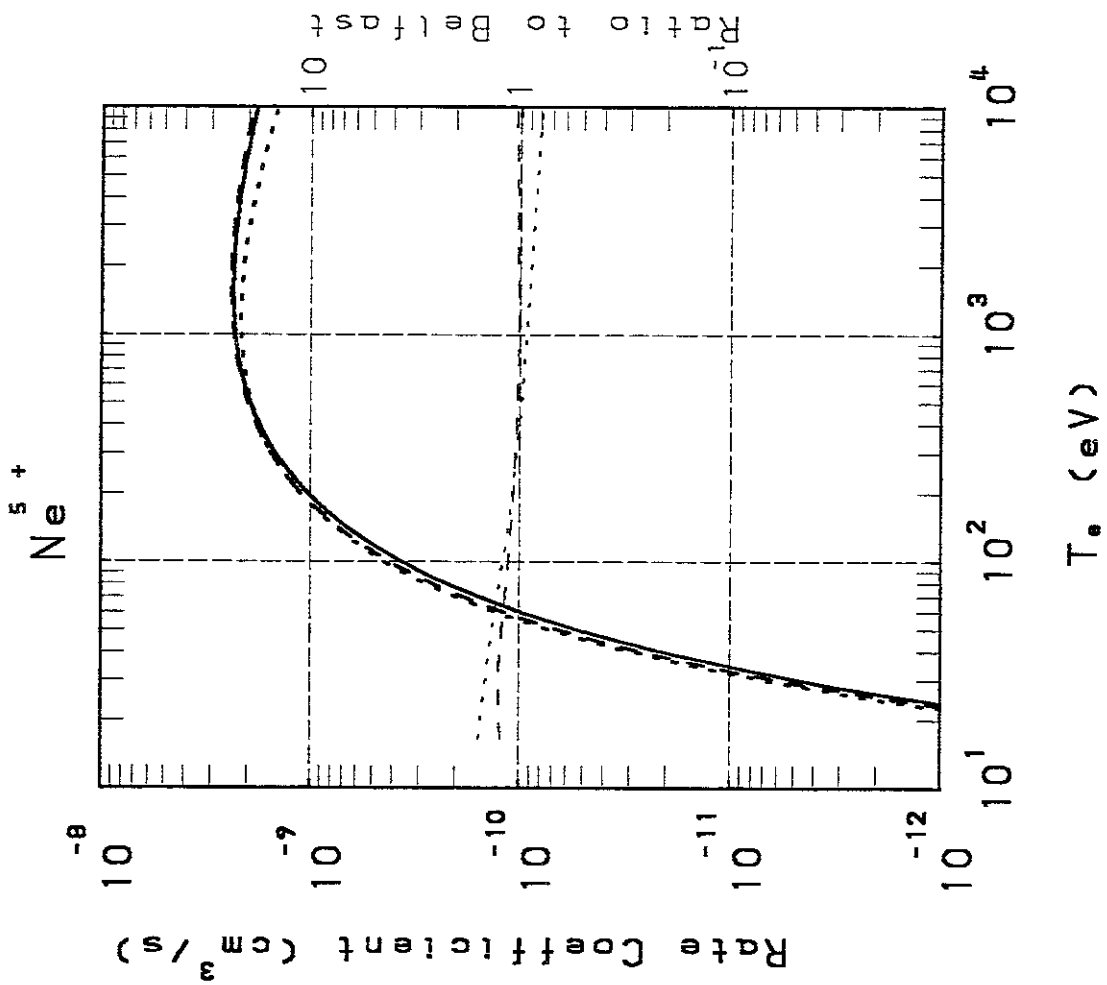
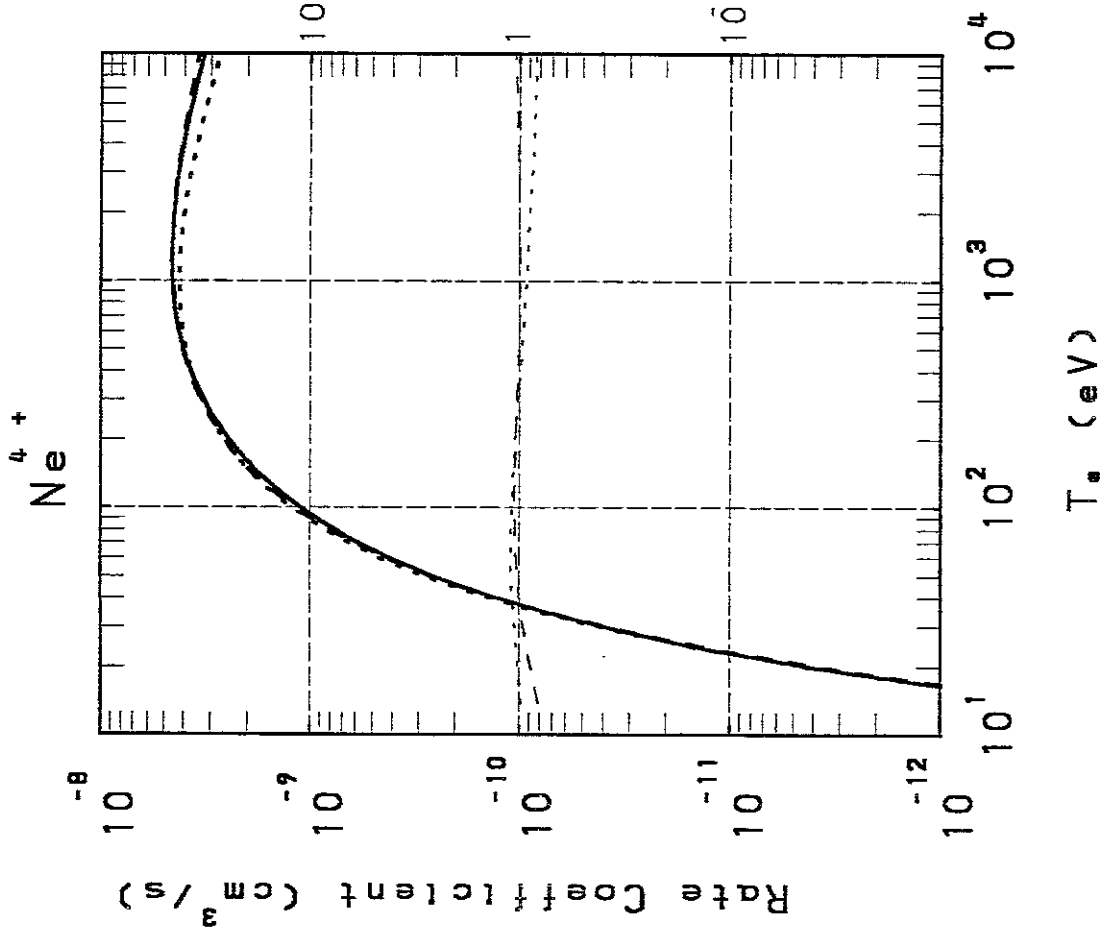
Ne¹⁺

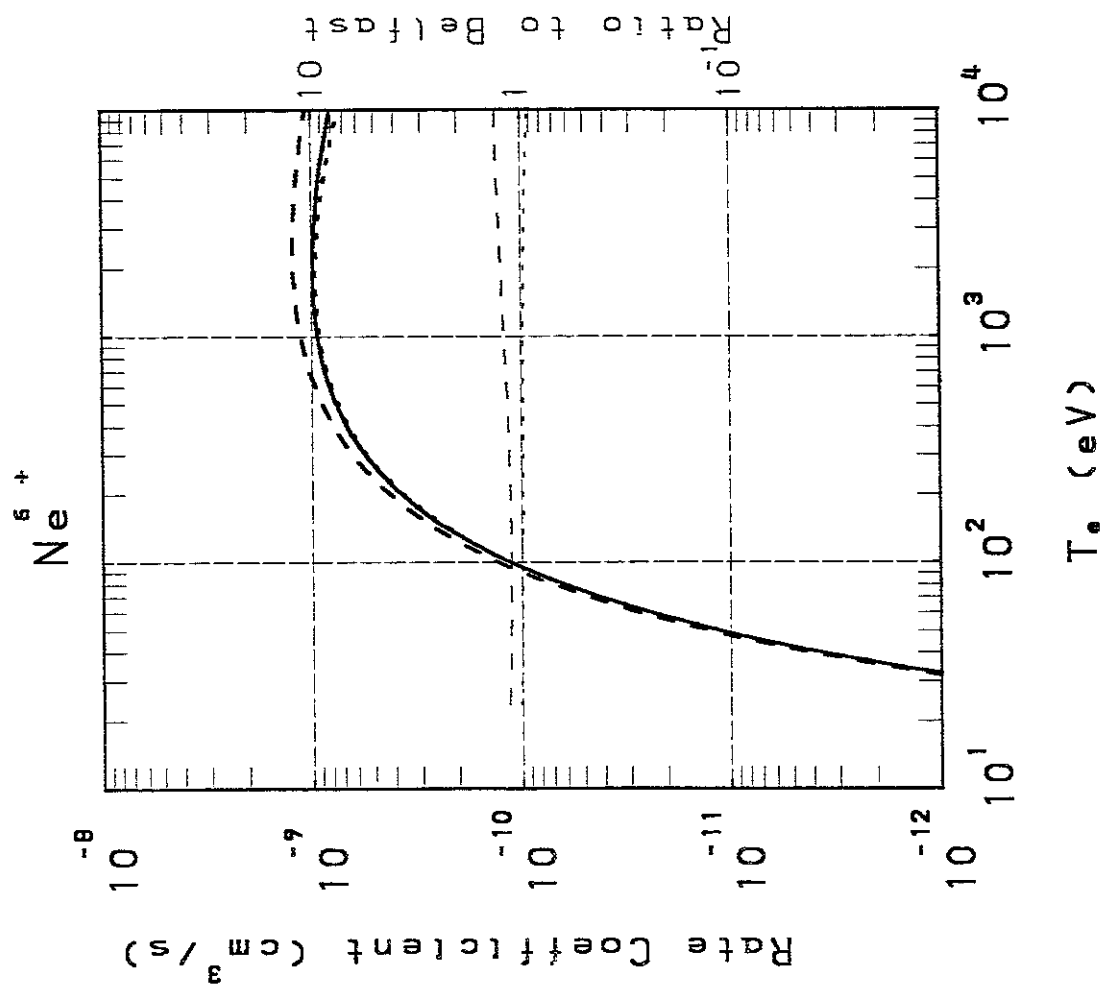
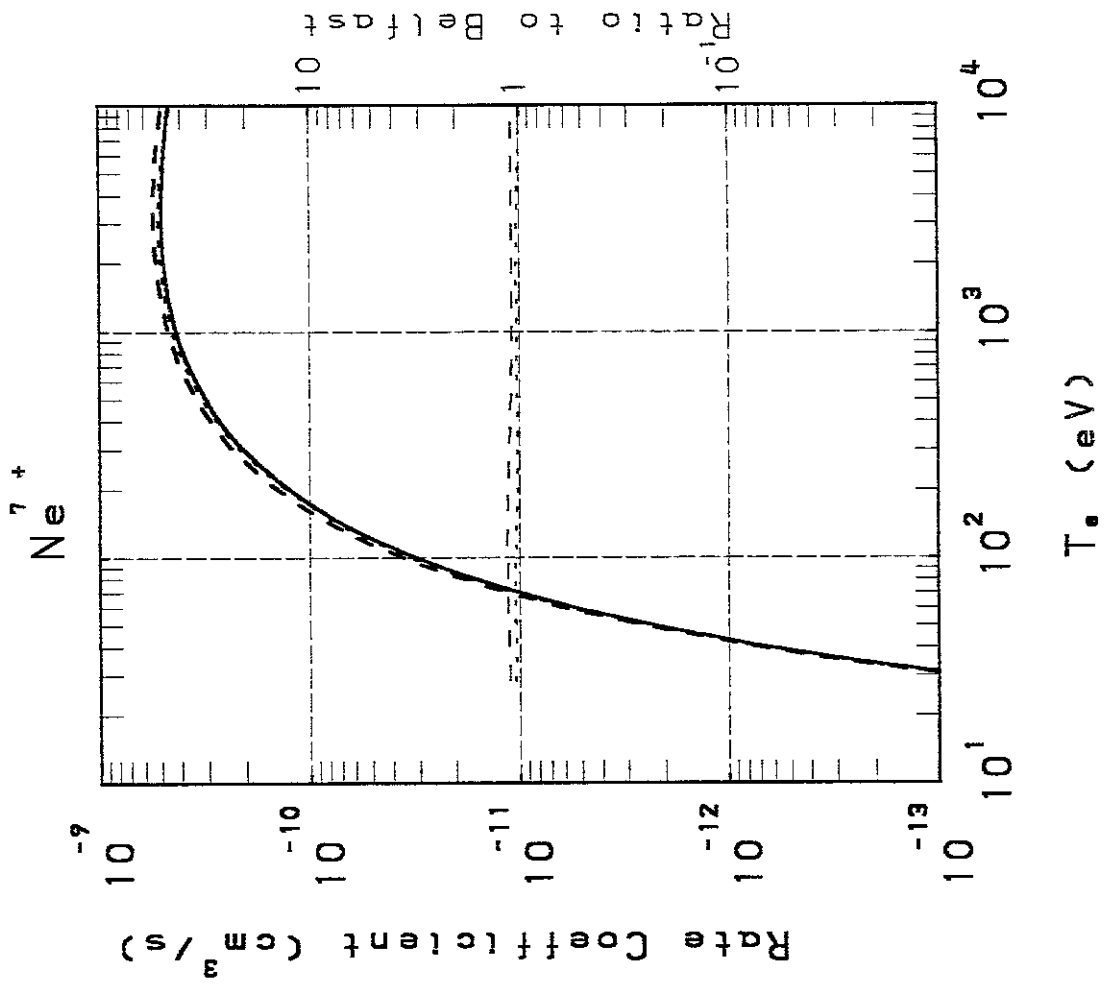


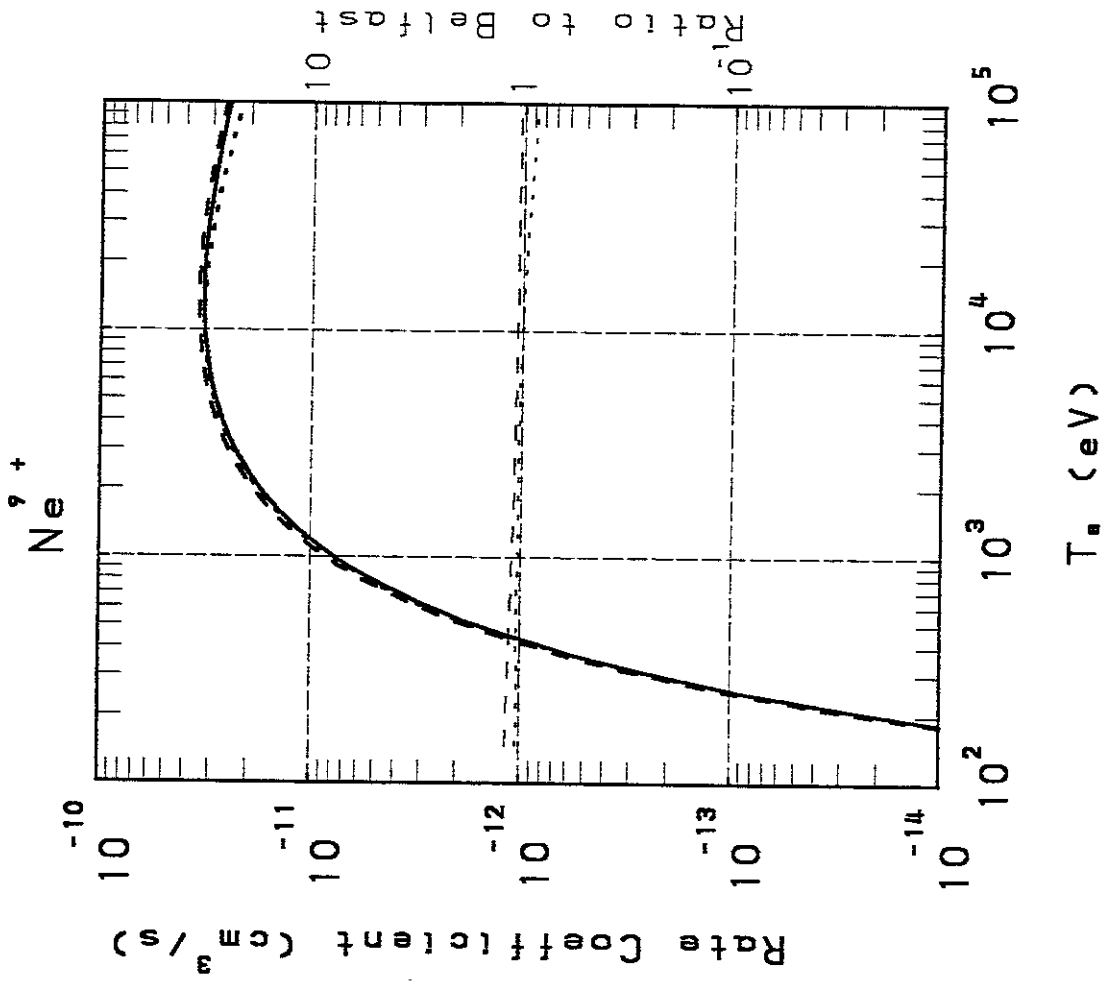
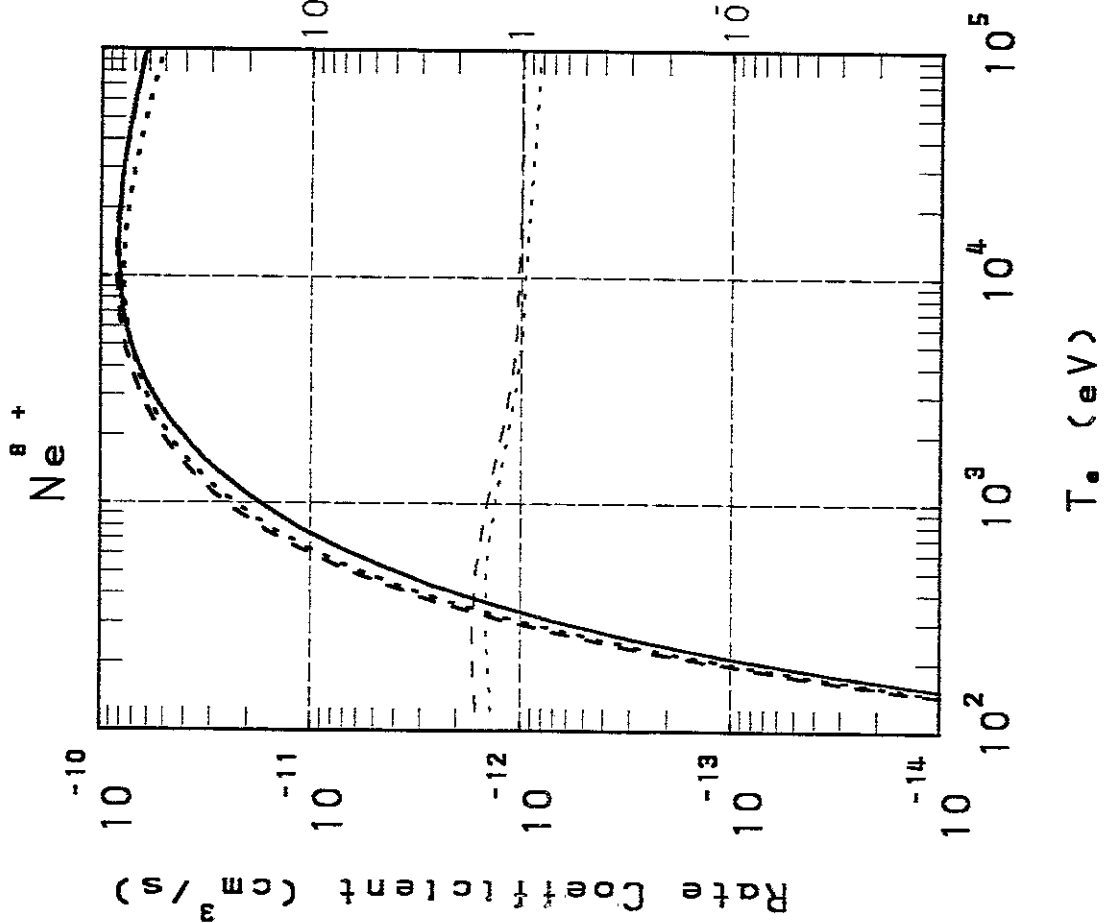
Ne

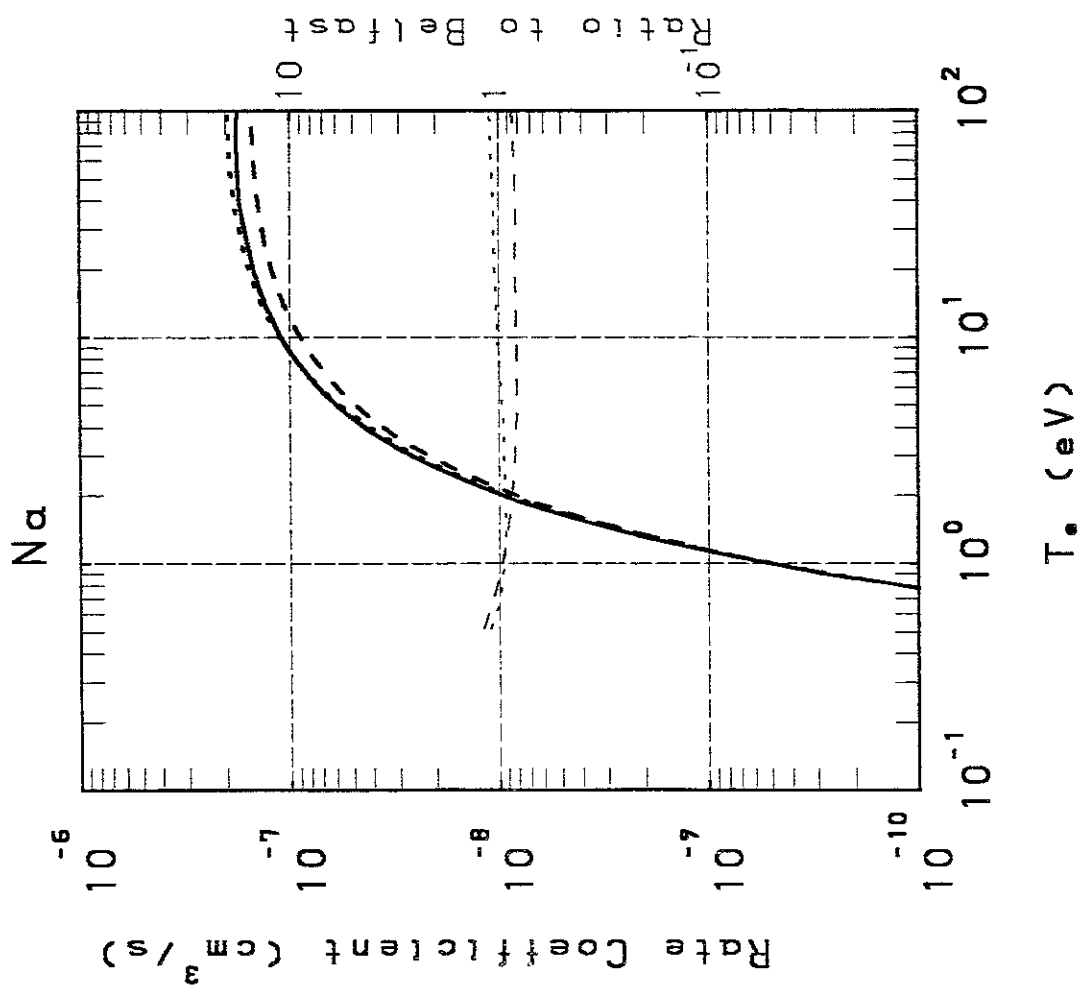
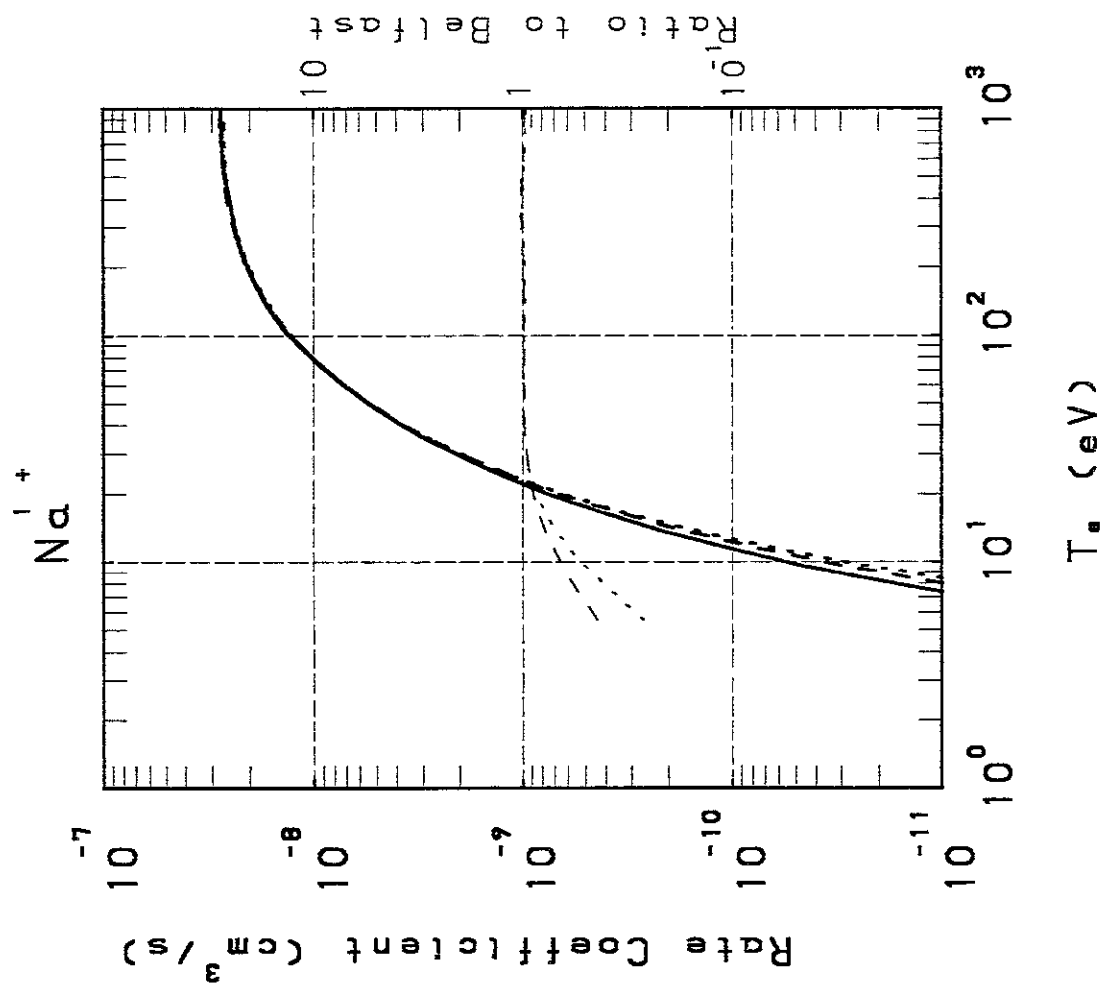


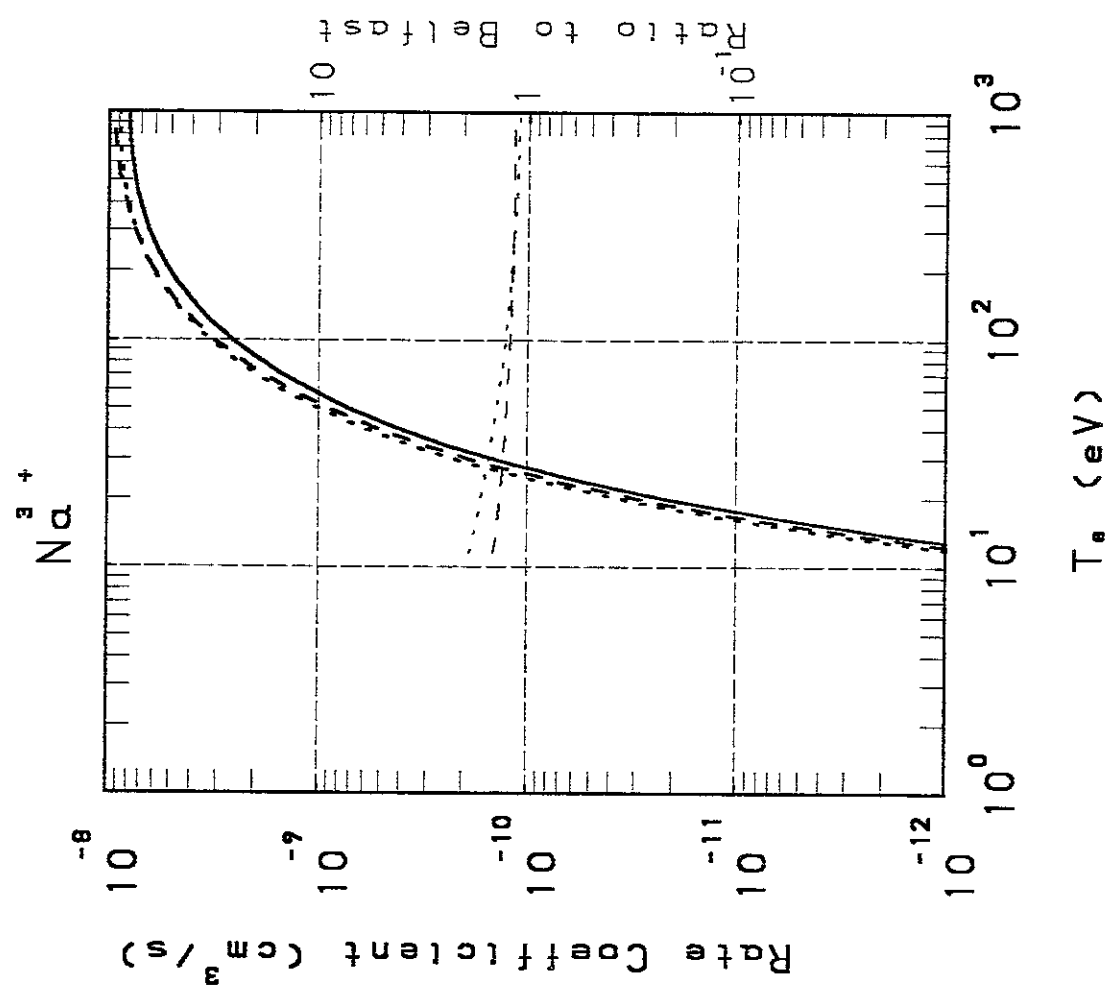
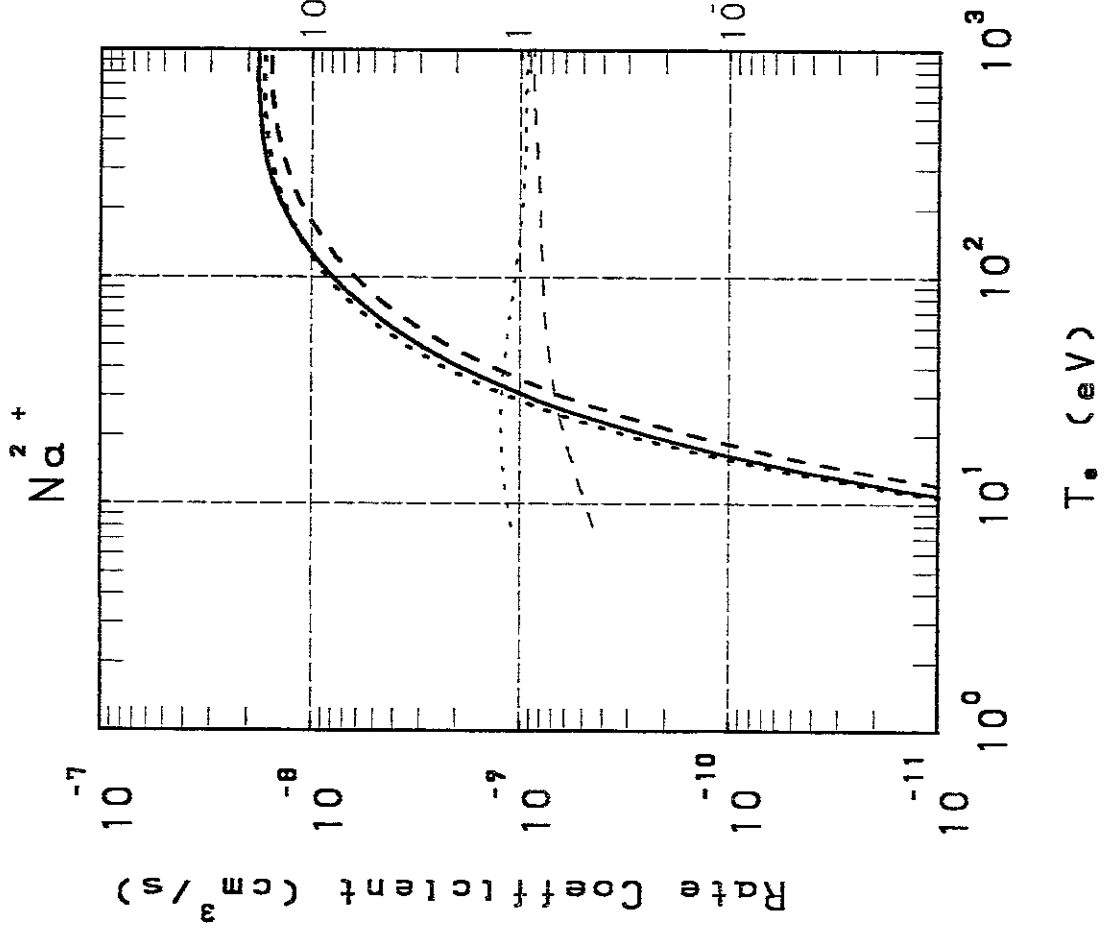


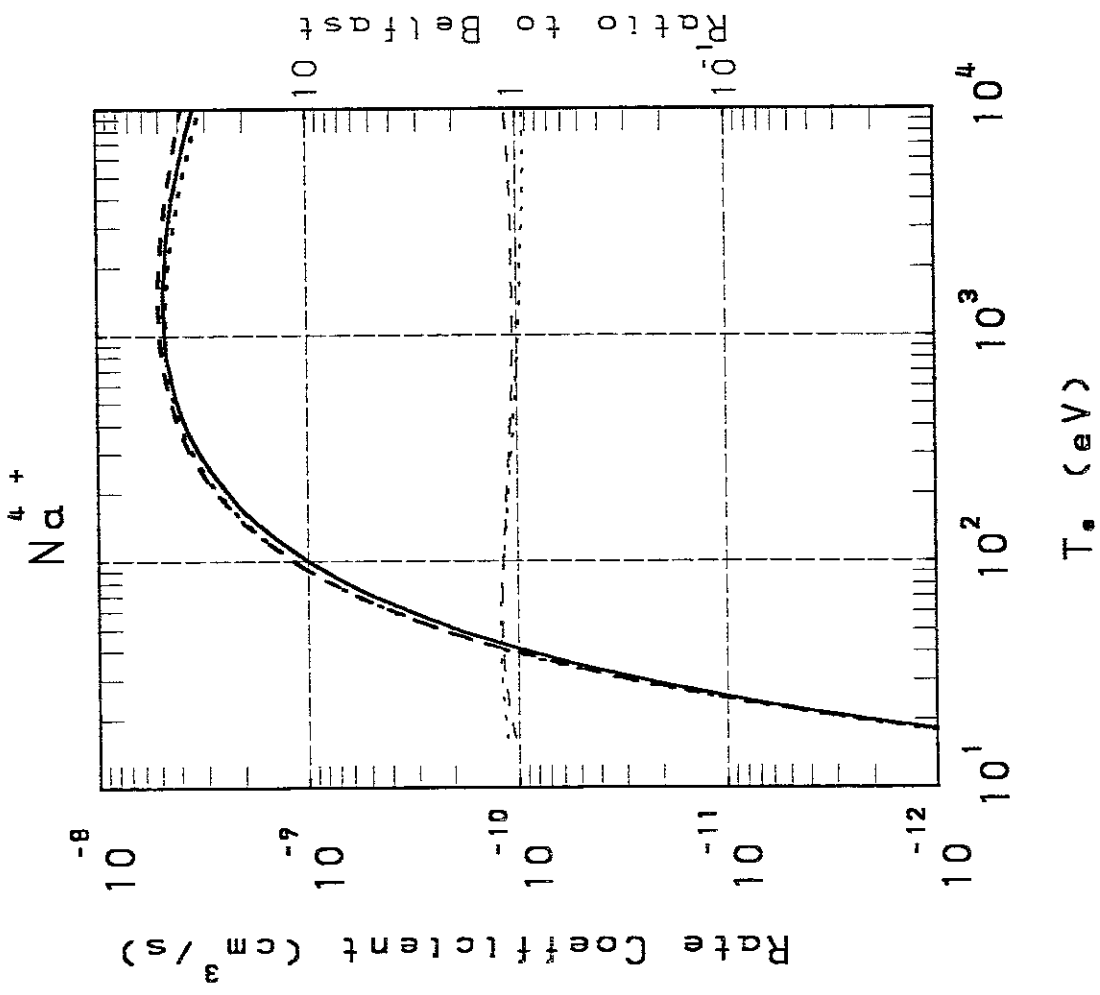
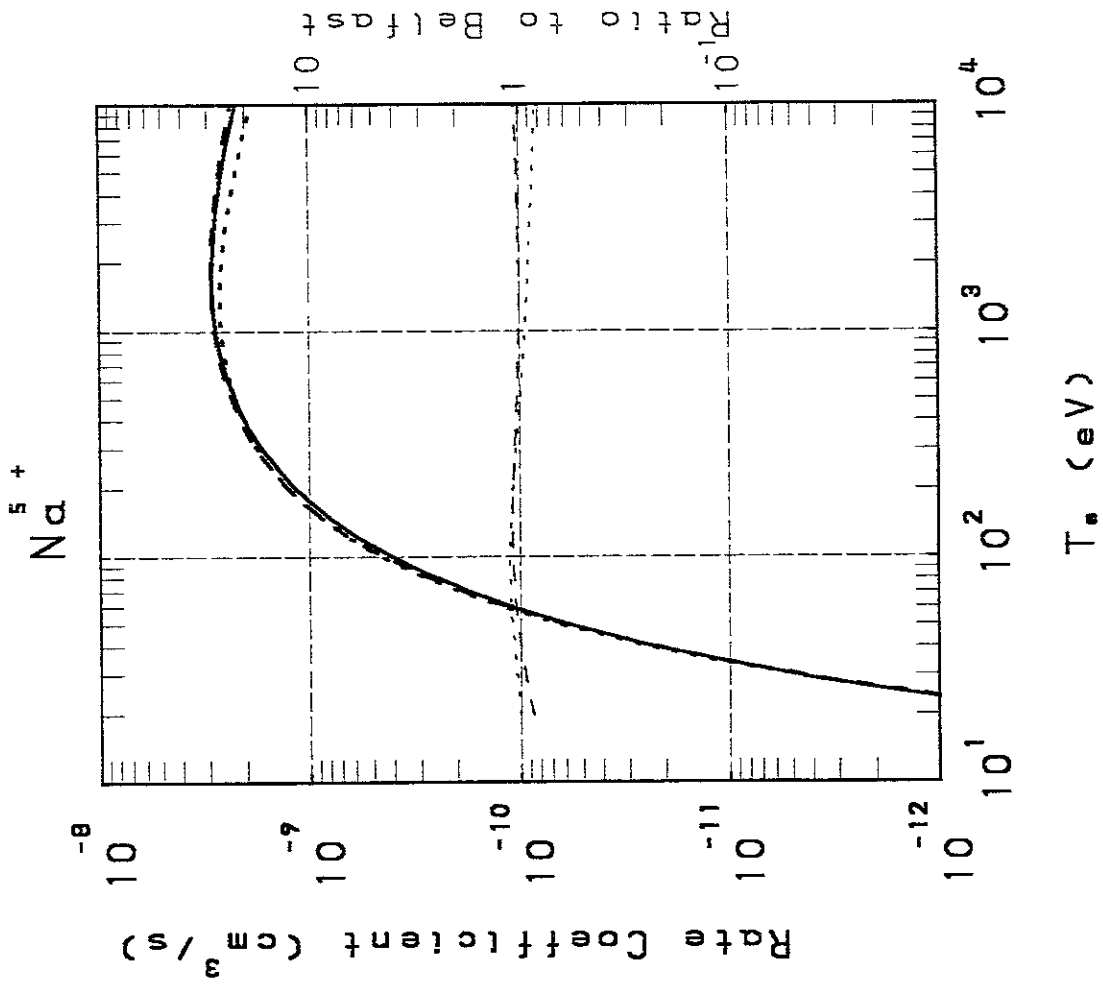


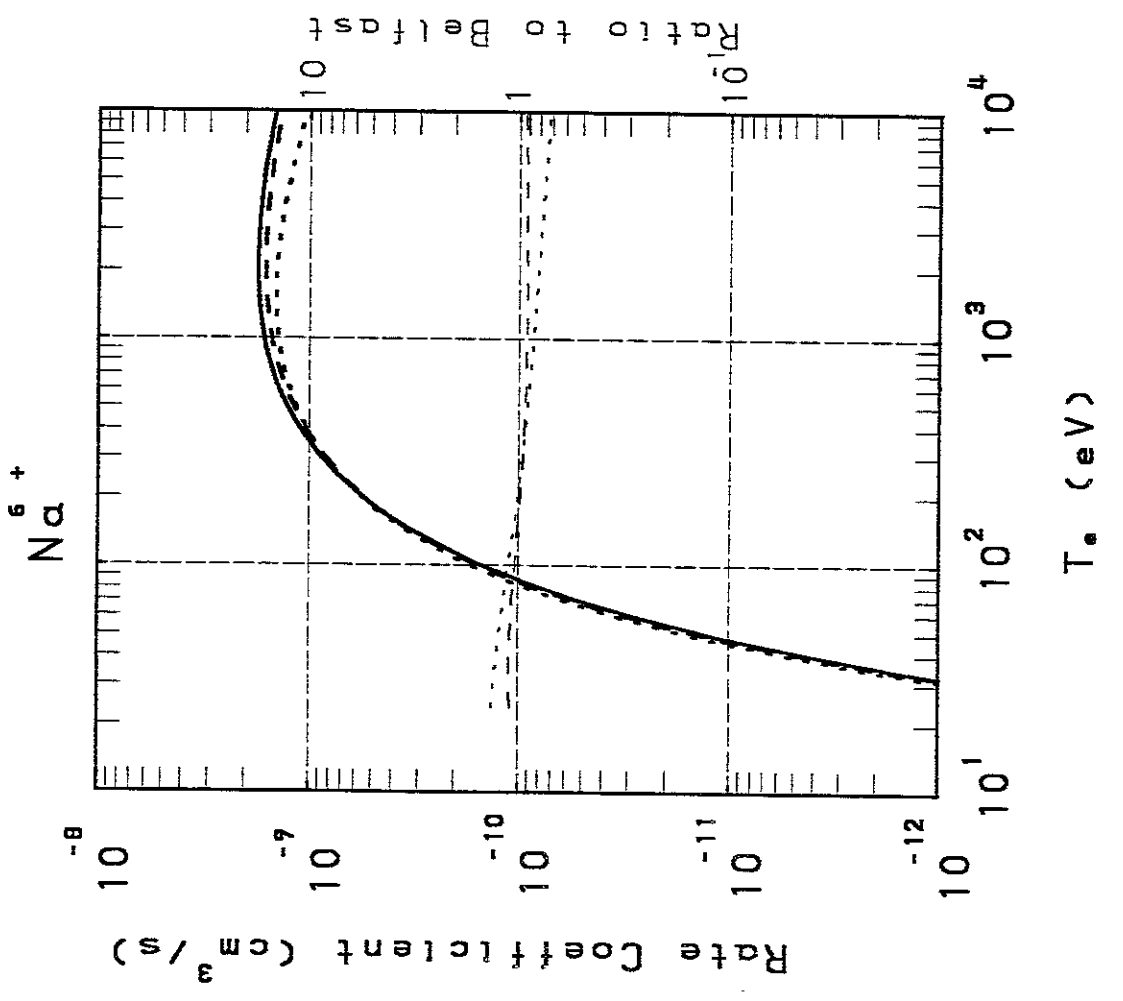
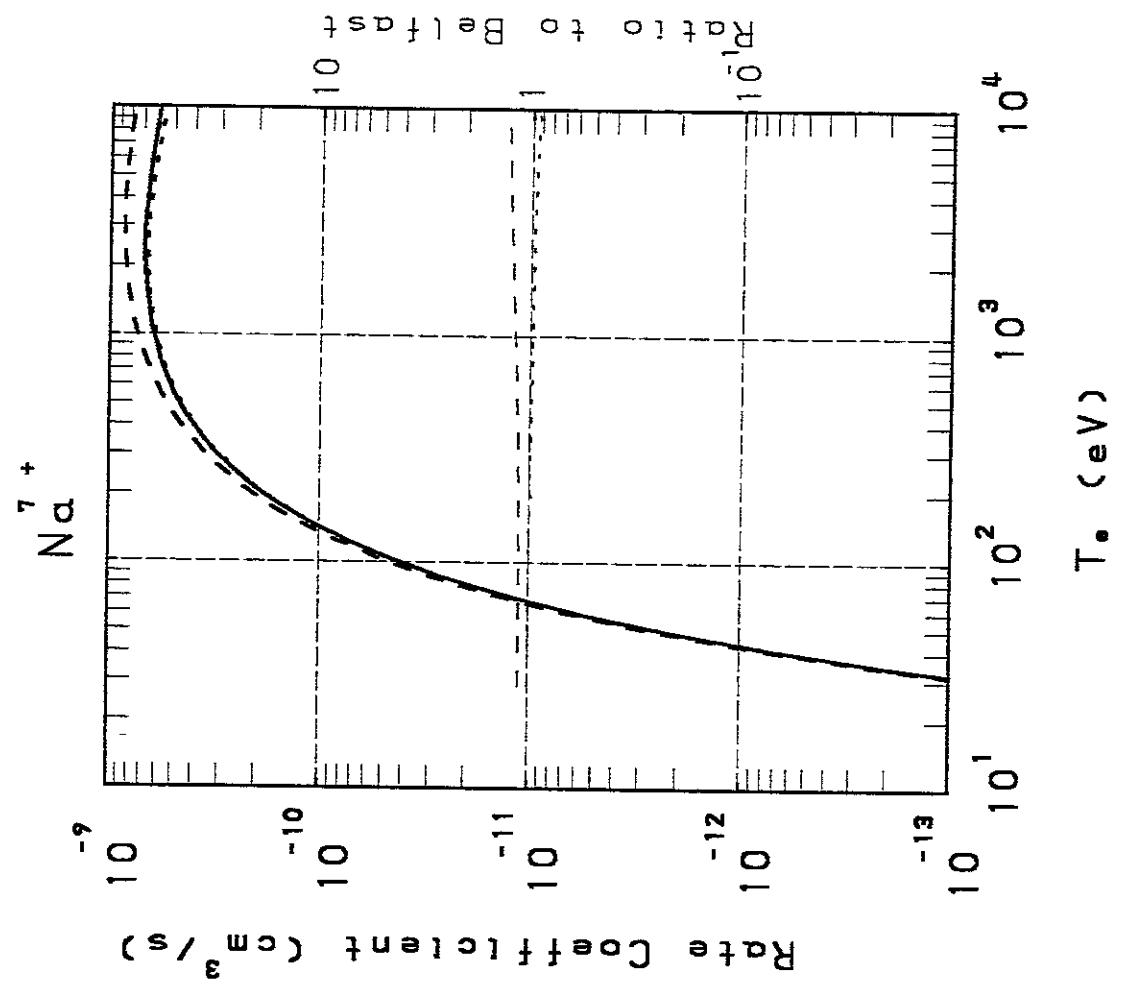


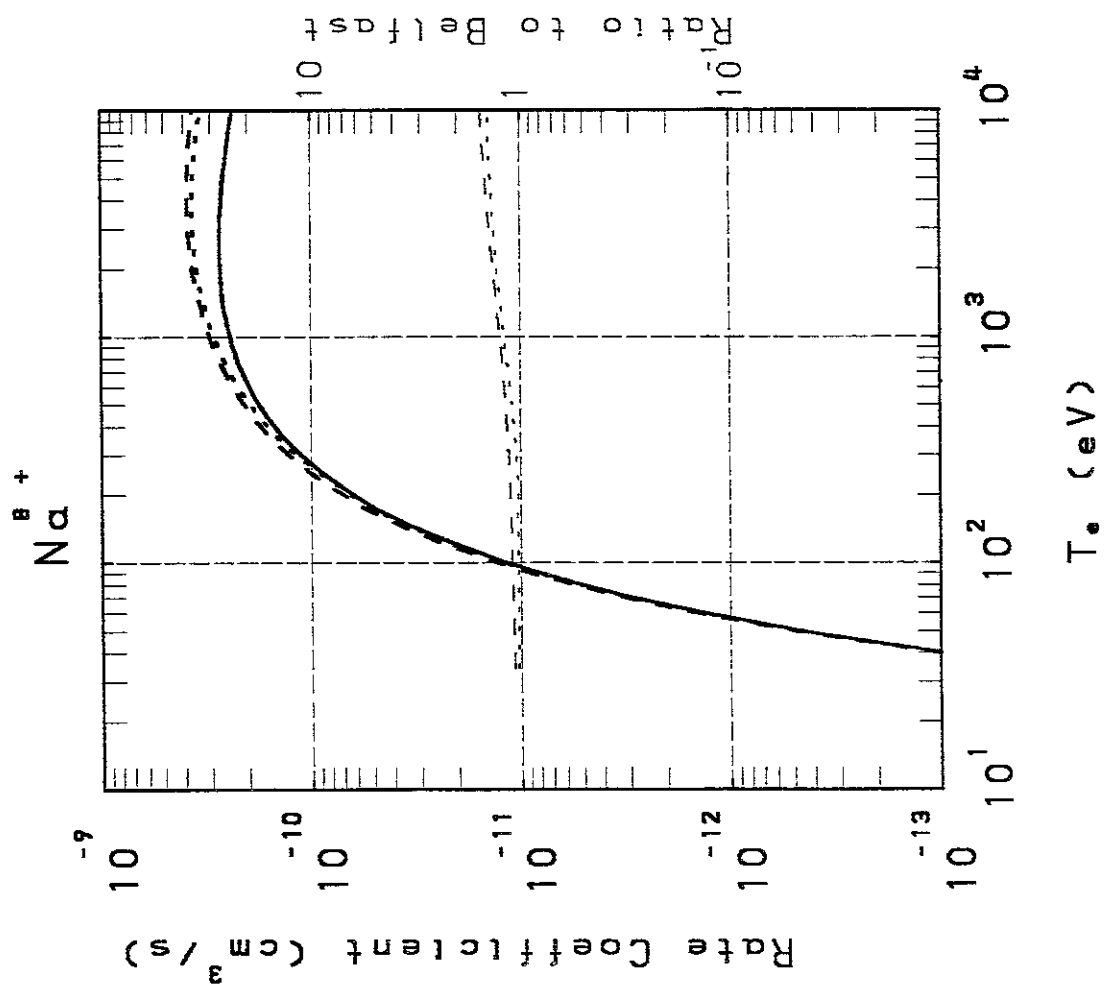
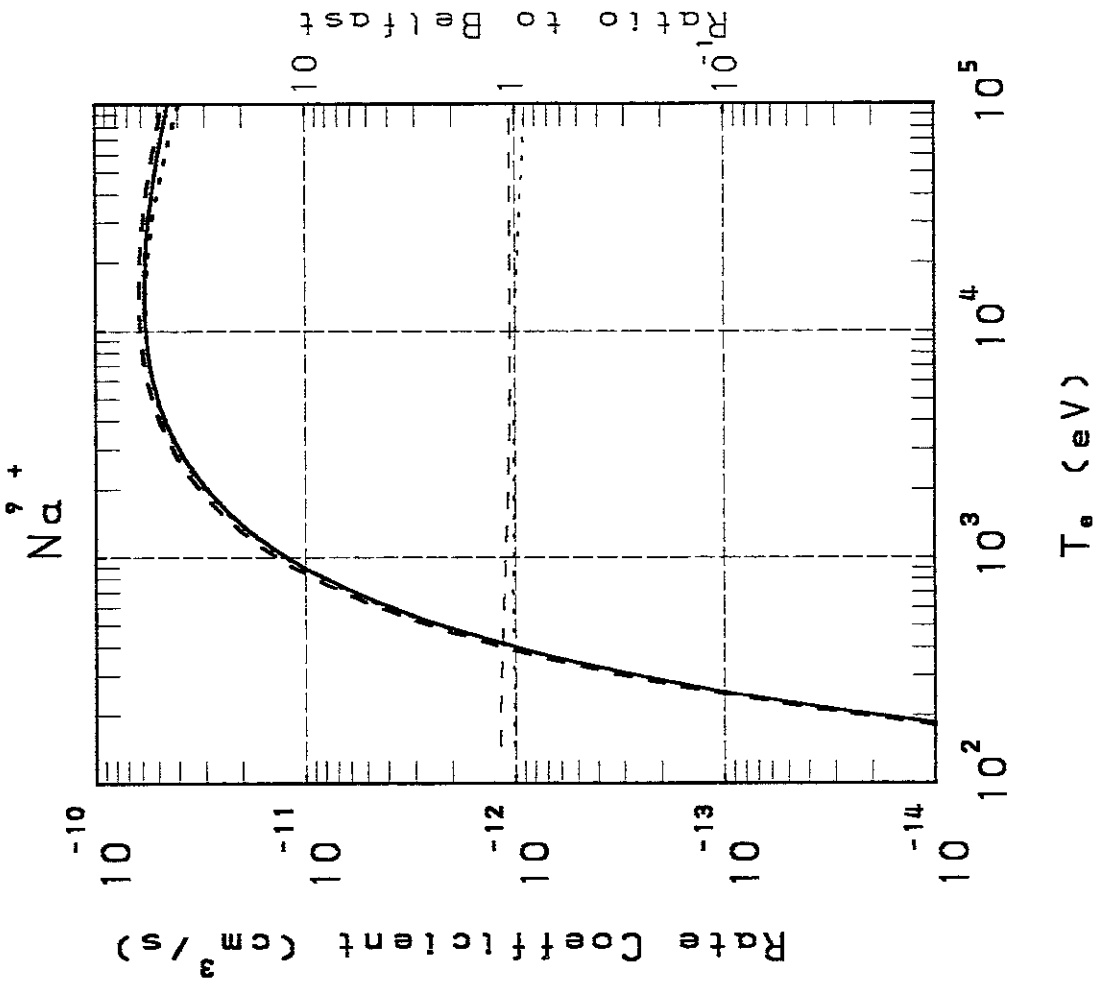


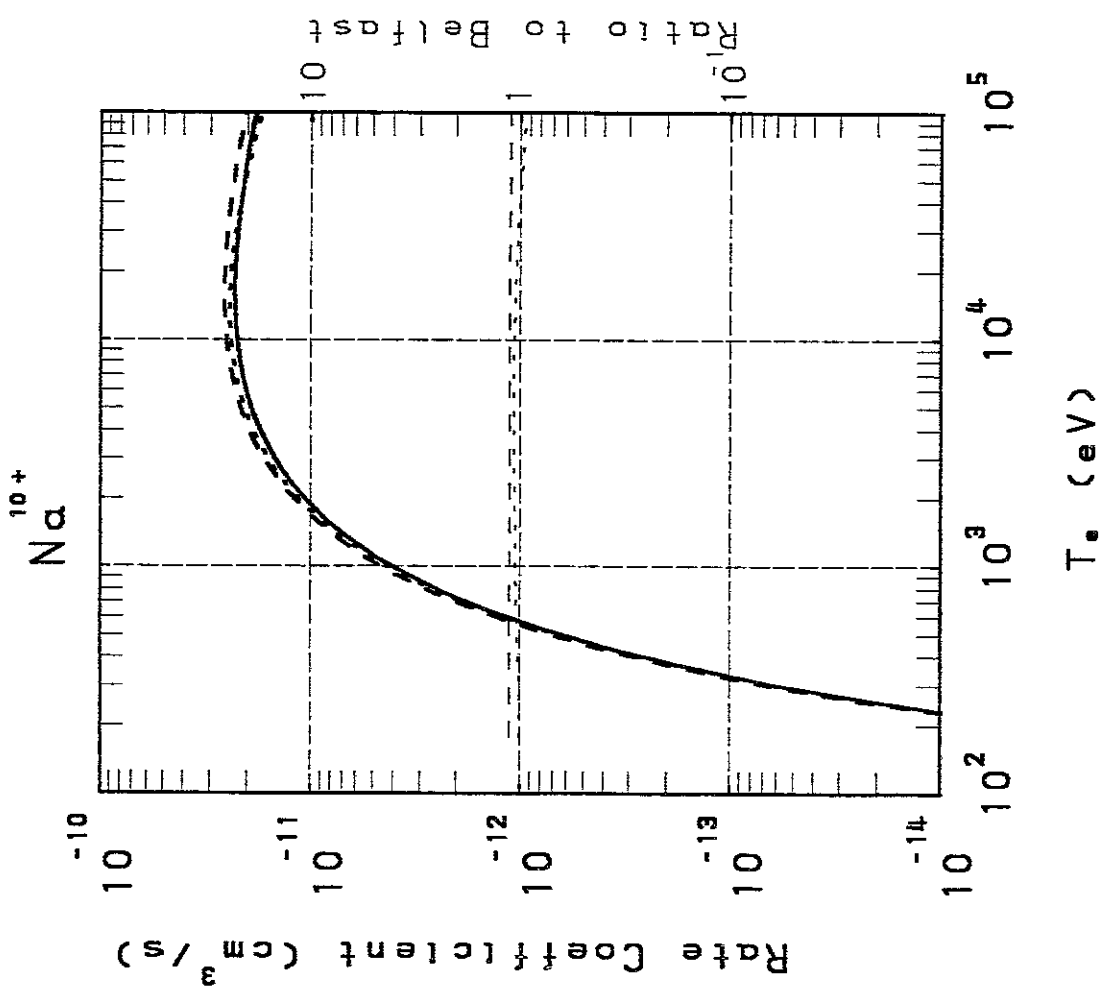


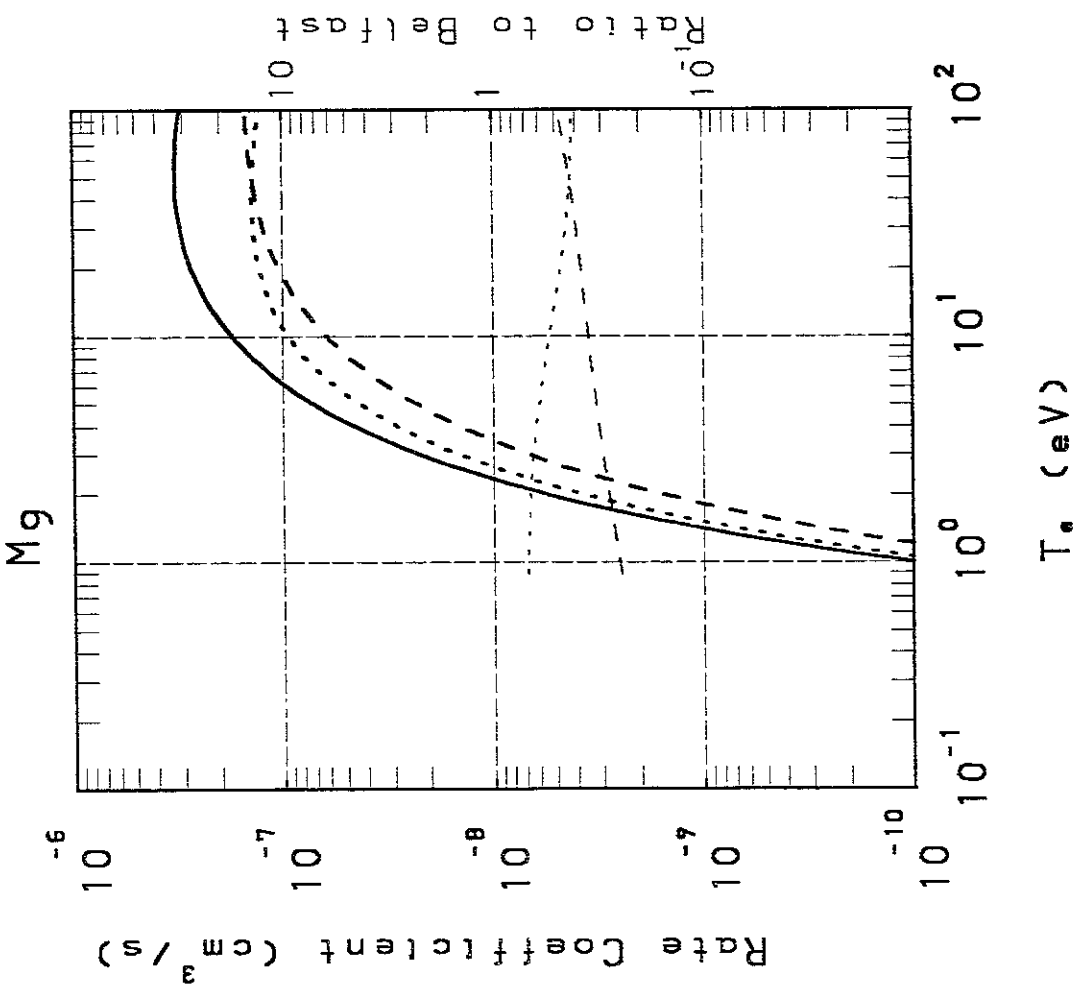
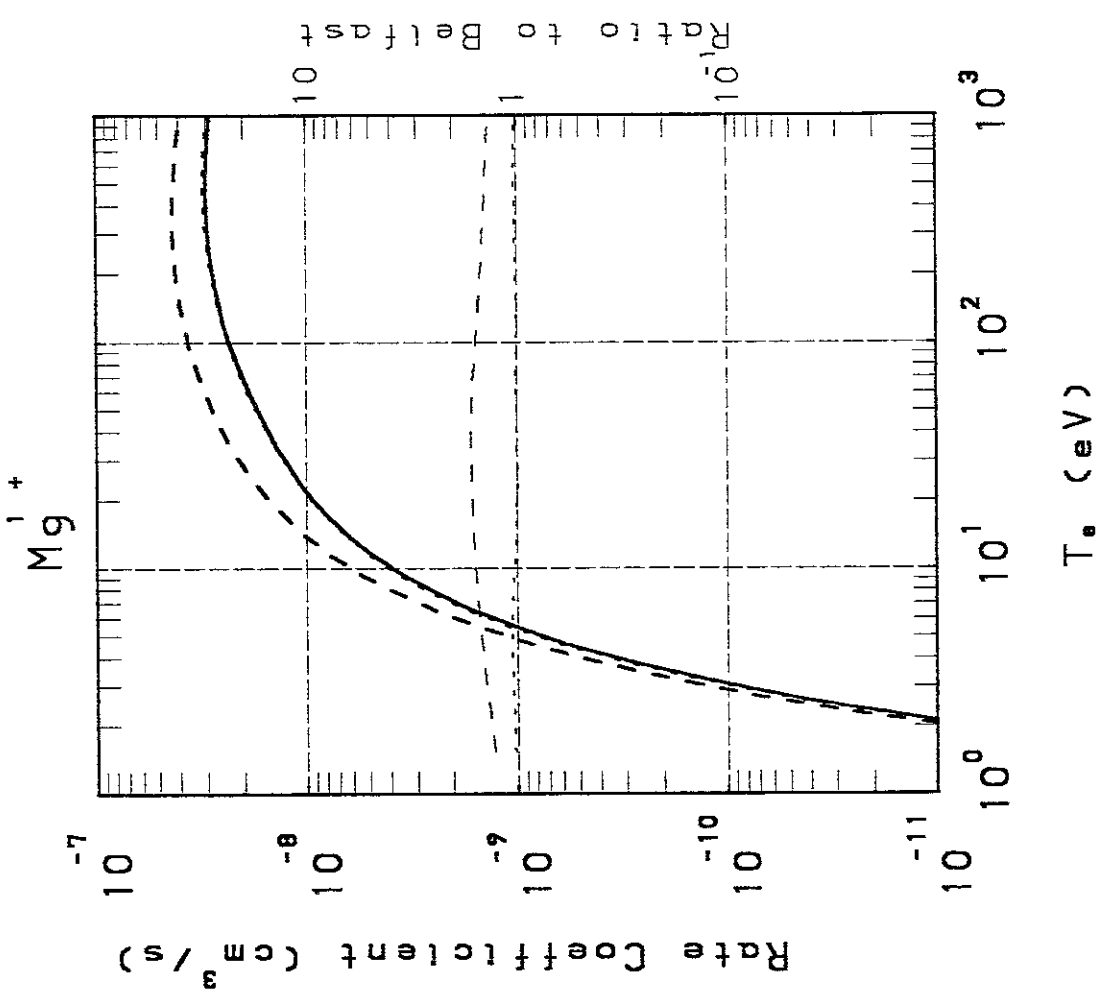


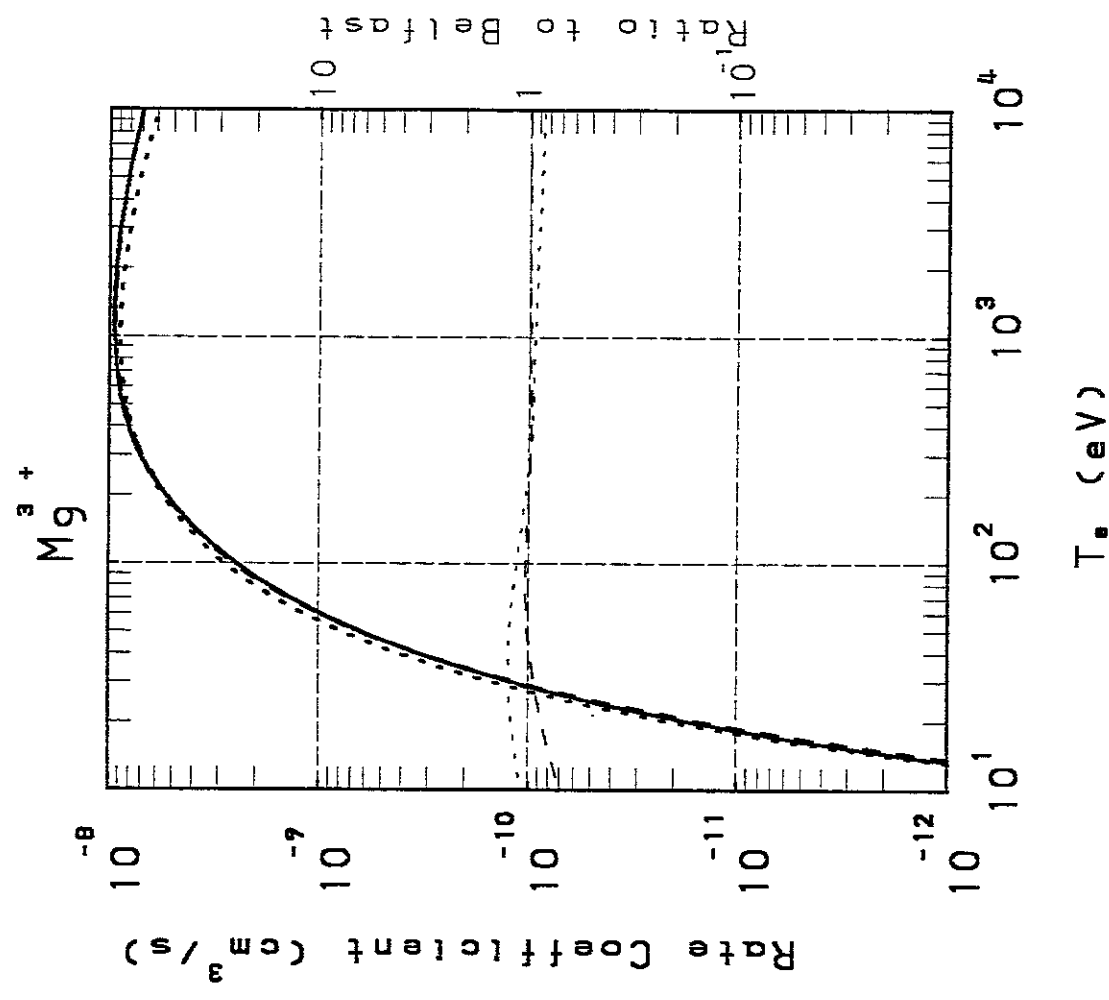
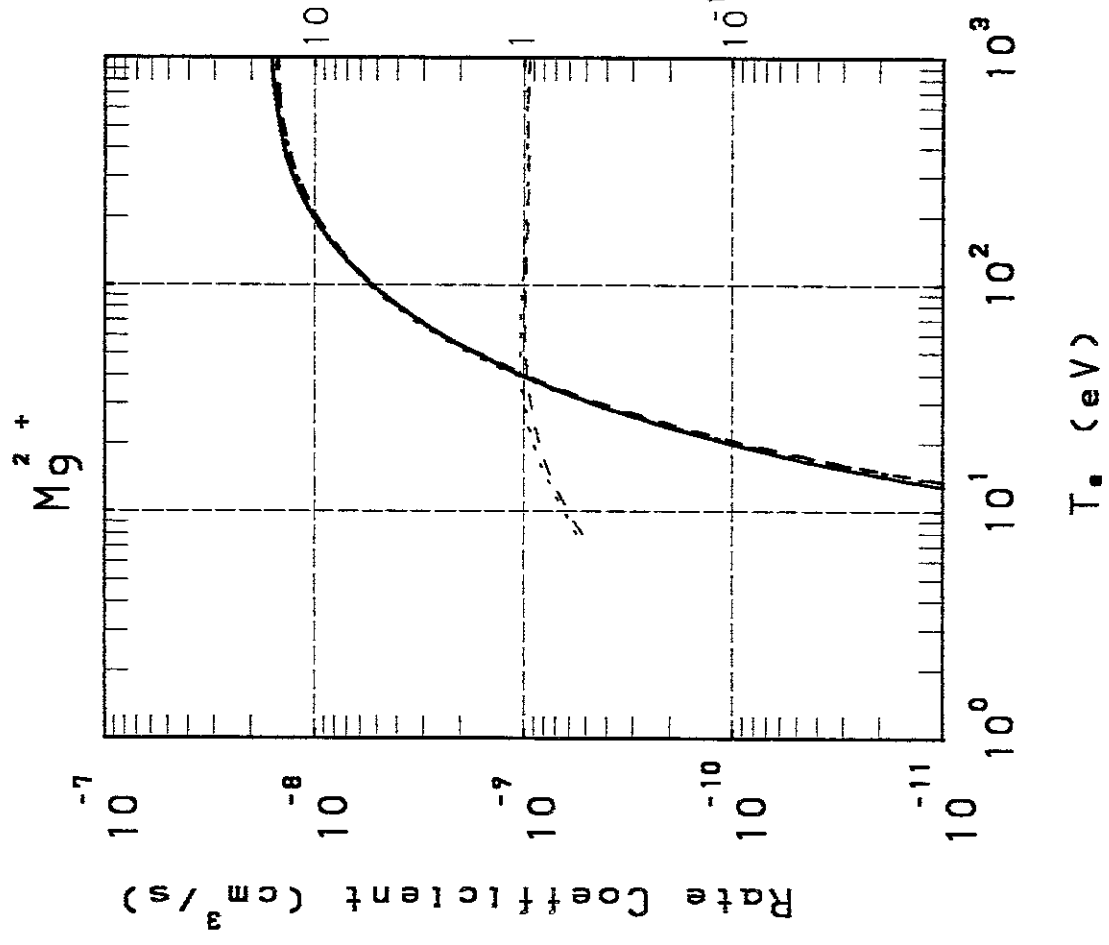


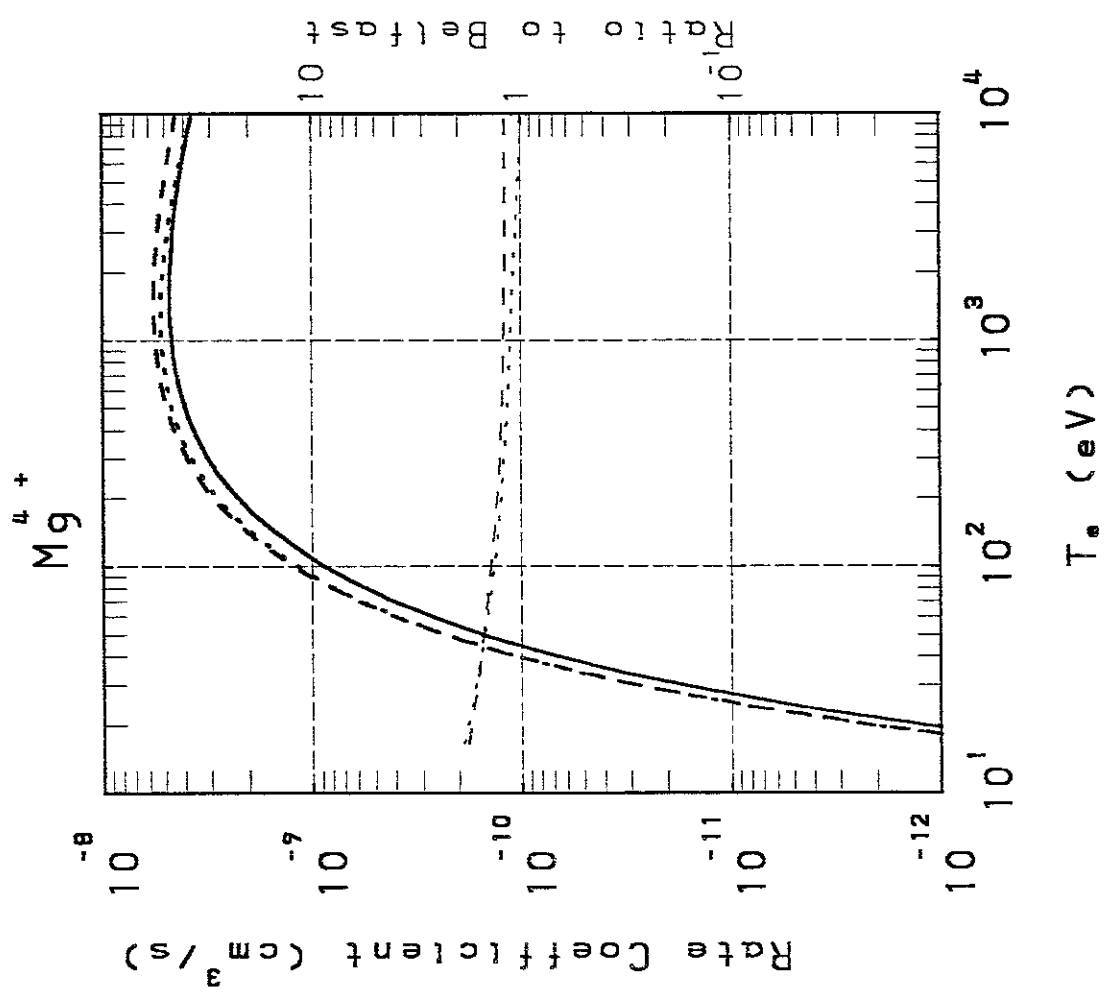
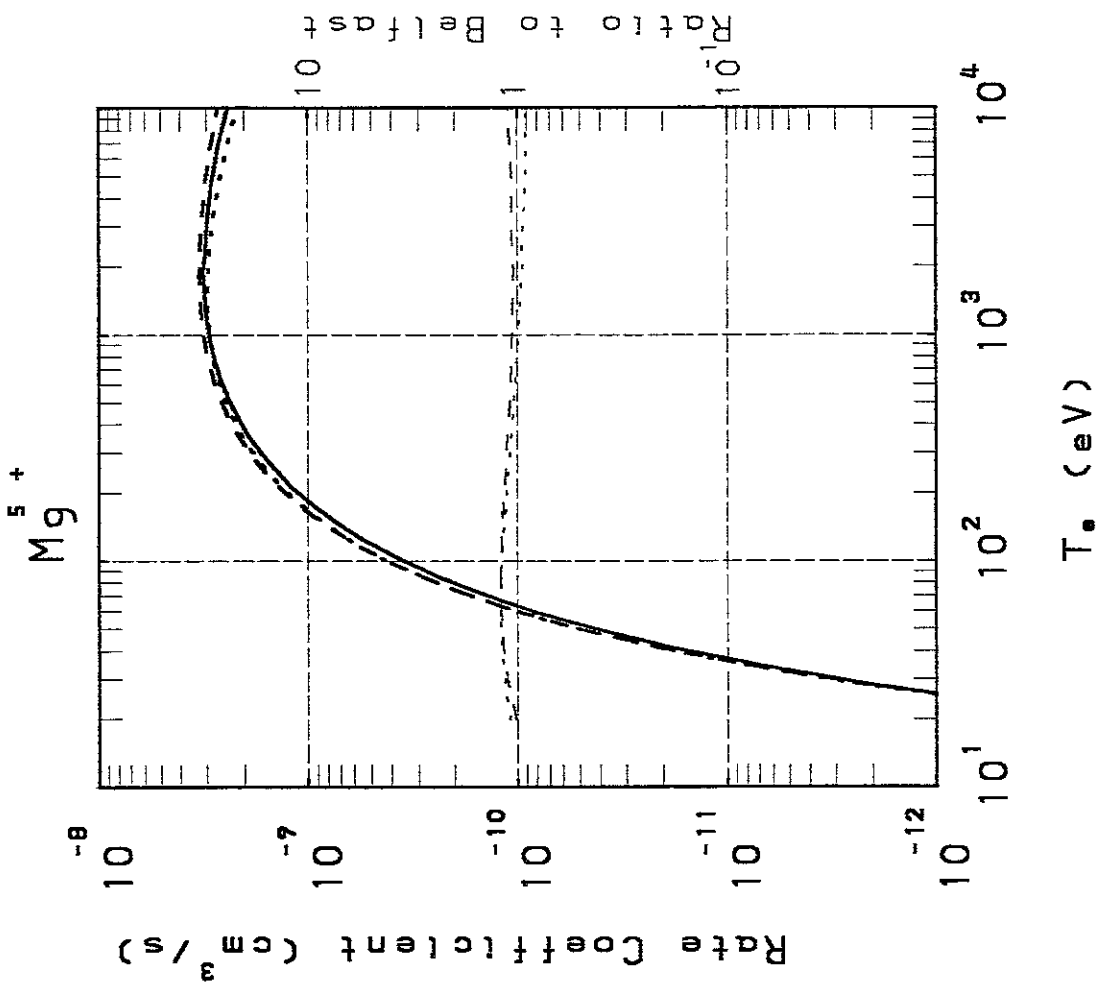


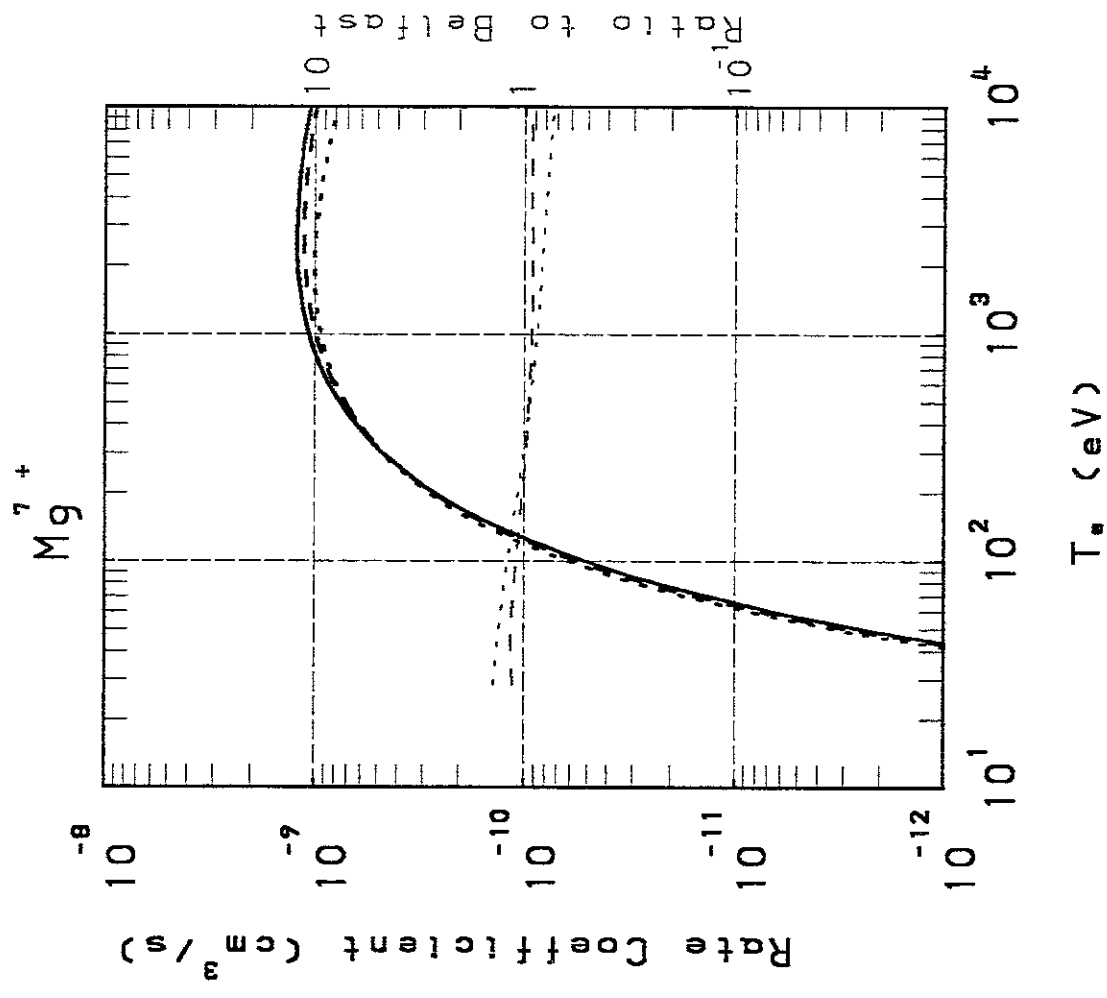
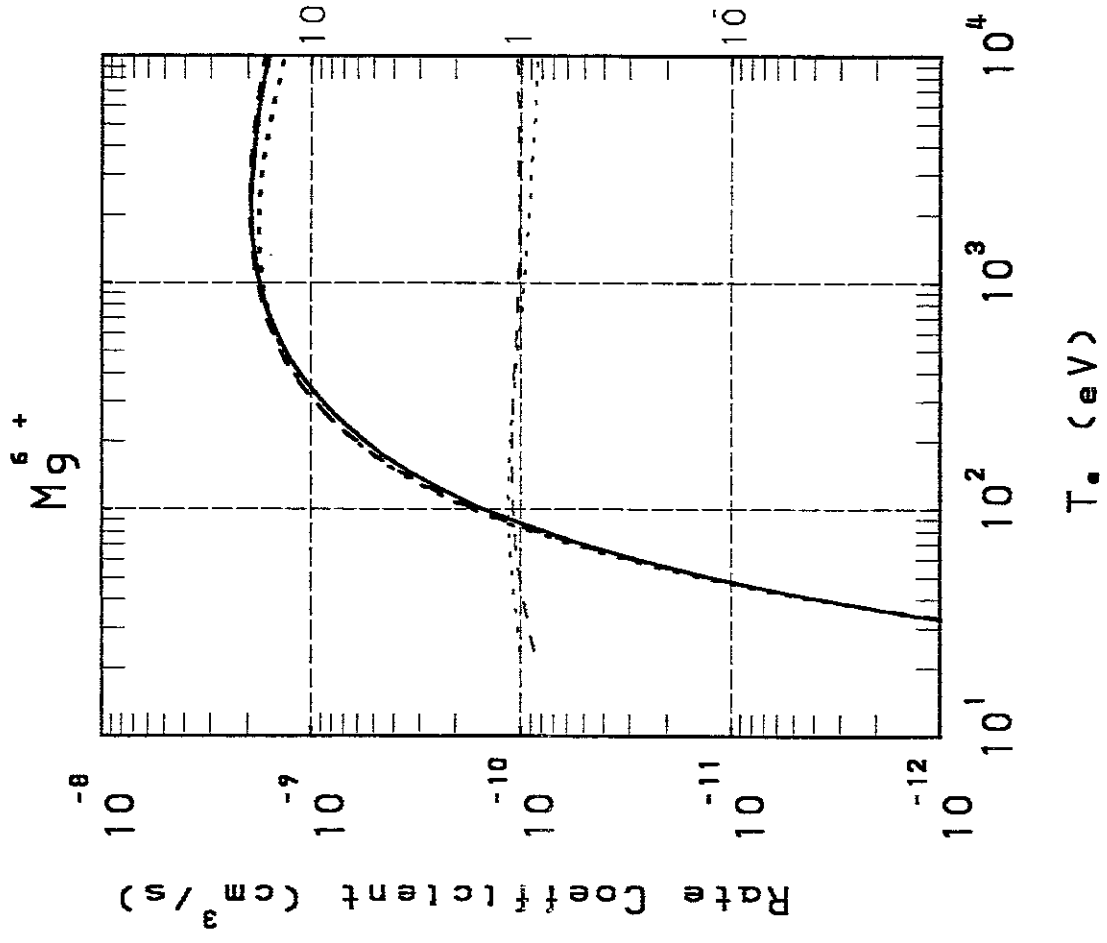


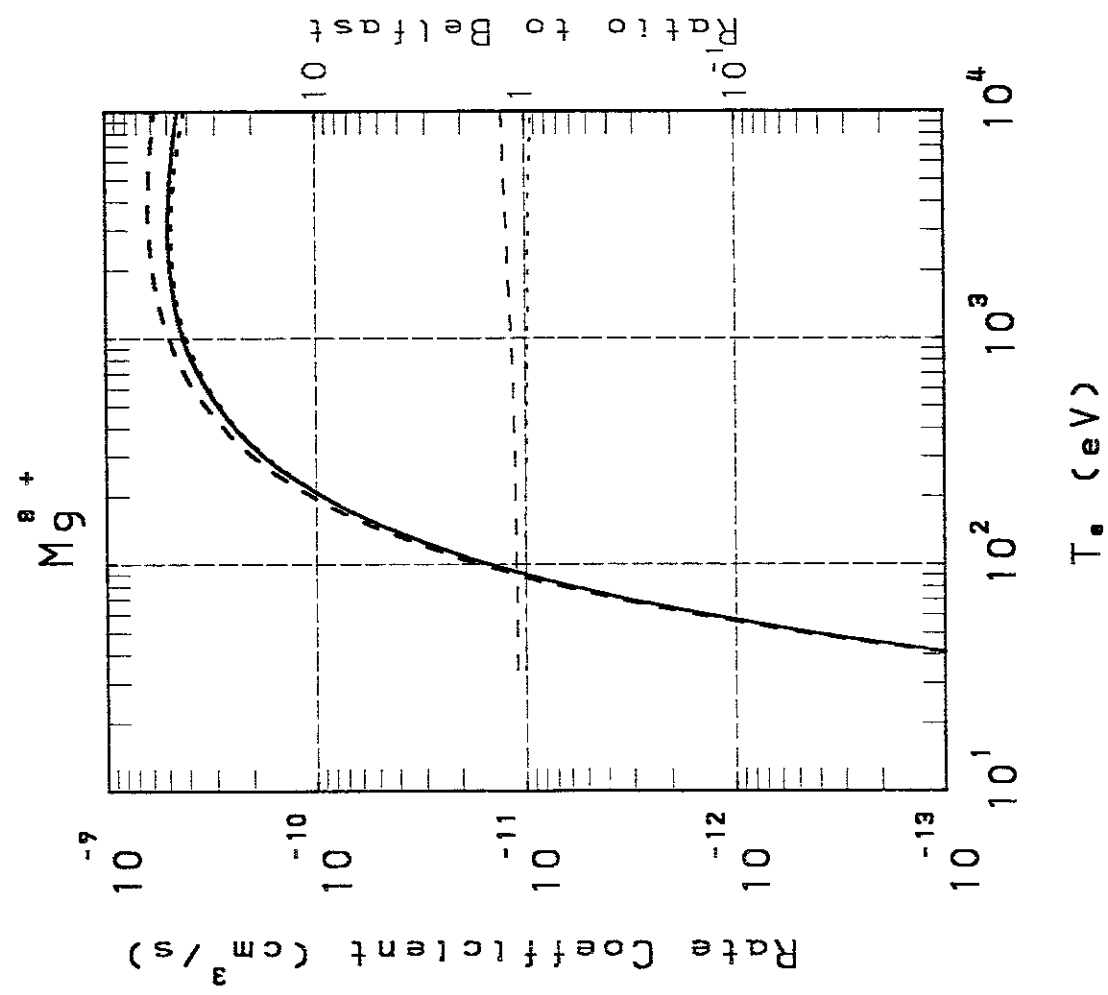
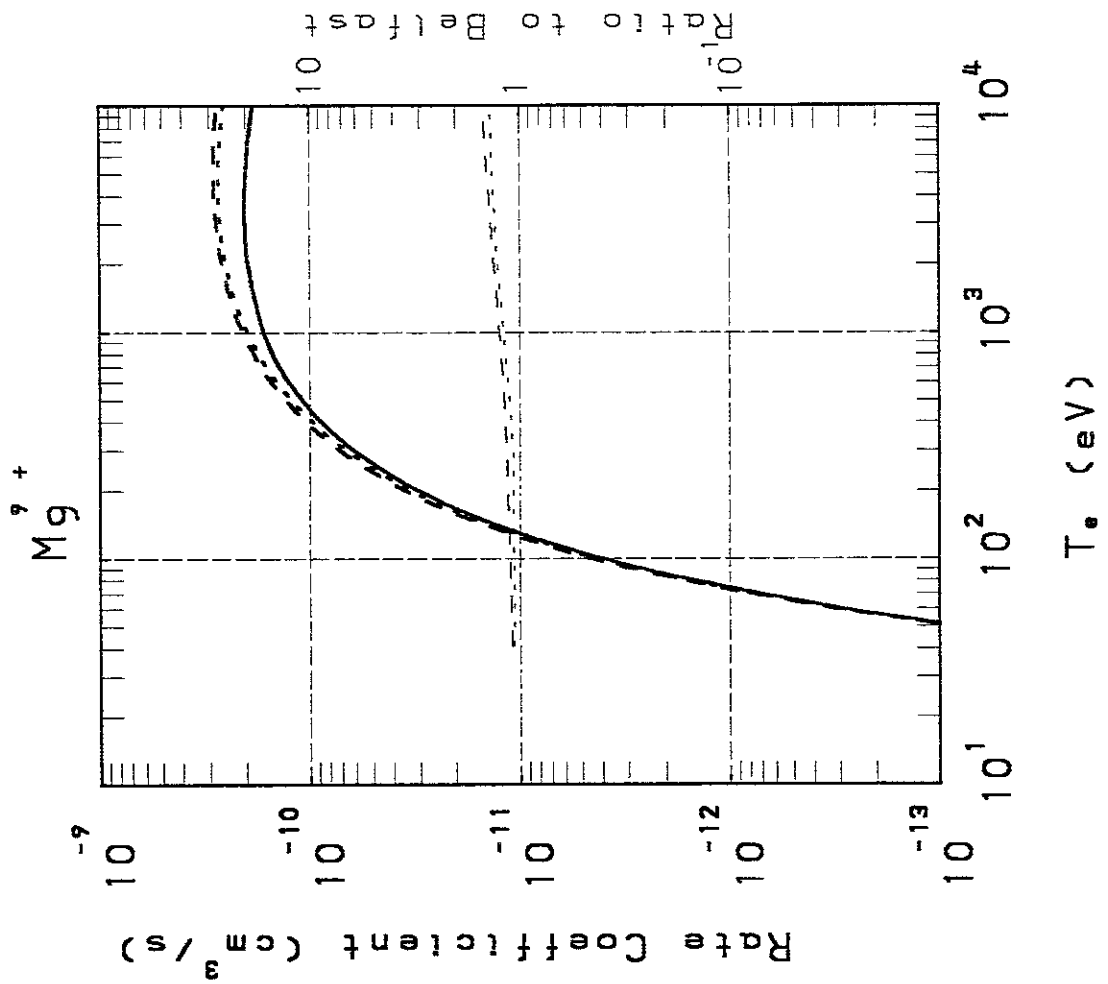


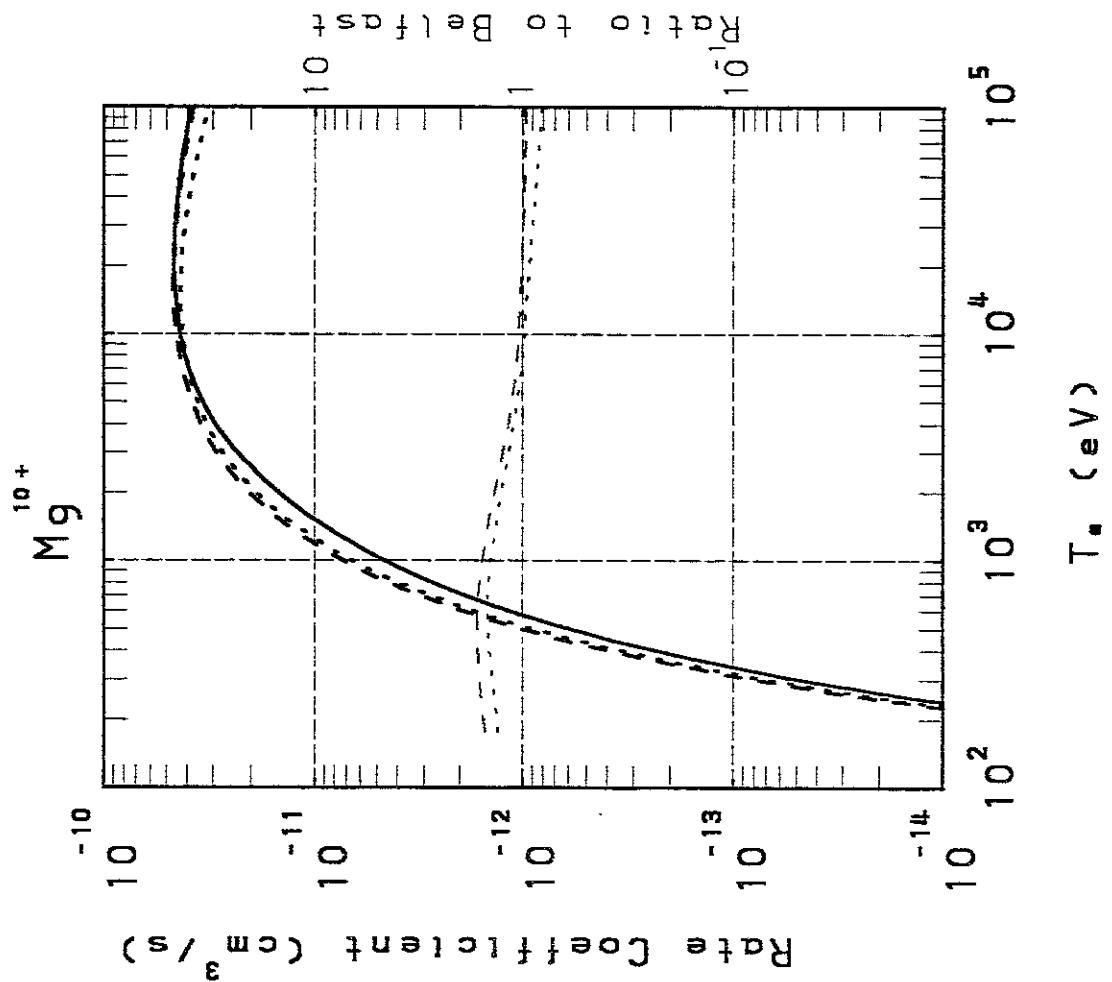
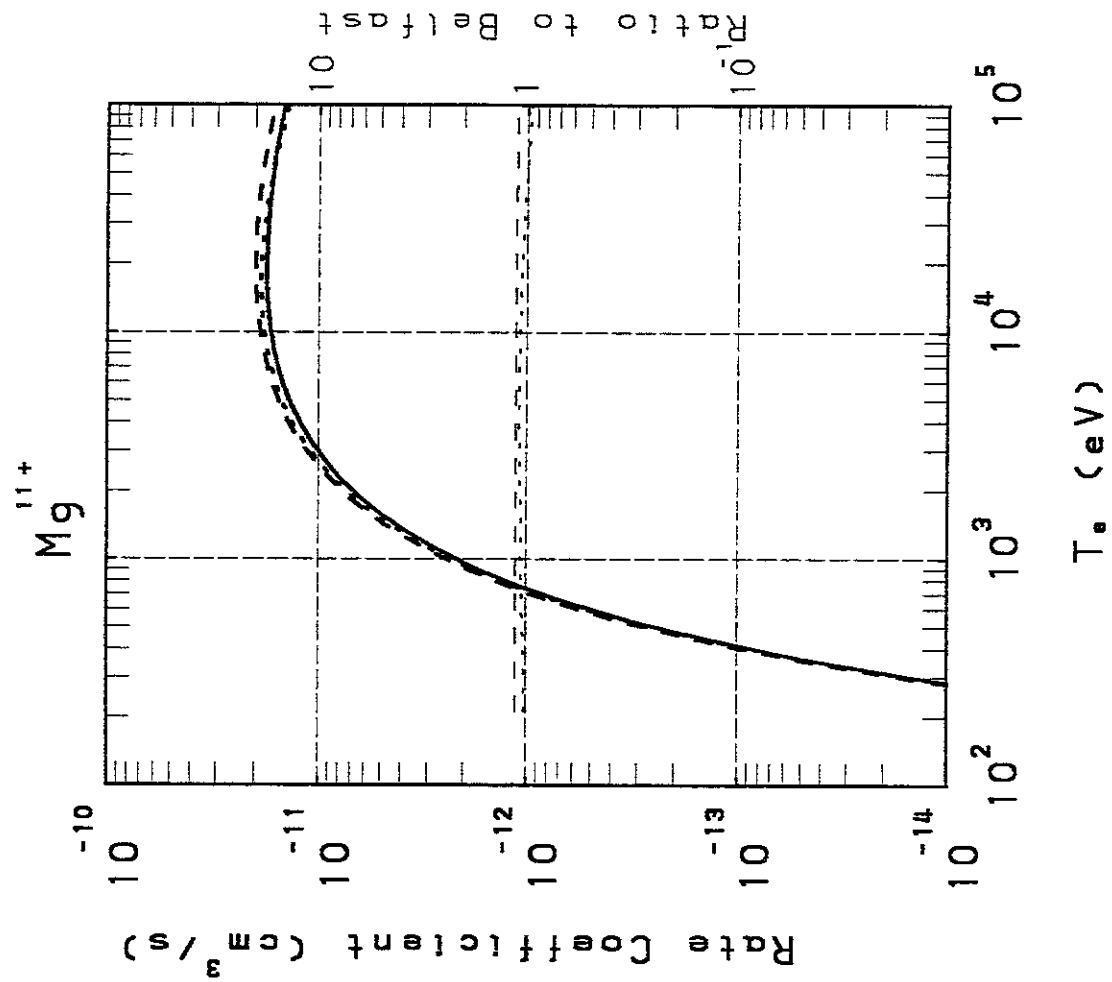


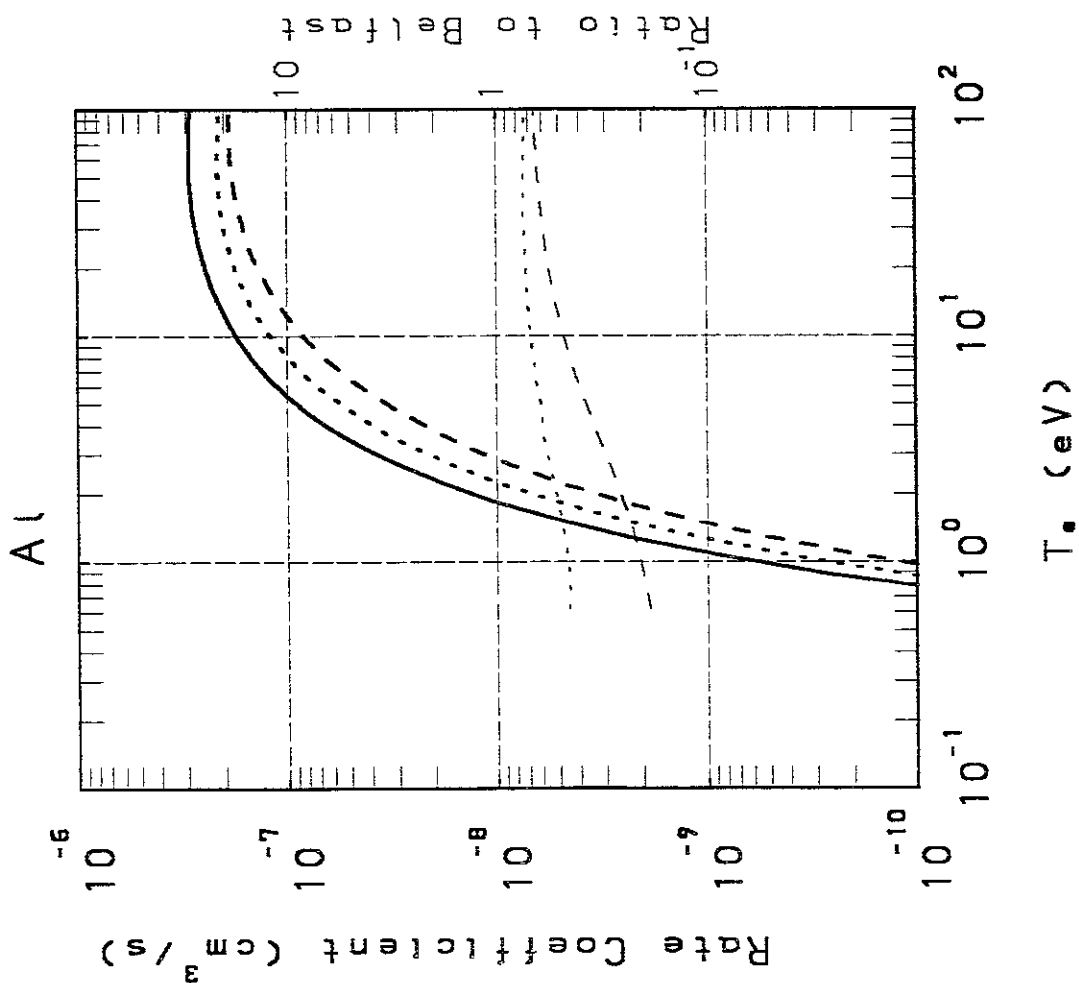
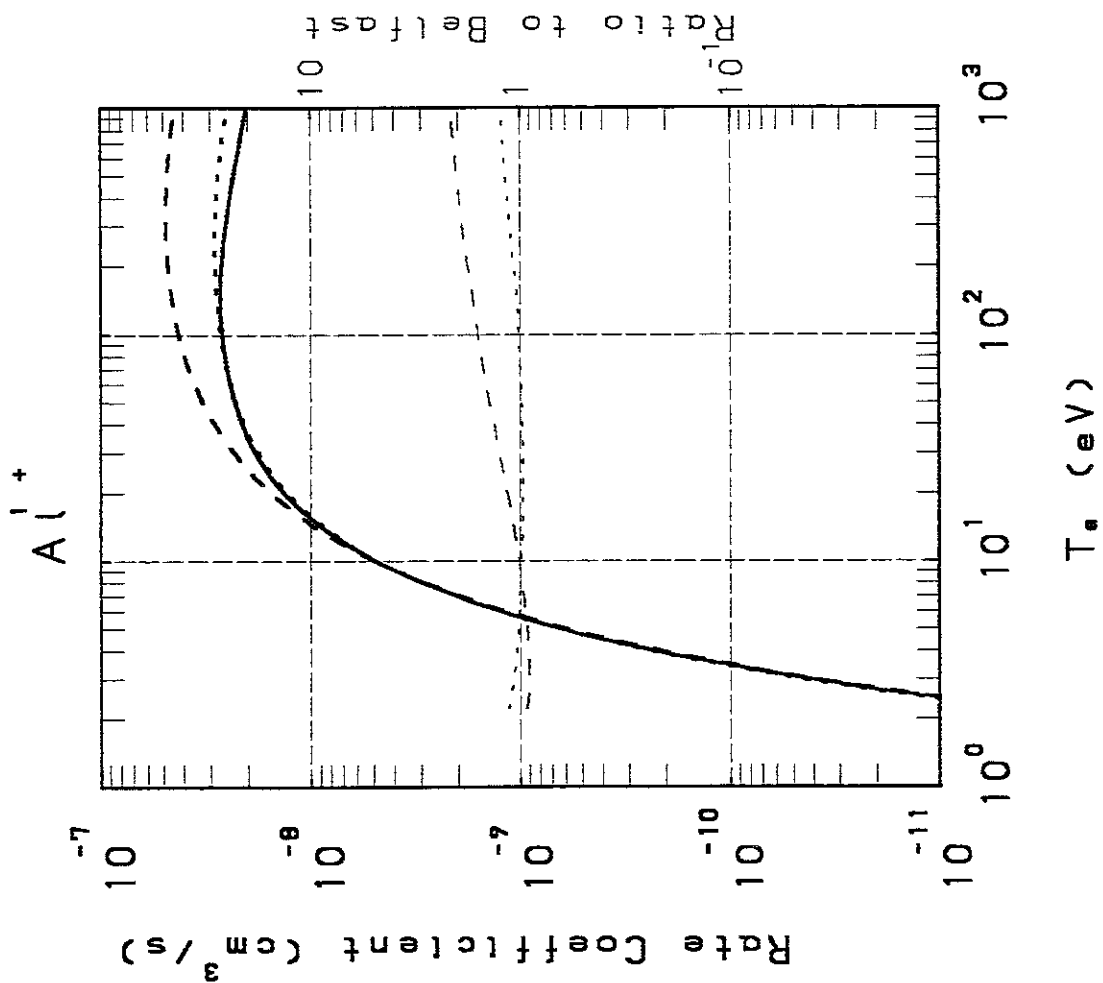






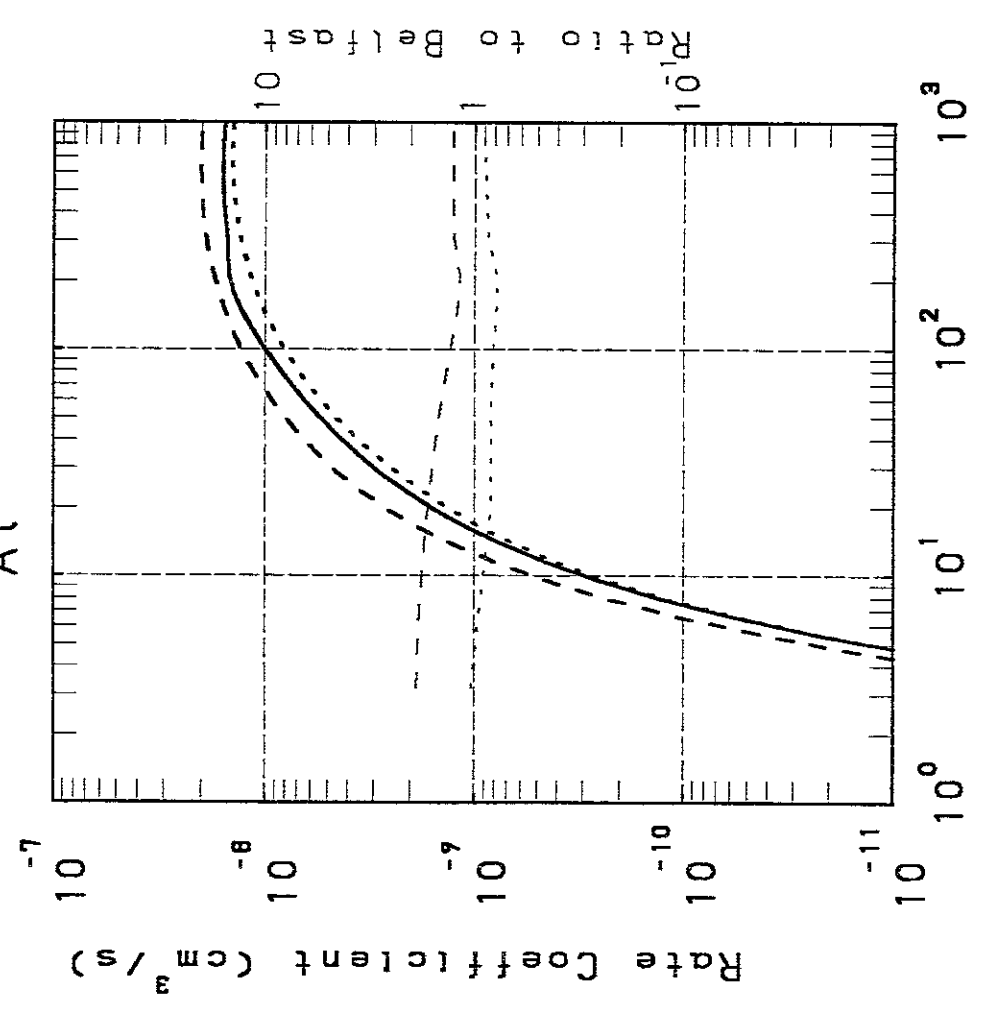
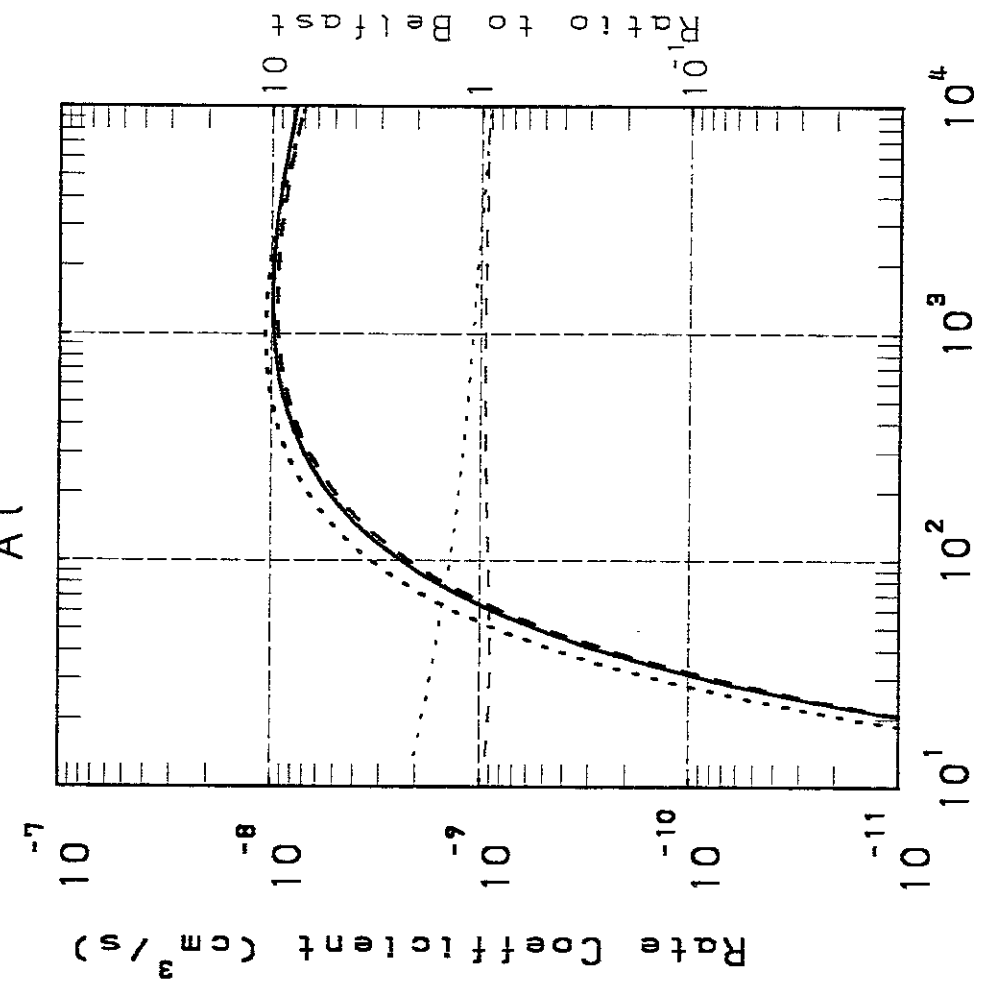






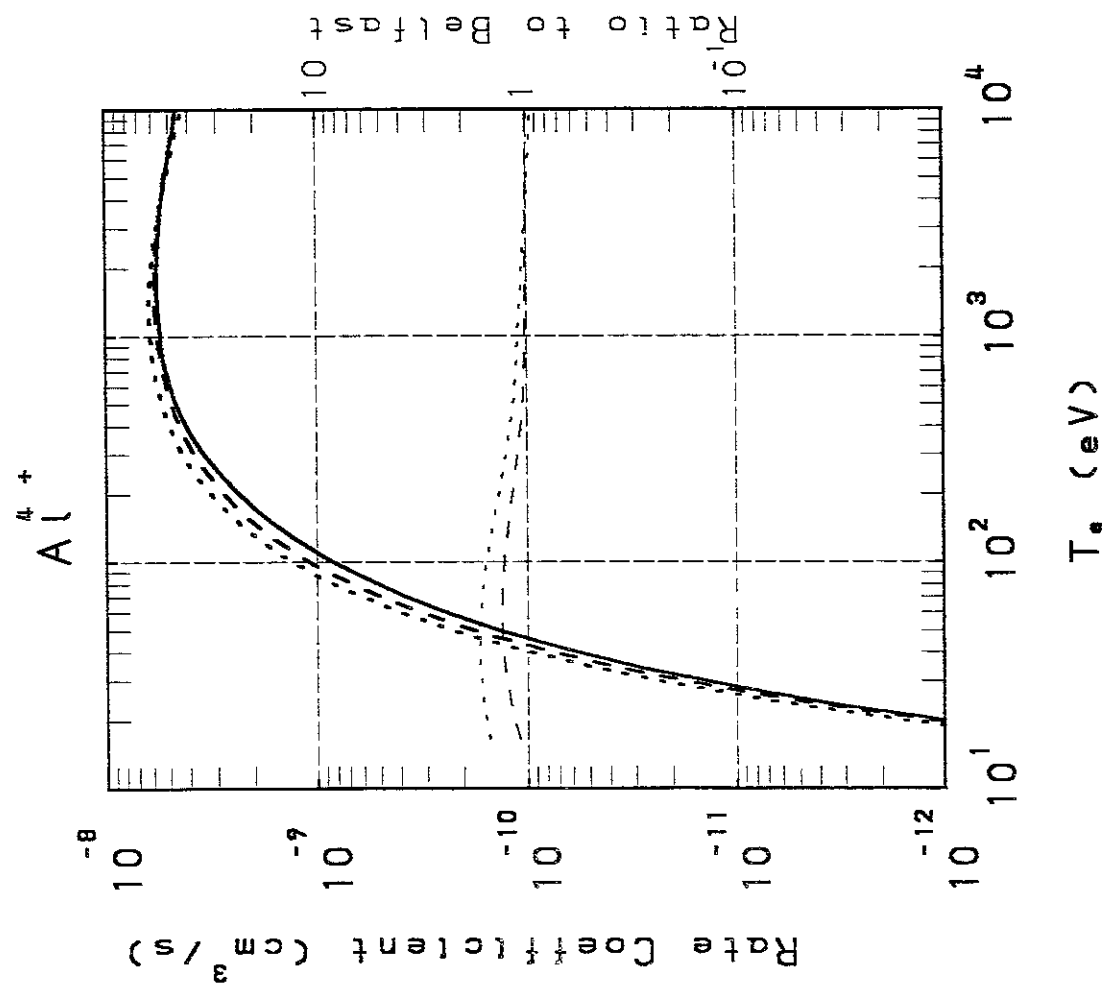
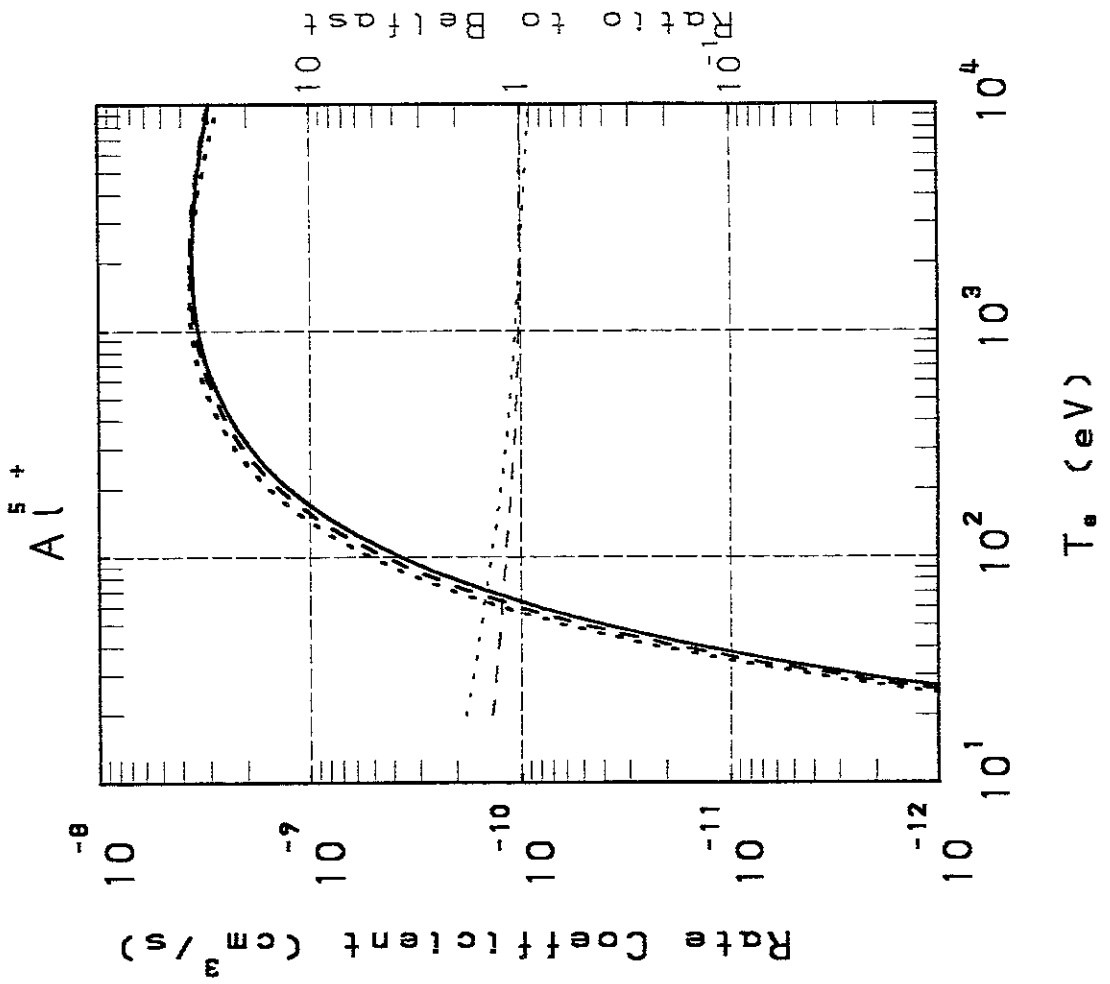
Al^{3+}

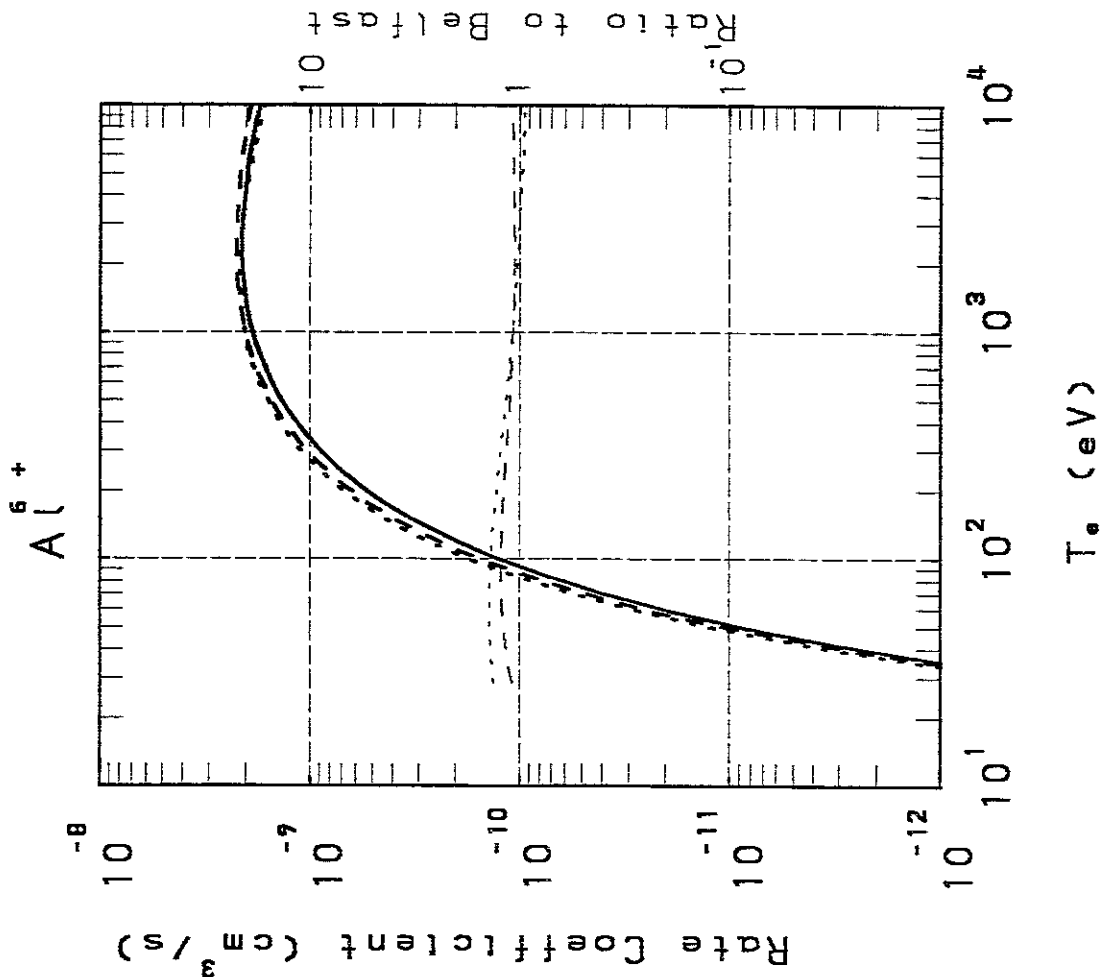
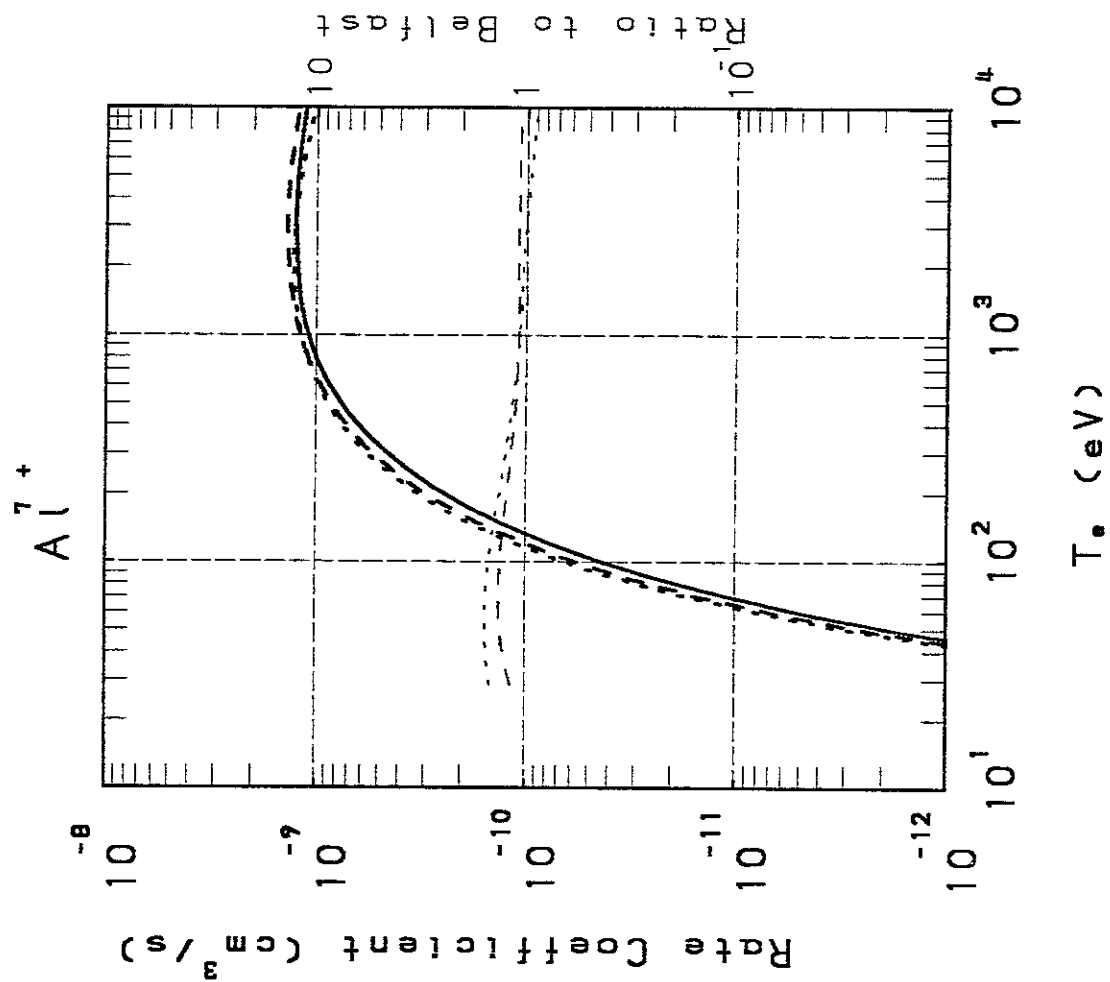
Al^{2+}

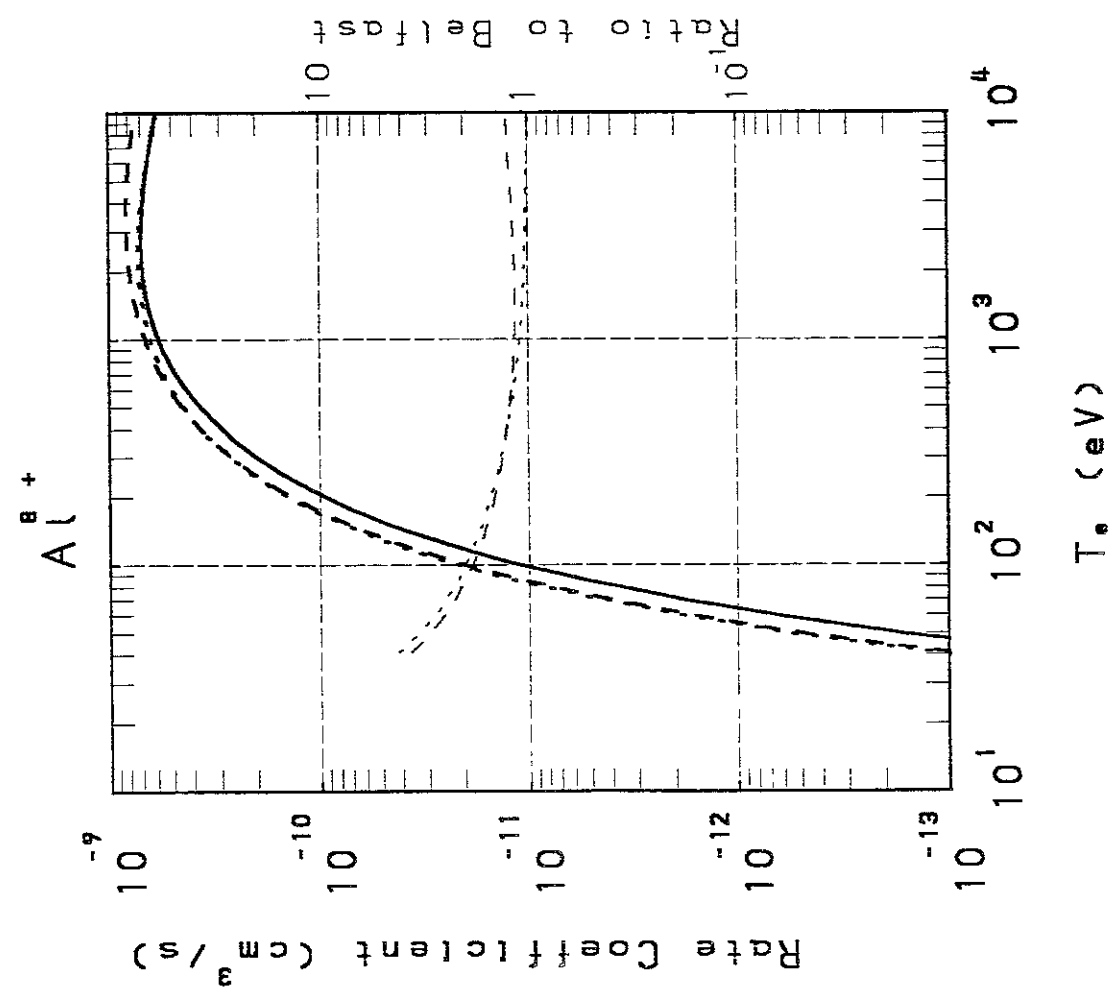
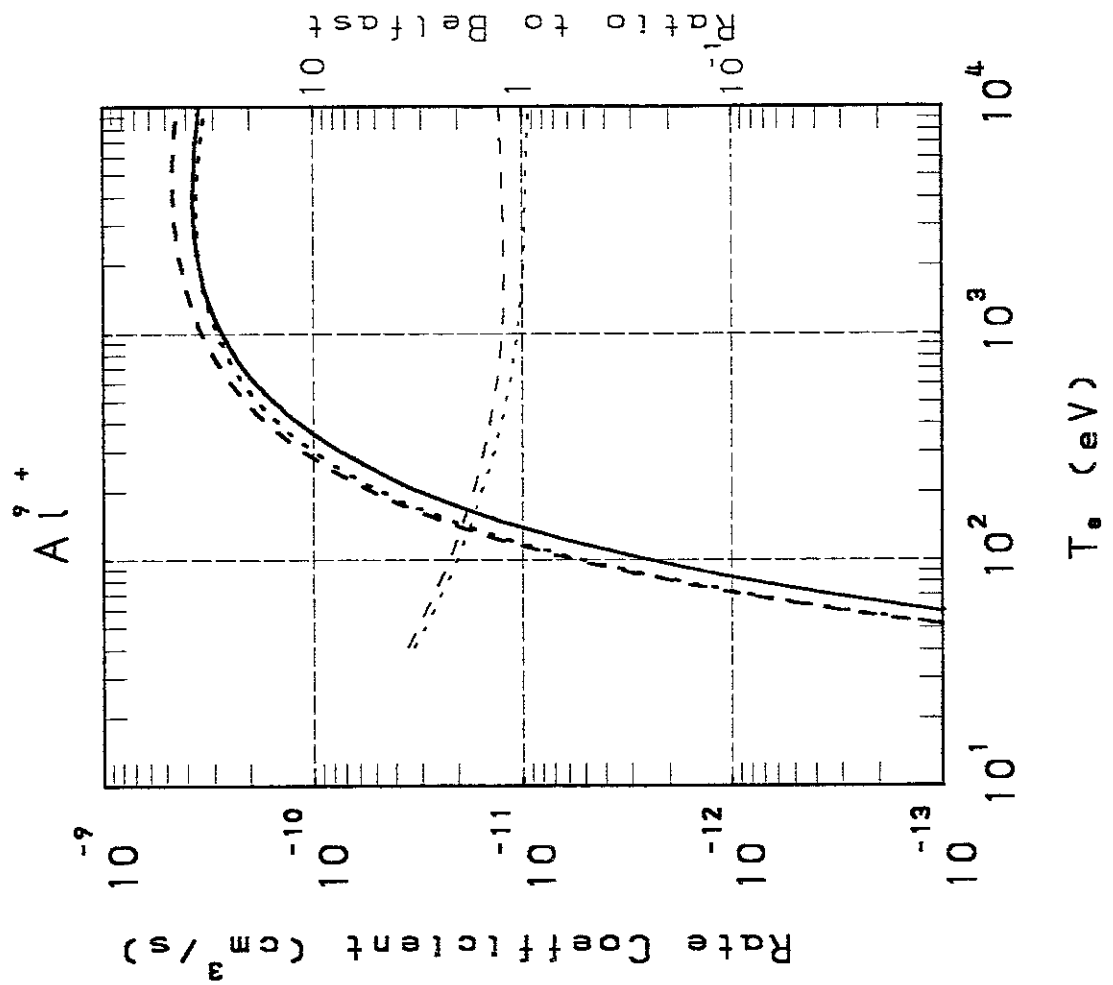


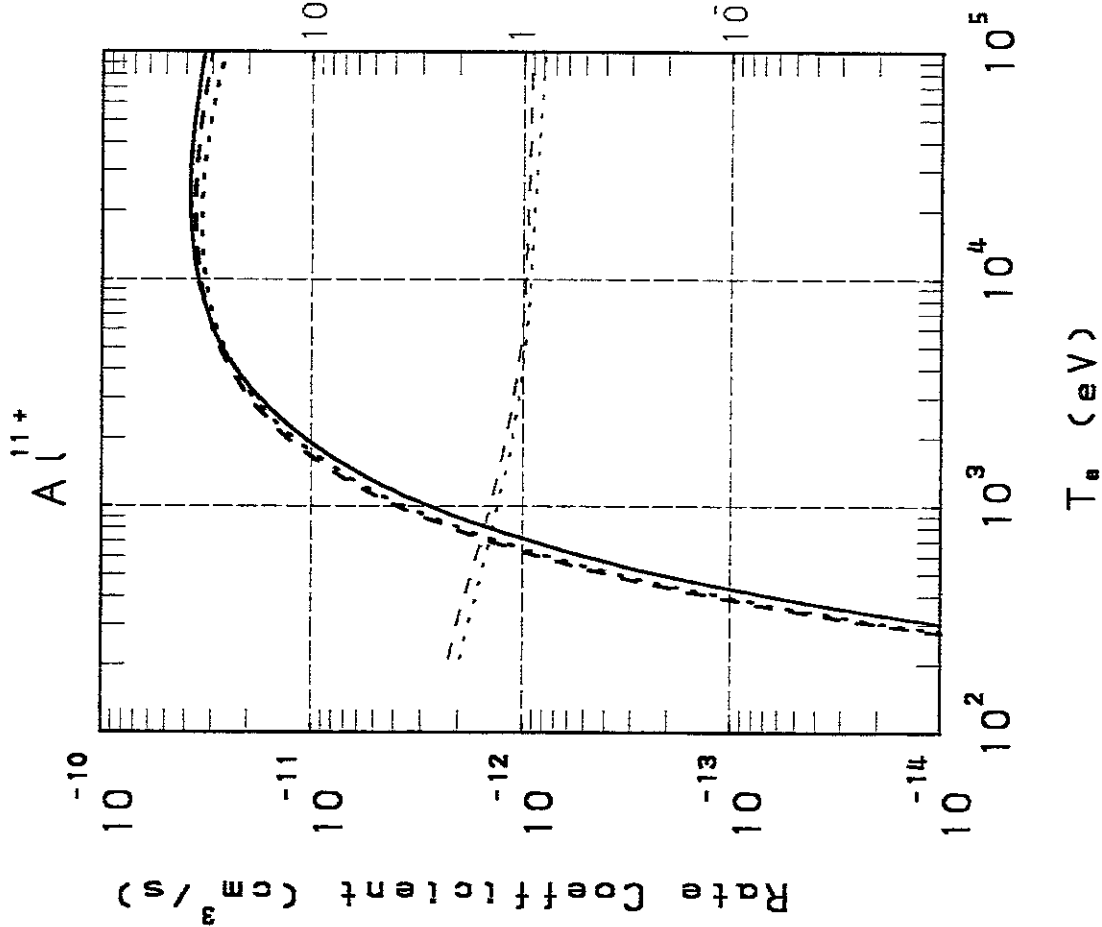
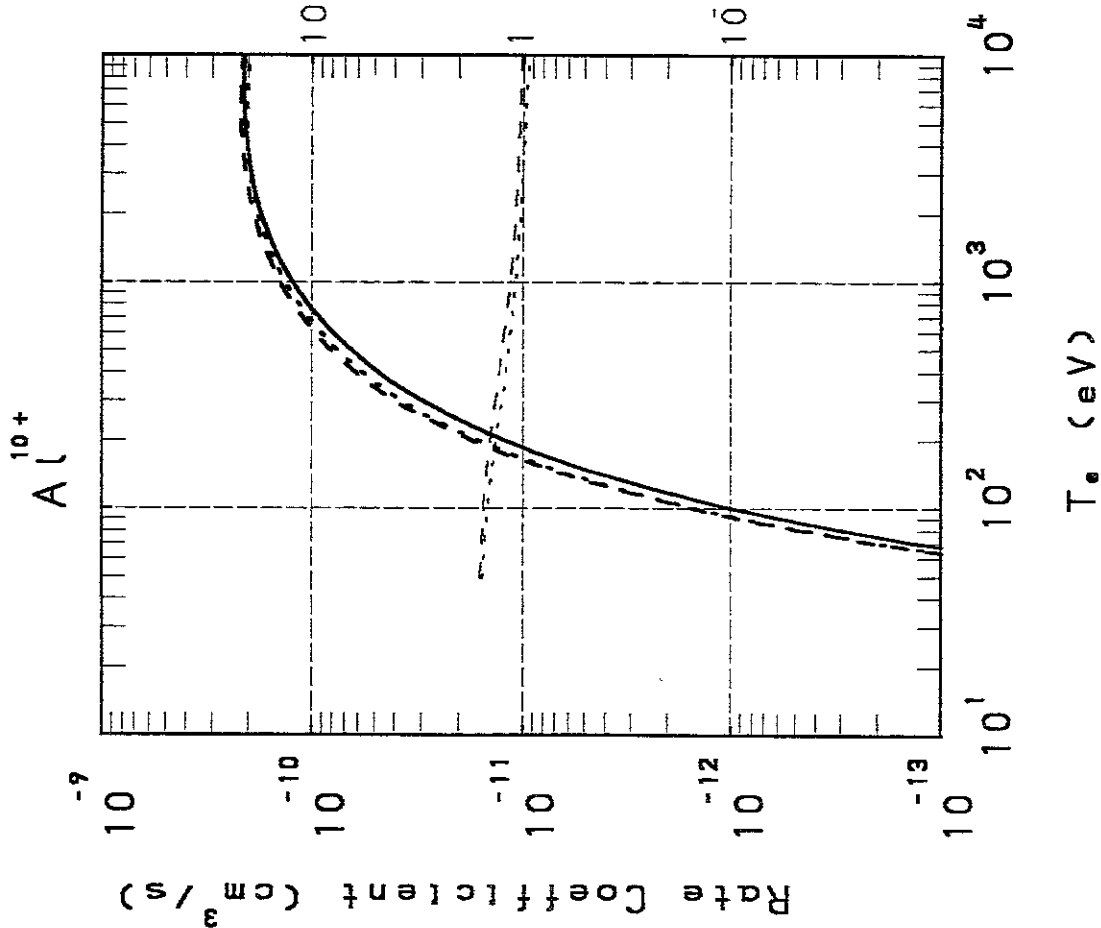
T_e (eV)

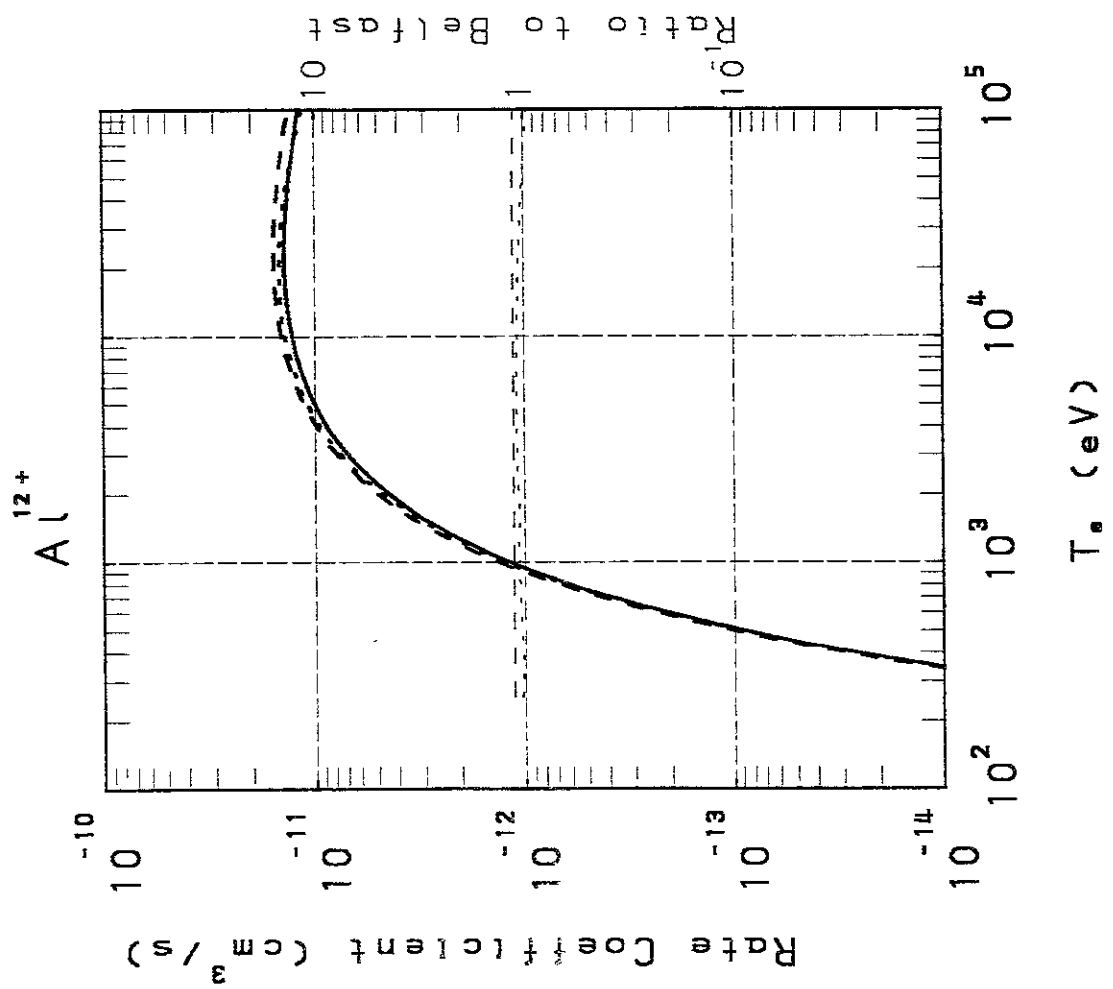
T_e (eV)

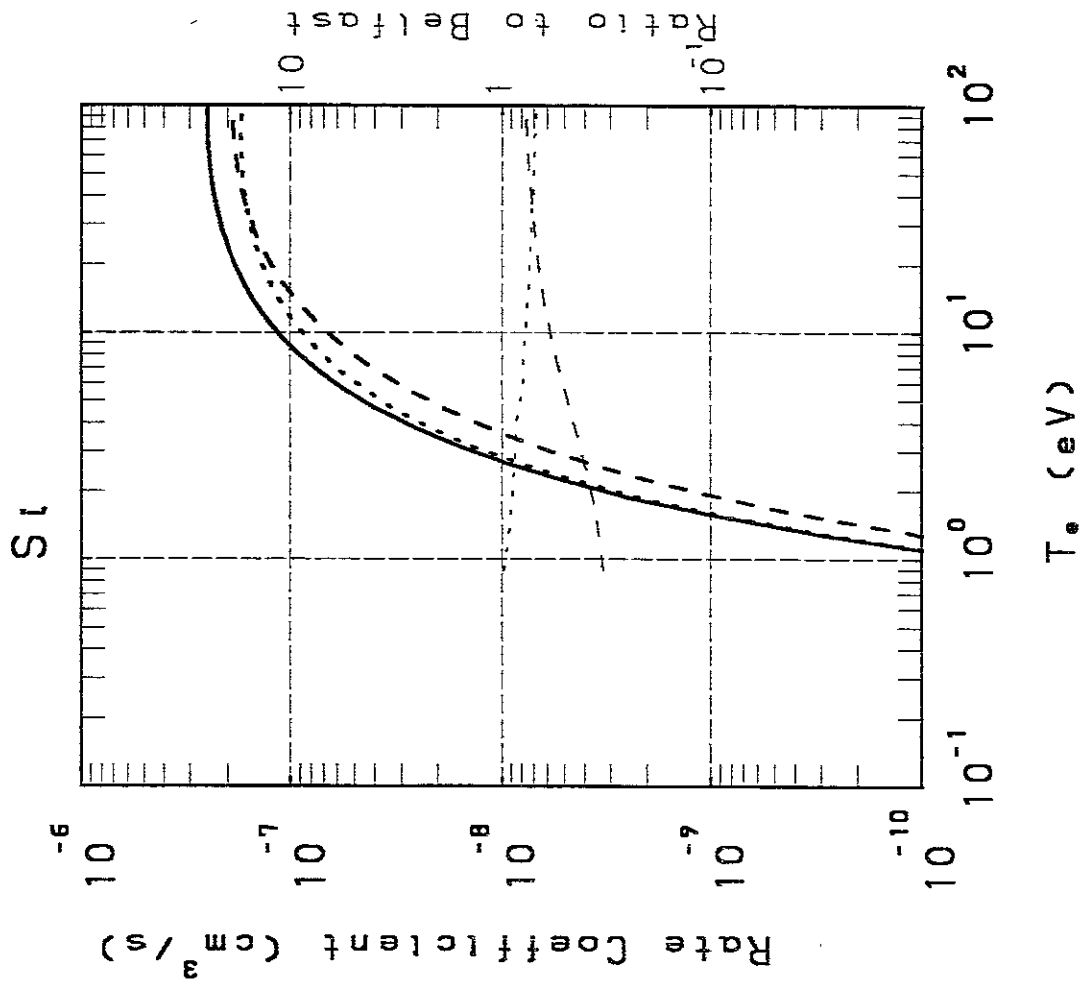
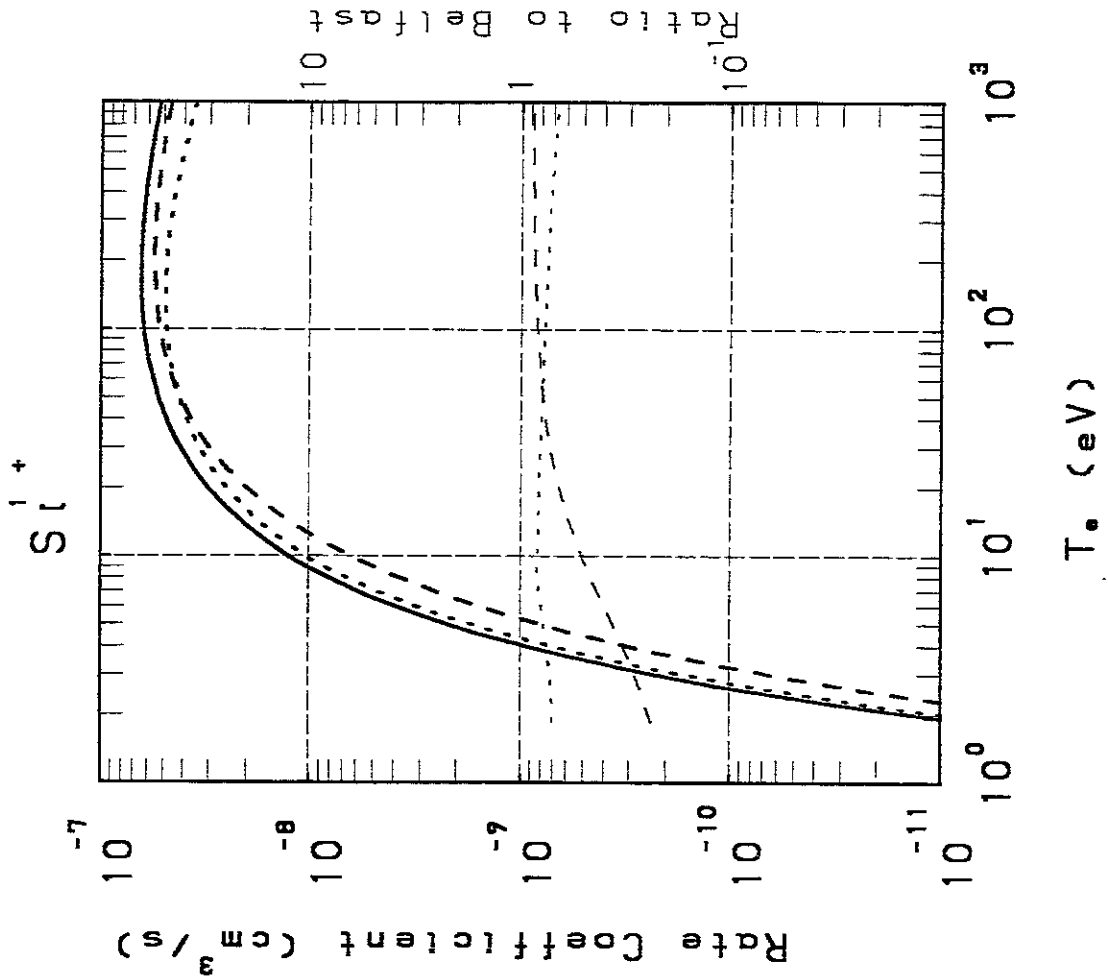


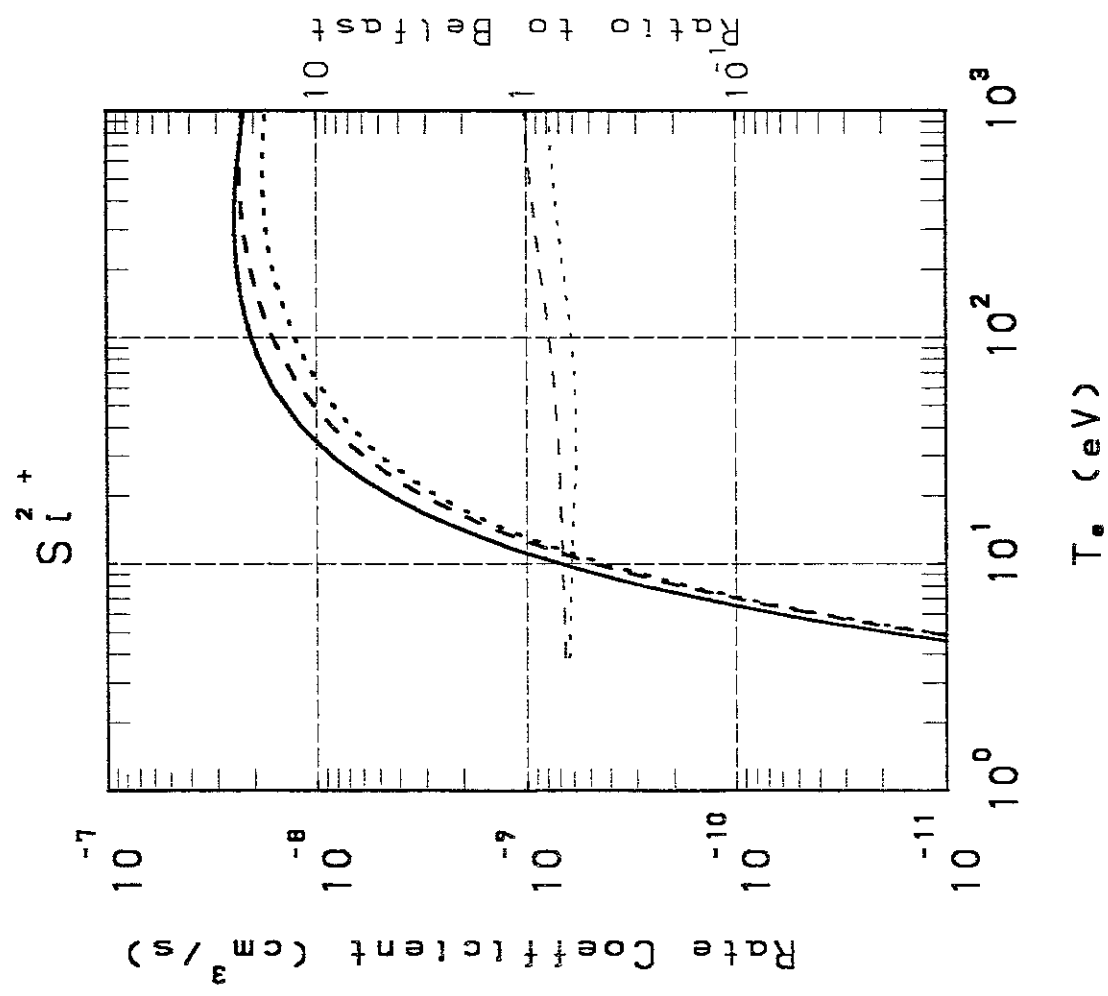
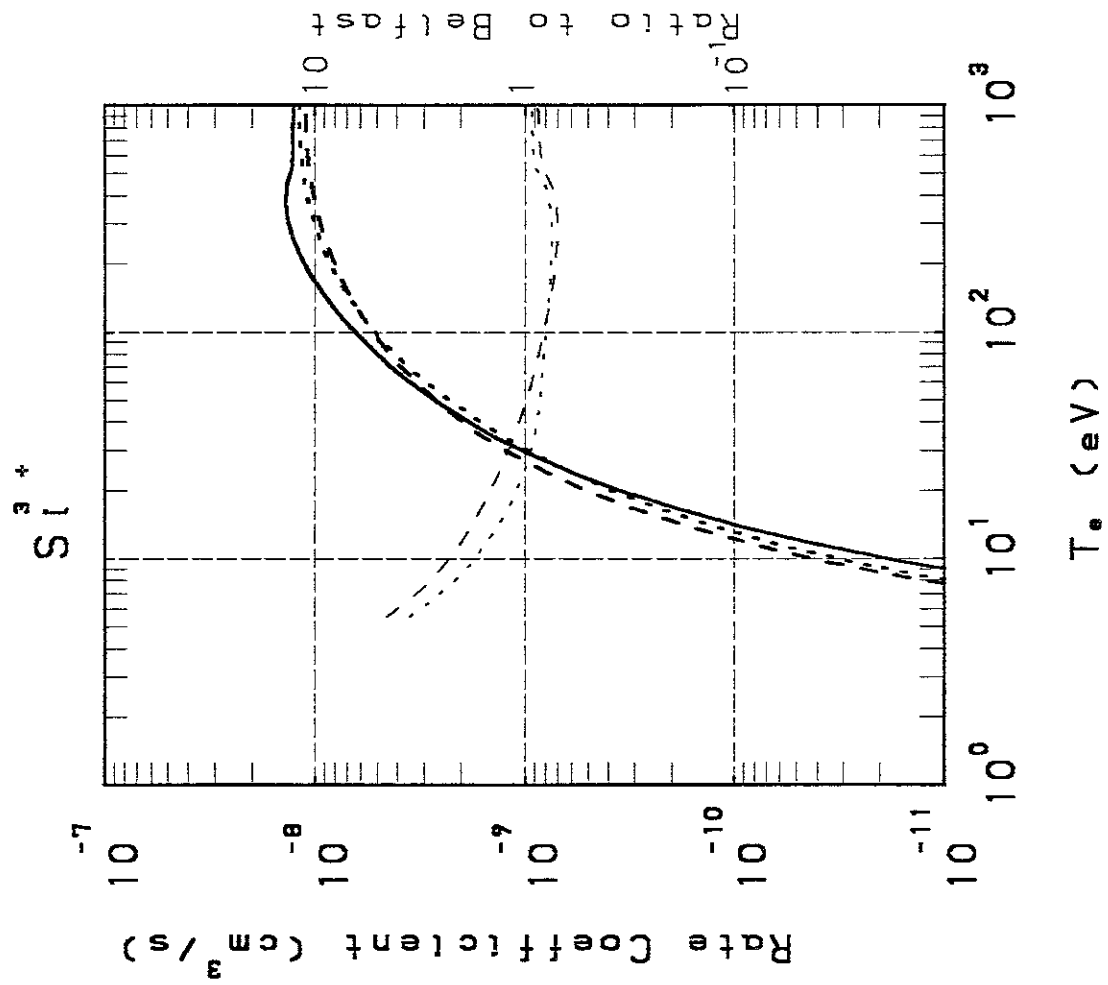


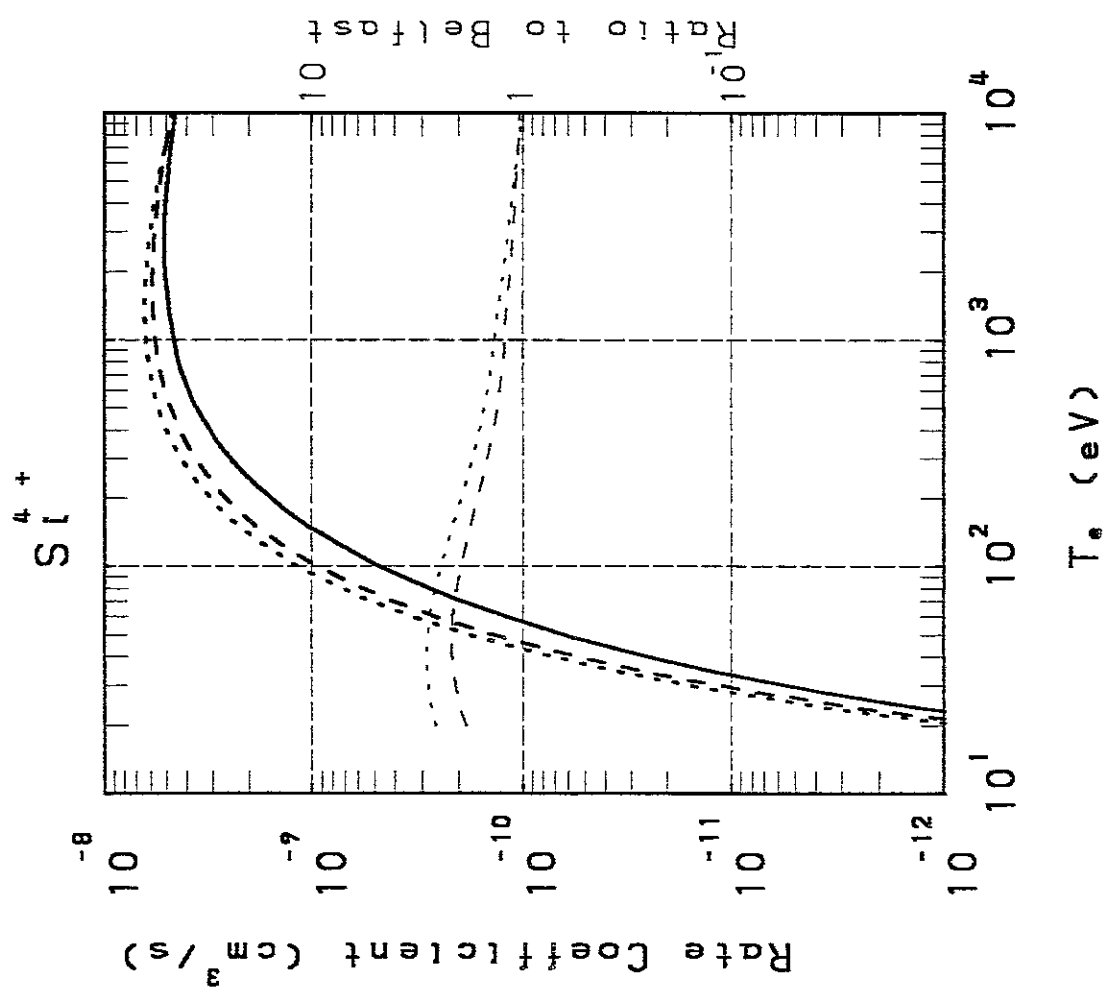
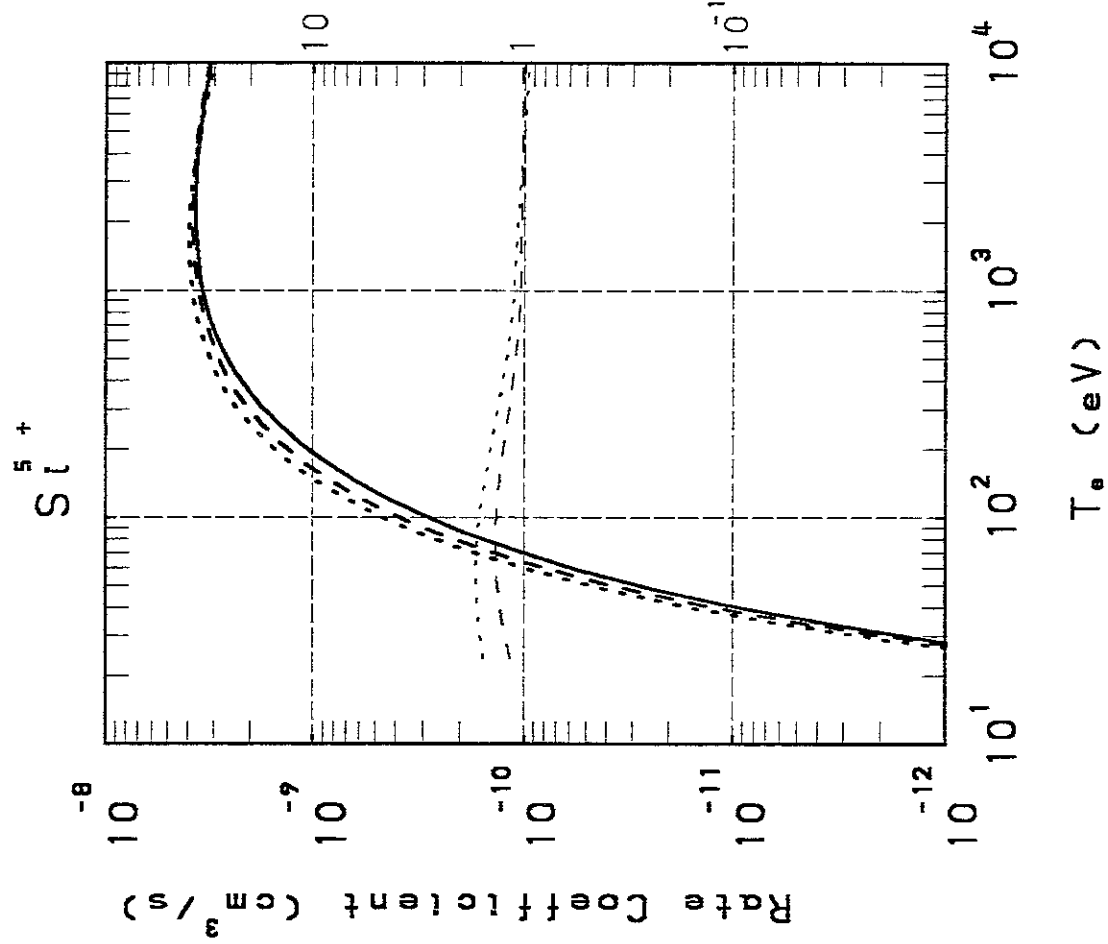


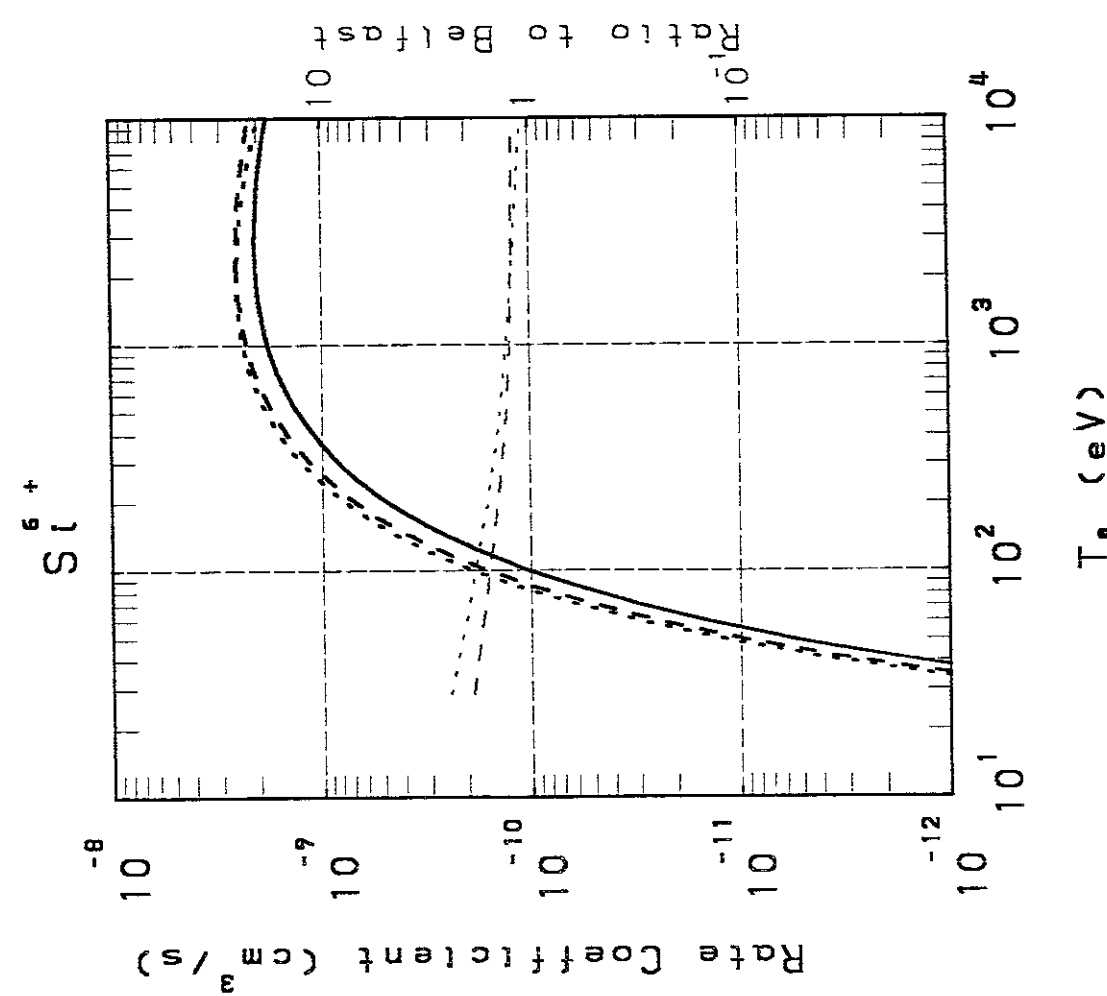
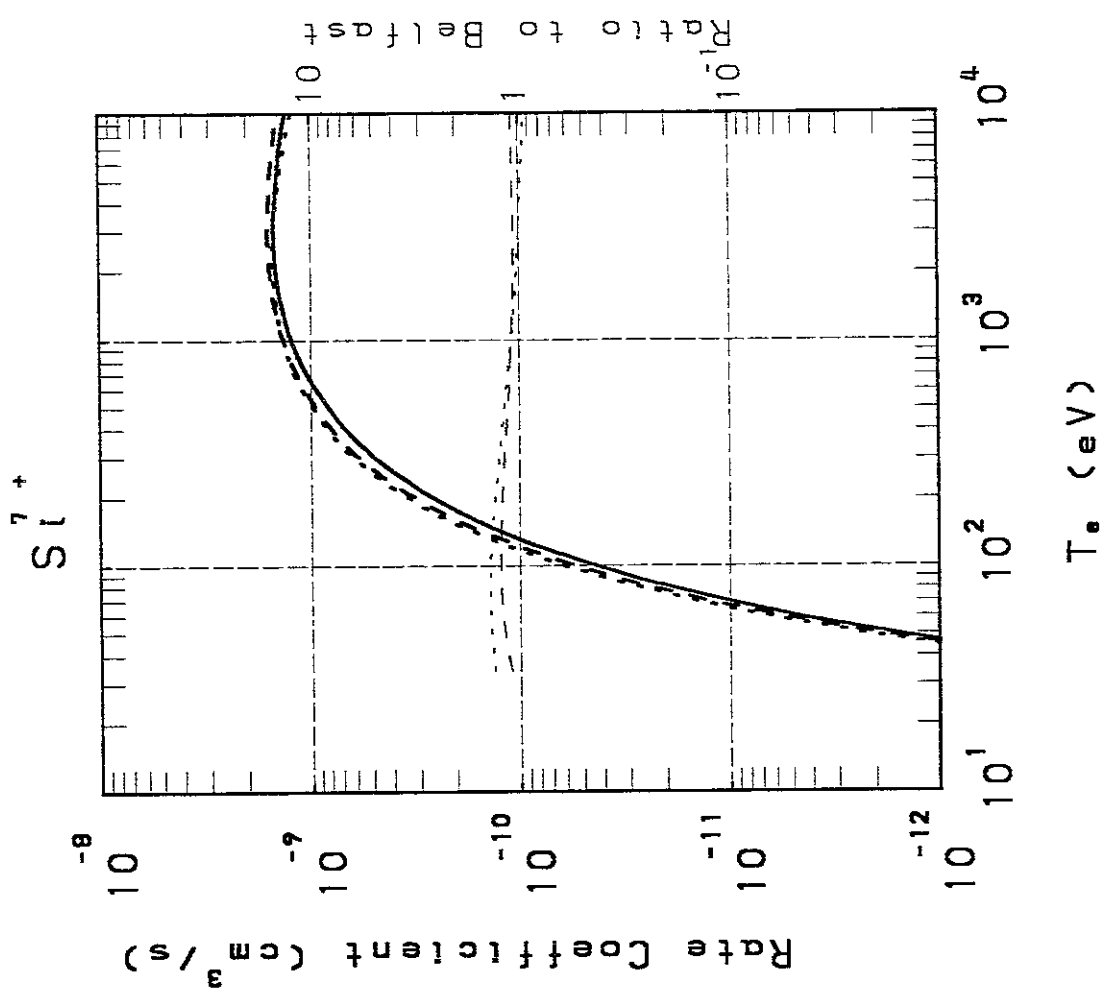


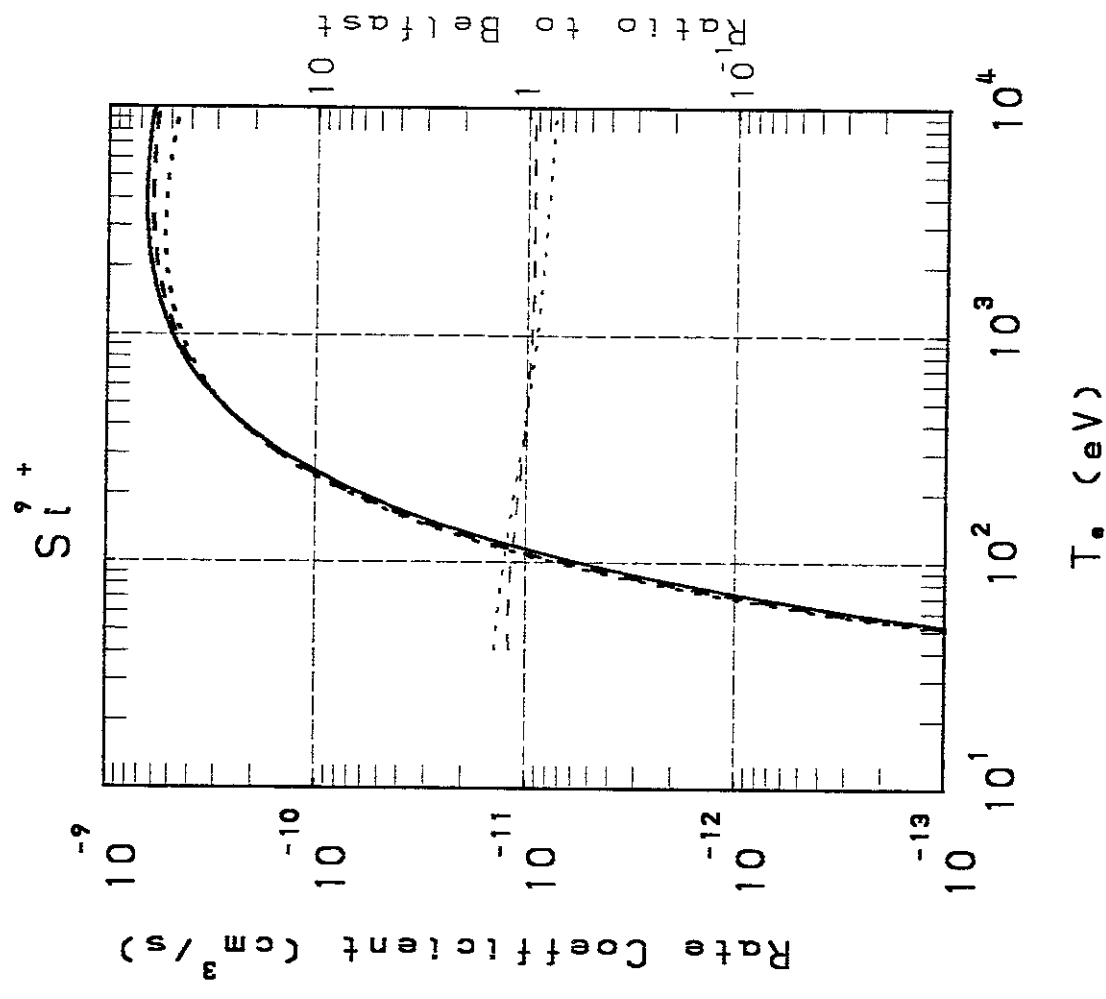
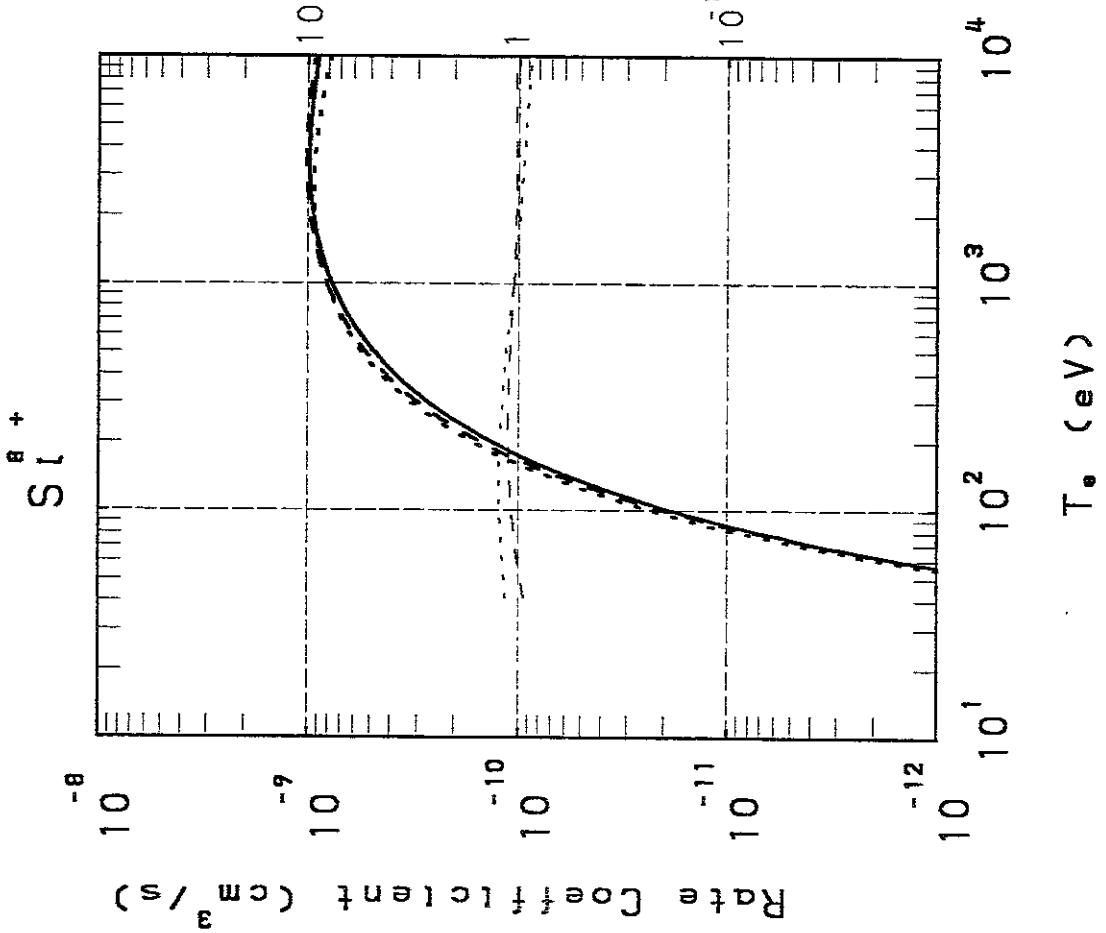


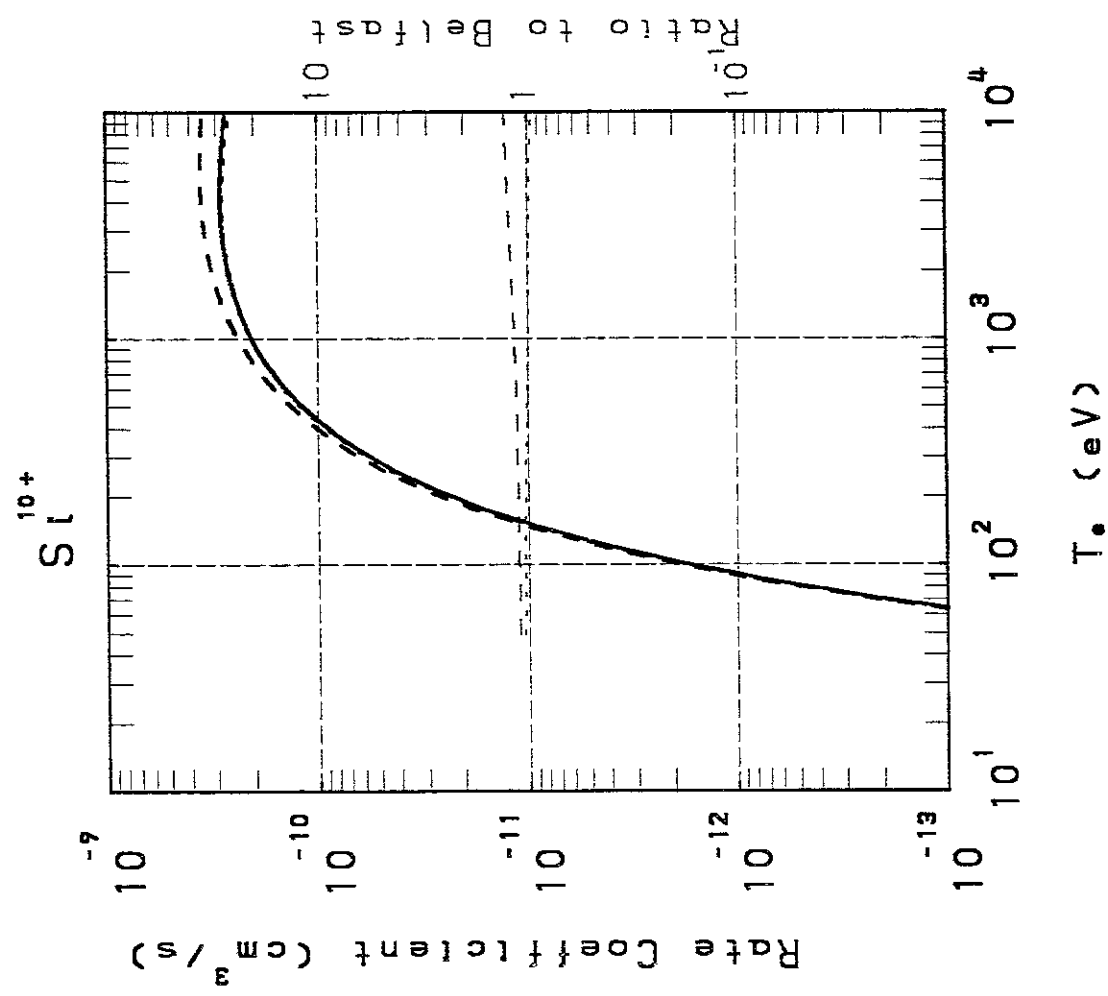
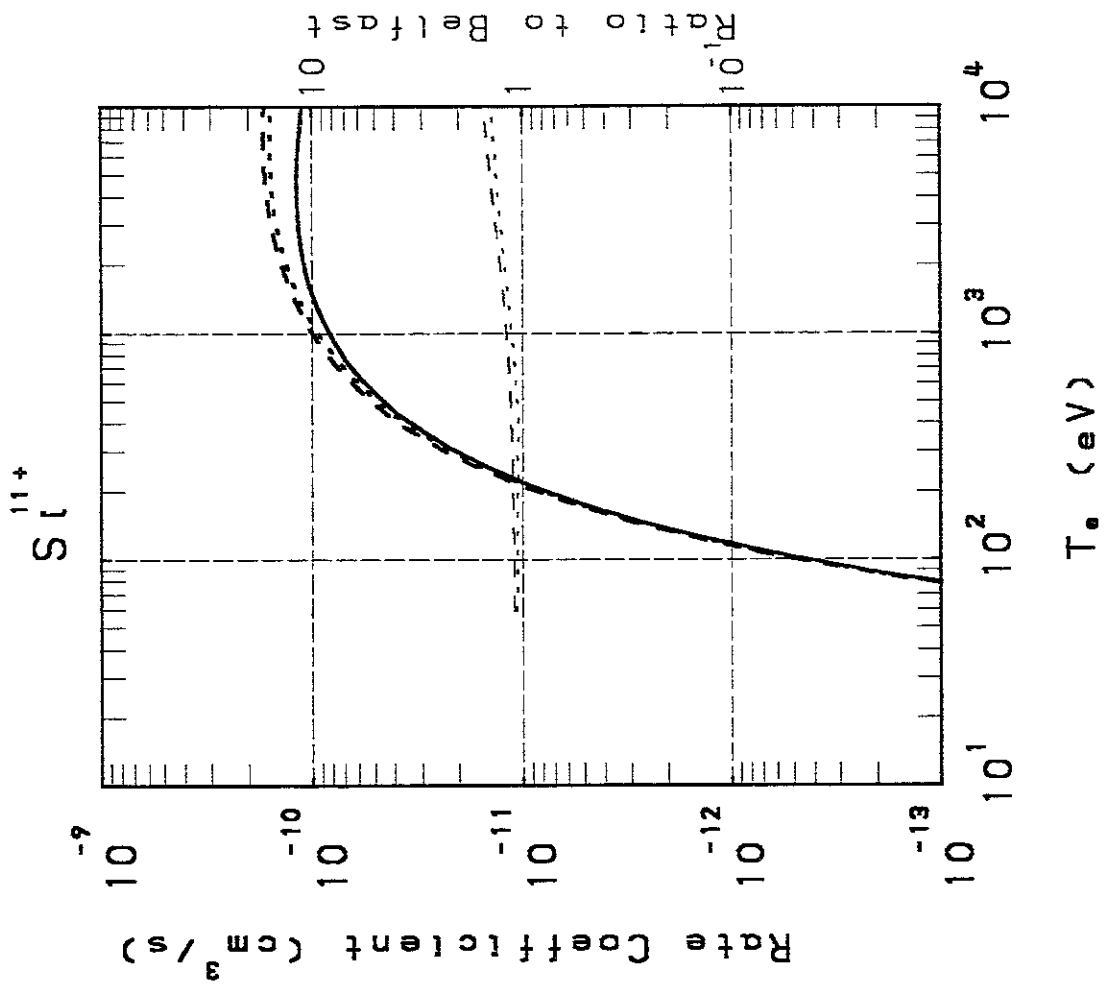


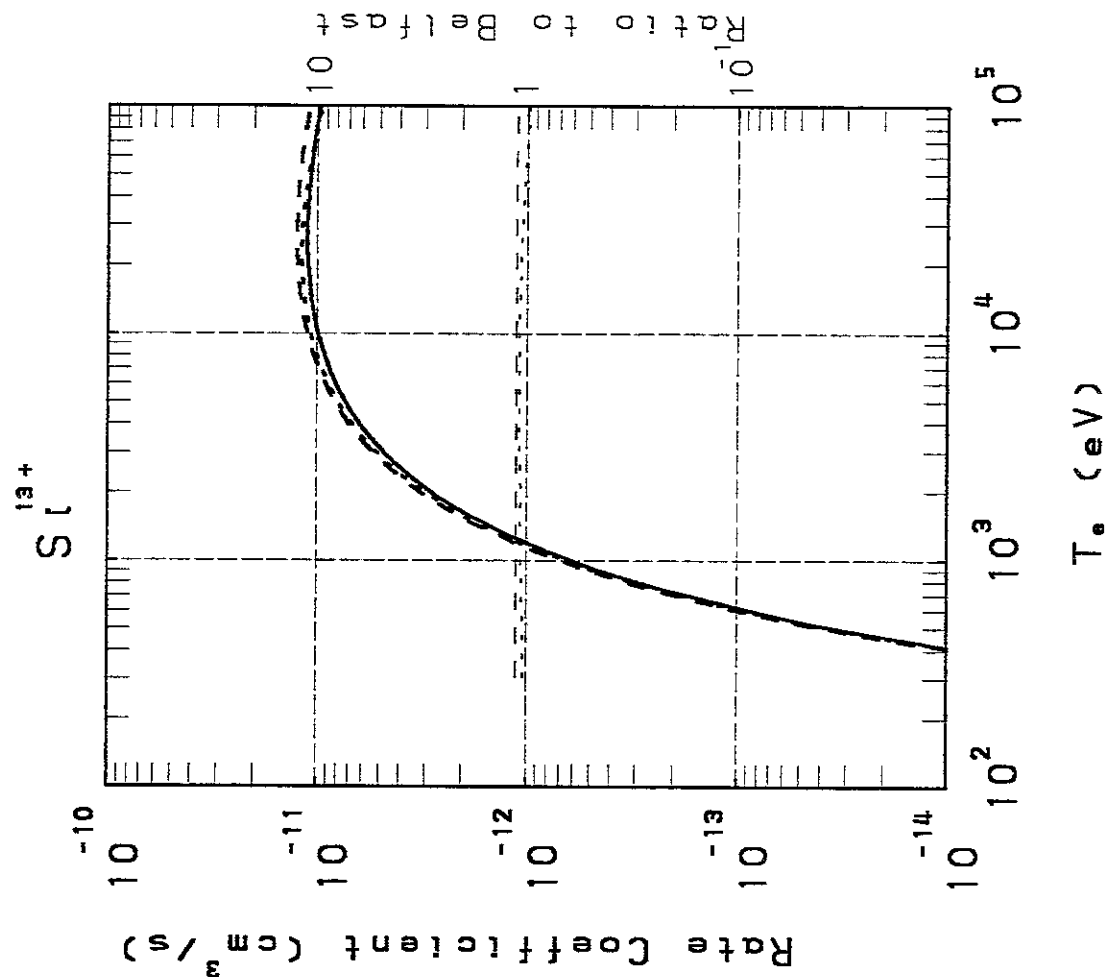
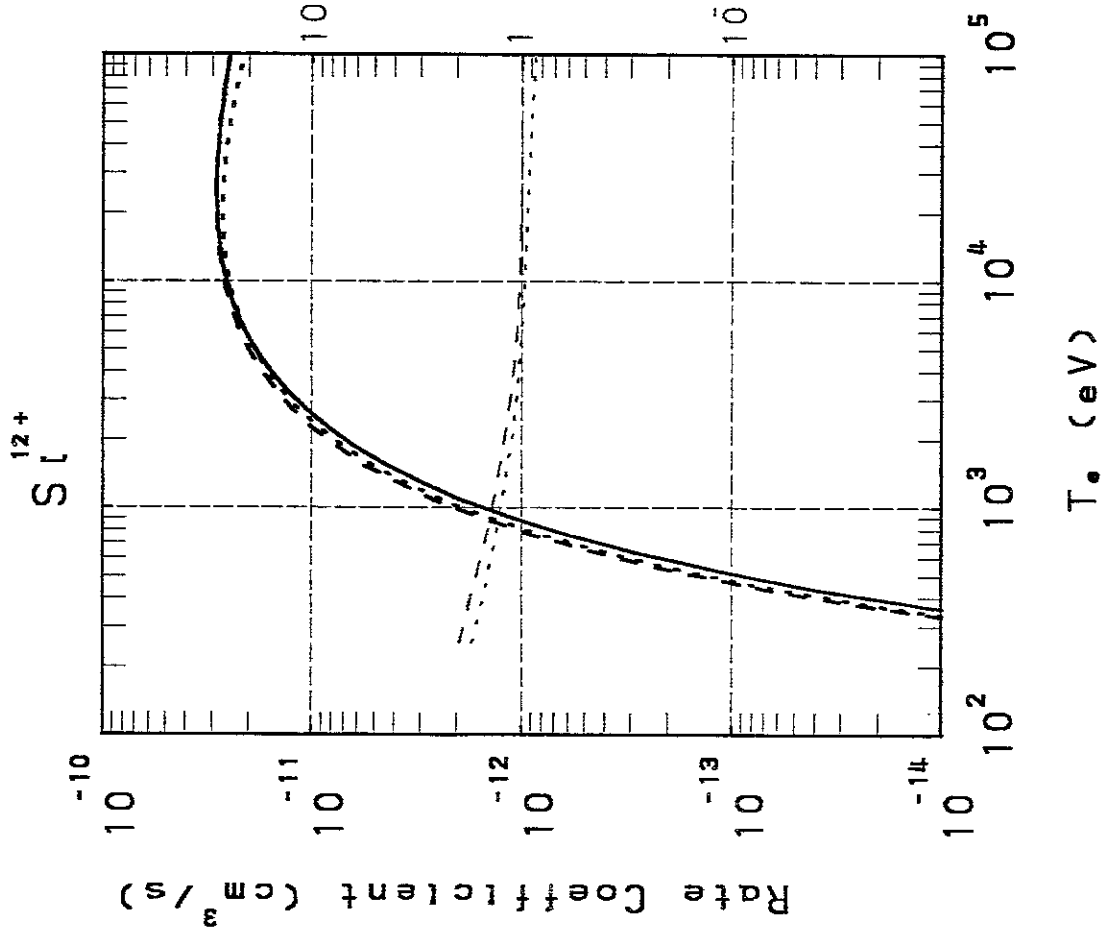


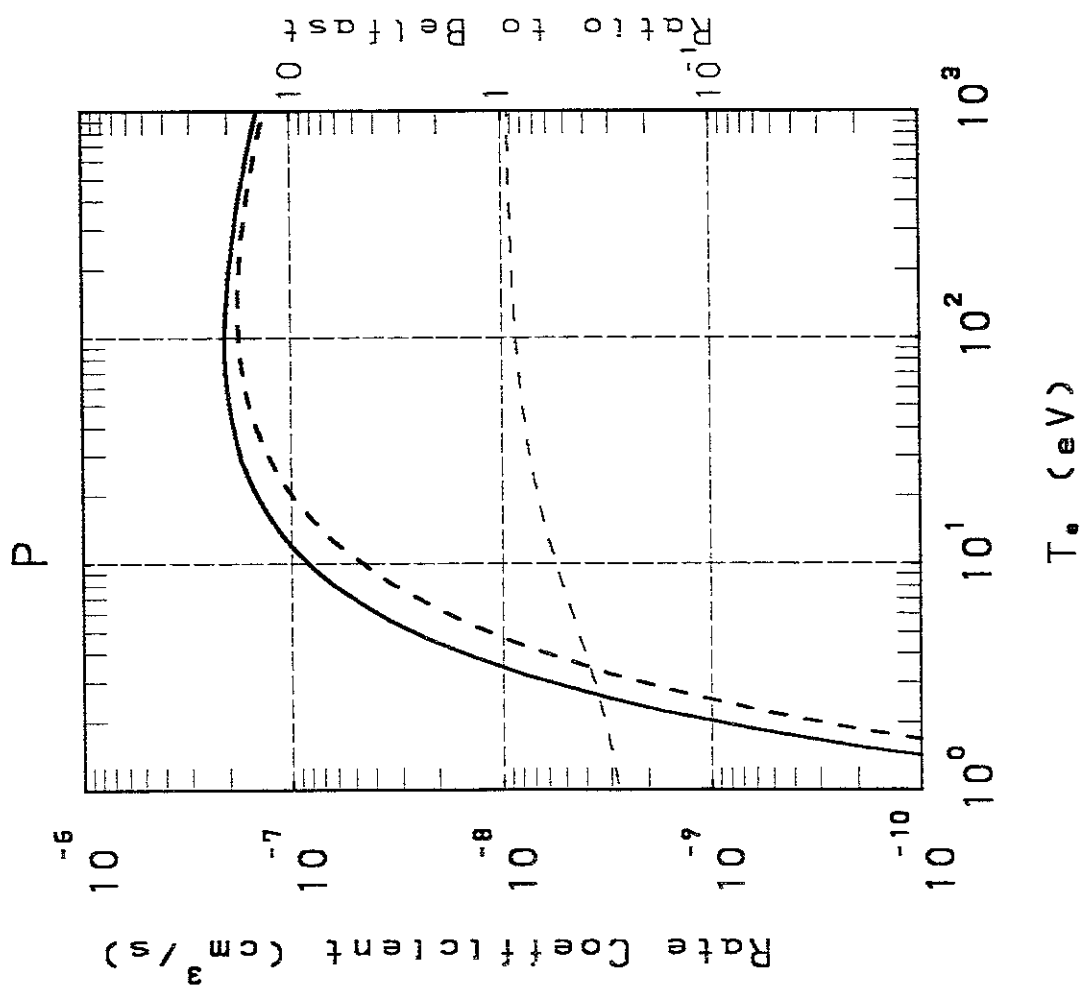
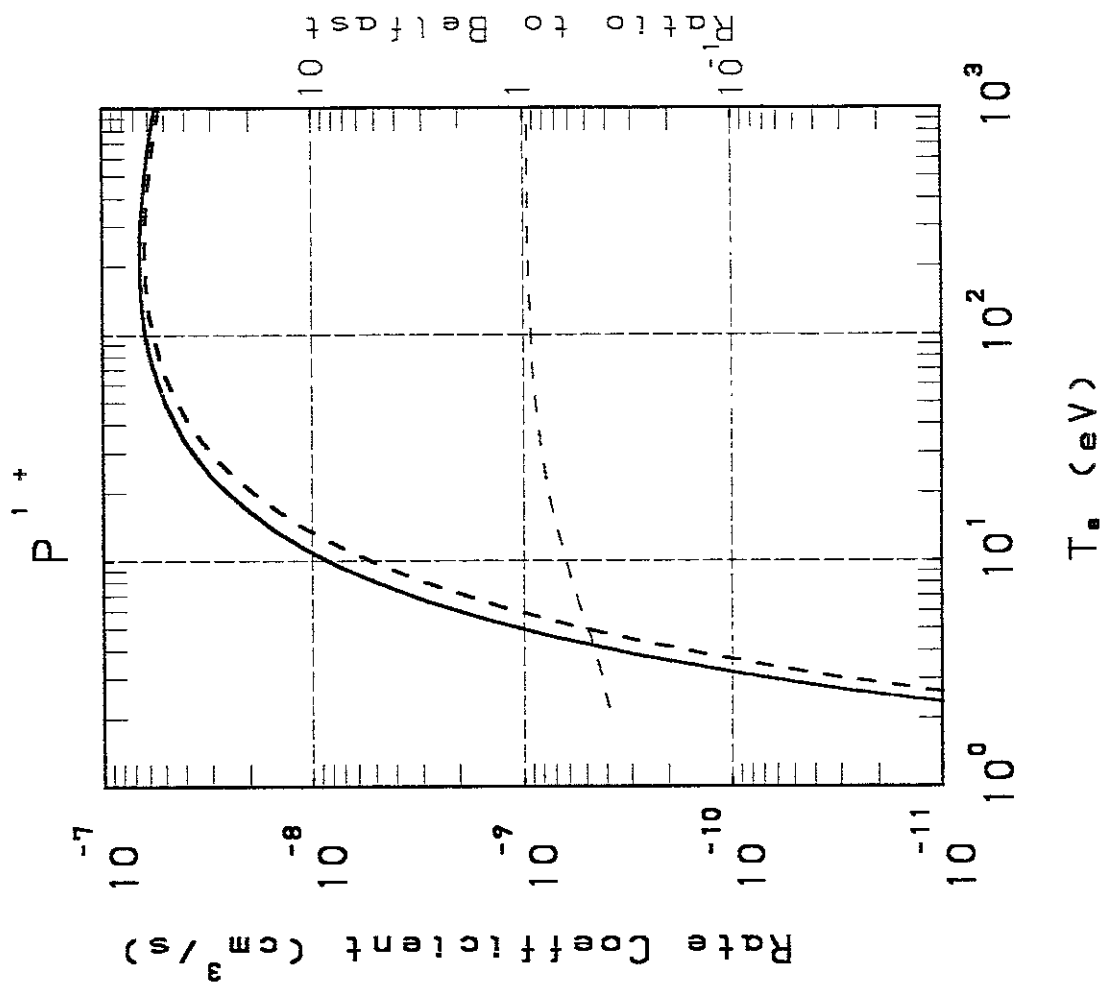


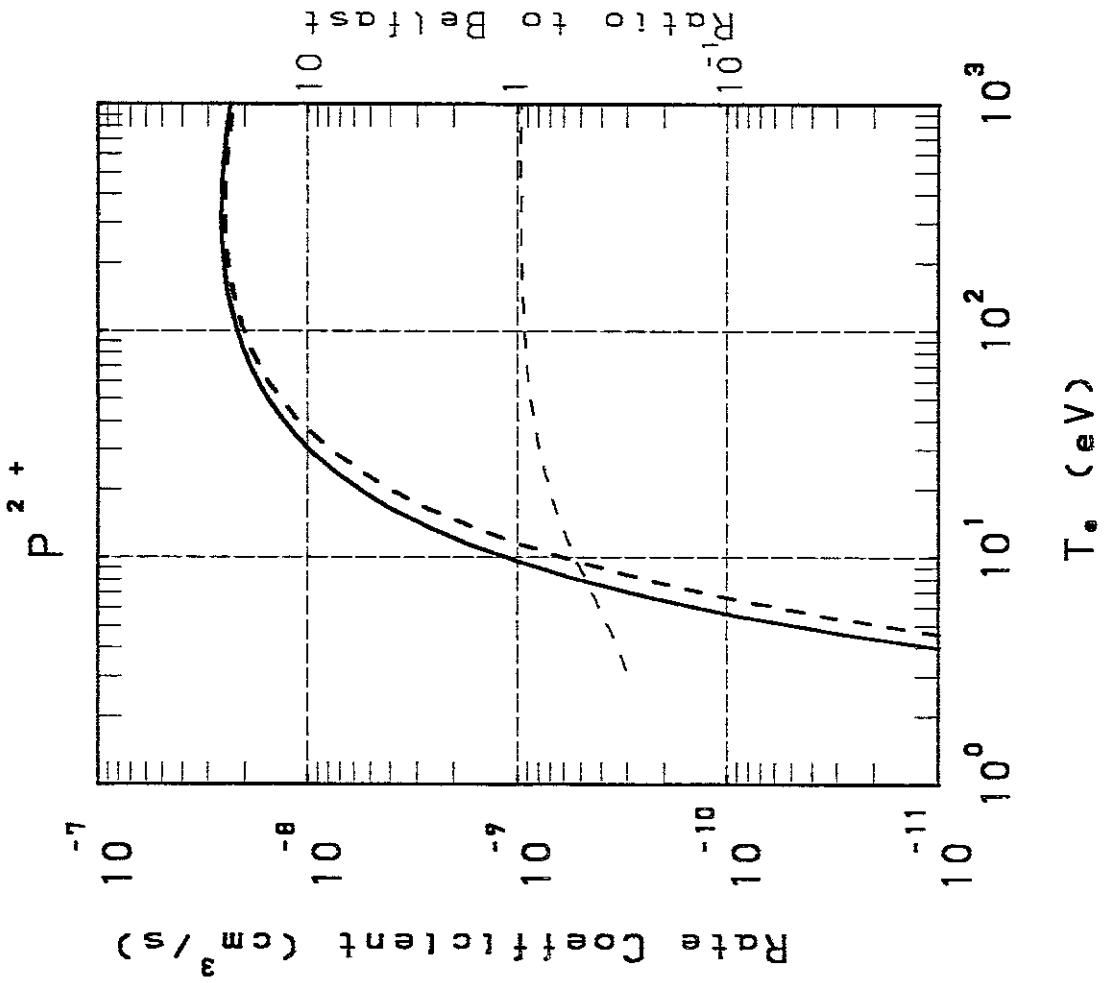
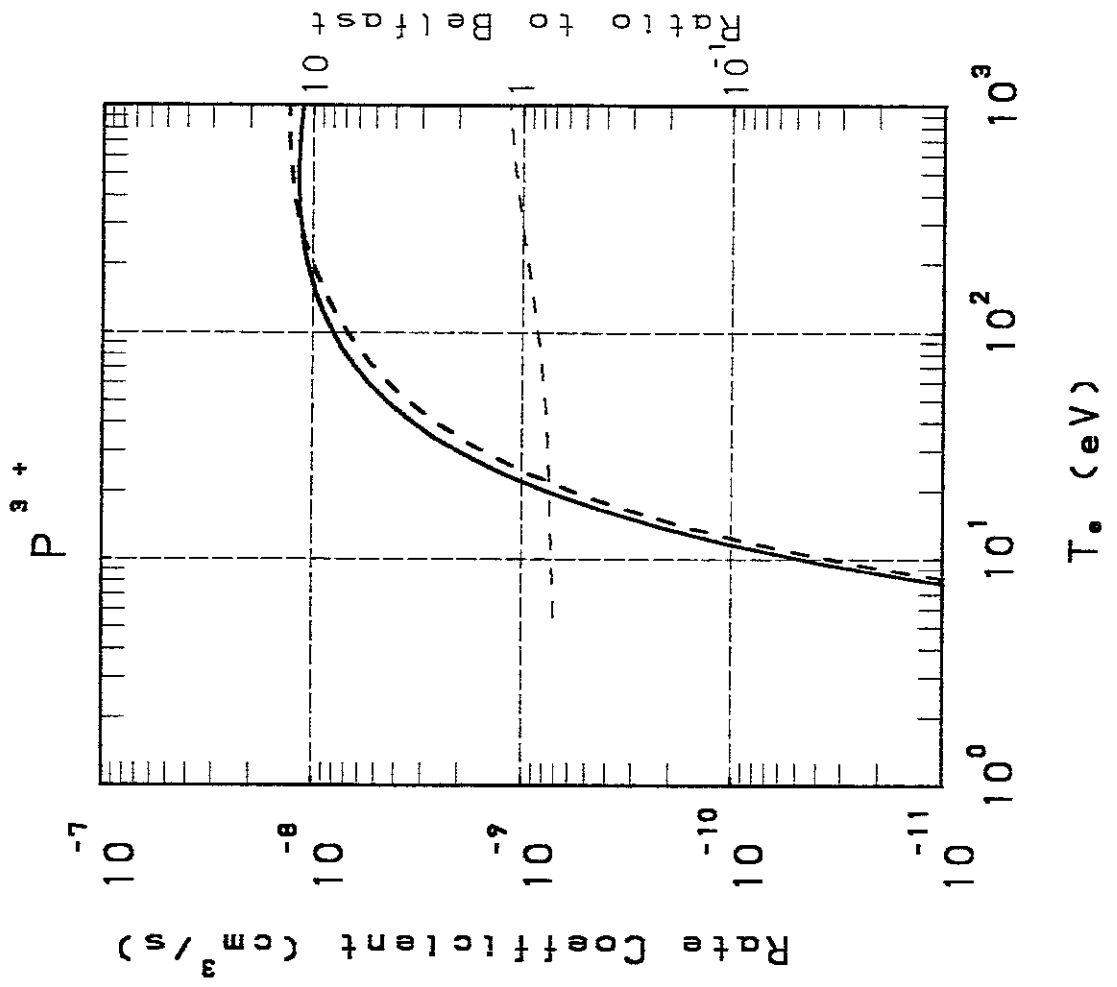


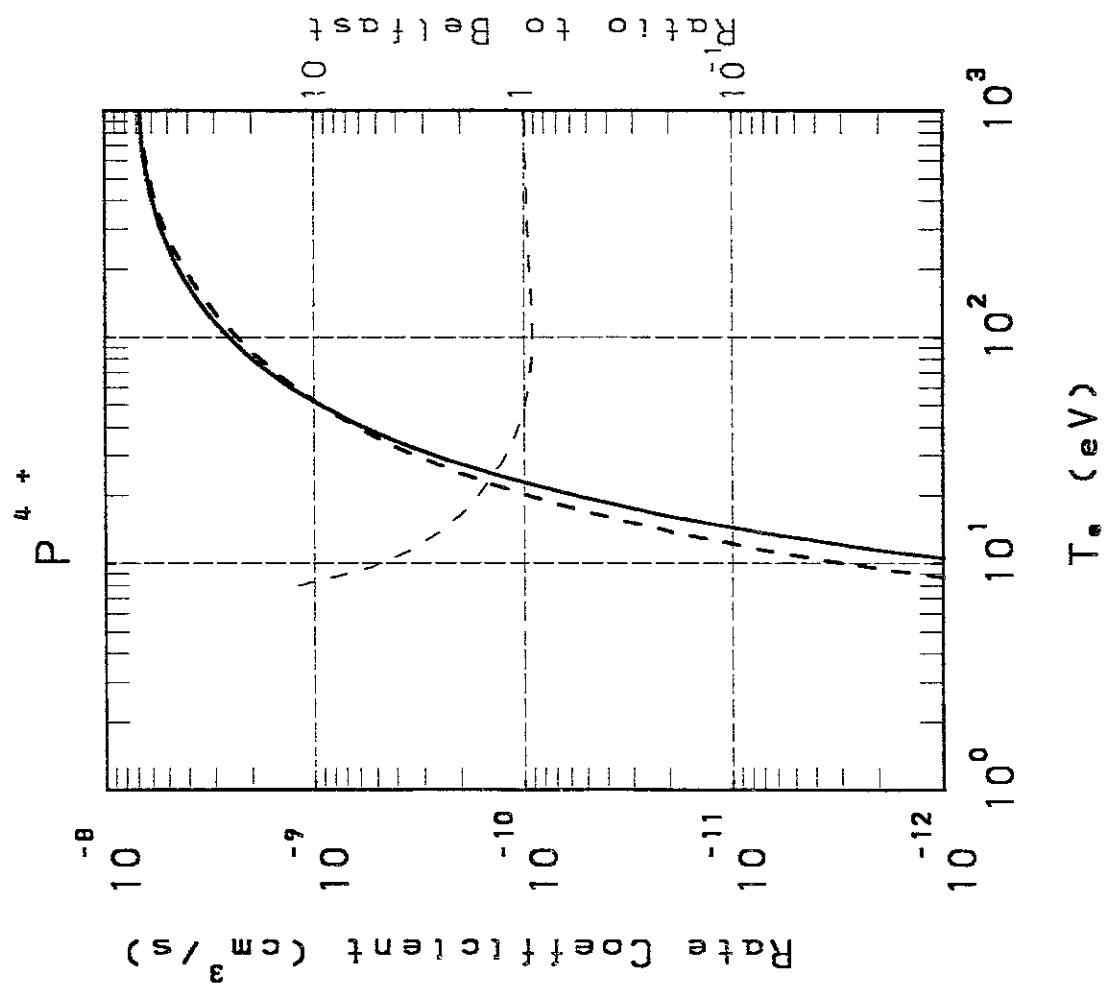
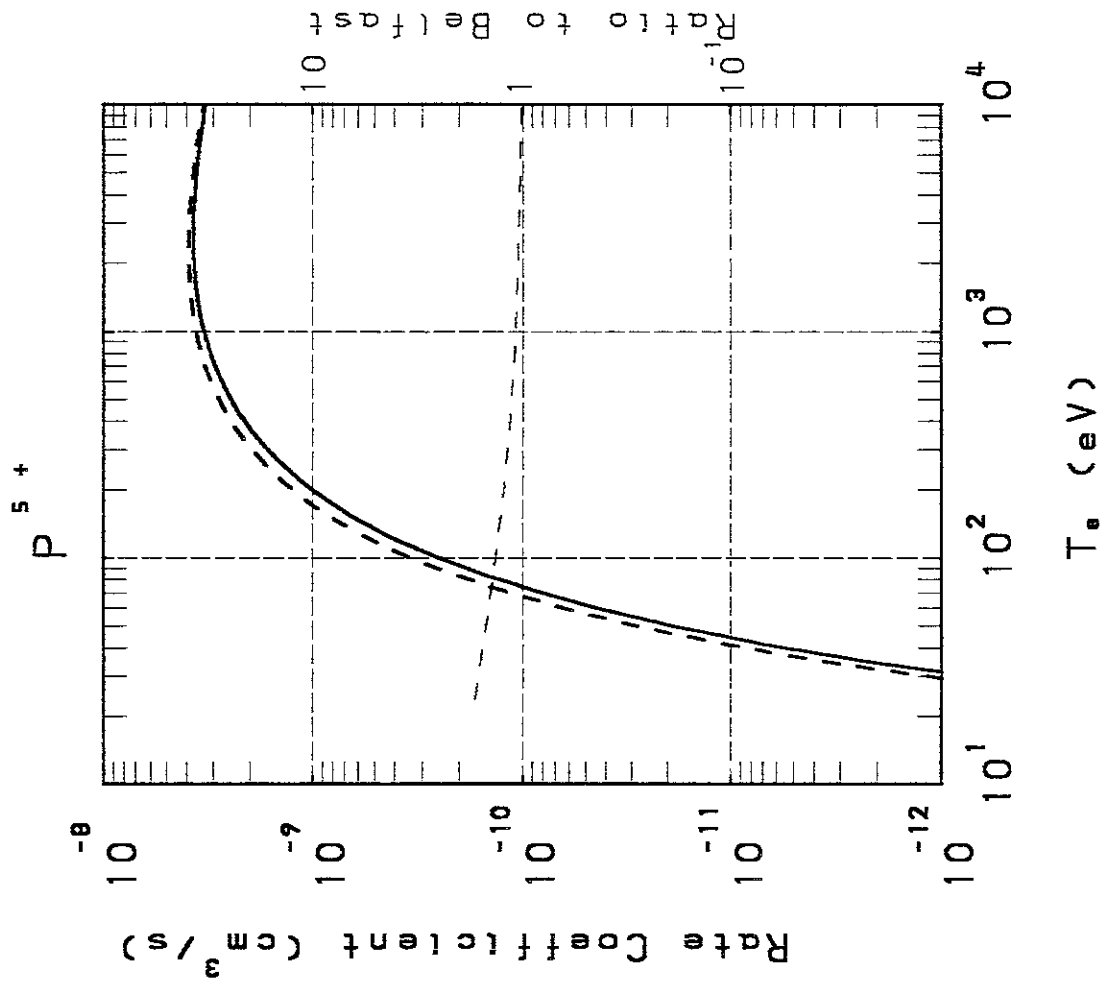


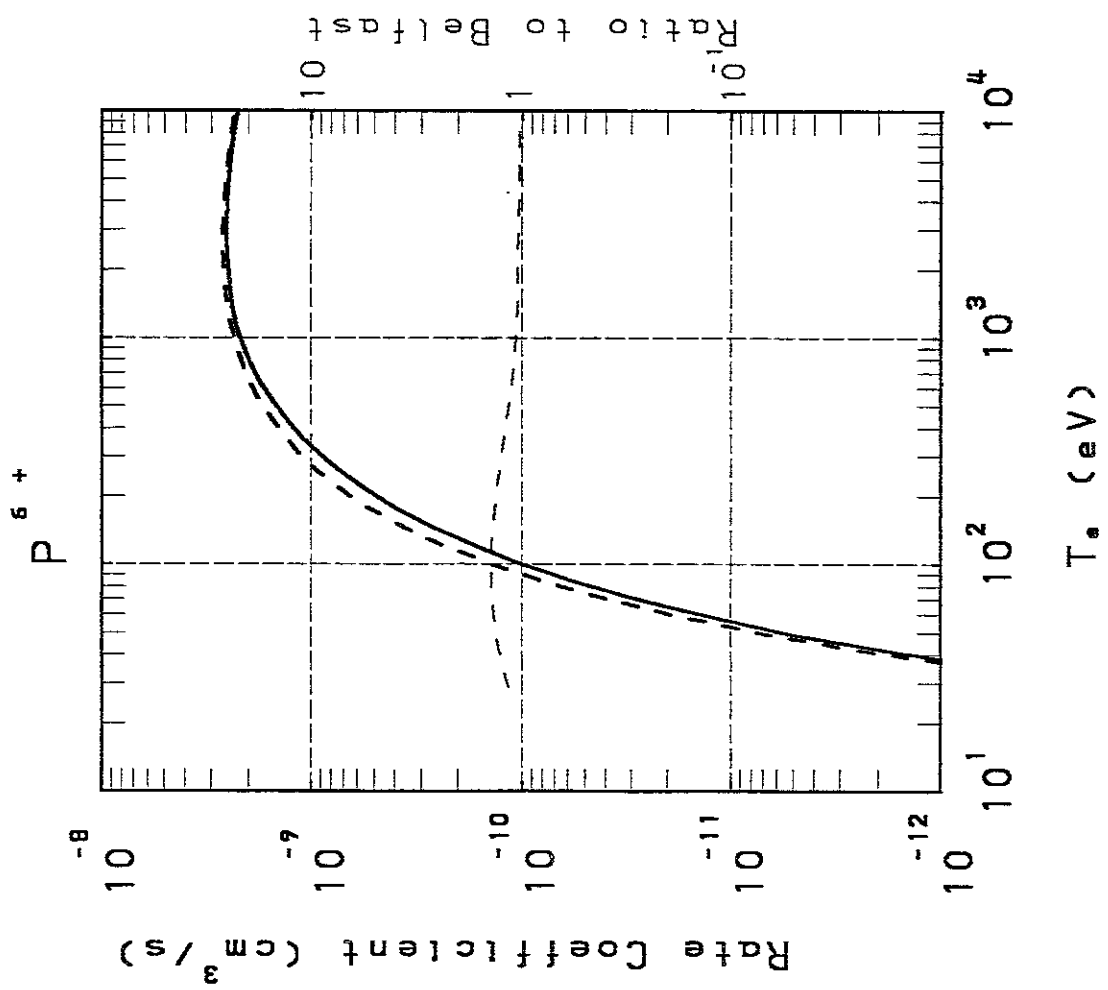
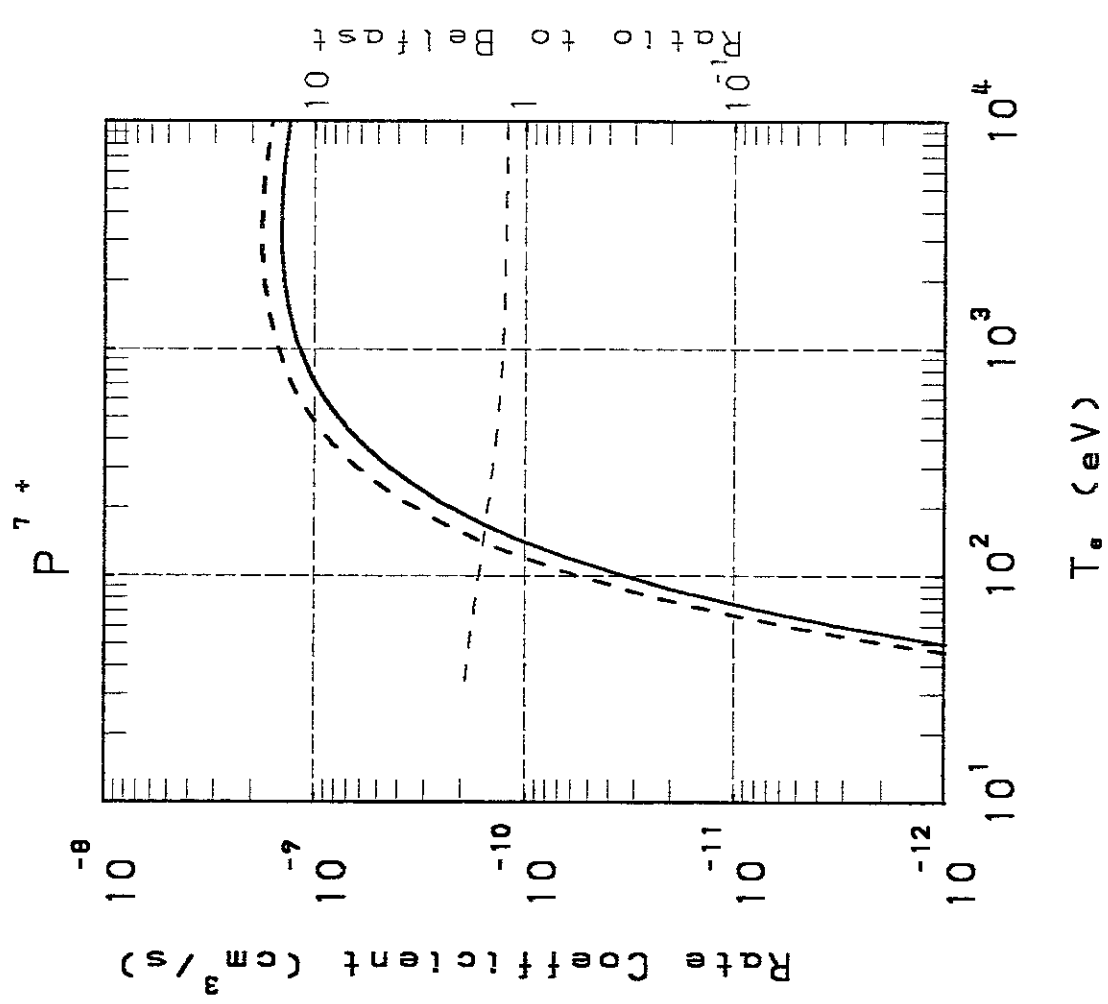


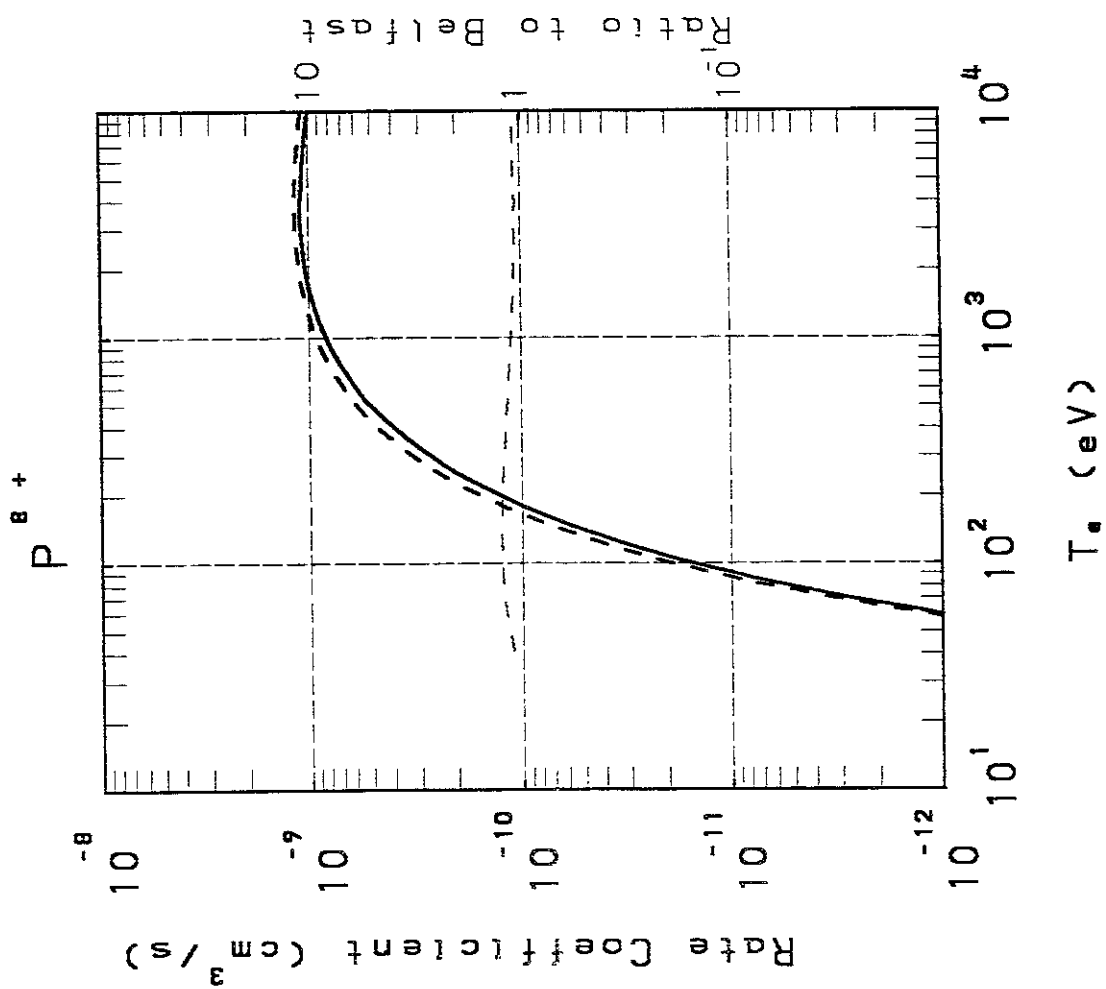
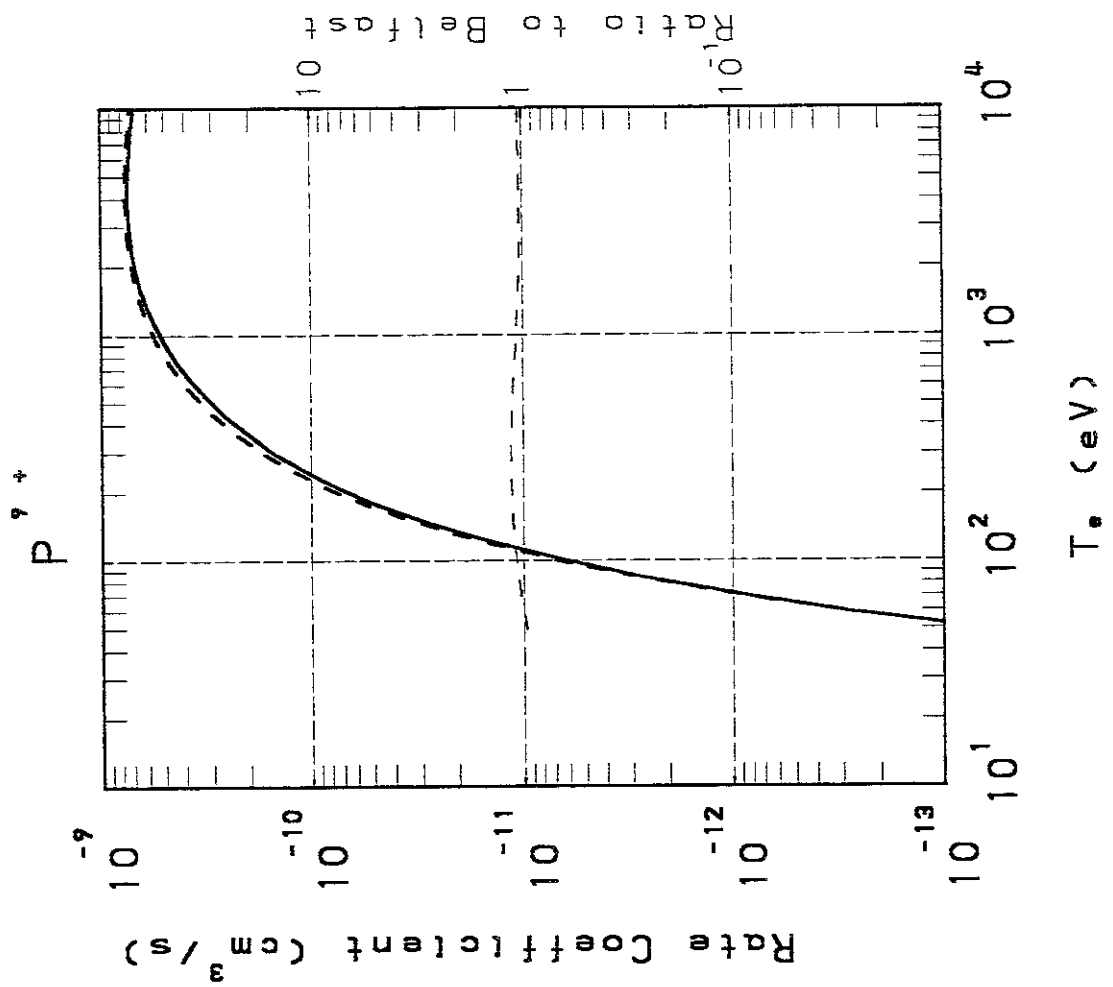


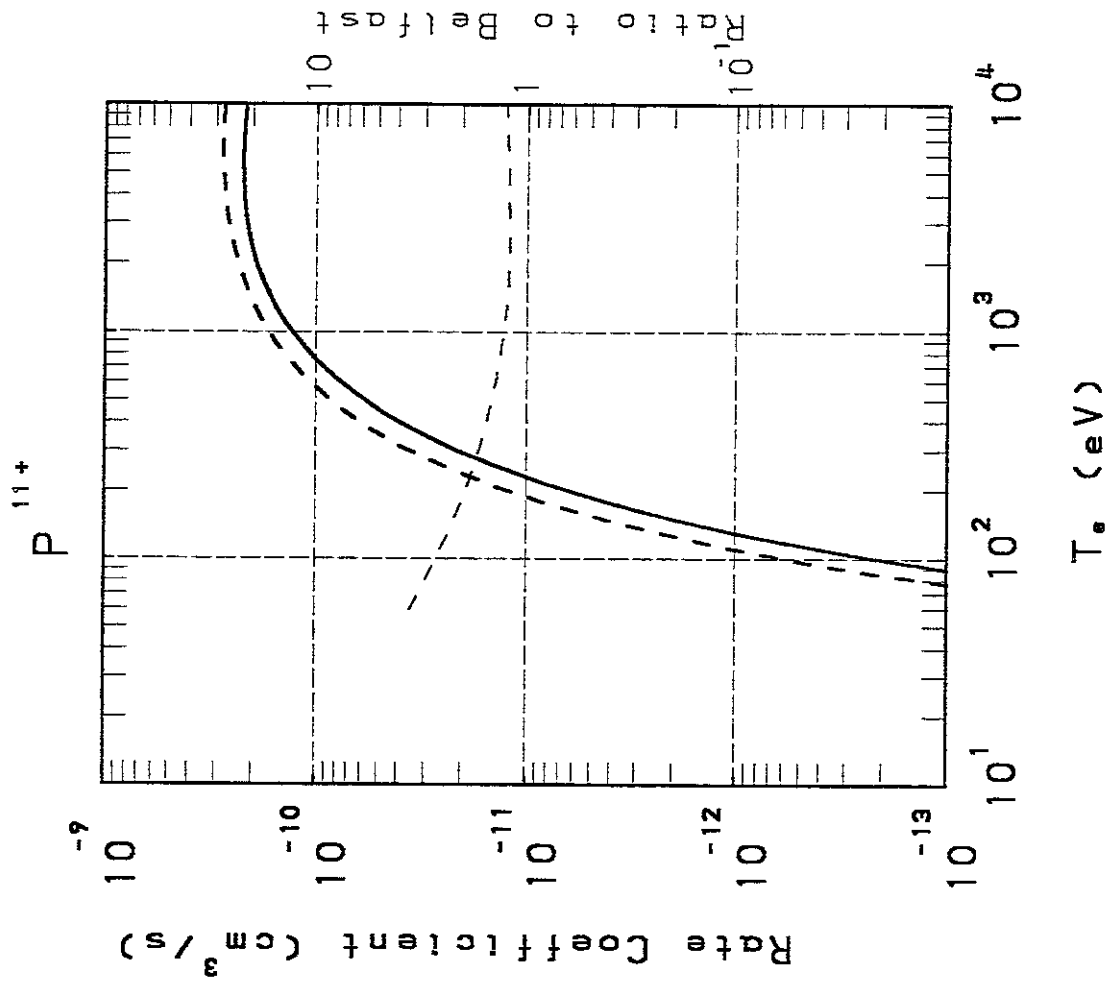
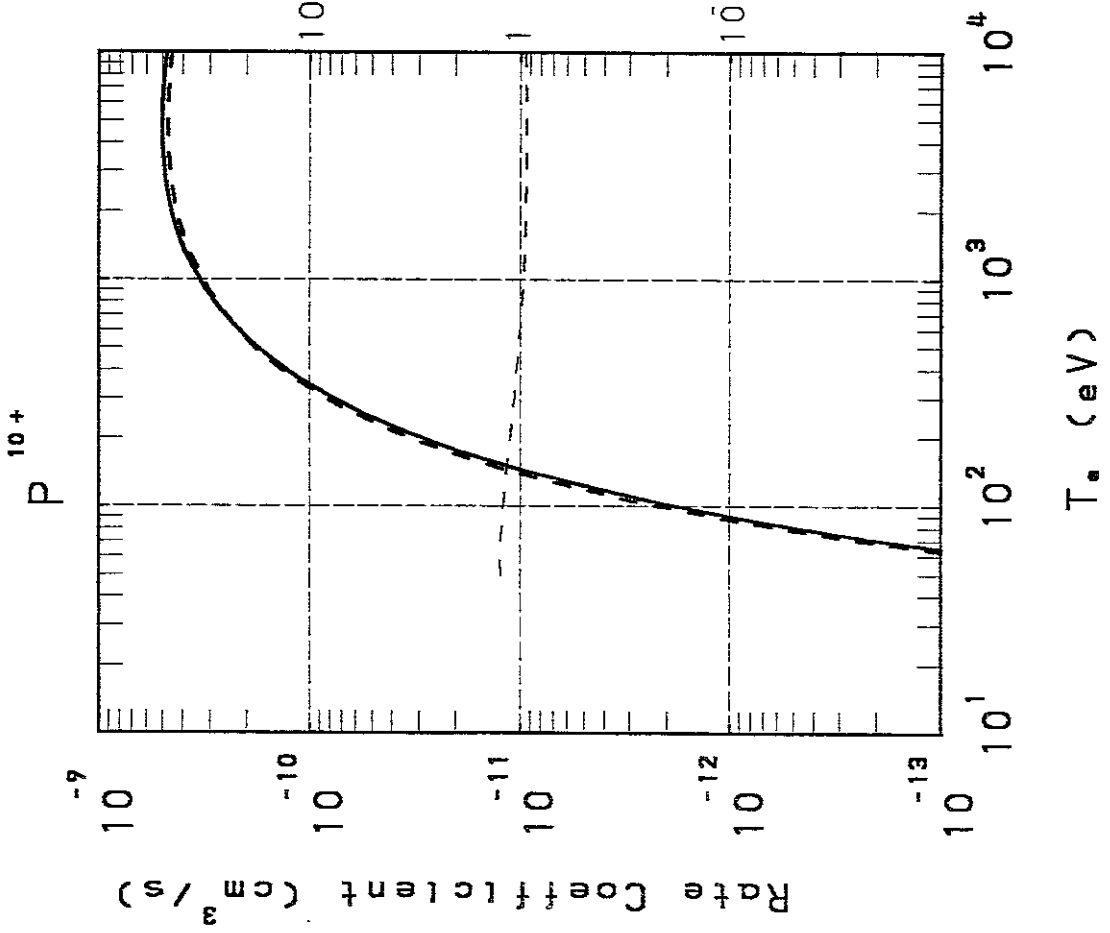


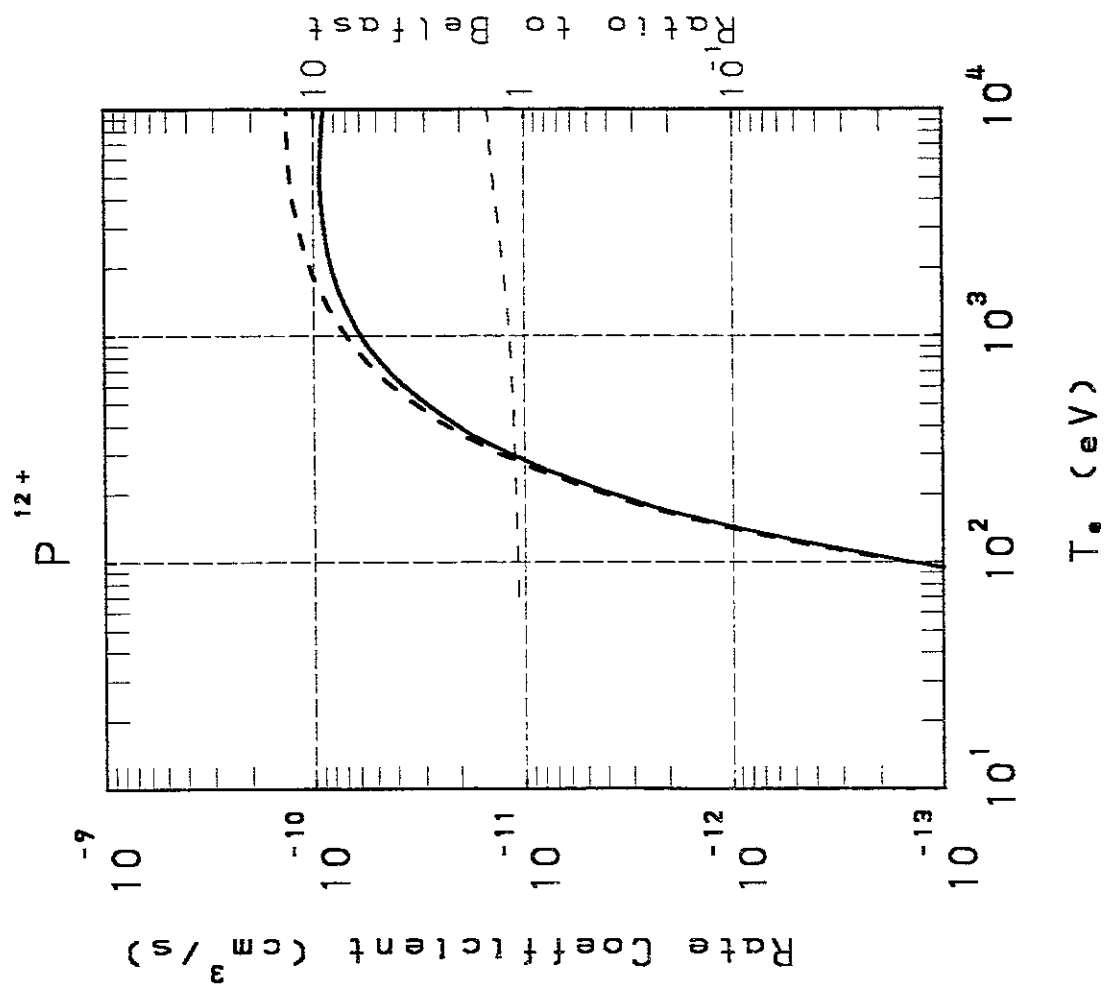
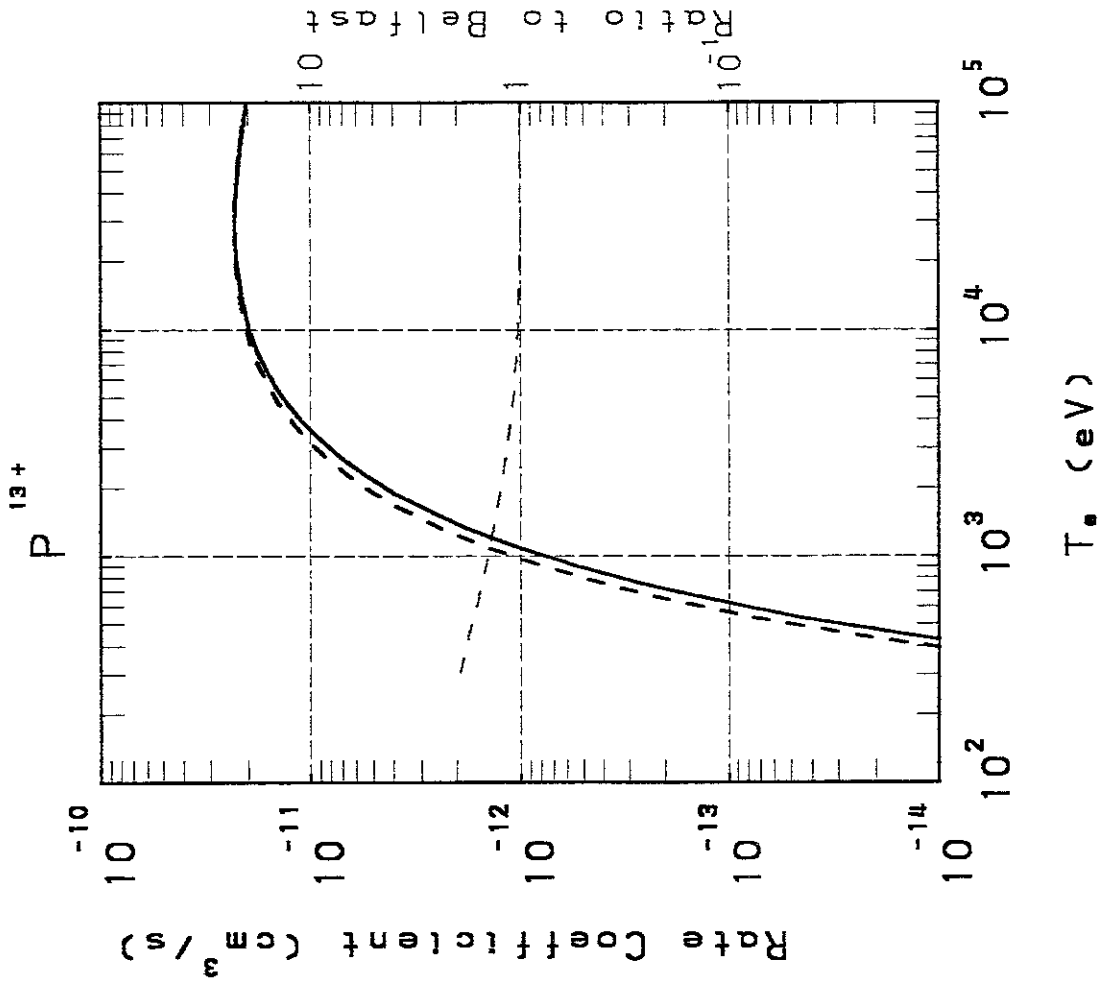


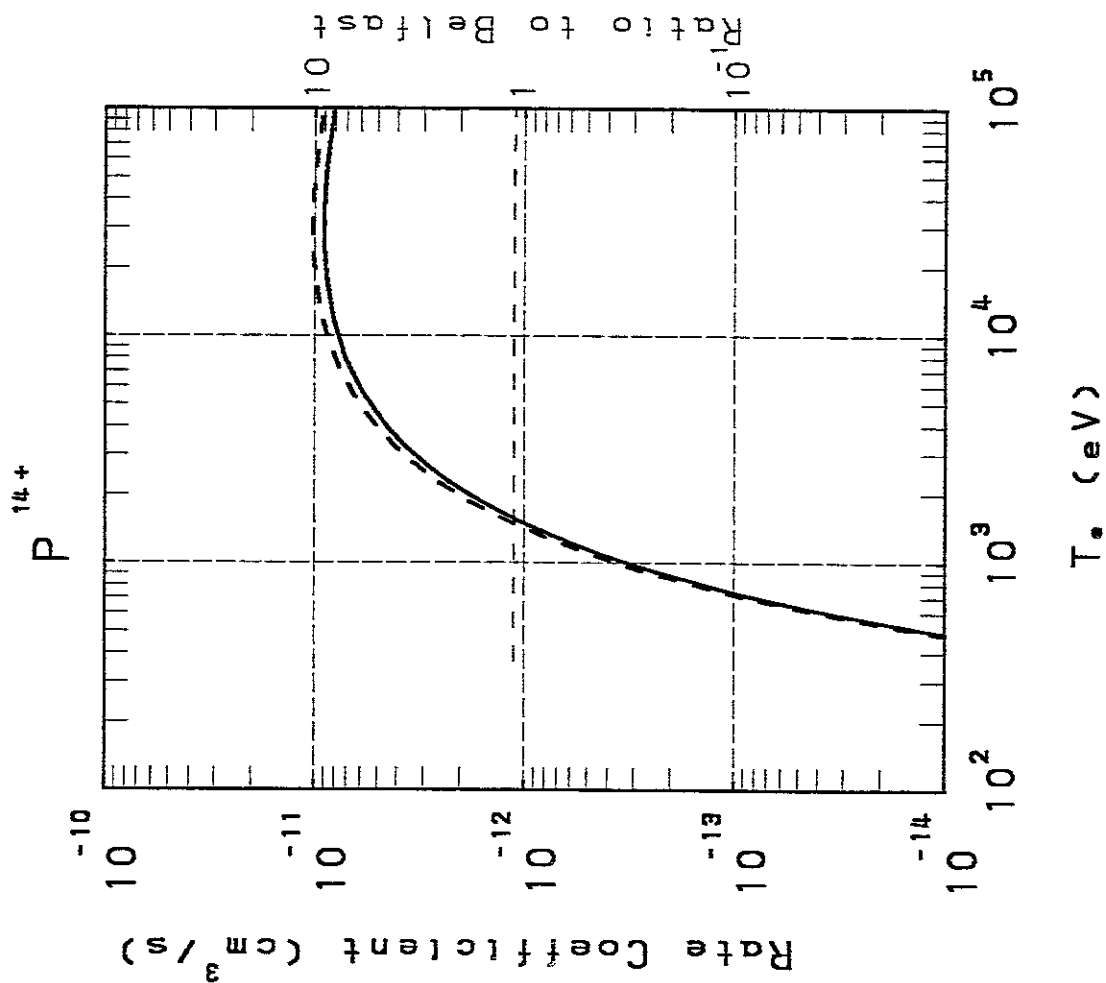


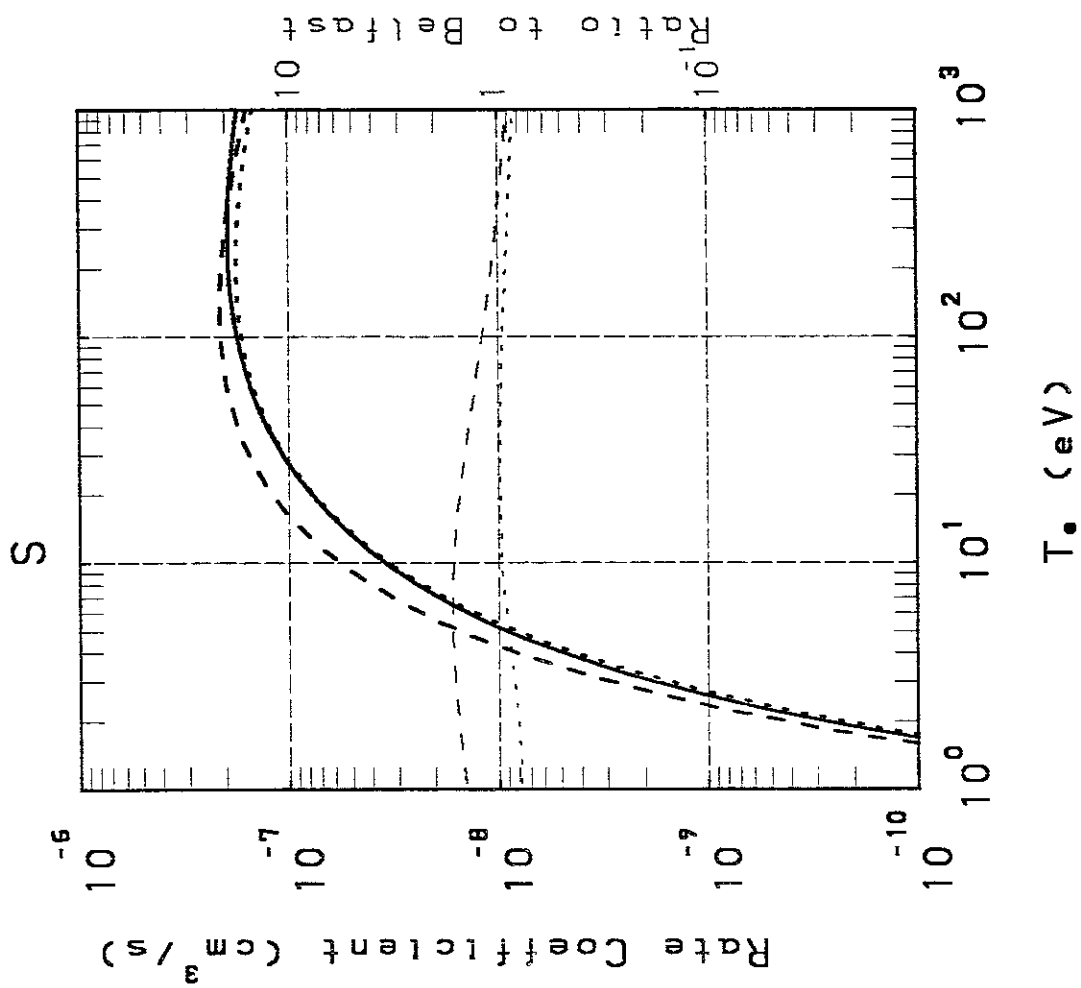
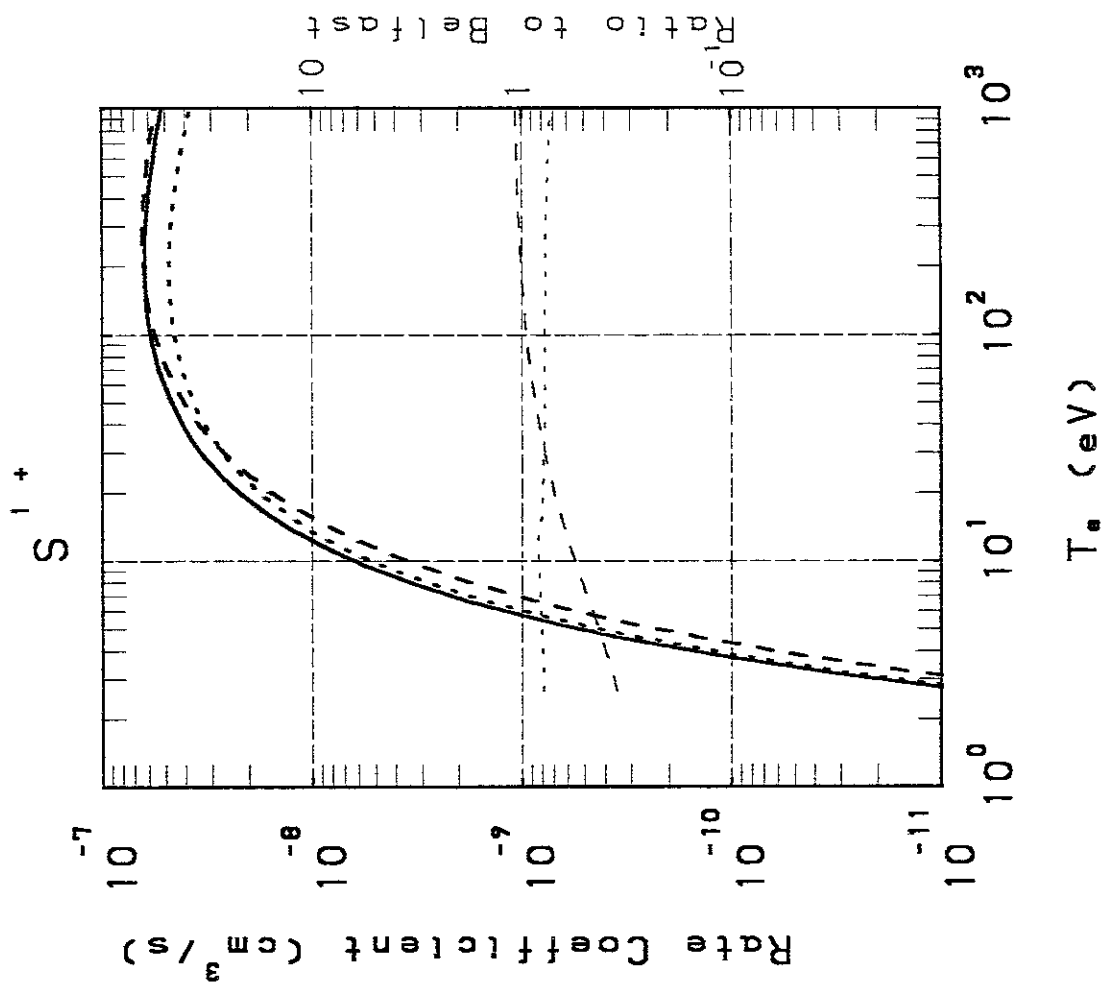


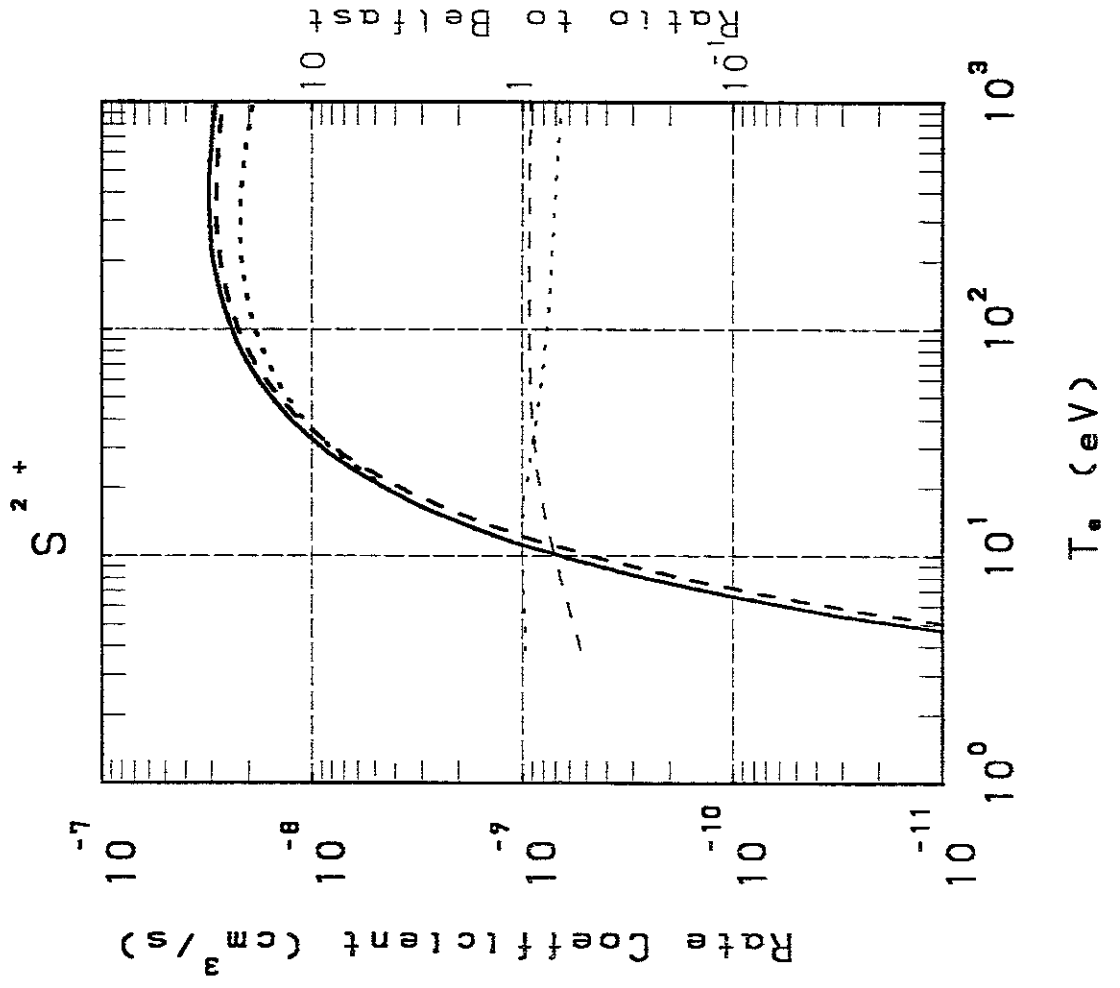
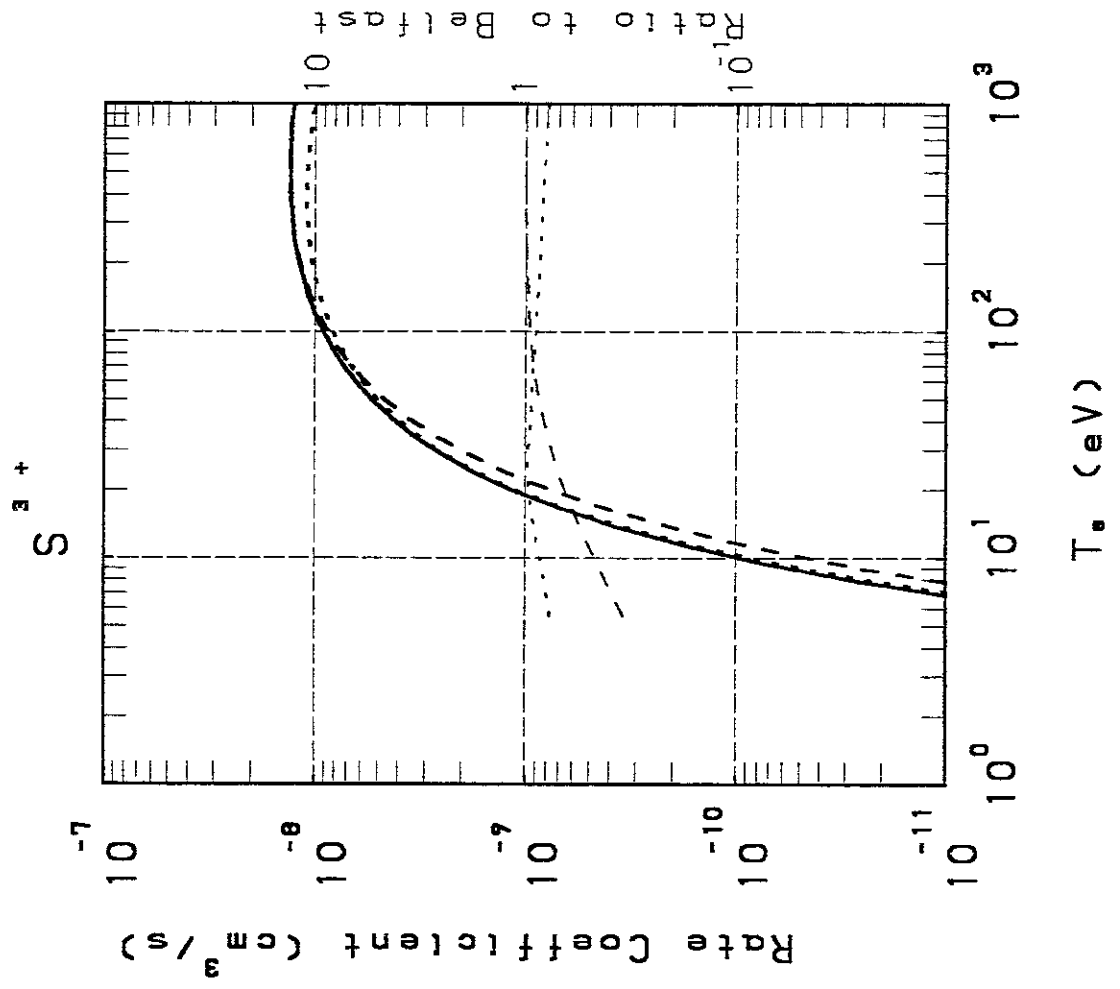


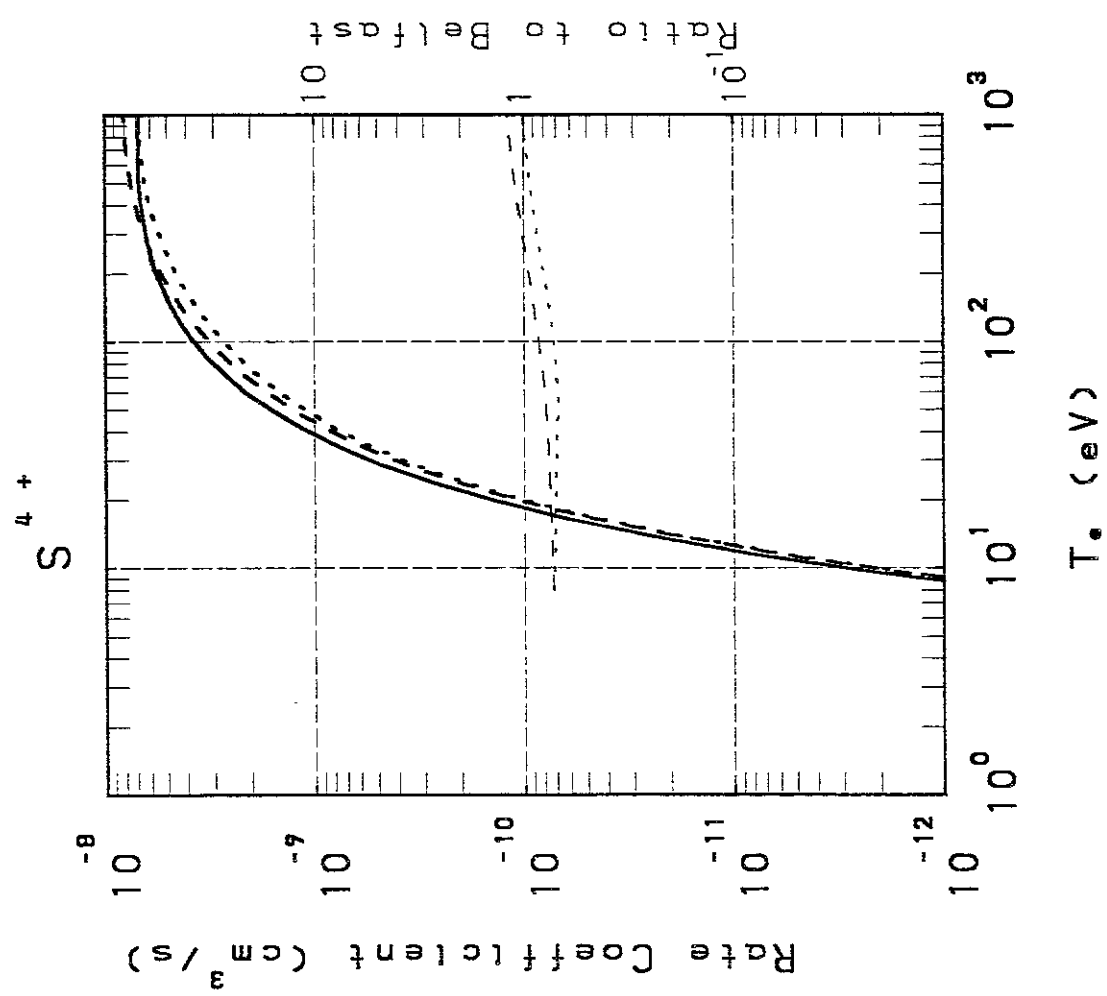
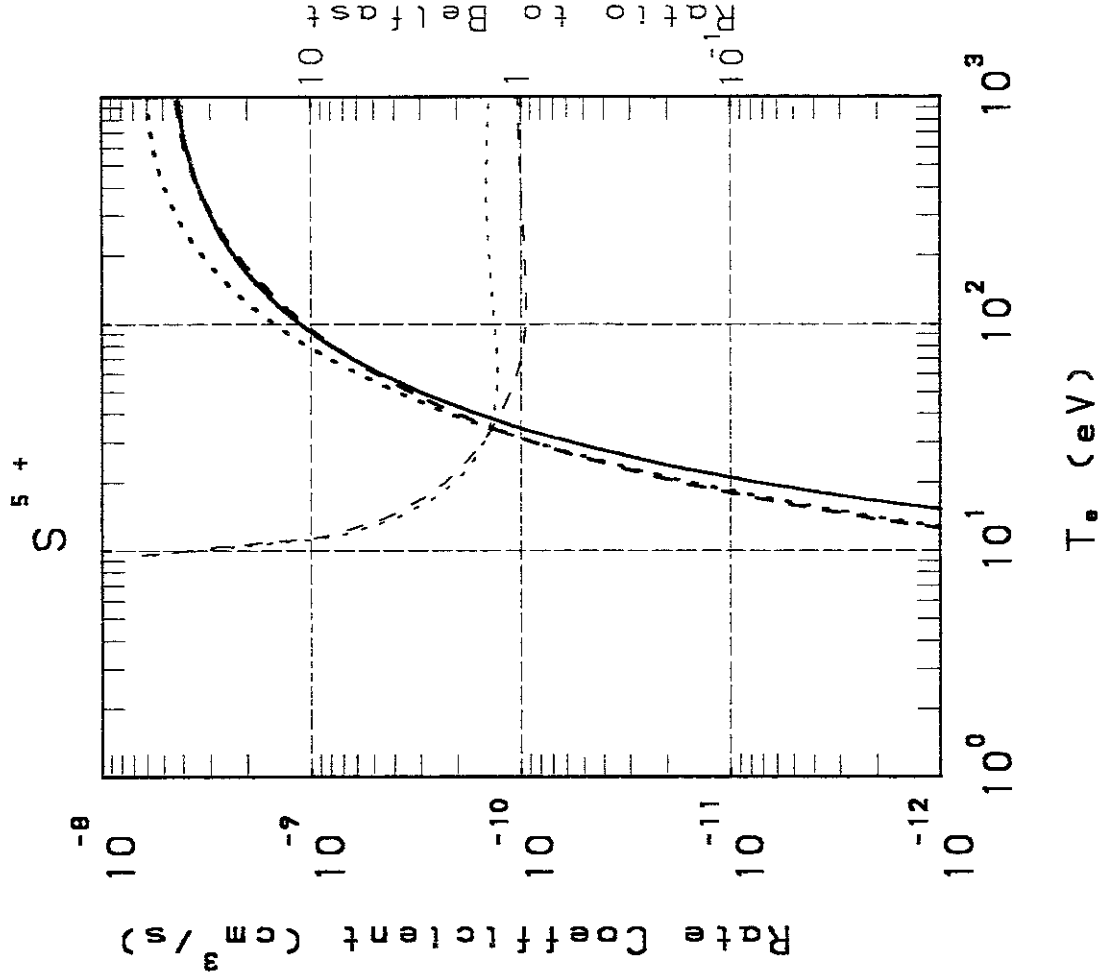


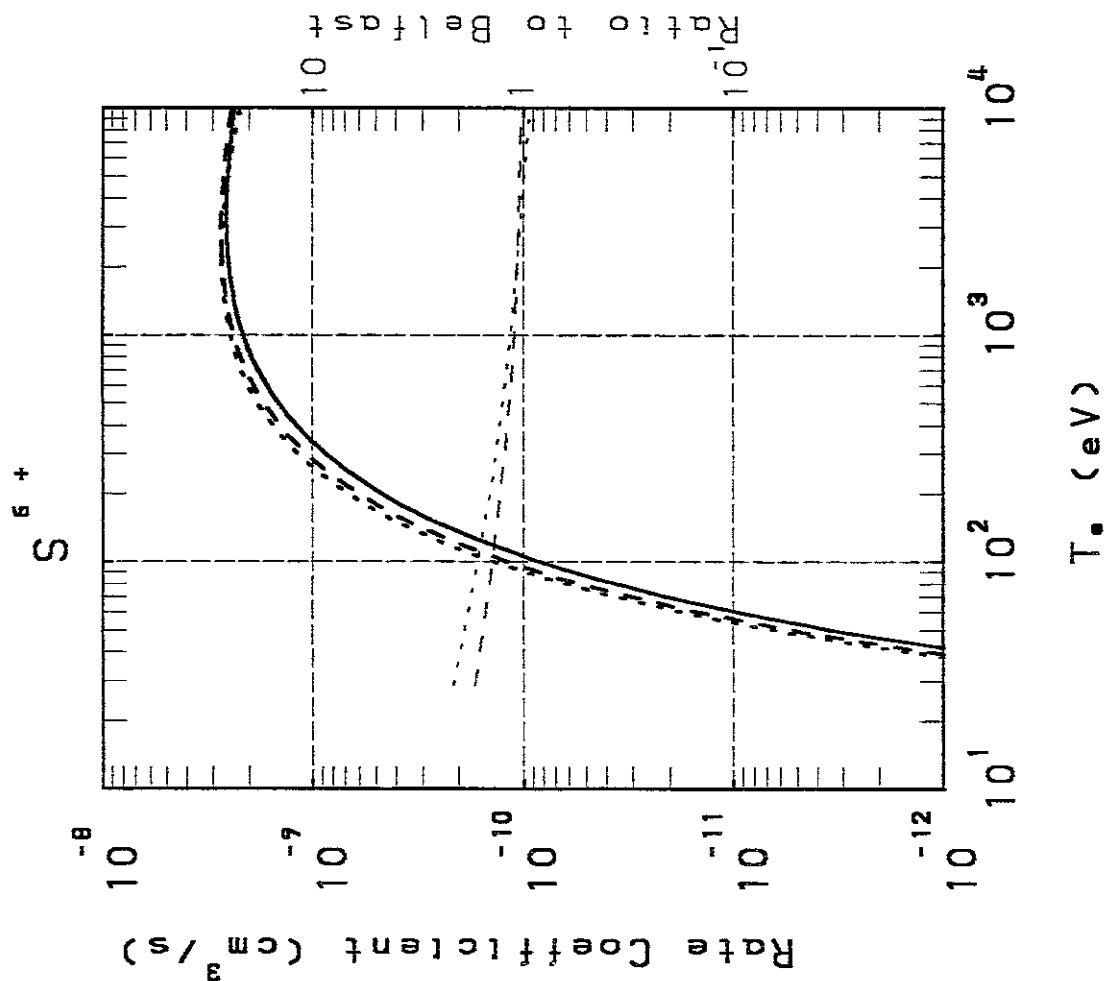
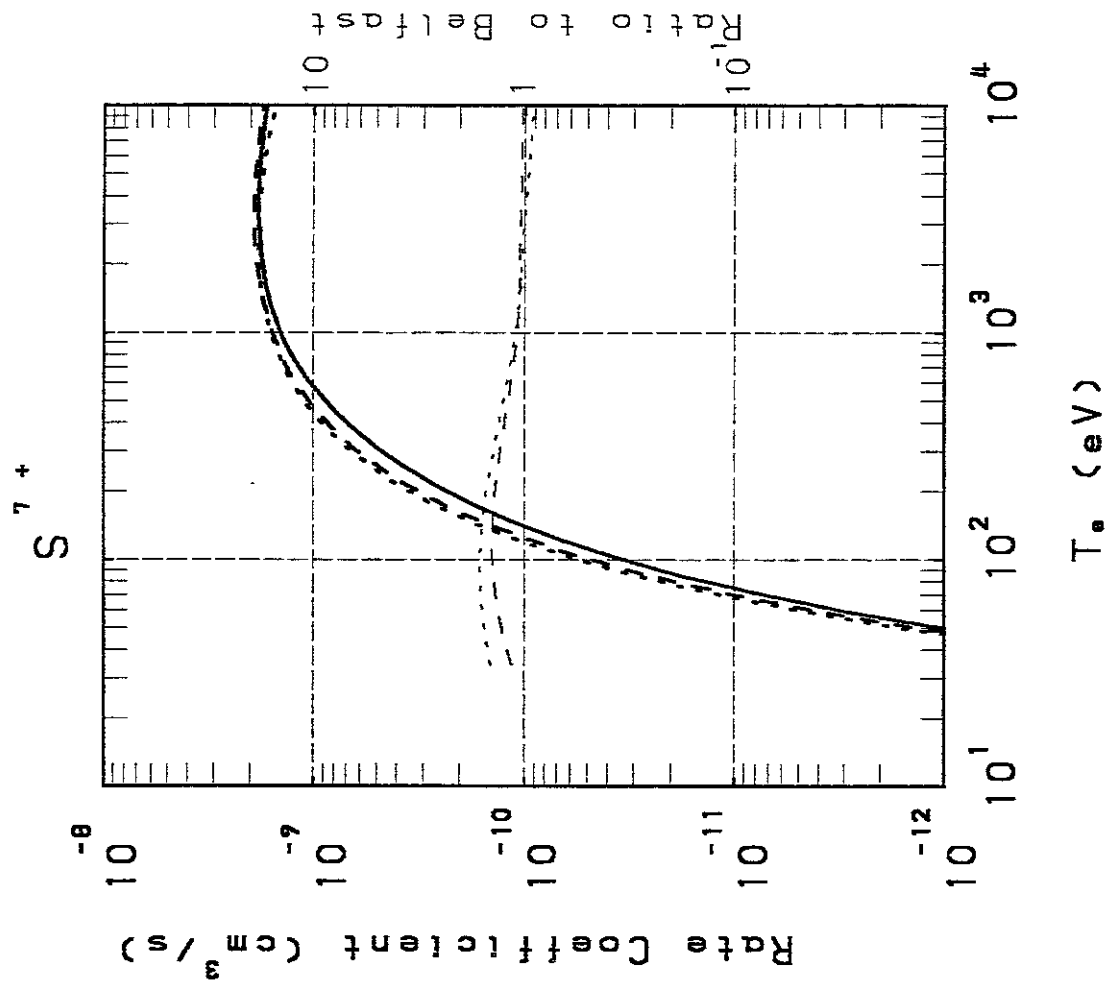


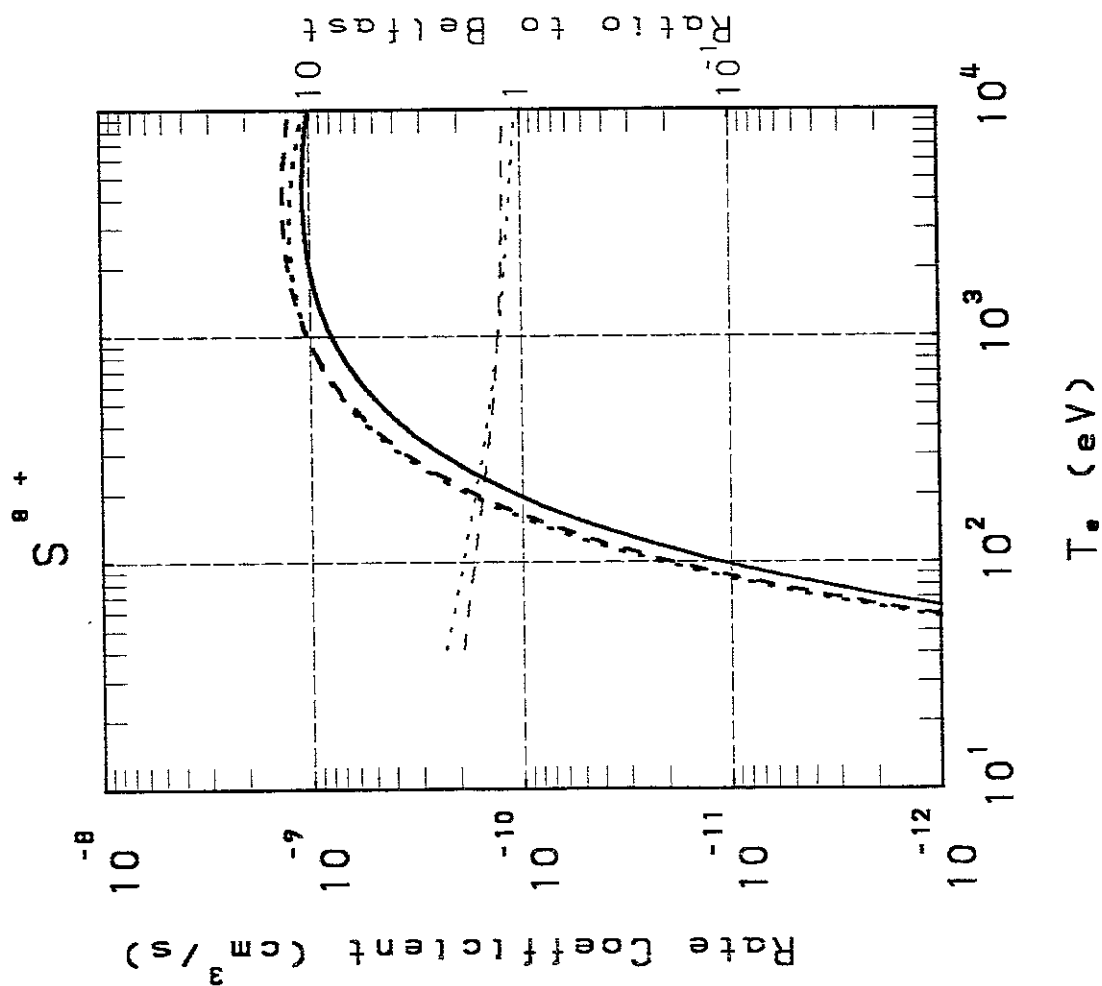
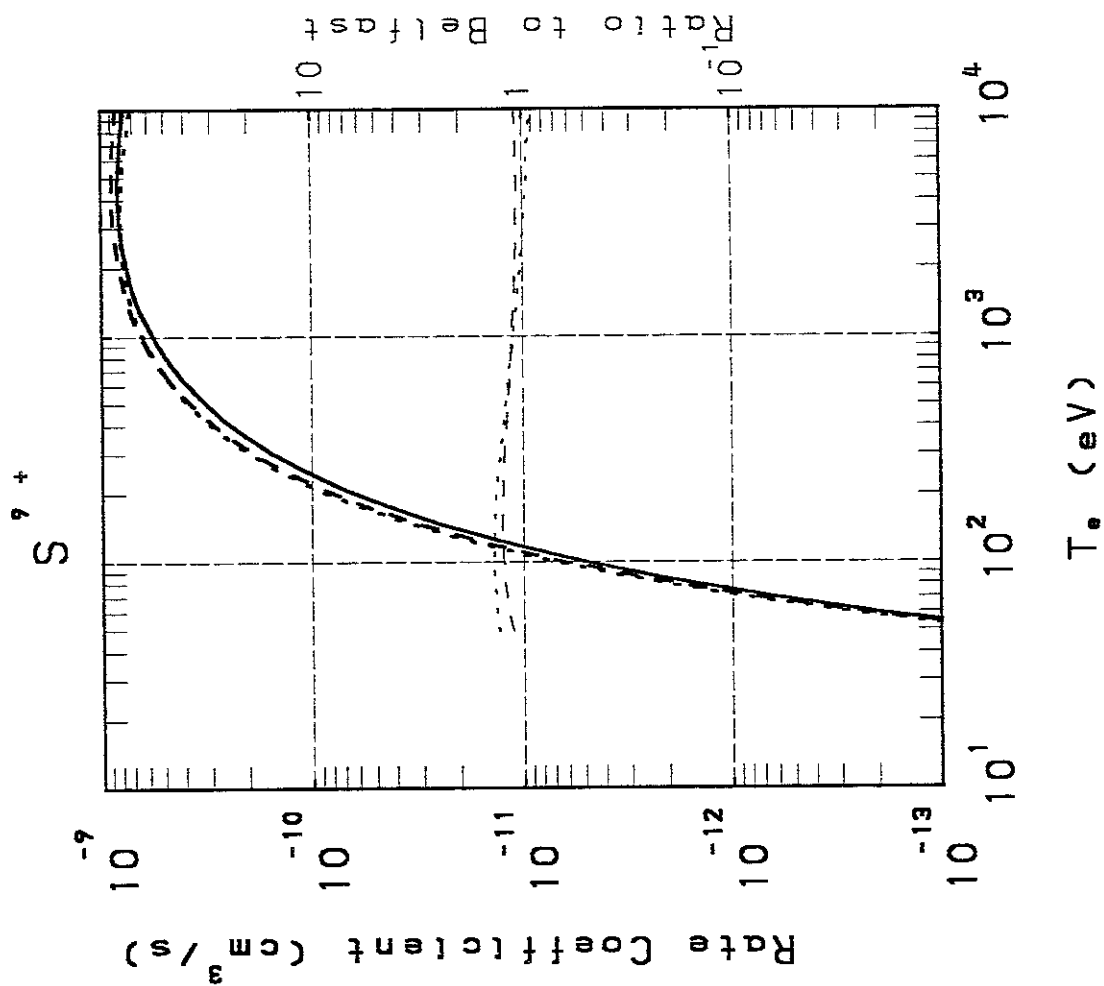


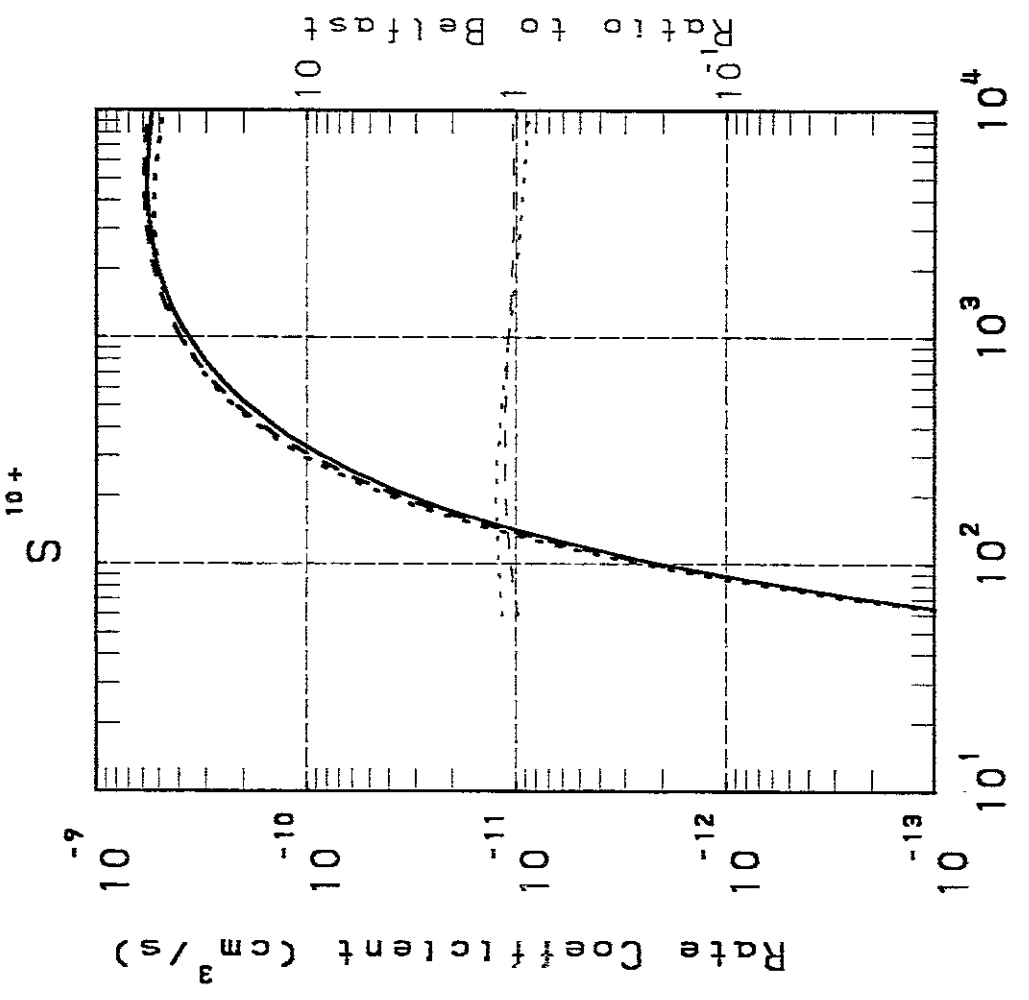
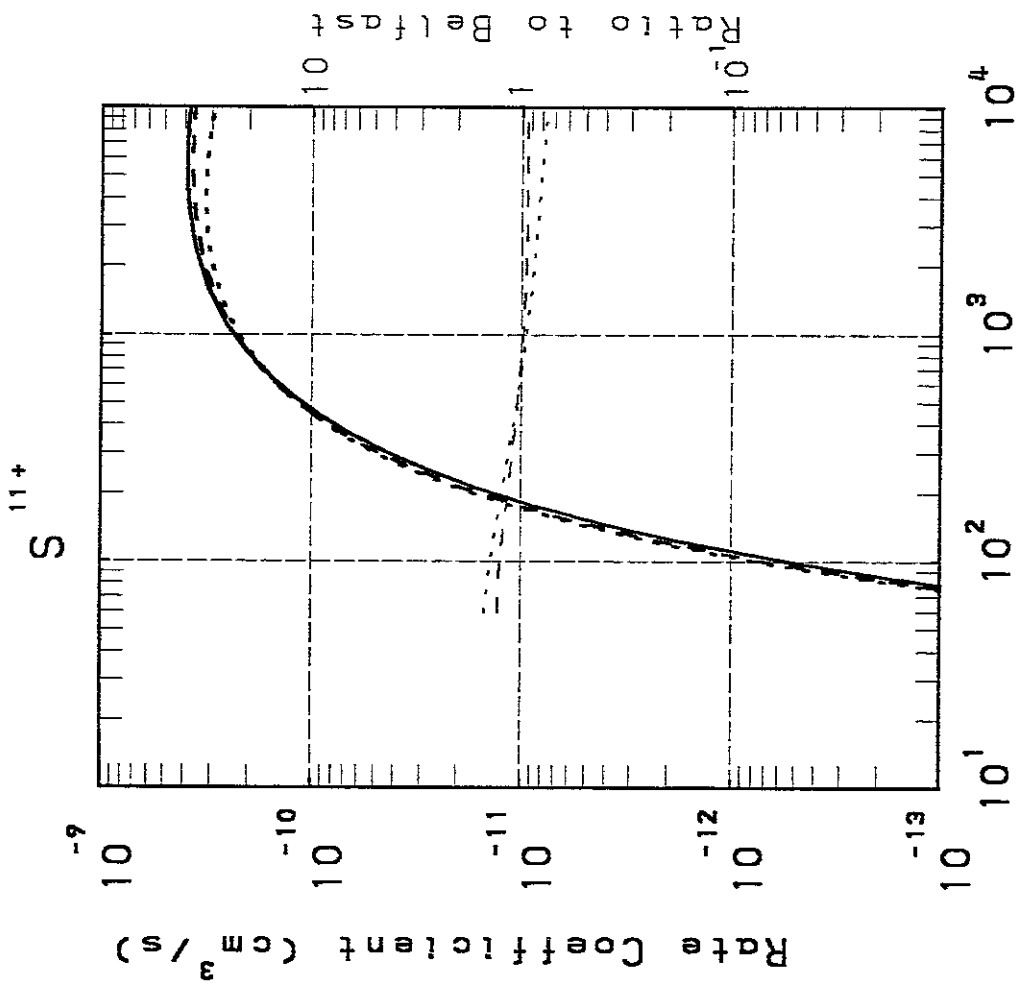


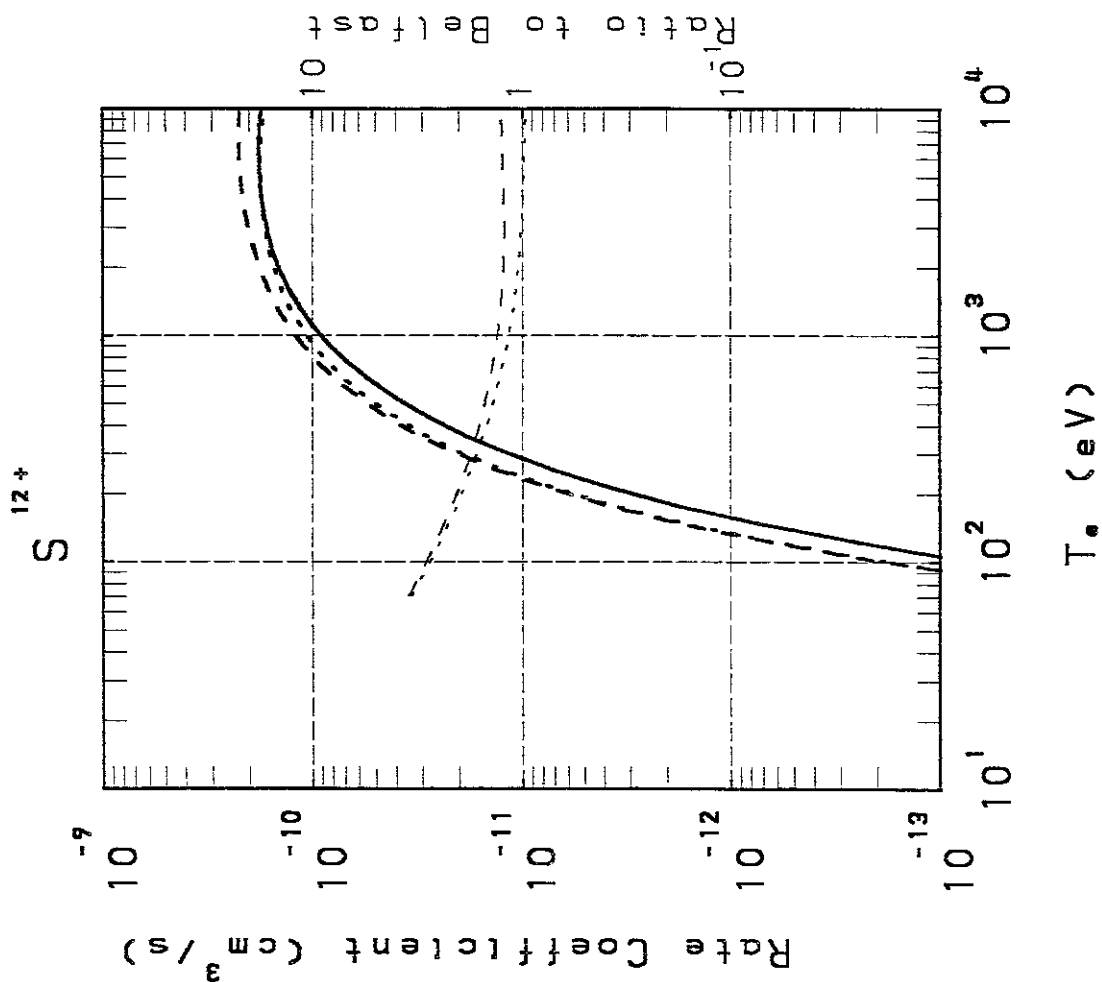
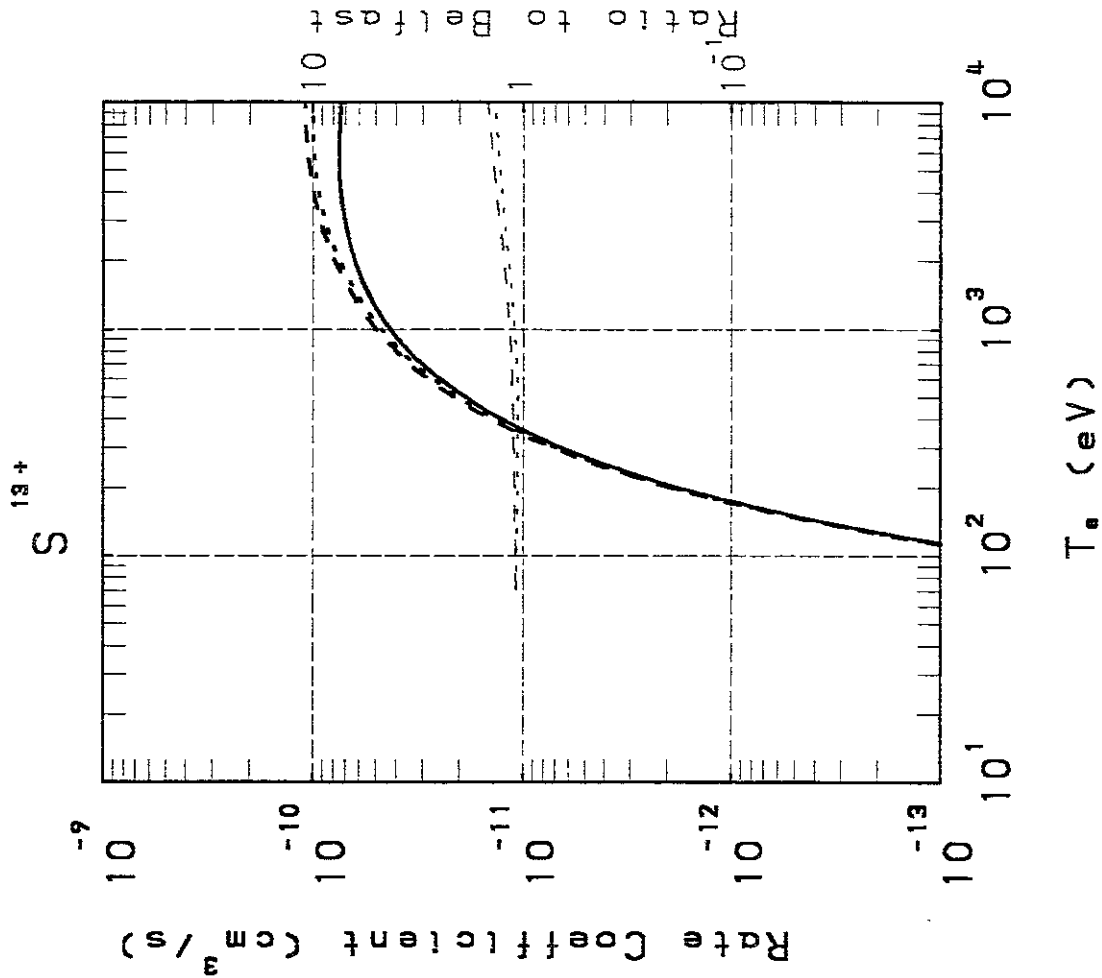


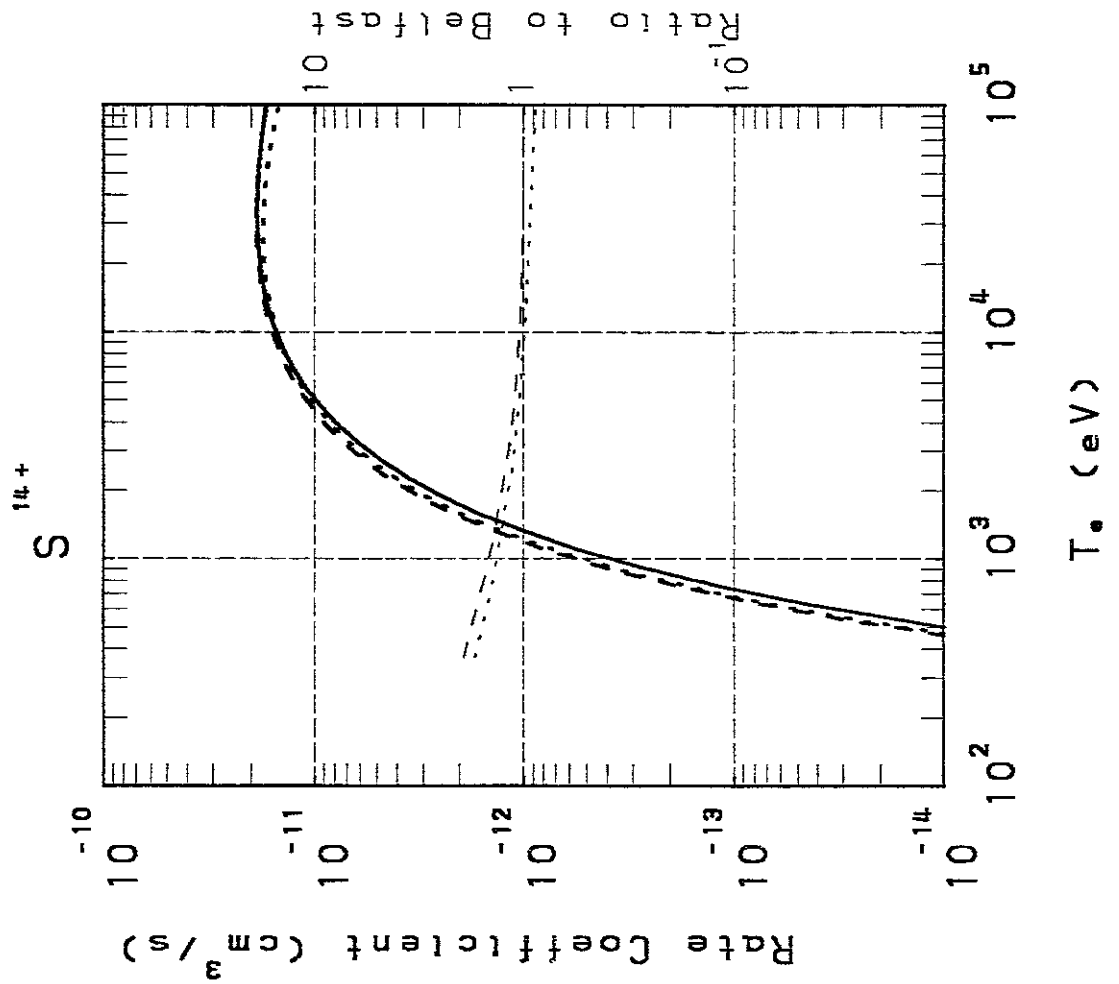
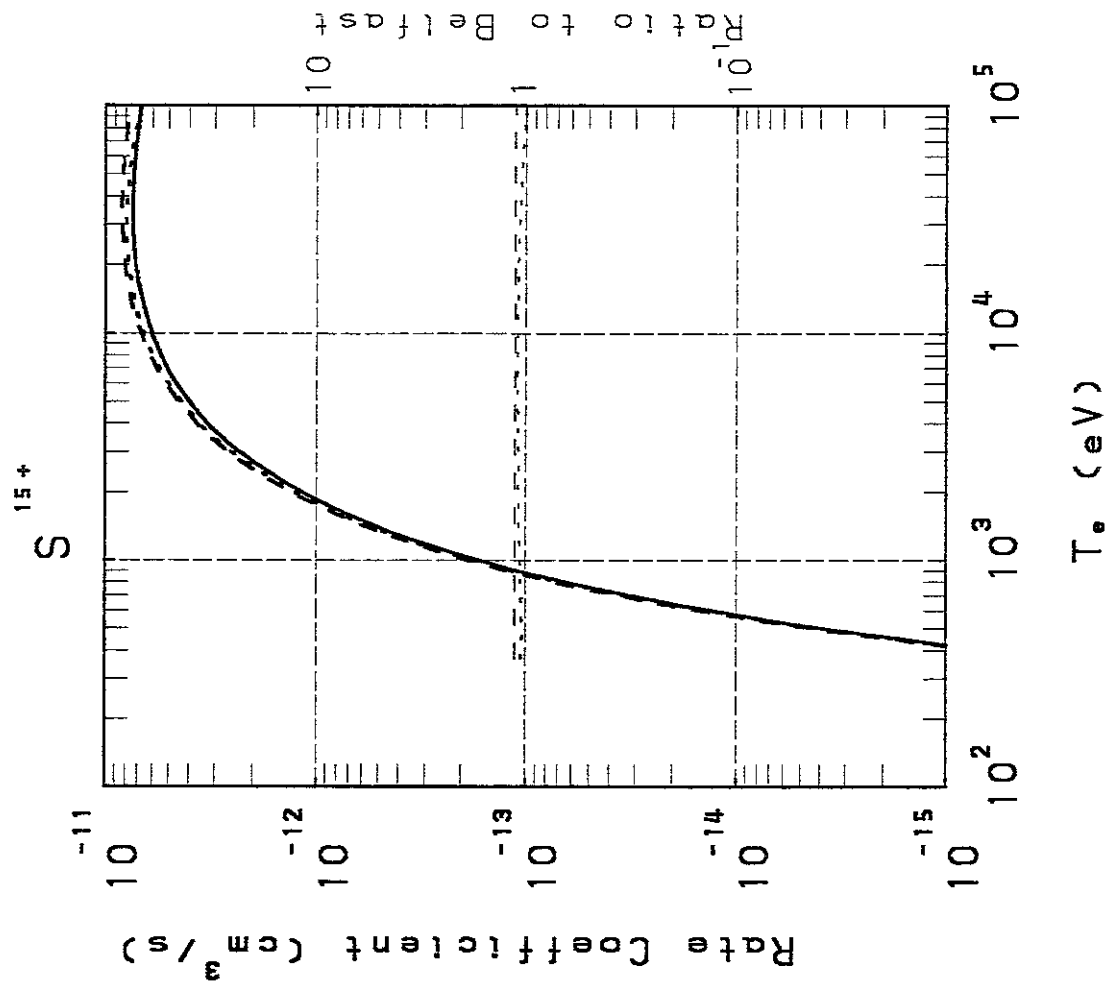


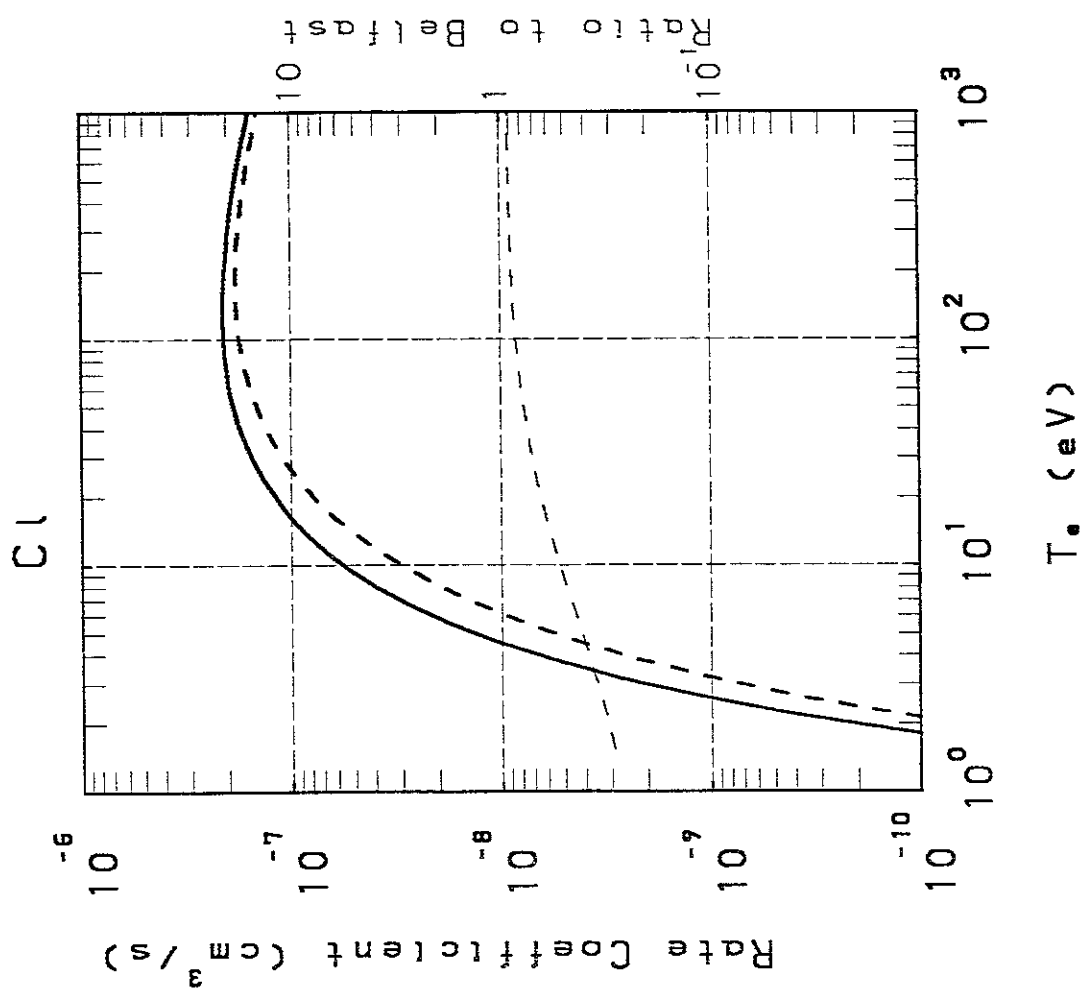
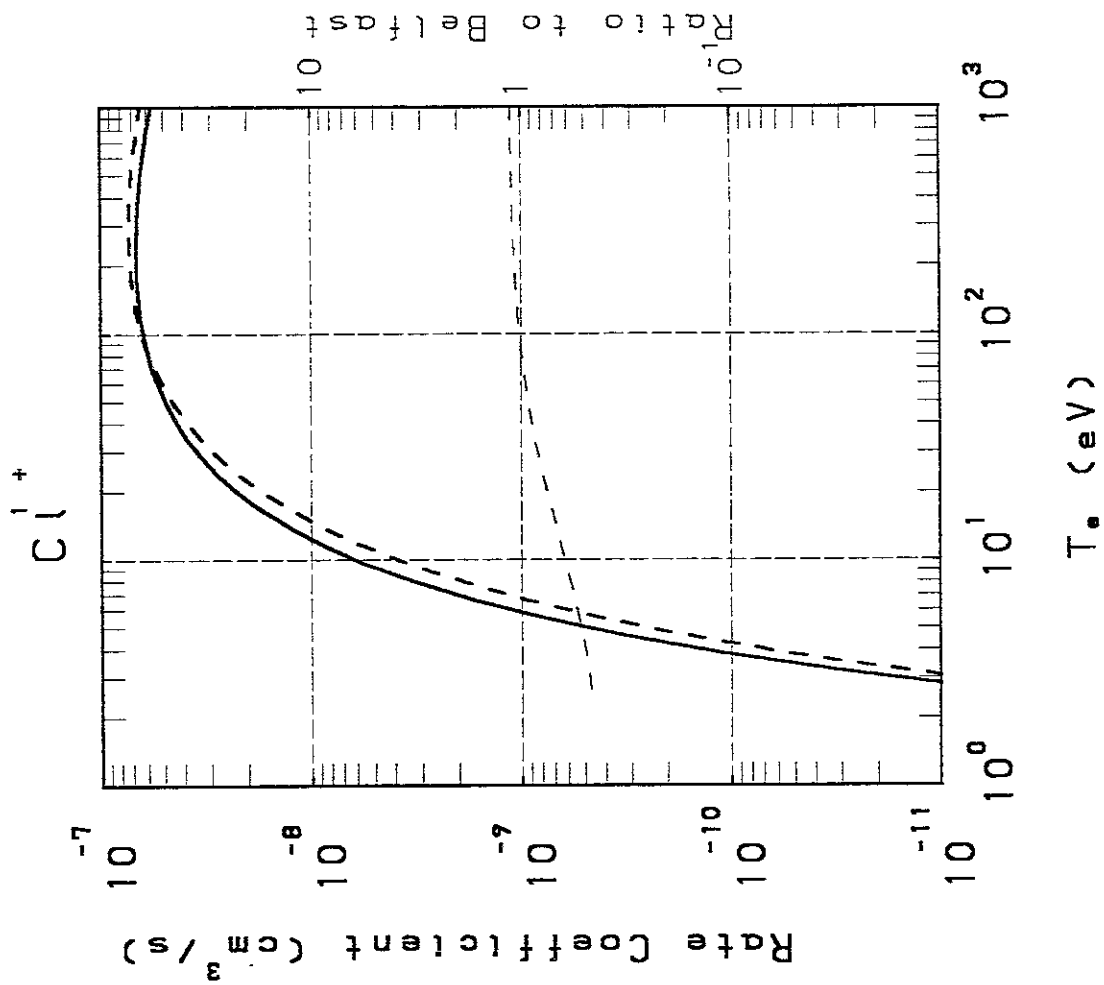


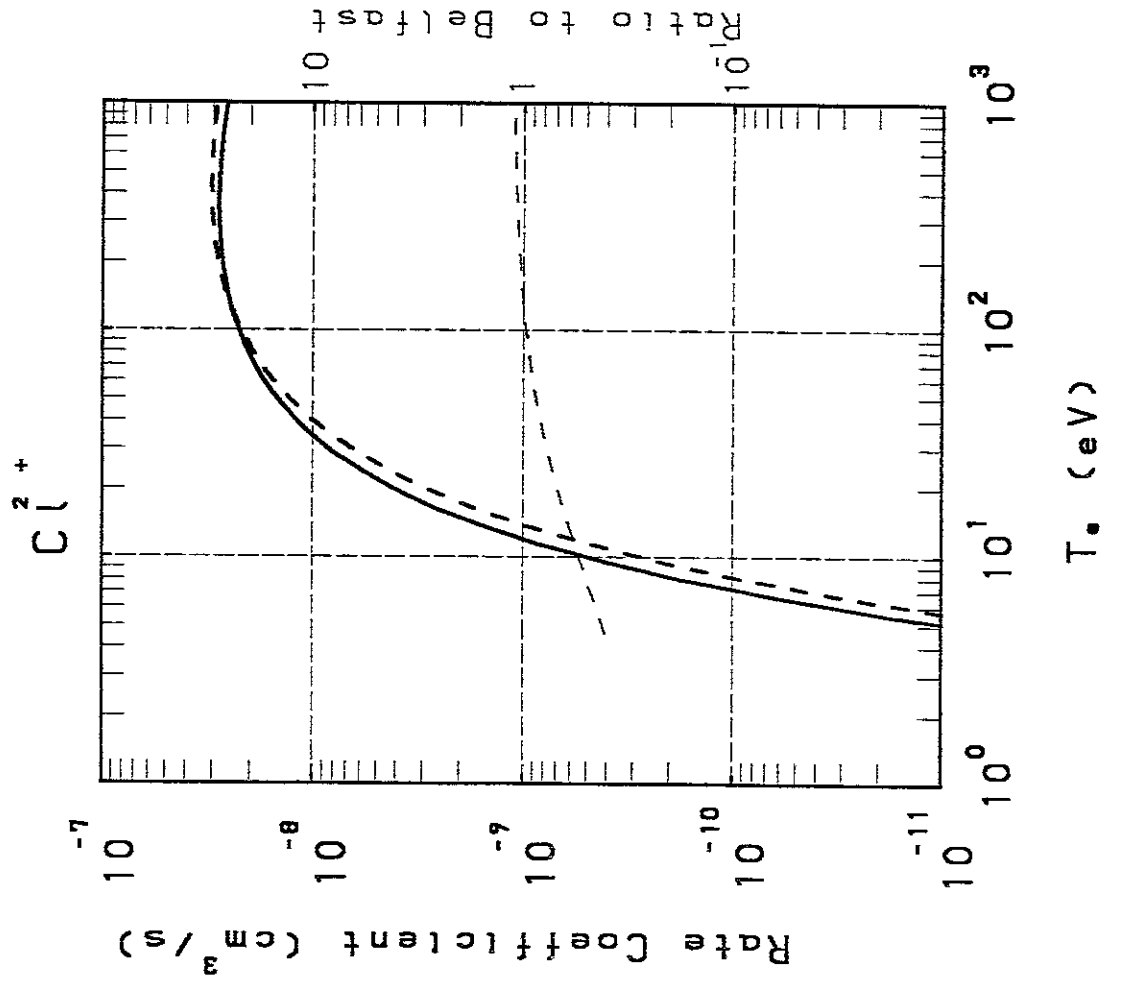
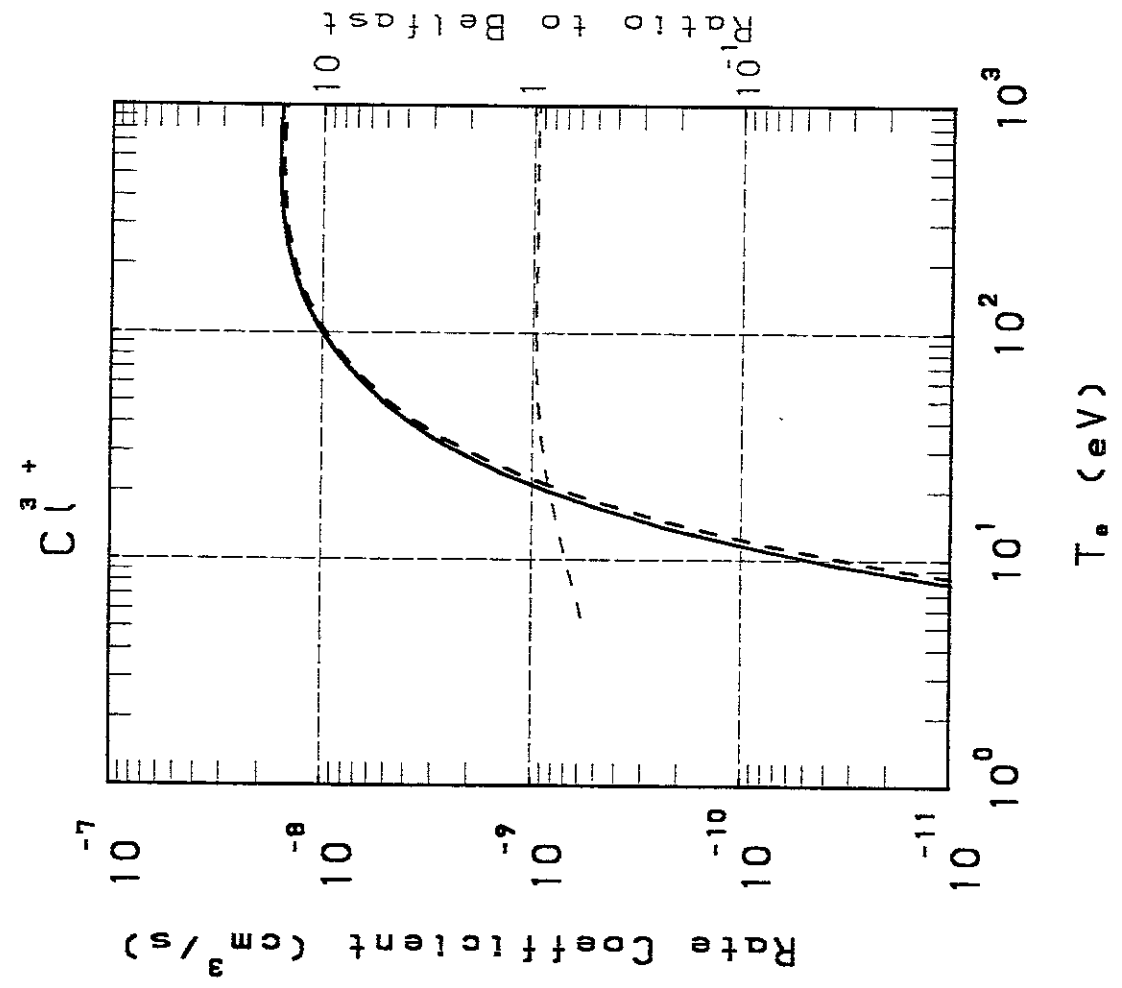


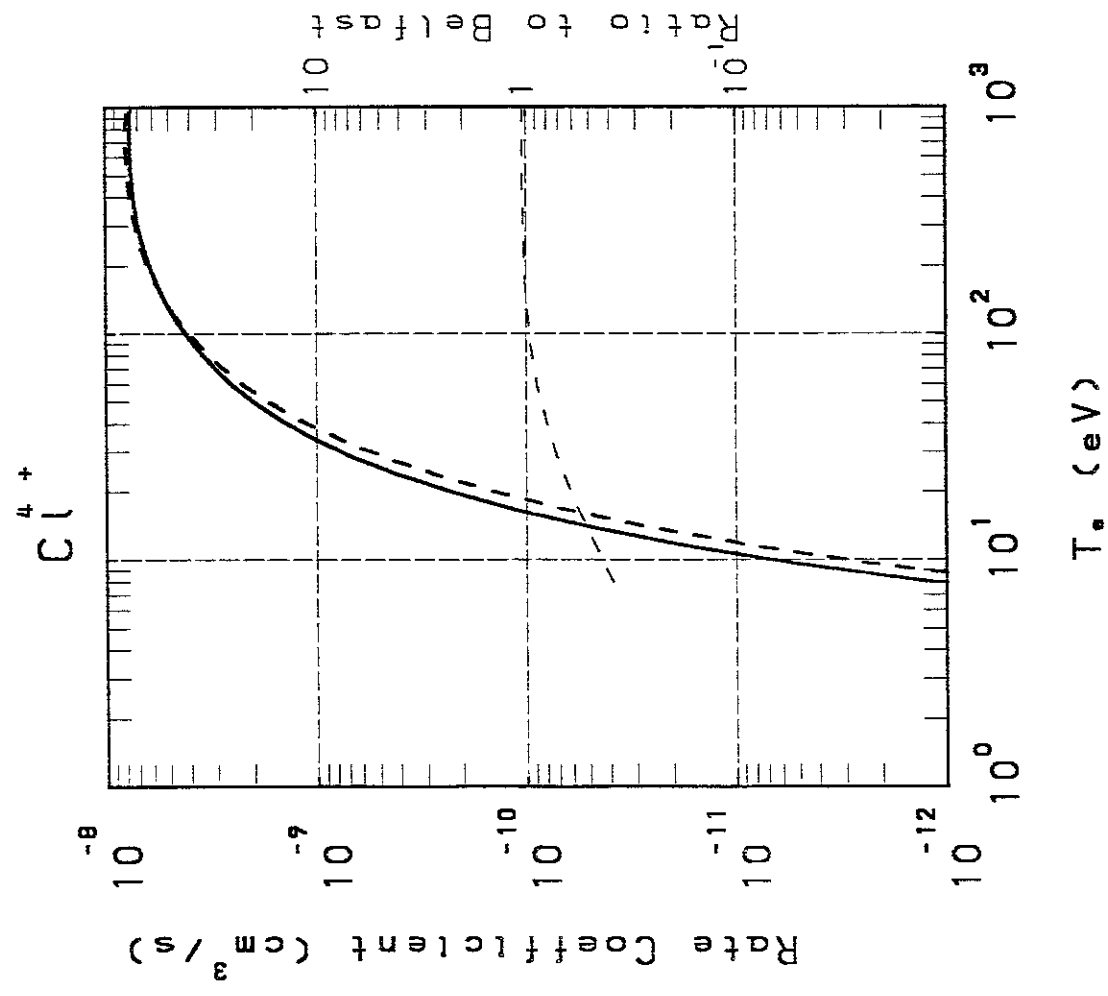
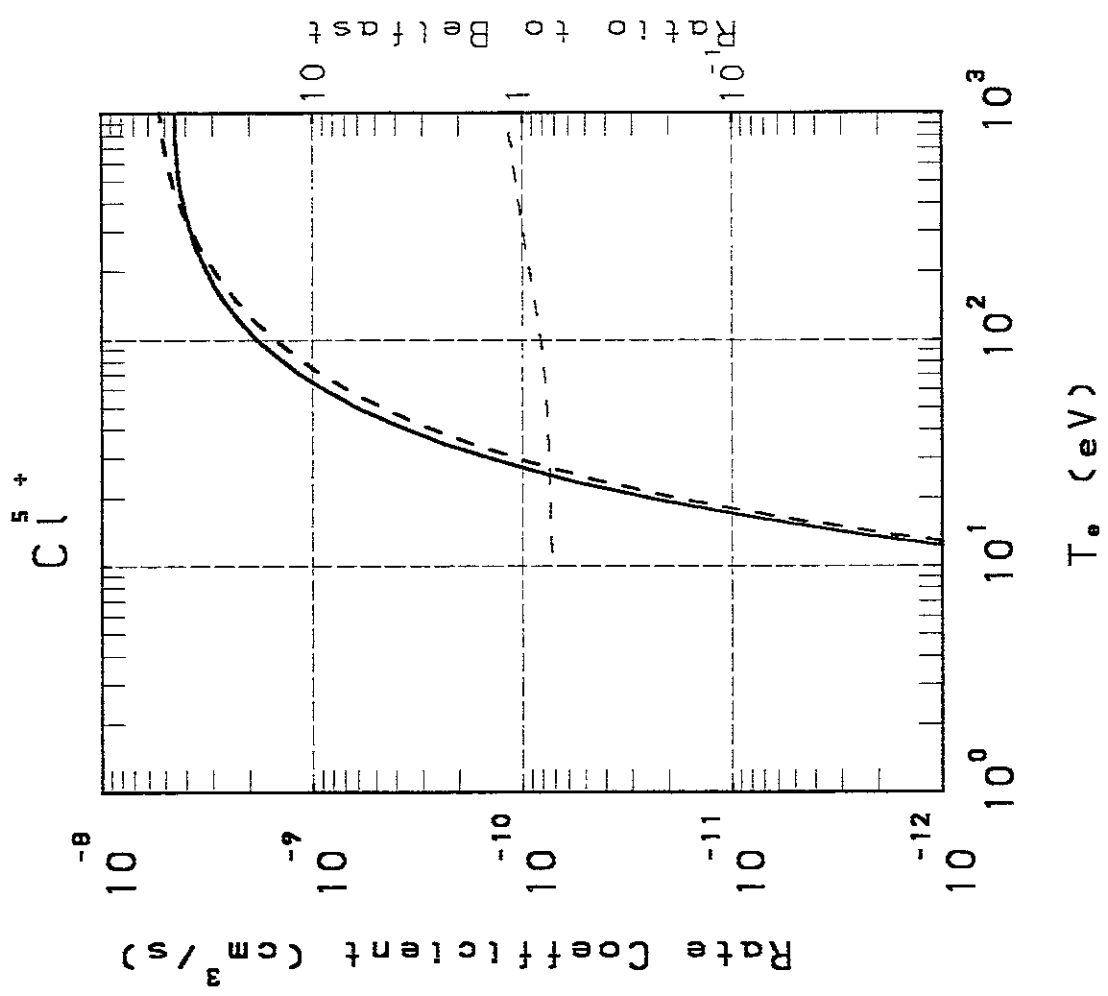


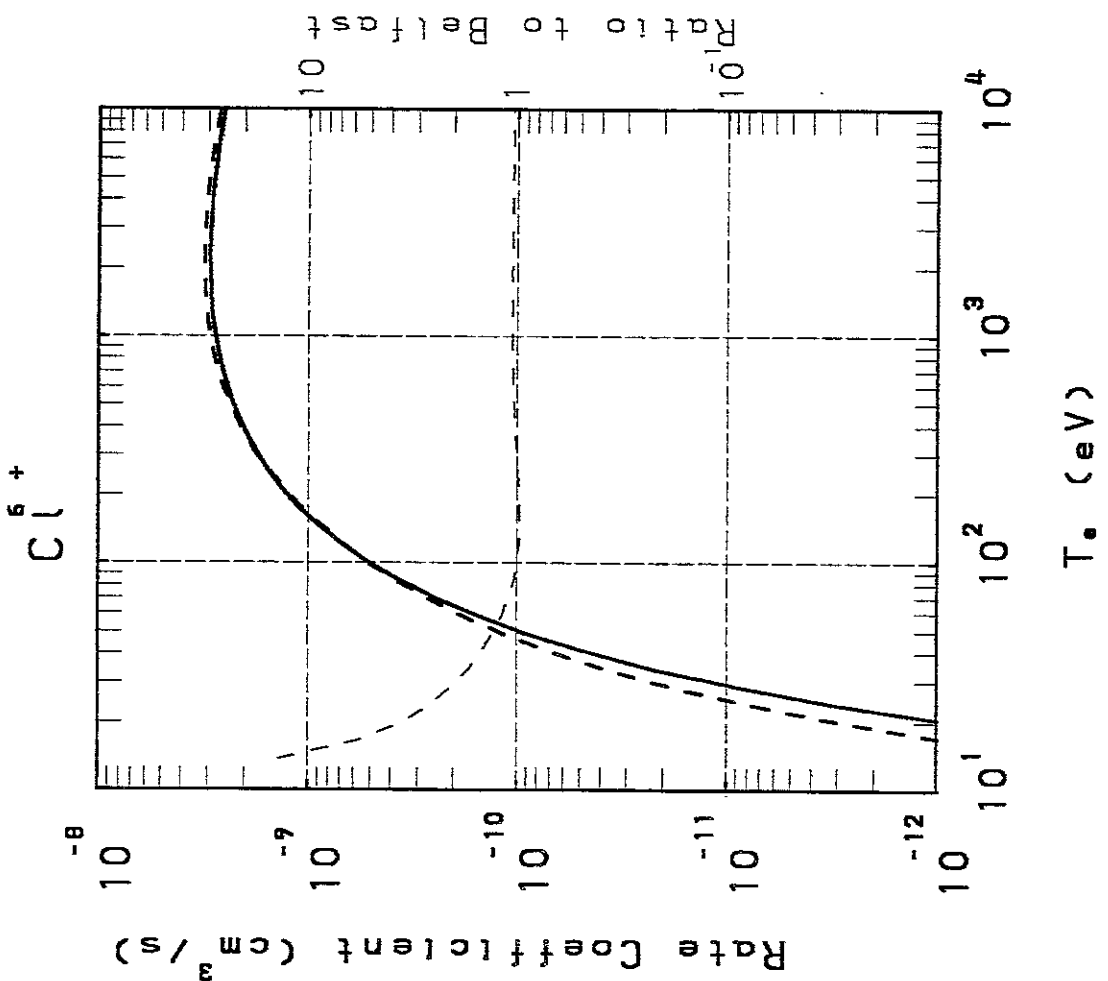
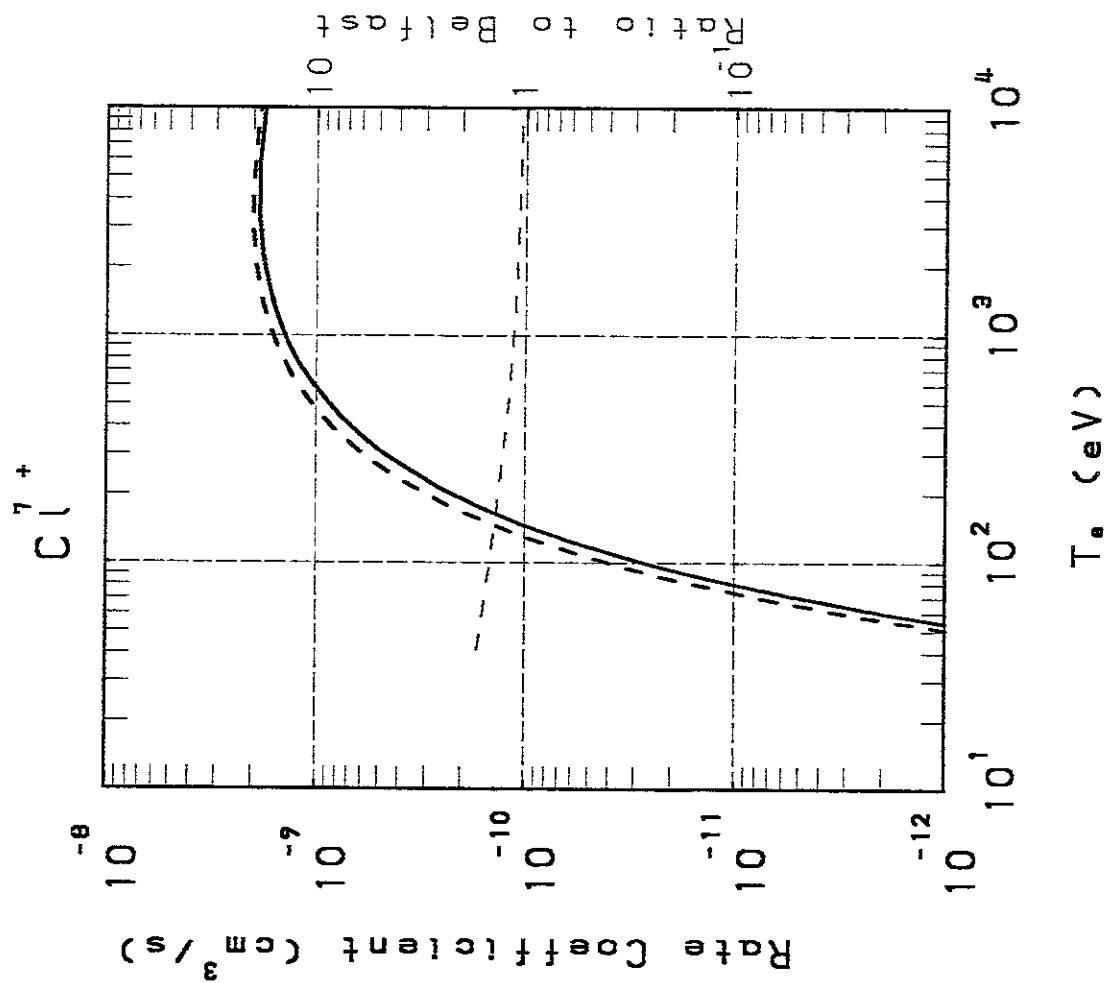


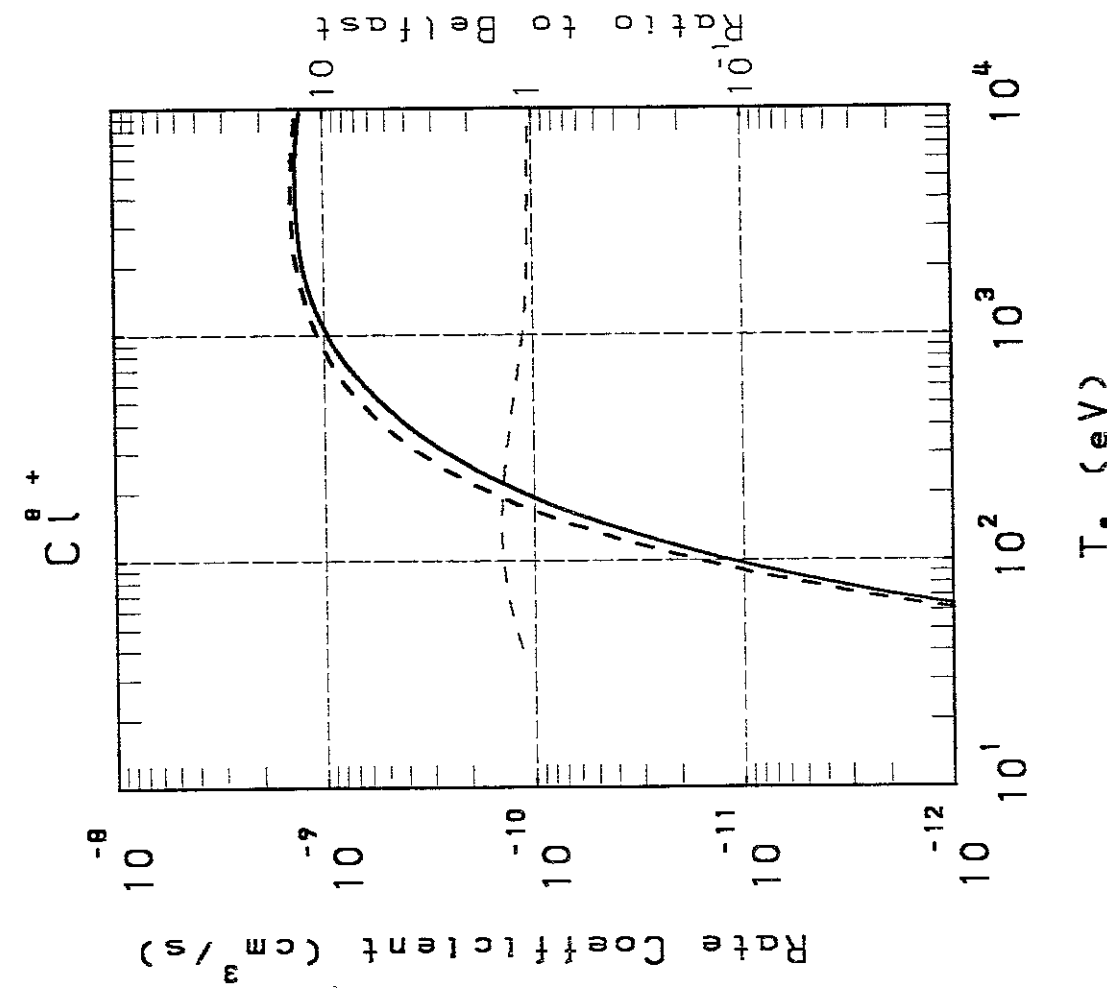
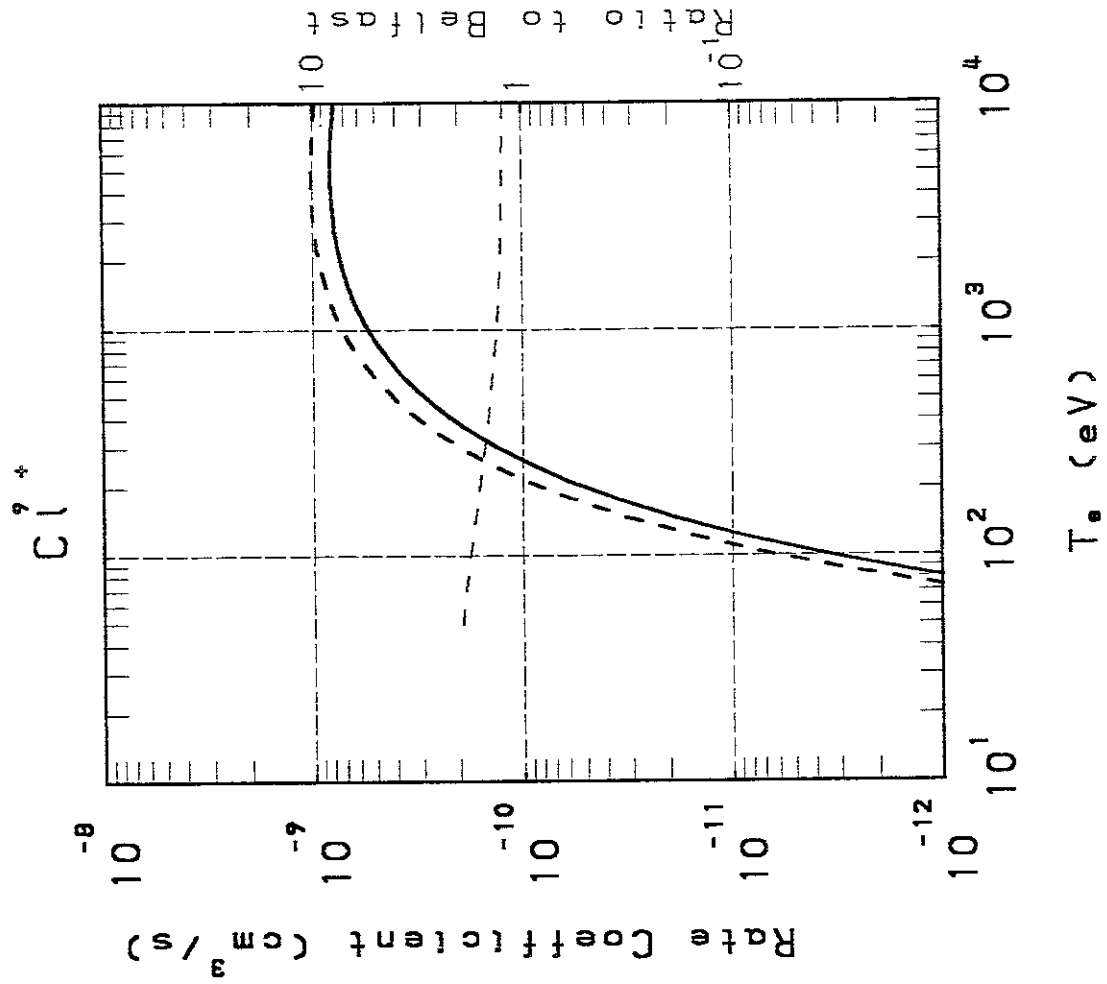


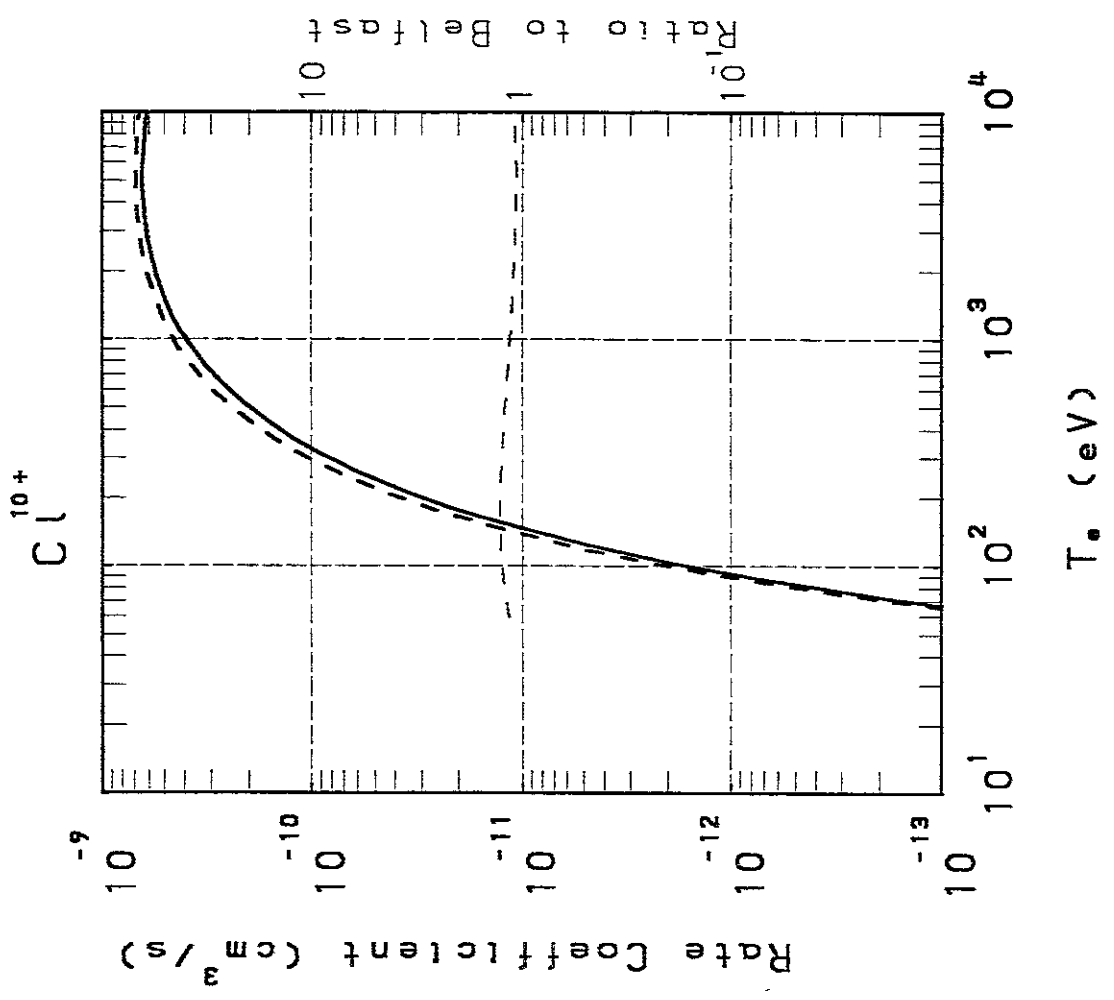
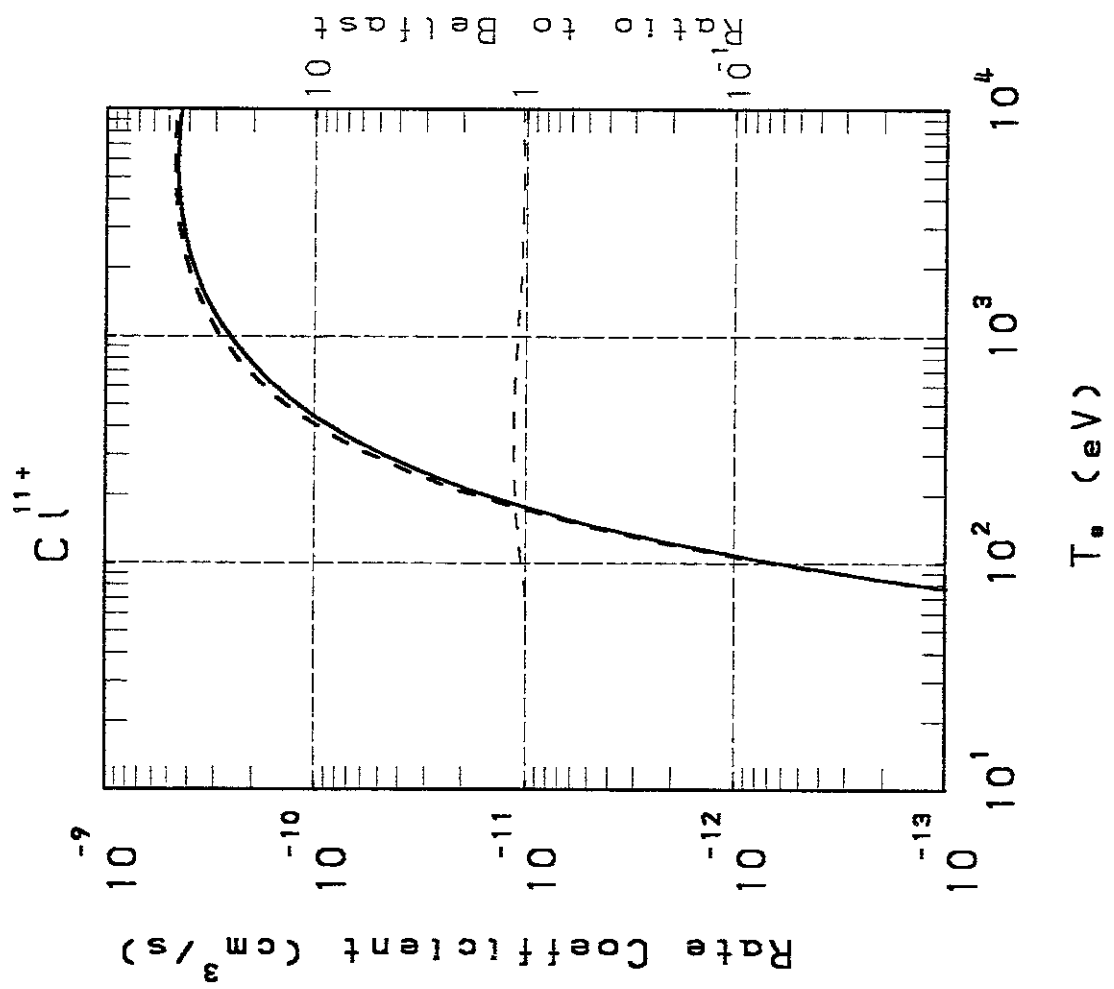


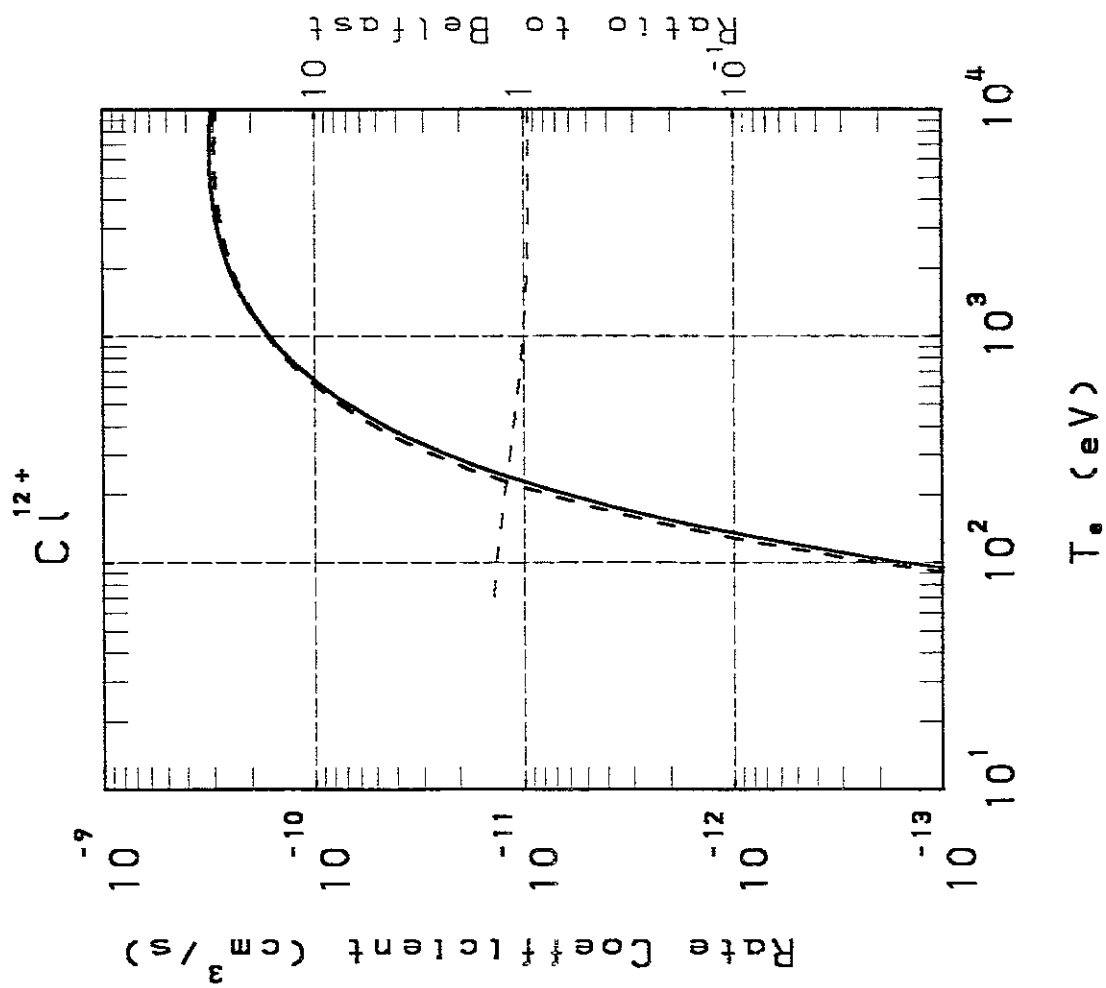
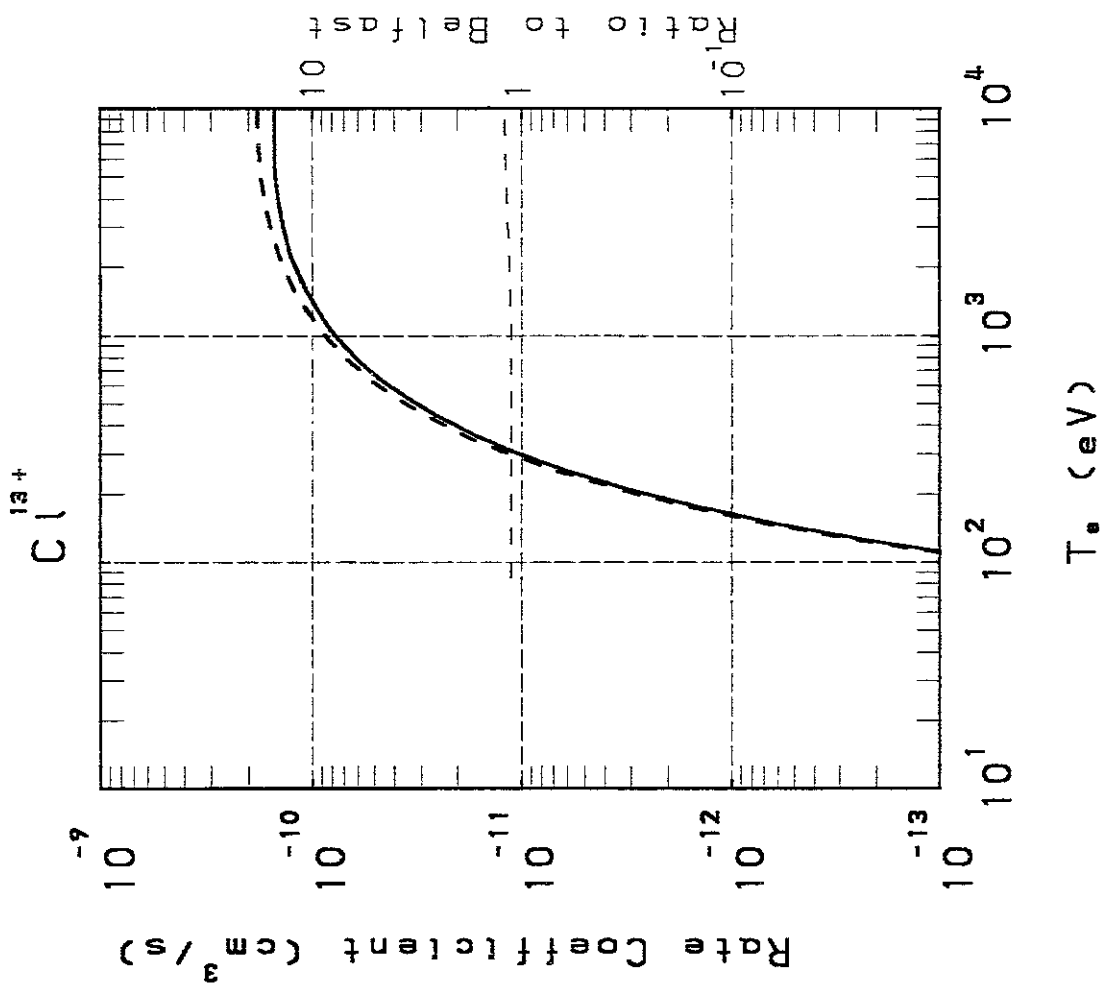


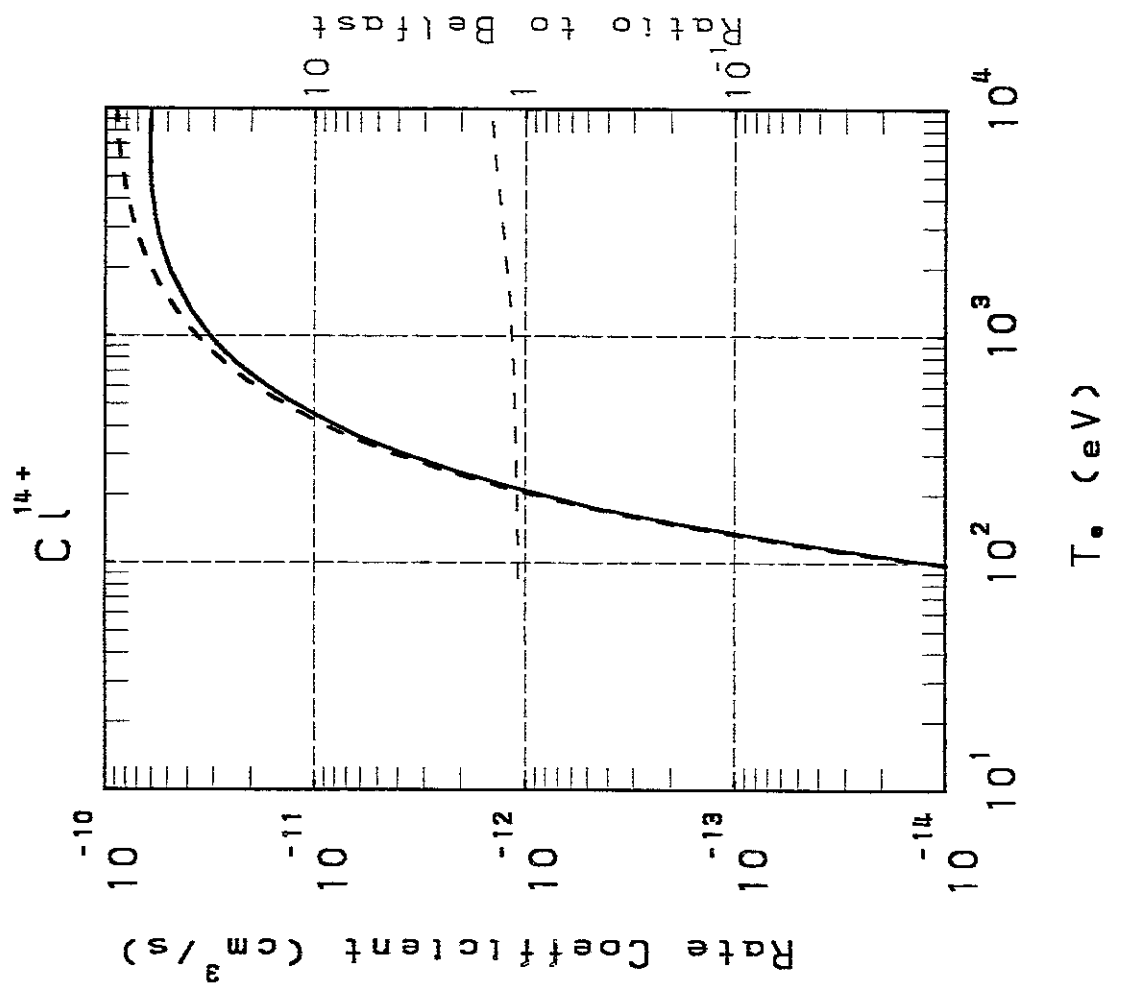
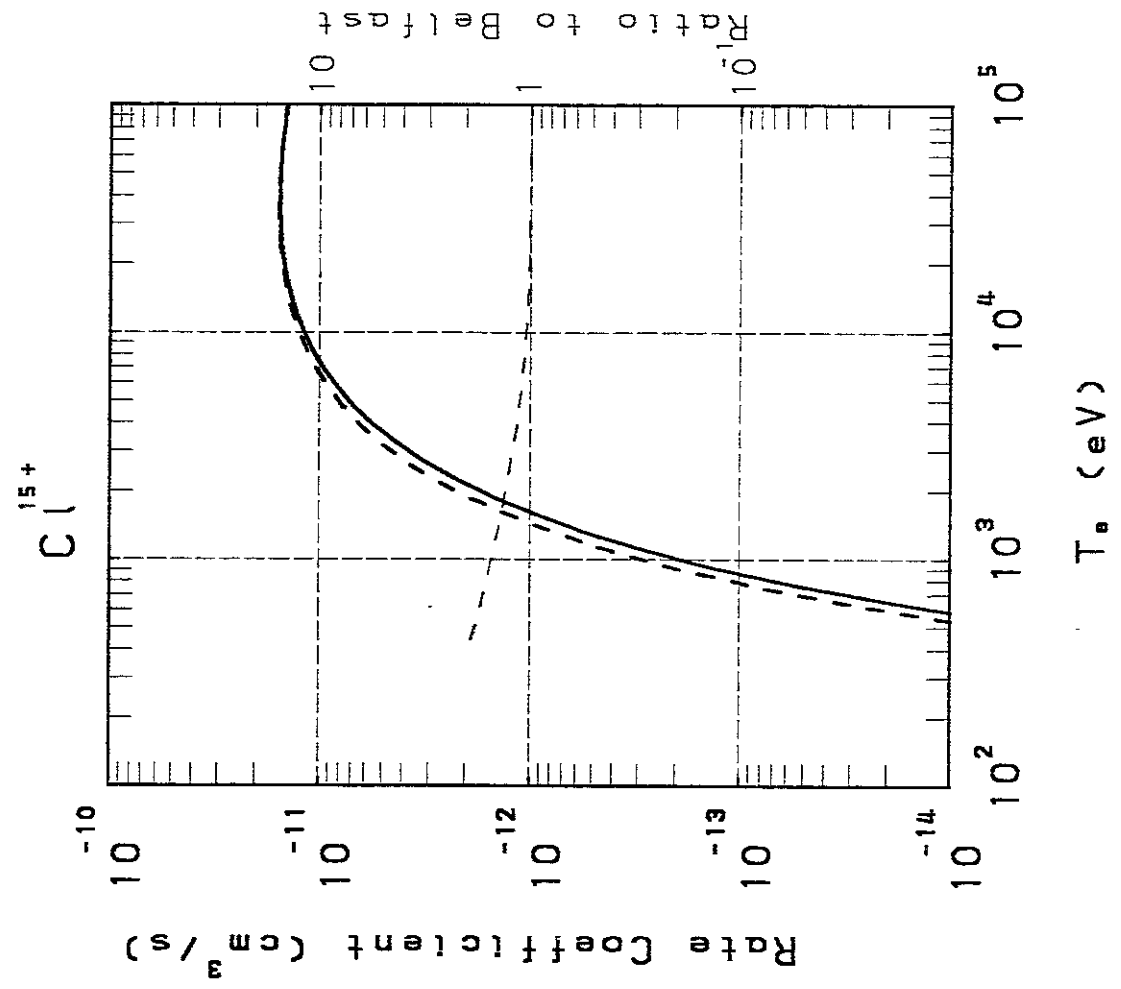


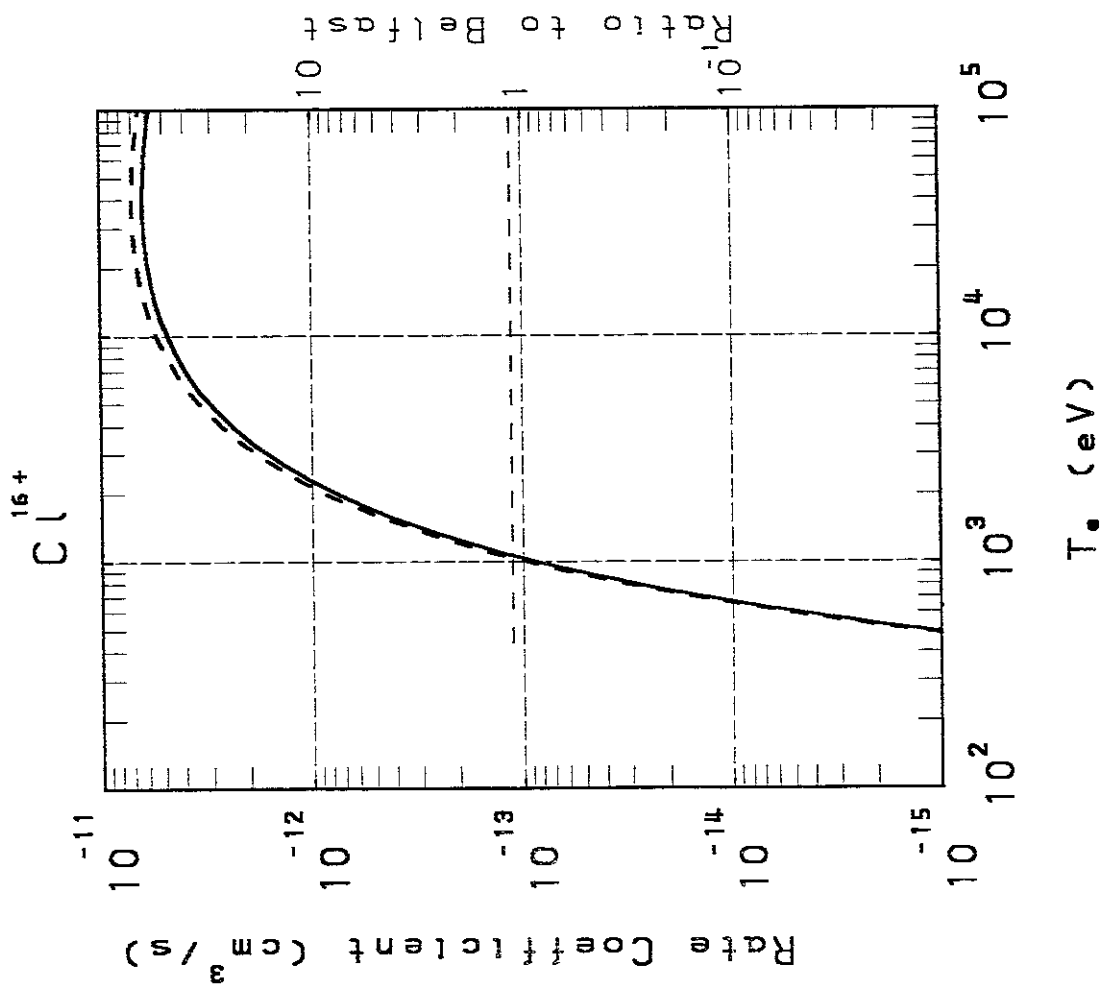


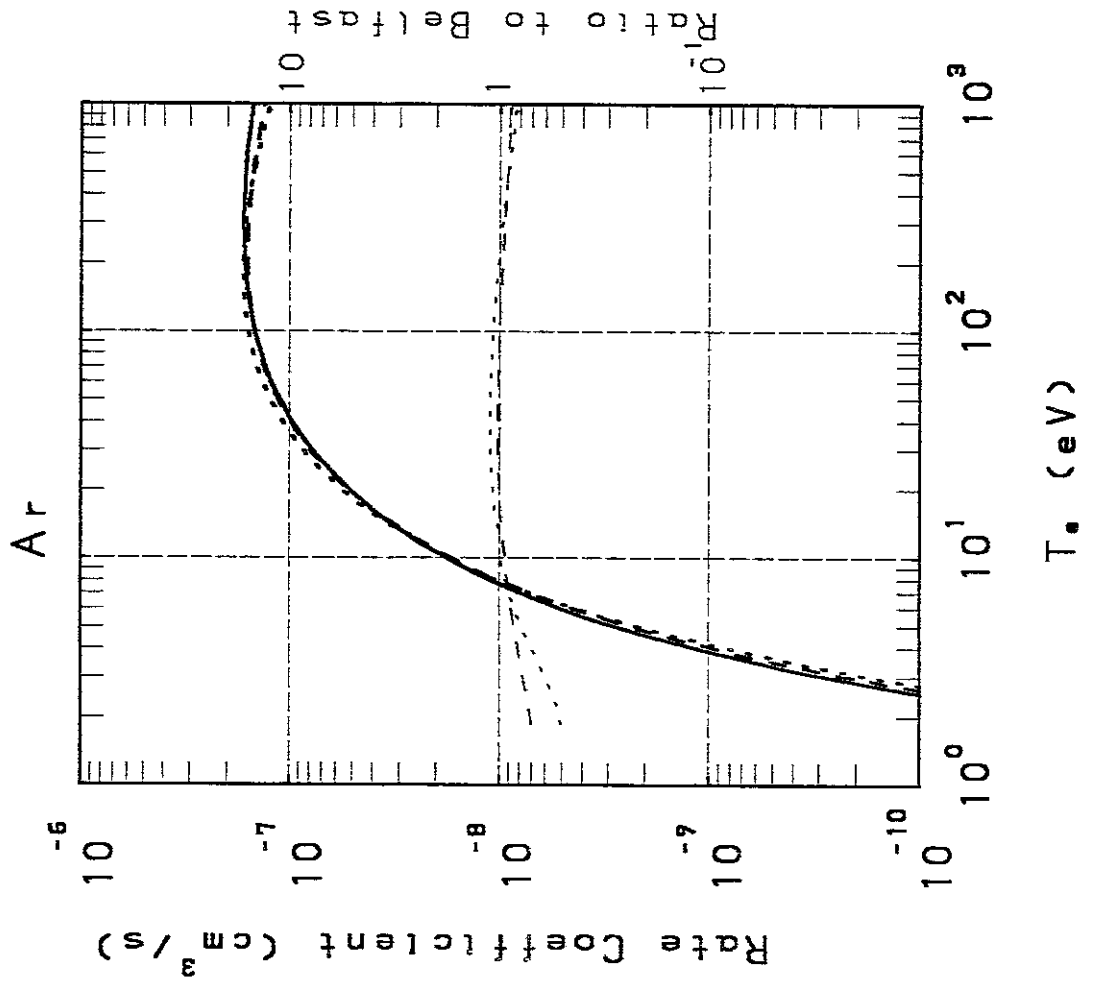
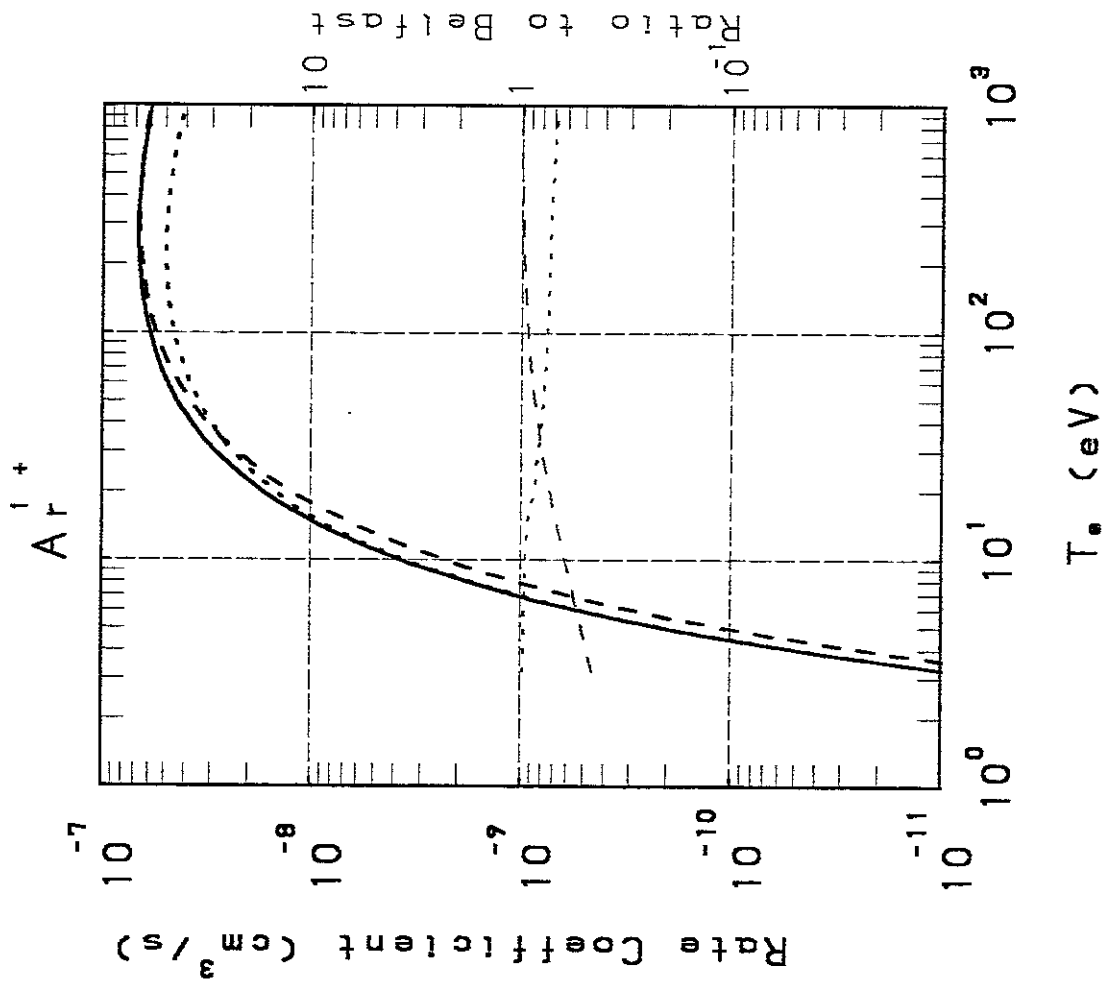


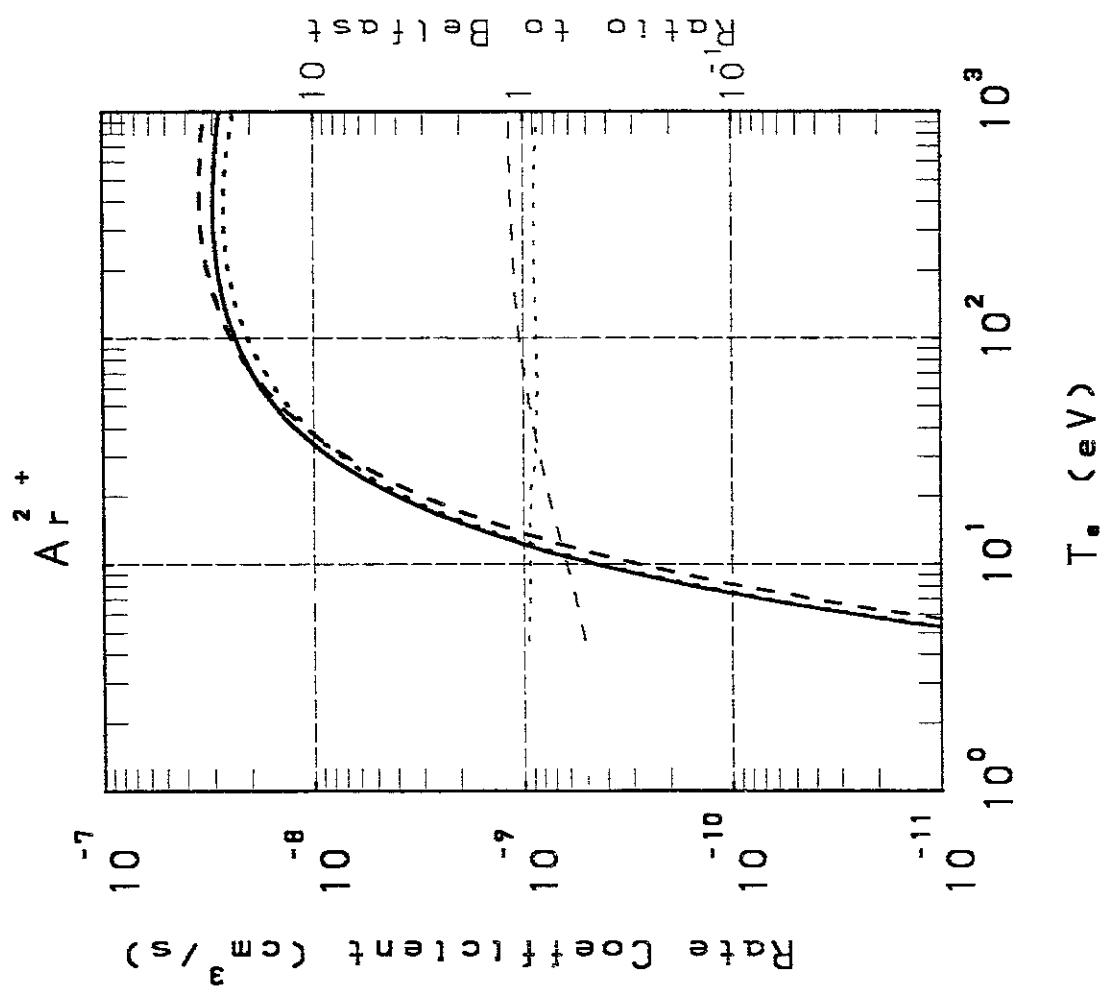
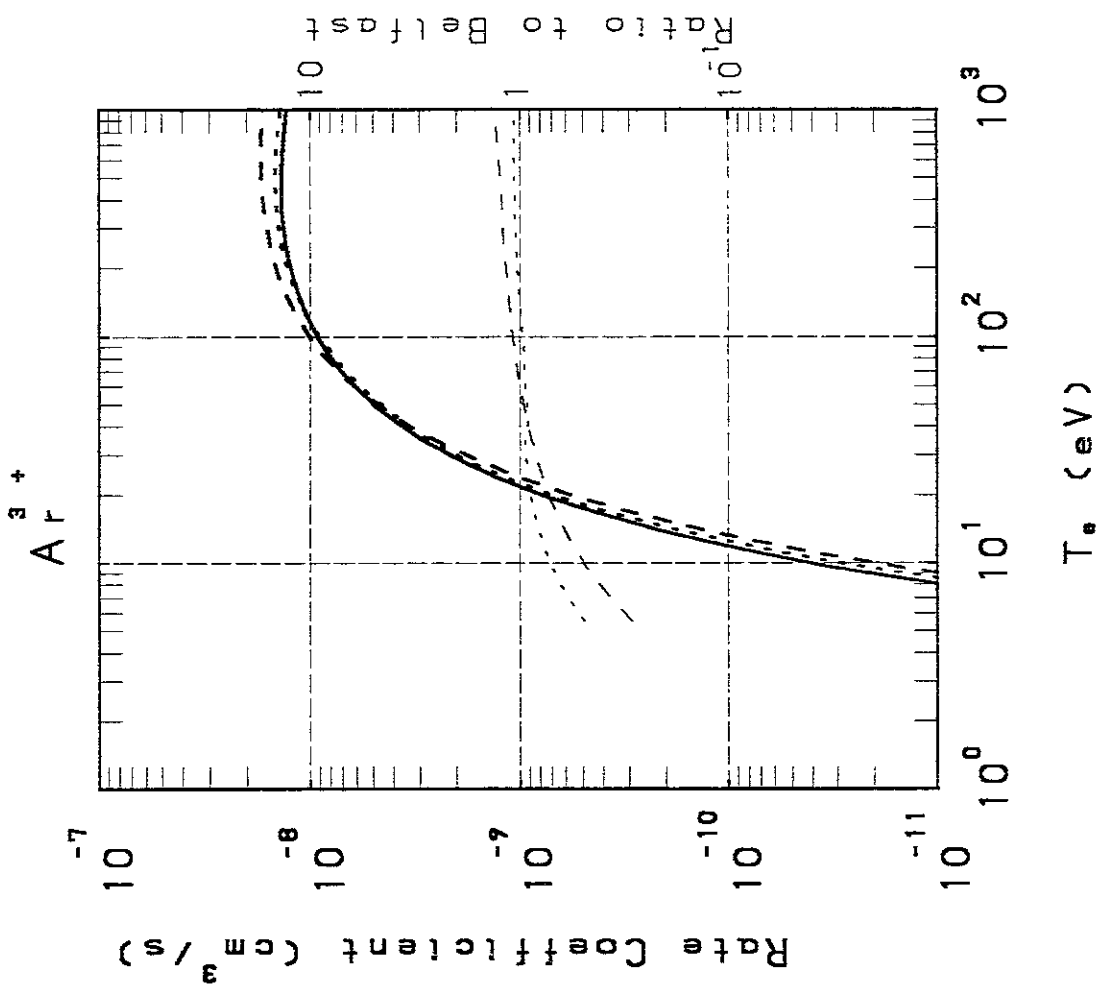


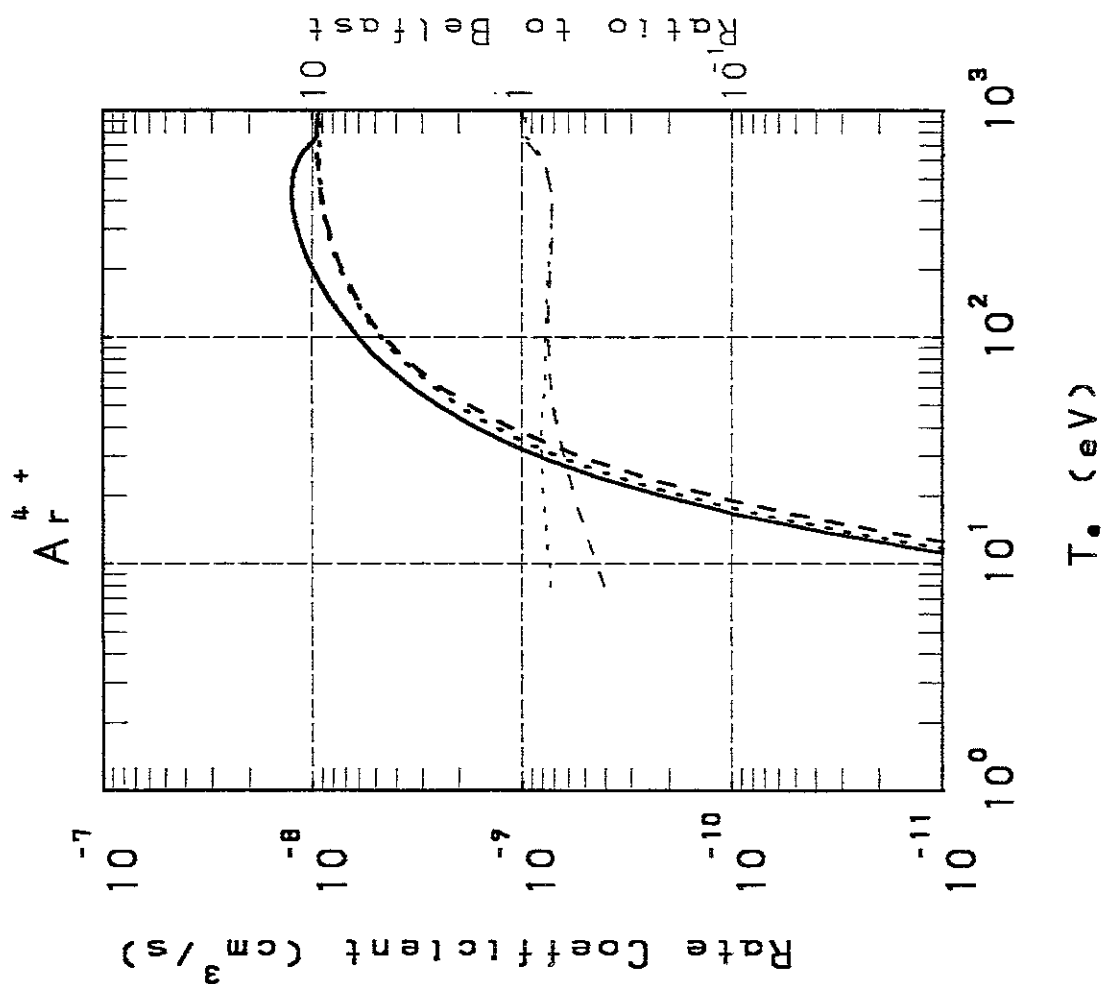
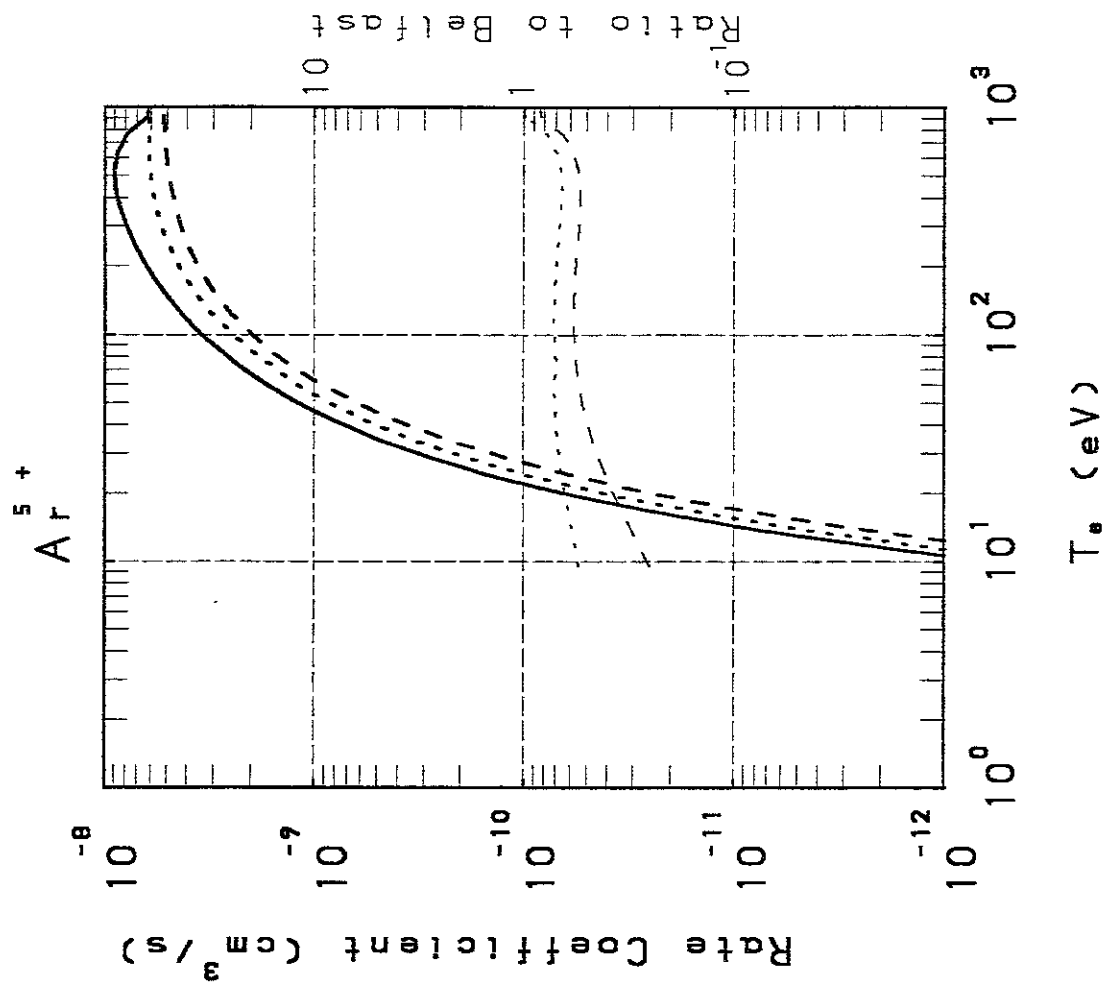


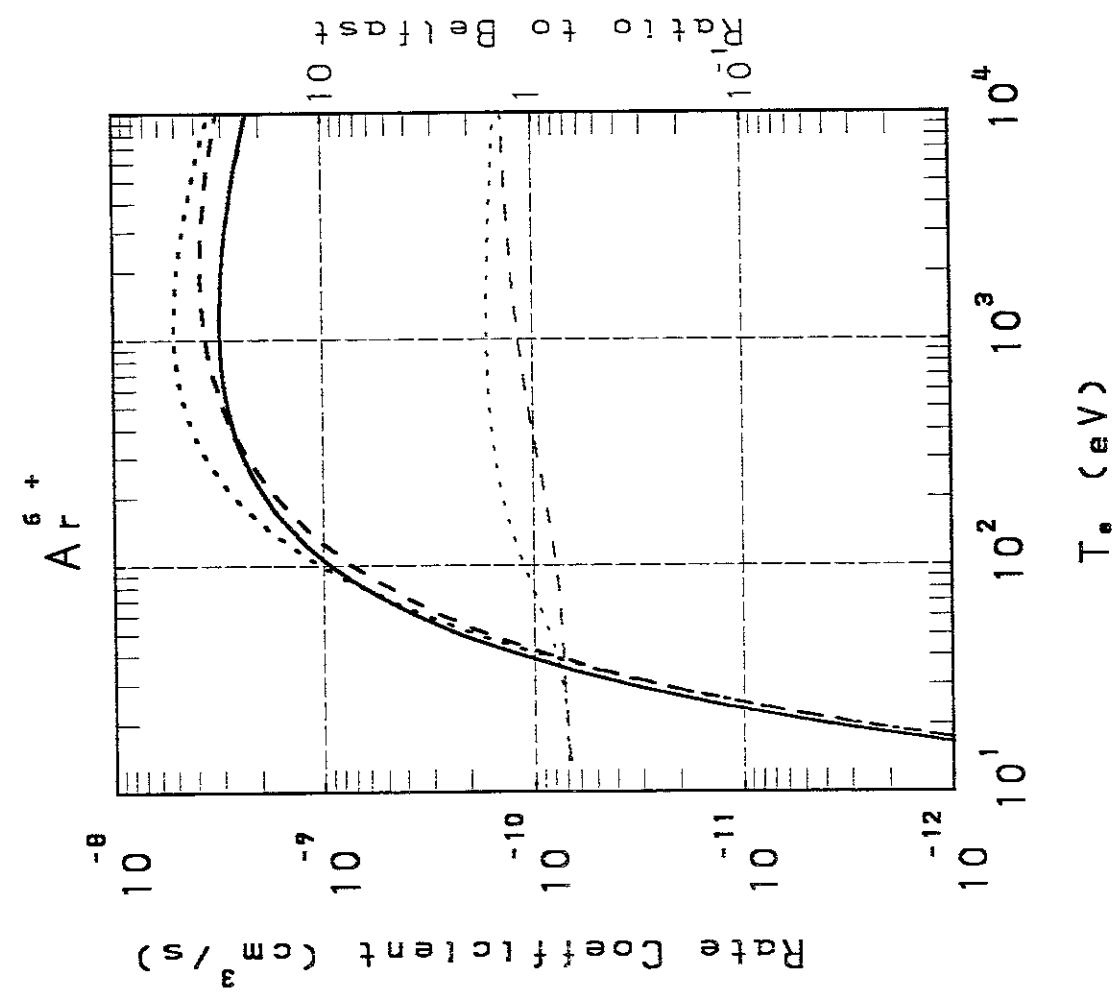
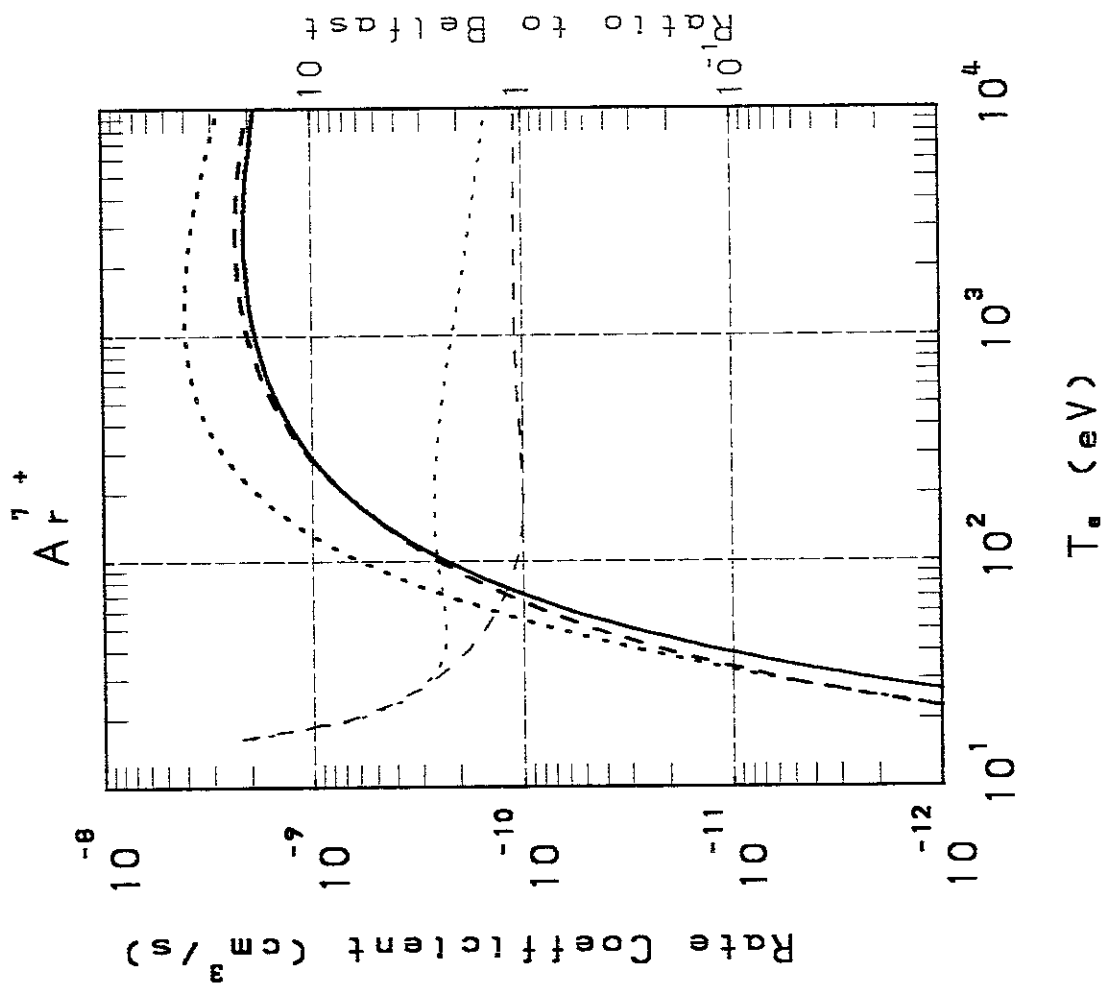


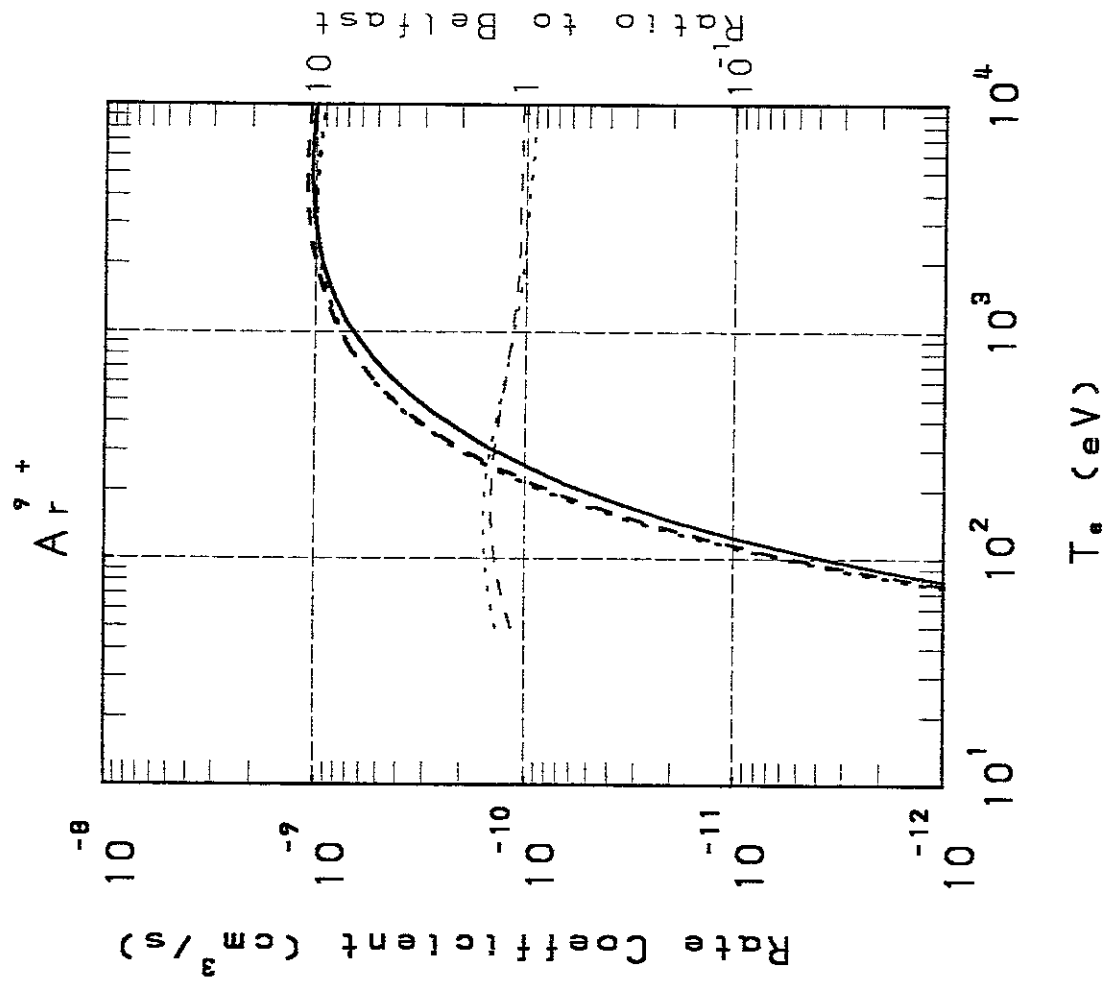
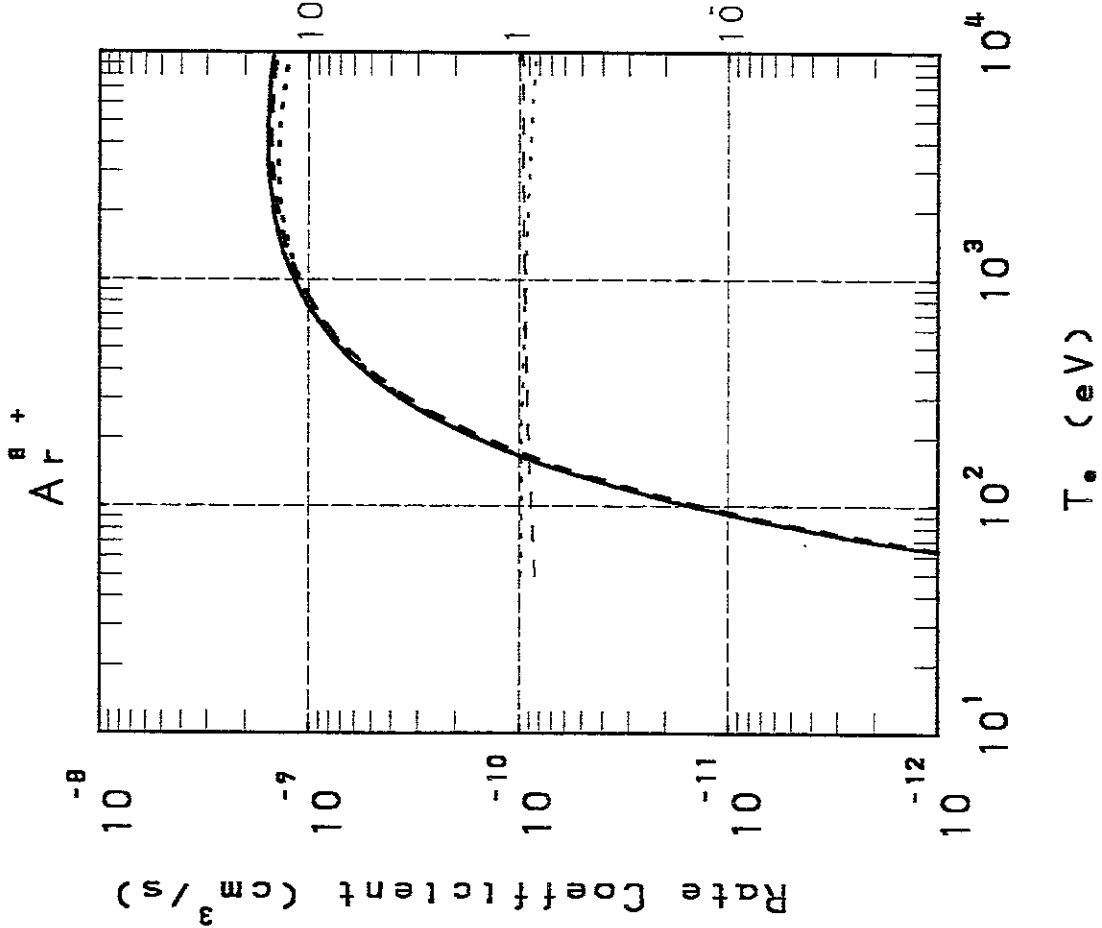


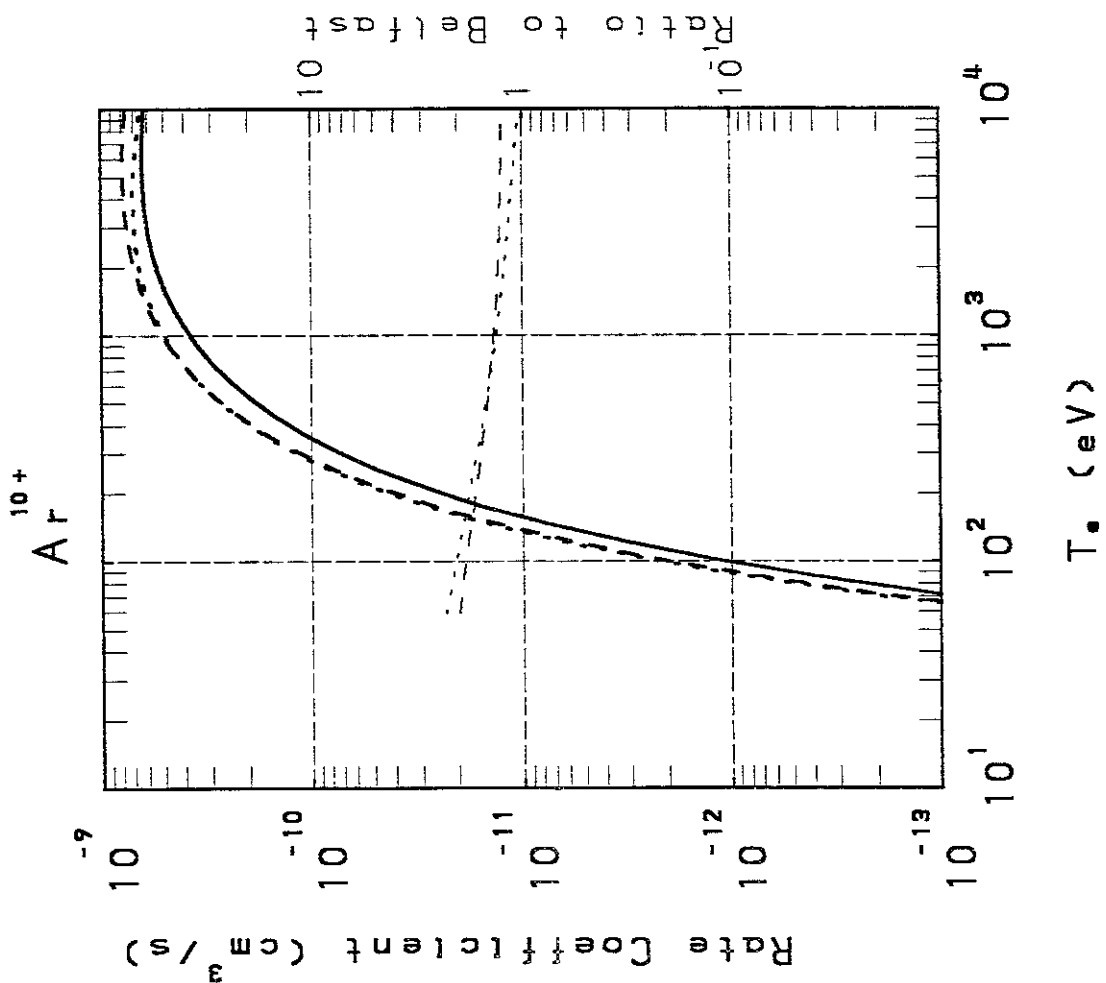
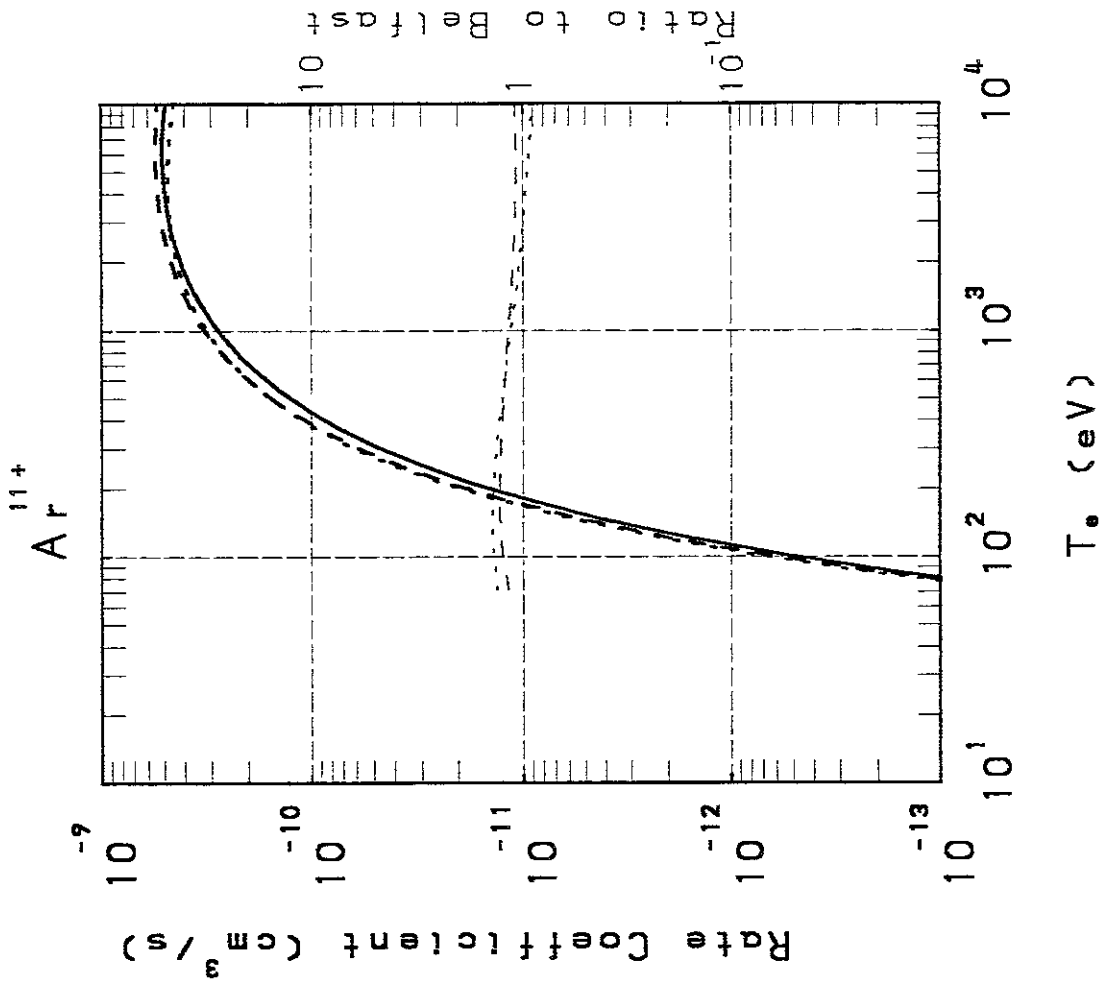


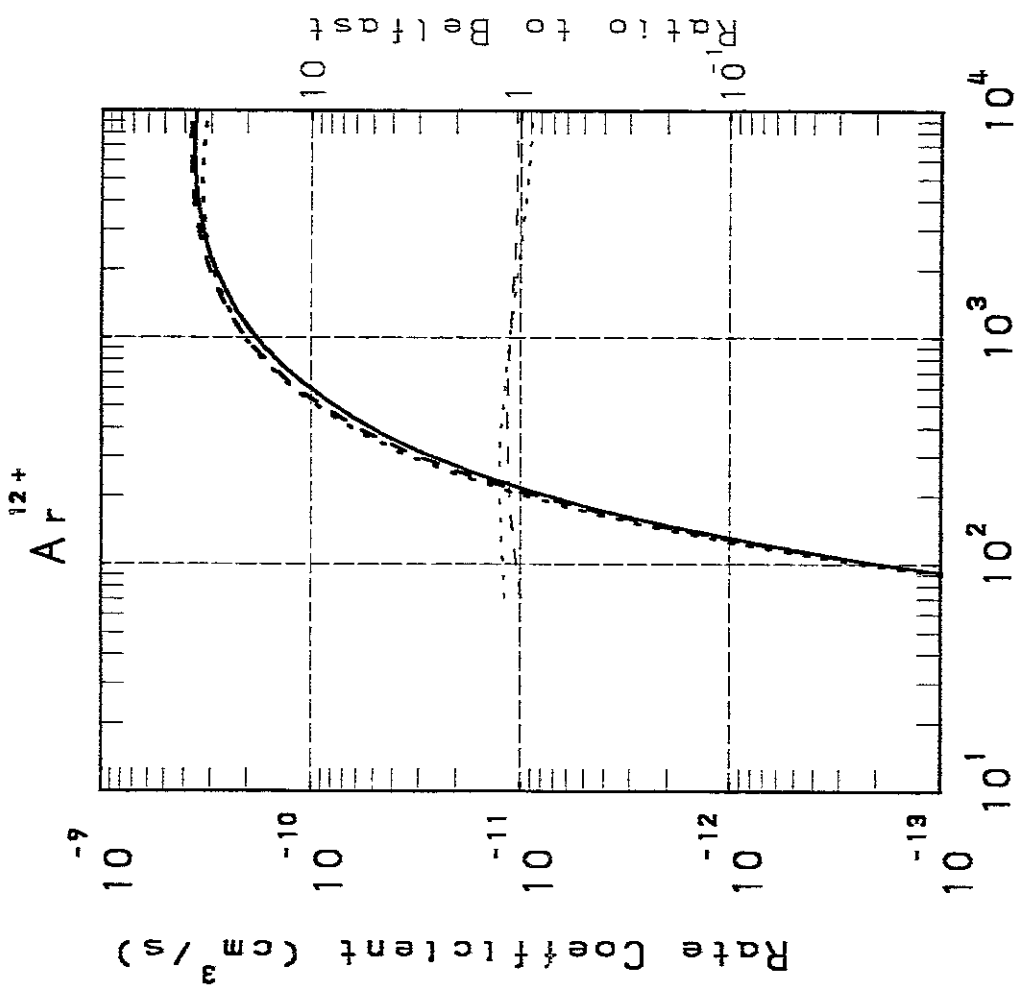
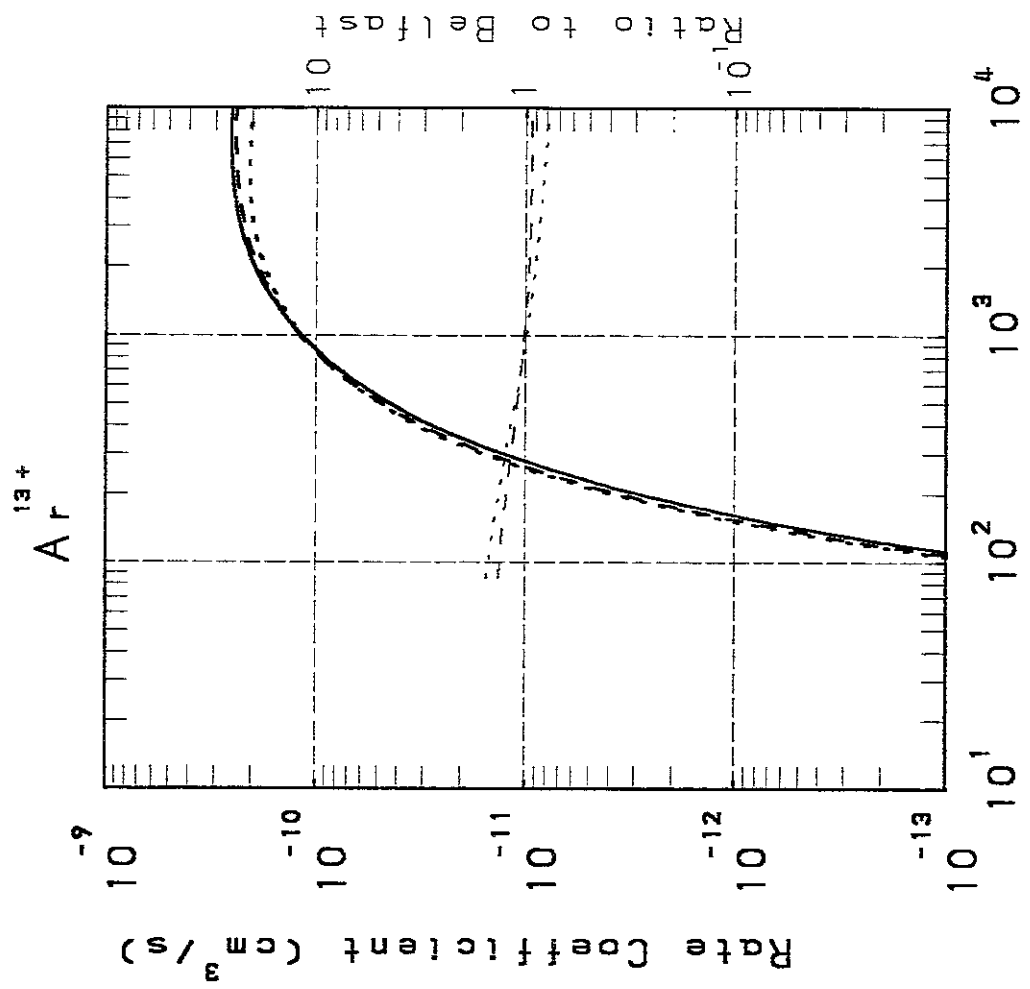


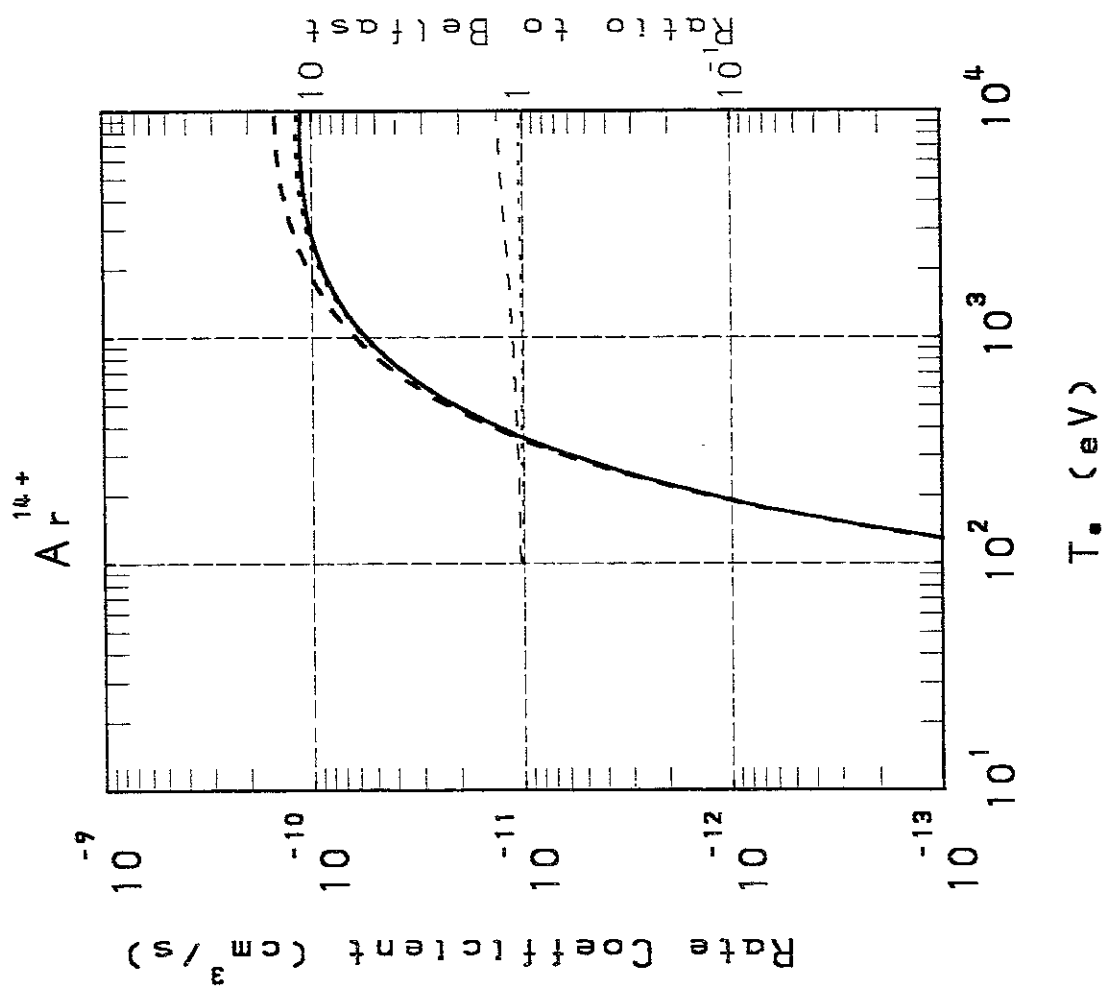
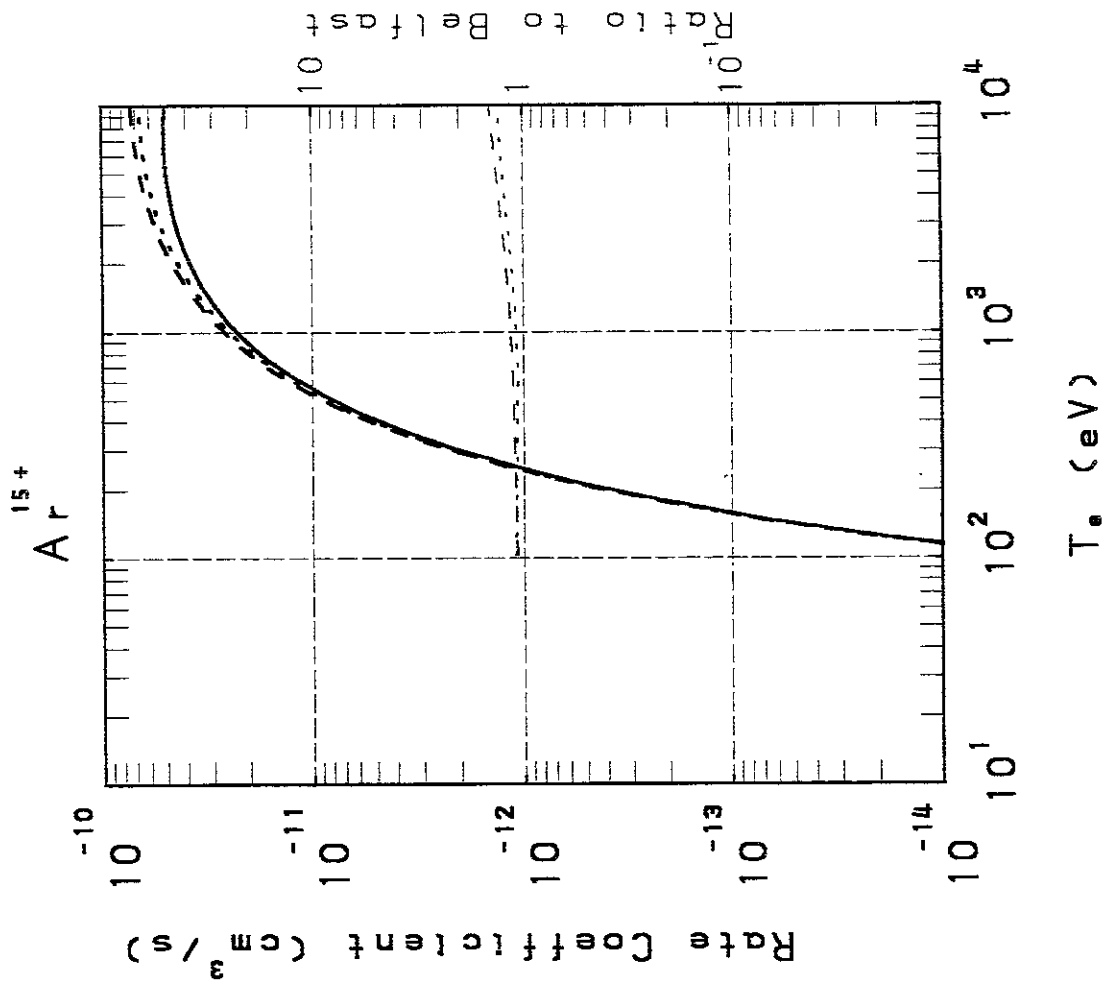


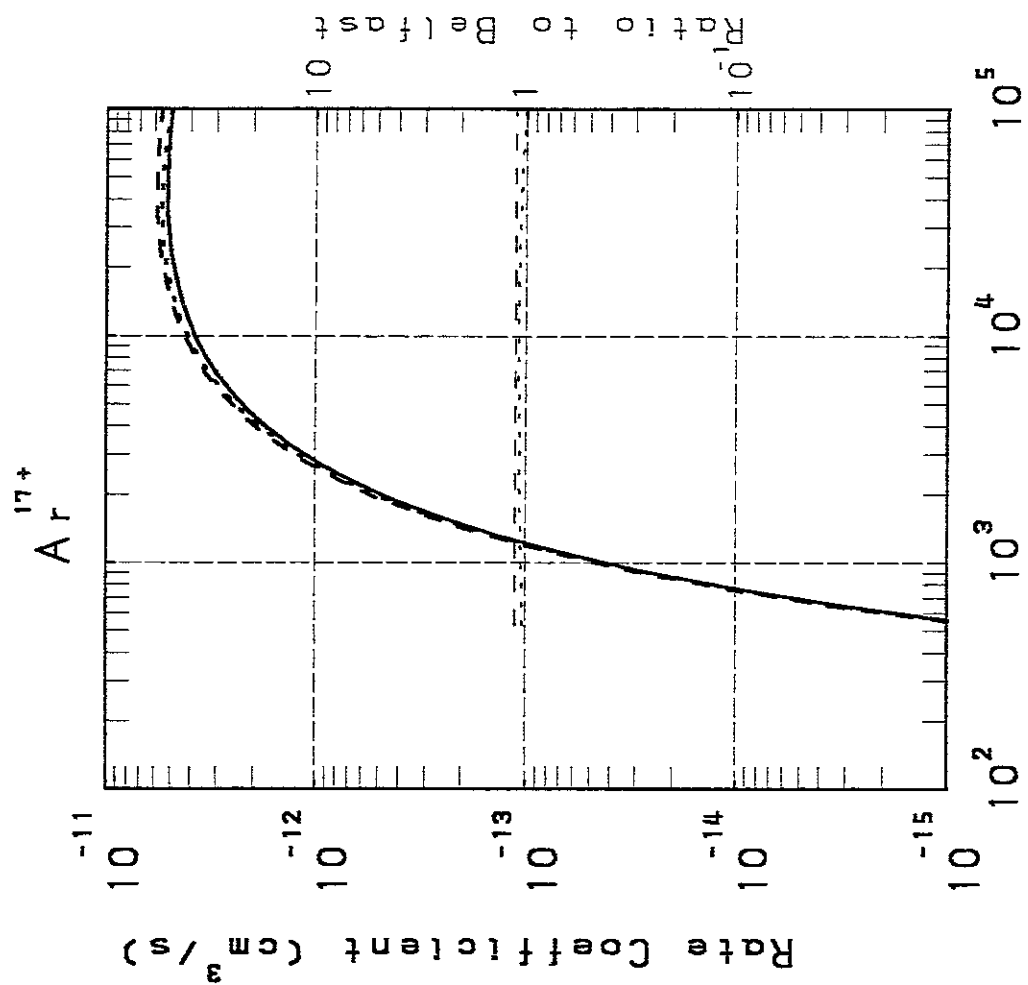




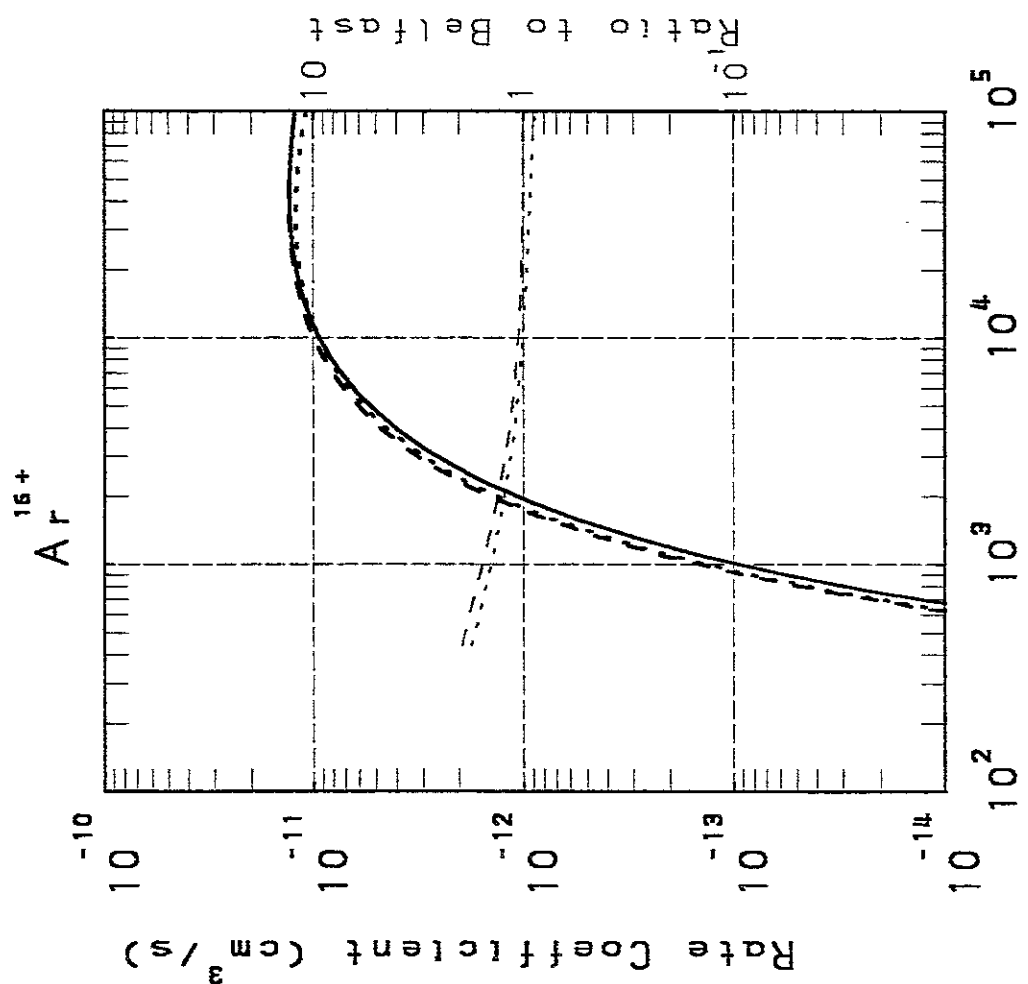




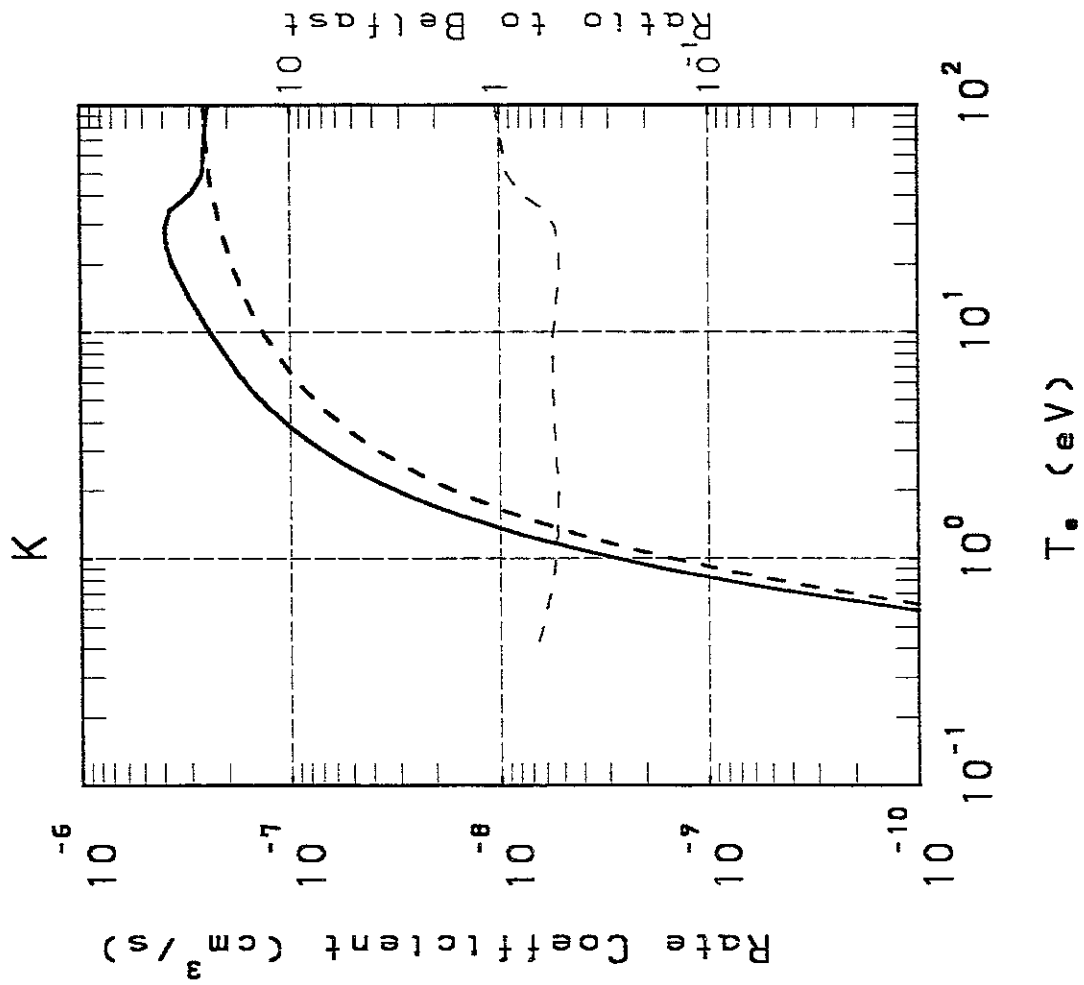
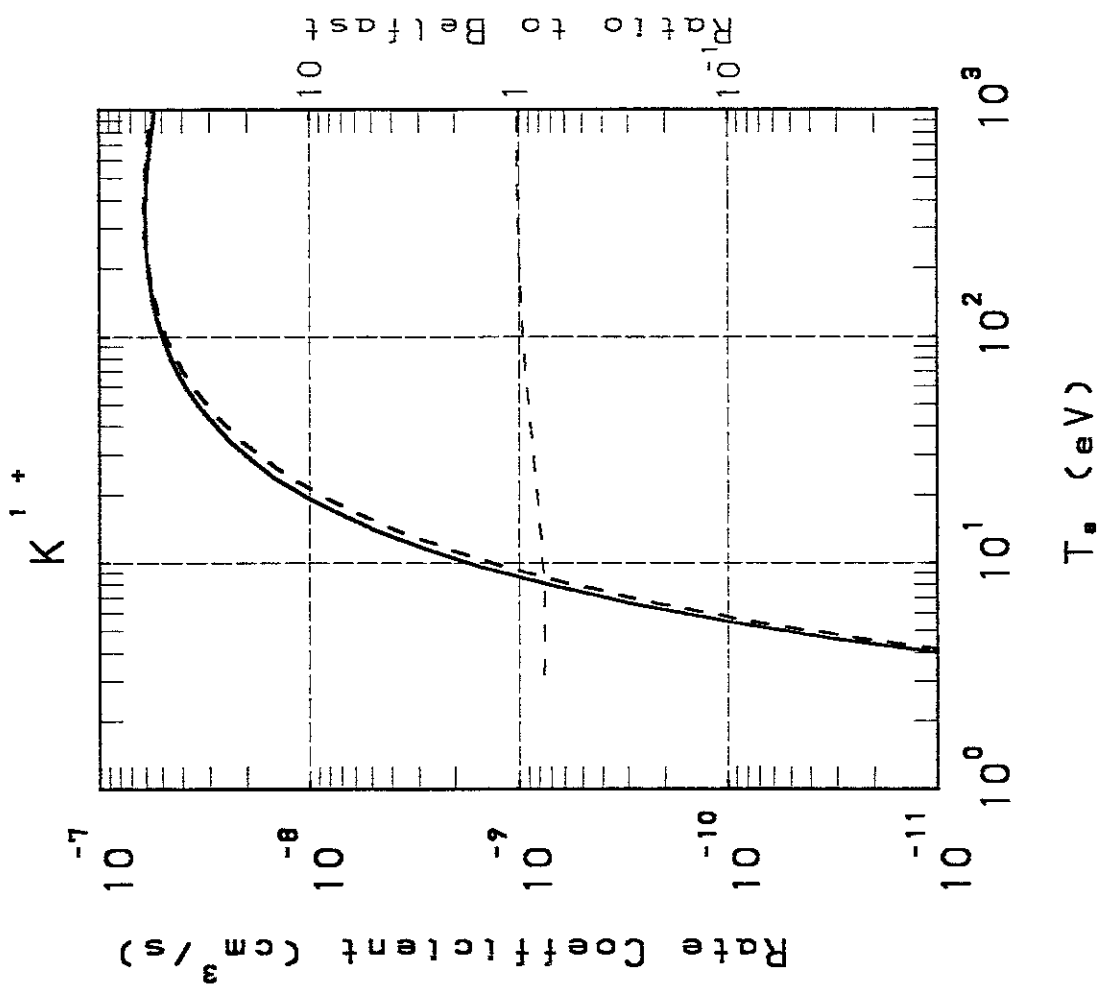


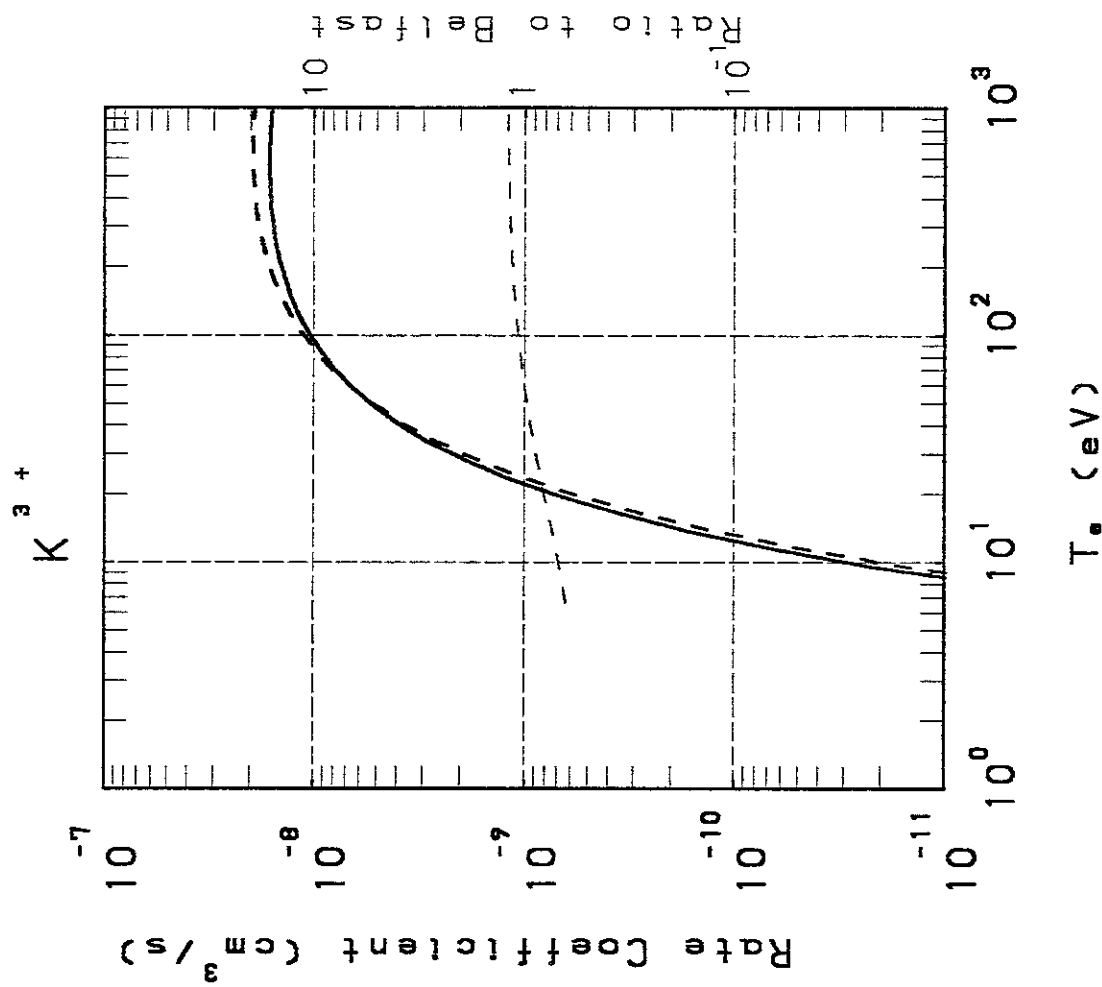
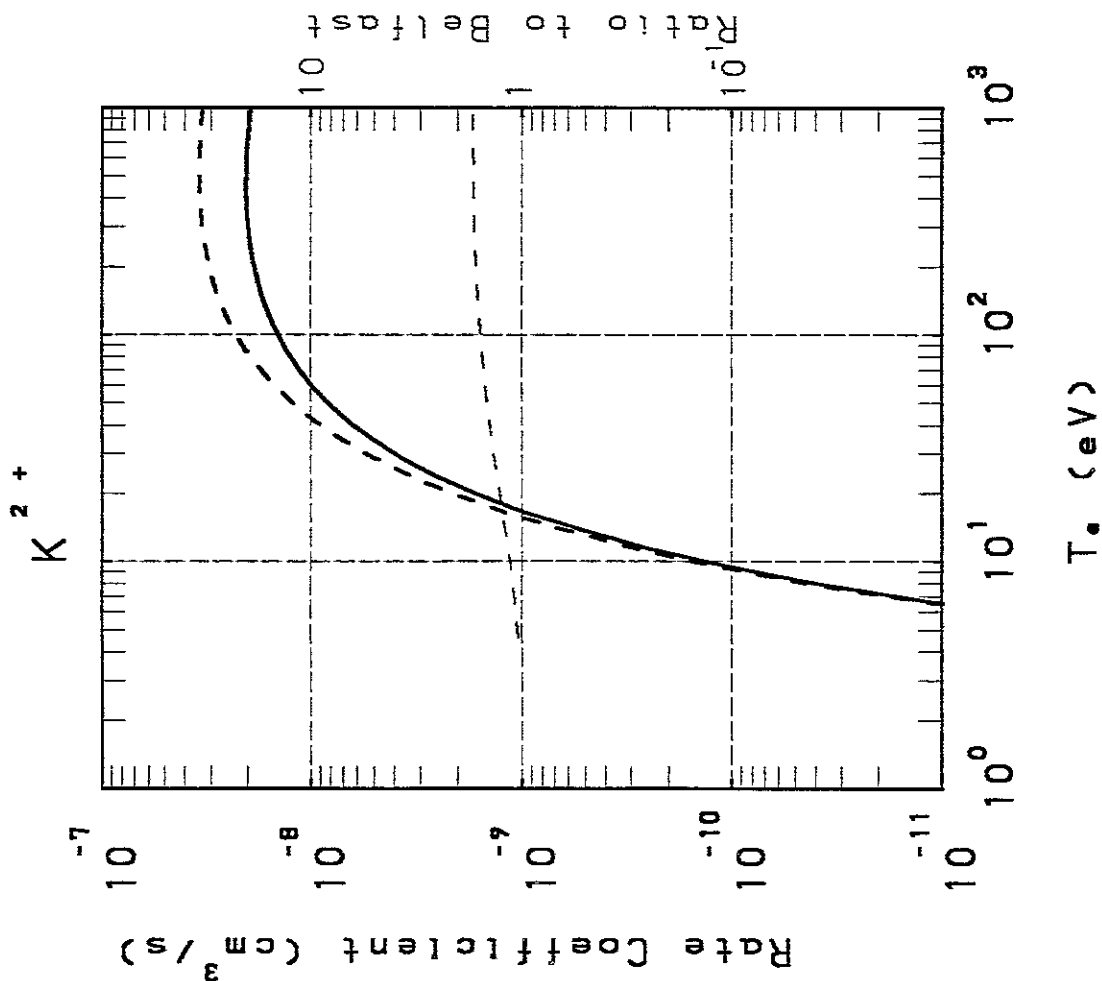


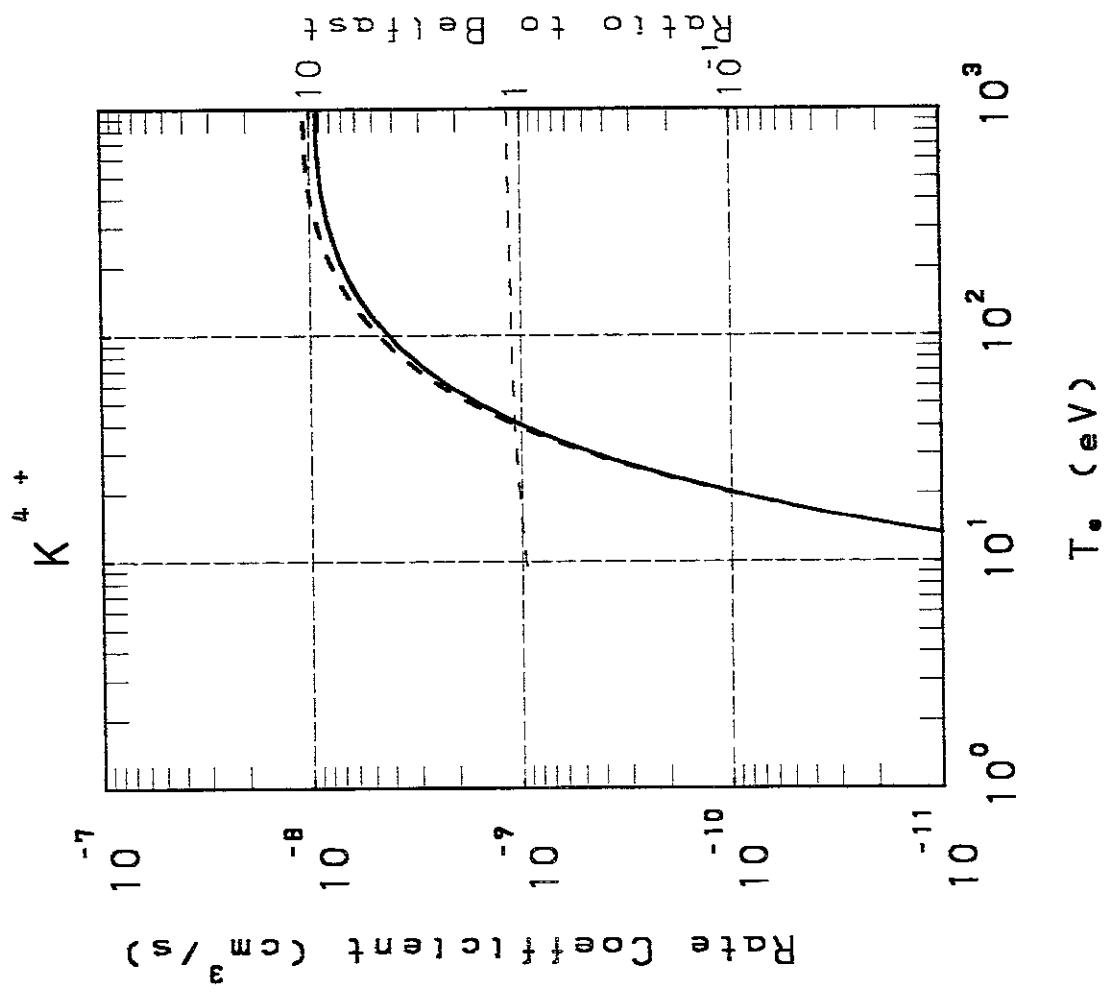
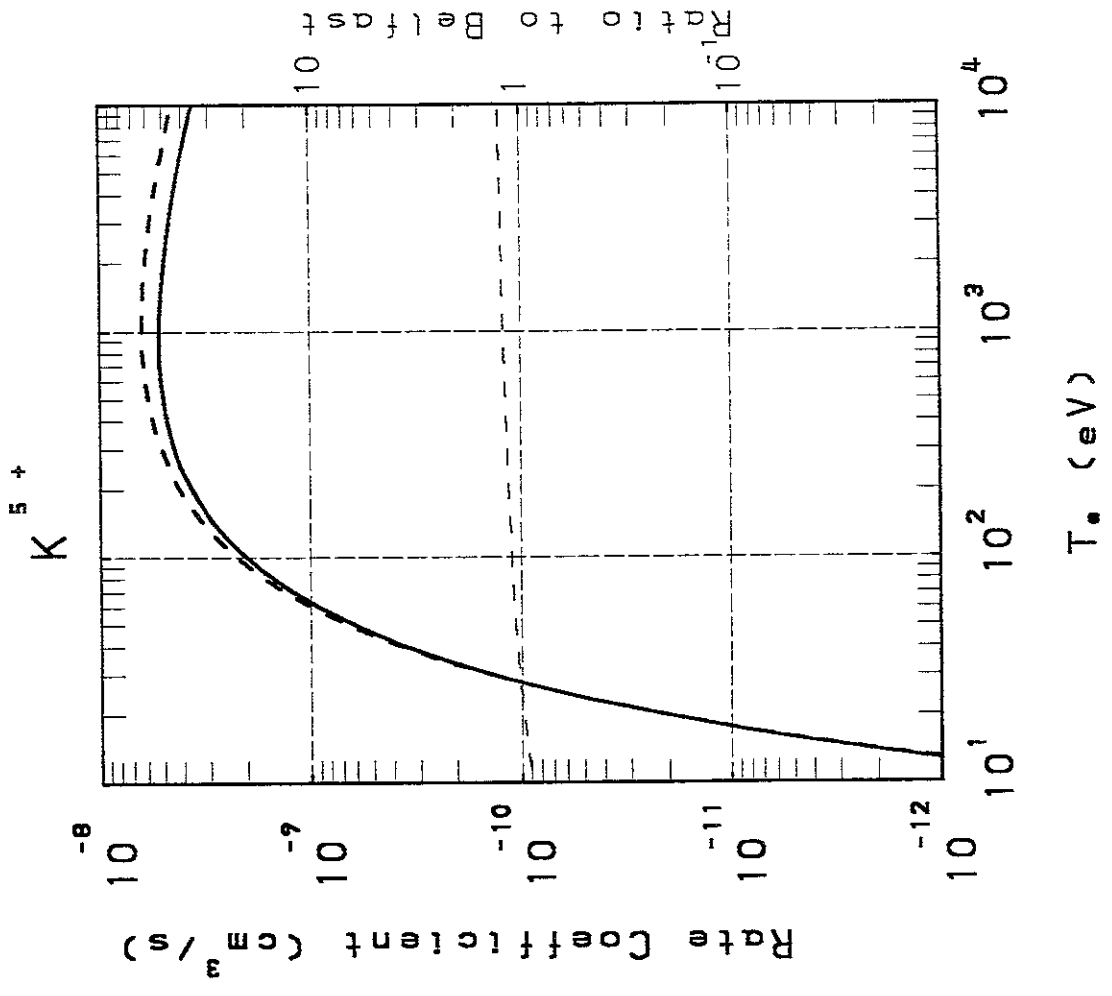
T_e (eV)

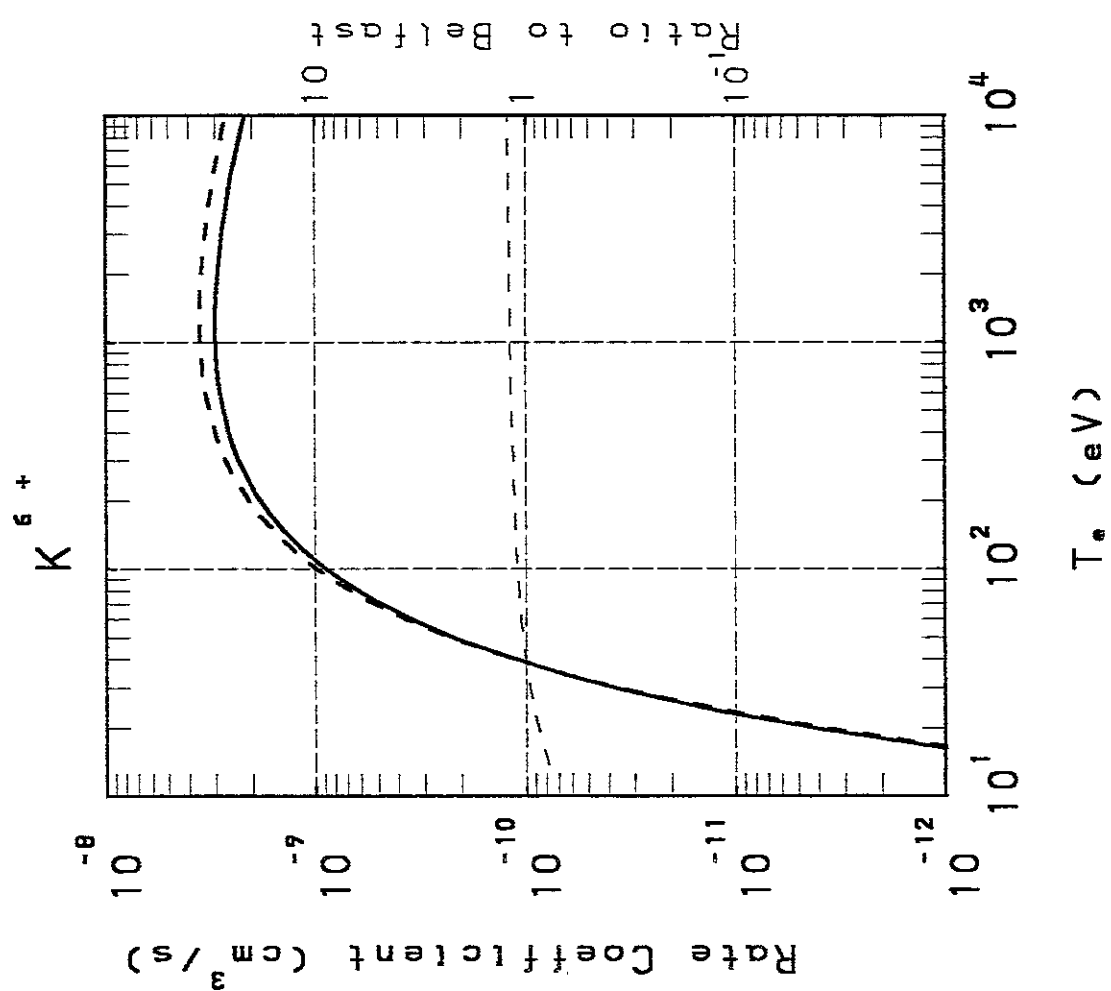
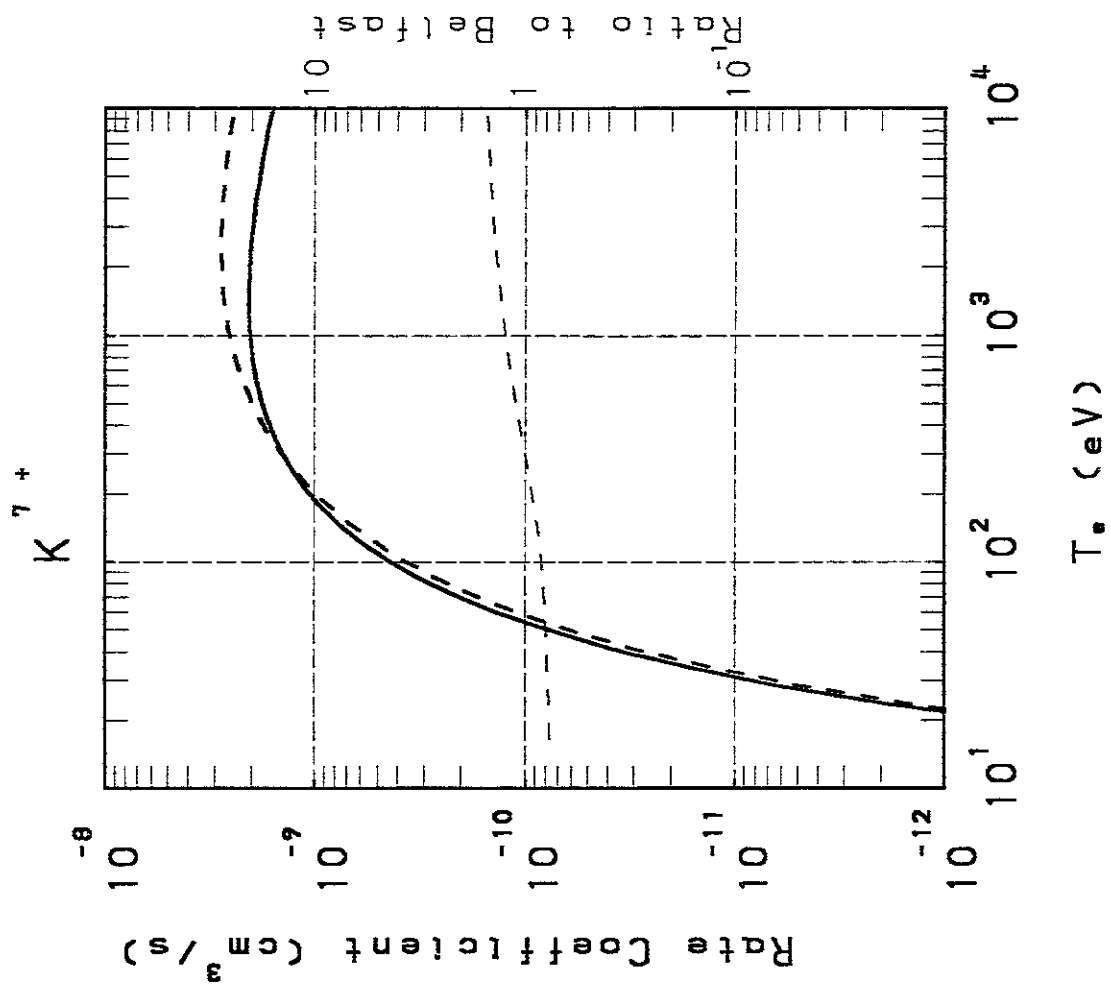


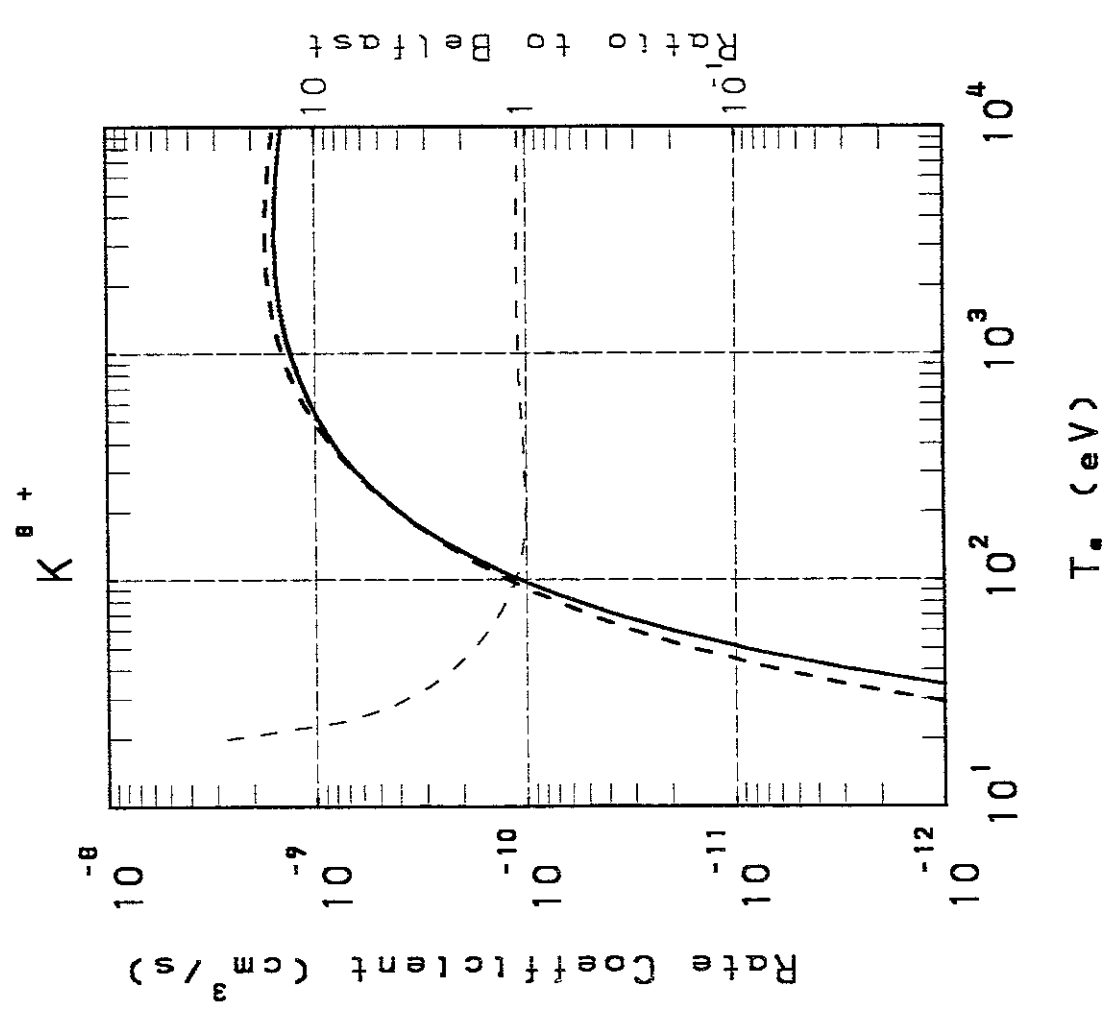
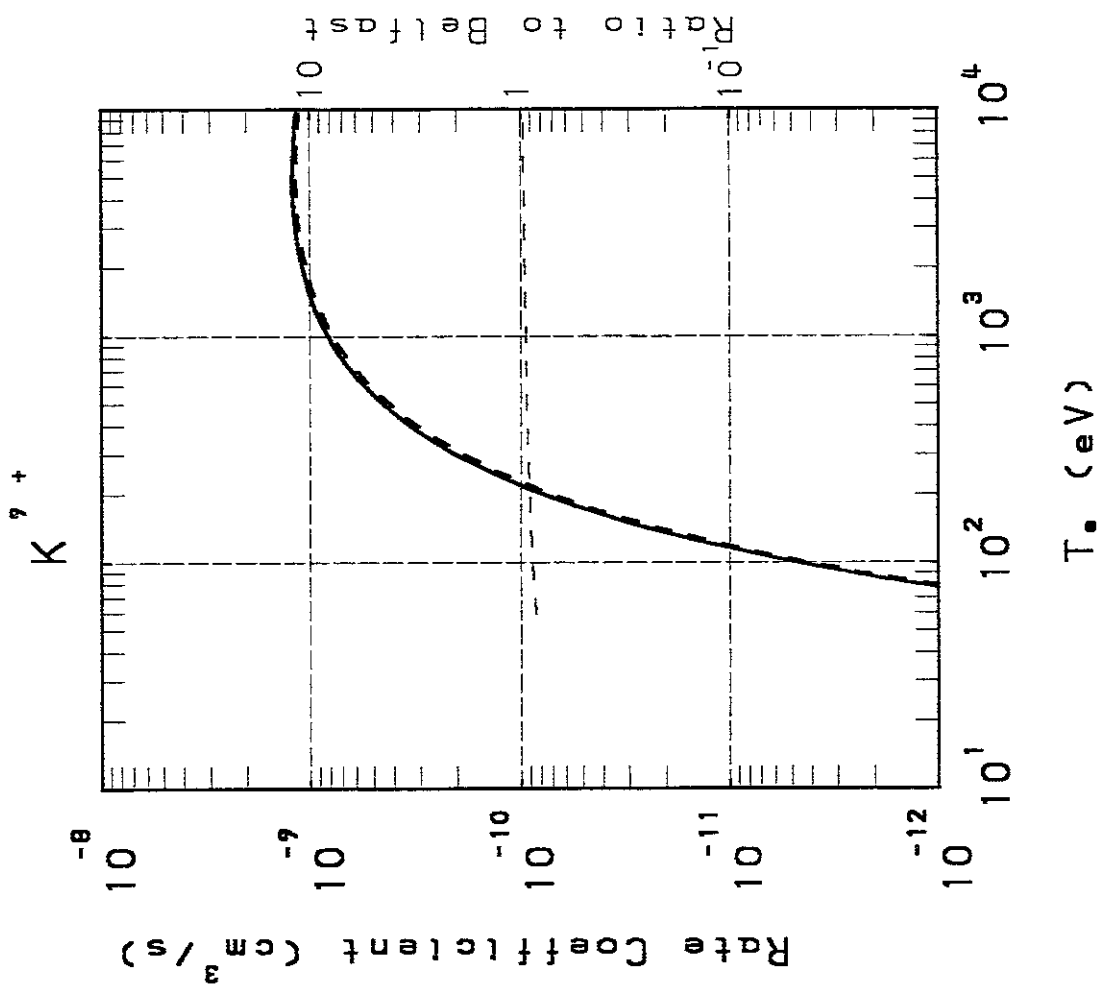
T_e (eV)

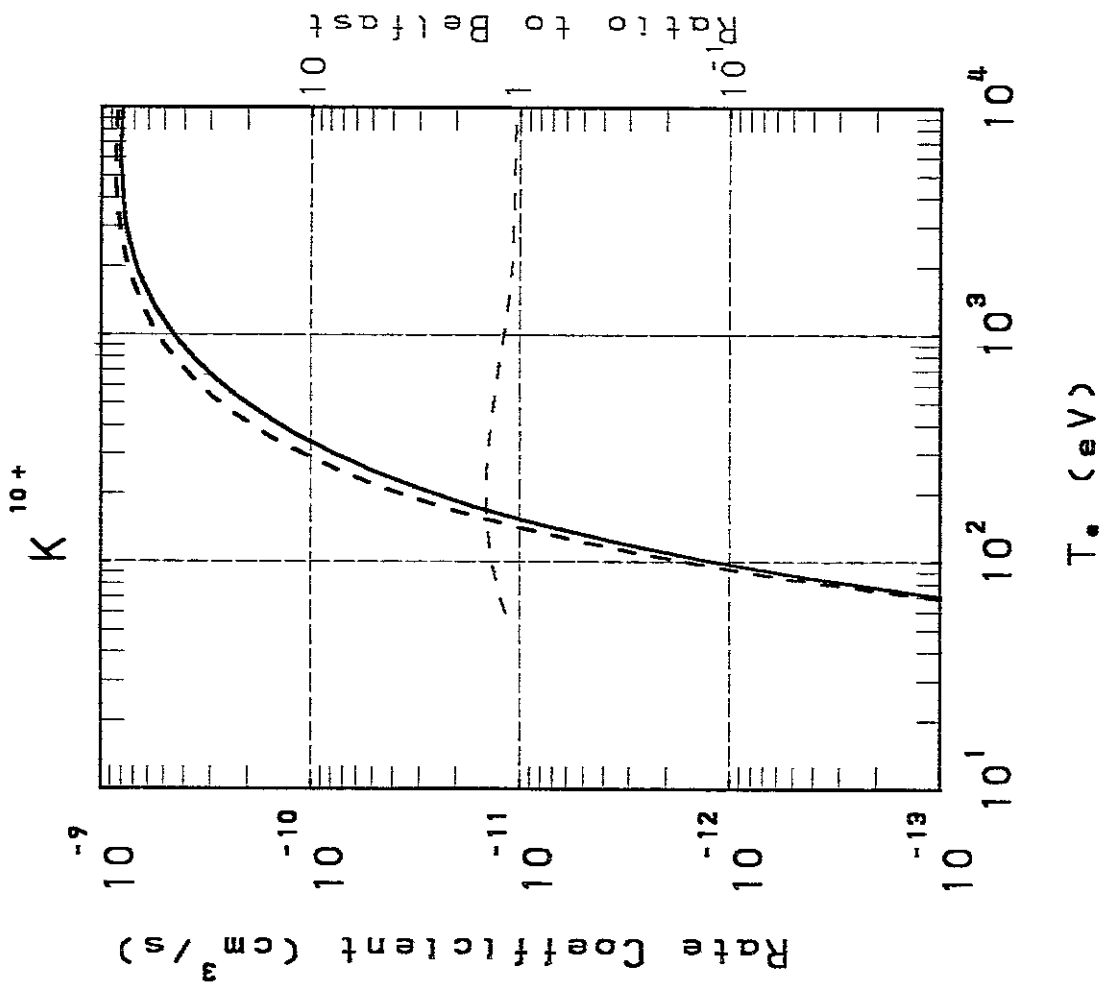
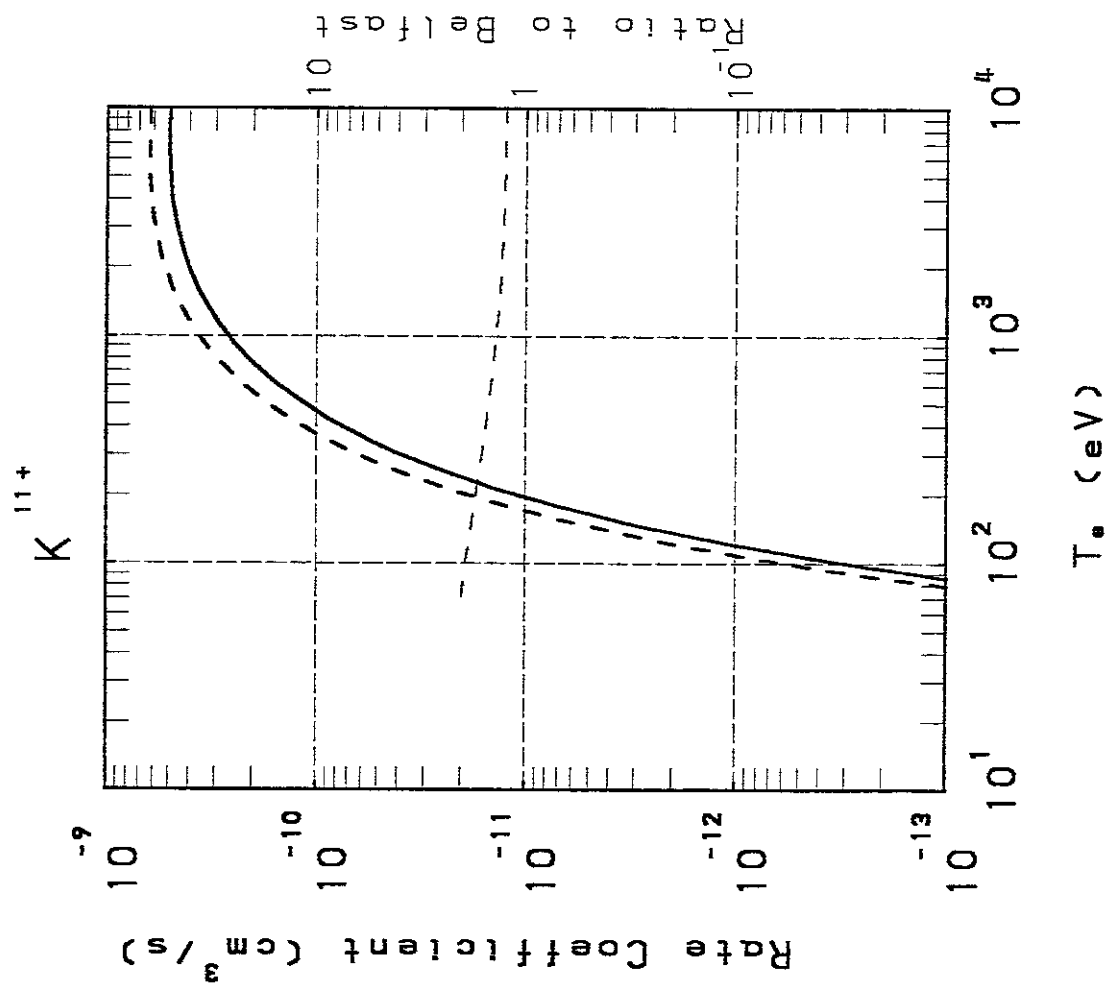


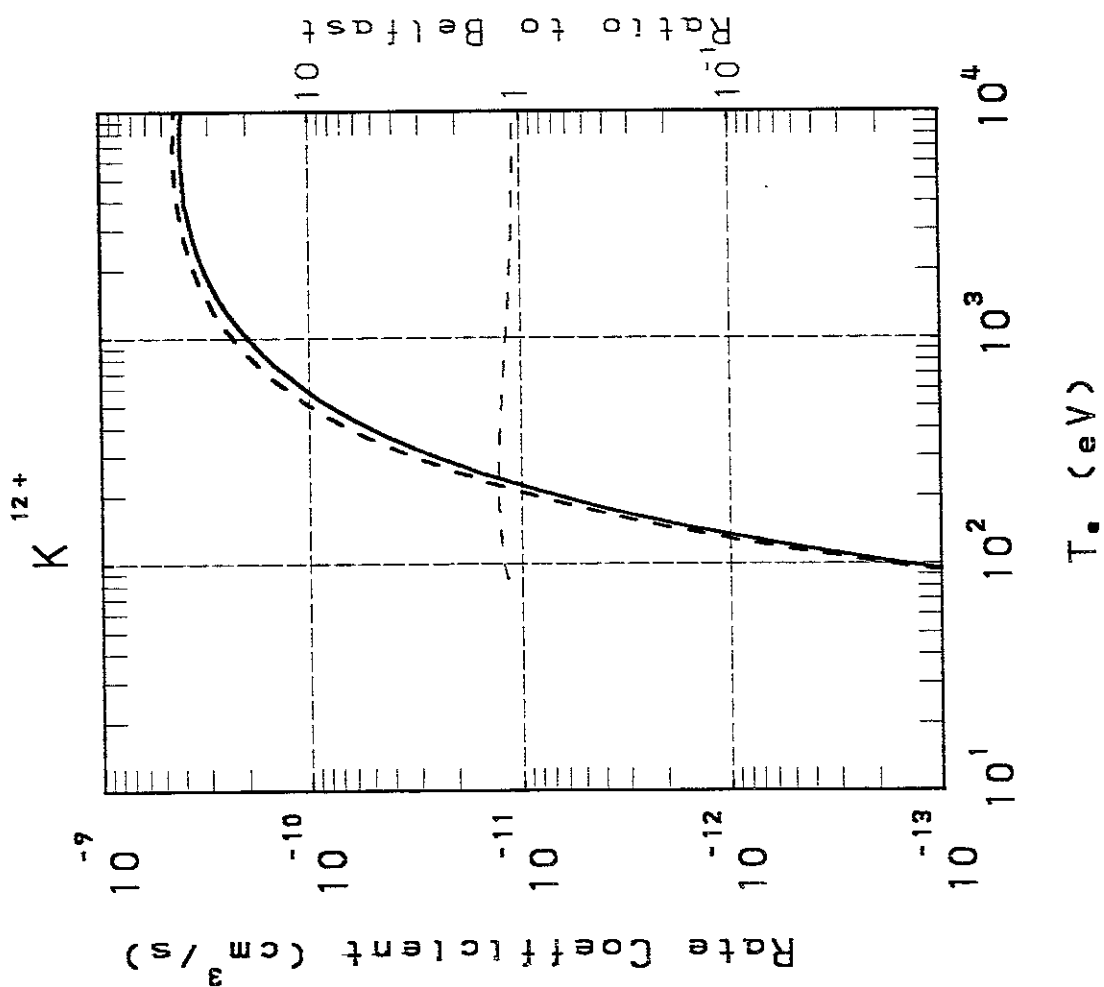
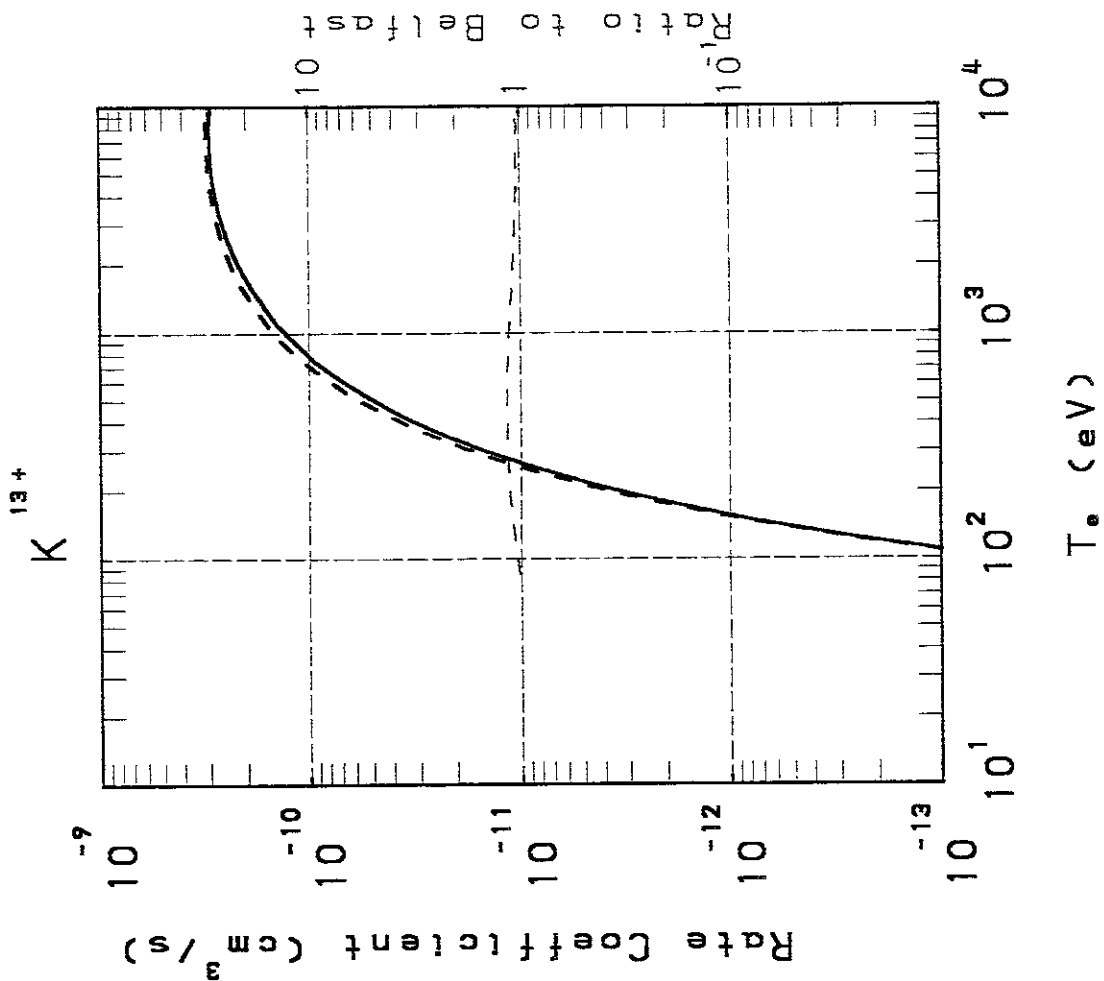


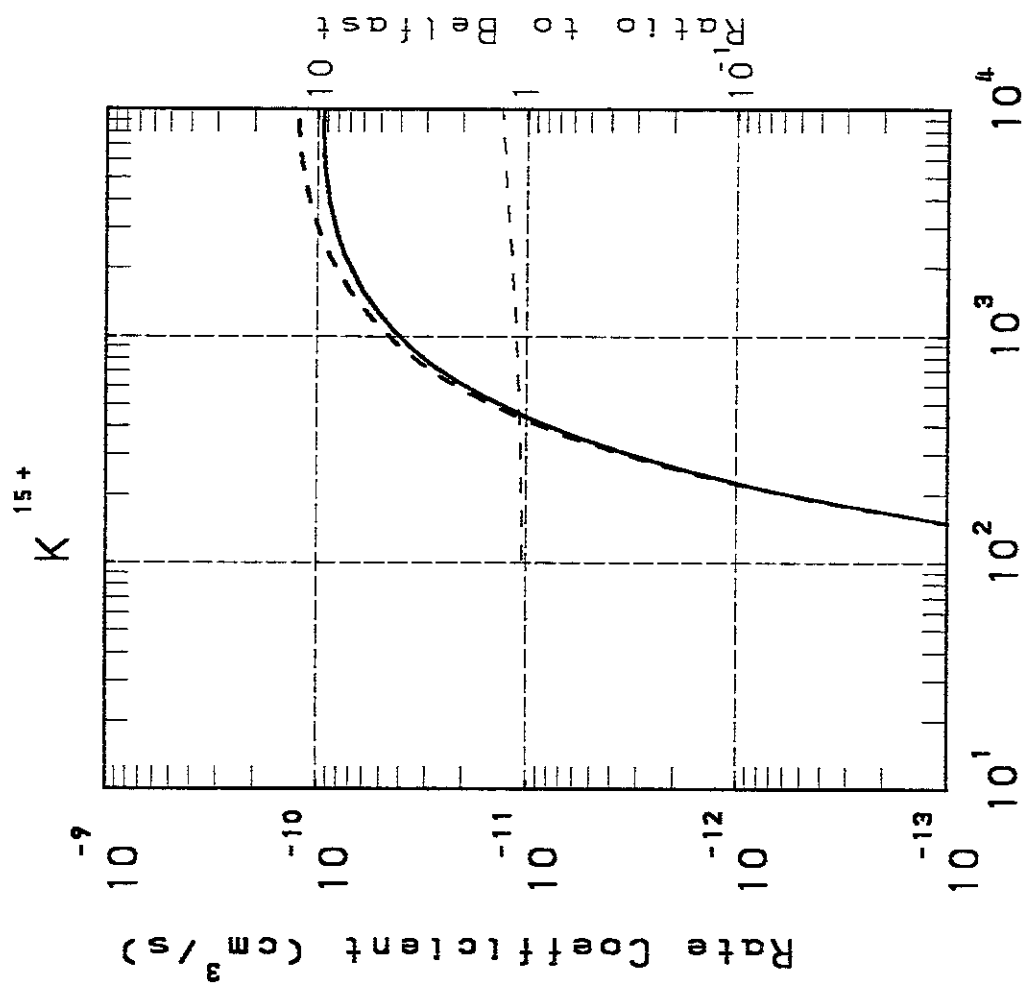




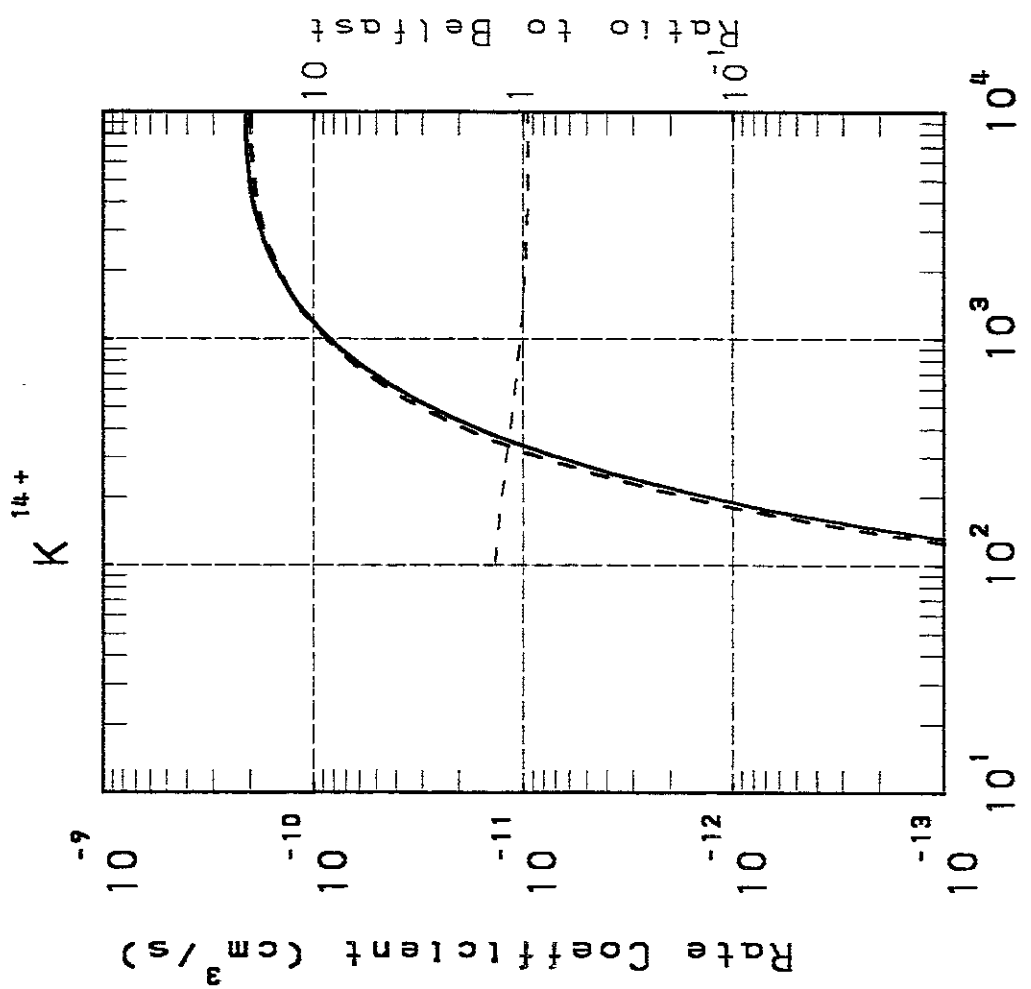




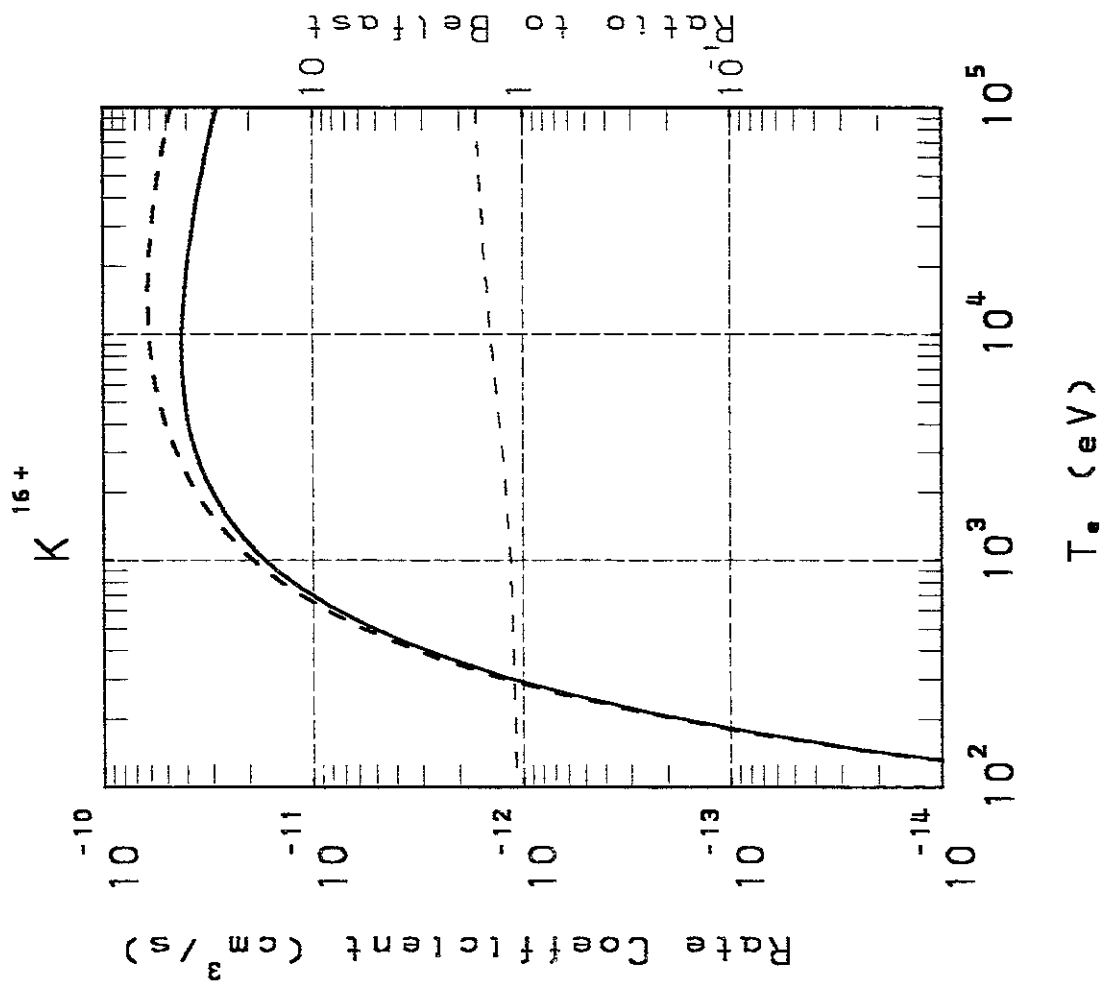
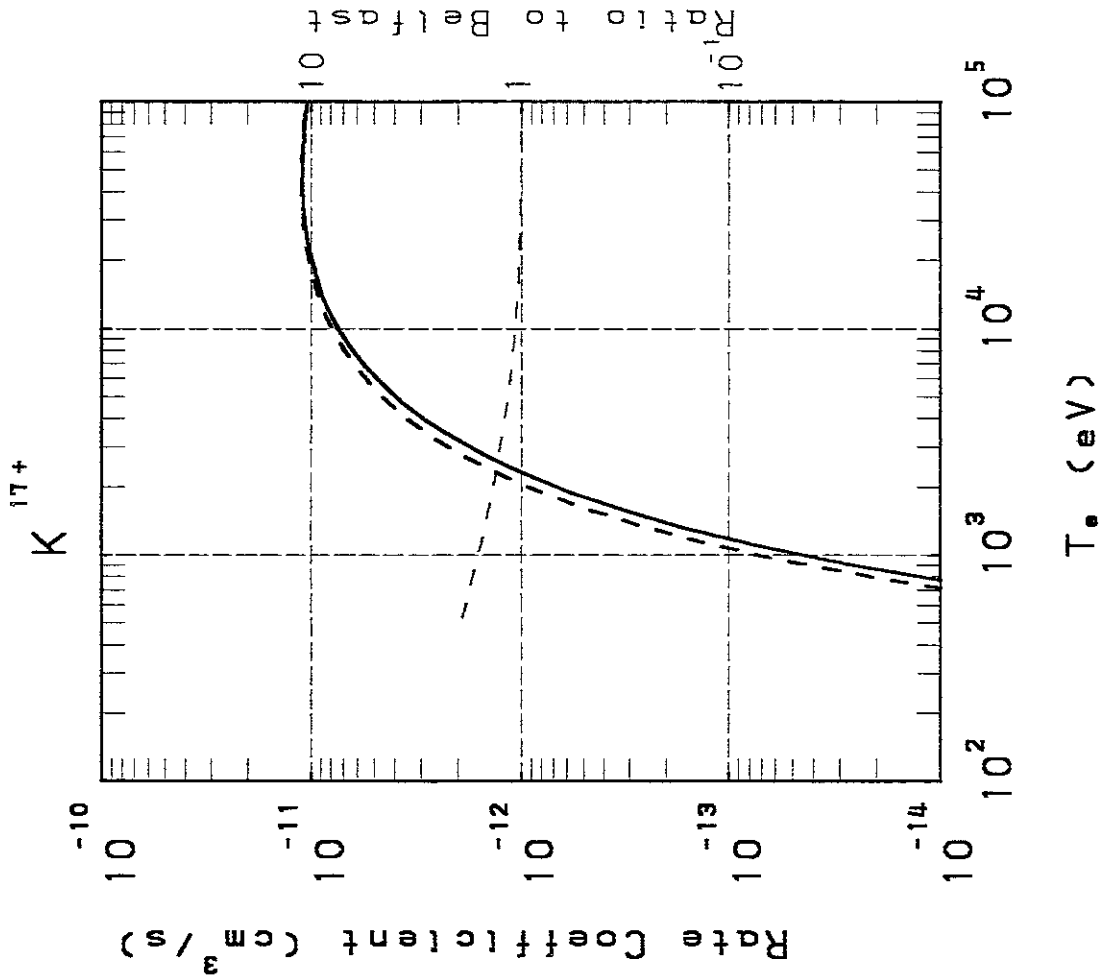


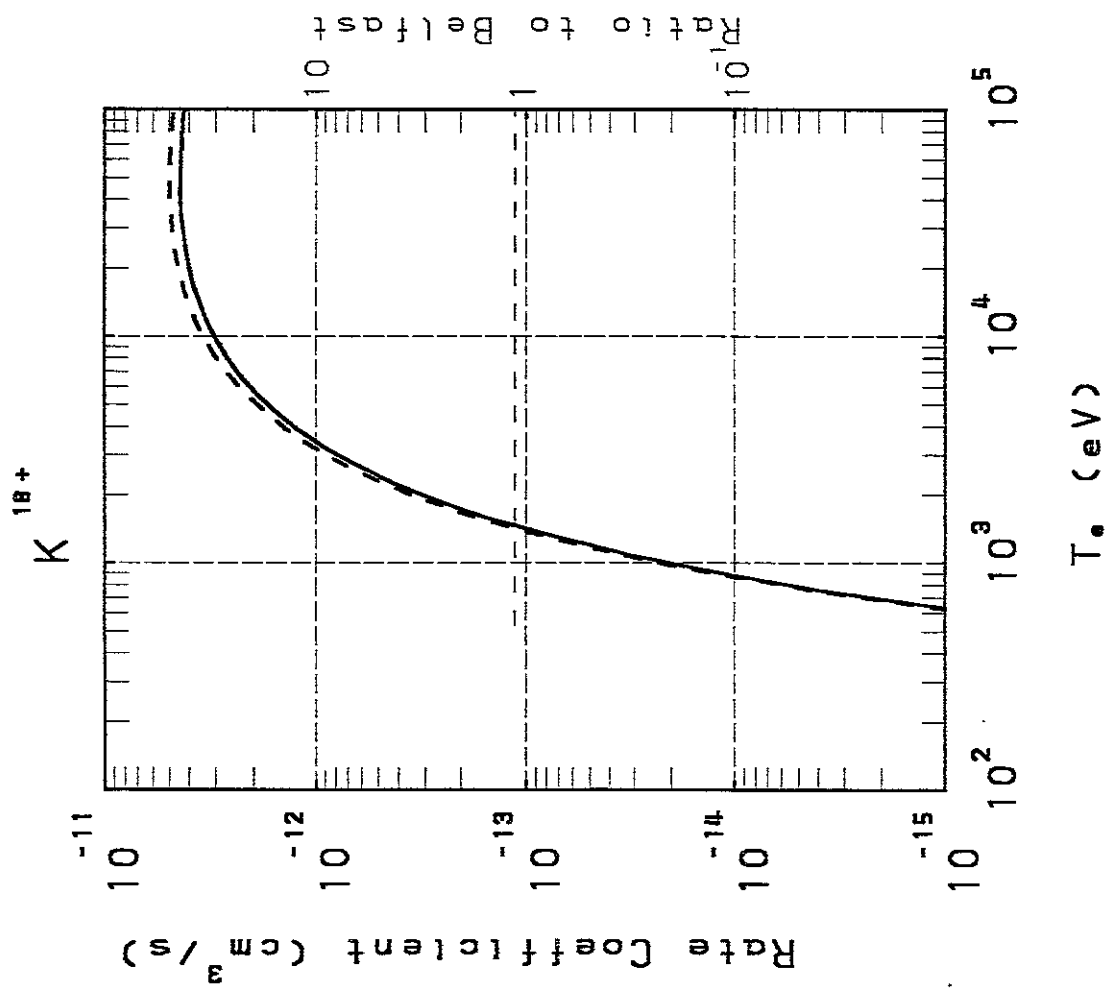


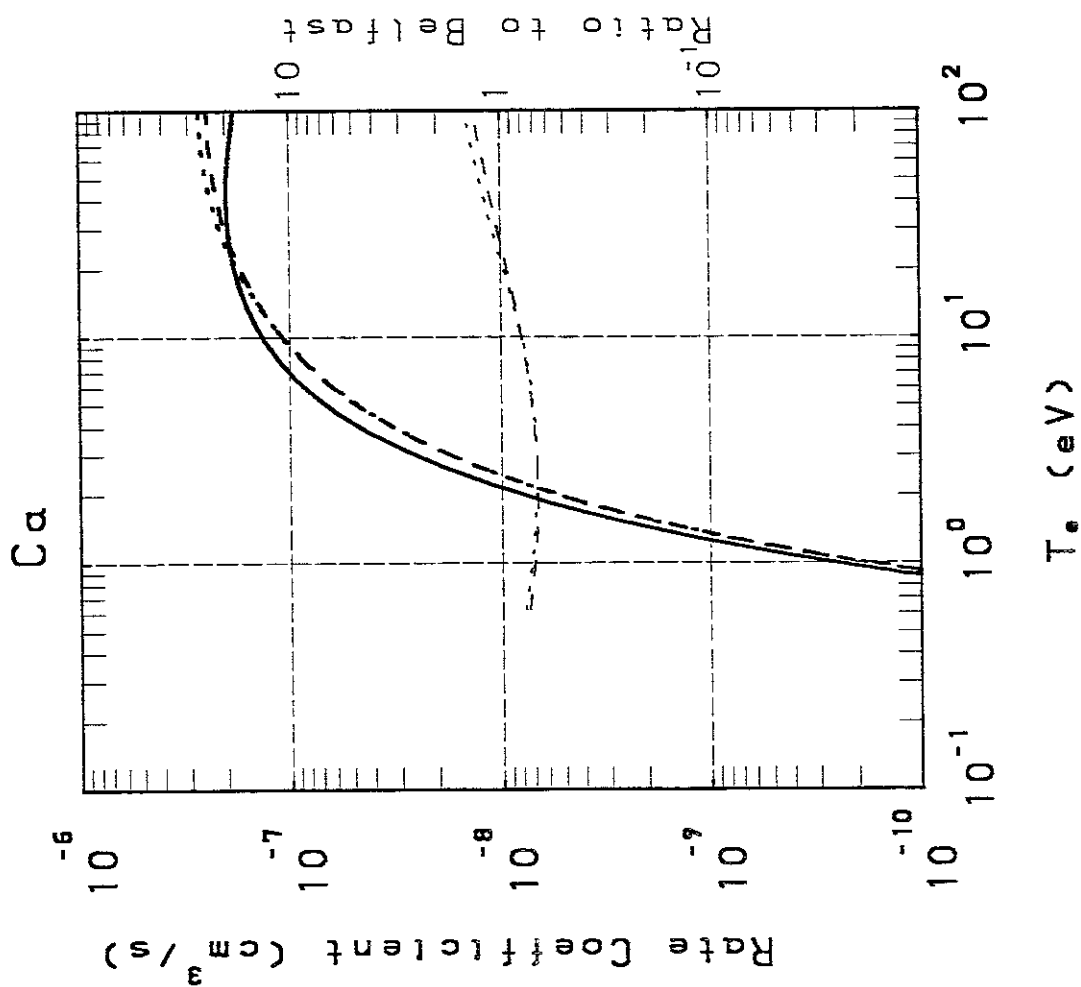
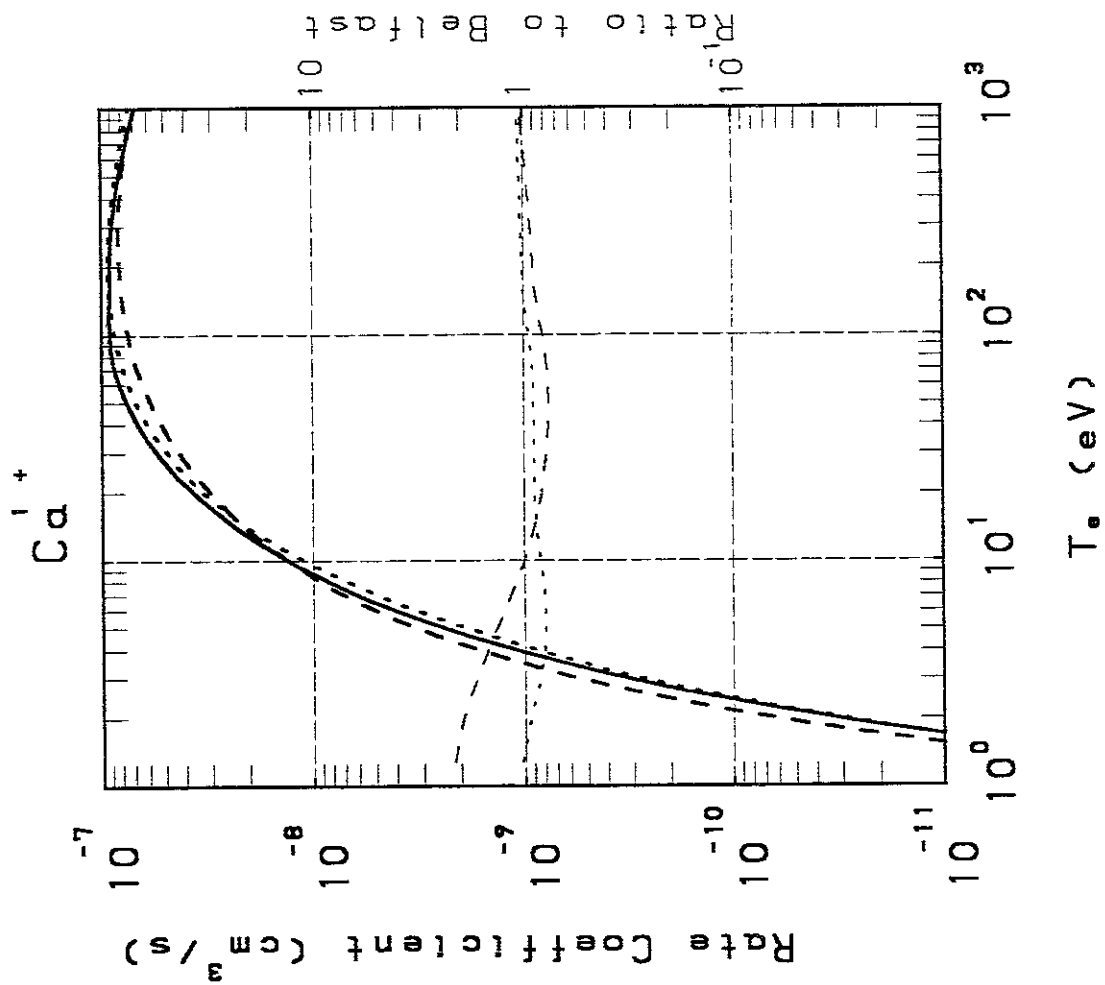
T_e (eV)

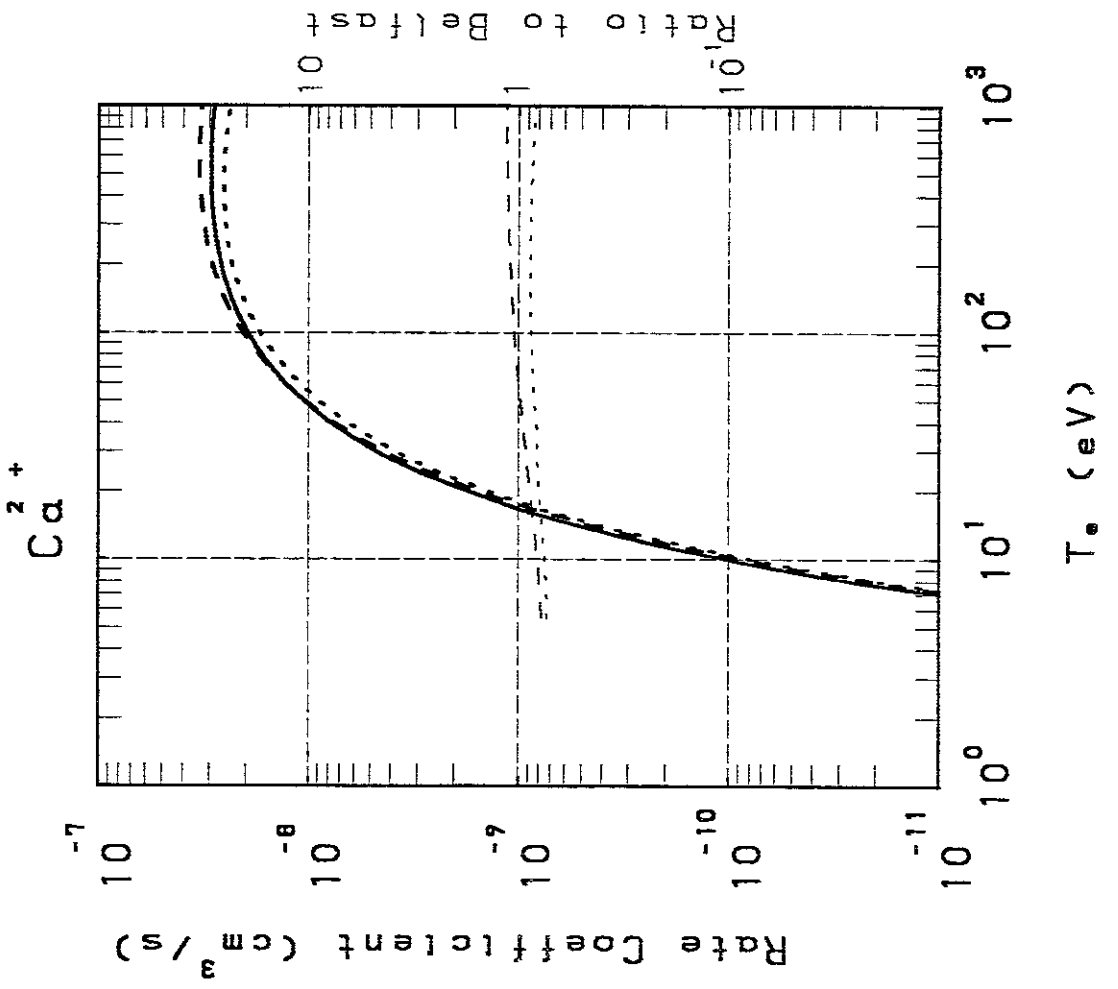
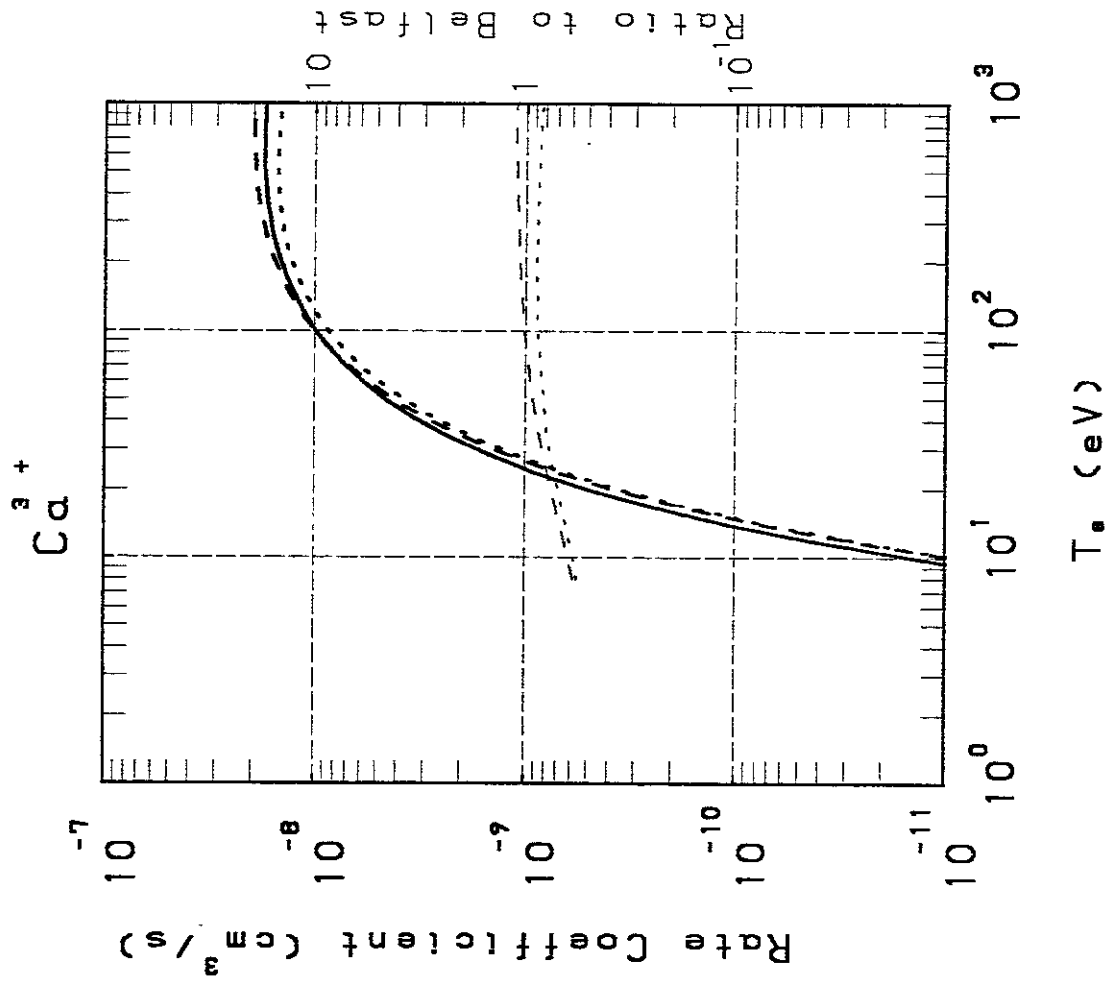


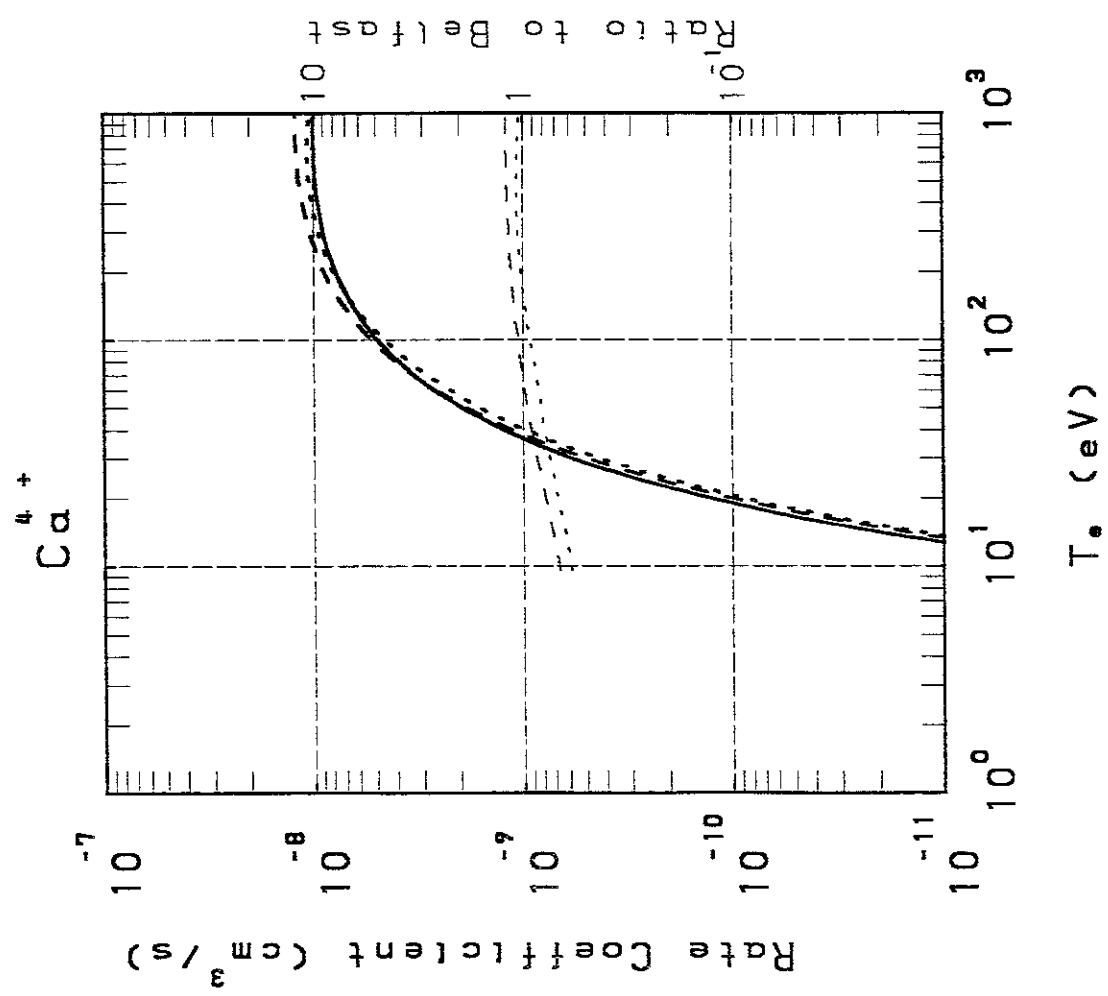
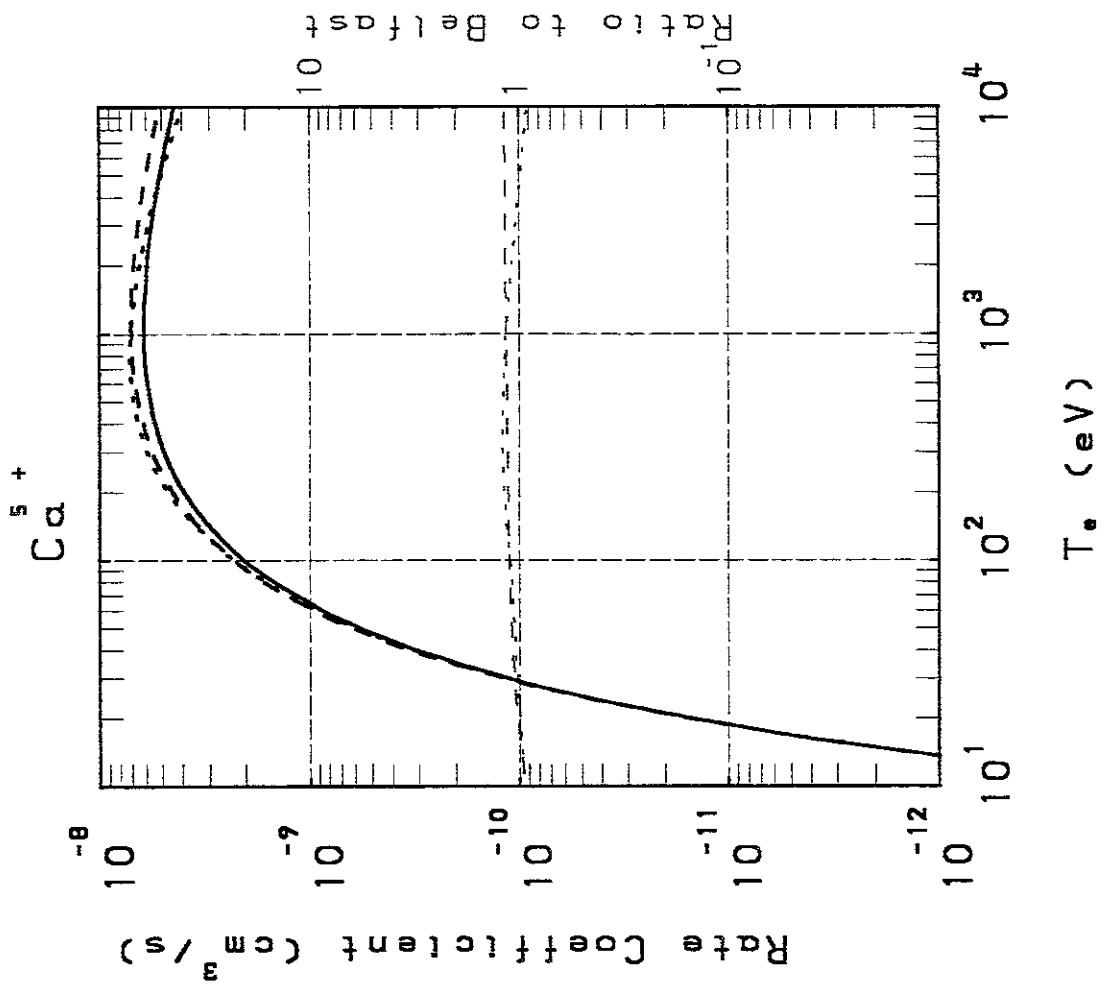
T_e (eV)

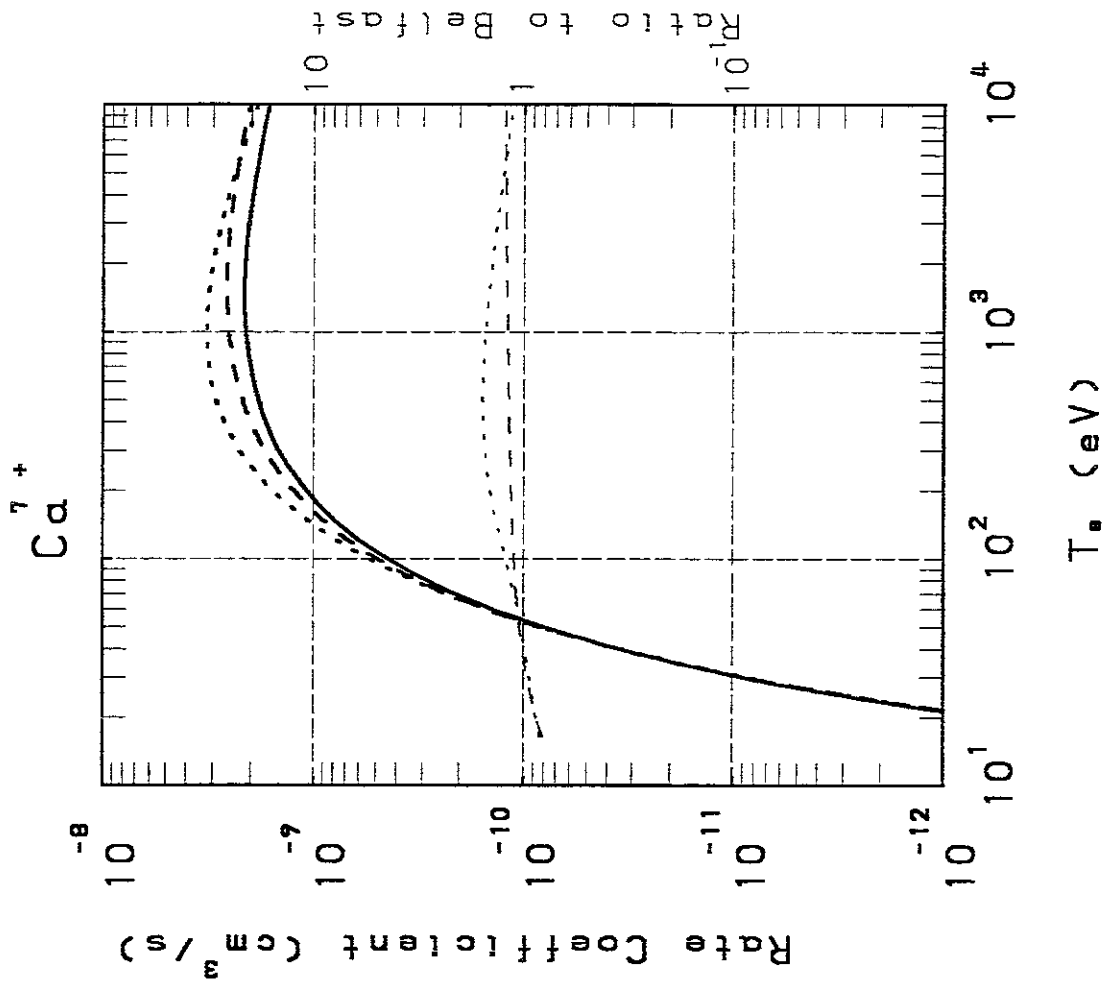
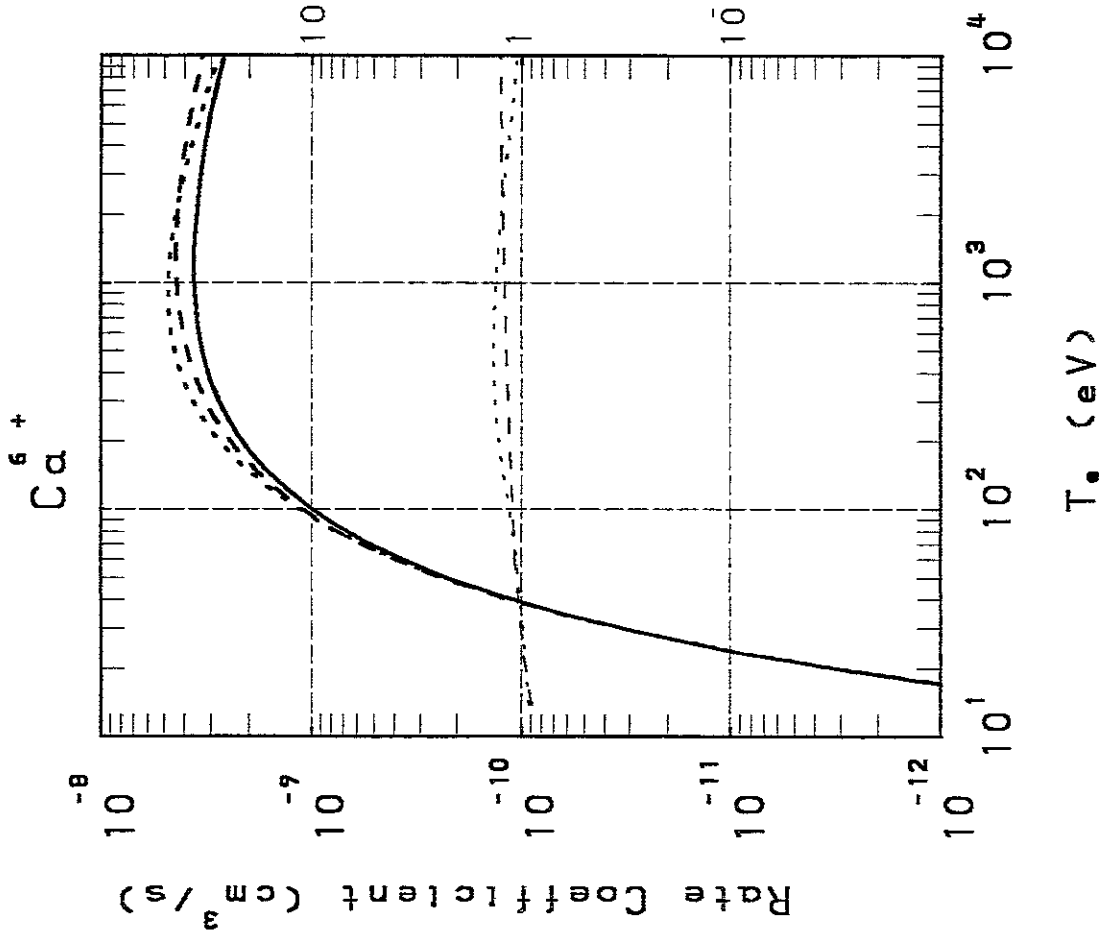


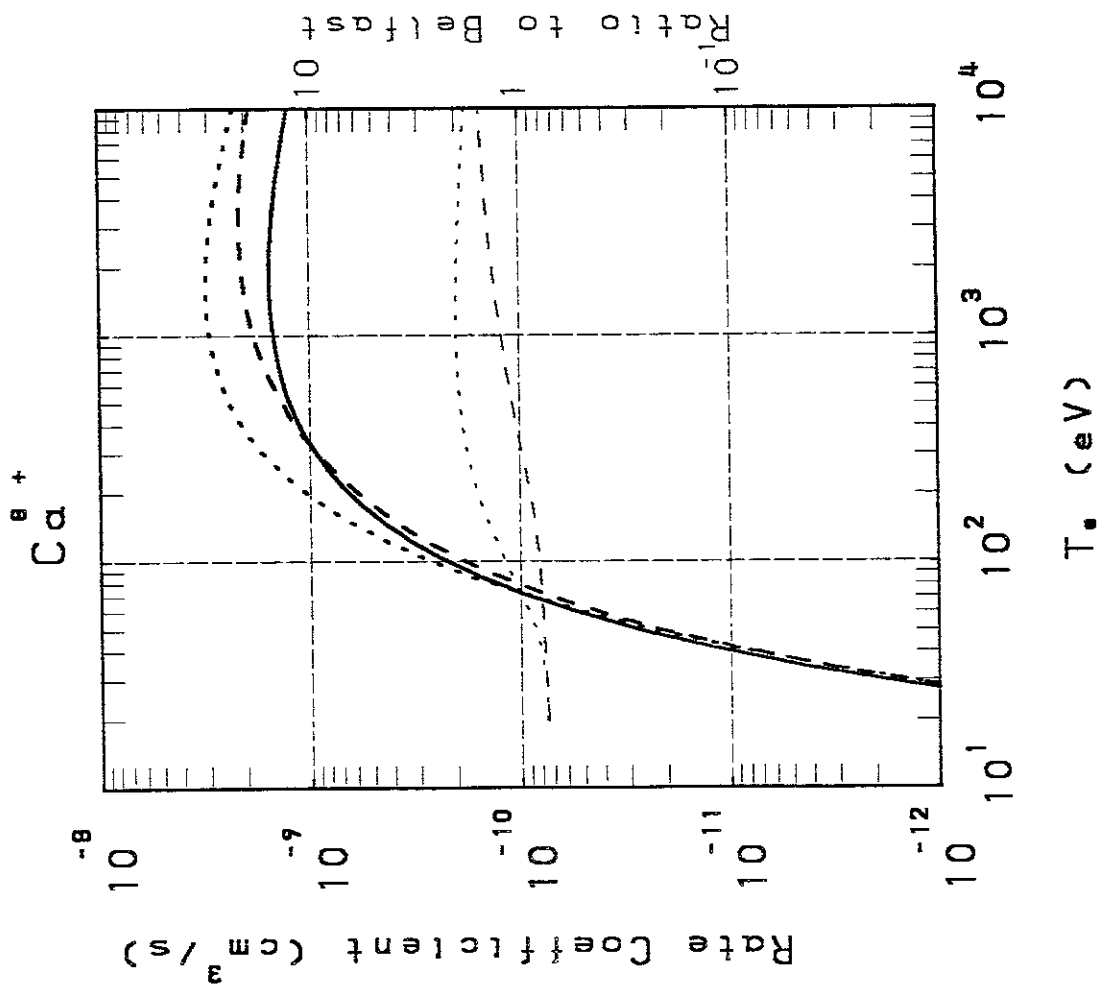
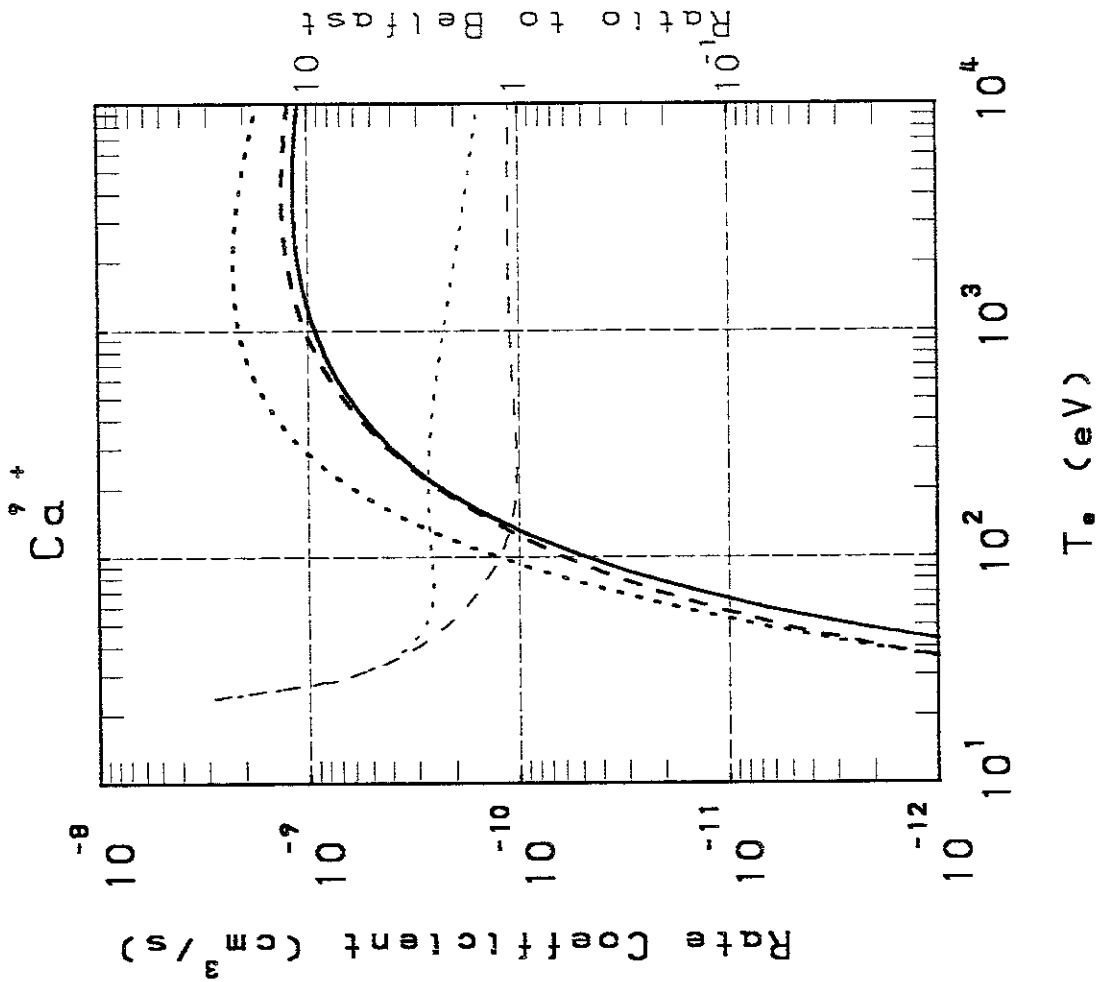


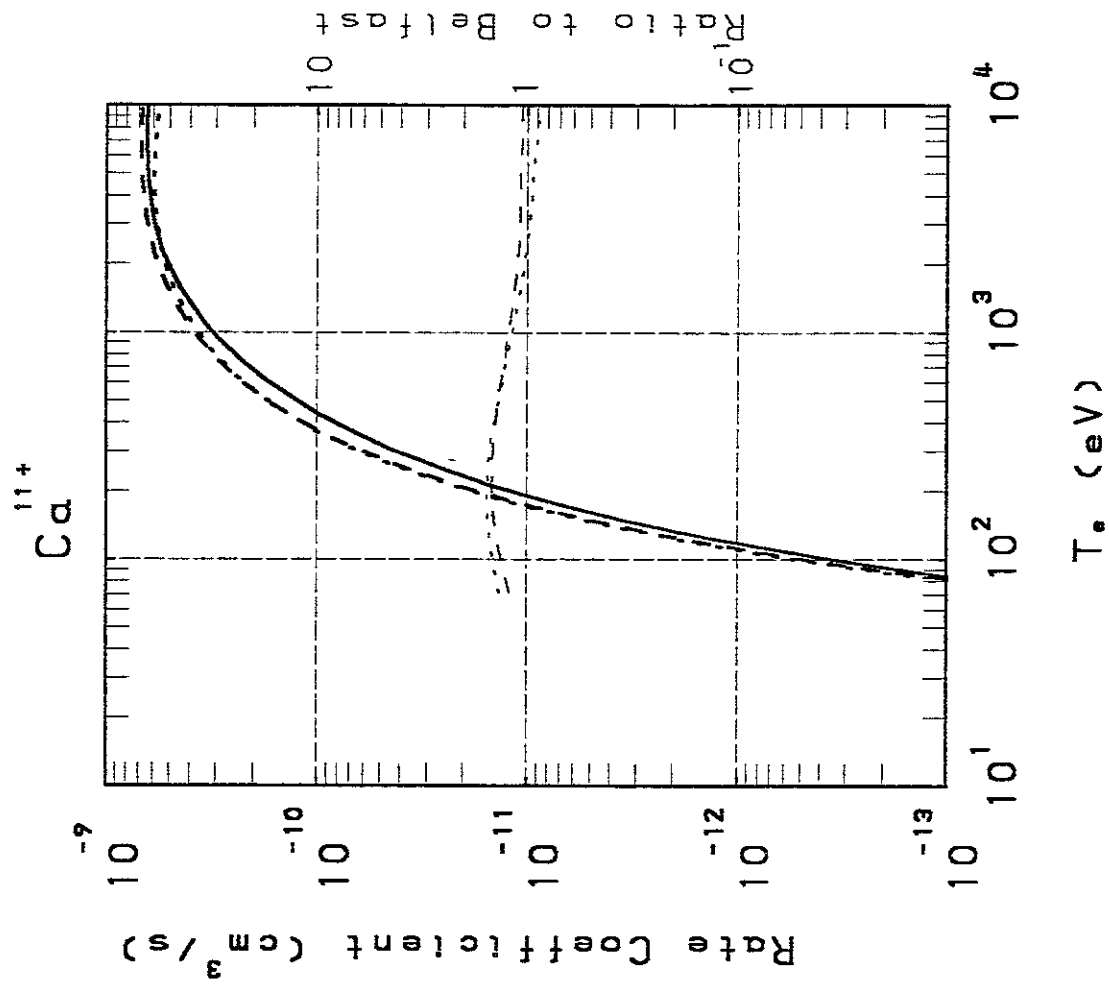
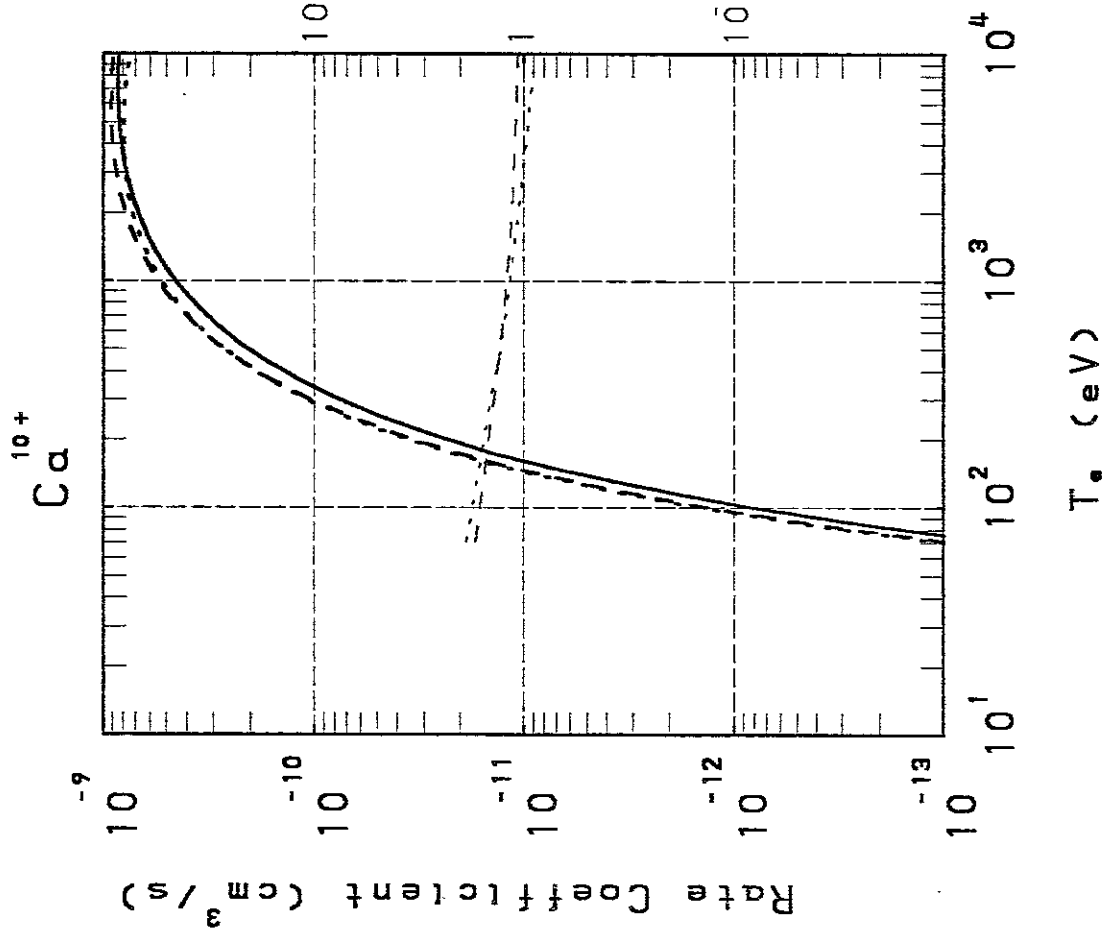


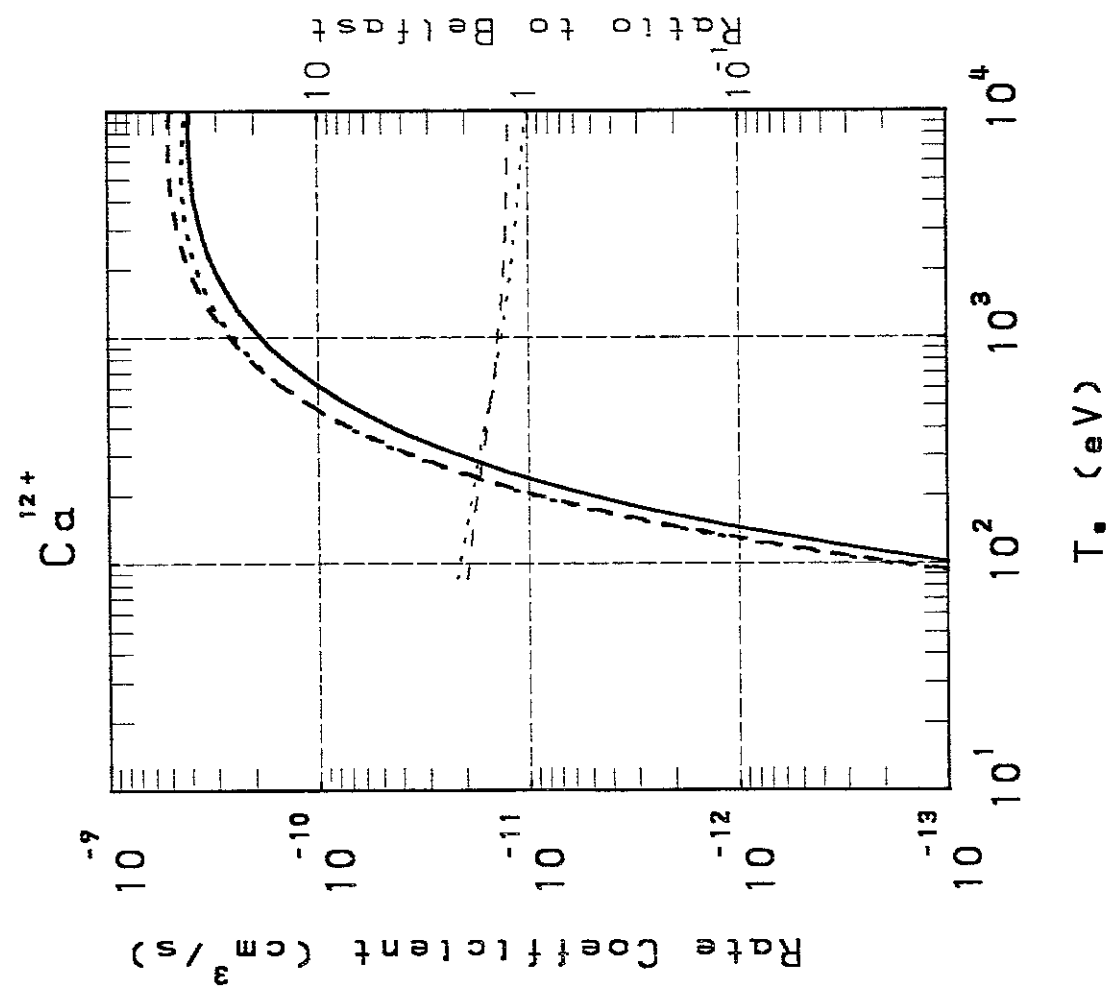
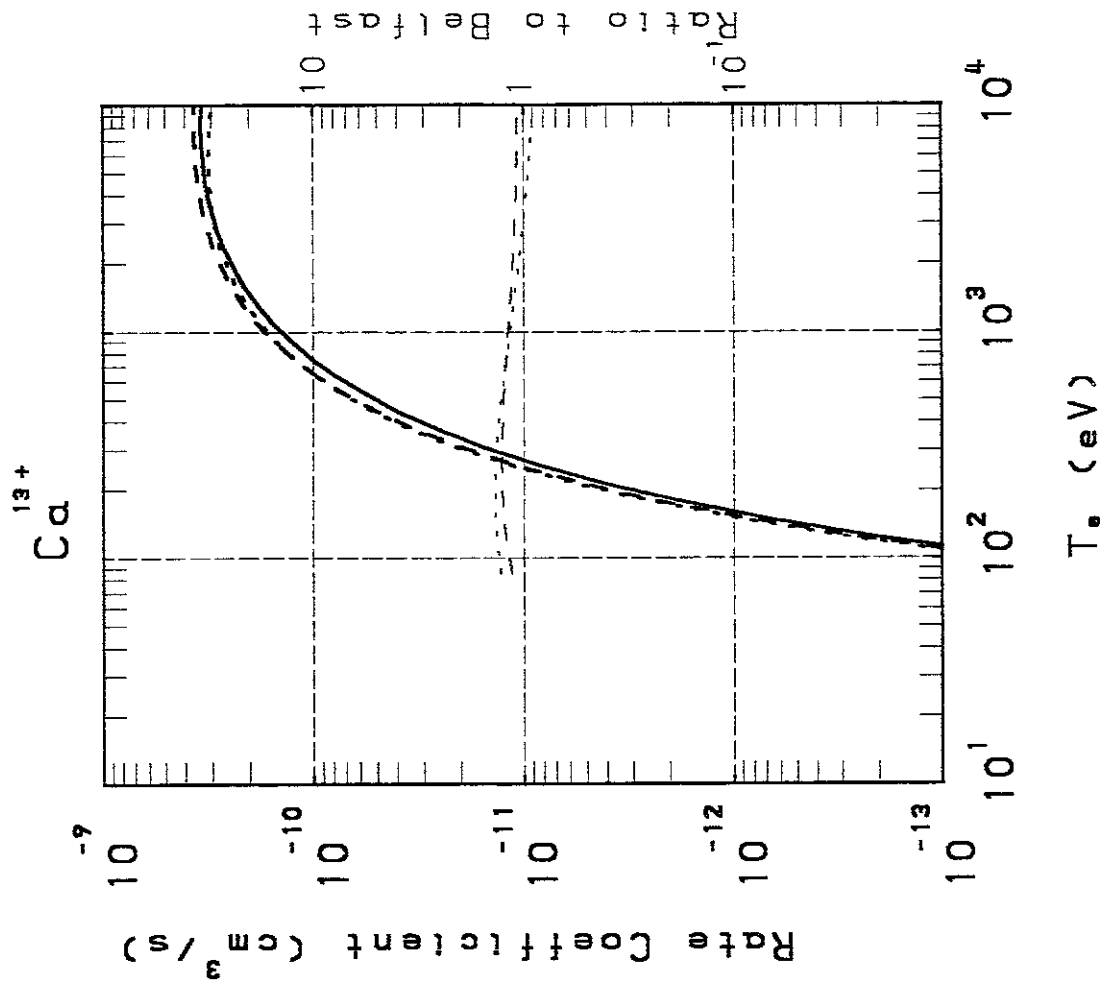


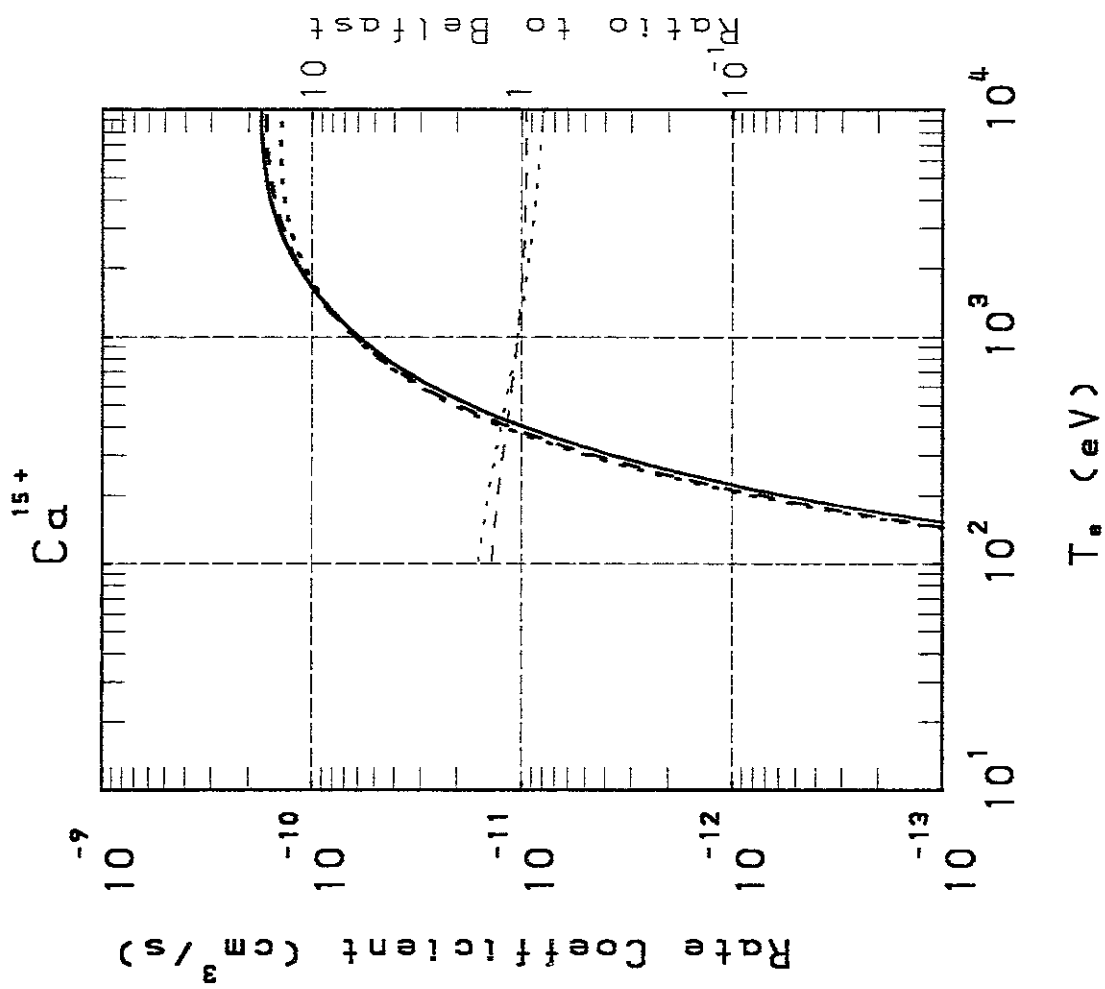
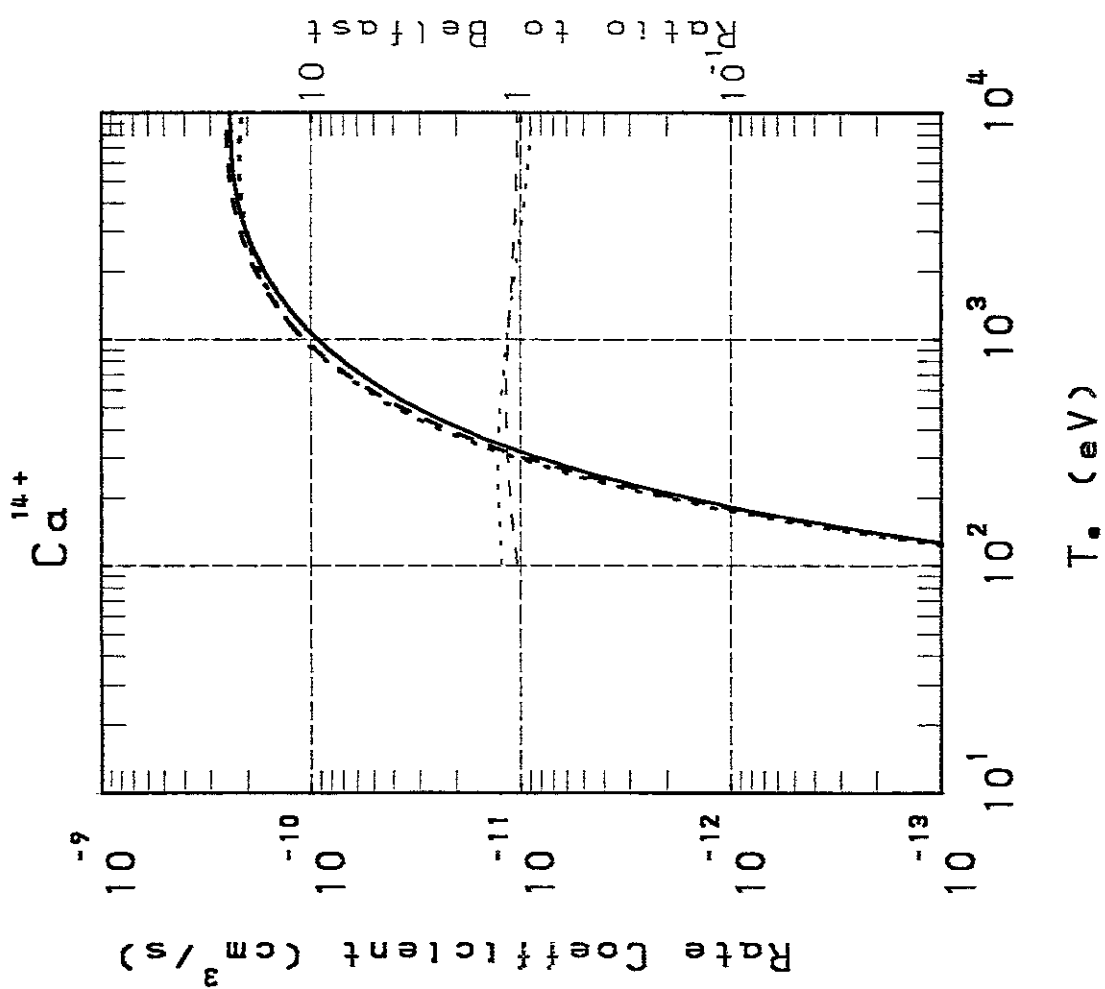


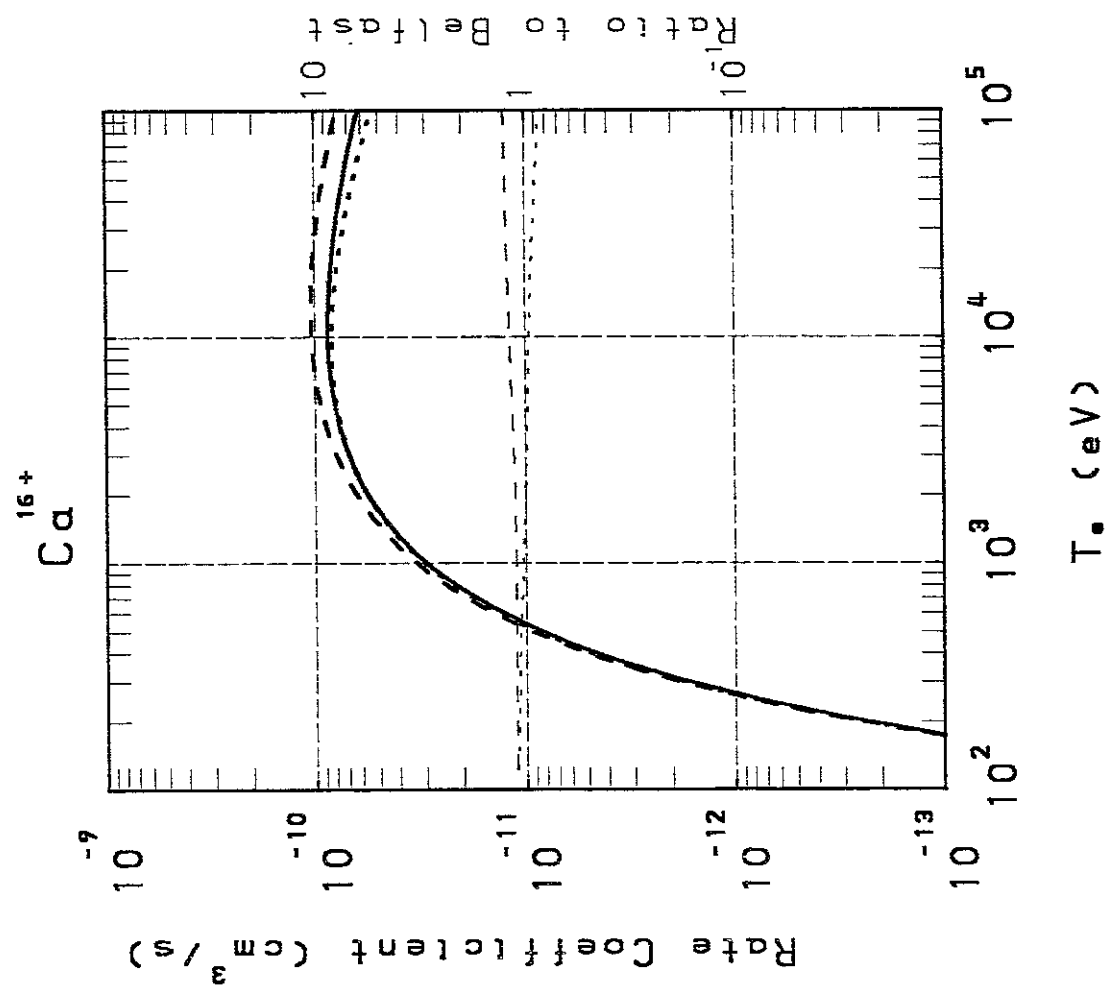
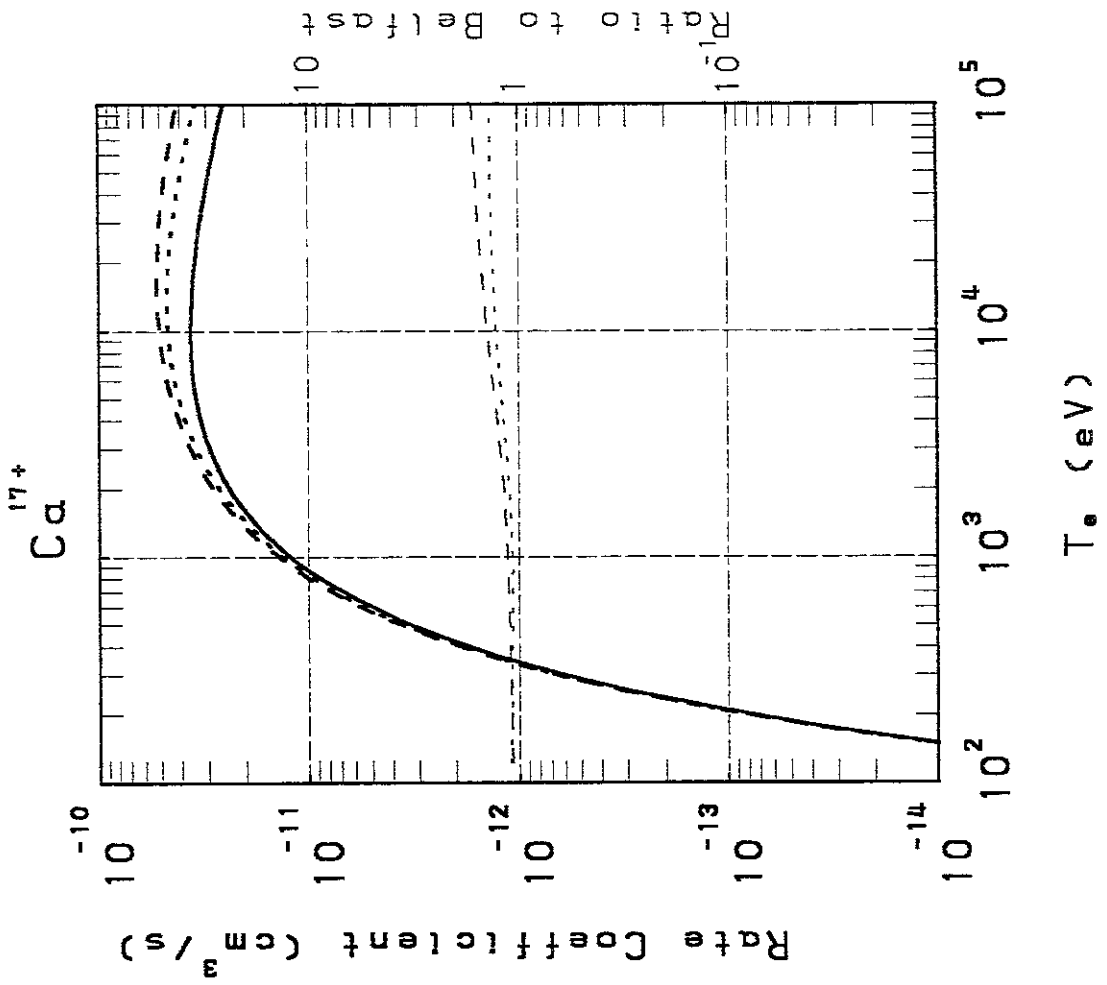


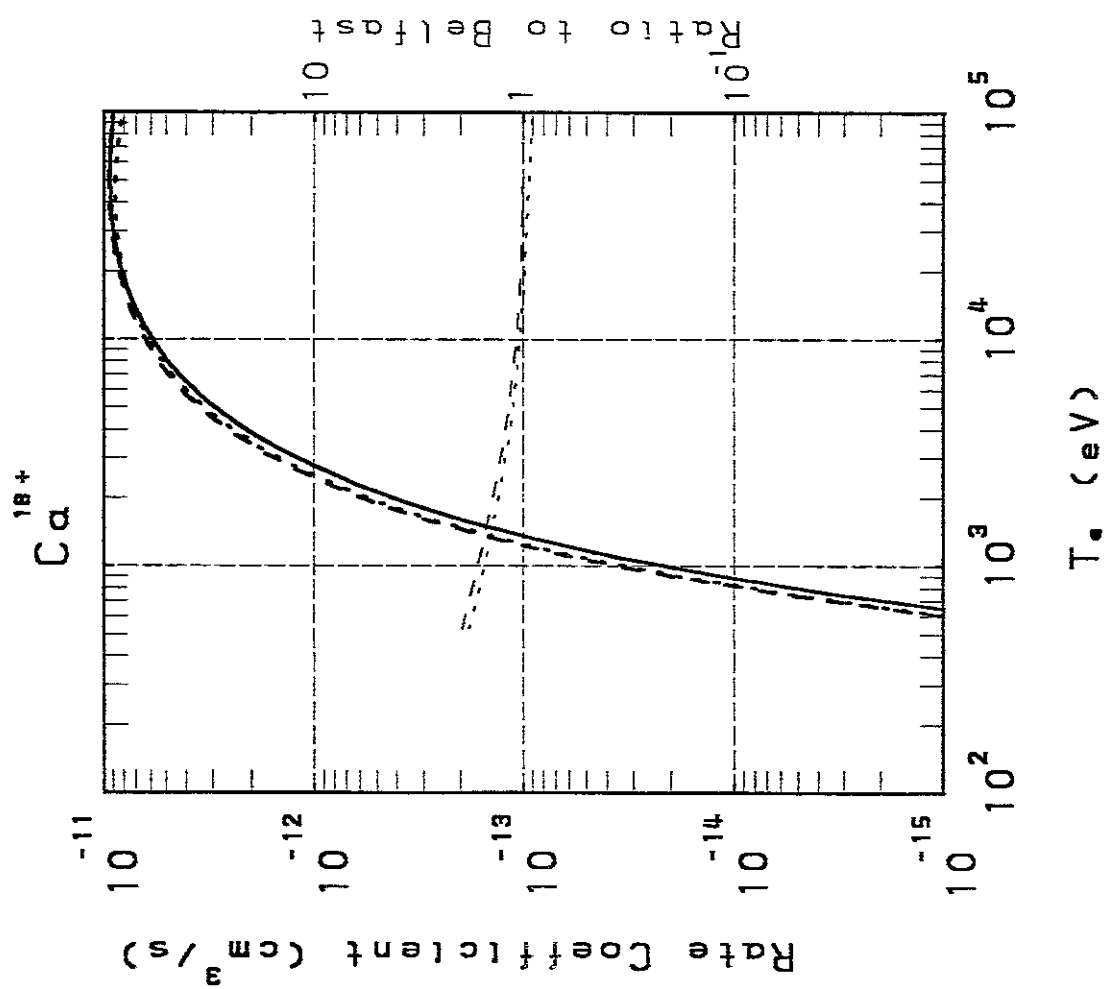
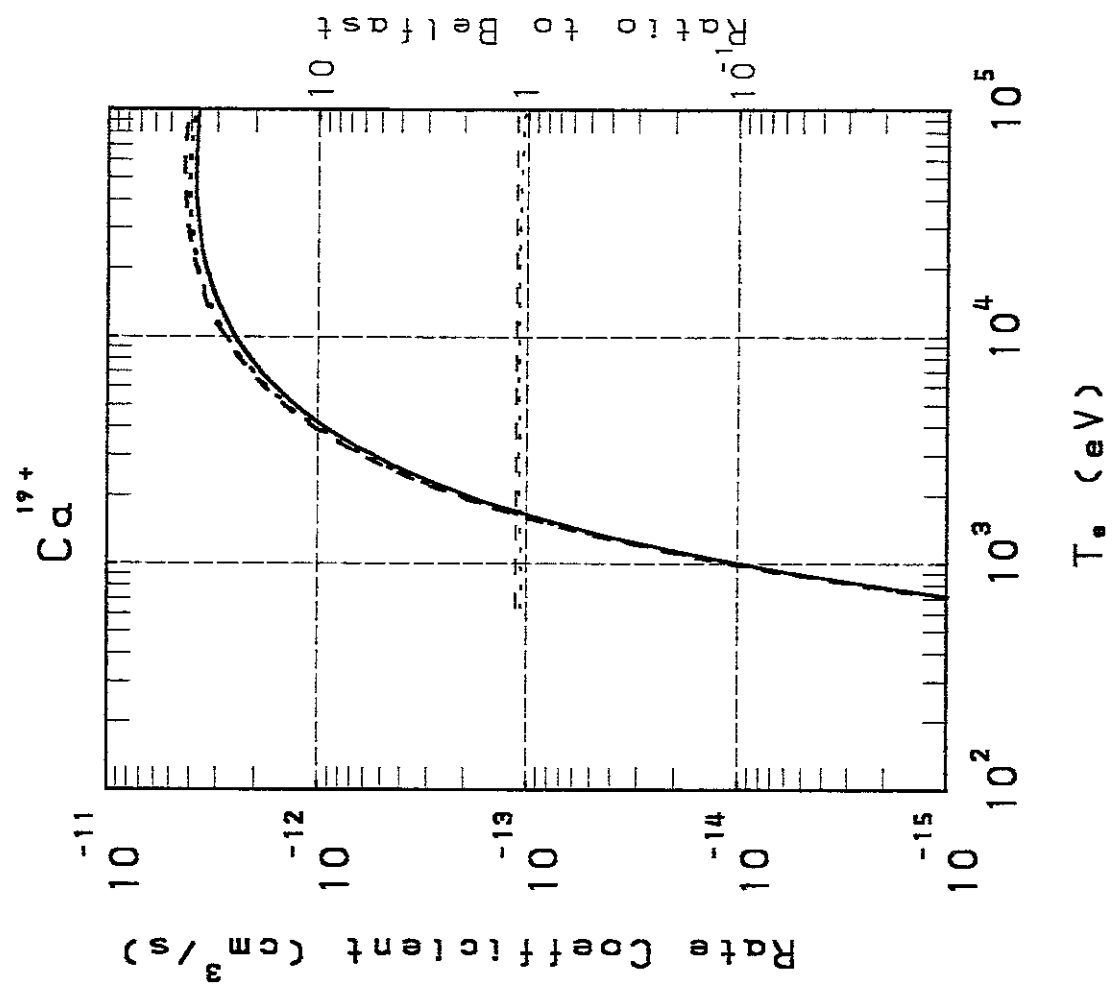


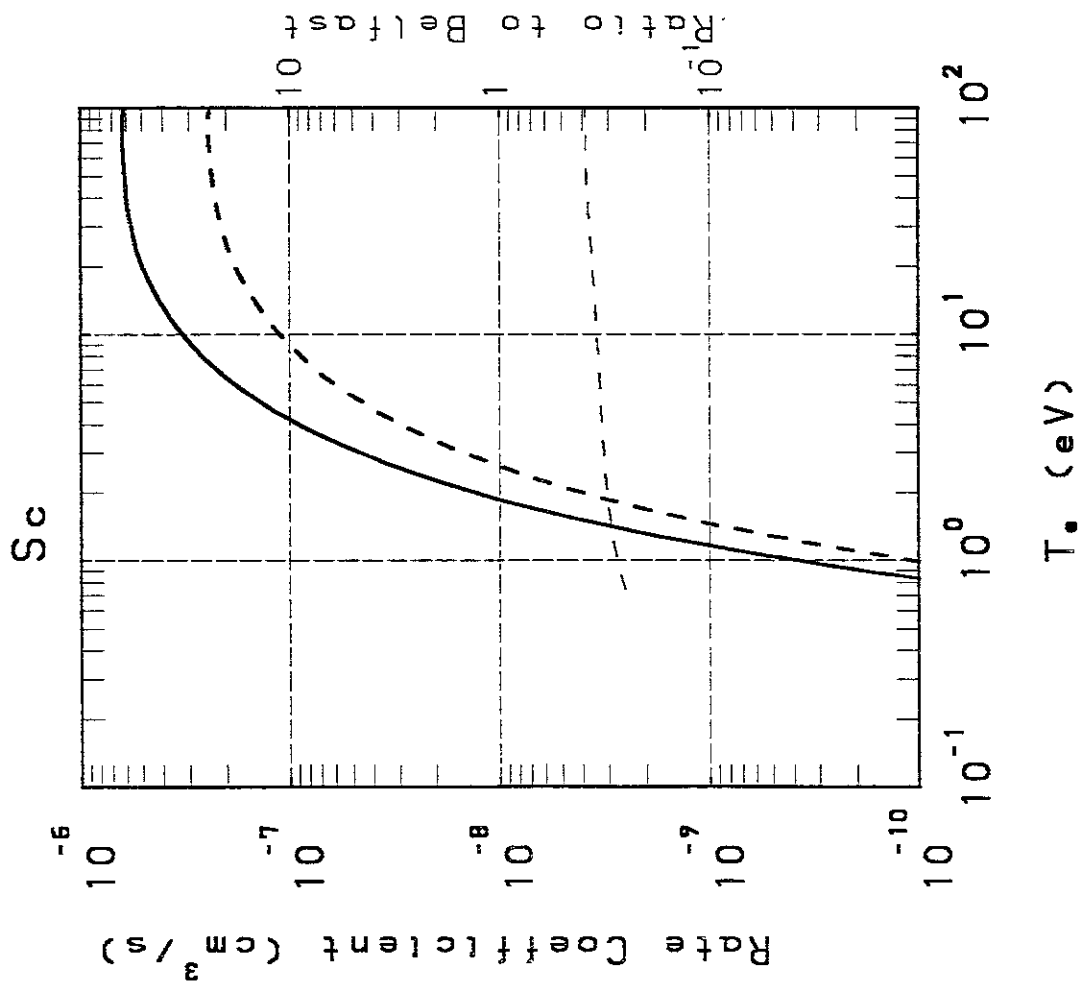
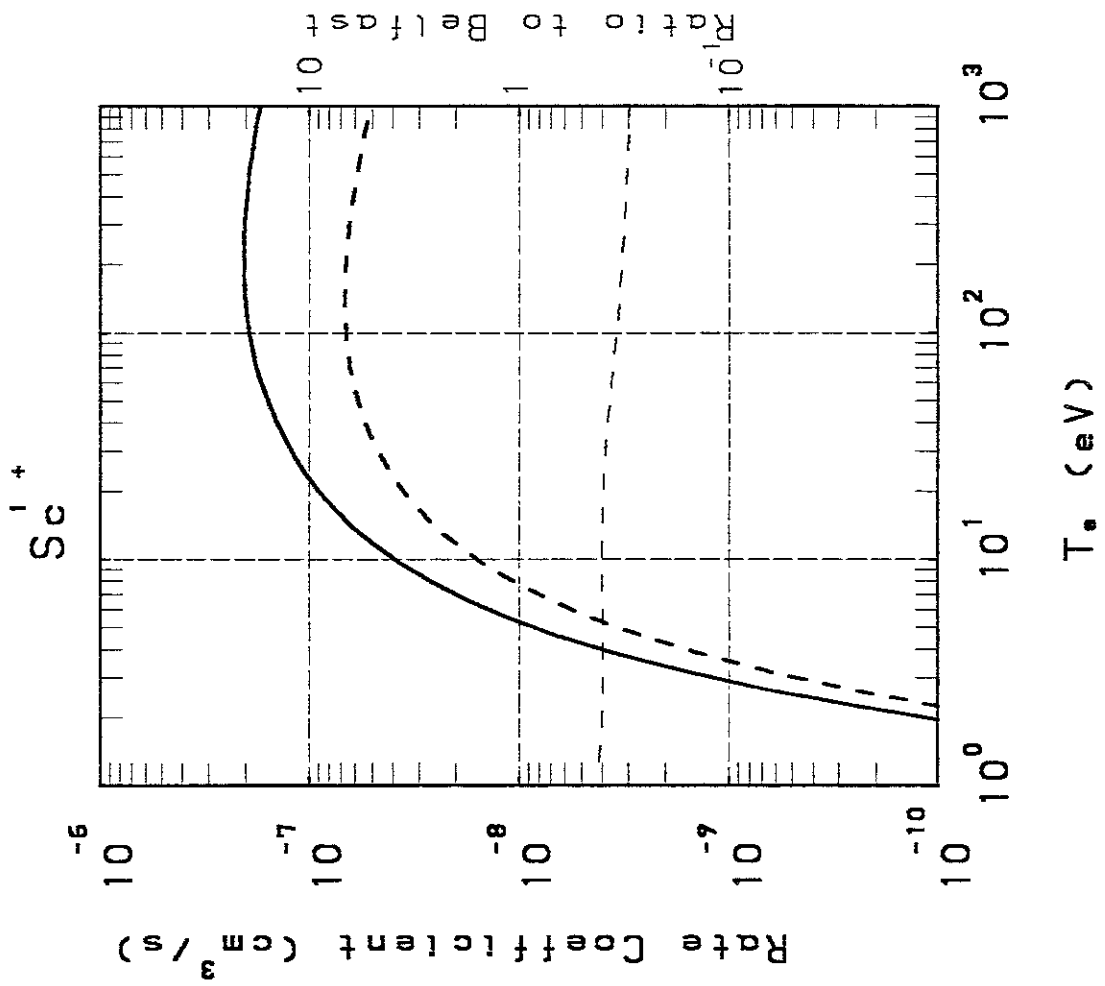


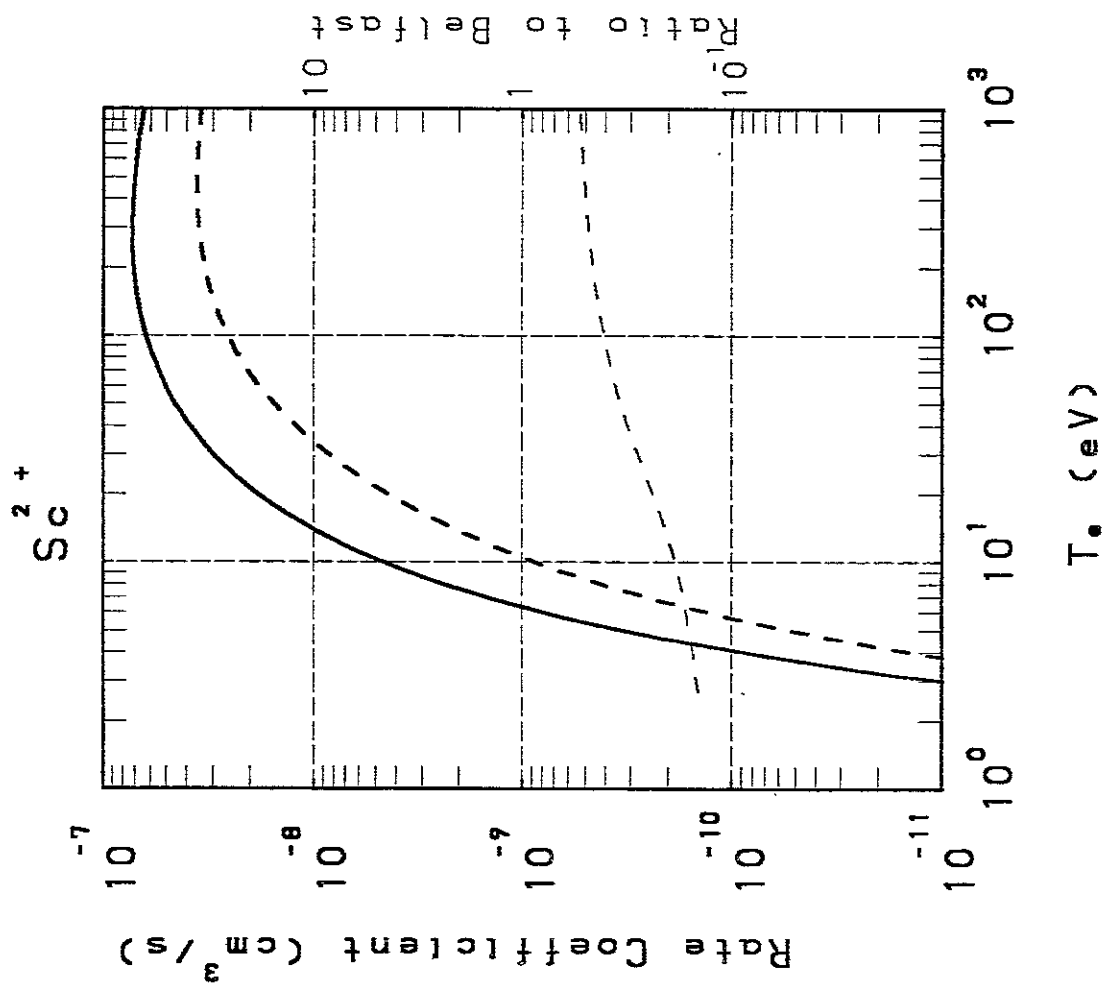
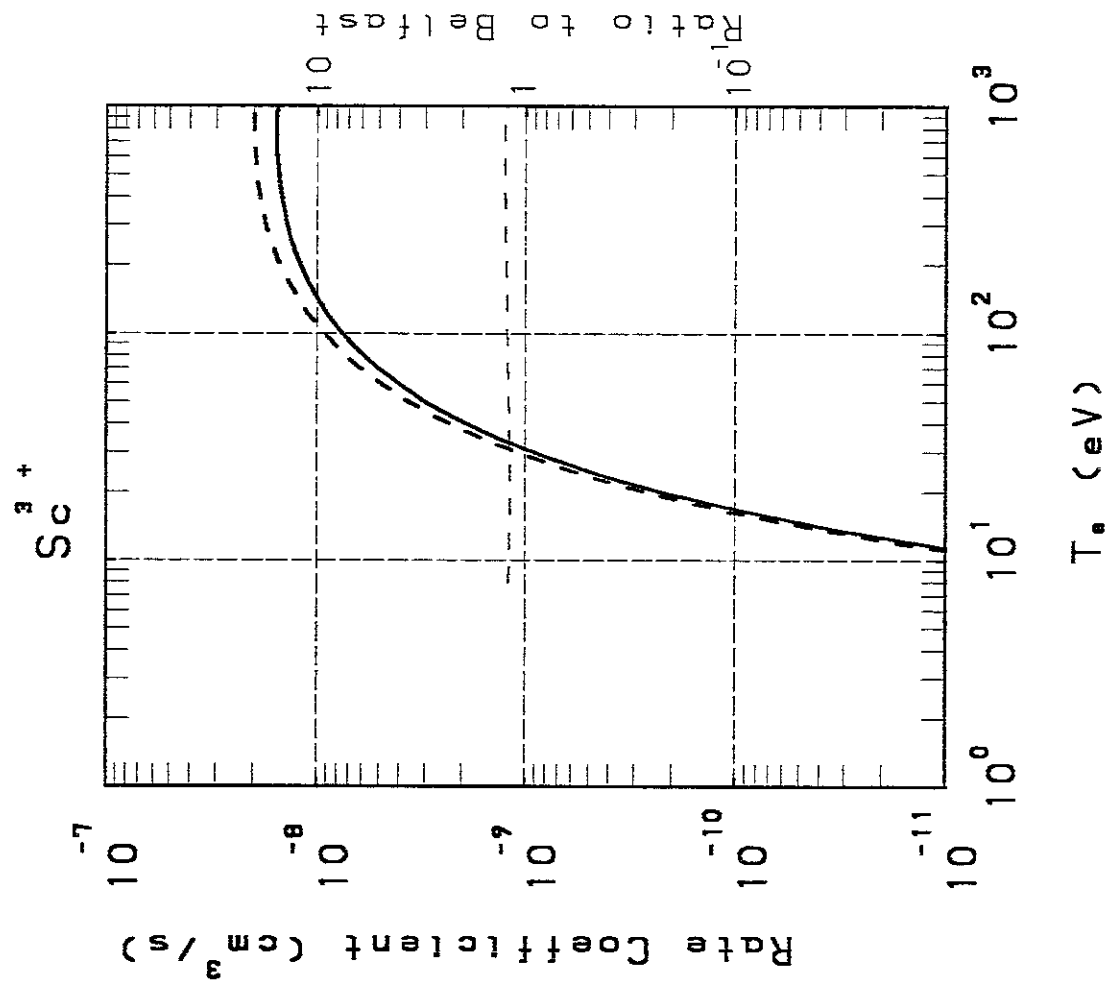


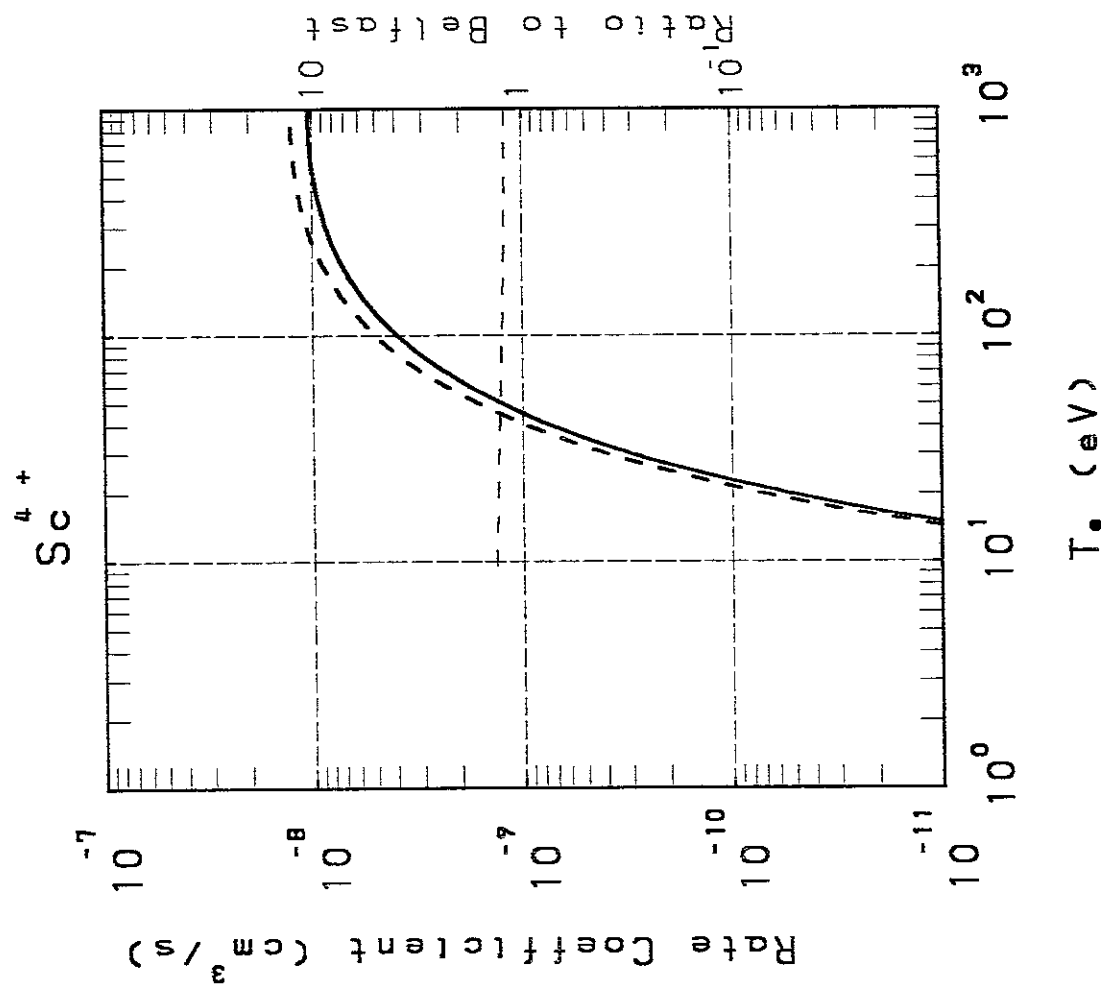
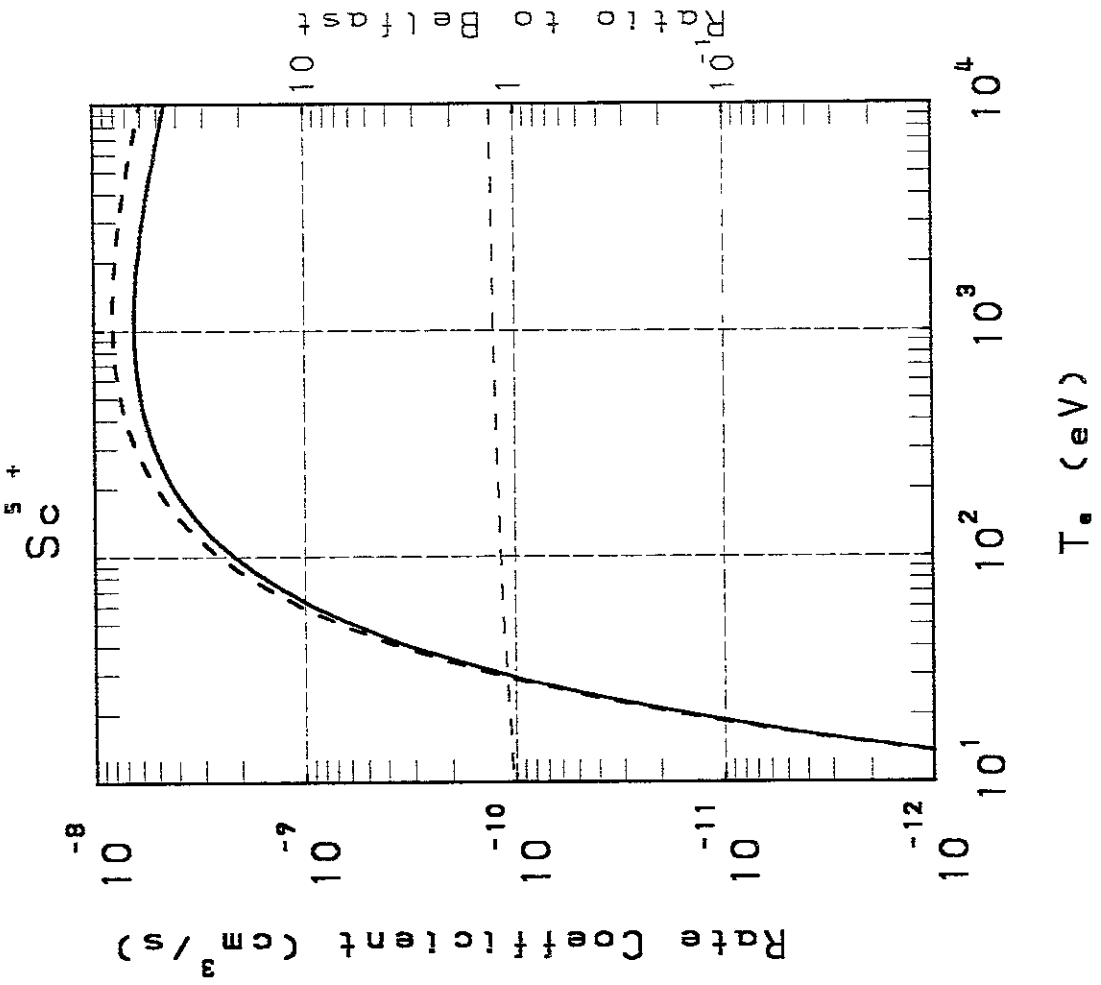


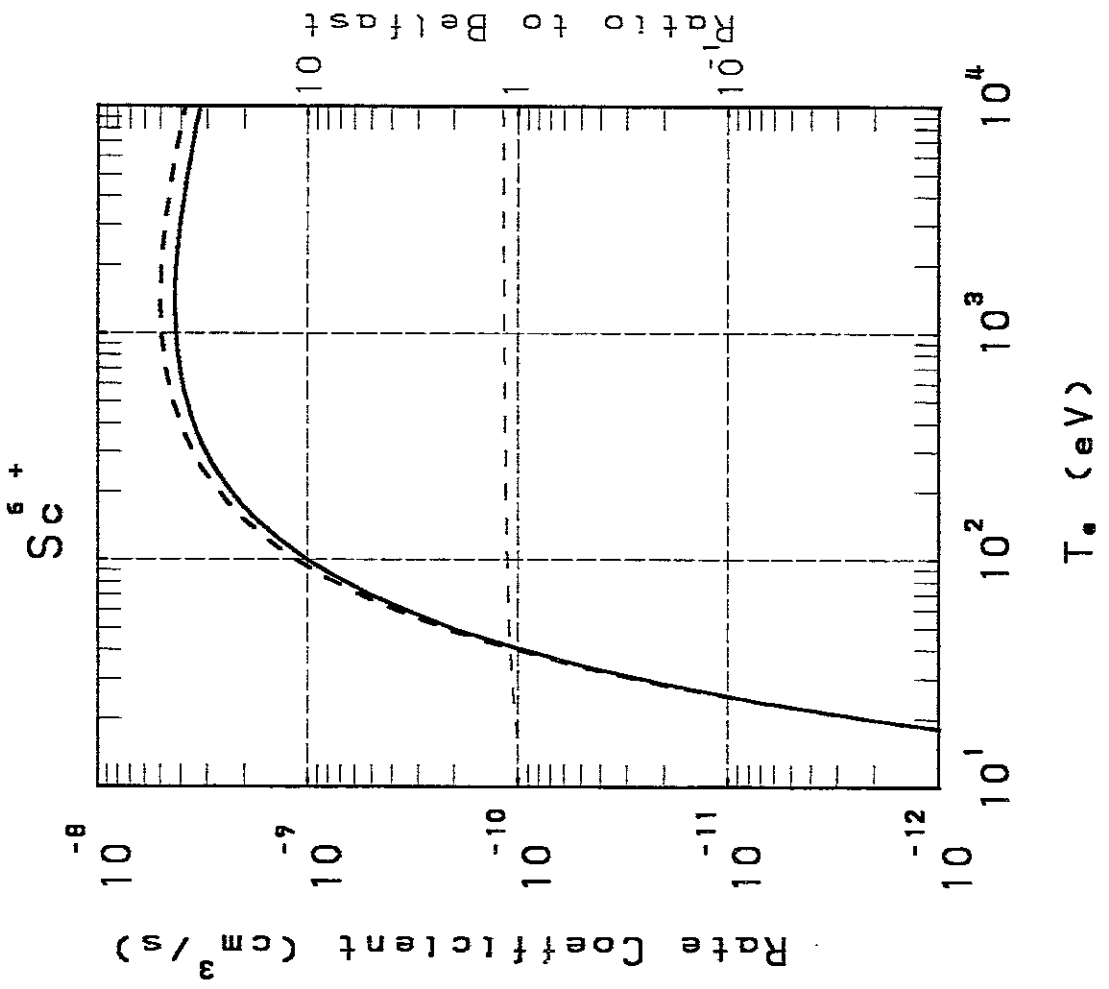
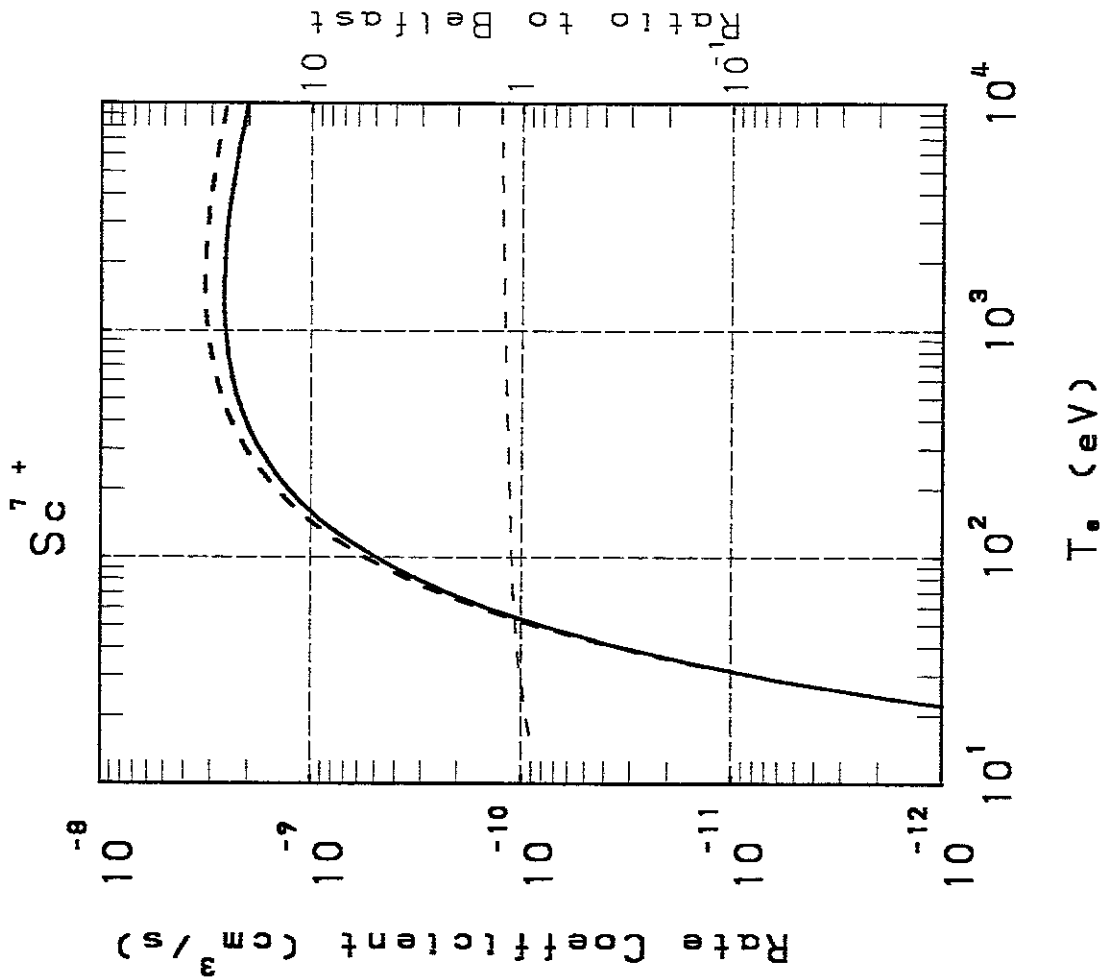


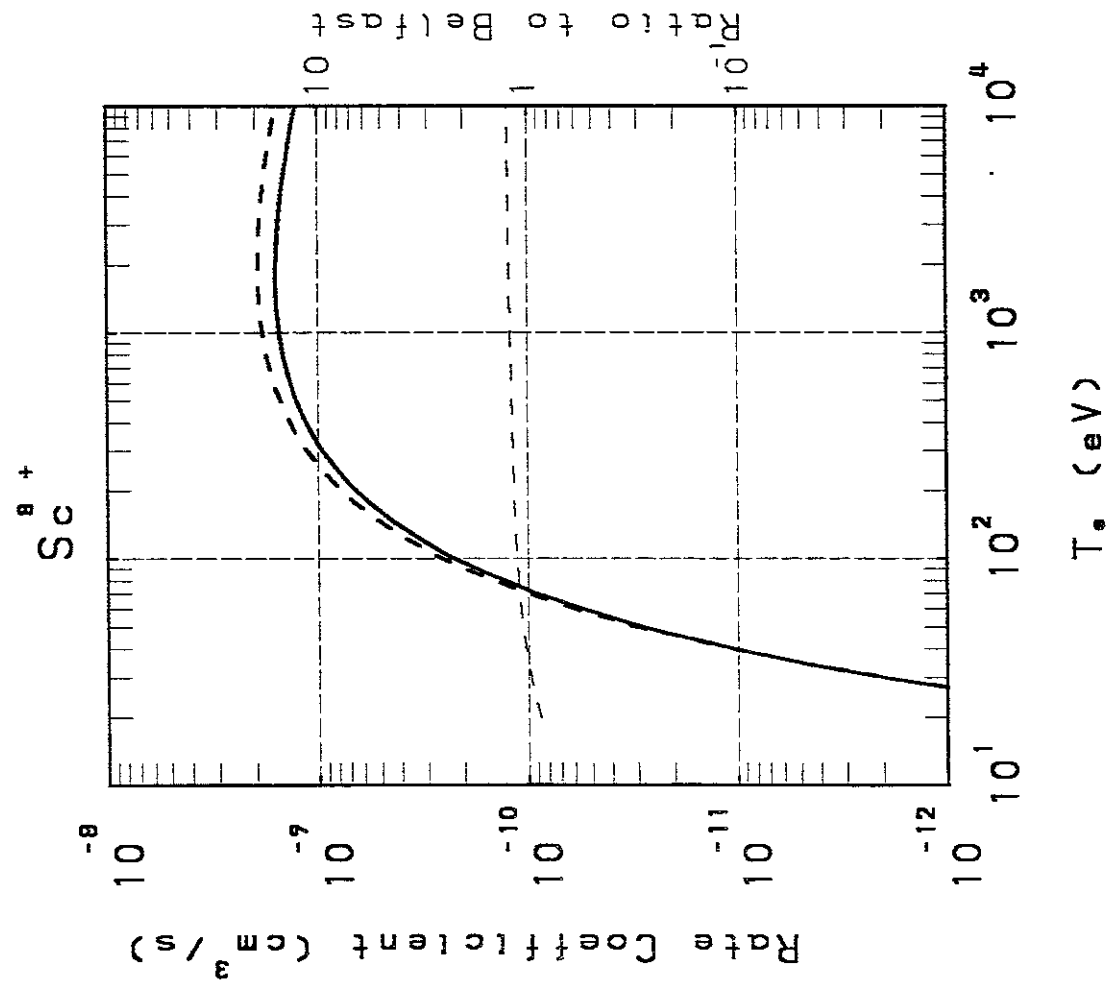
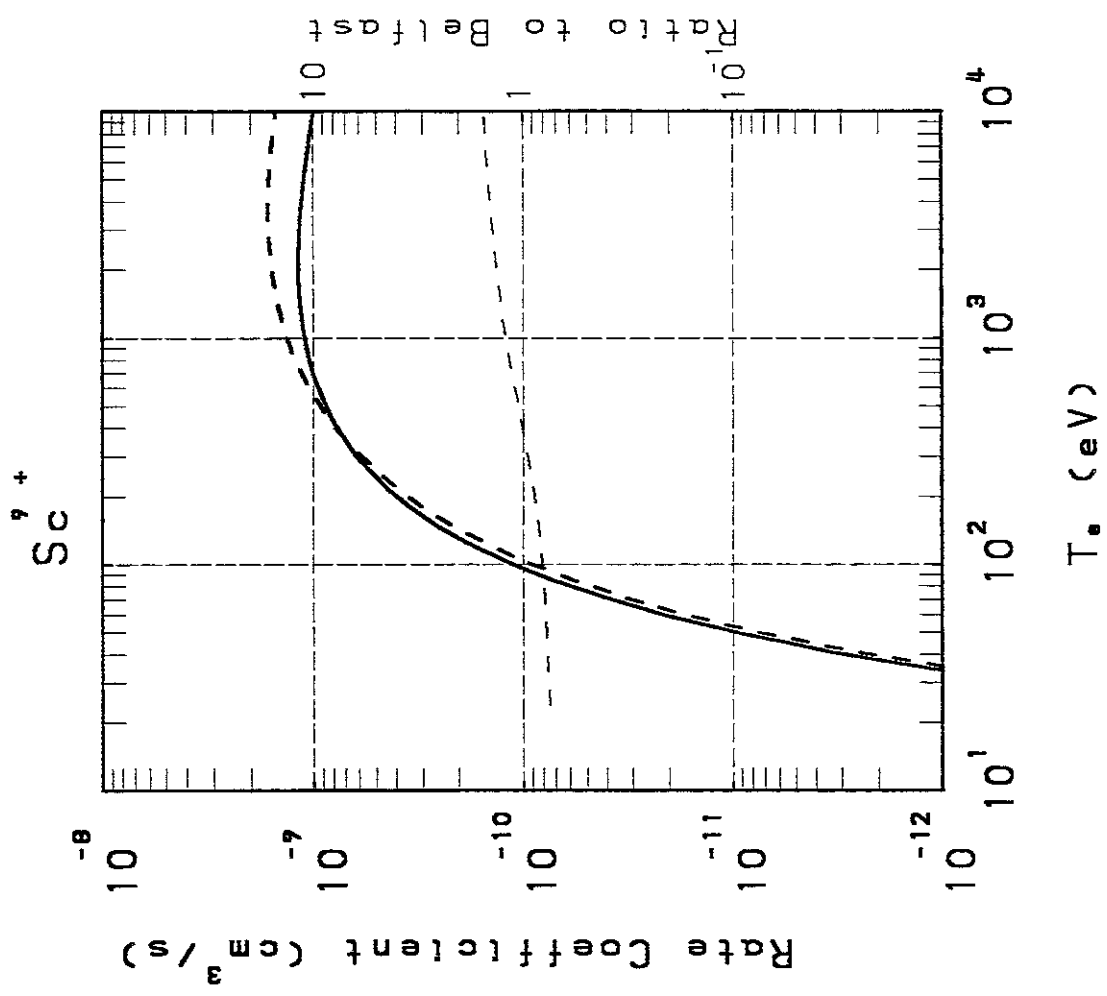


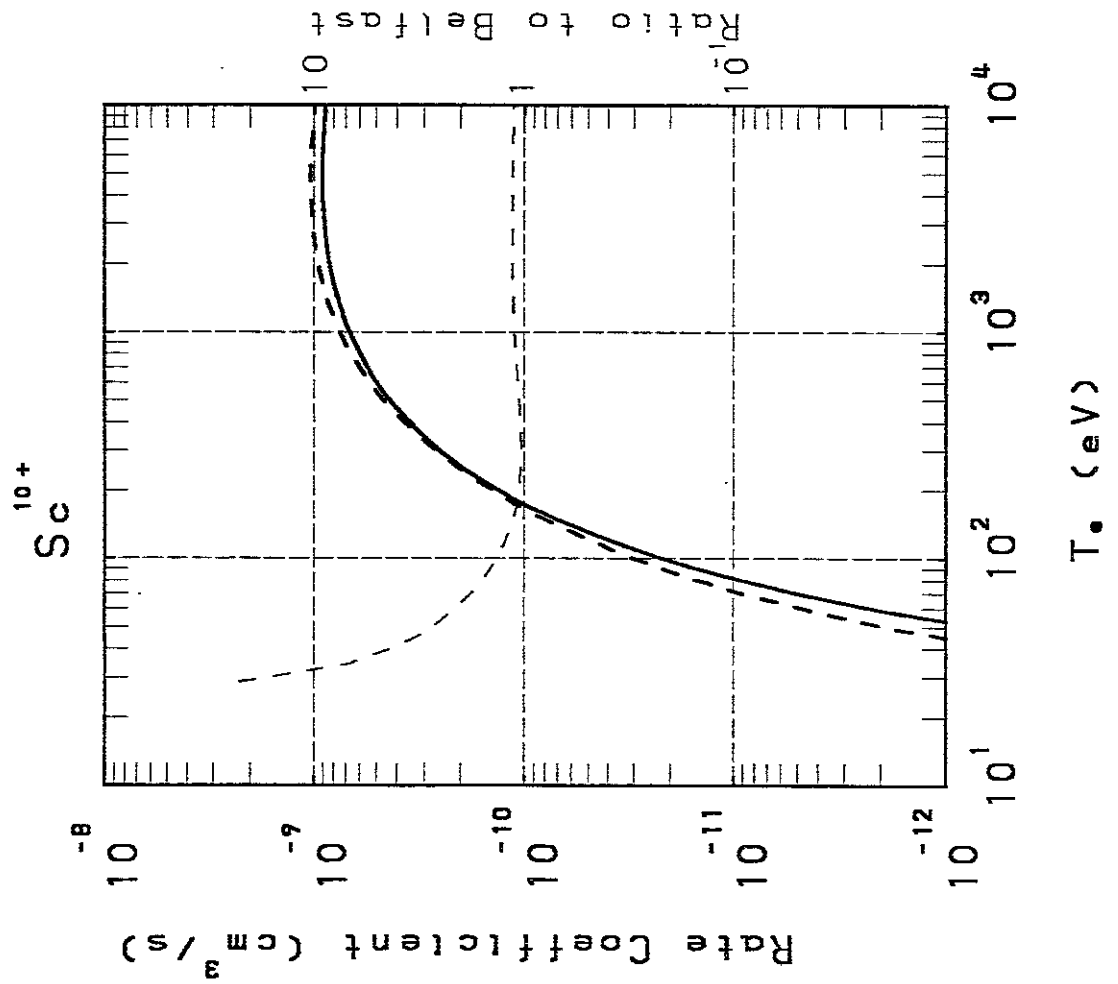
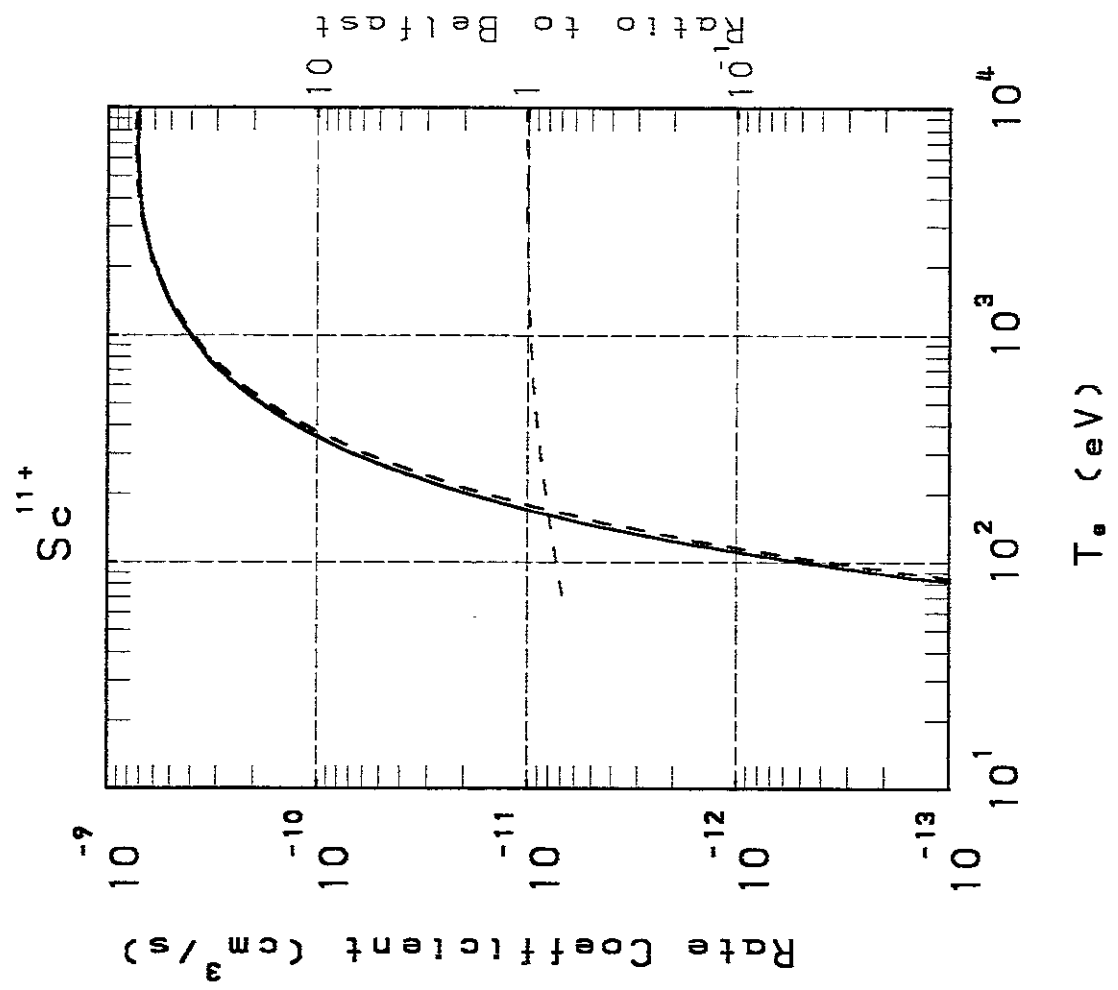


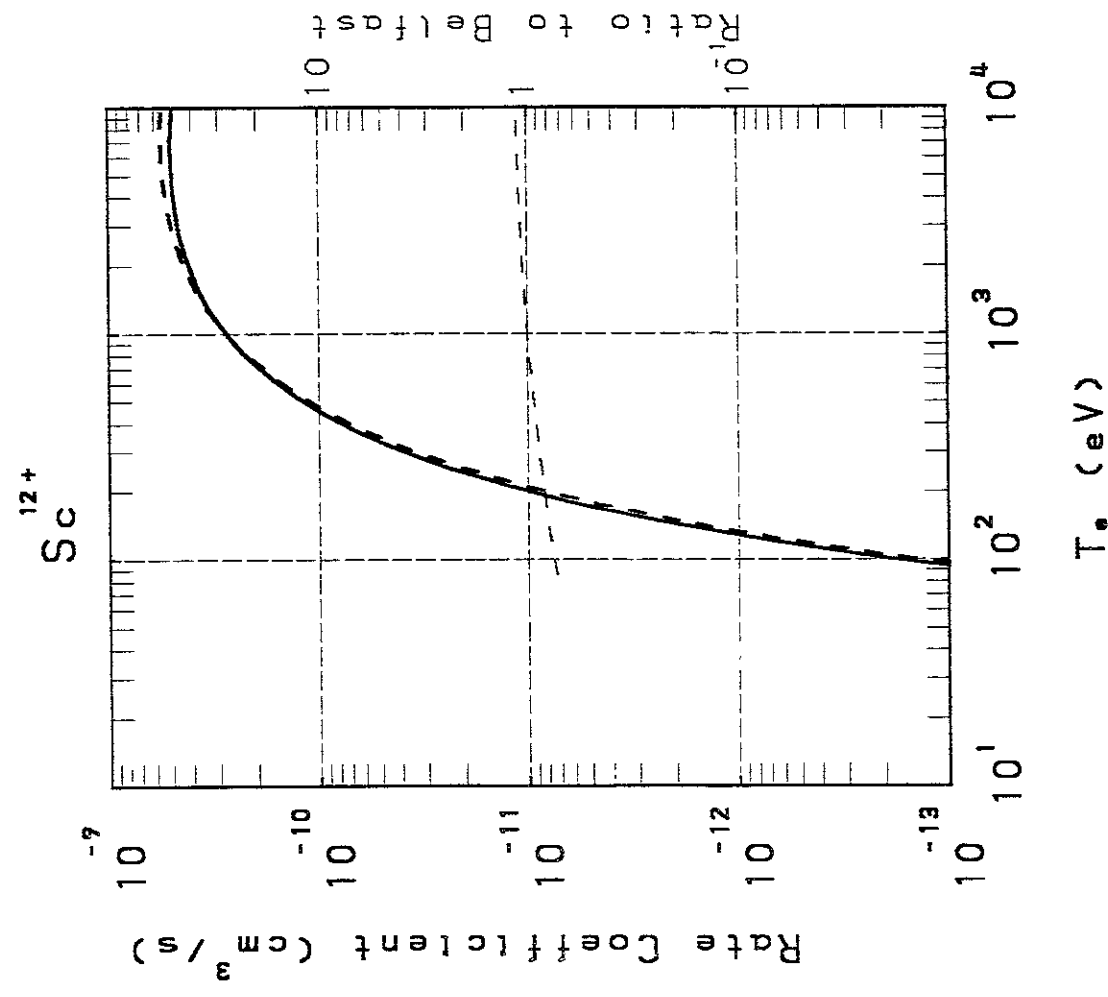
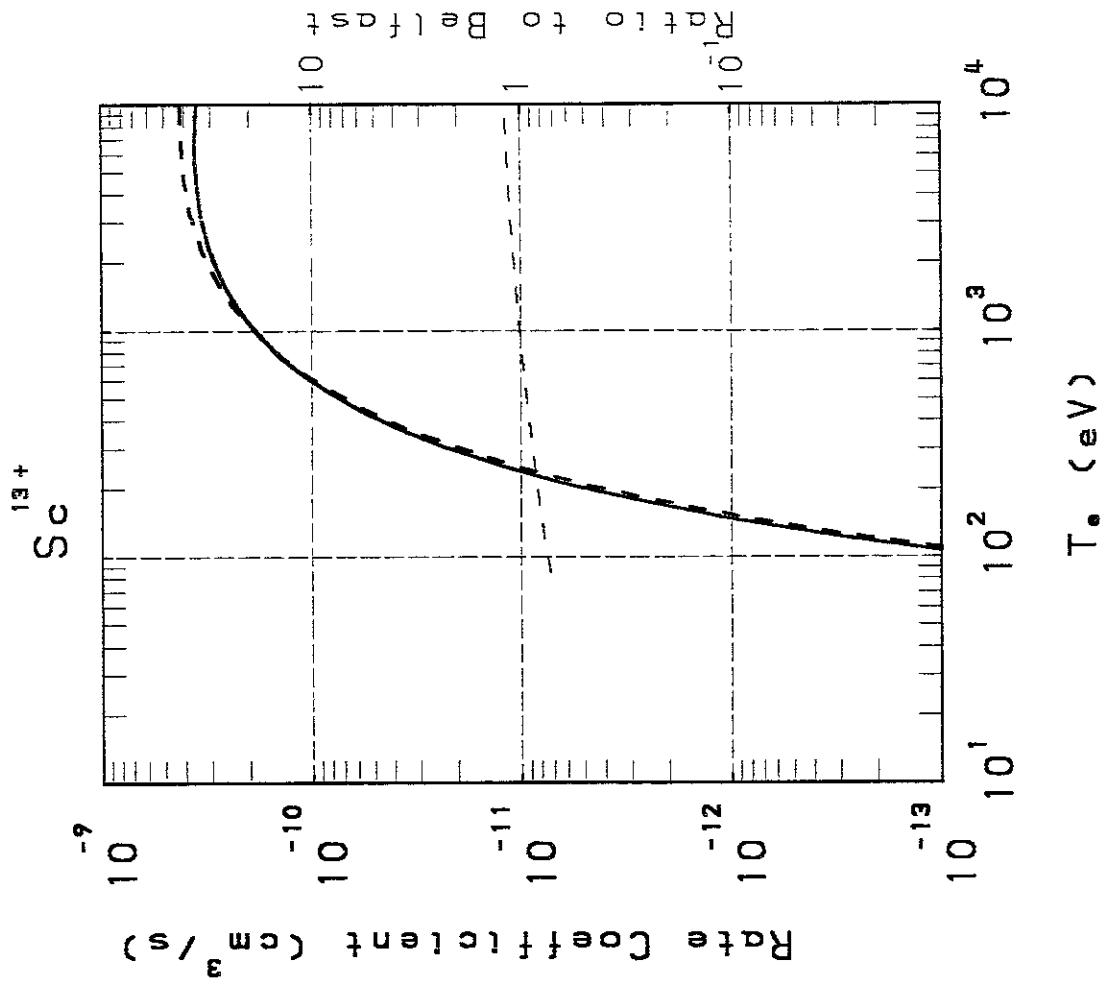


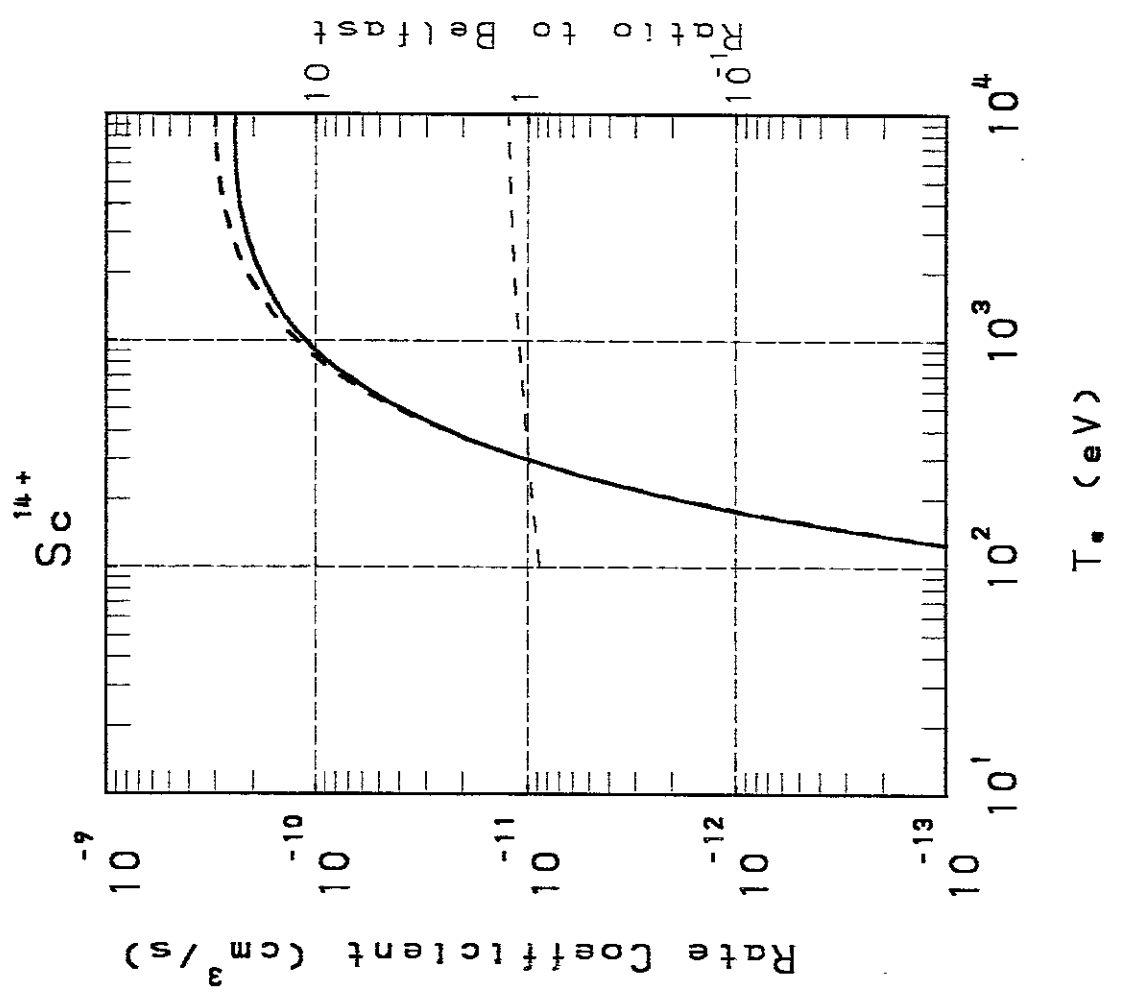
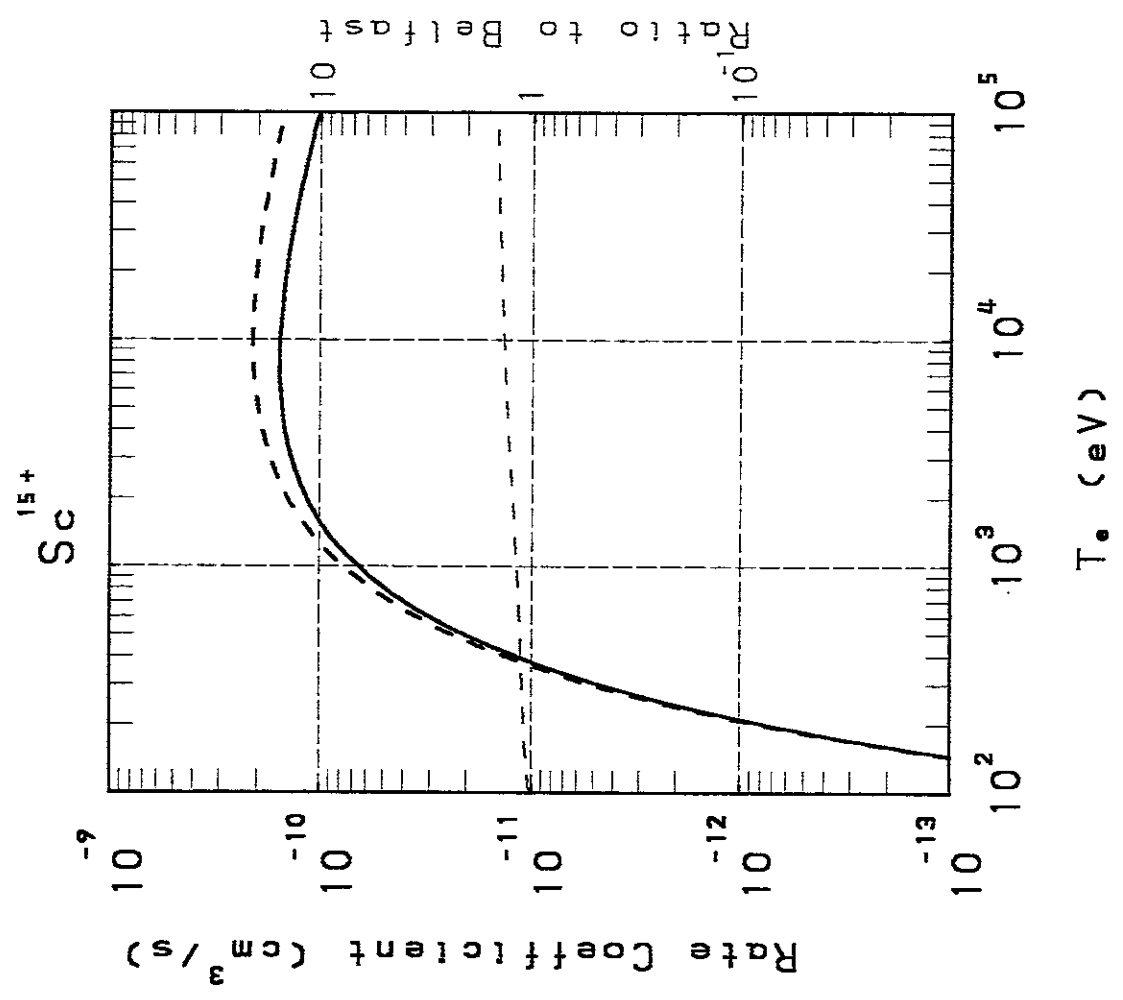


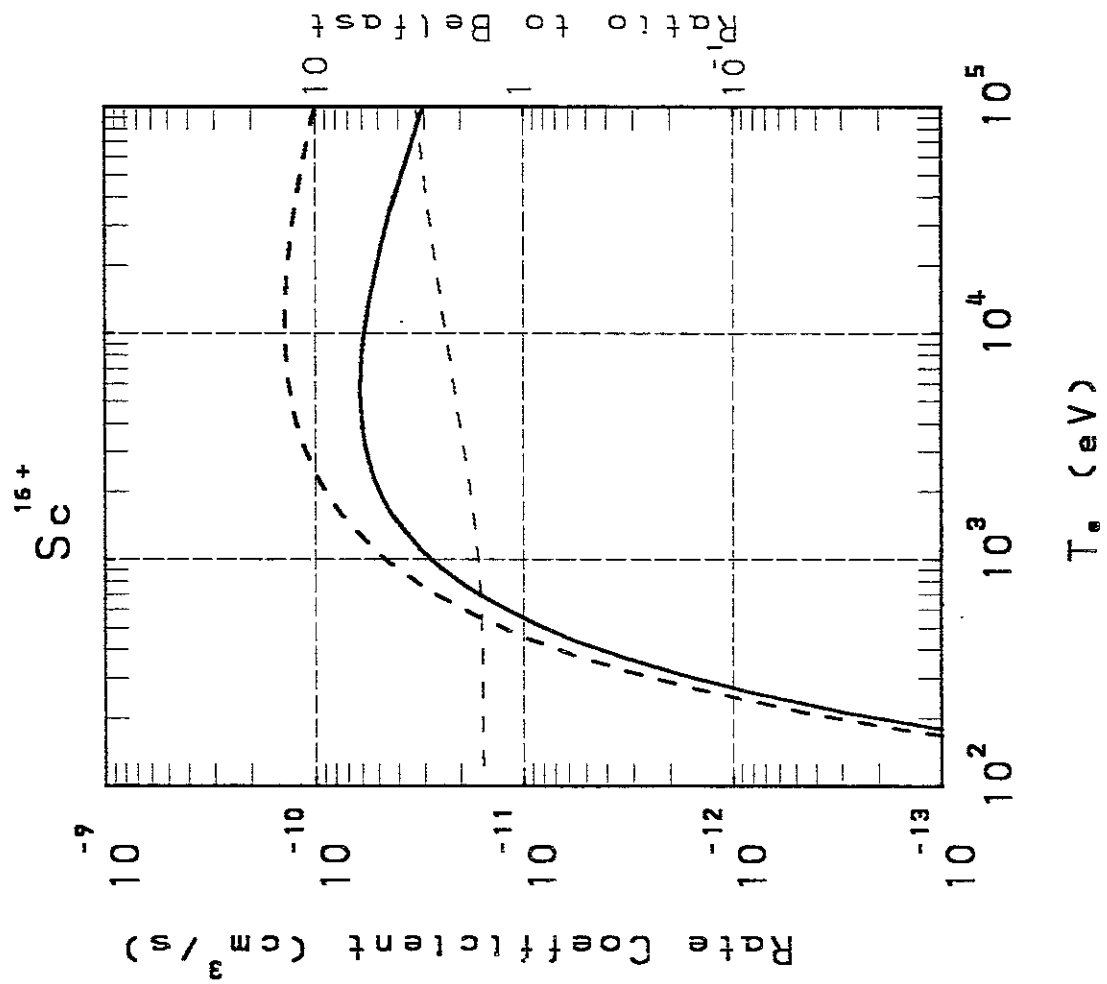
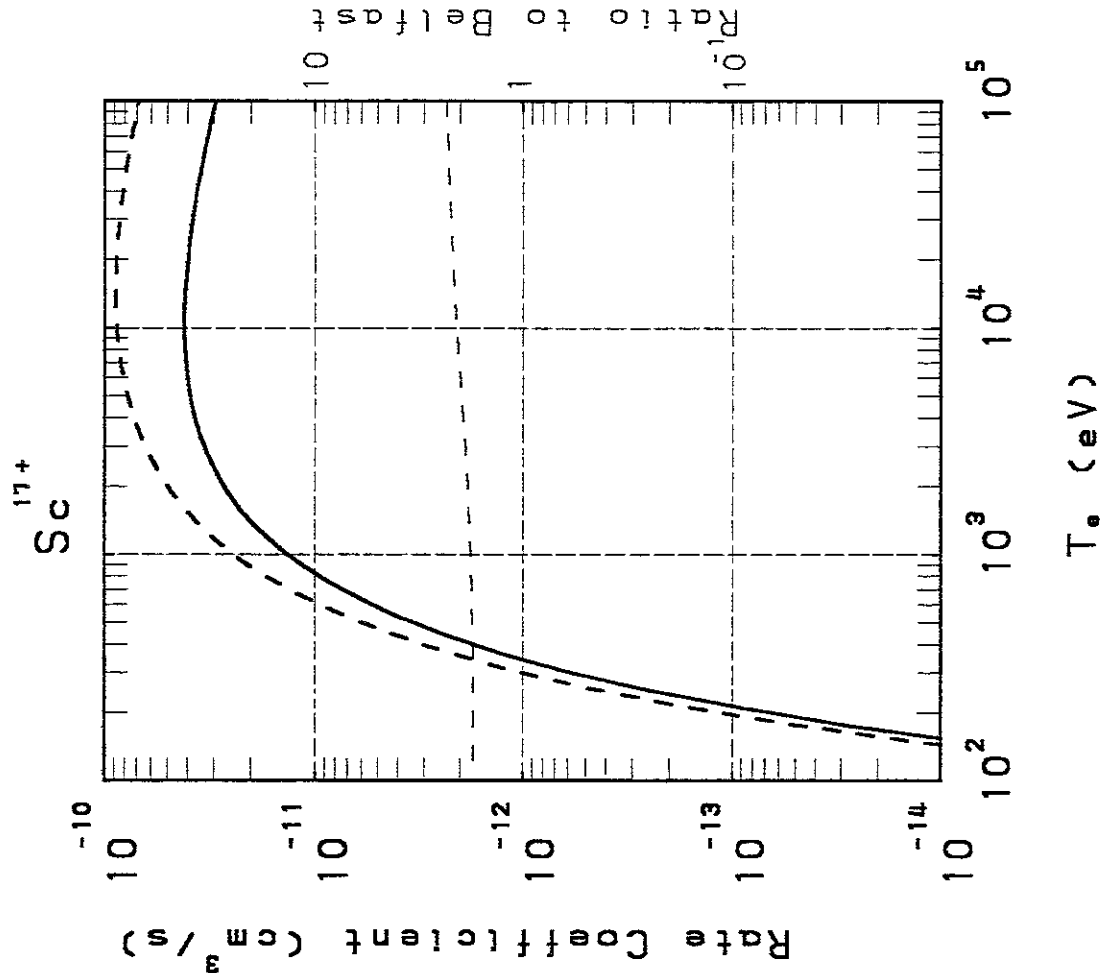


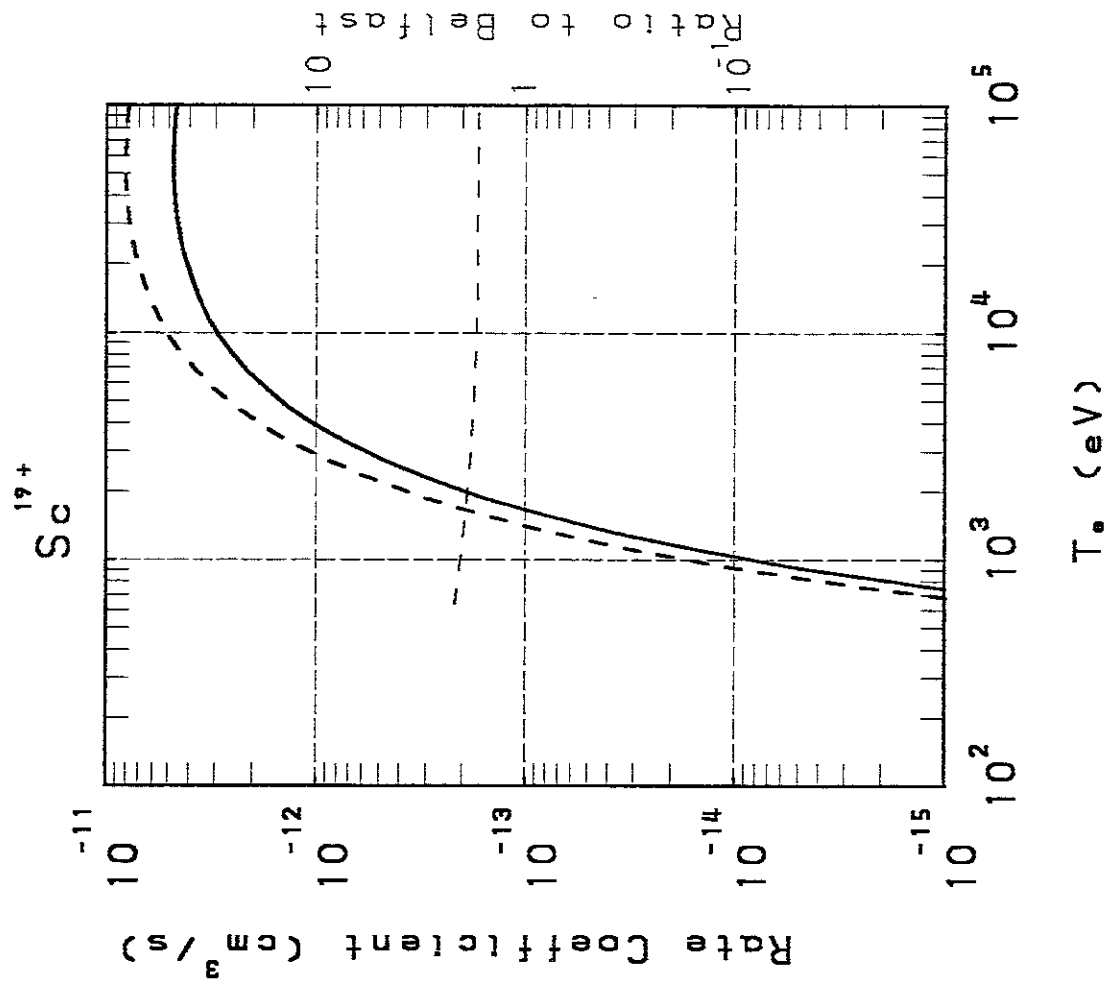
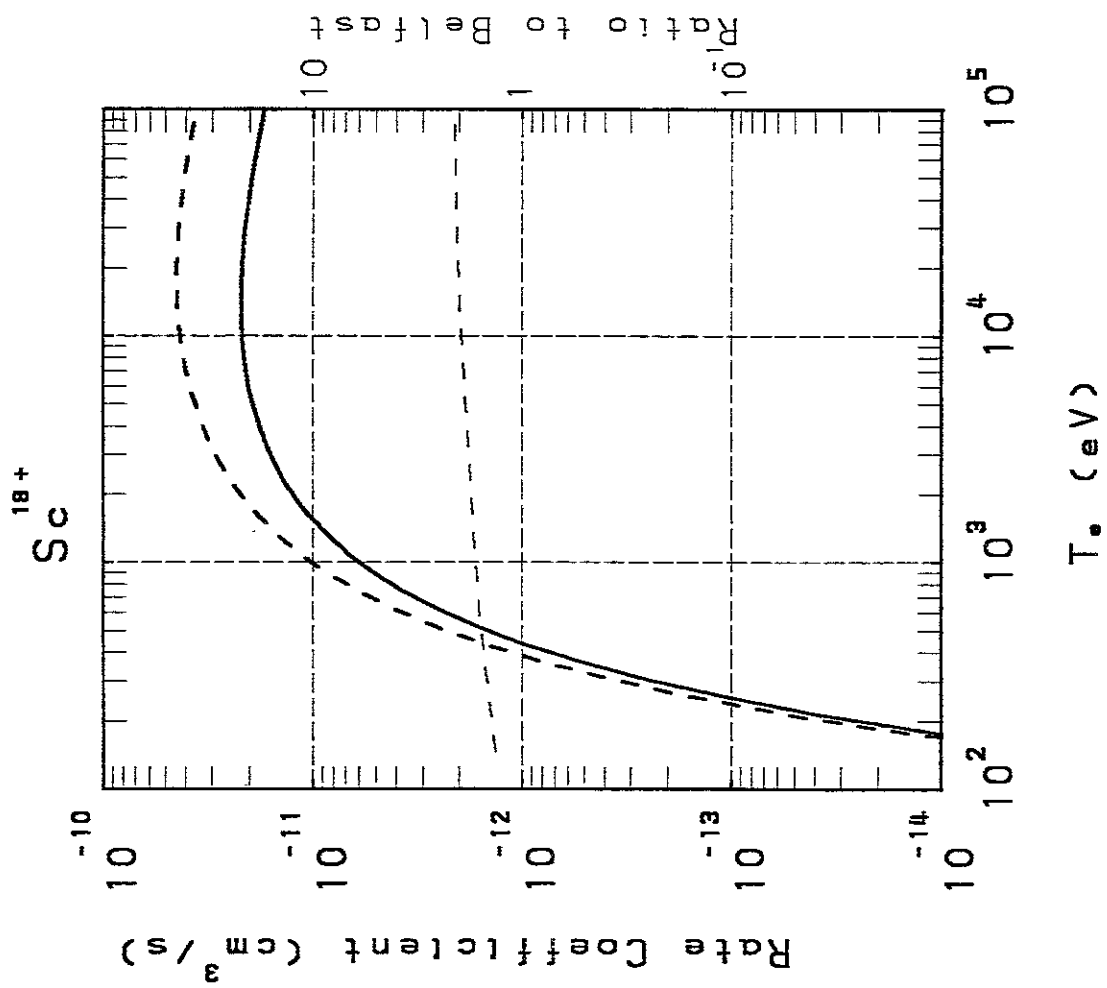


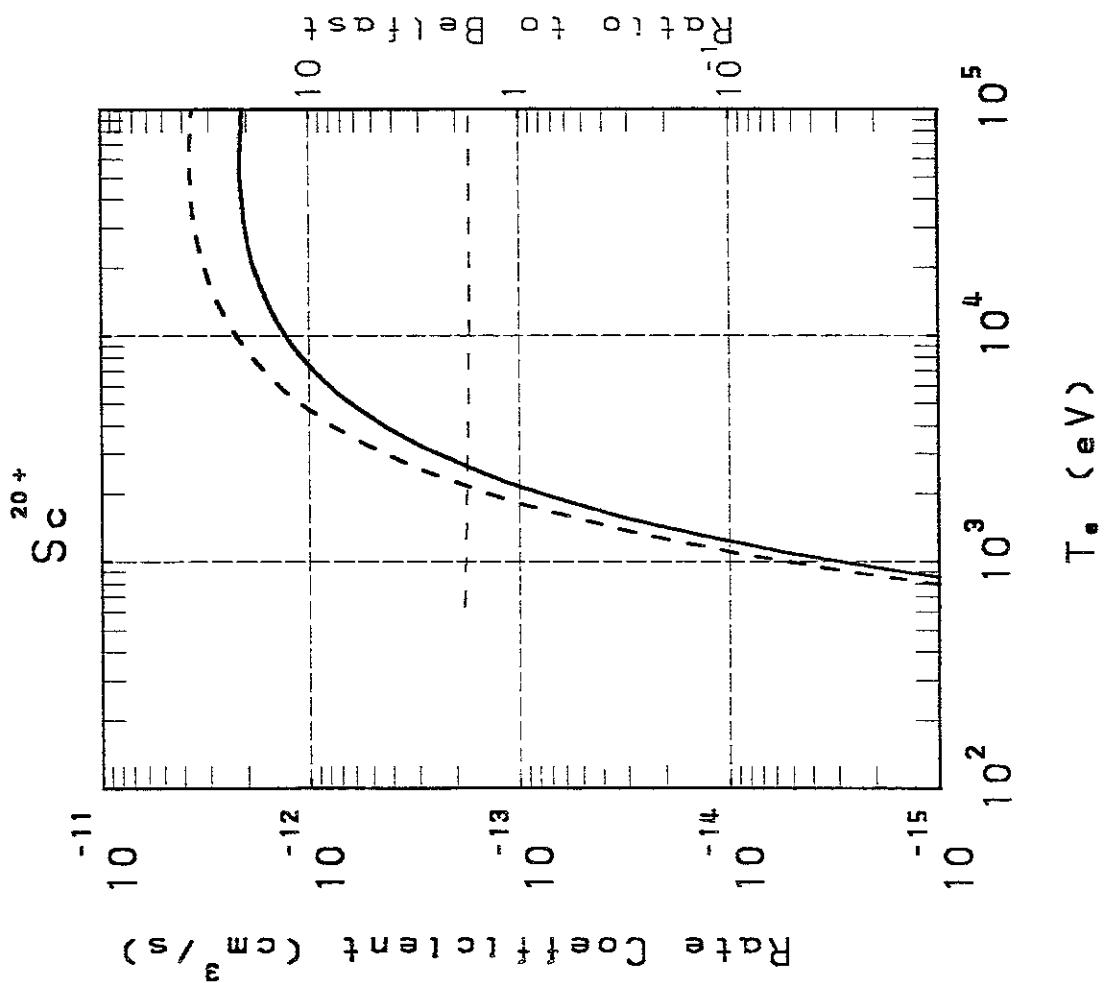


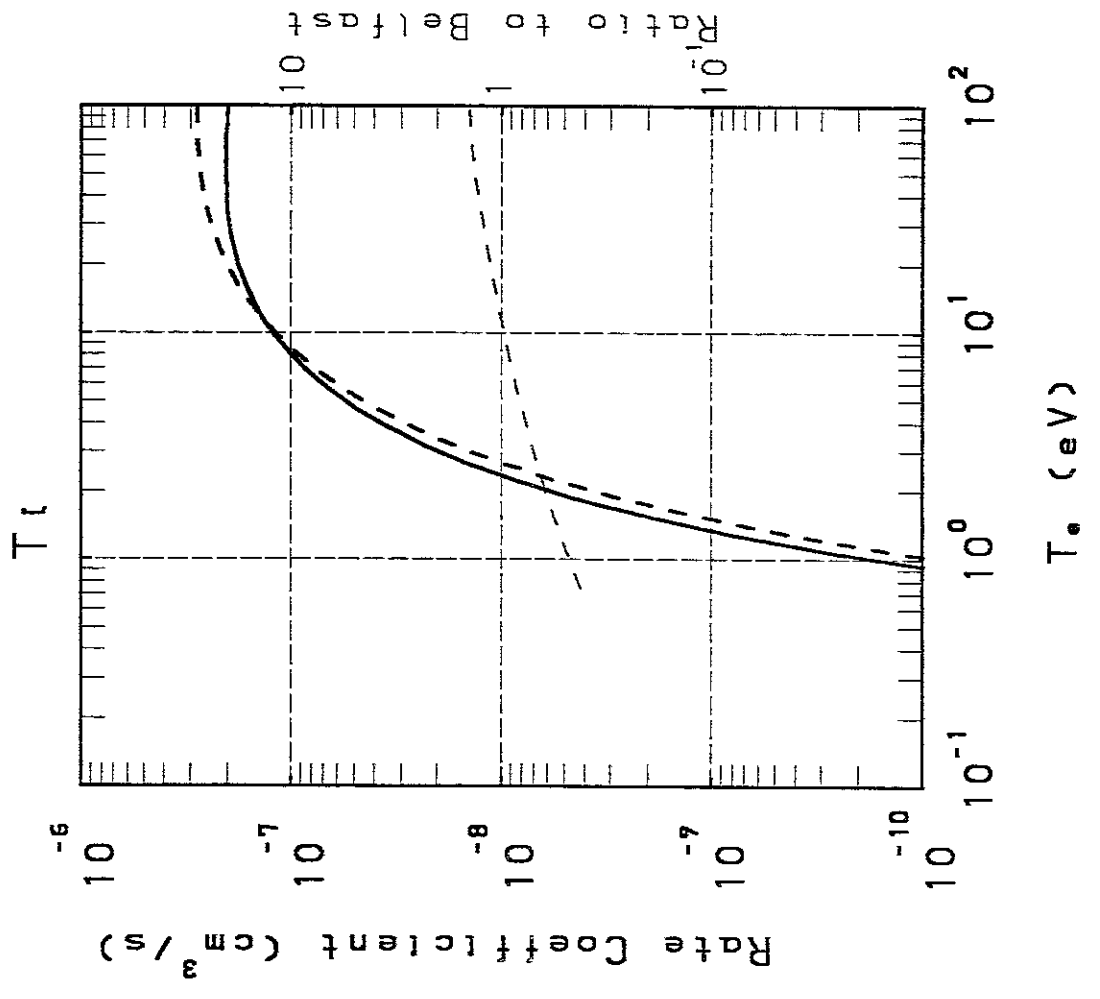
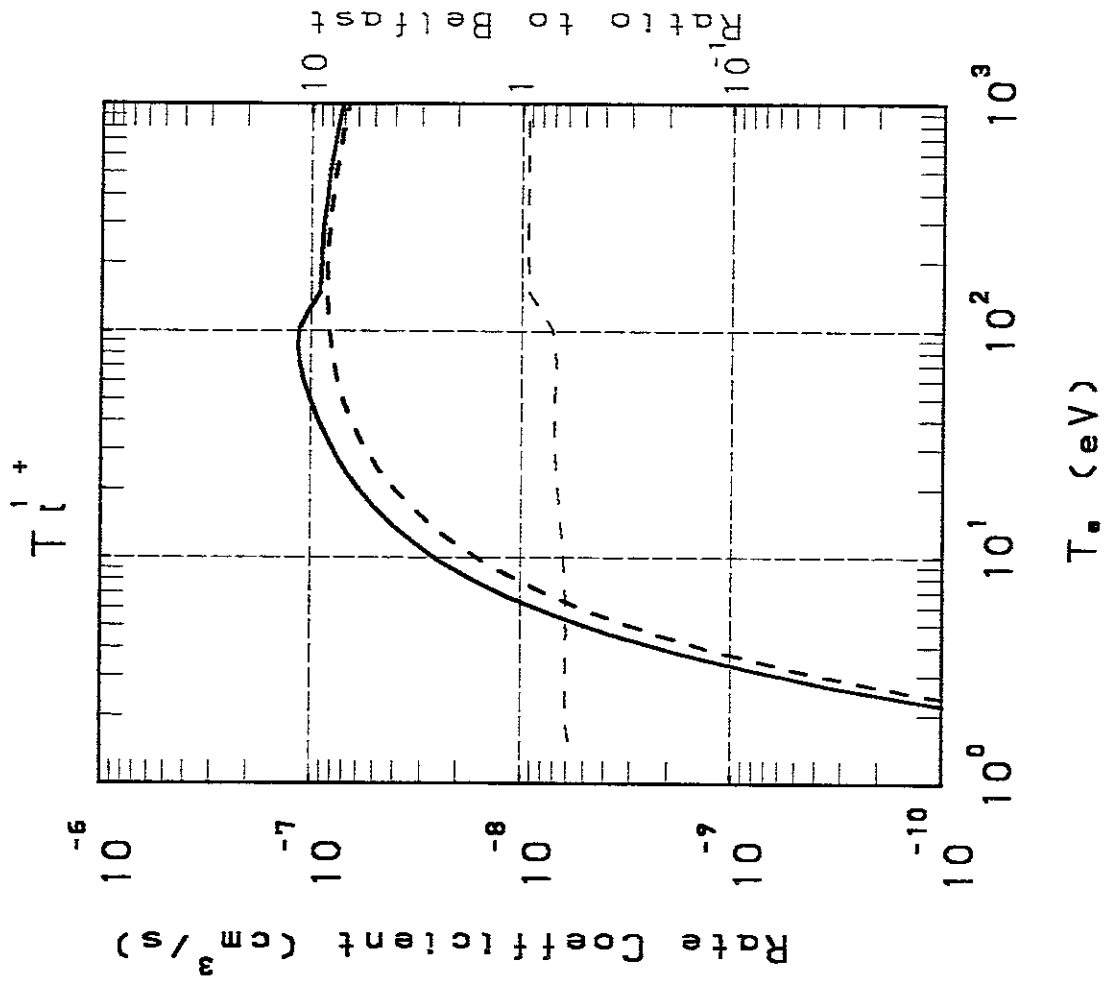


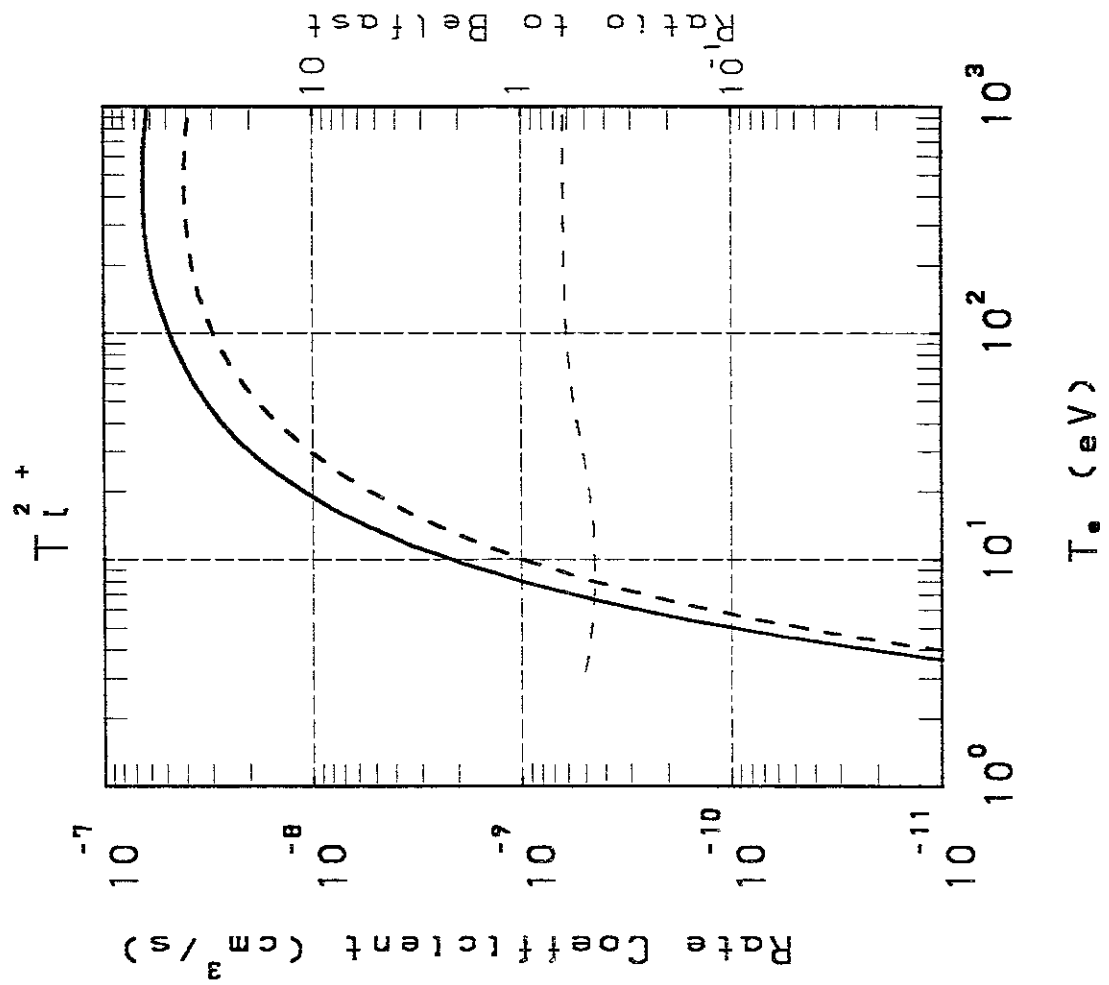
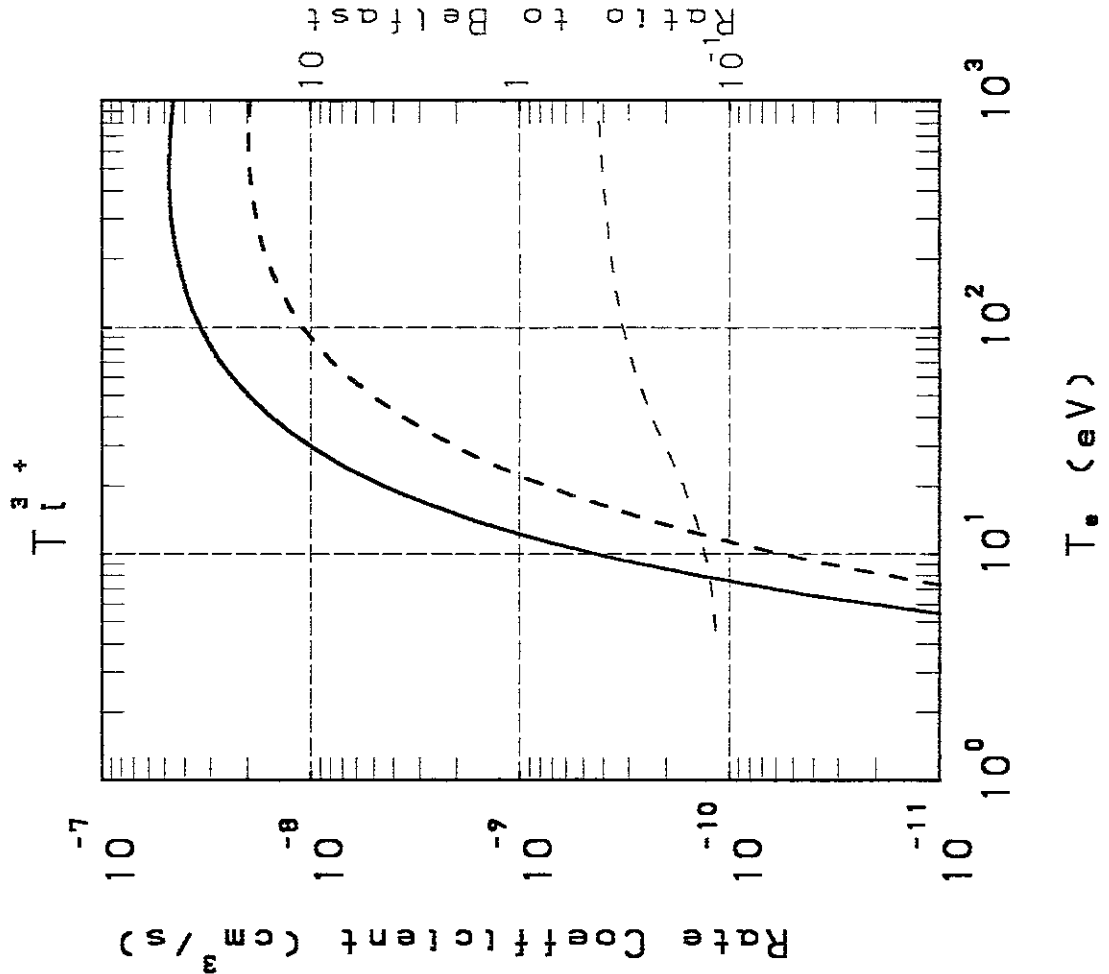


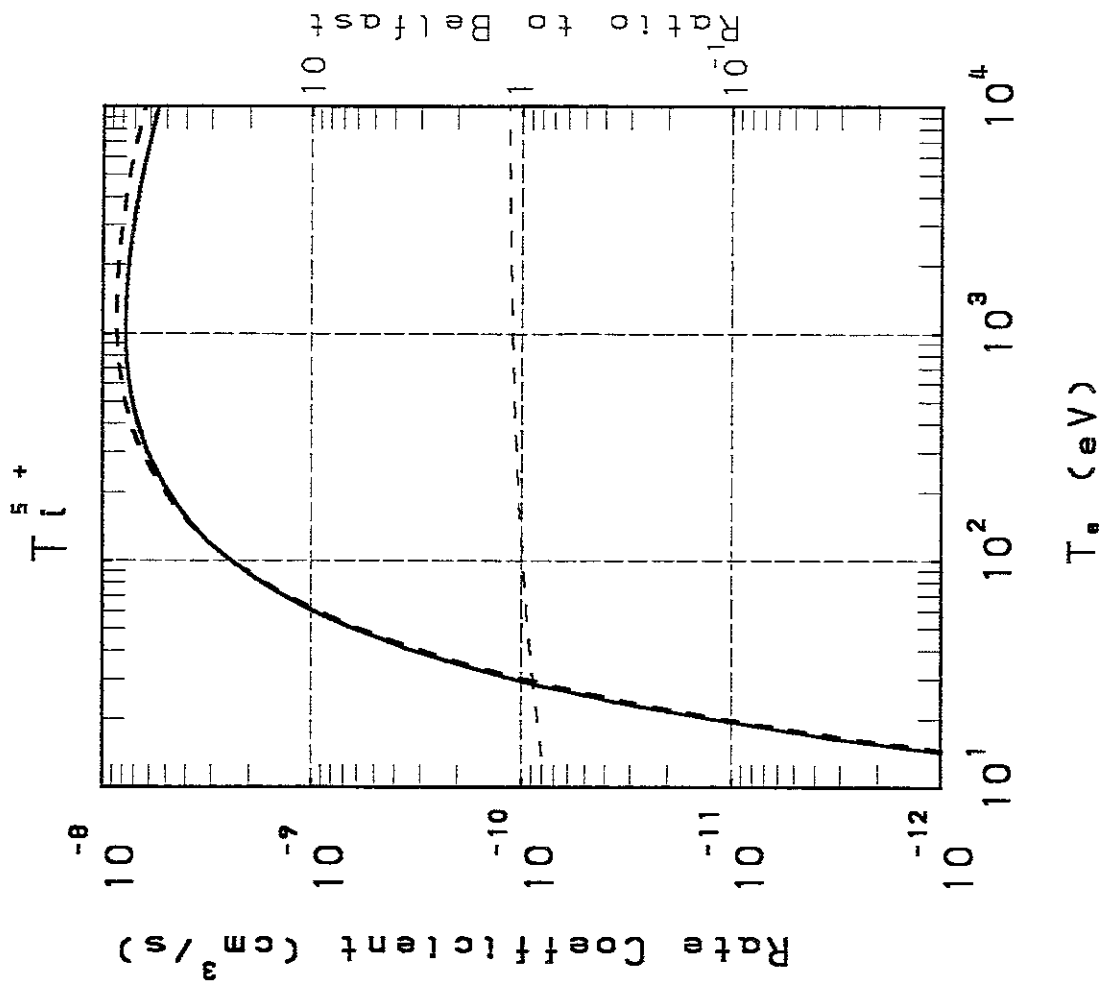
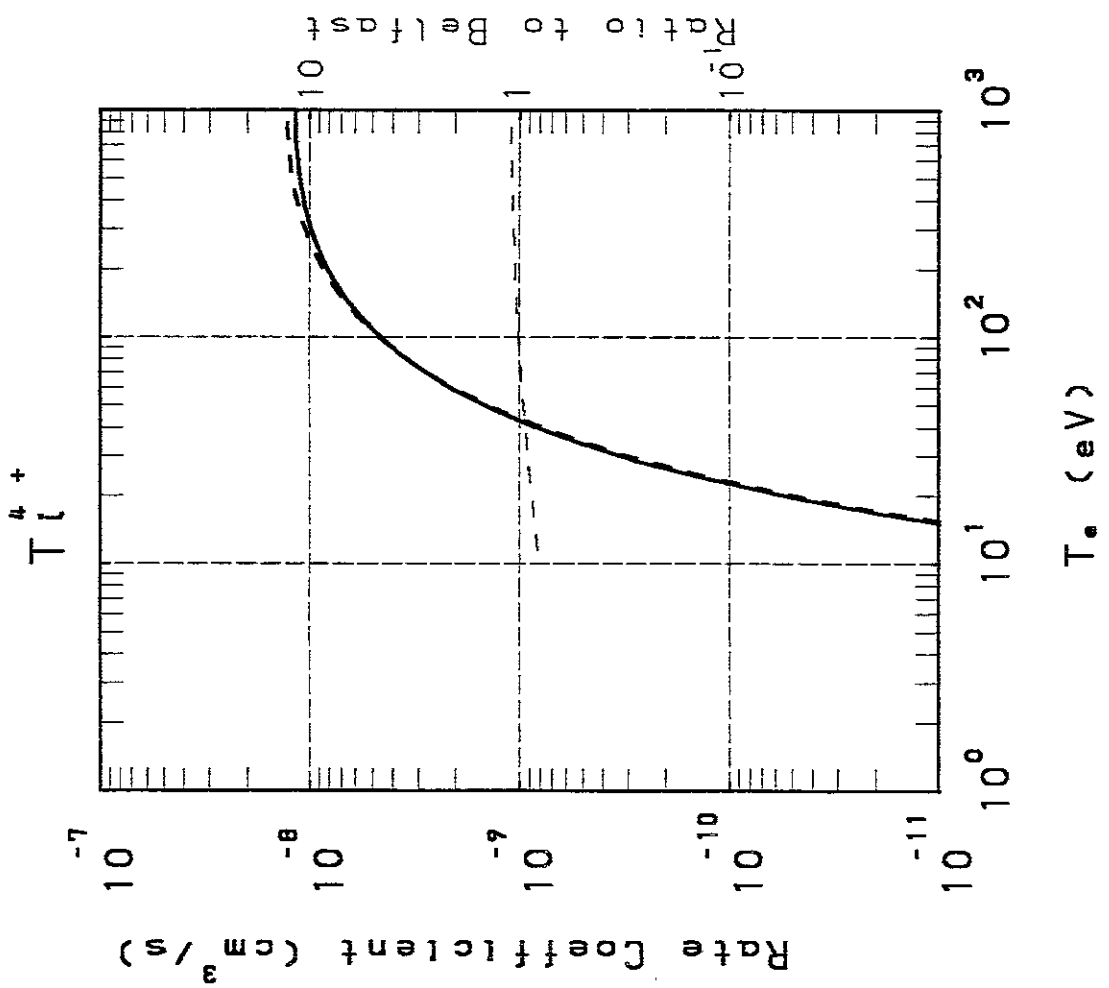


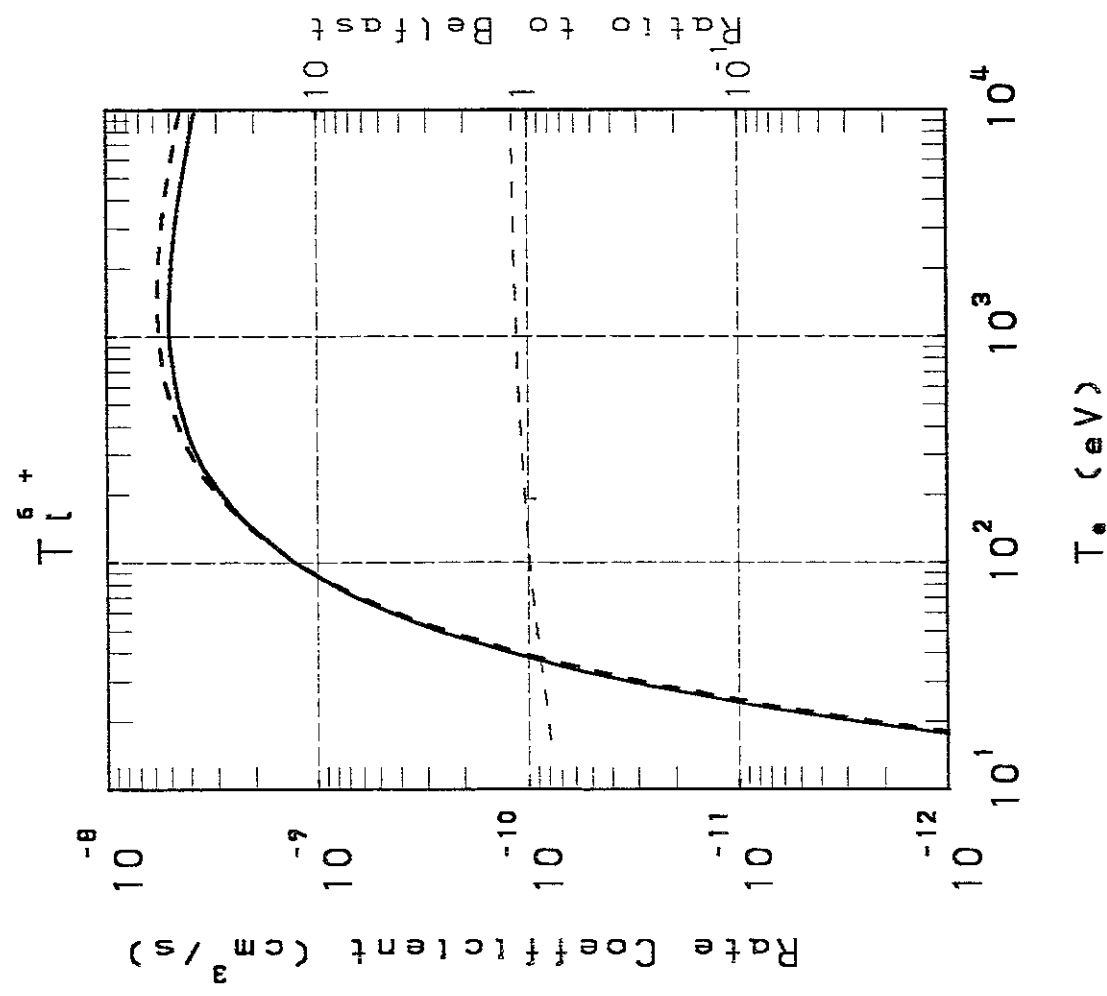
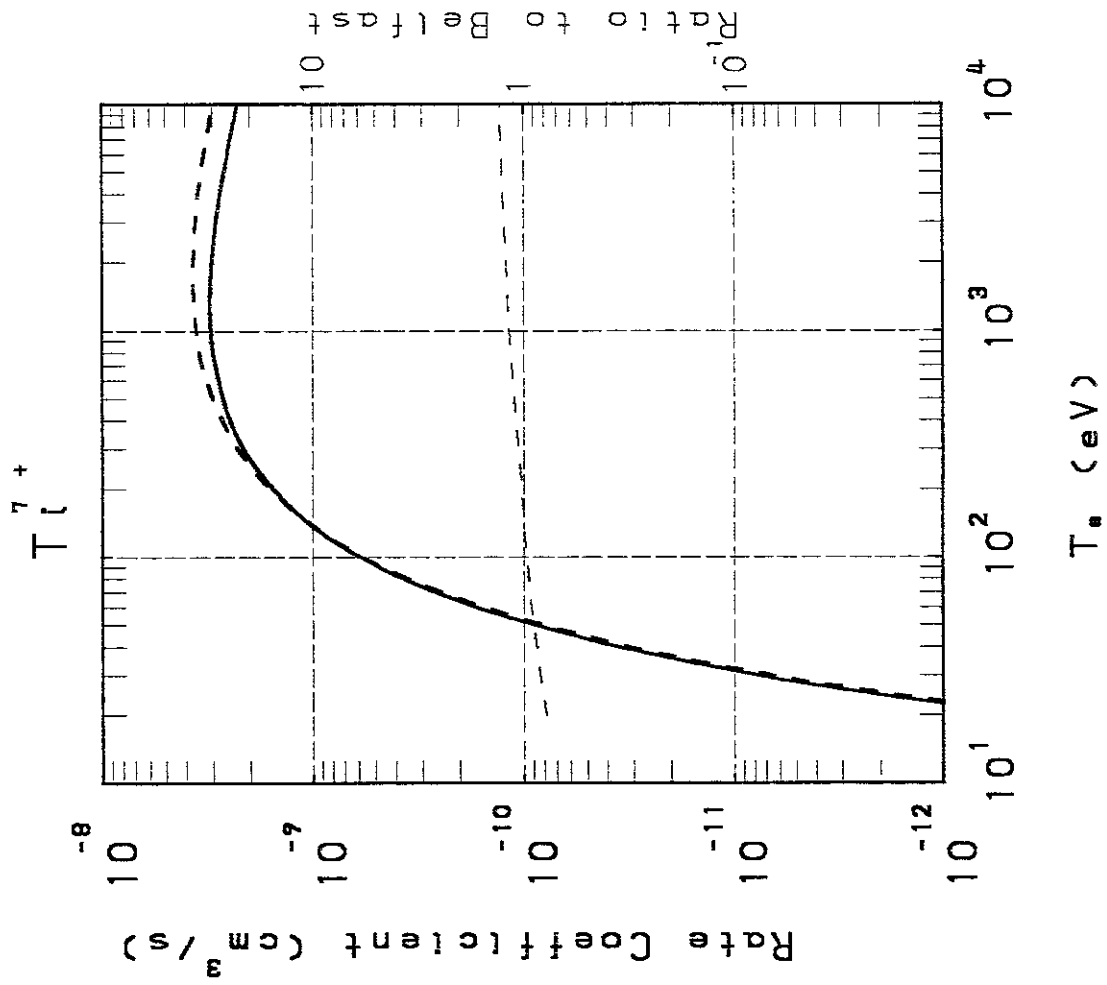


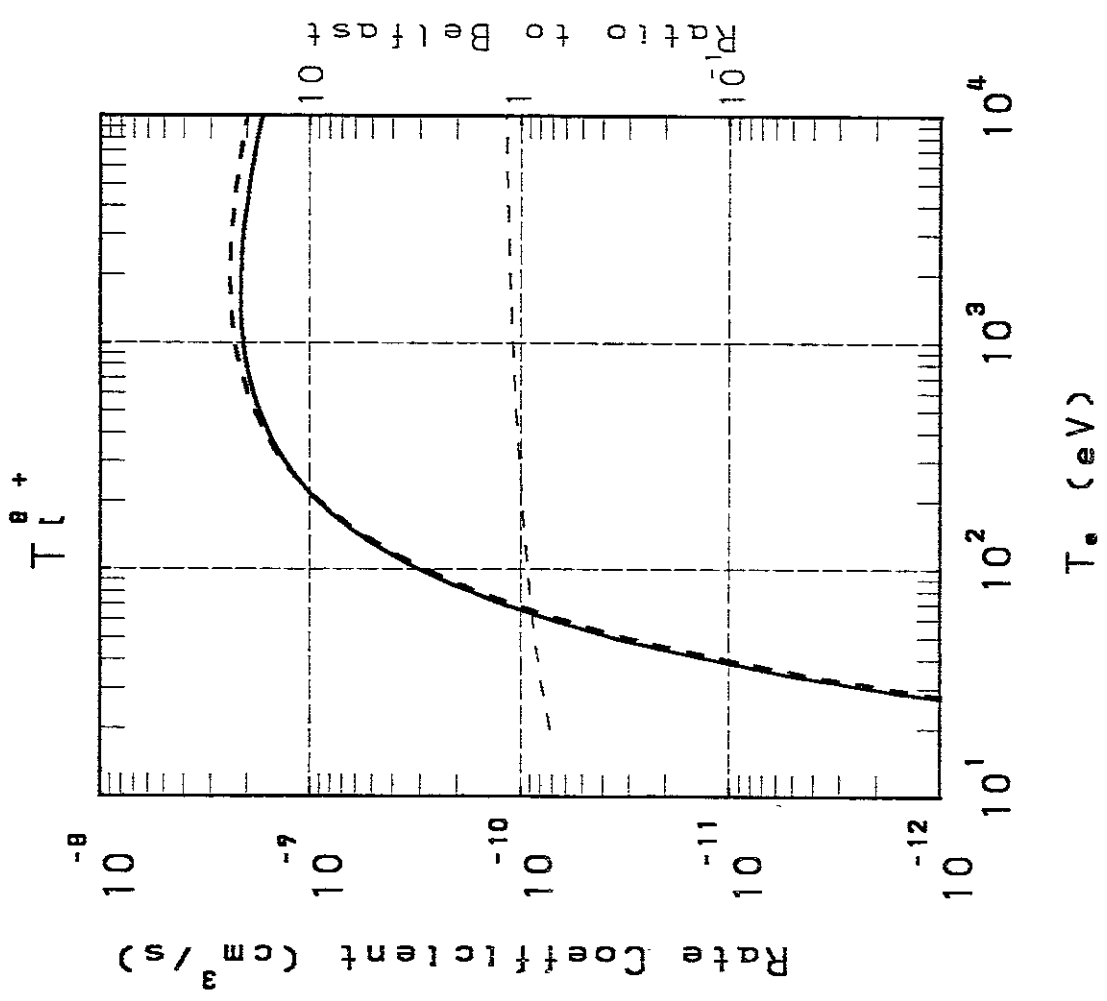
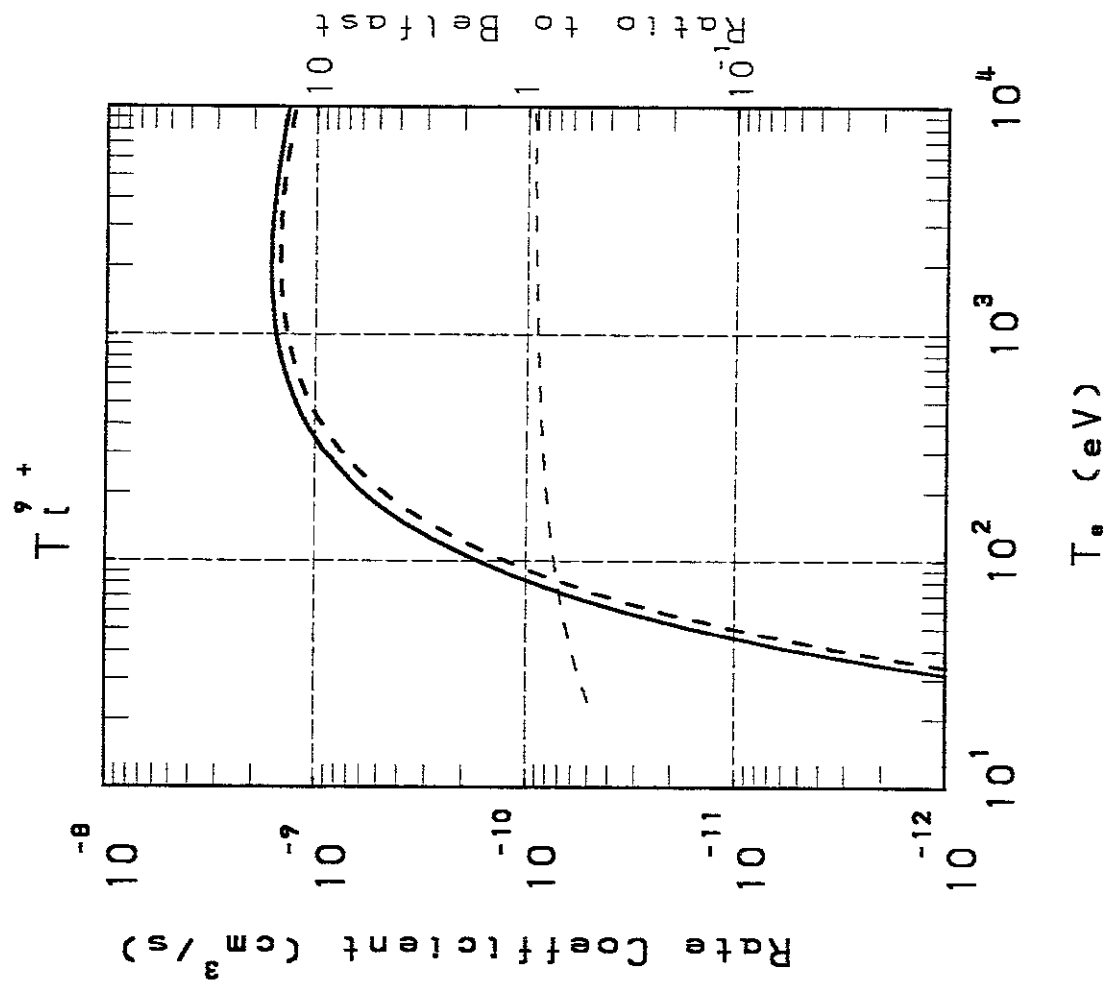


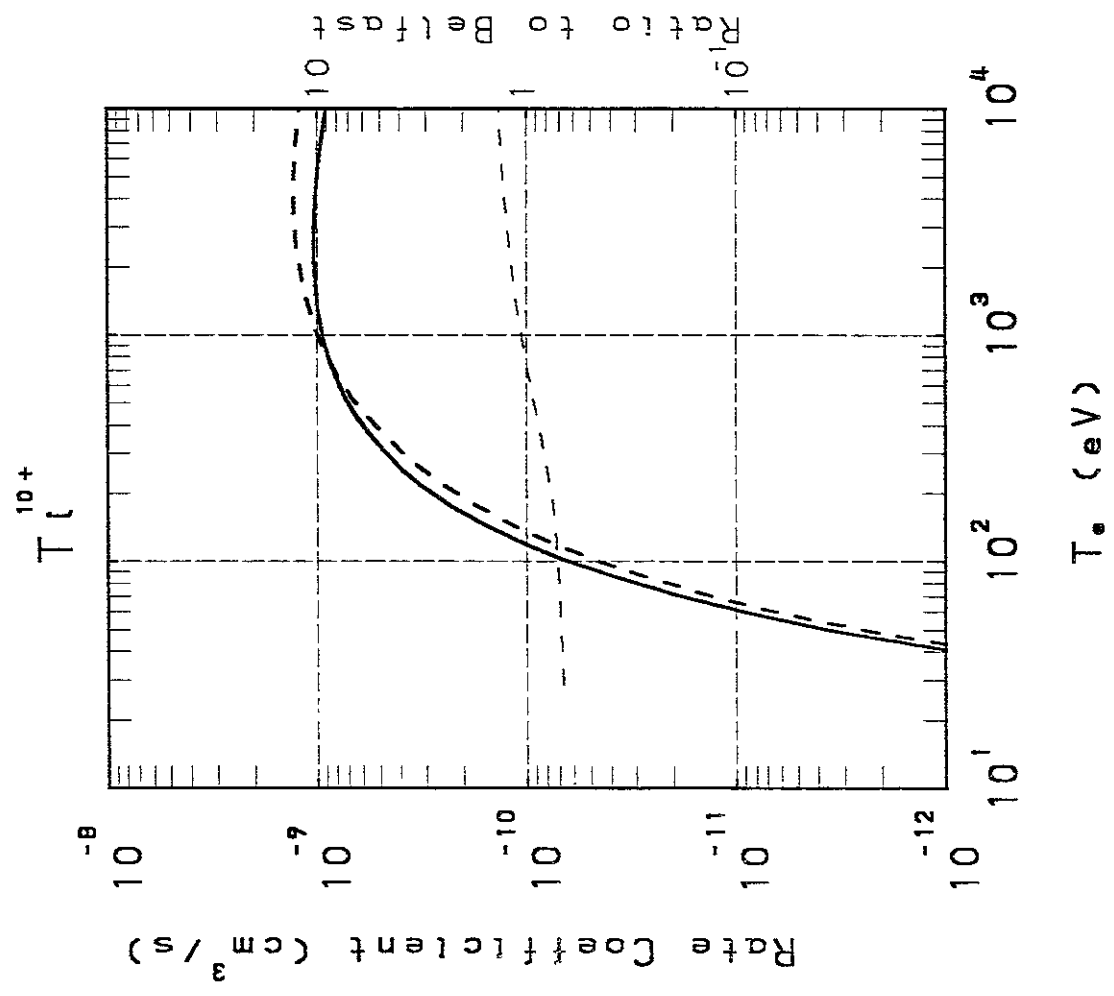
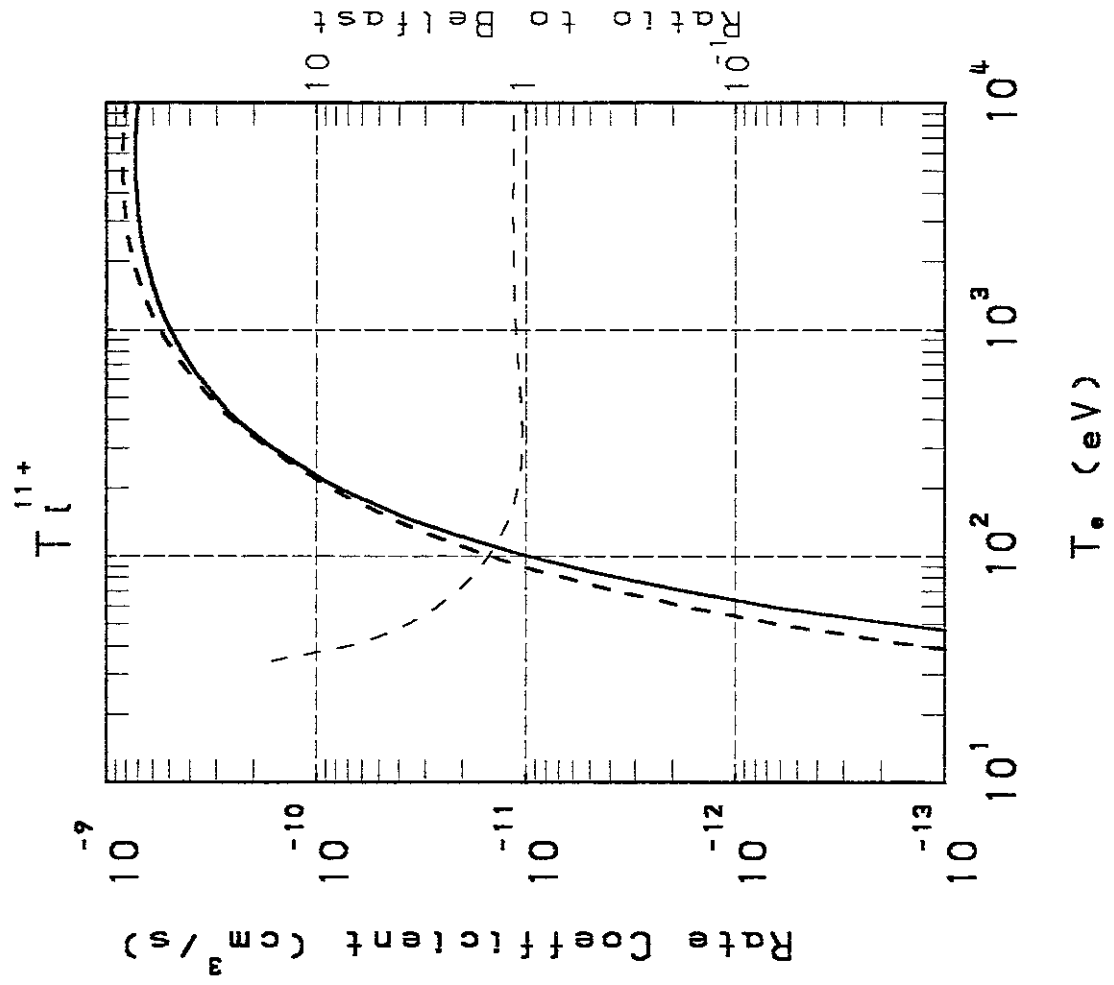


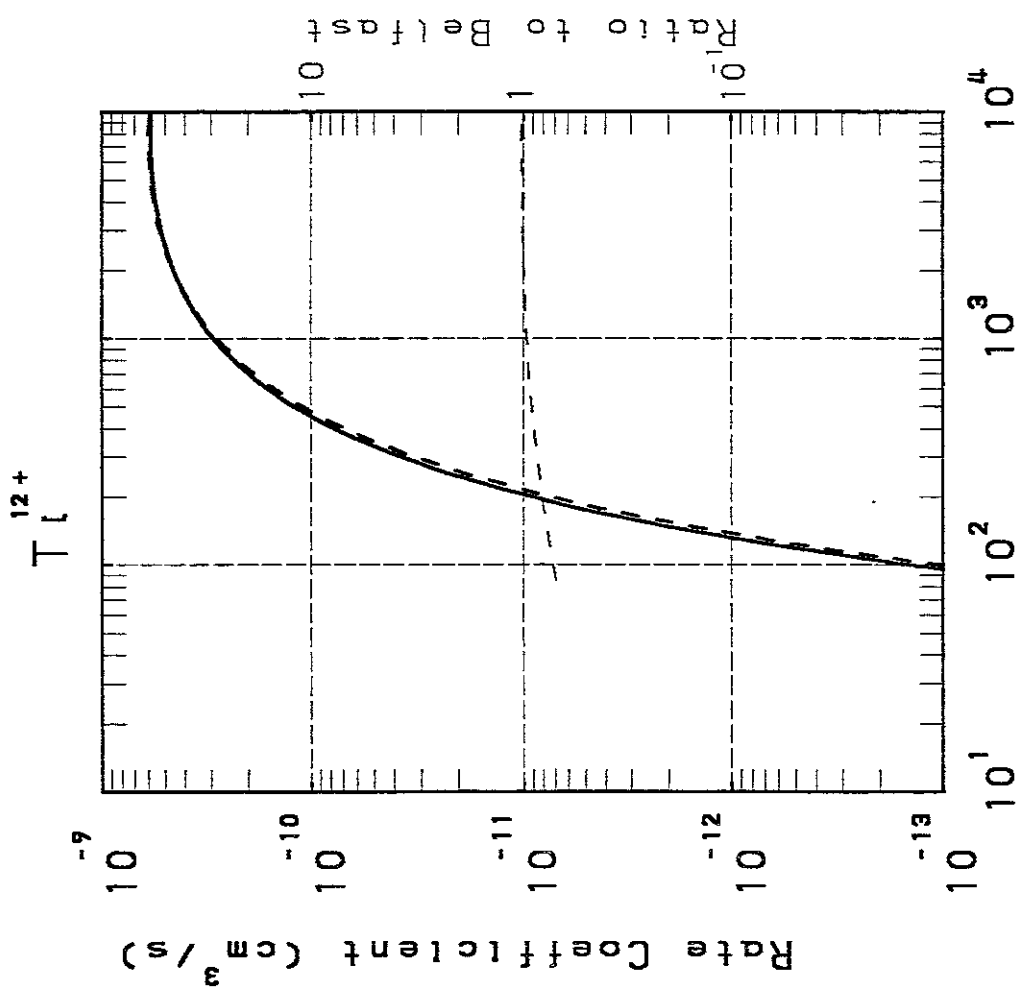
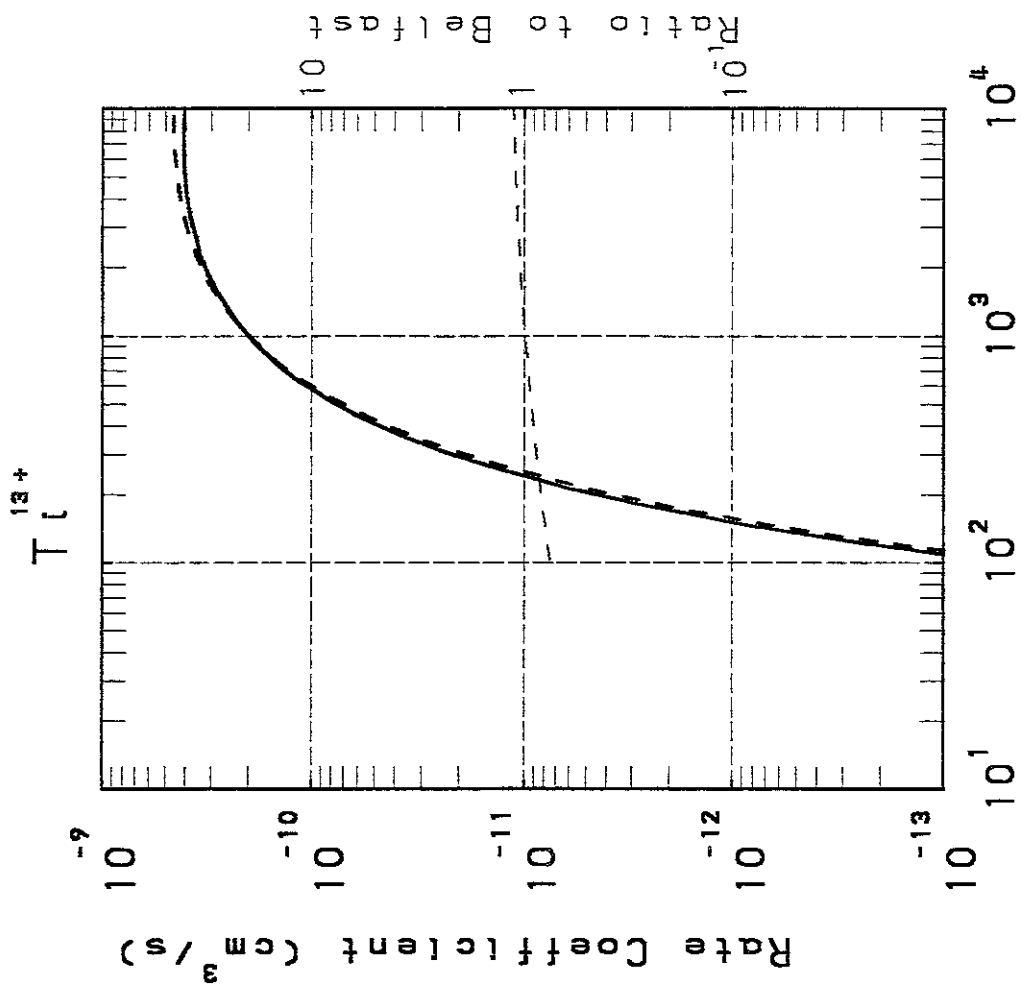


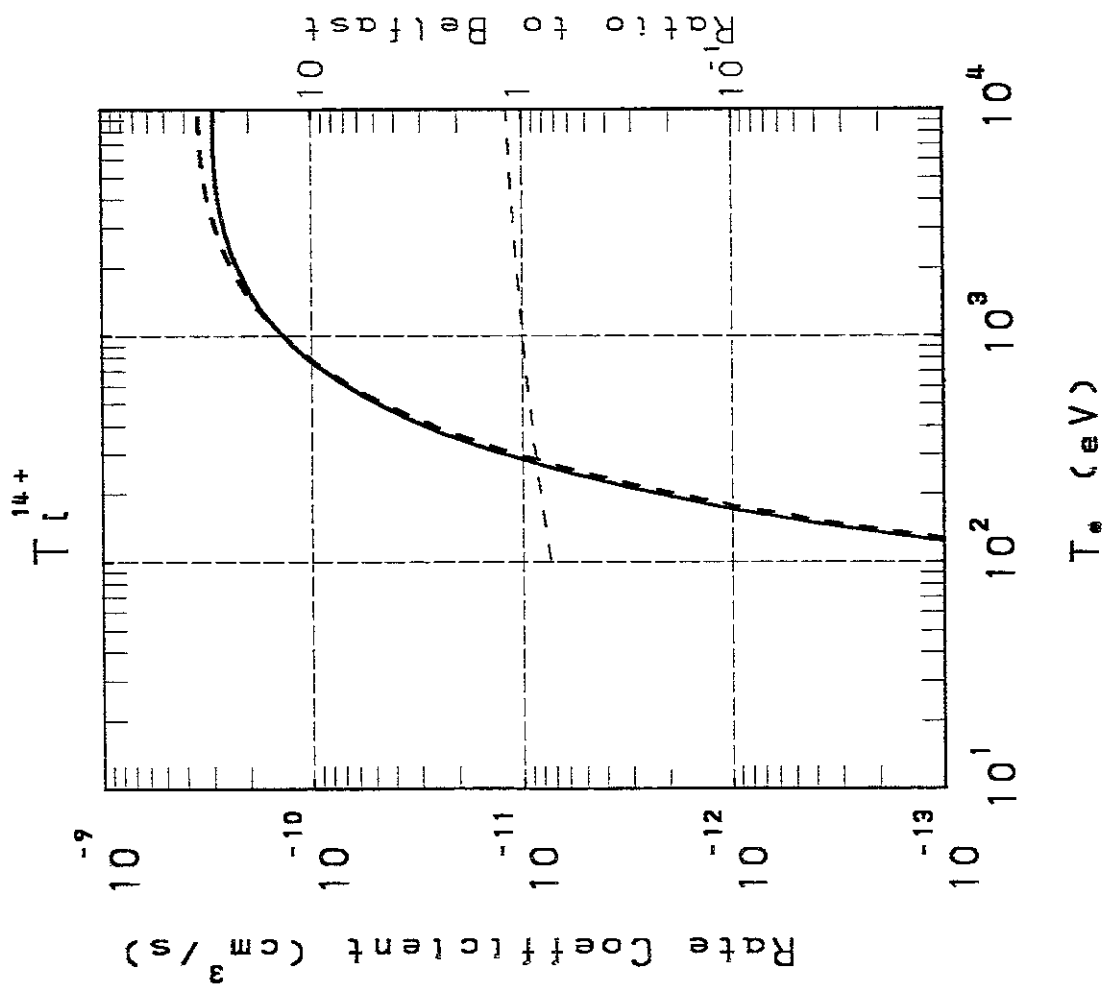
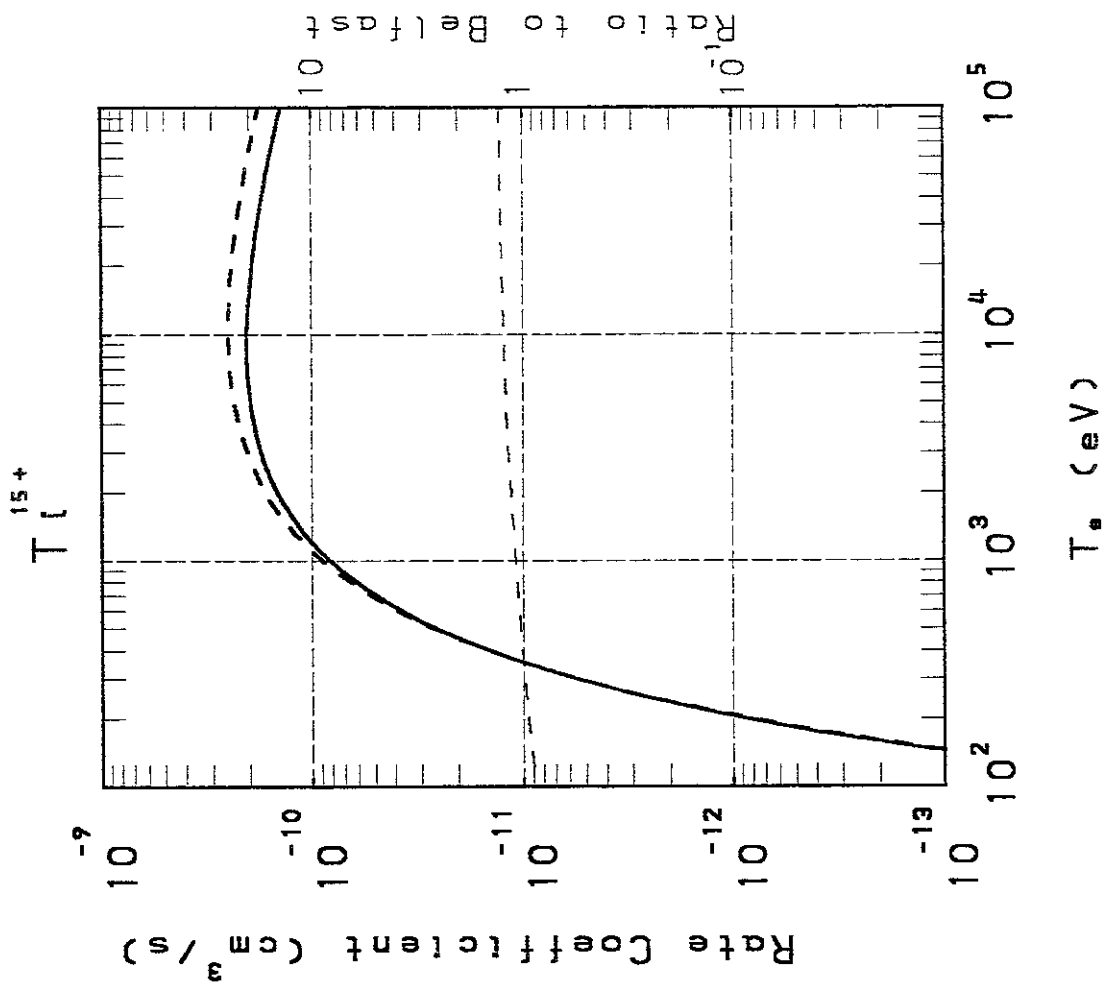


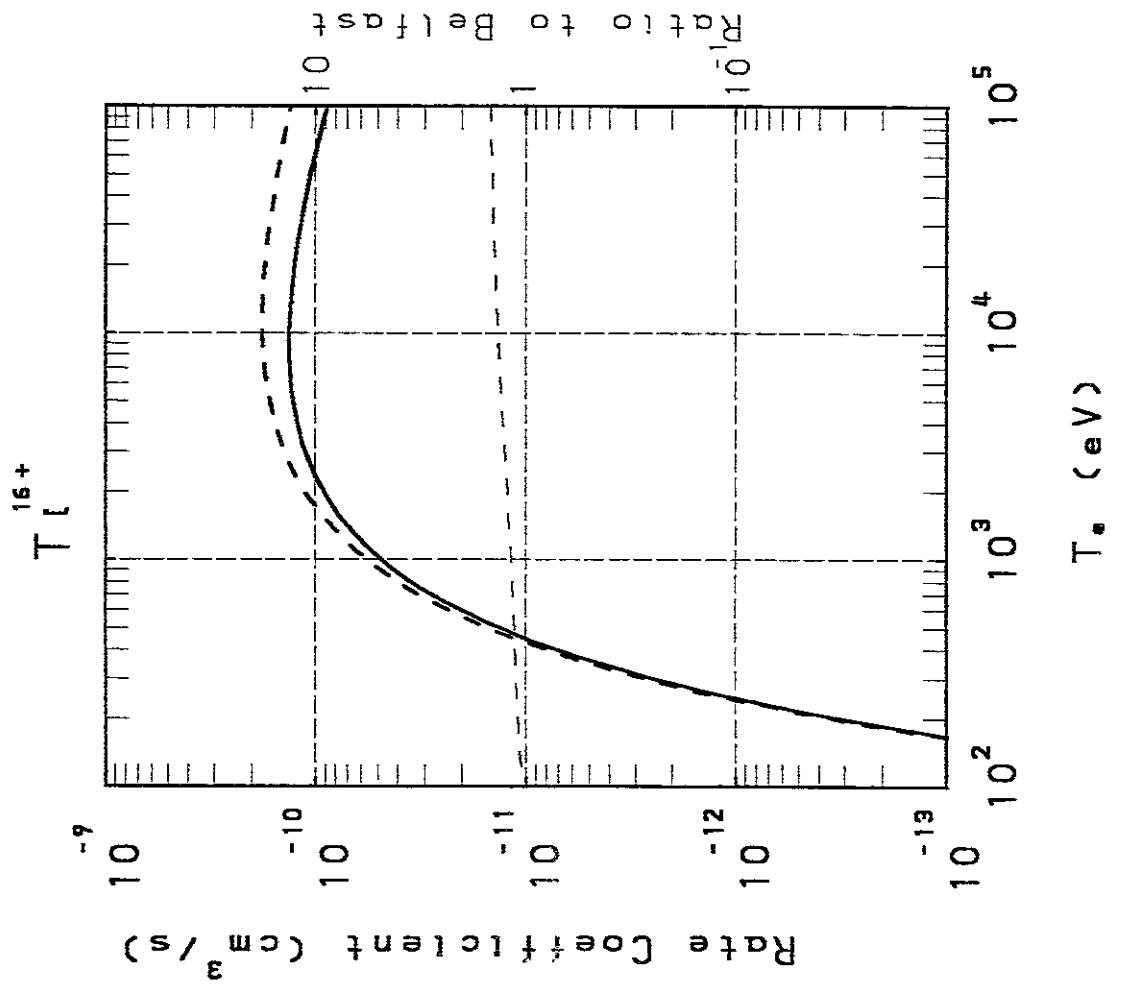
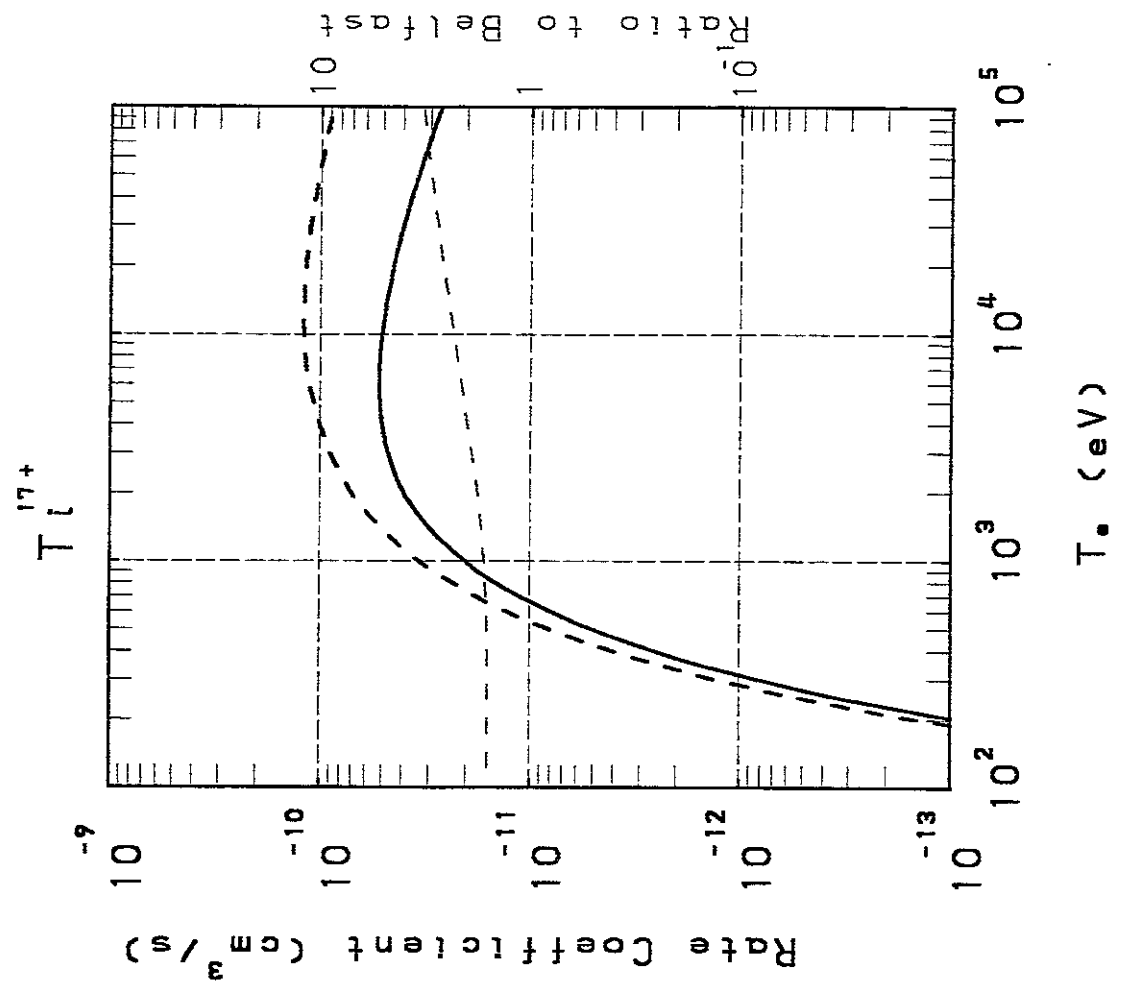


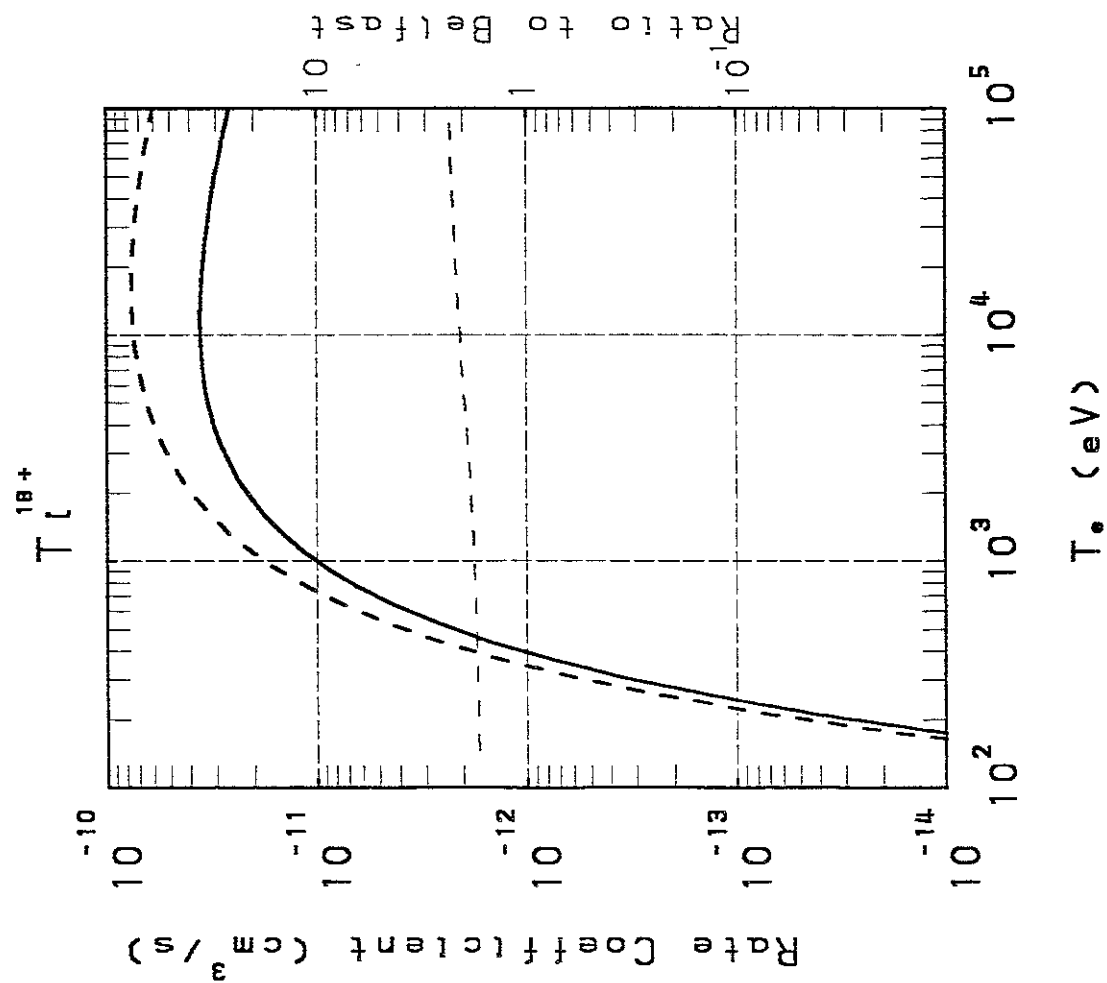
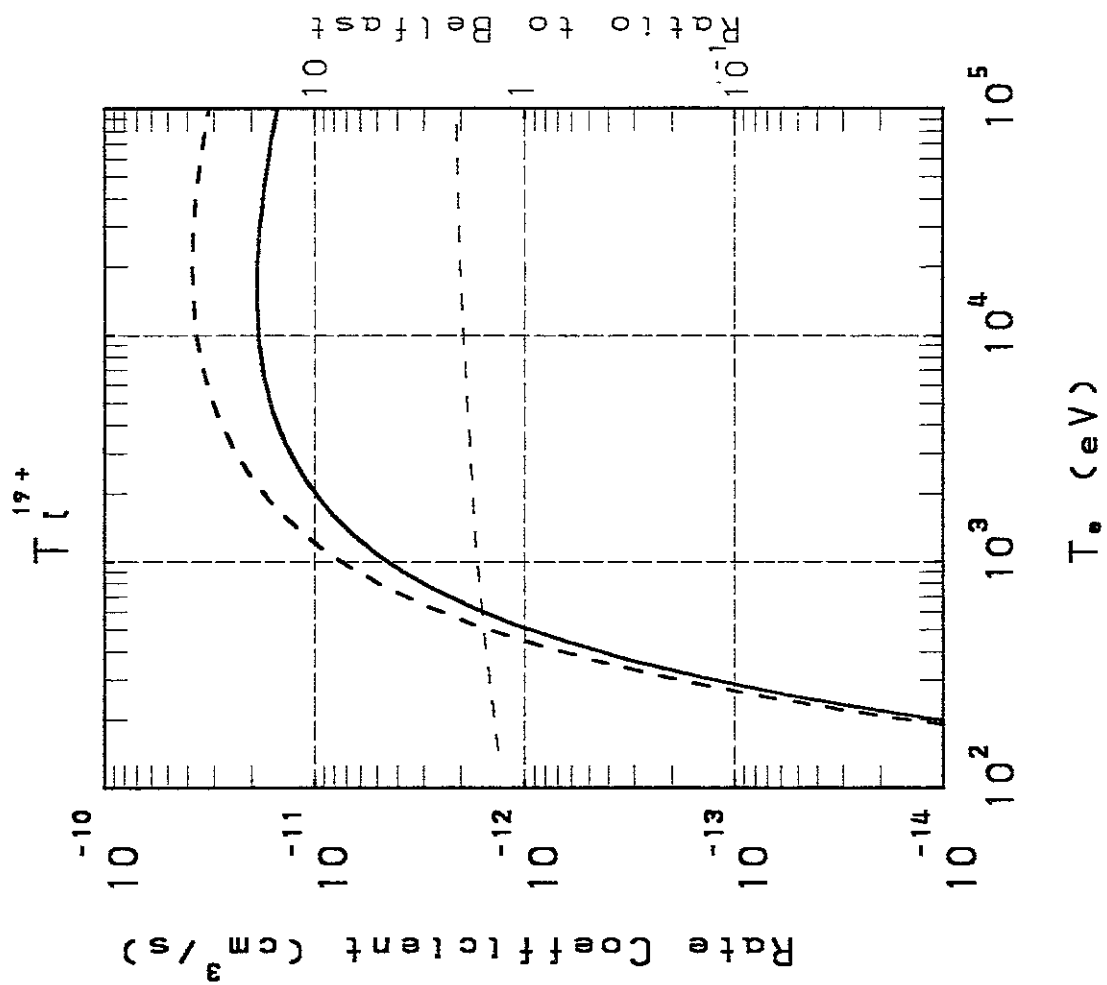


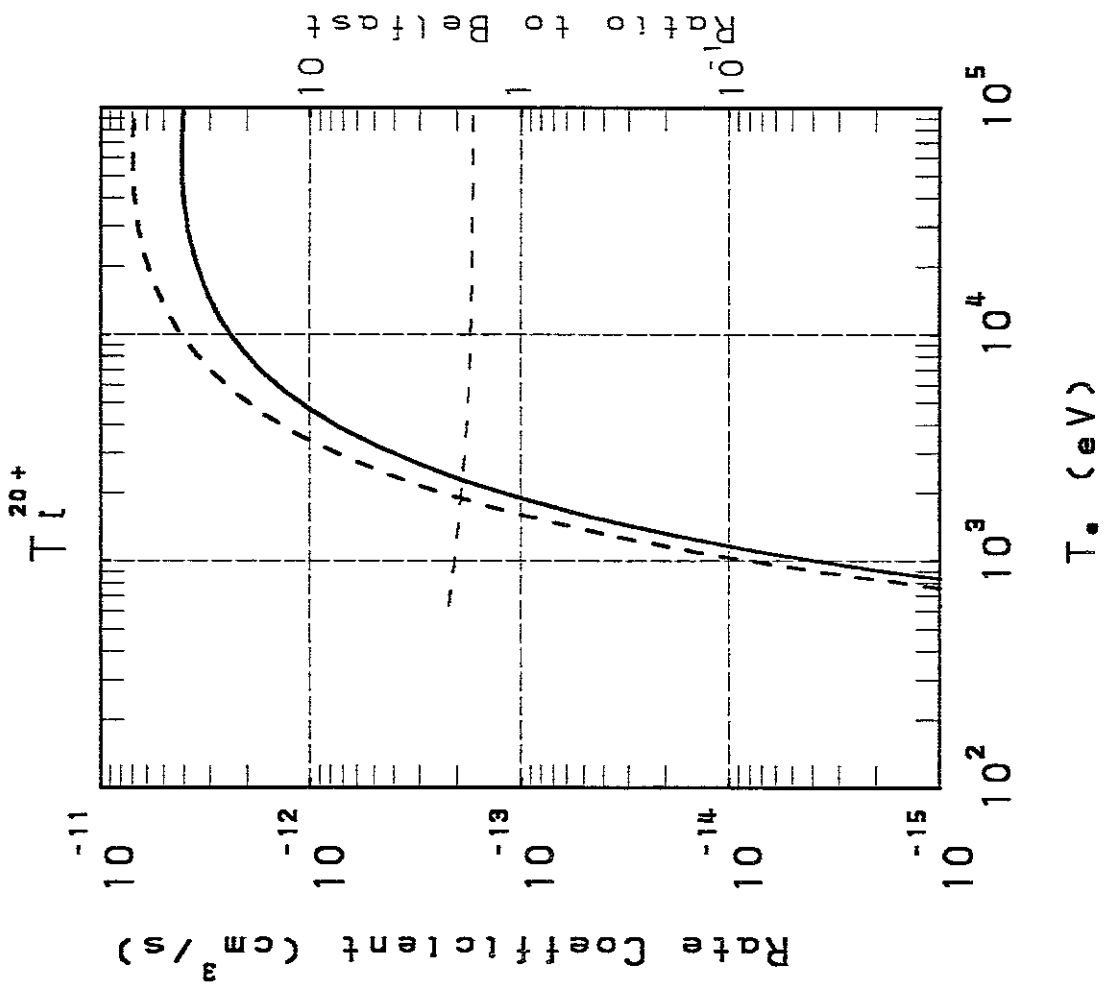
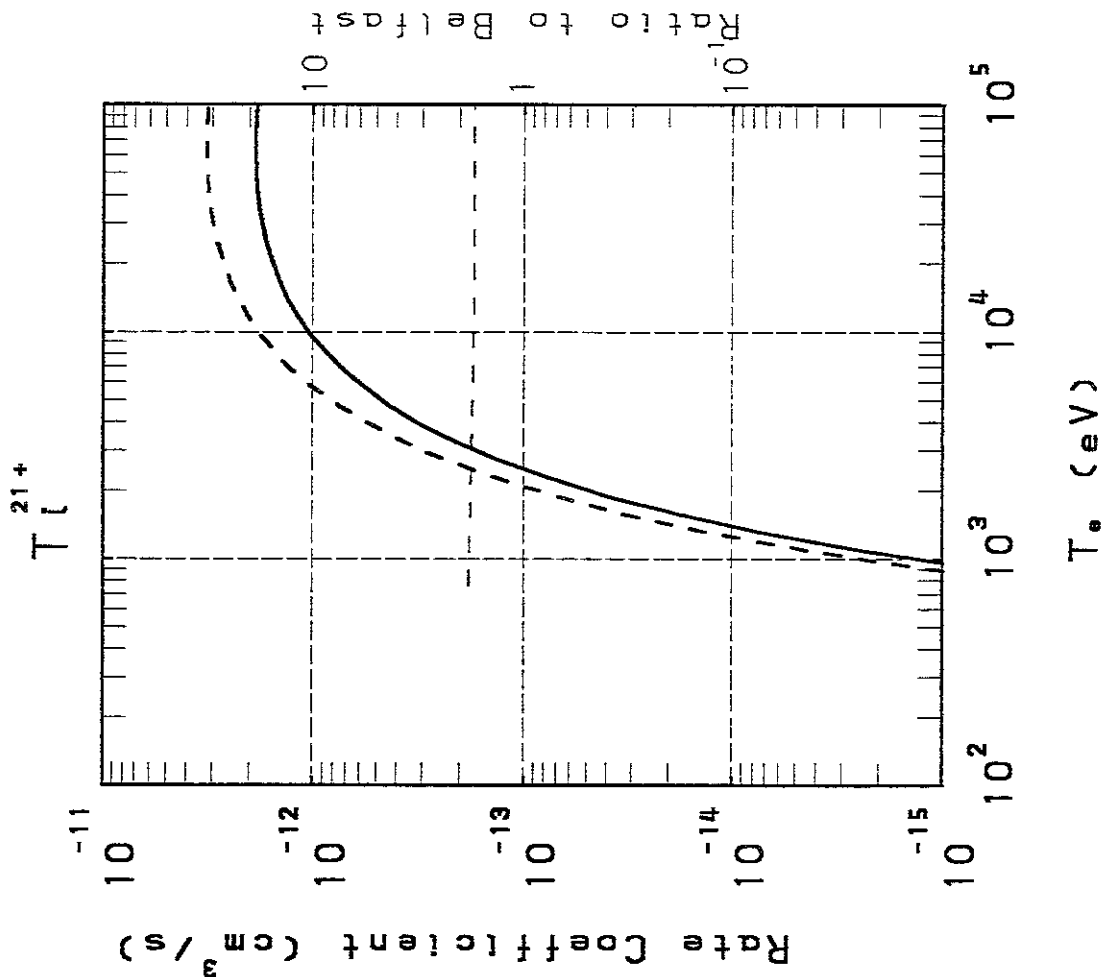


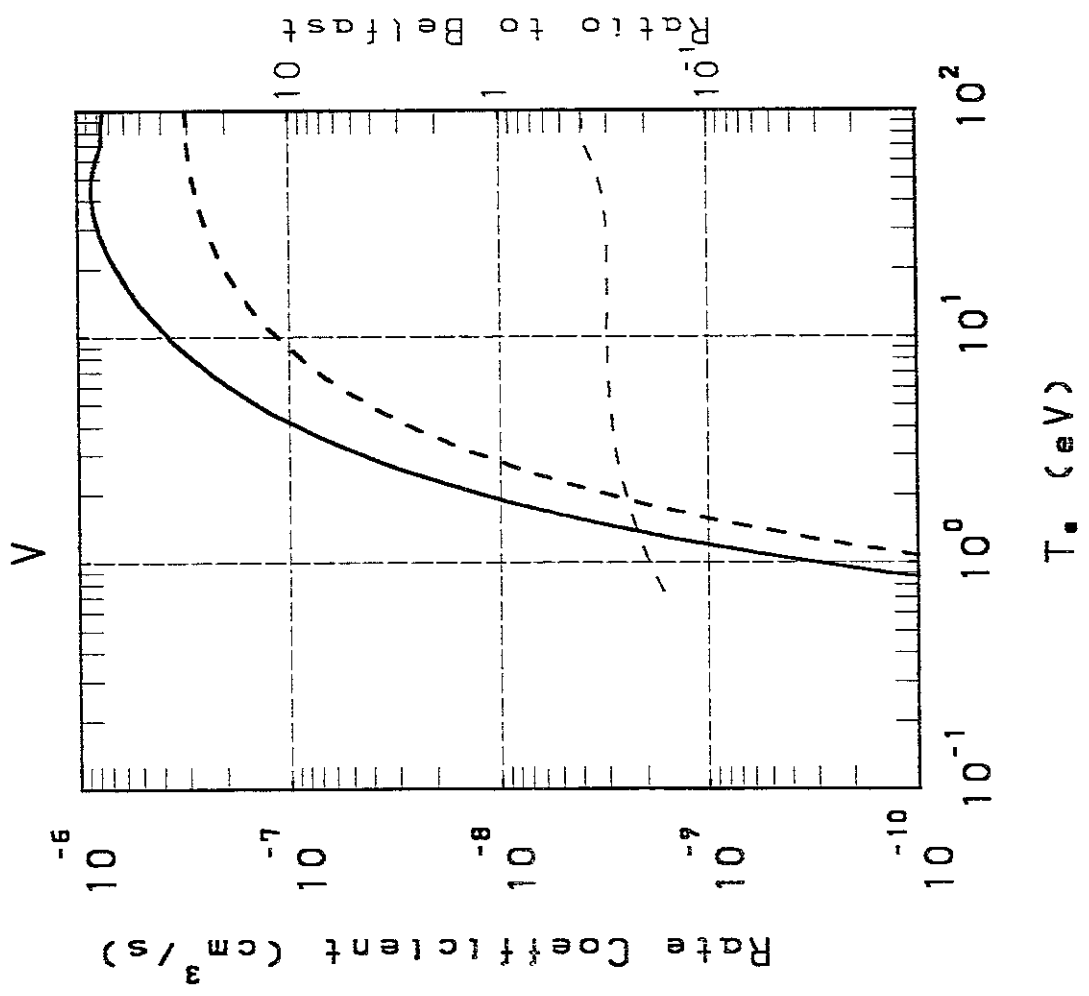
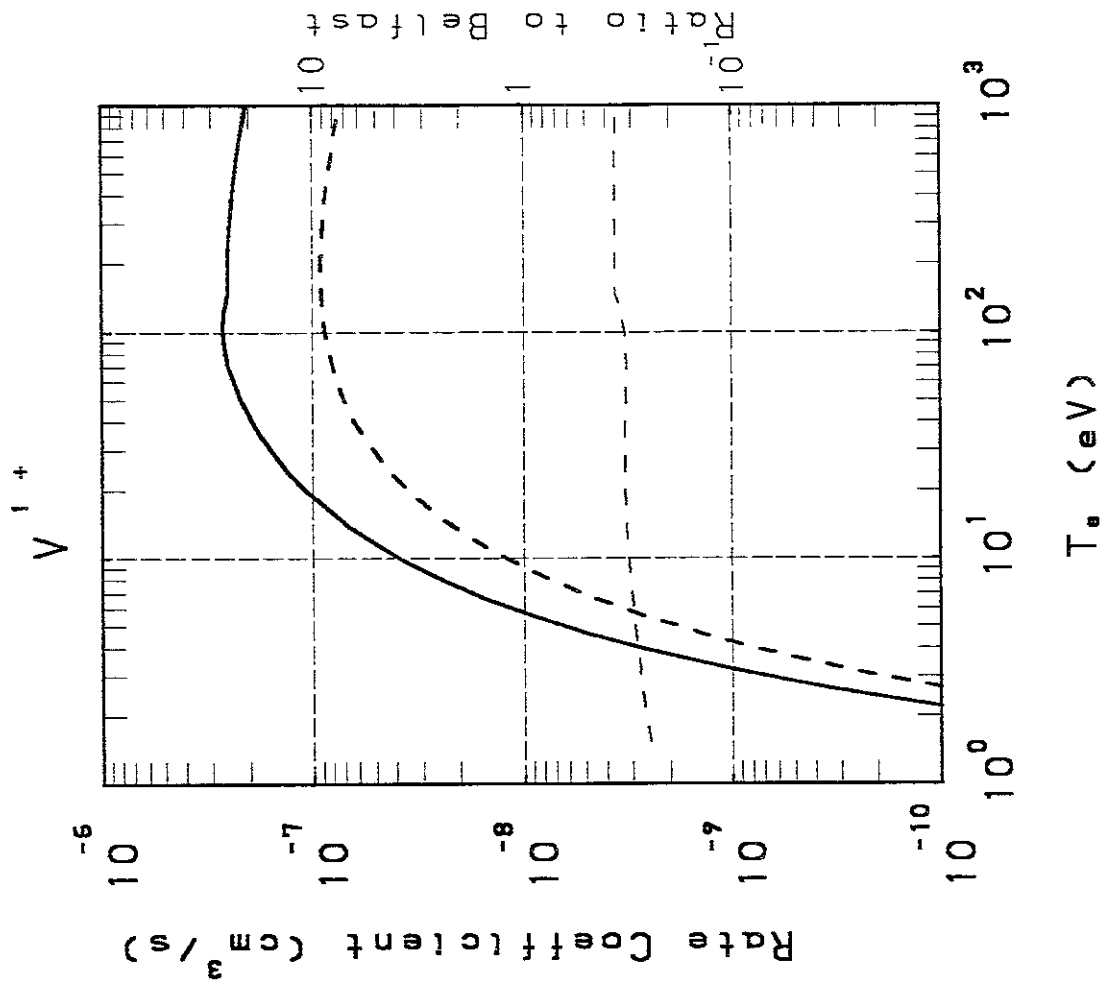


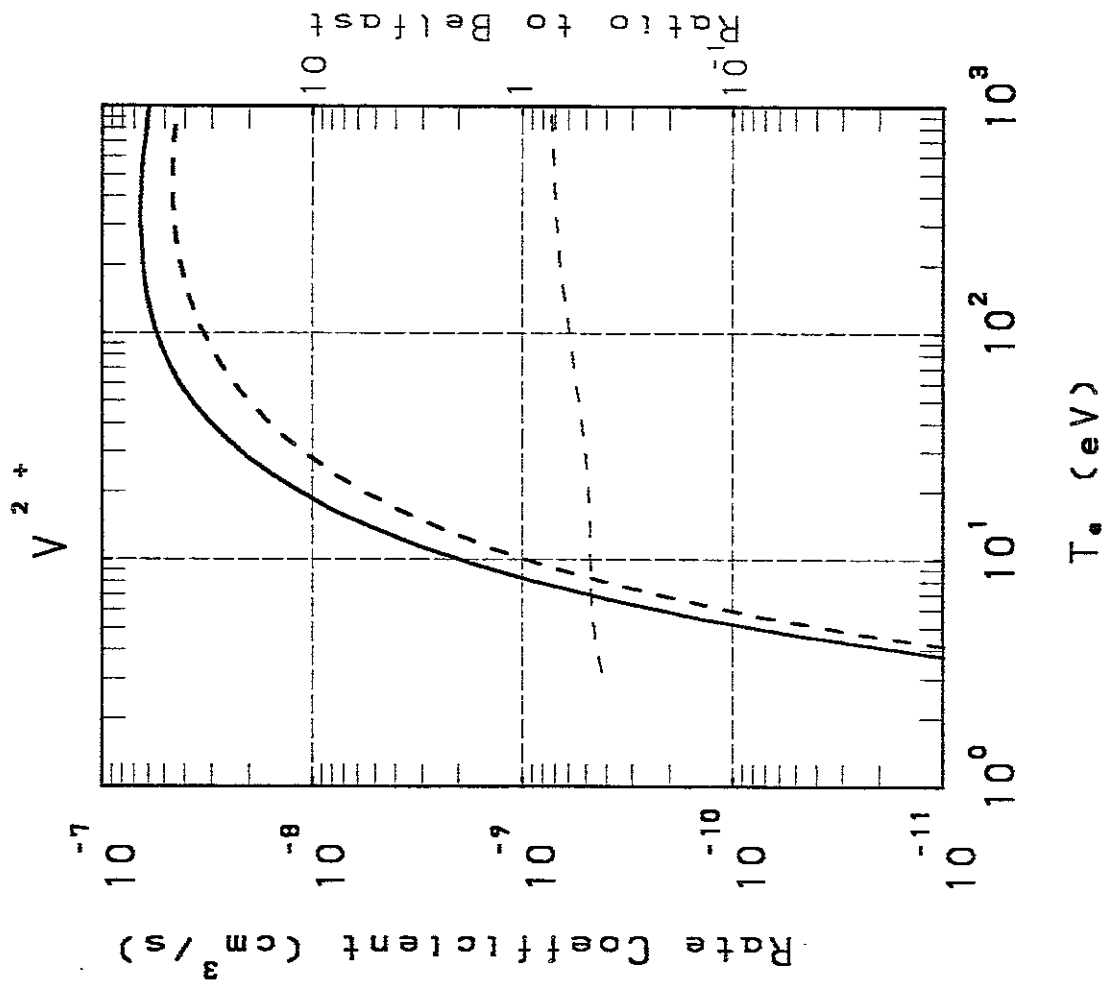
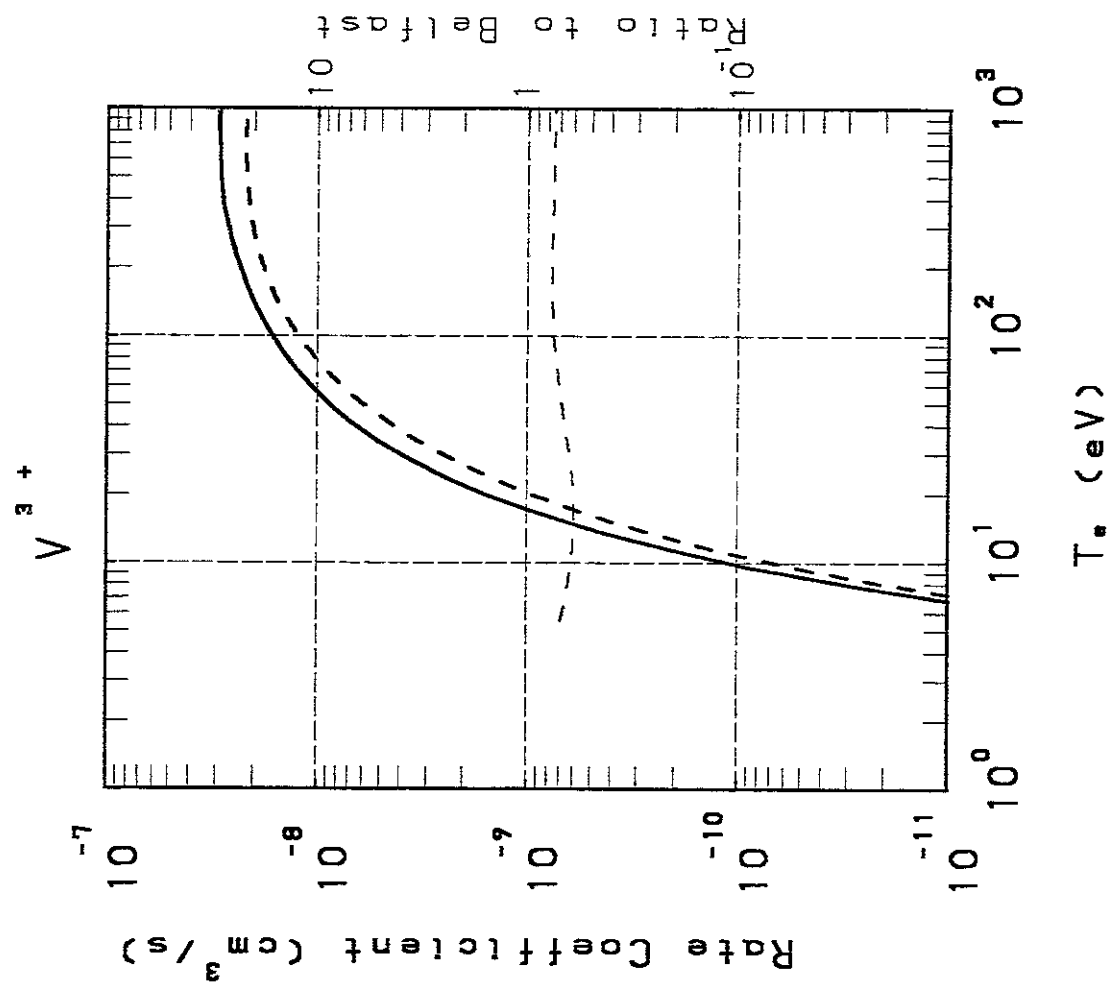


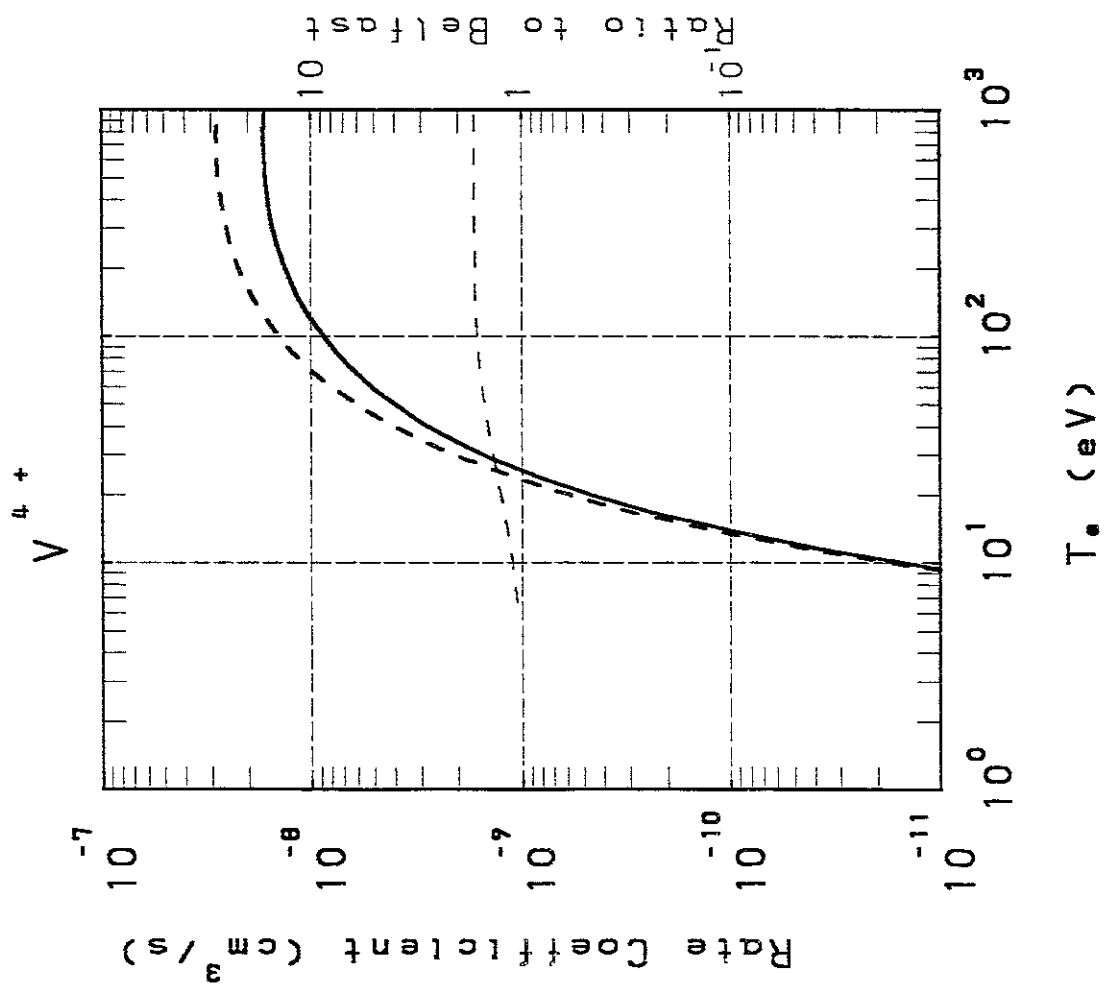
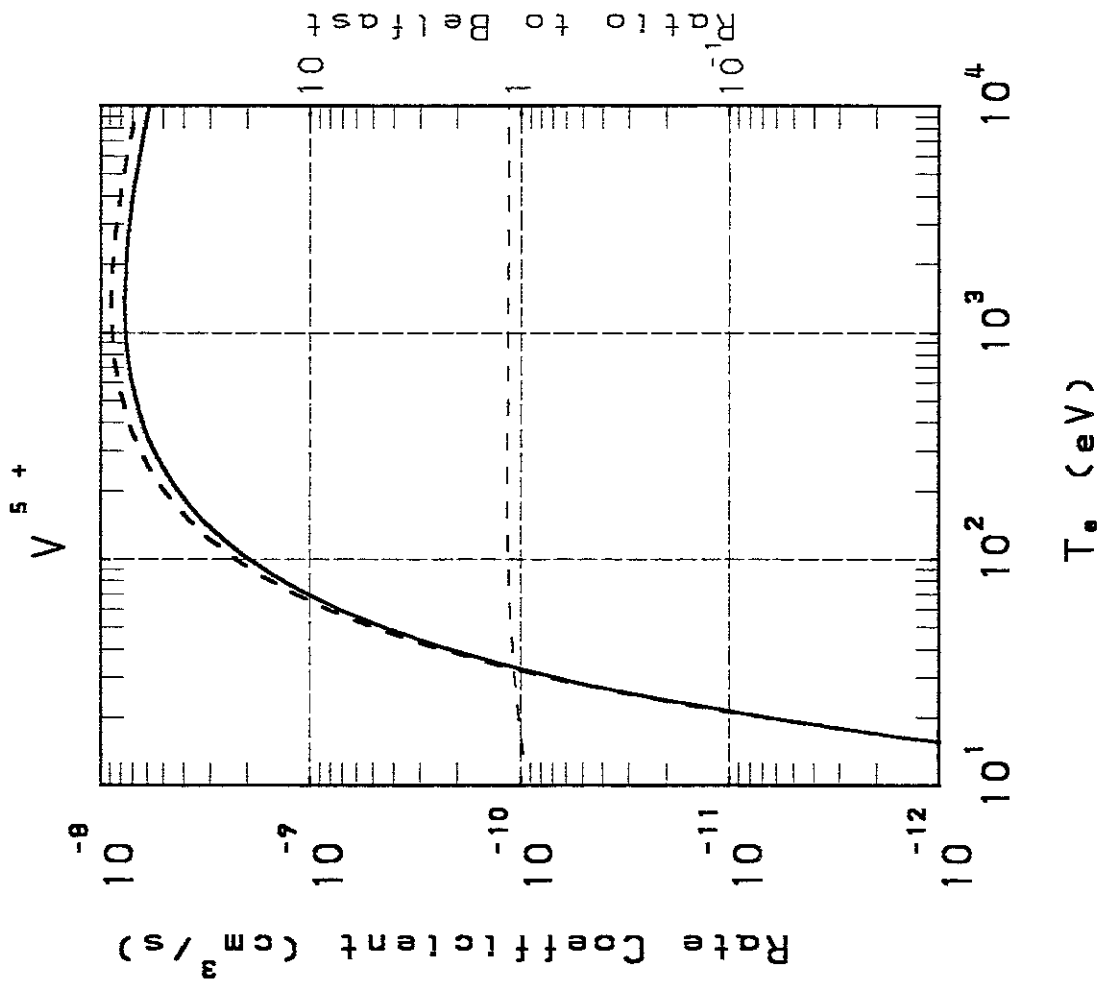


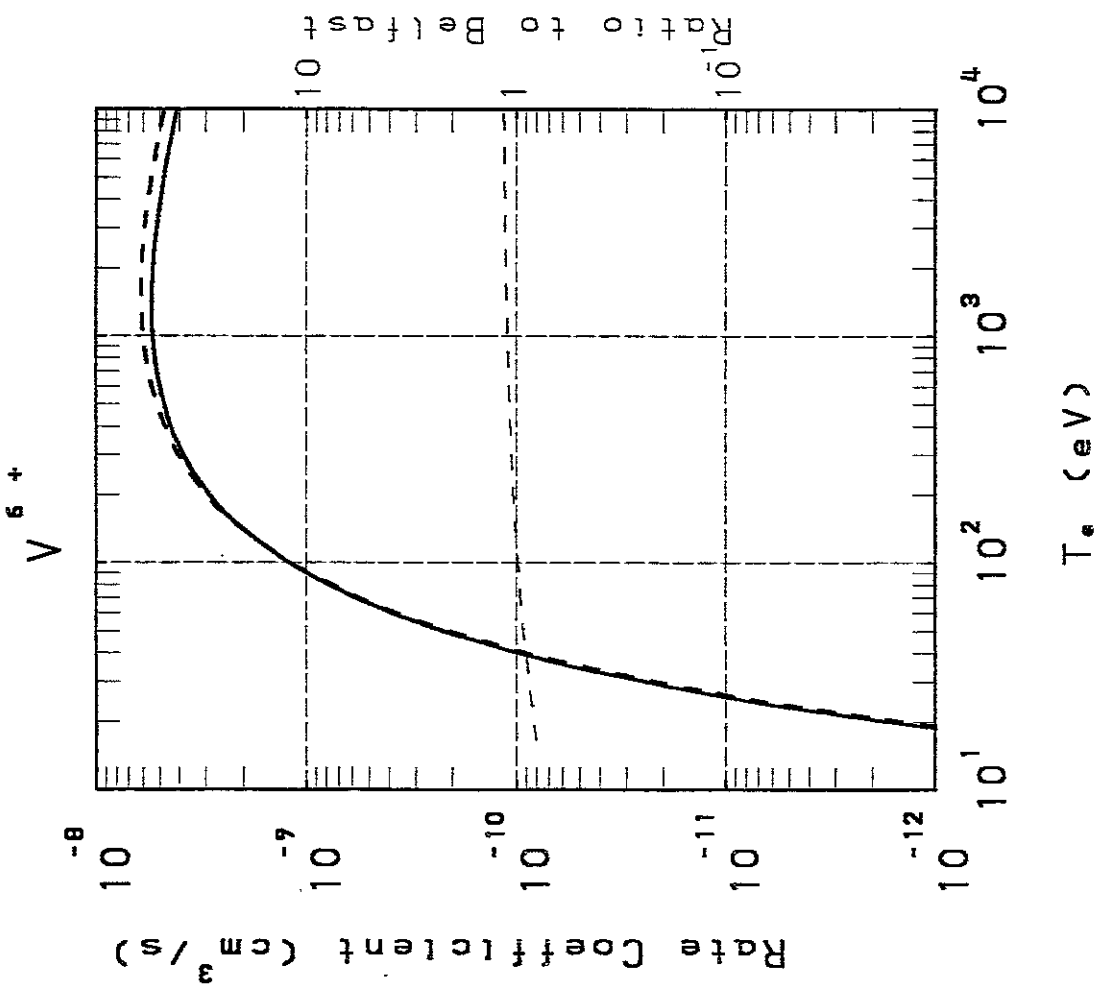
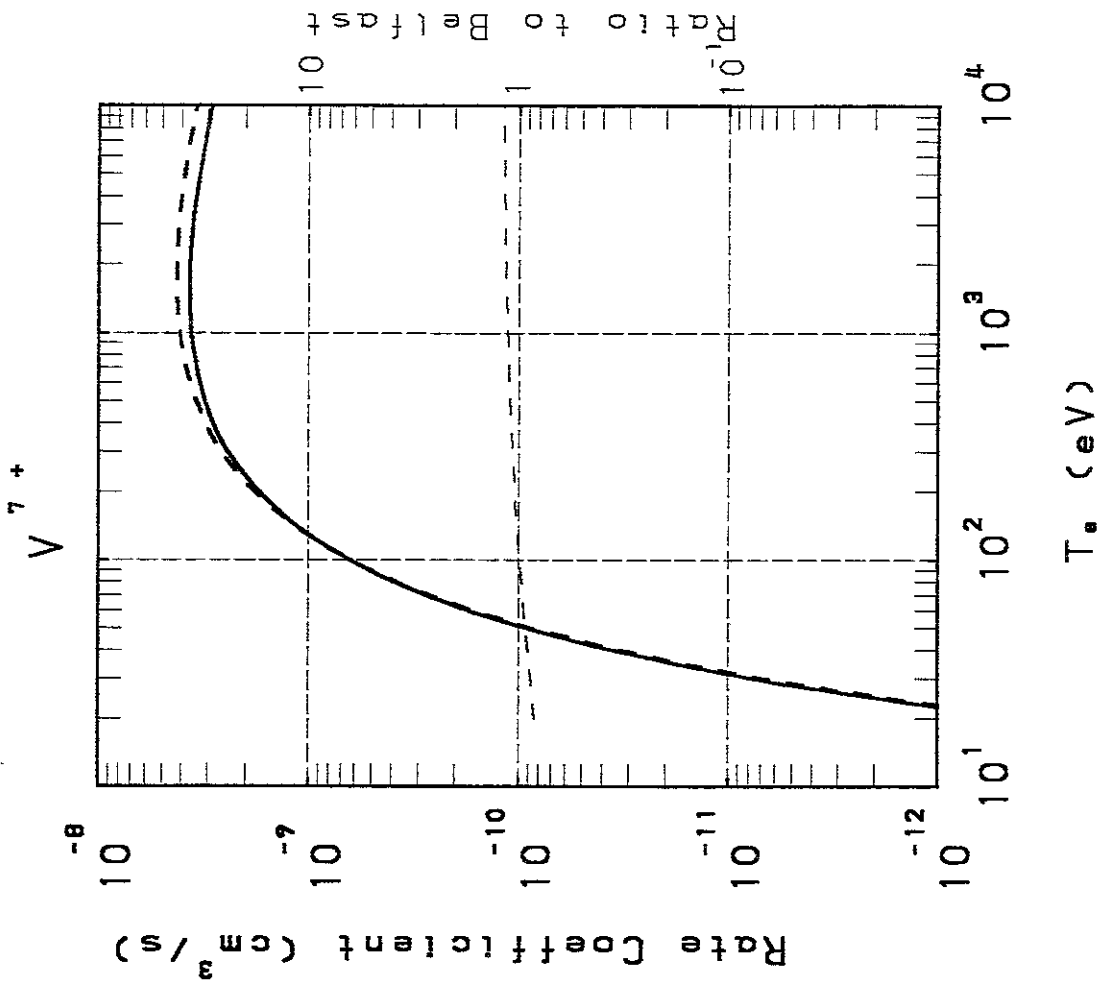


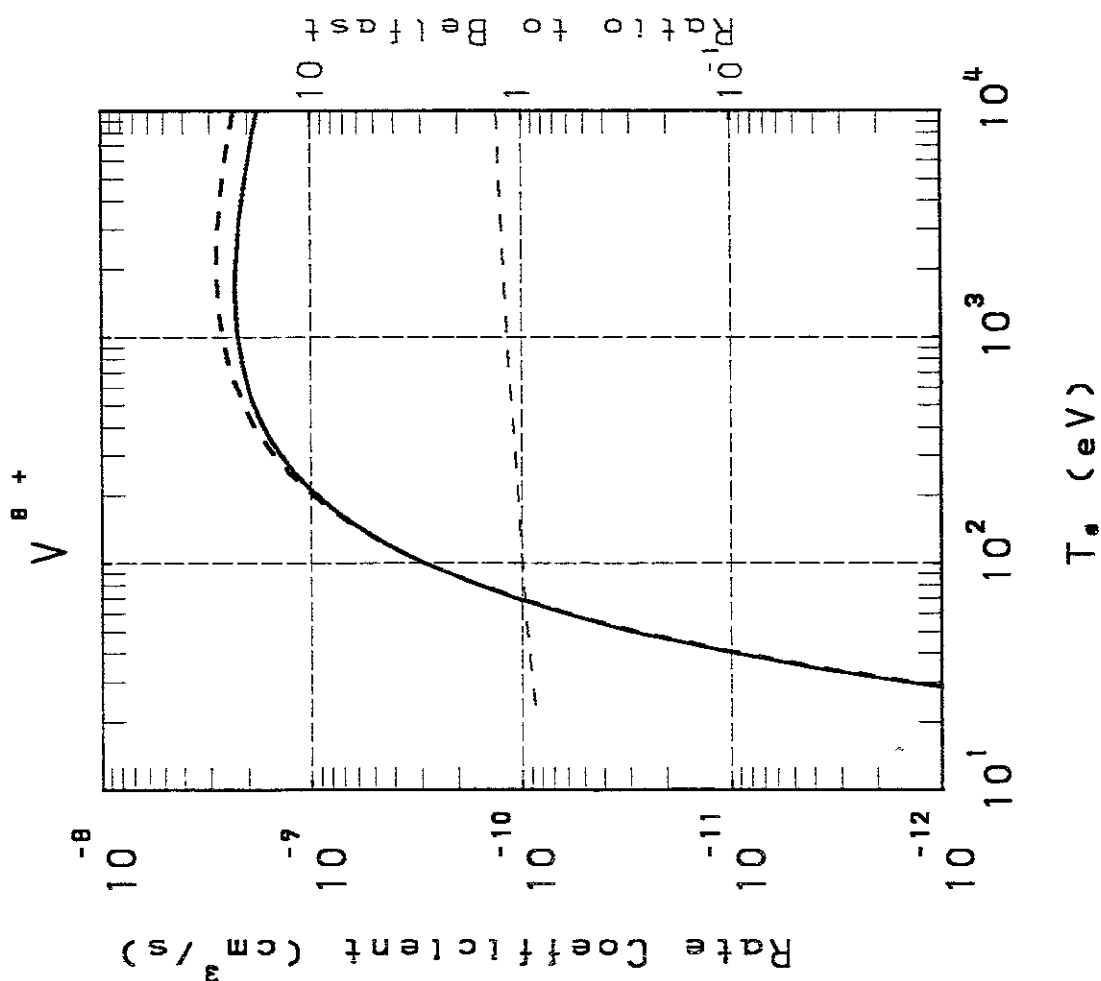
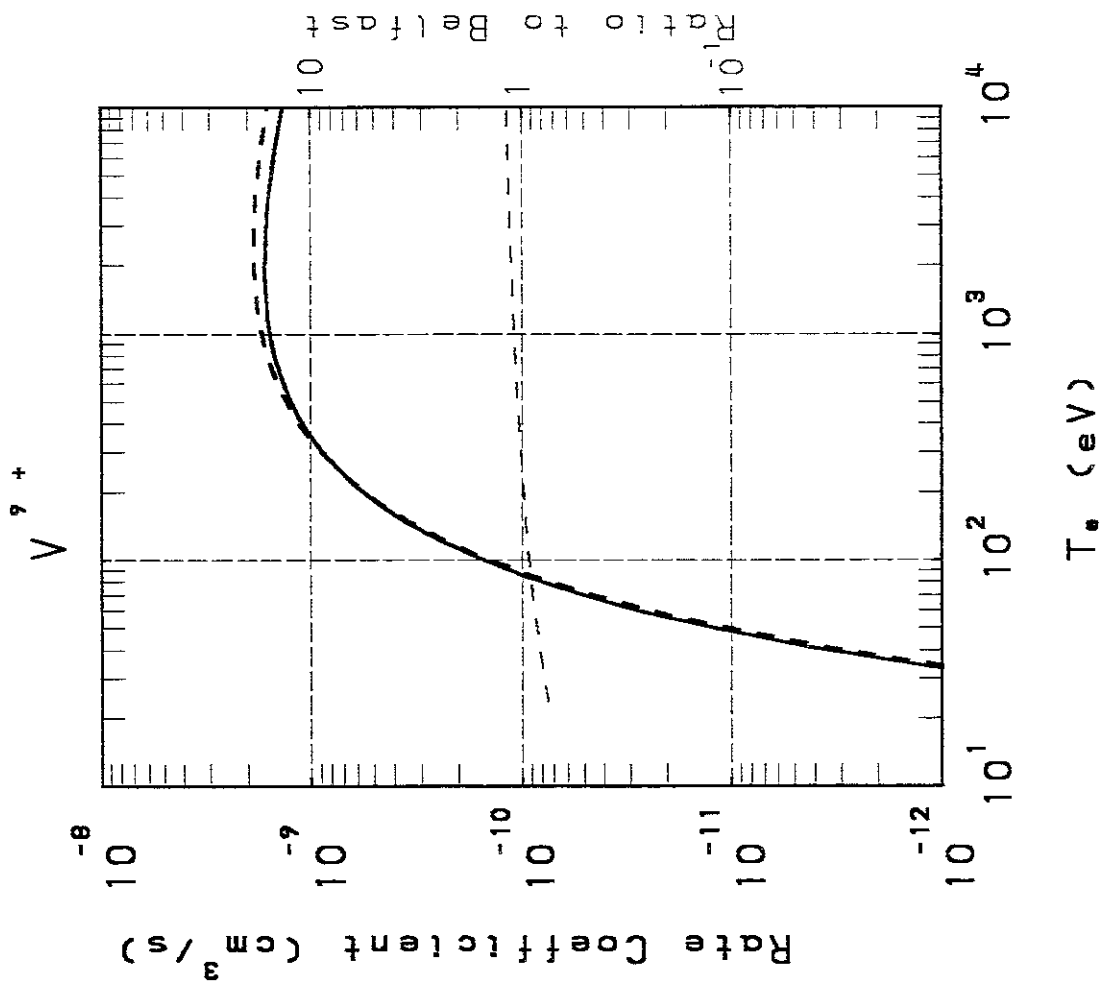


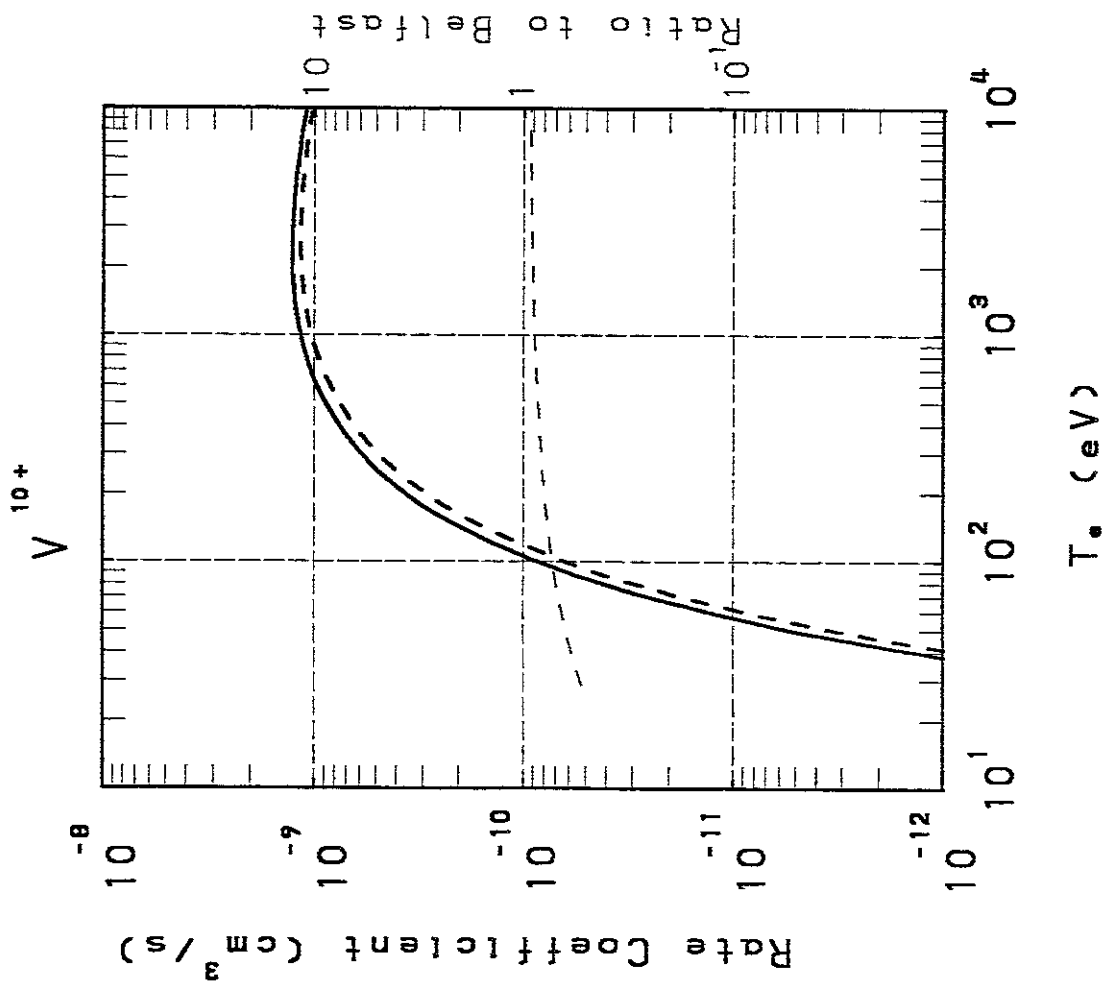
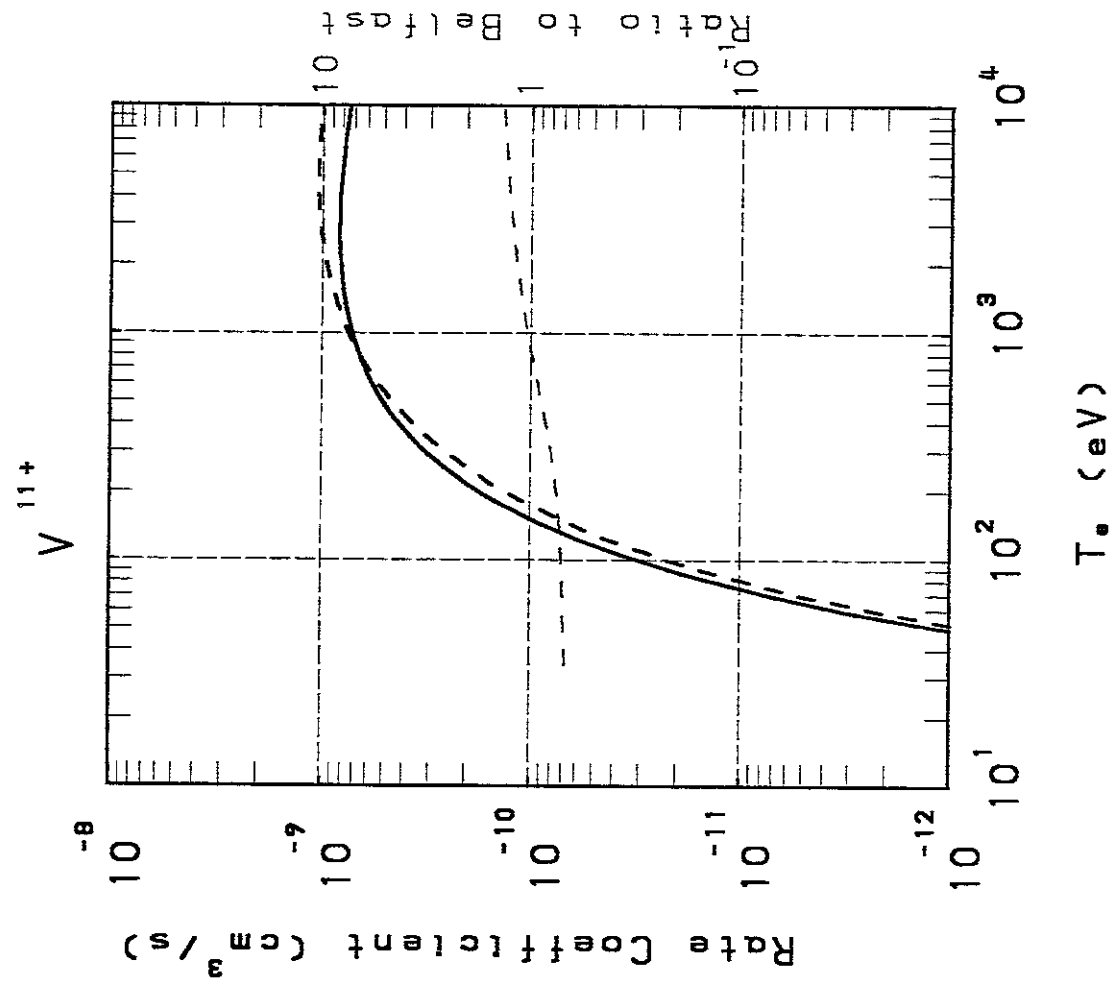


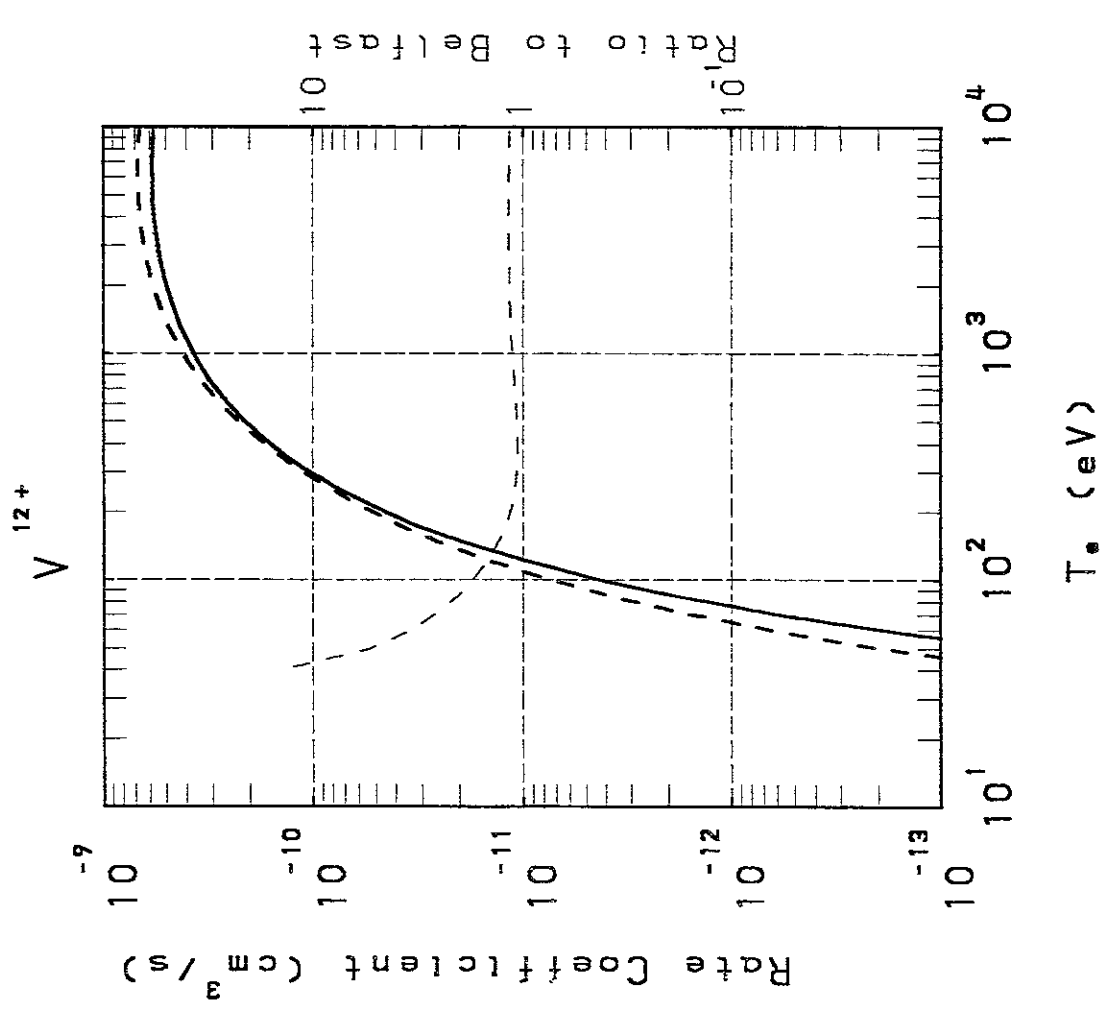
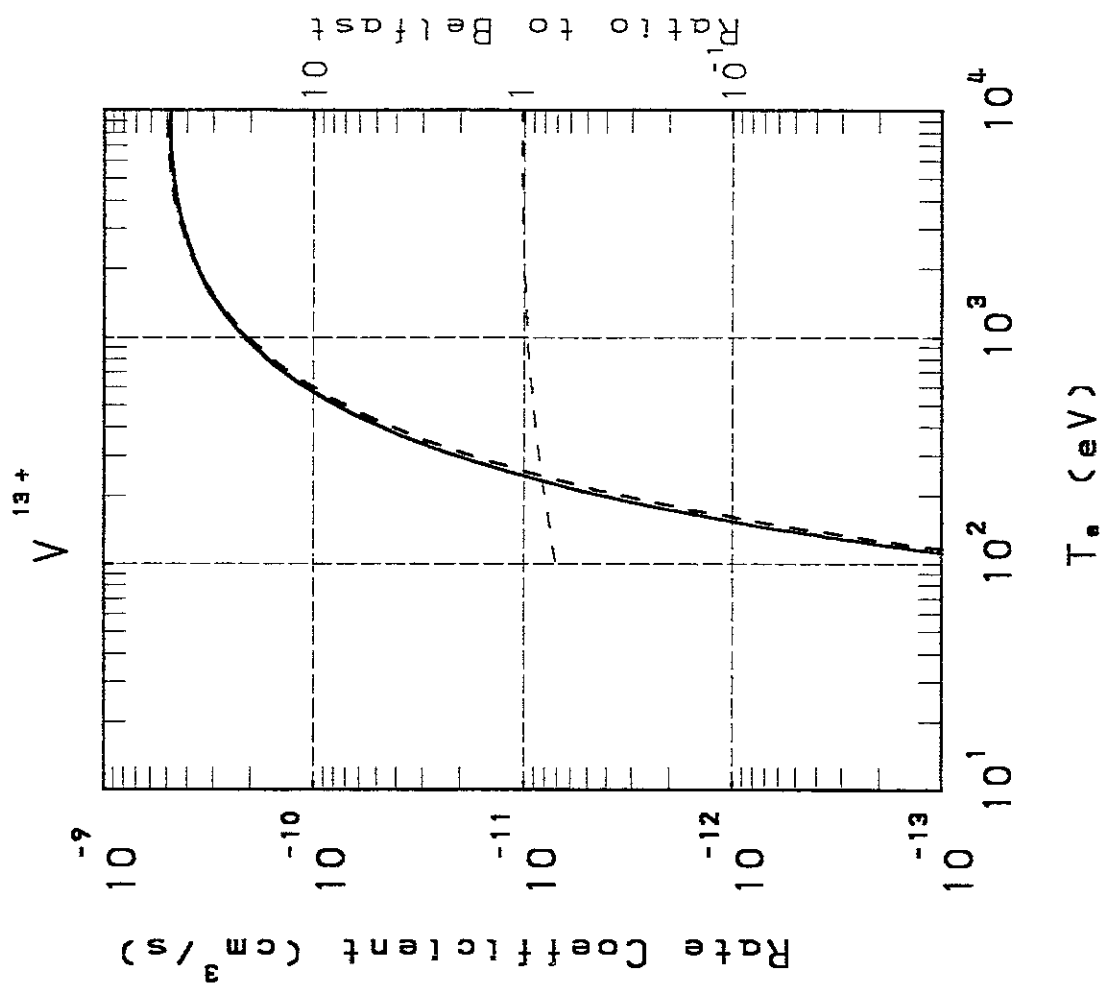


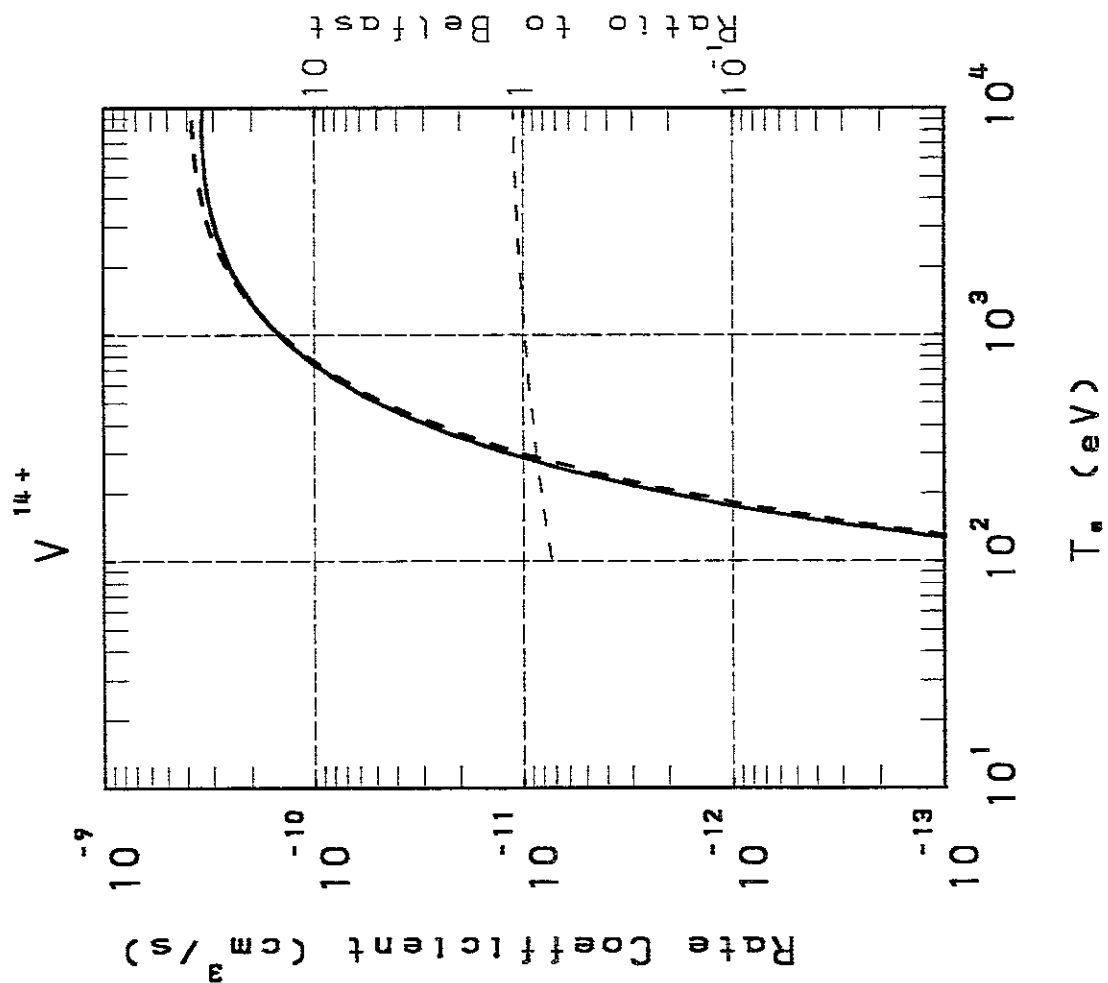
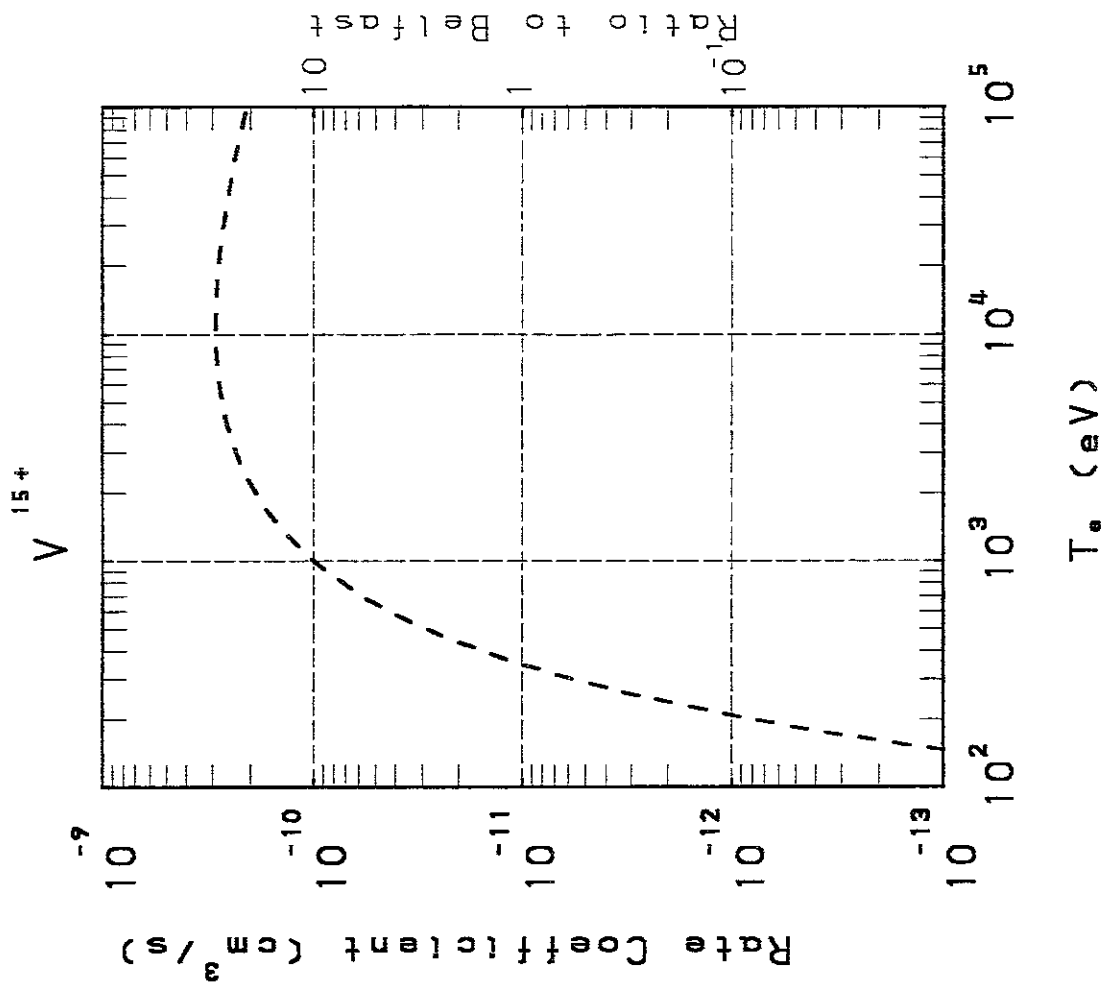


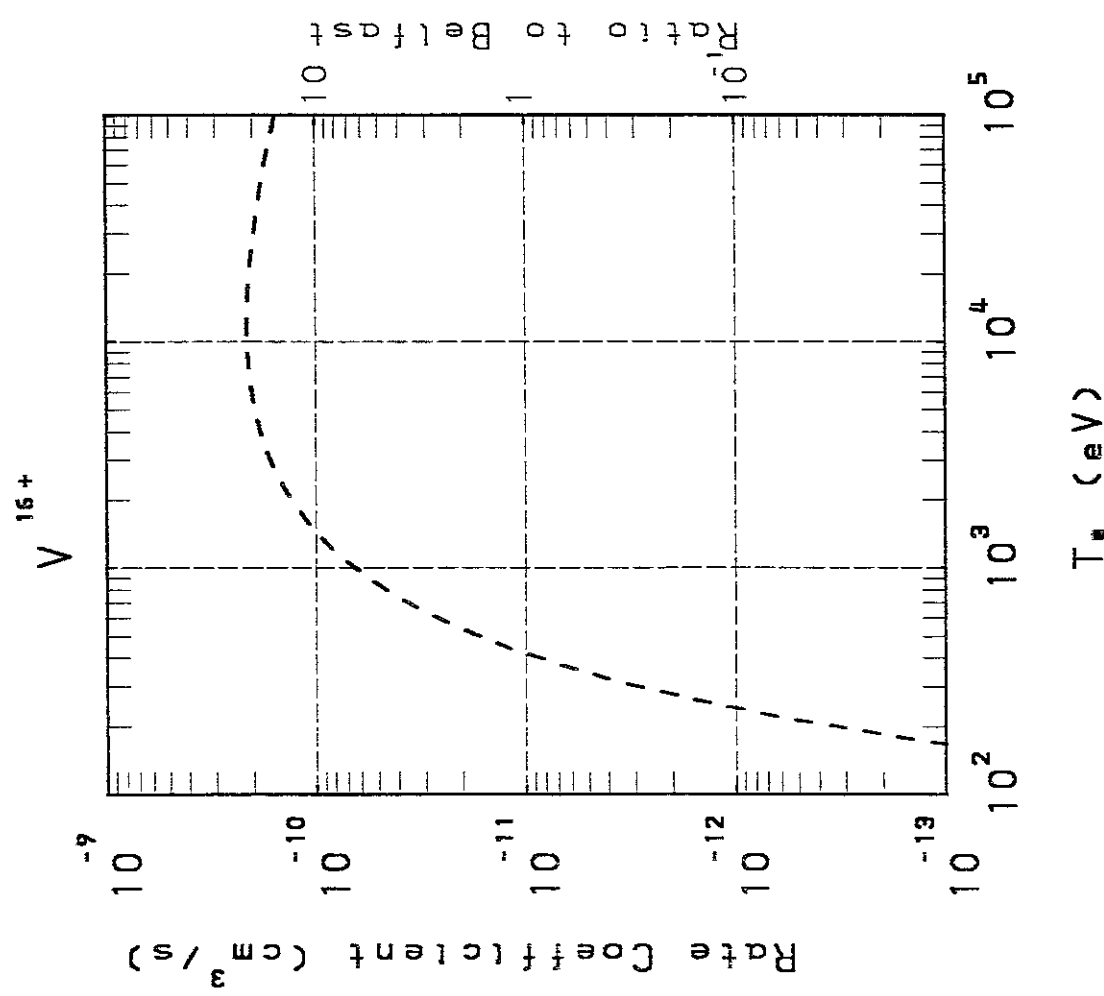
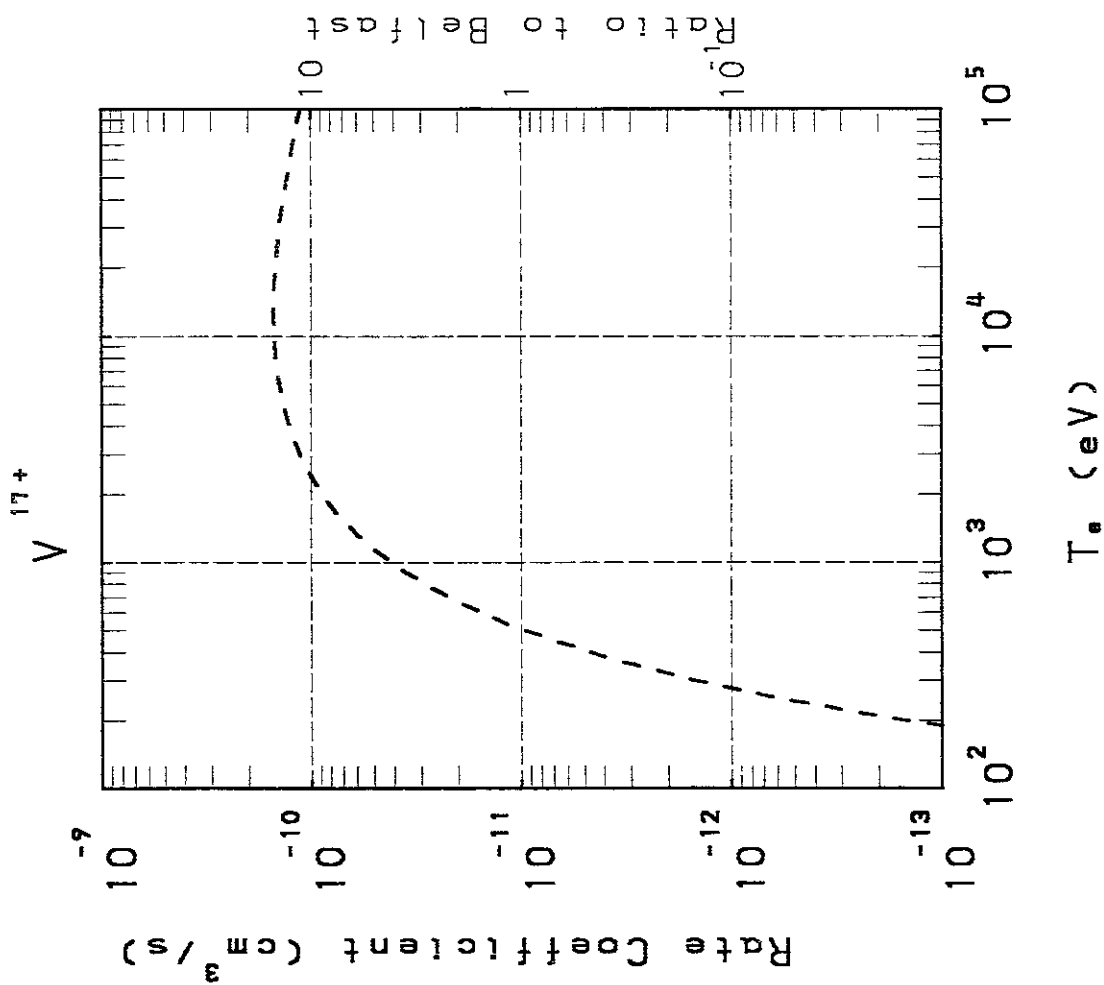


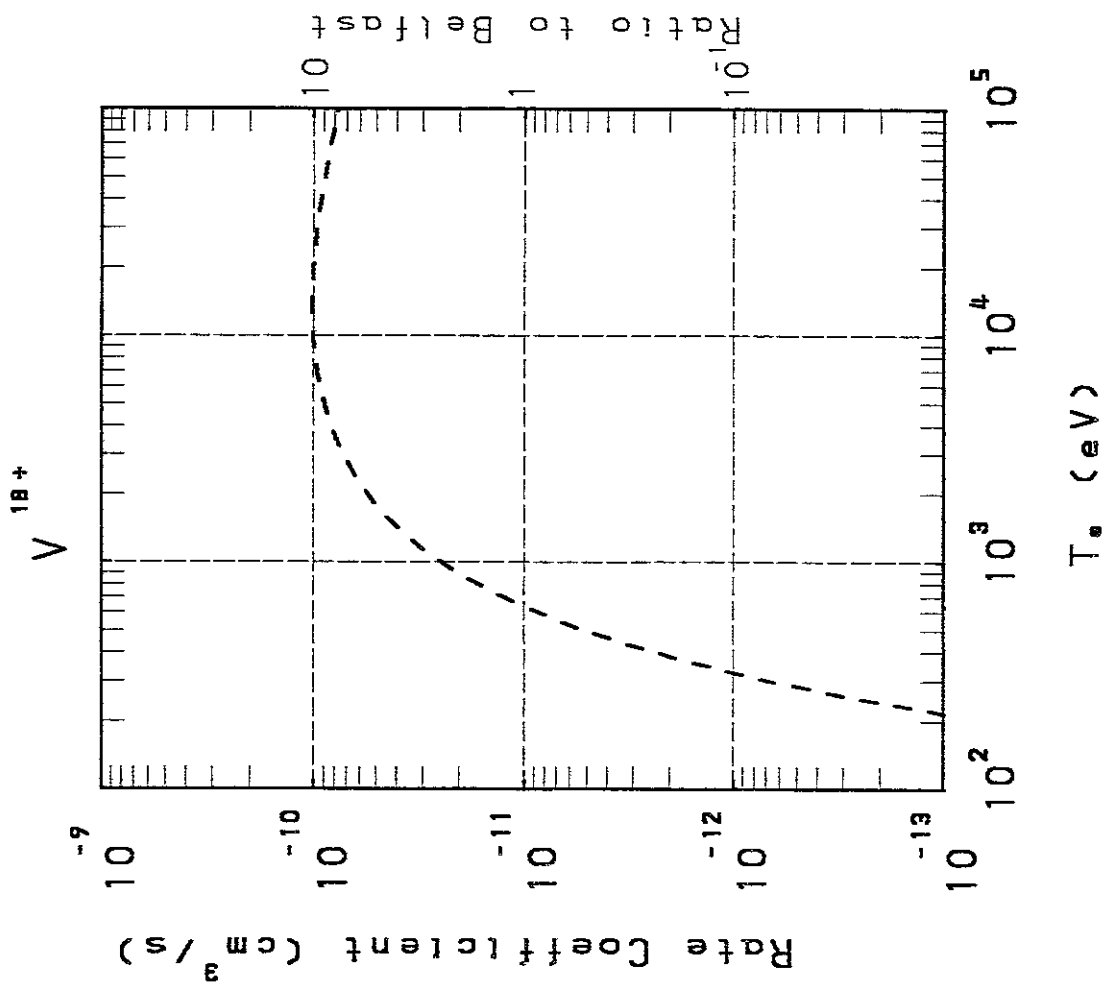
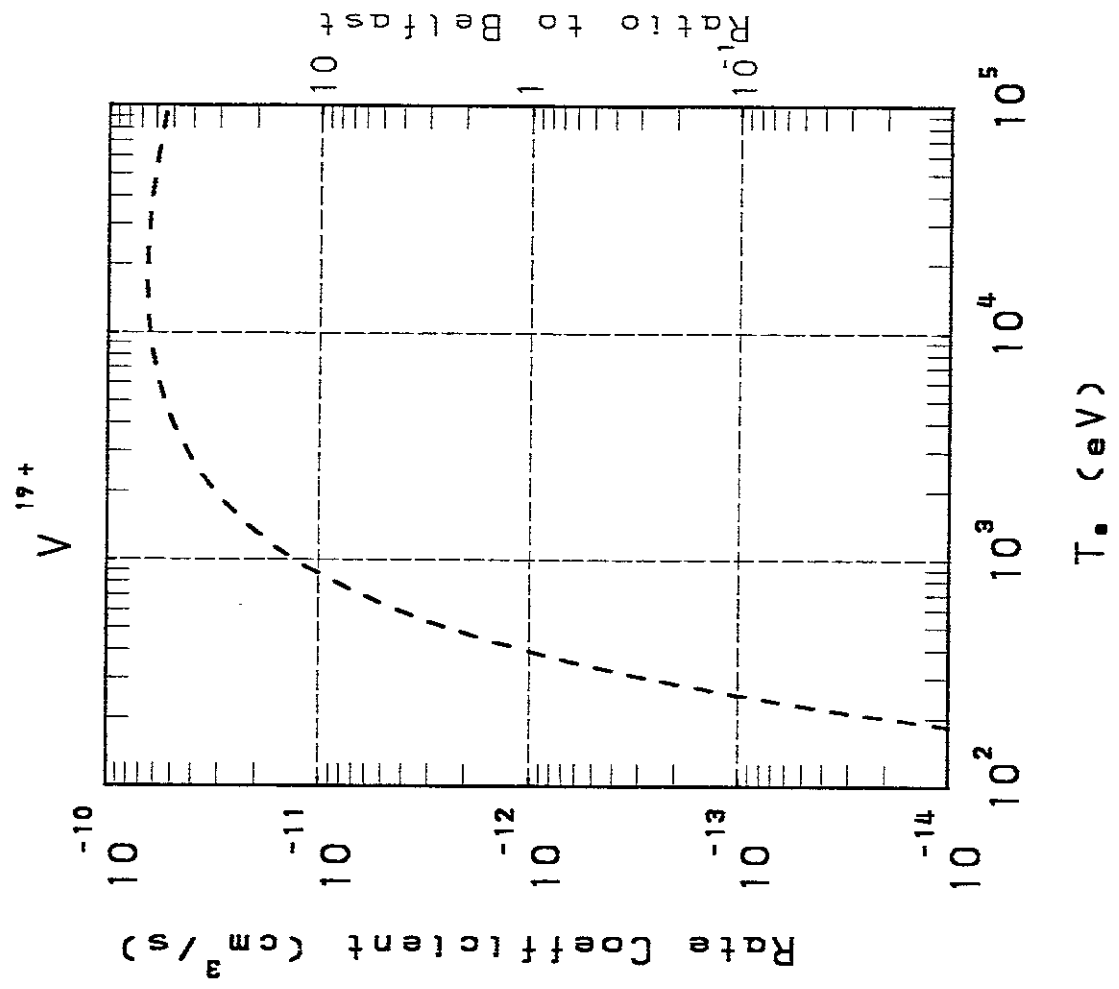


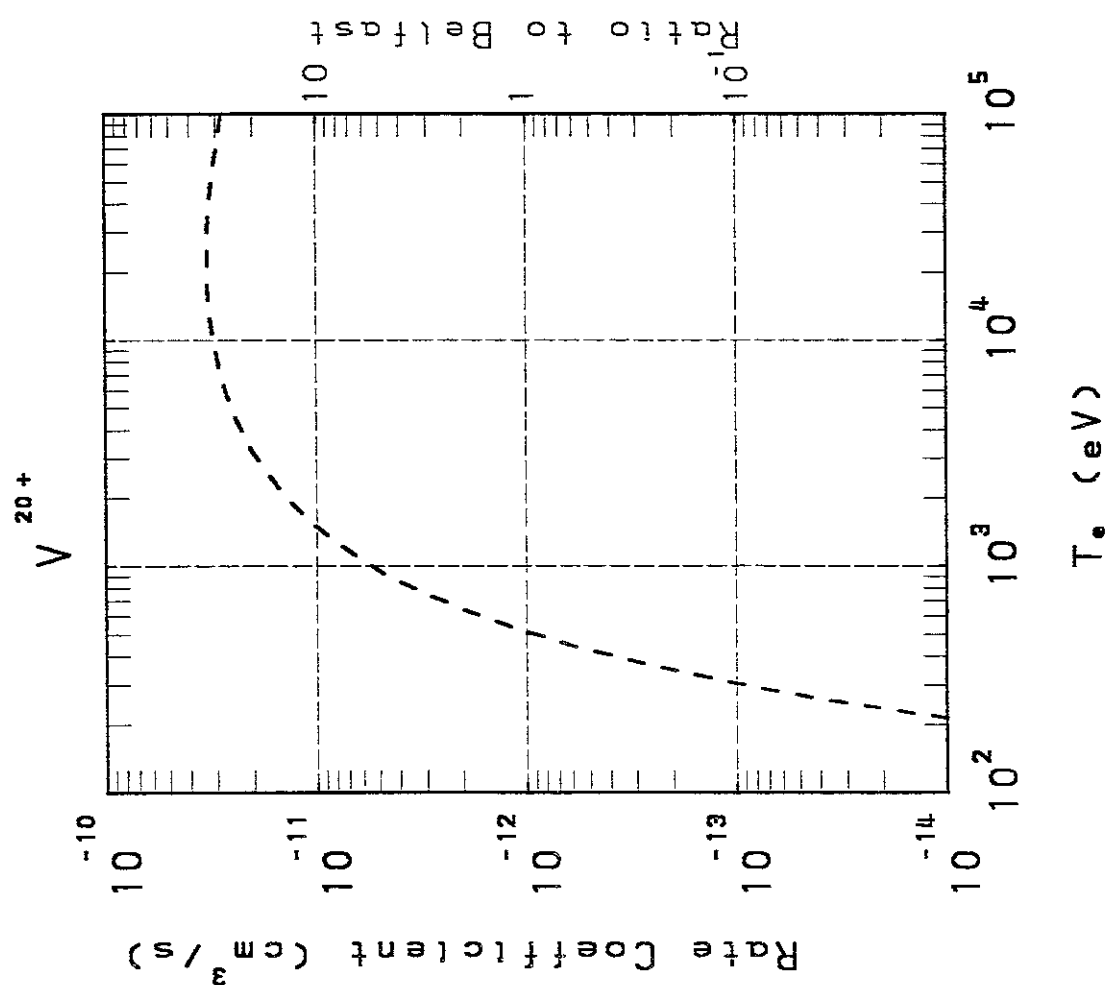
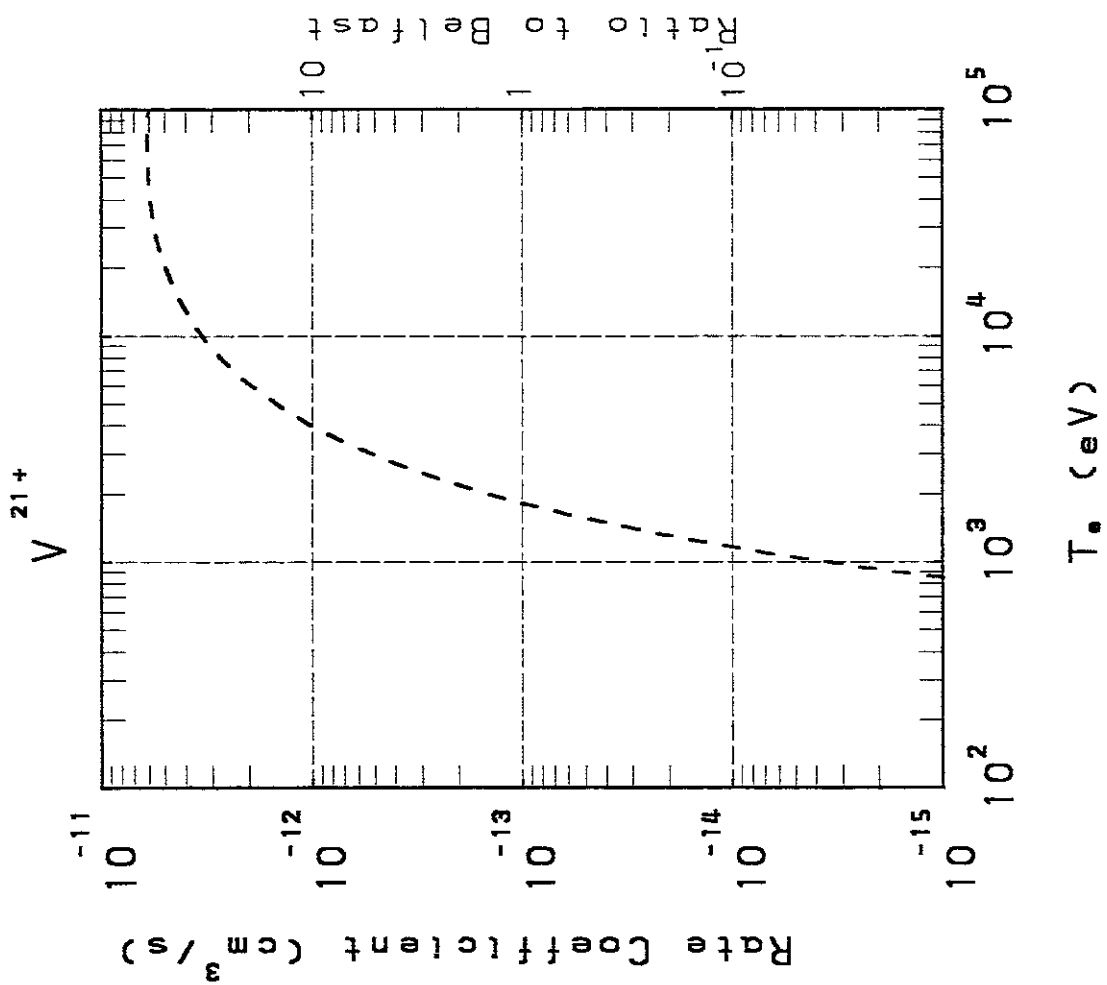


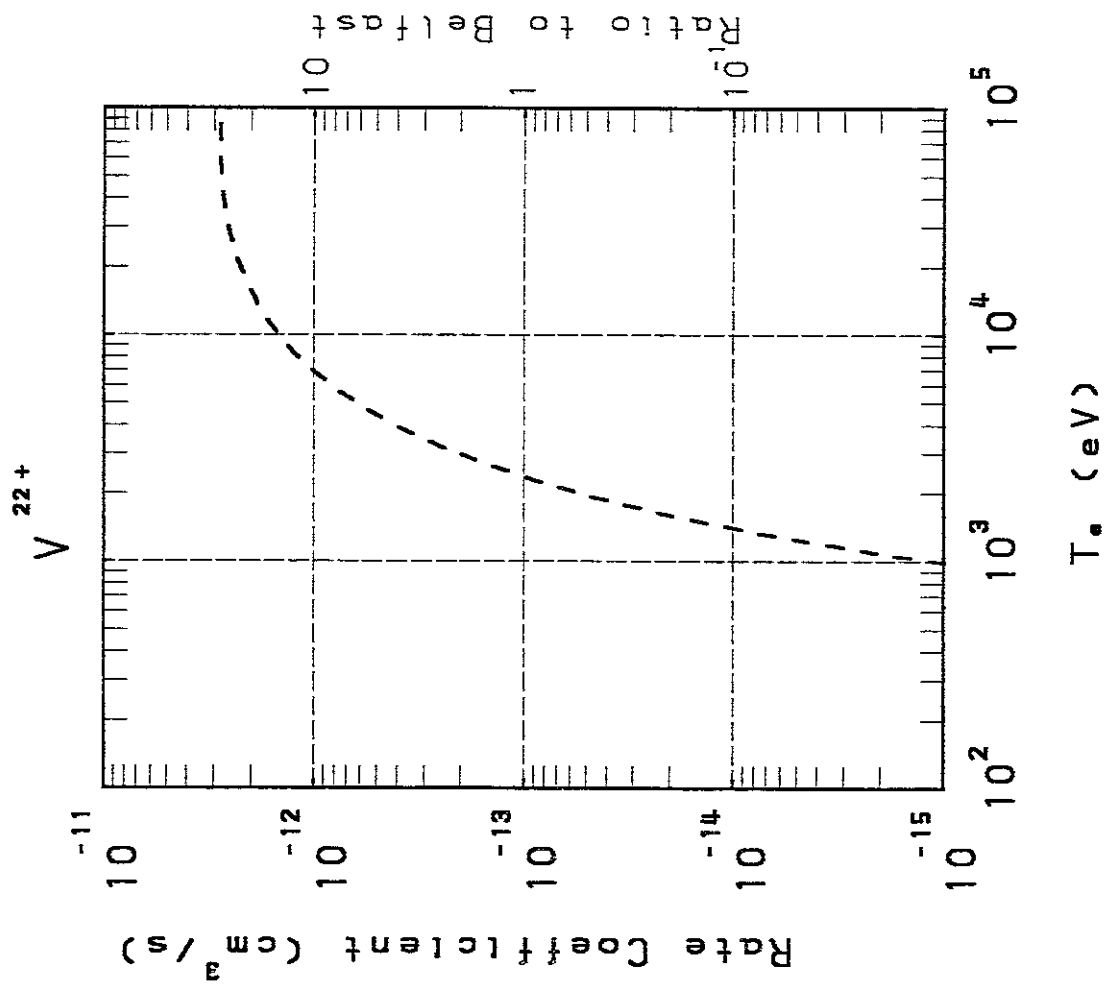


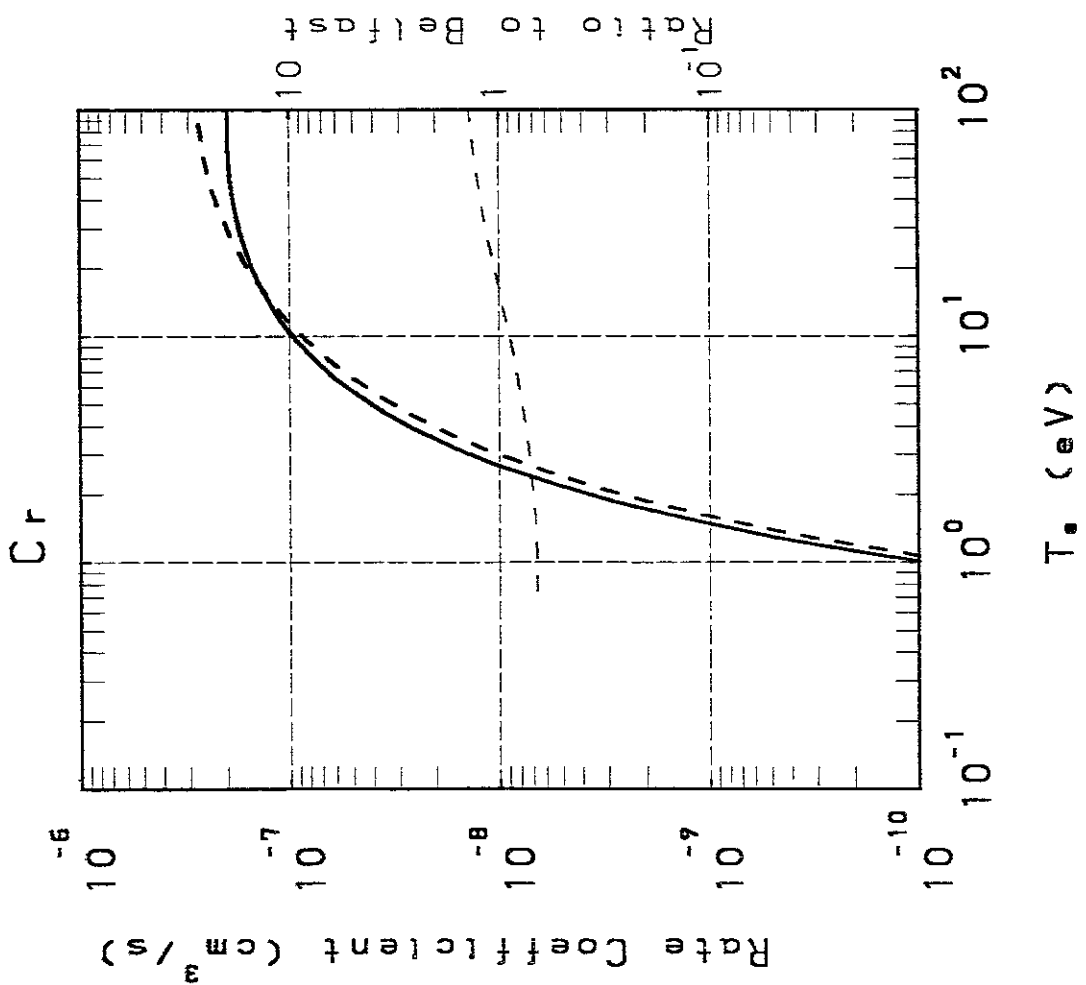
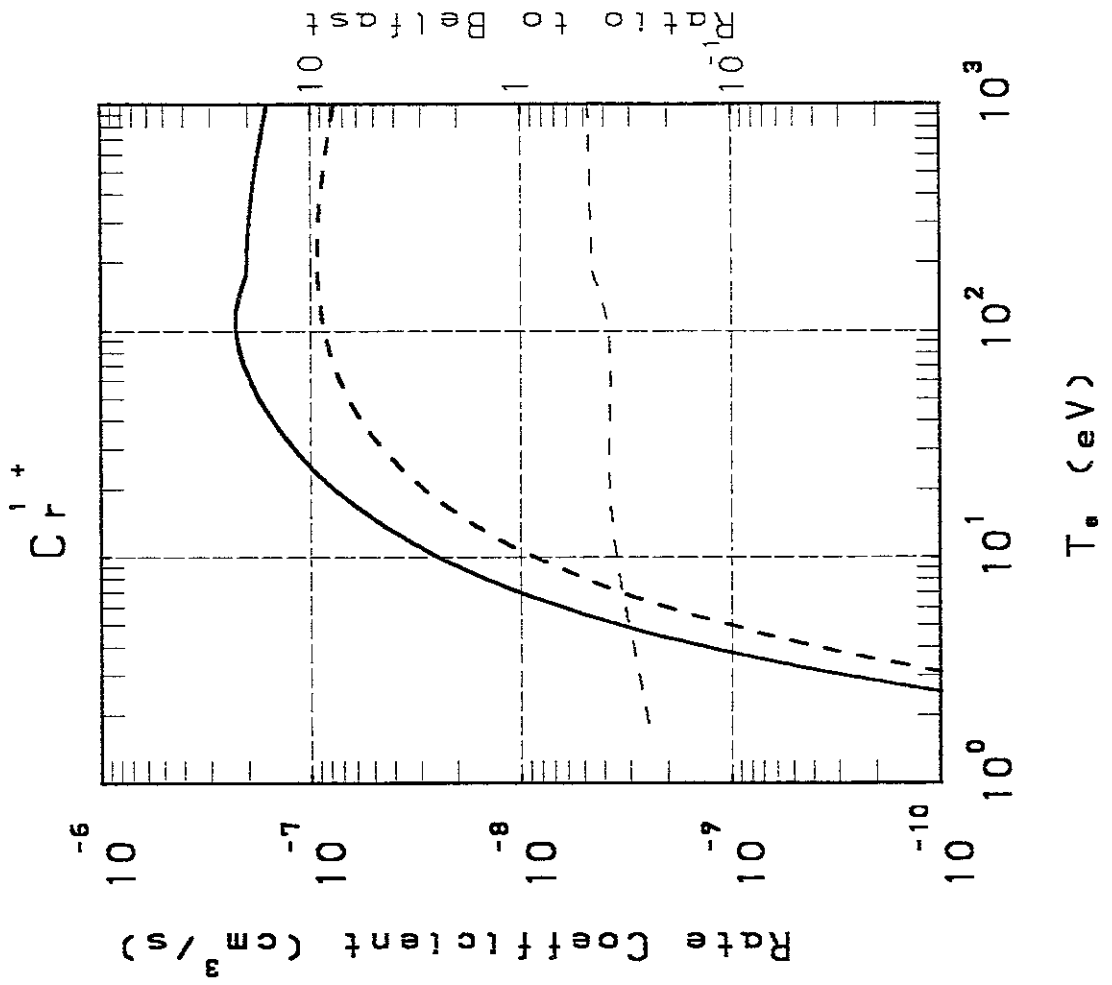


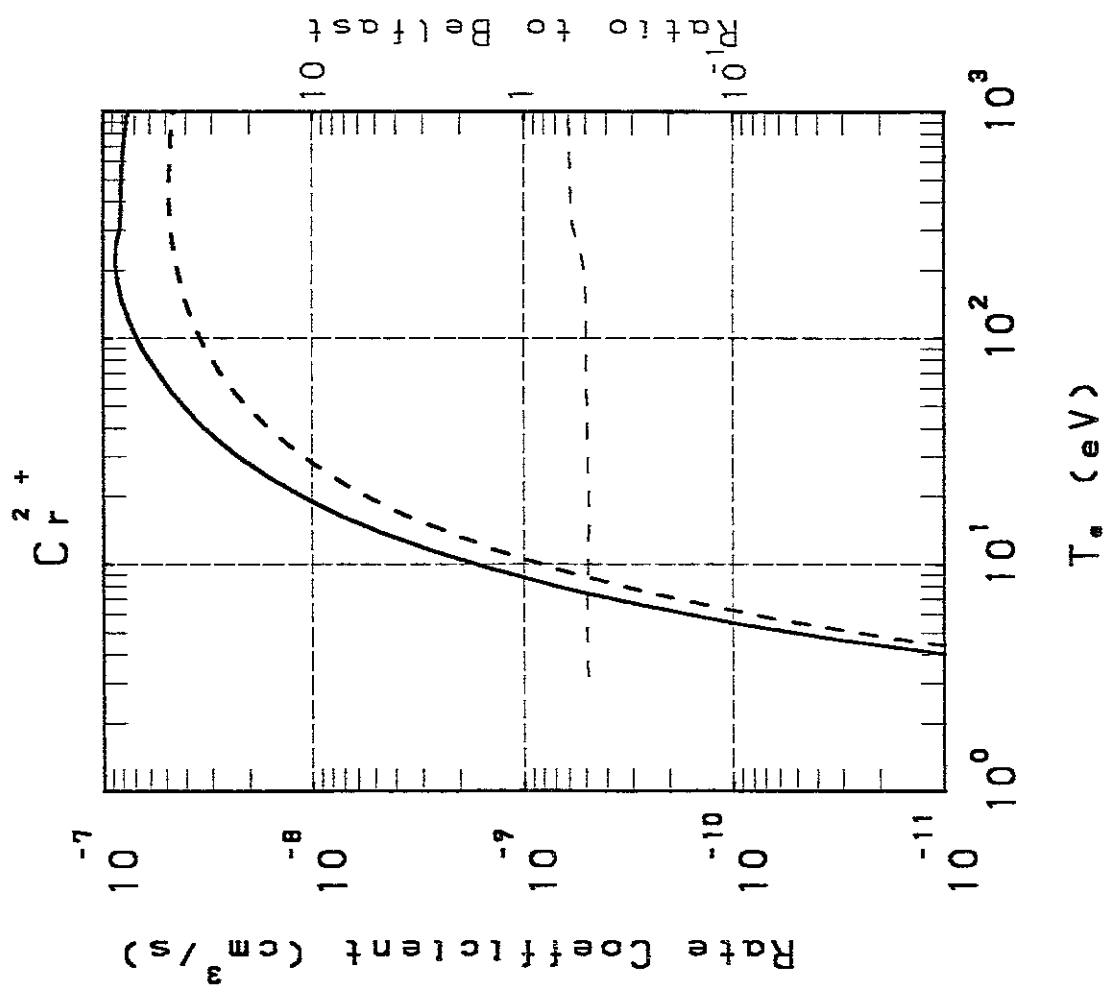
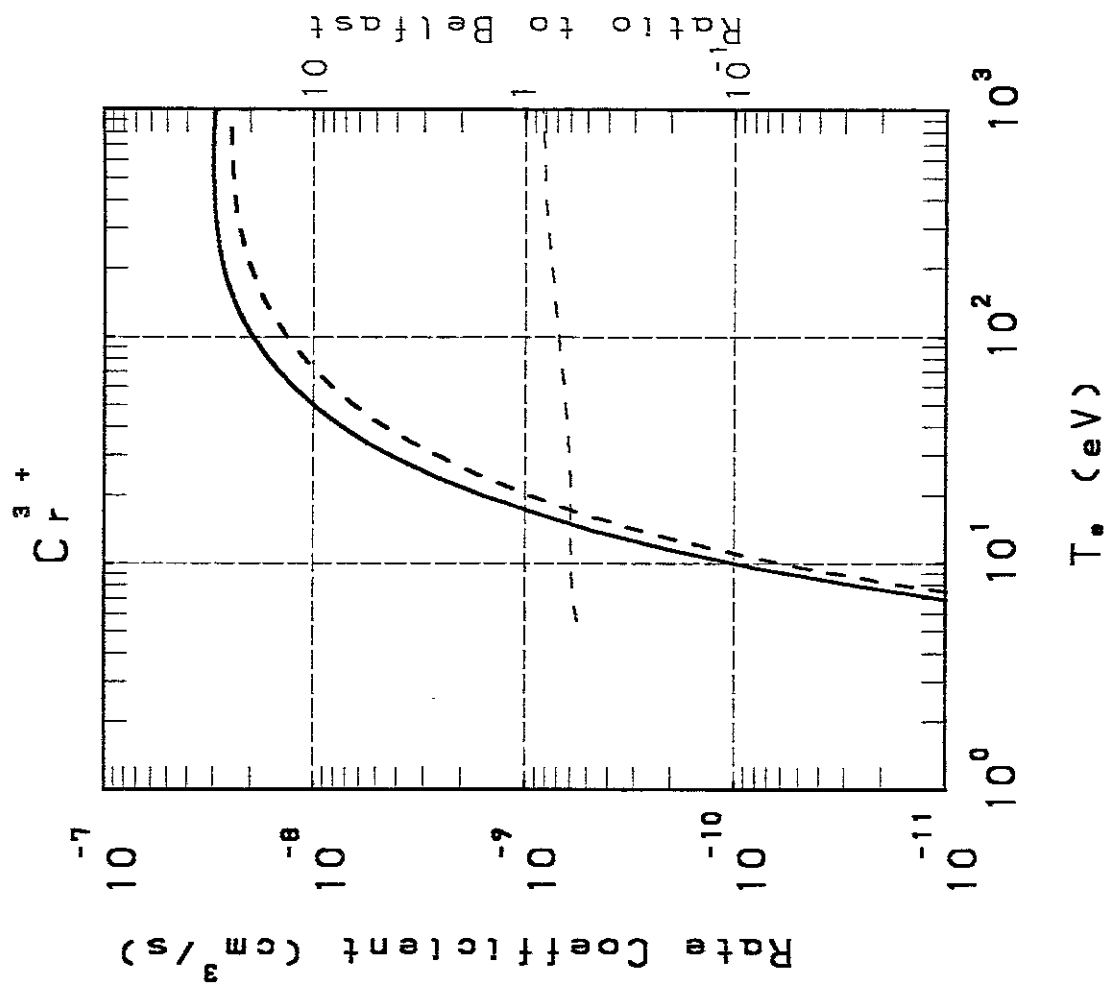


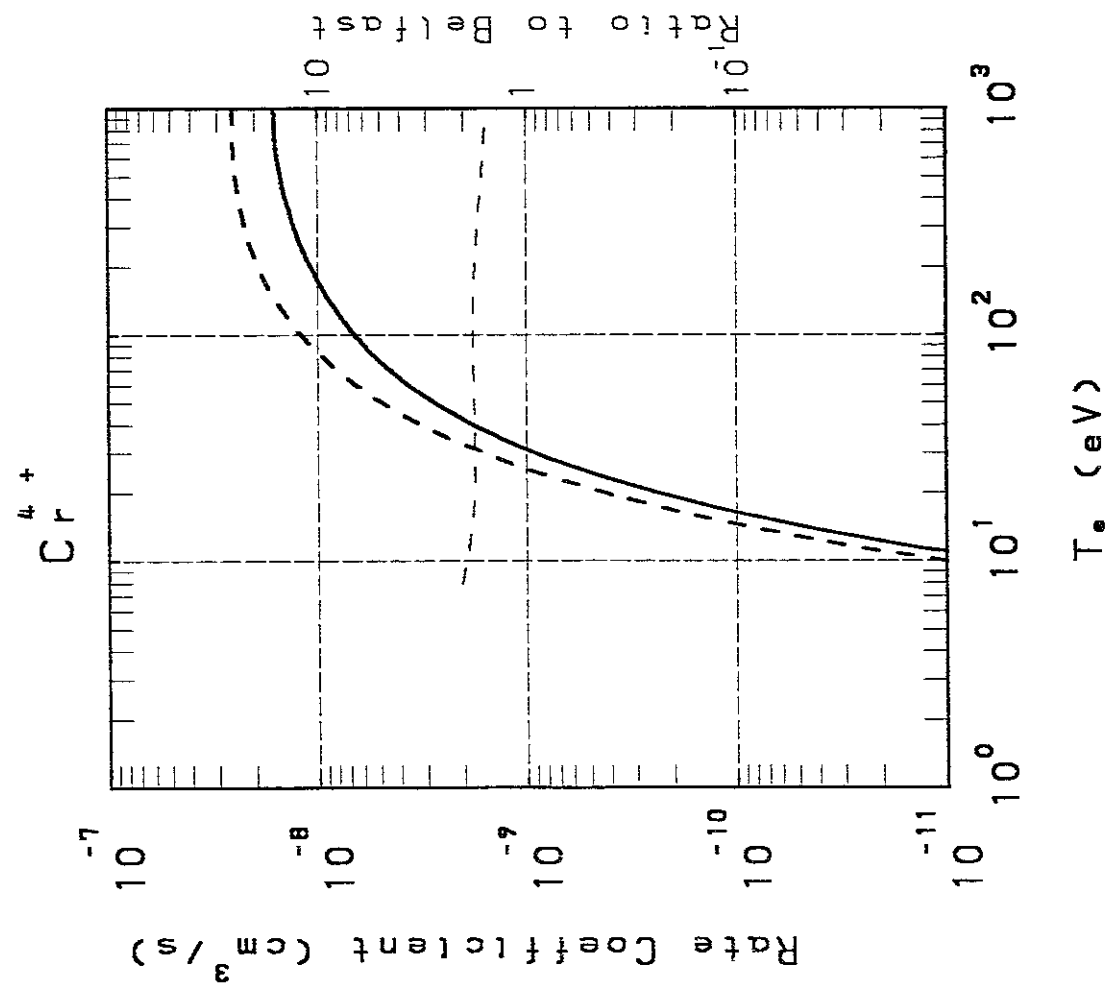
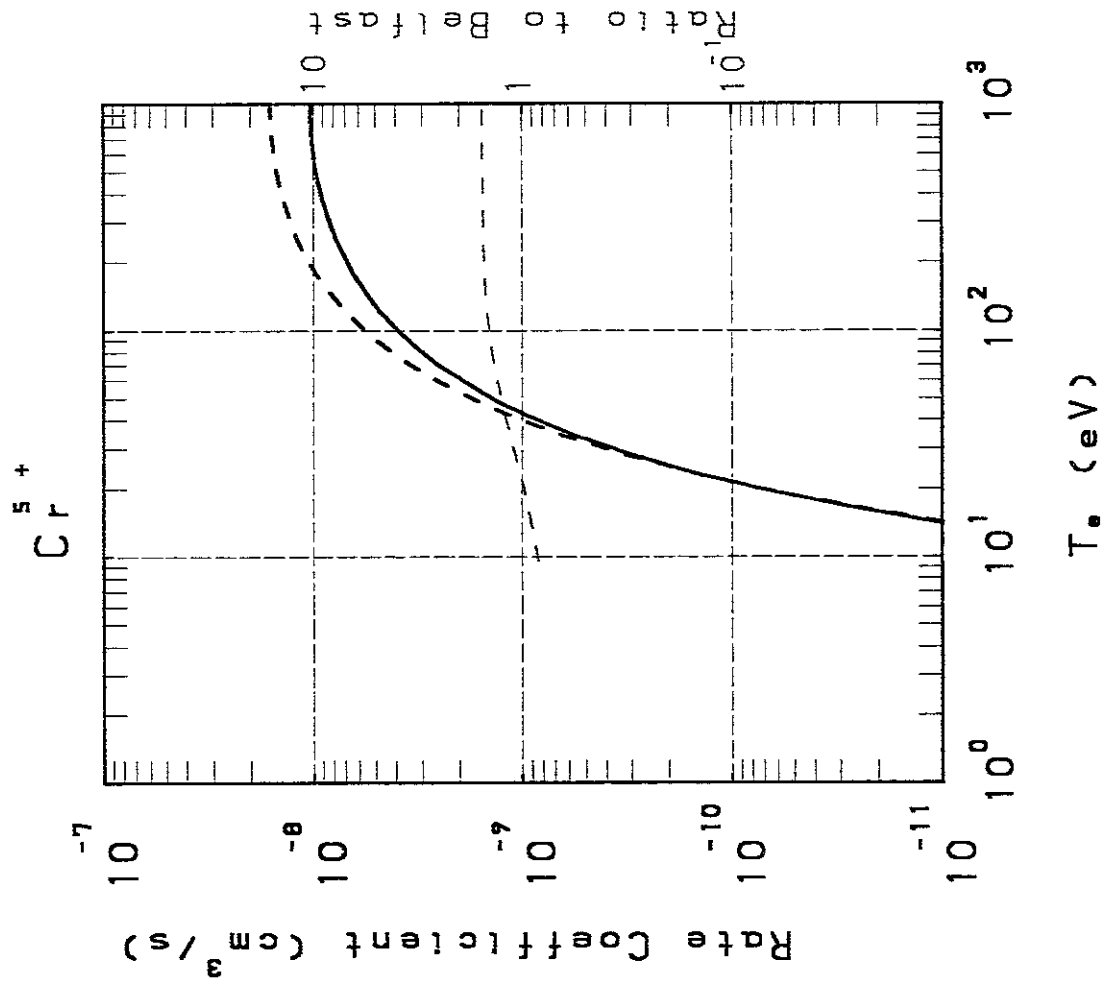


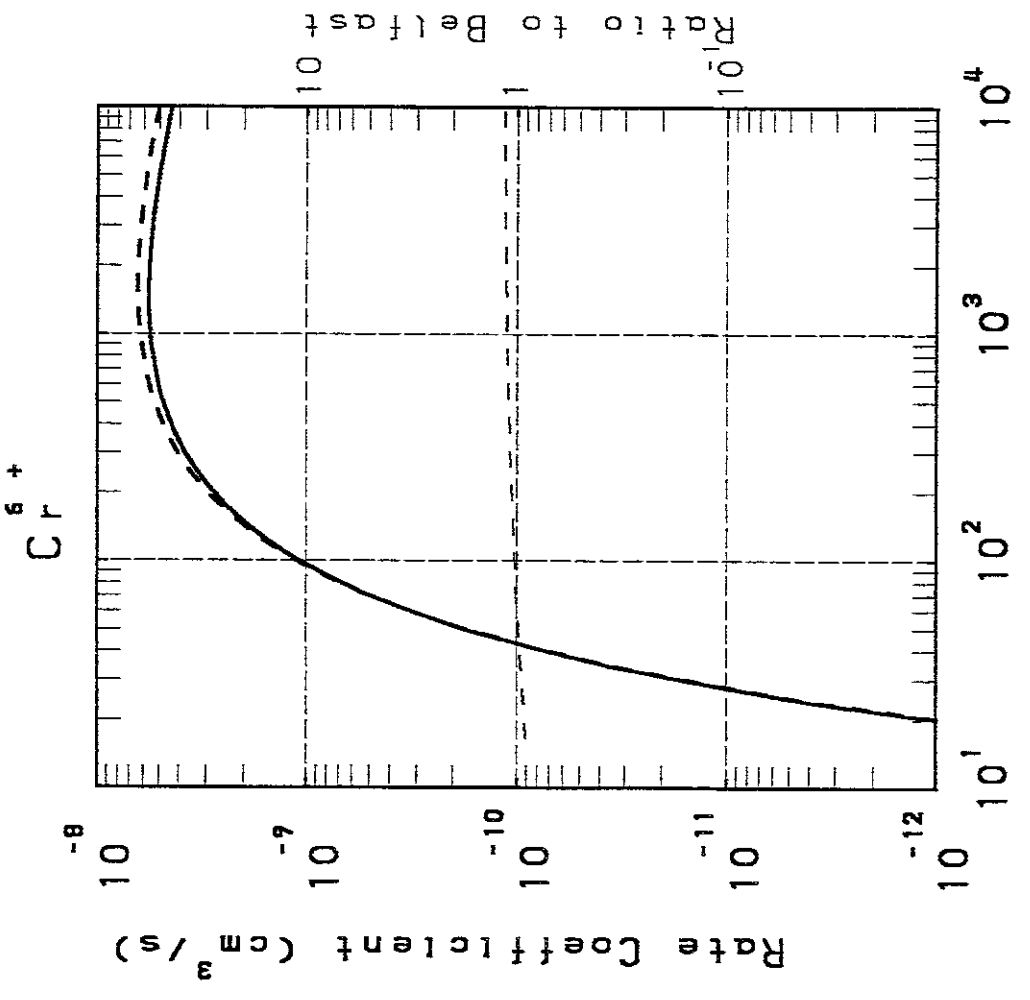
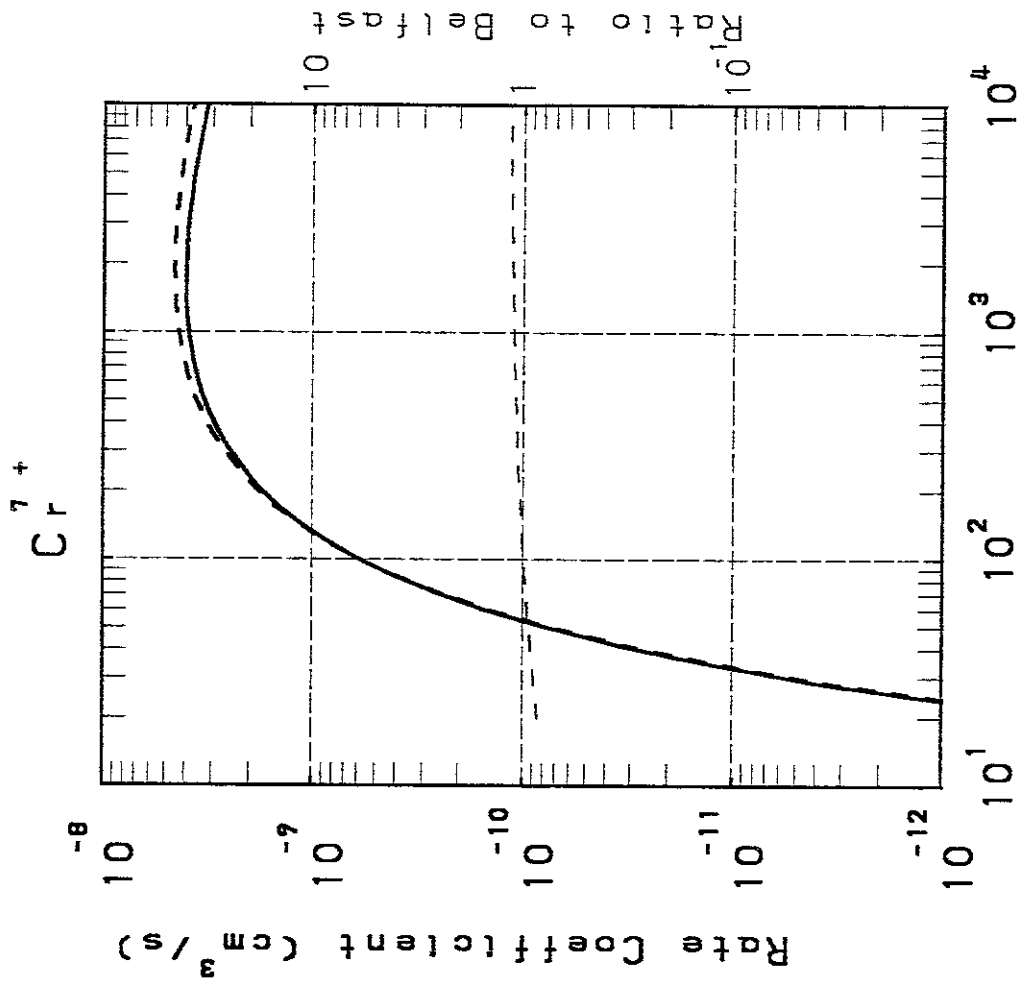


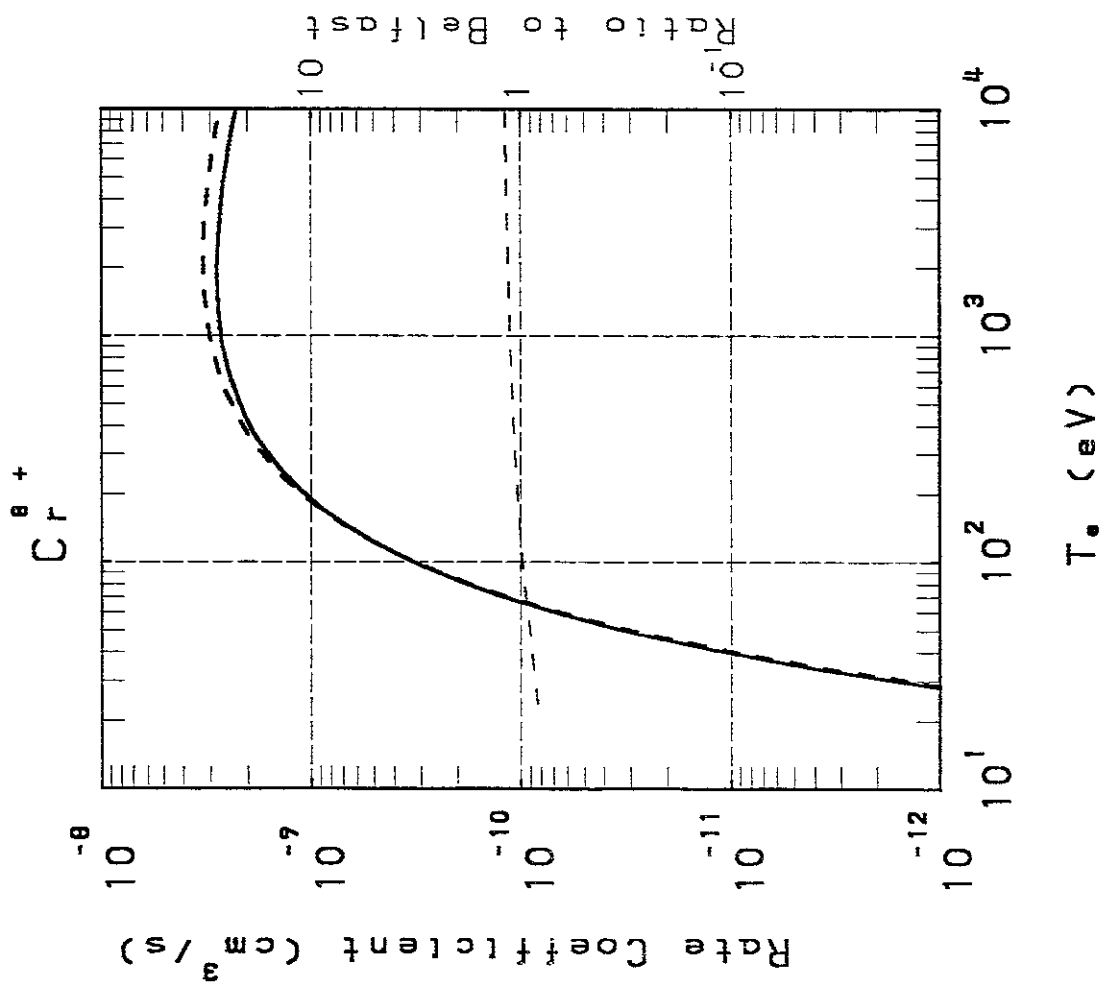
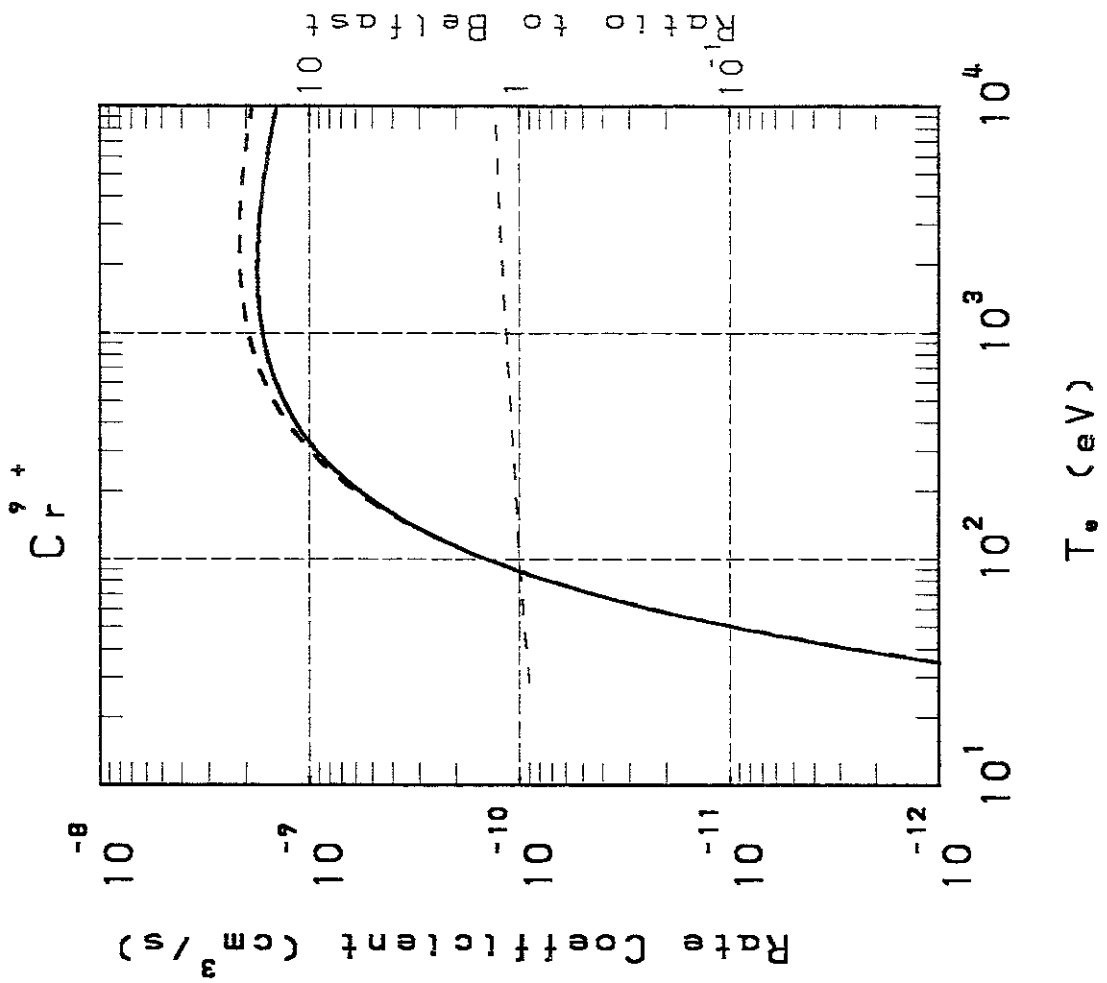


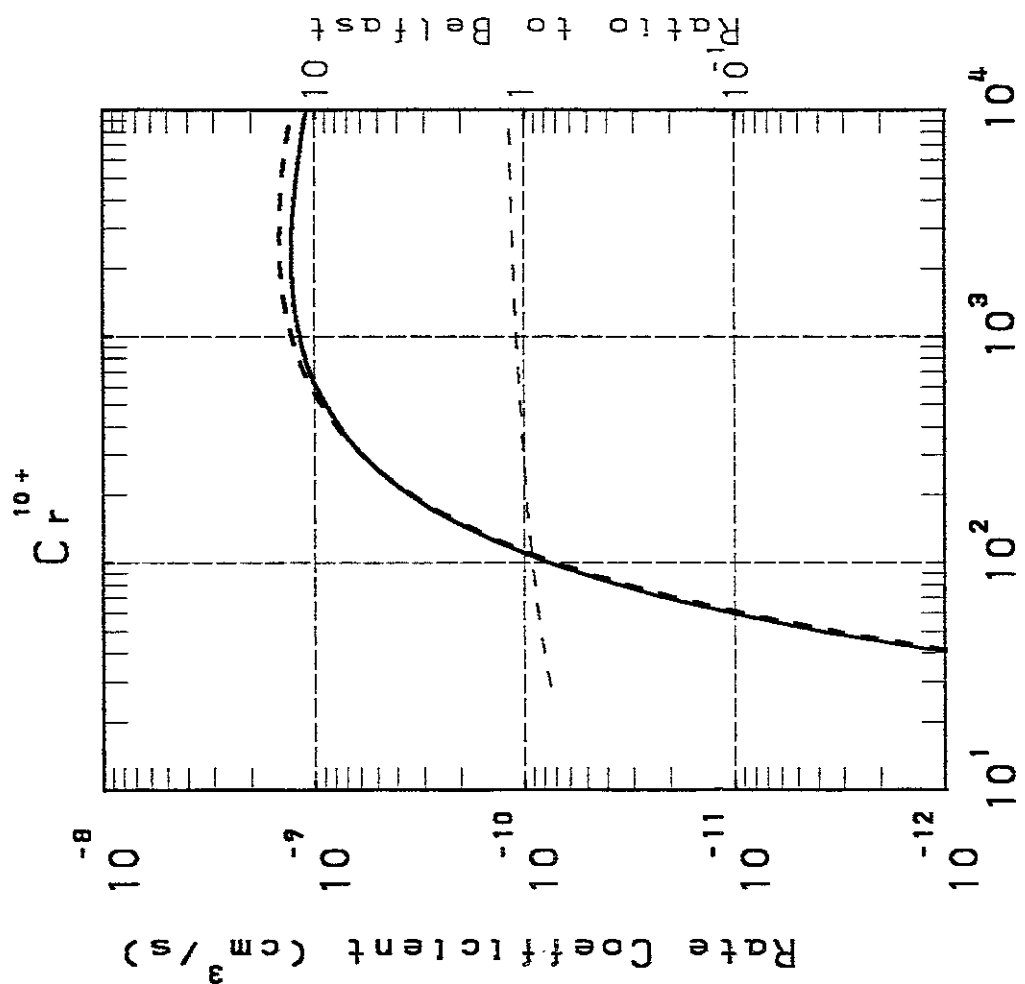
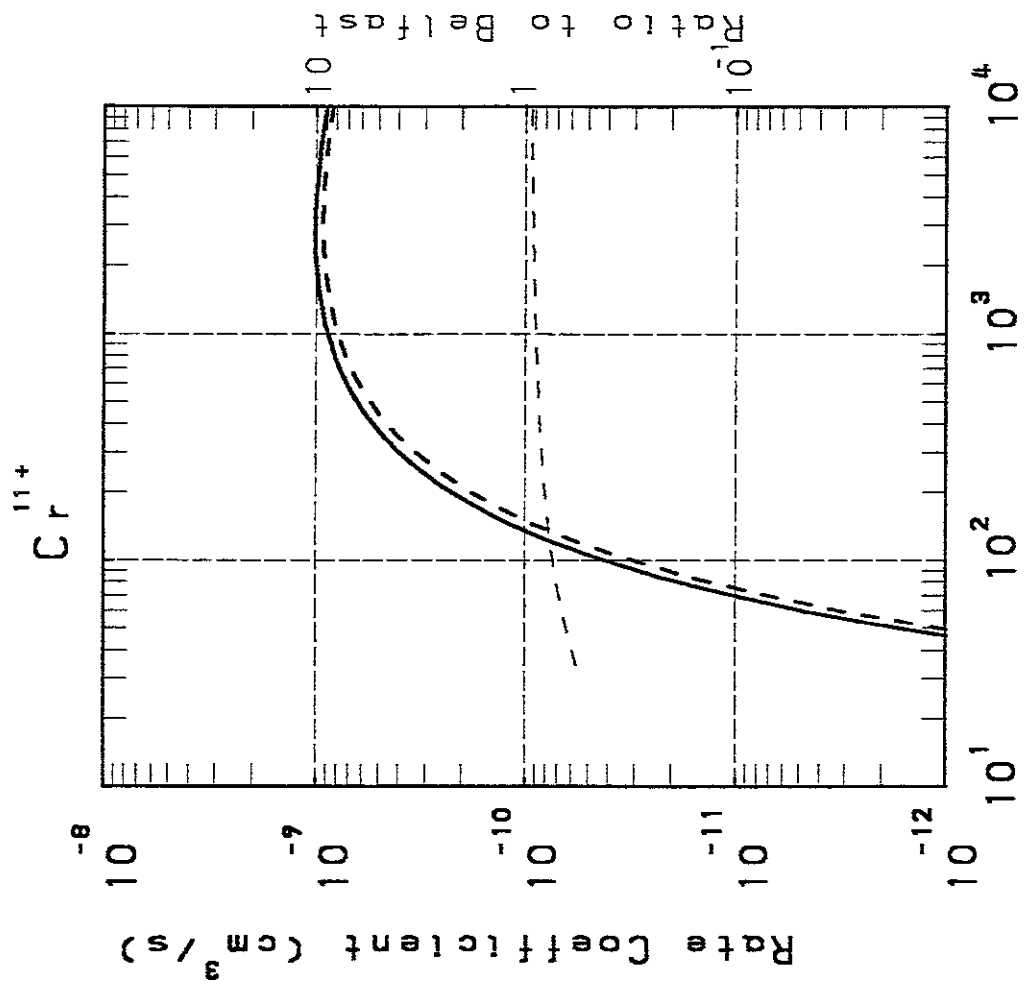


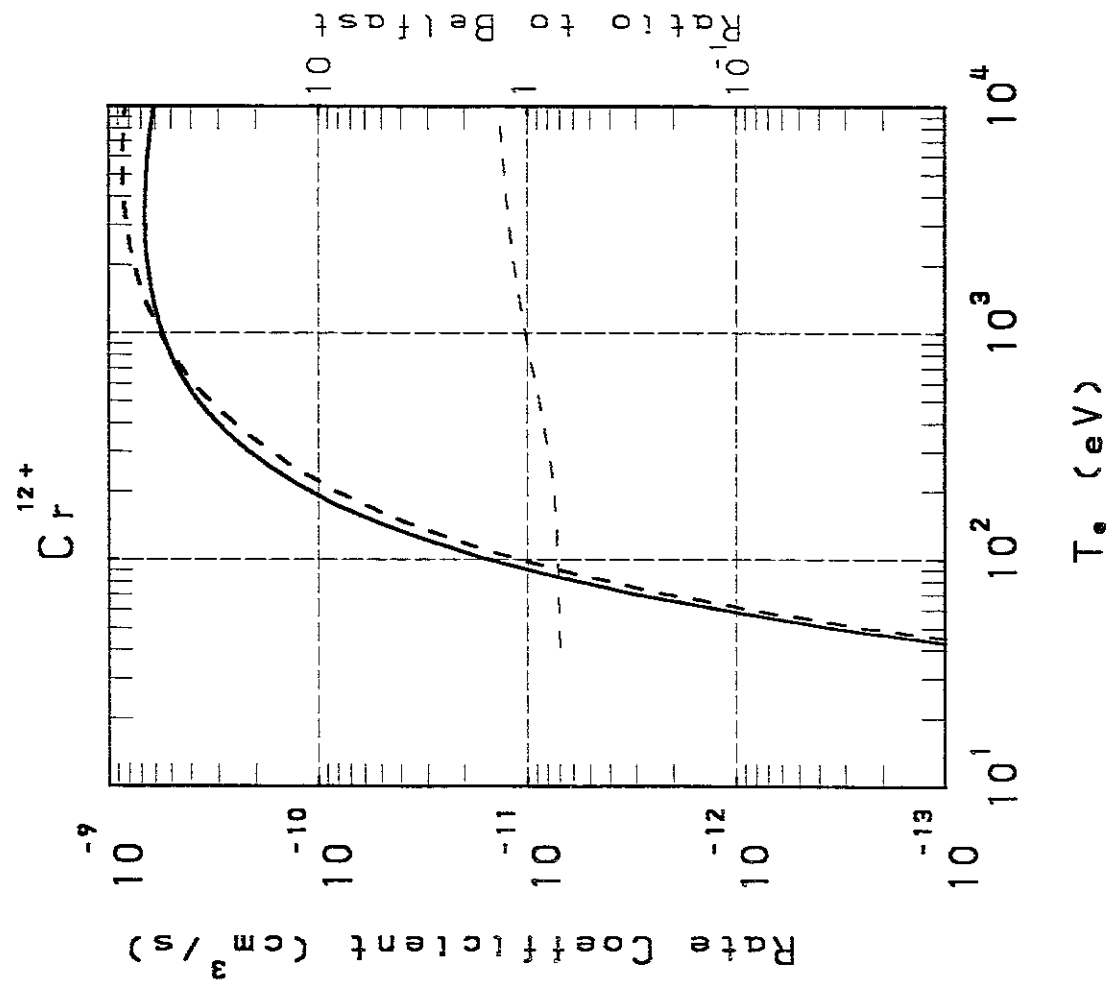
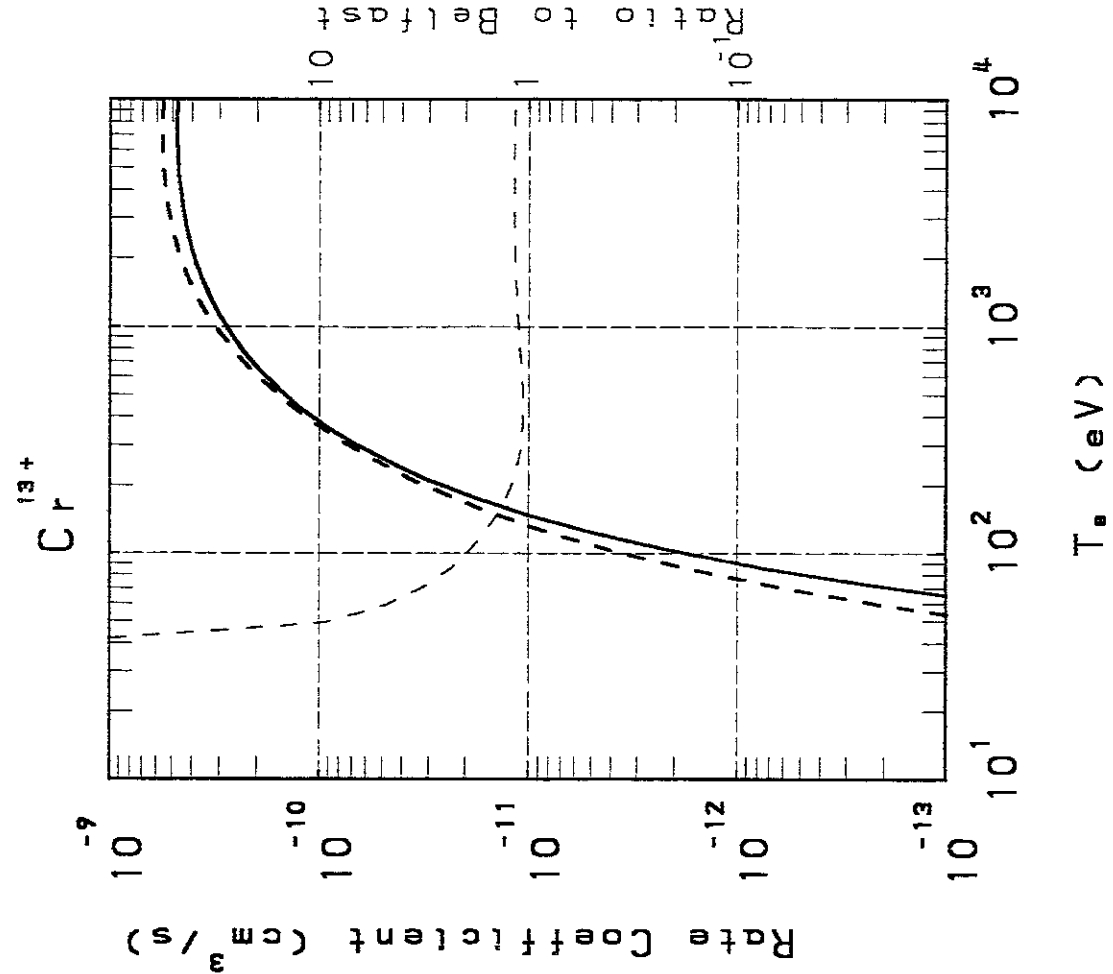


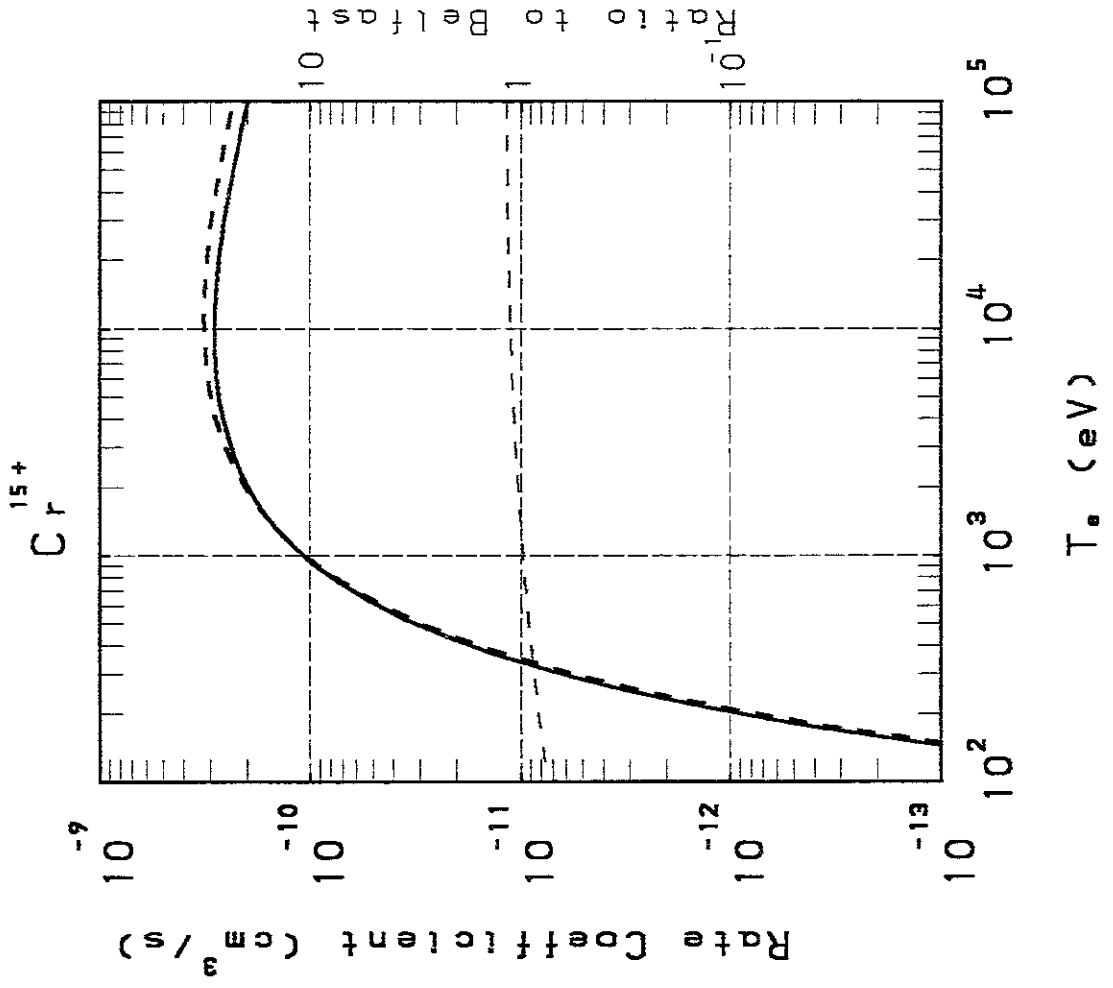
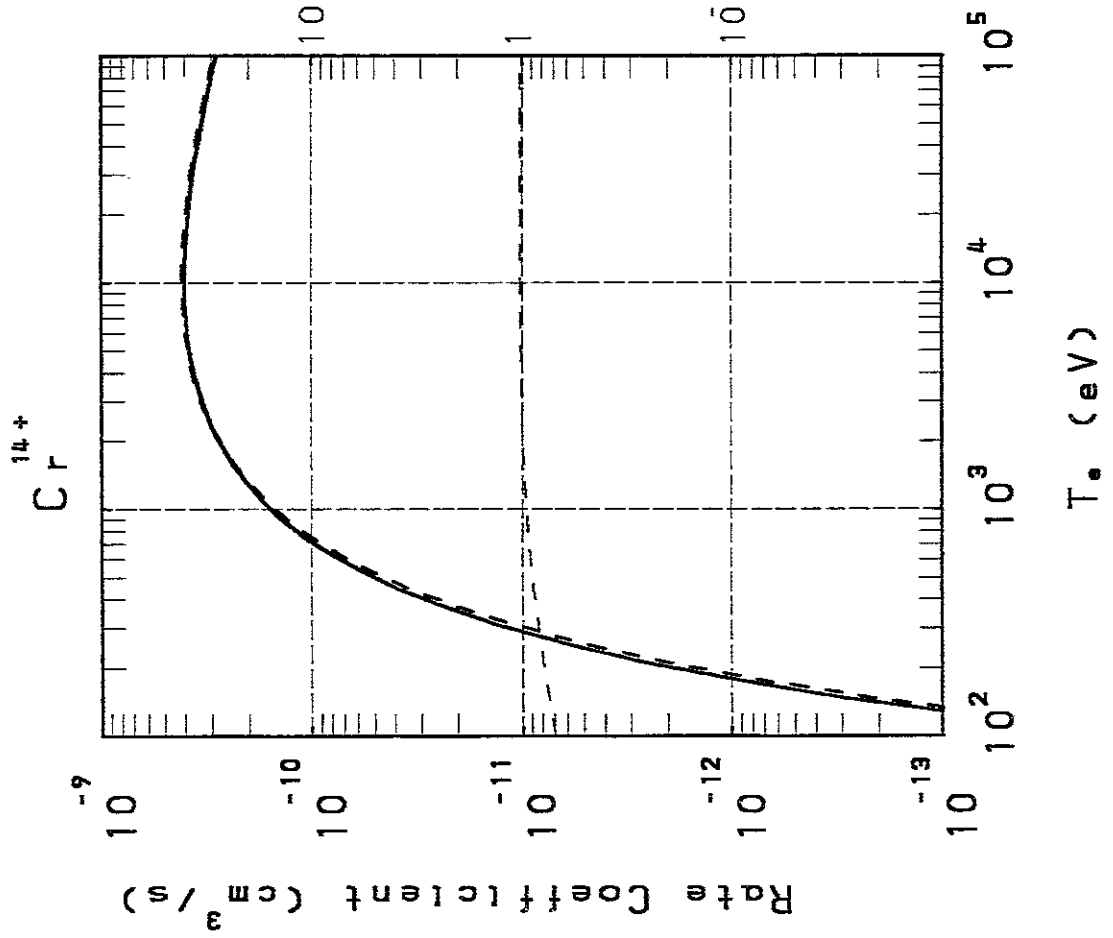


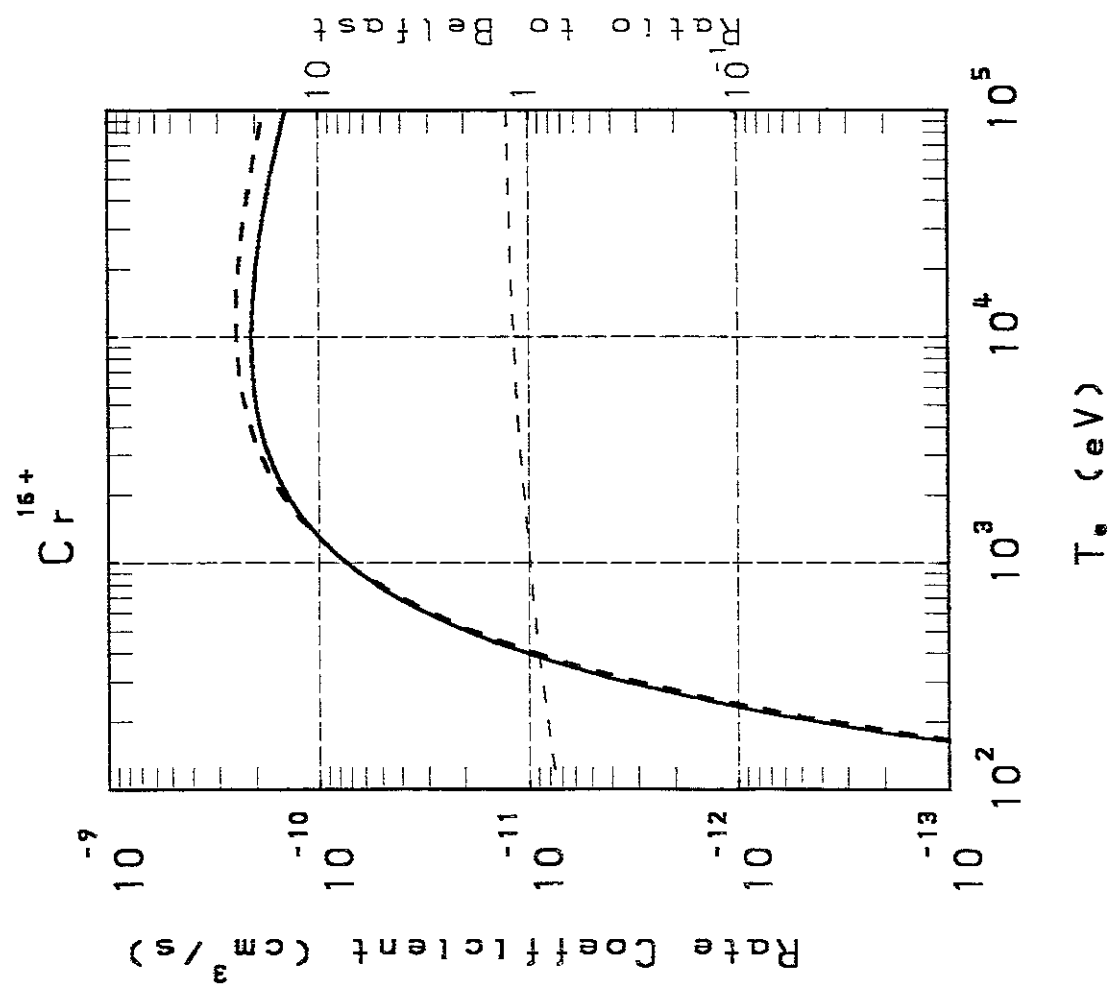
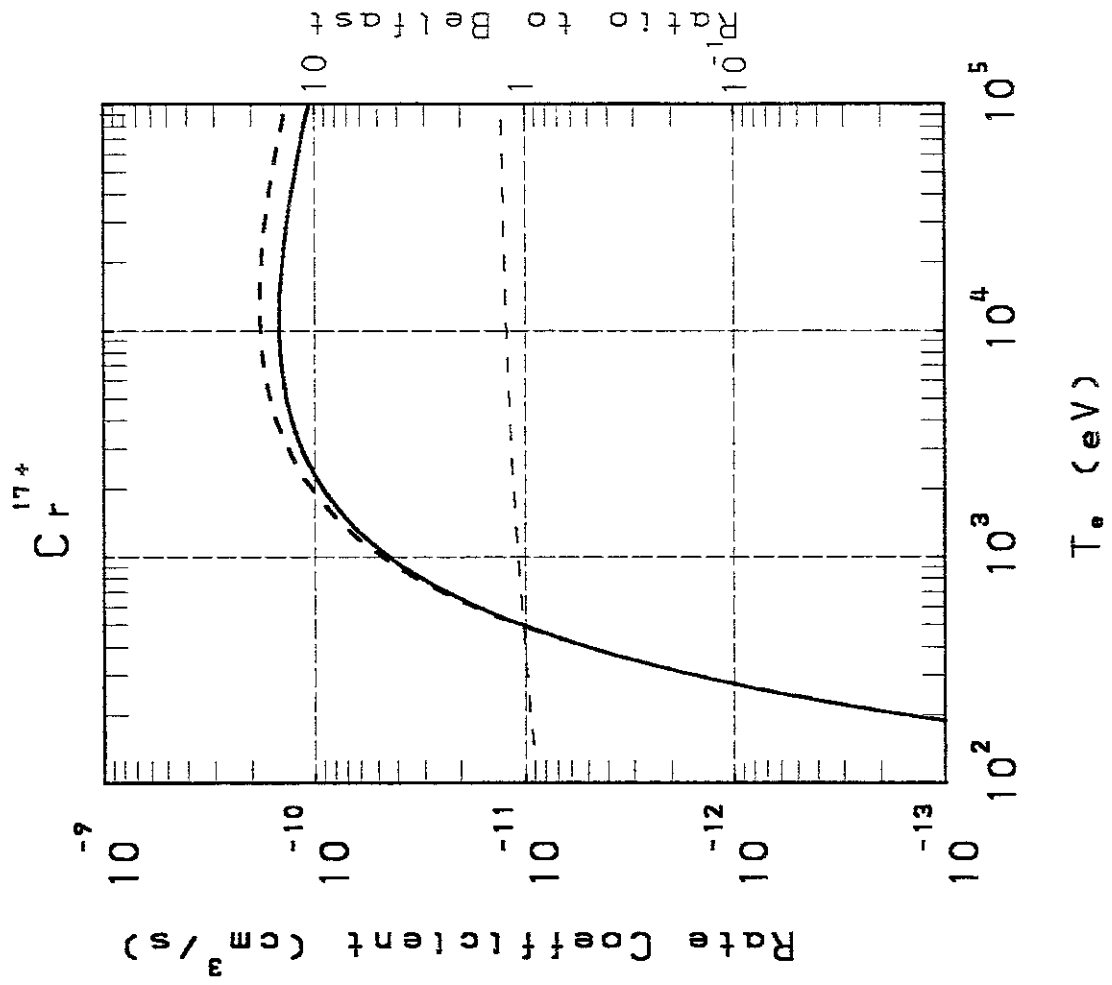


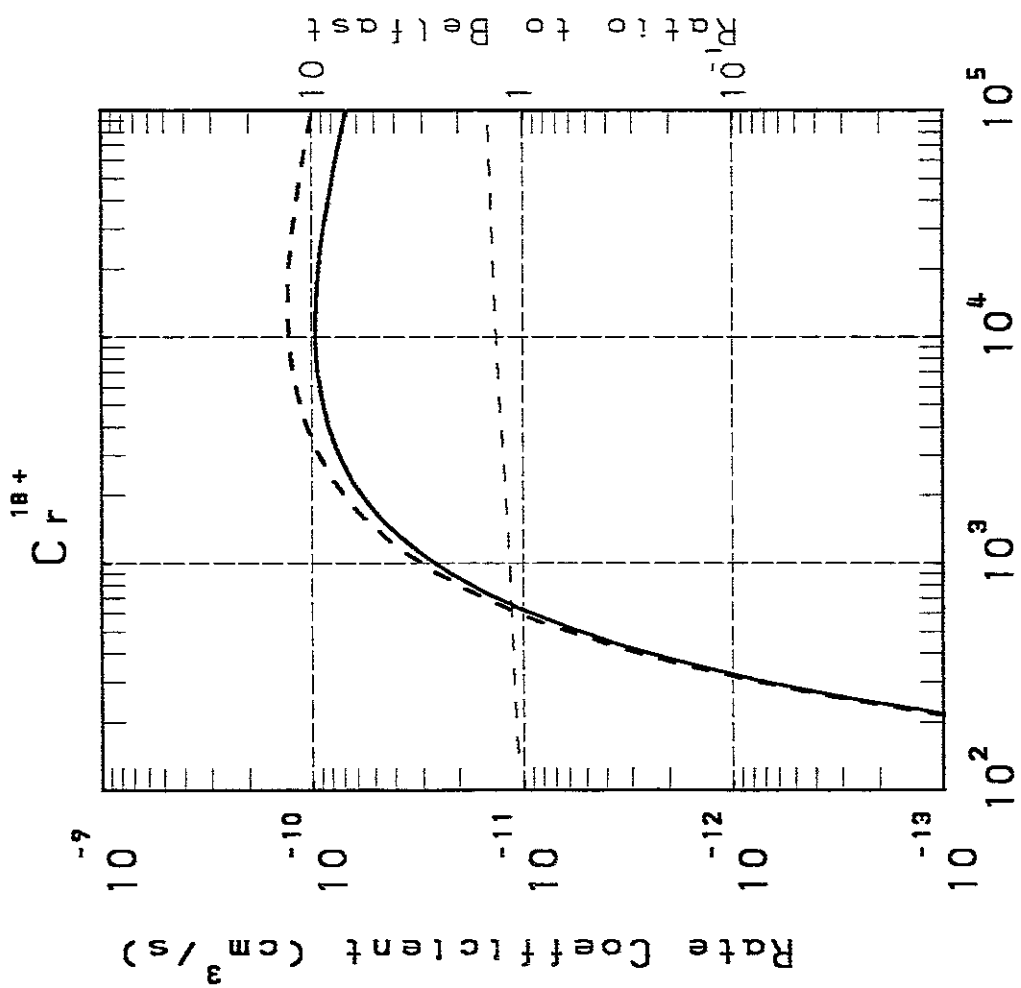




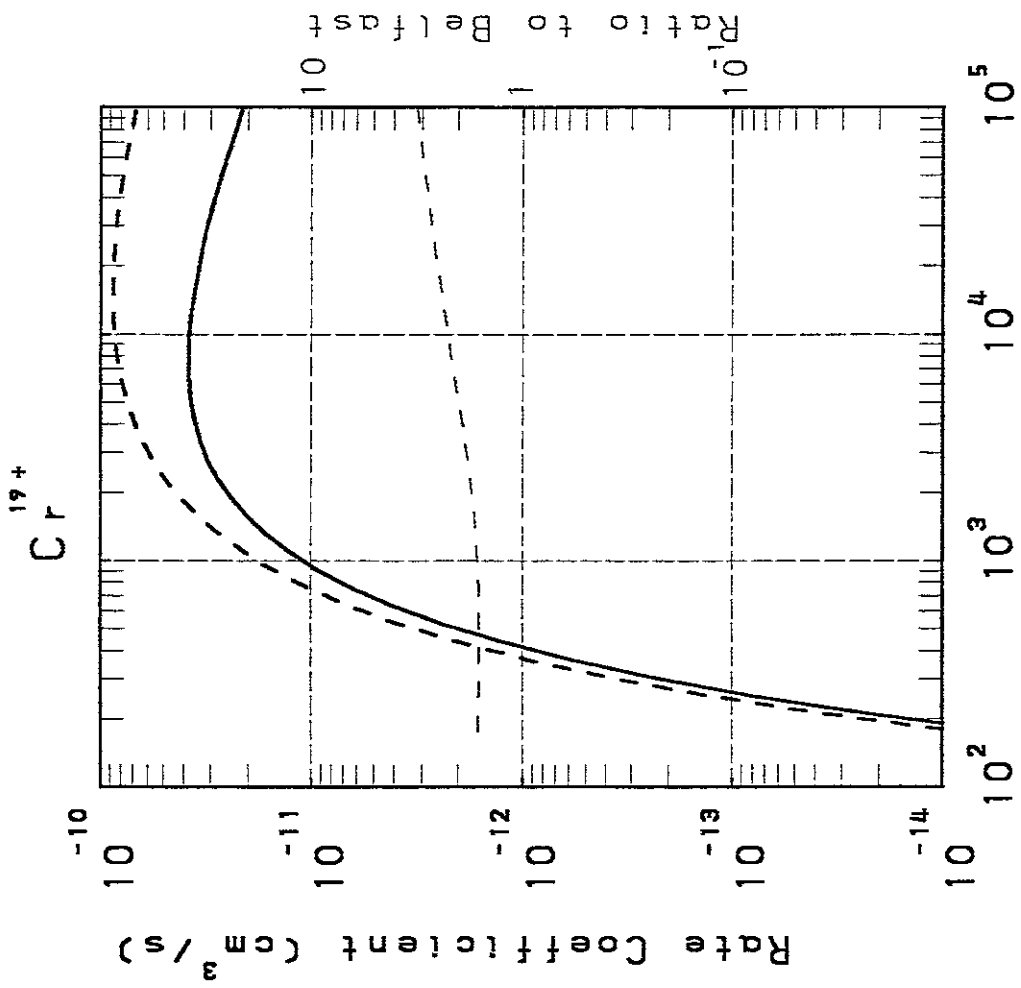




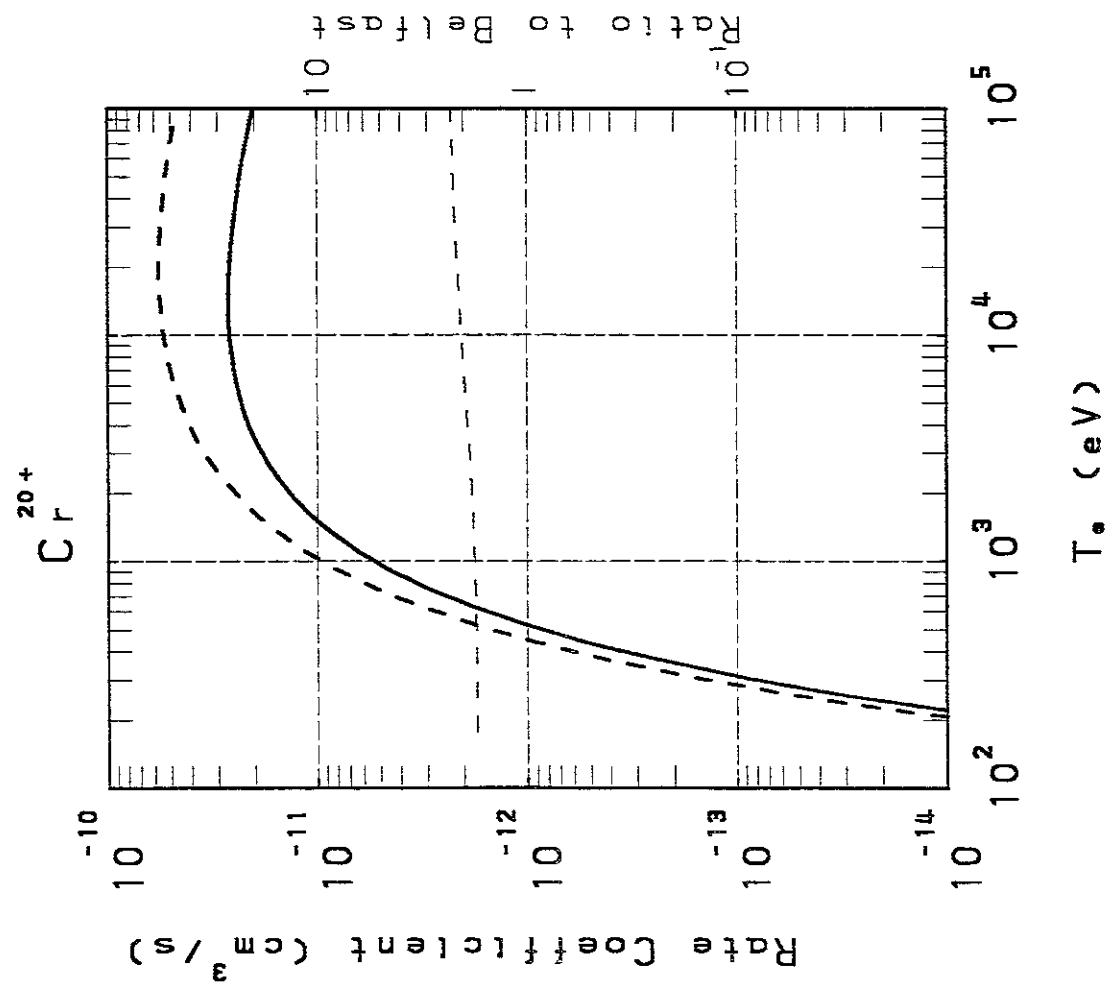
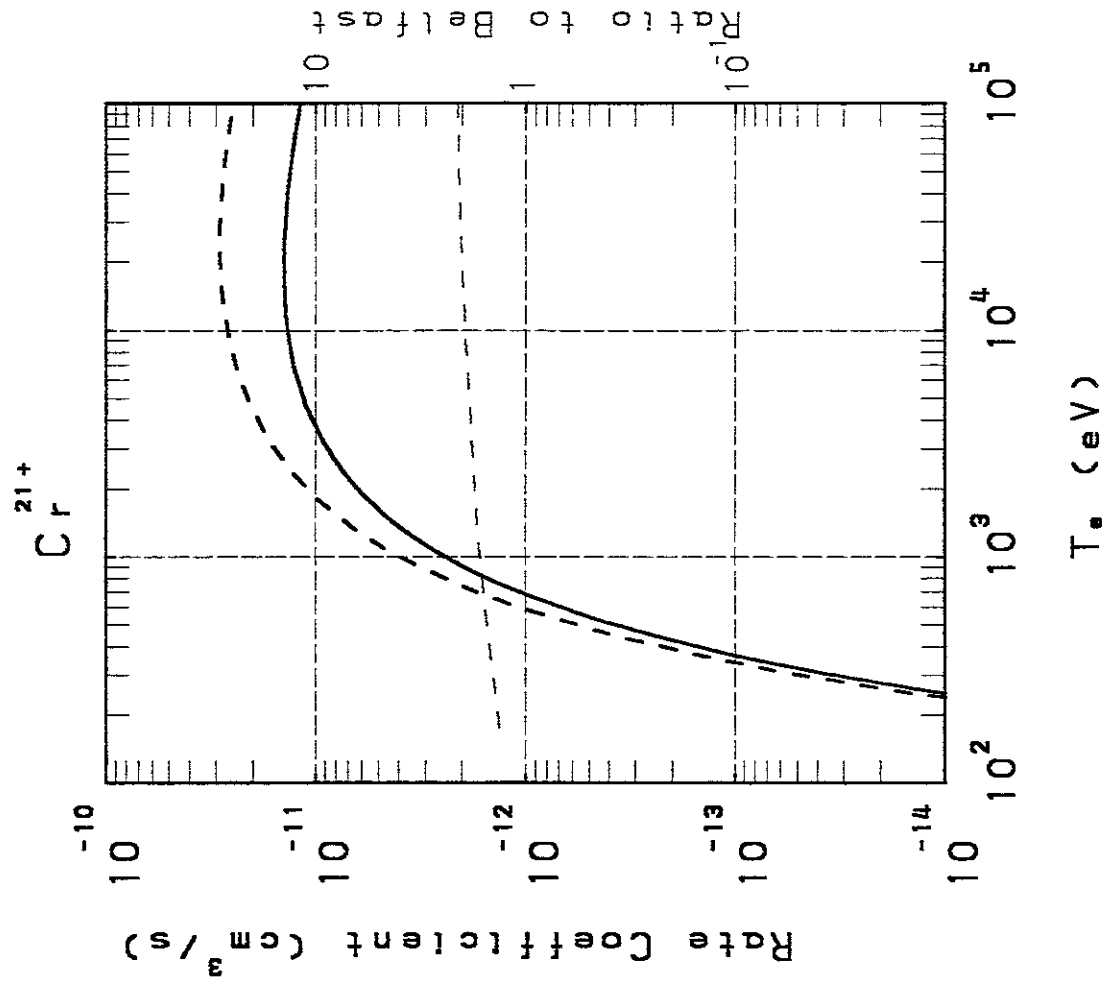


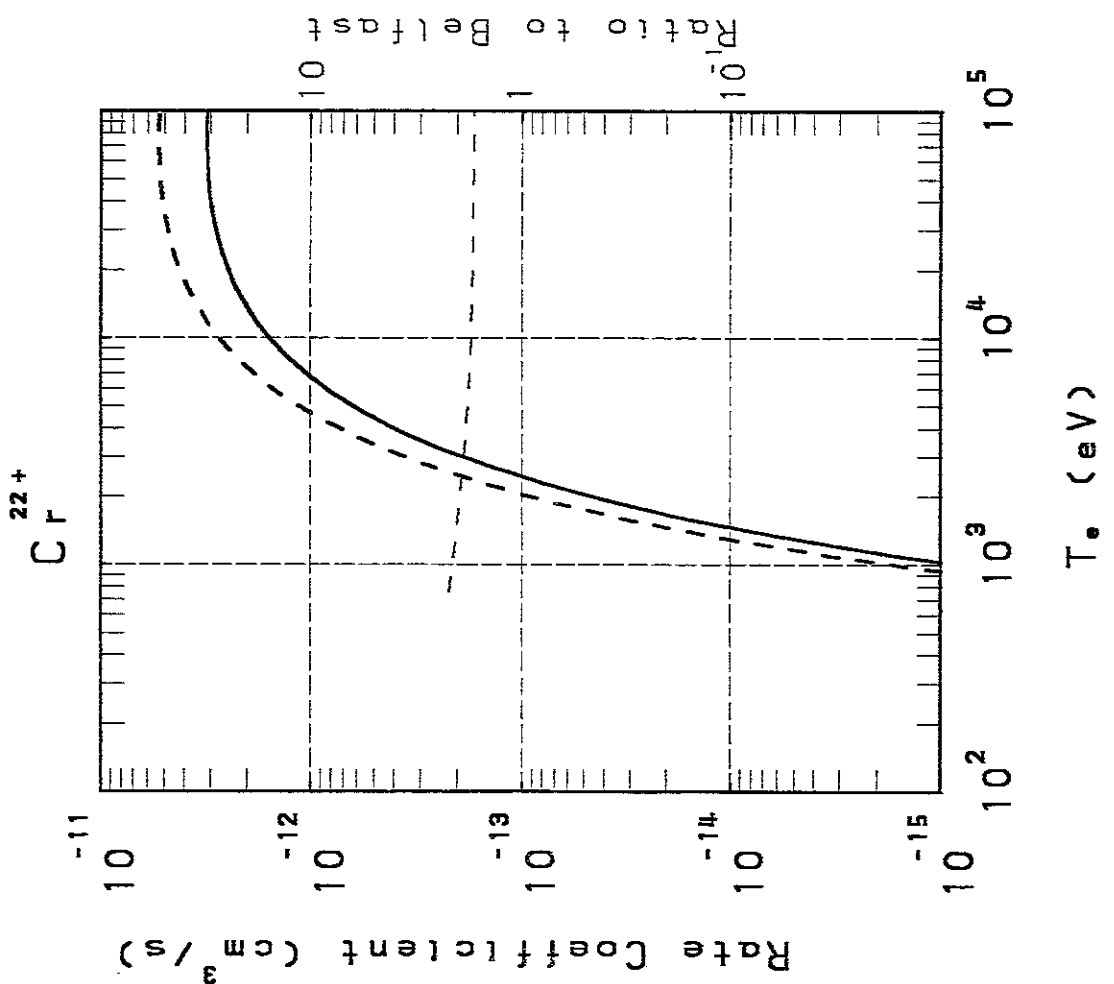
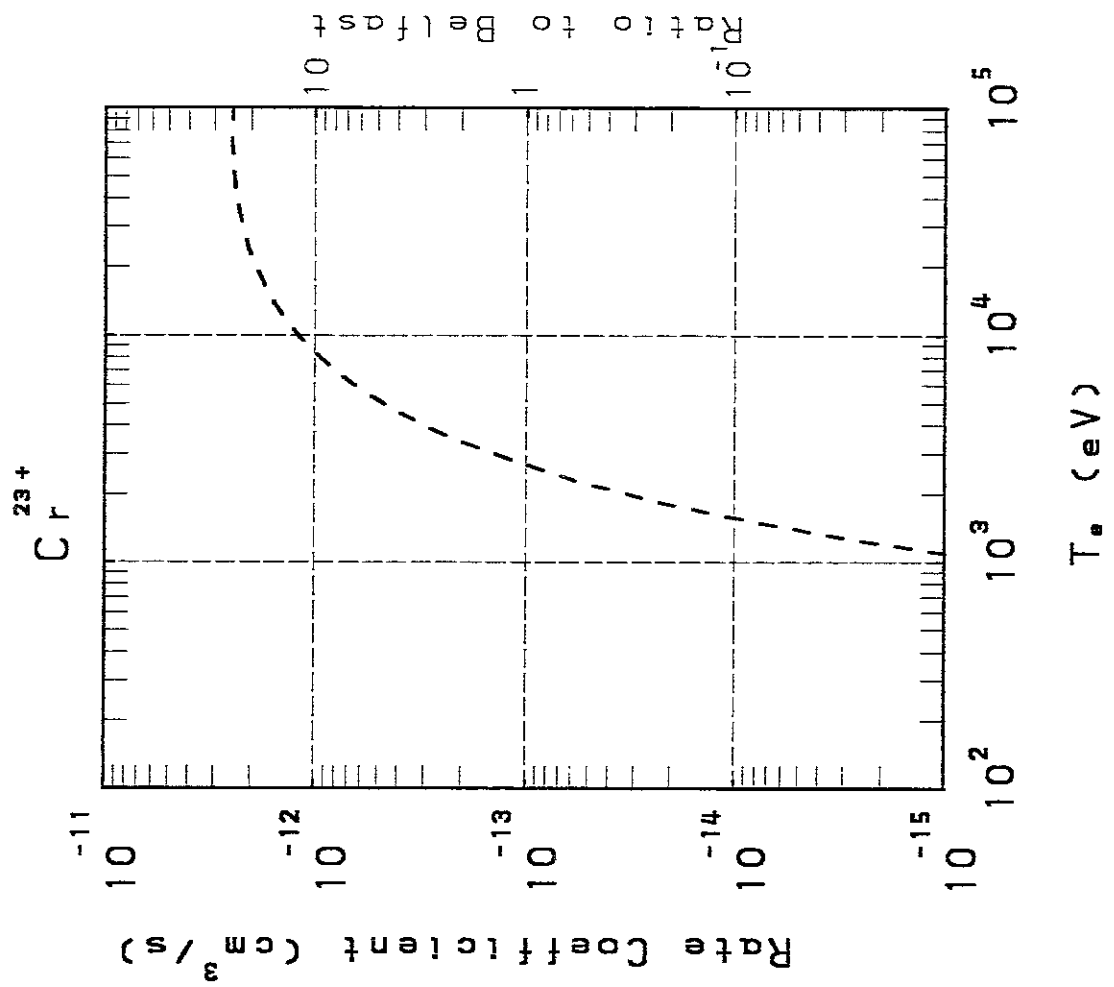


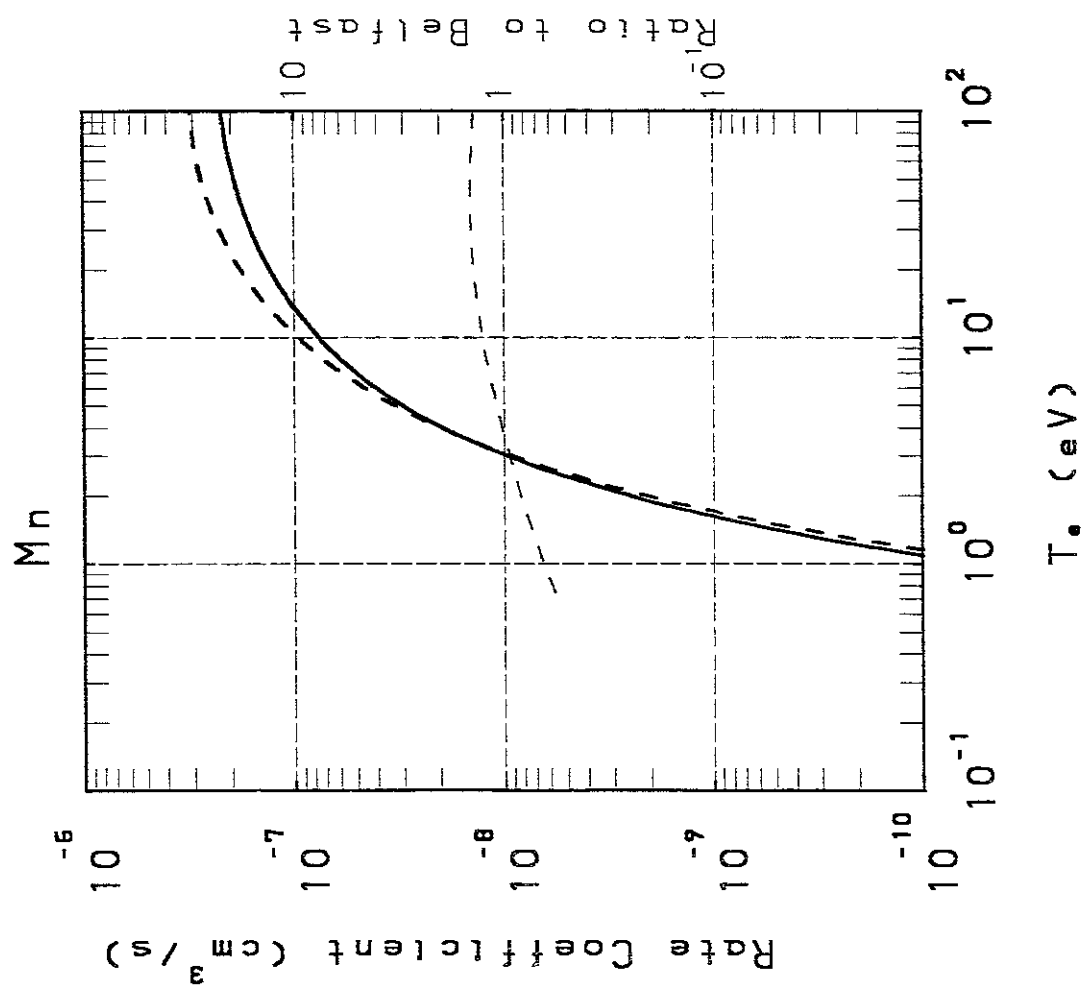
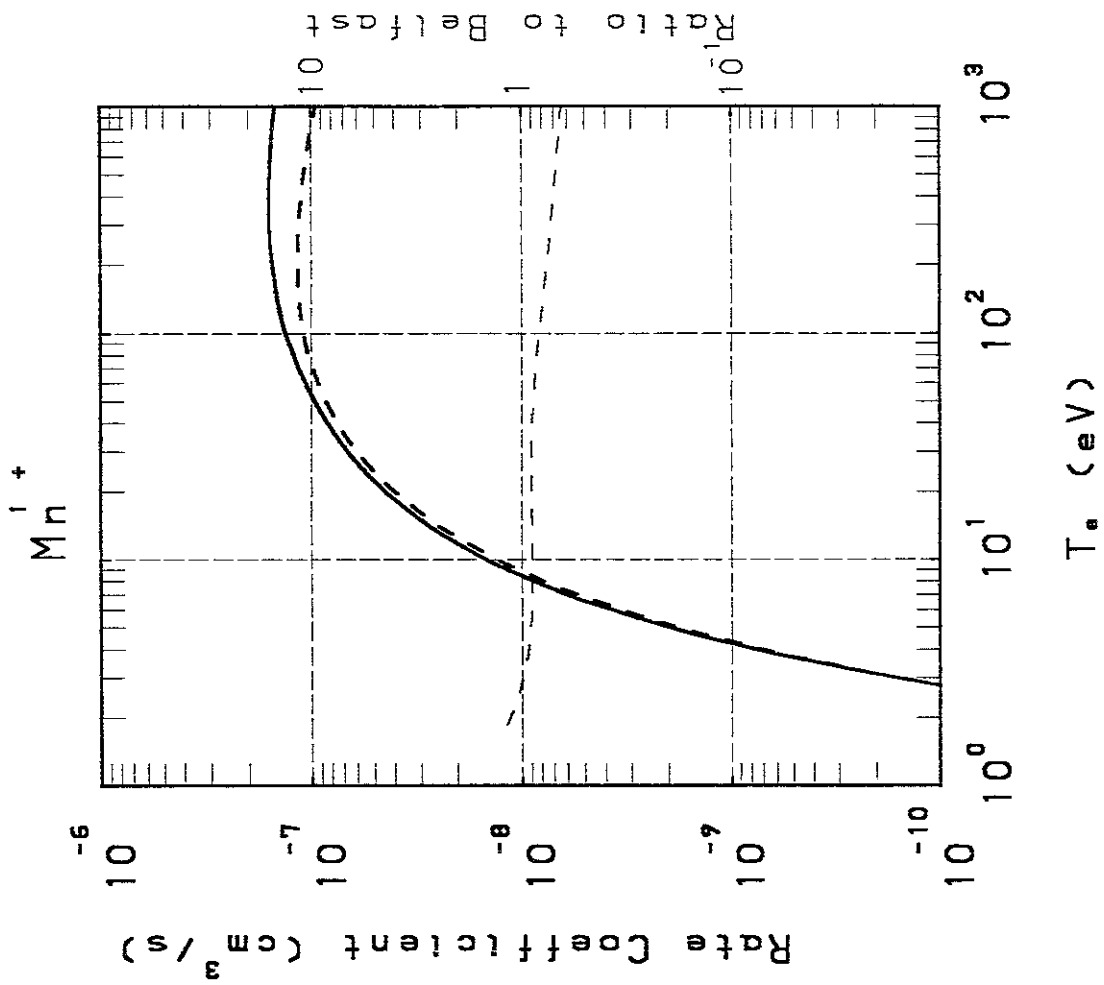
T^* (eV)

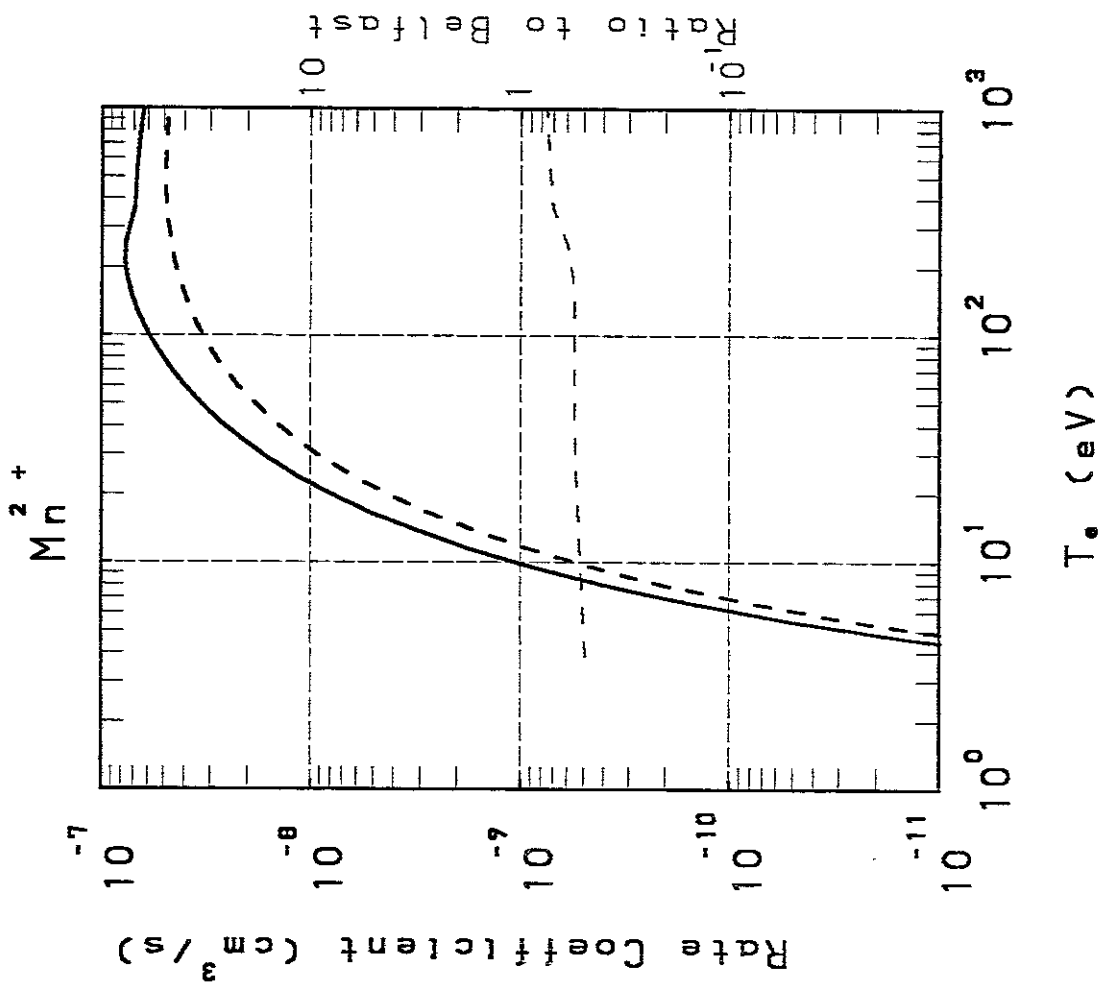
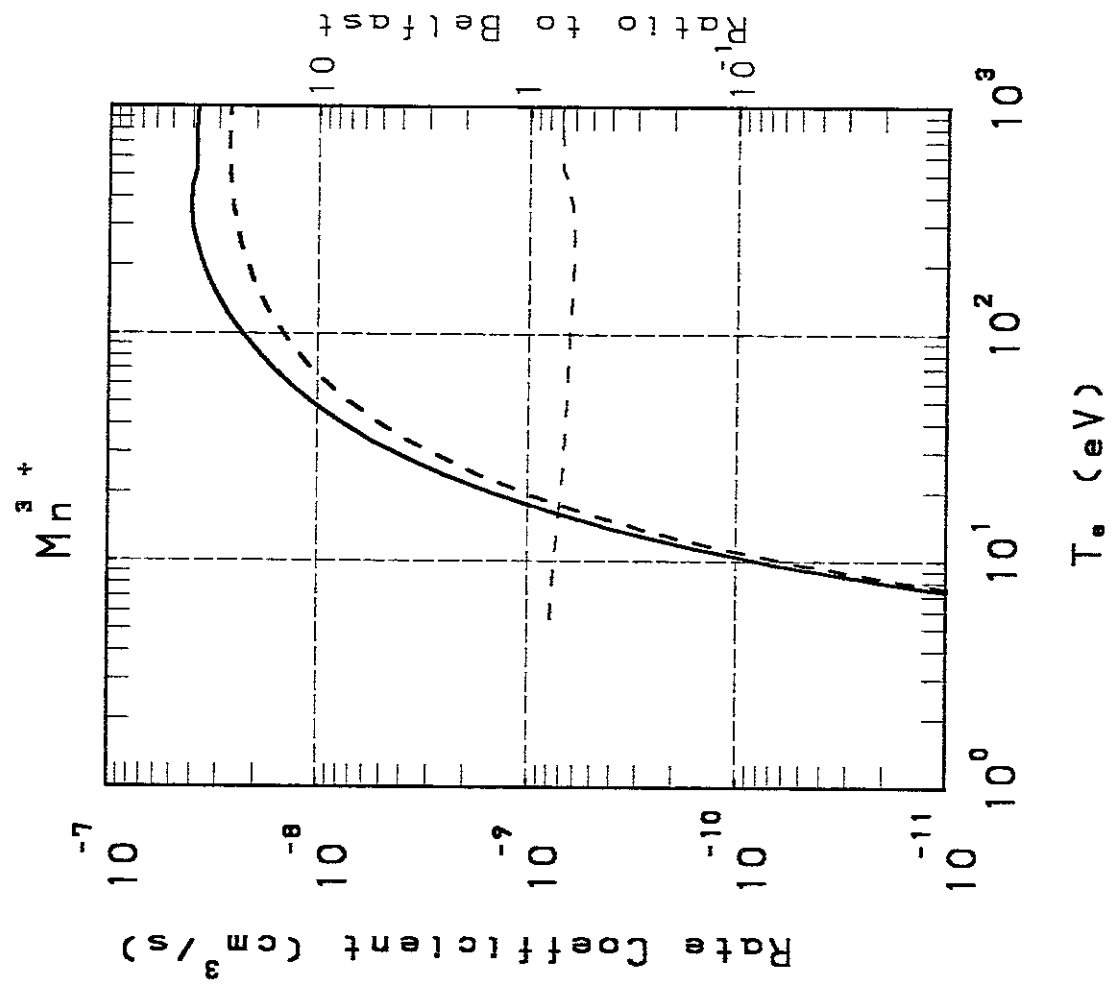


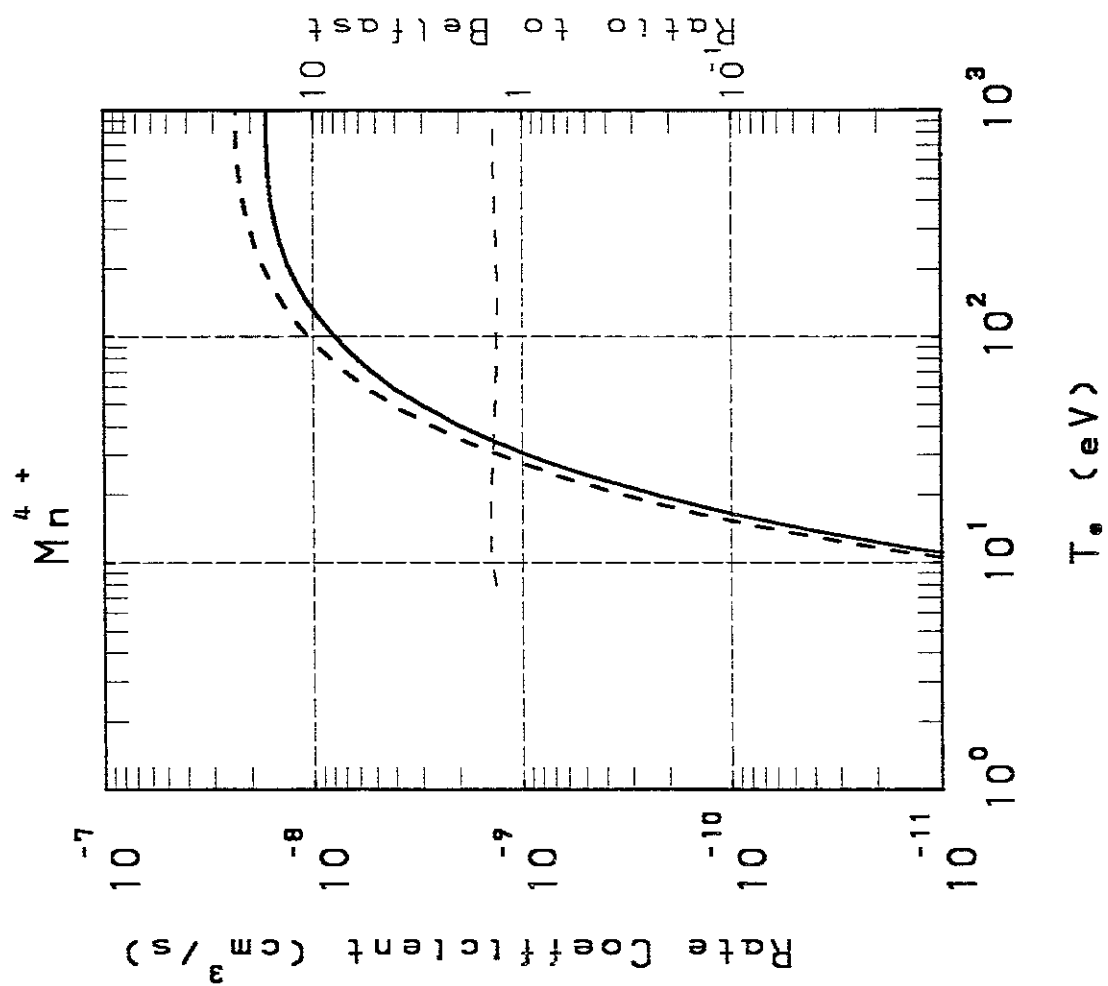
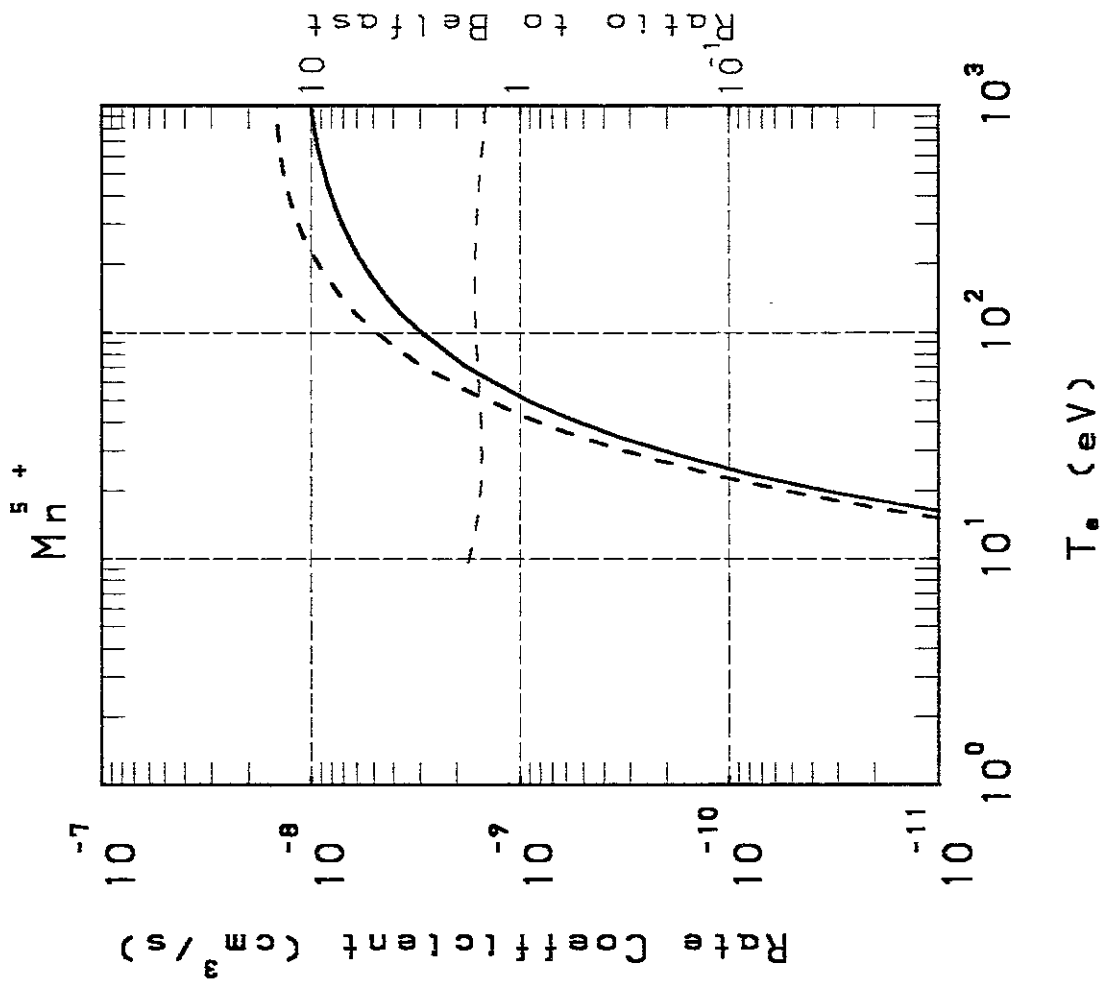
T^* (eV)

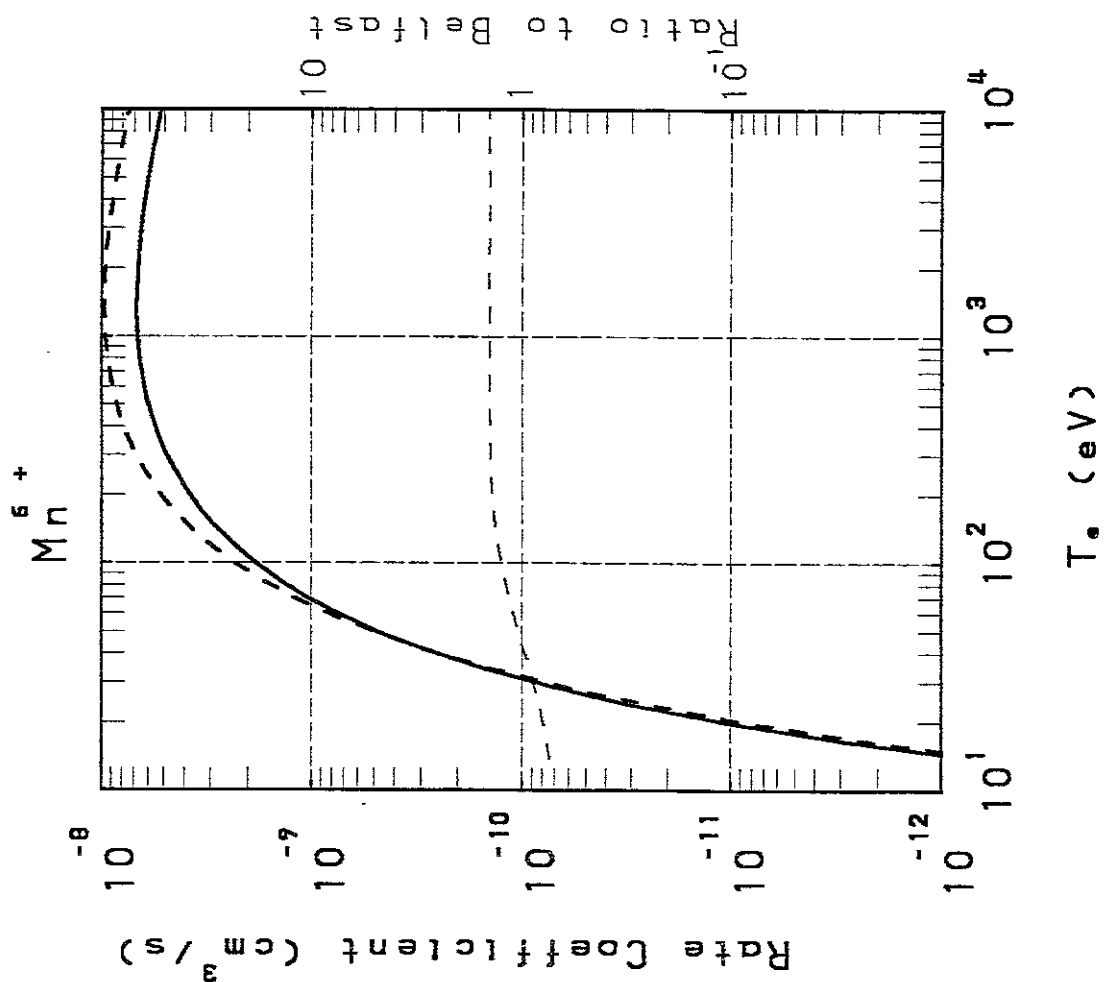
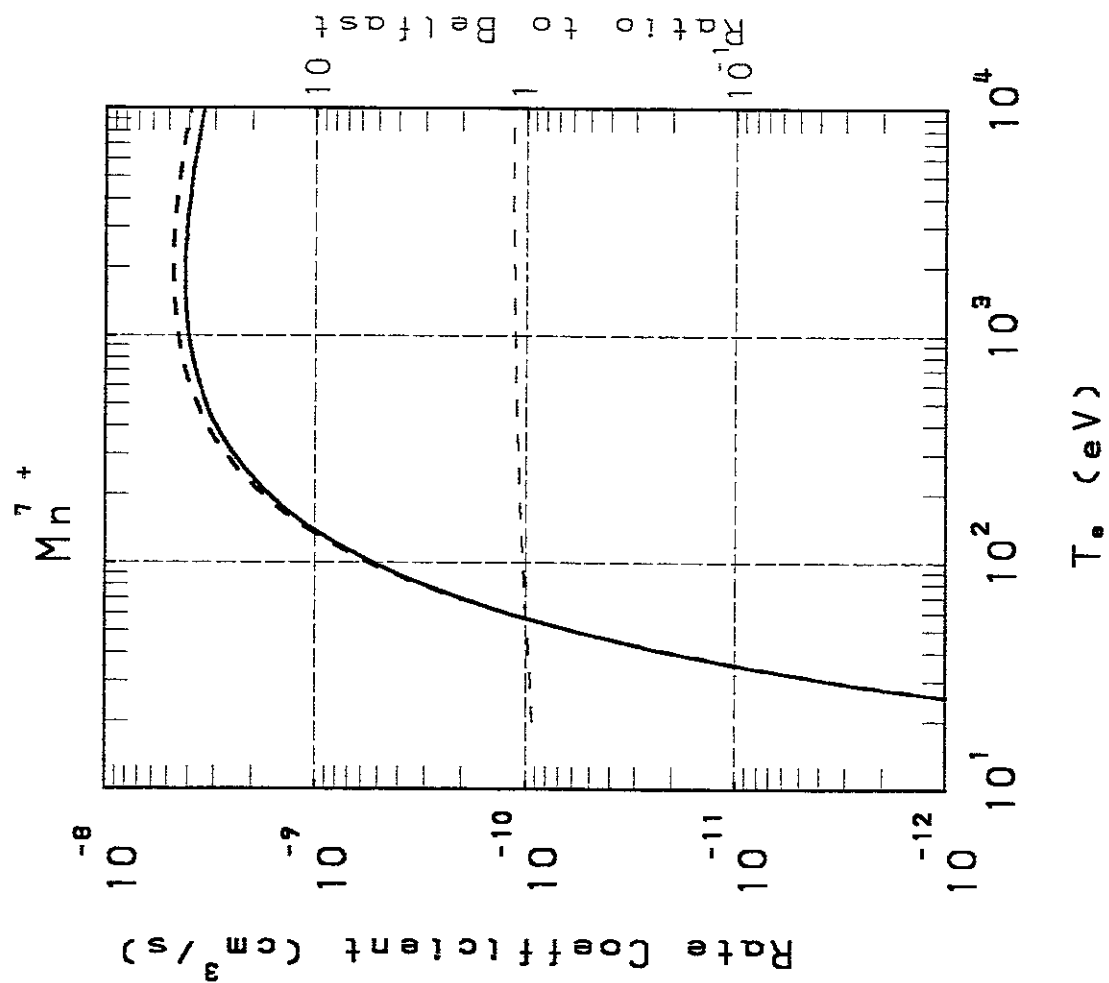


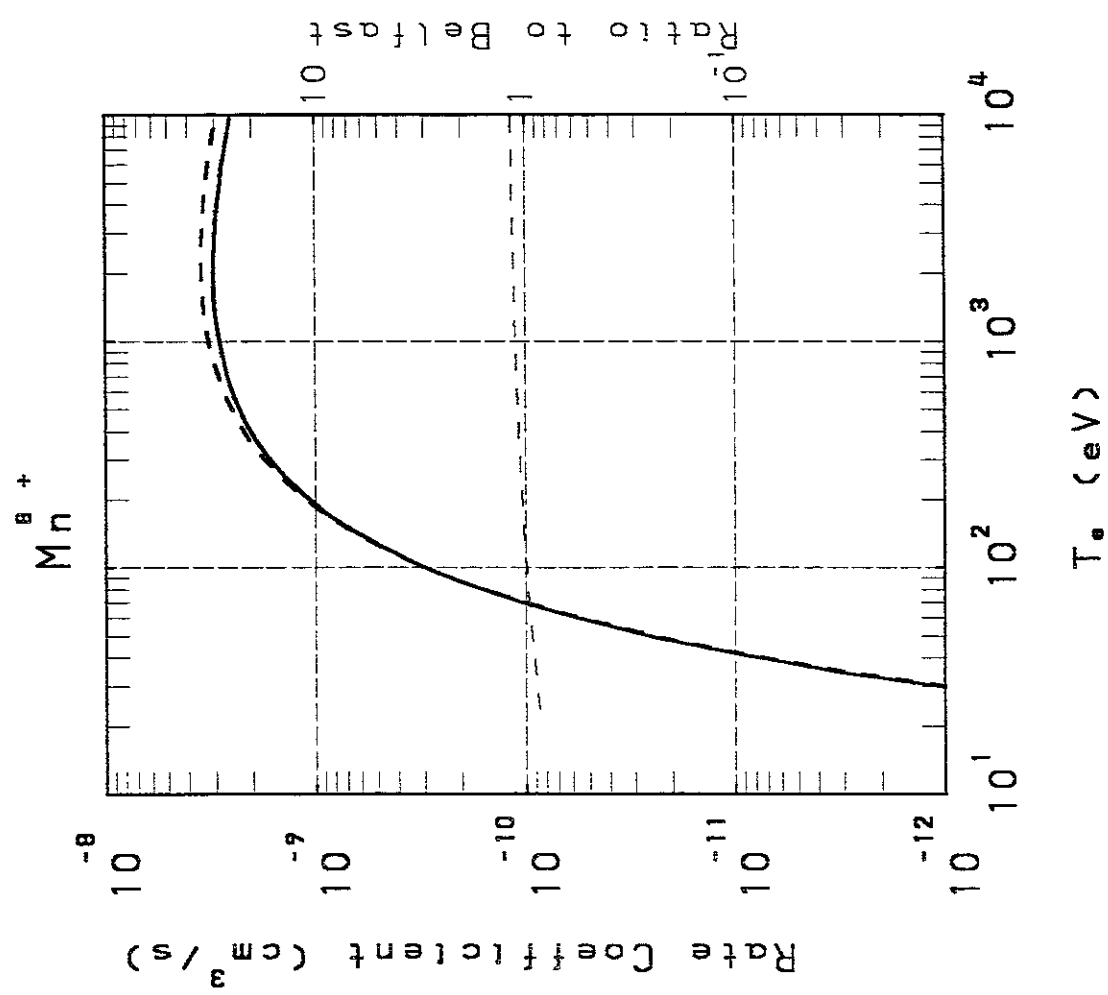
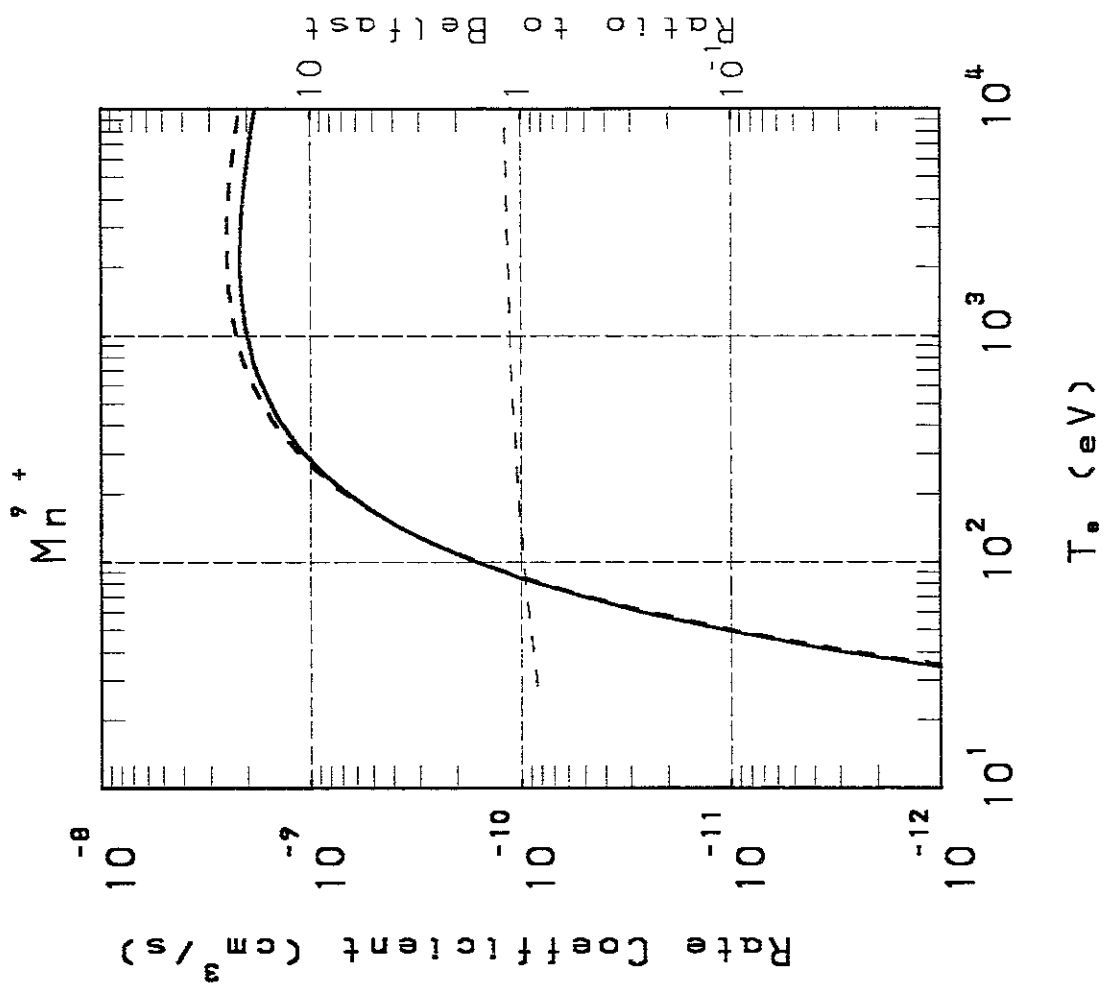


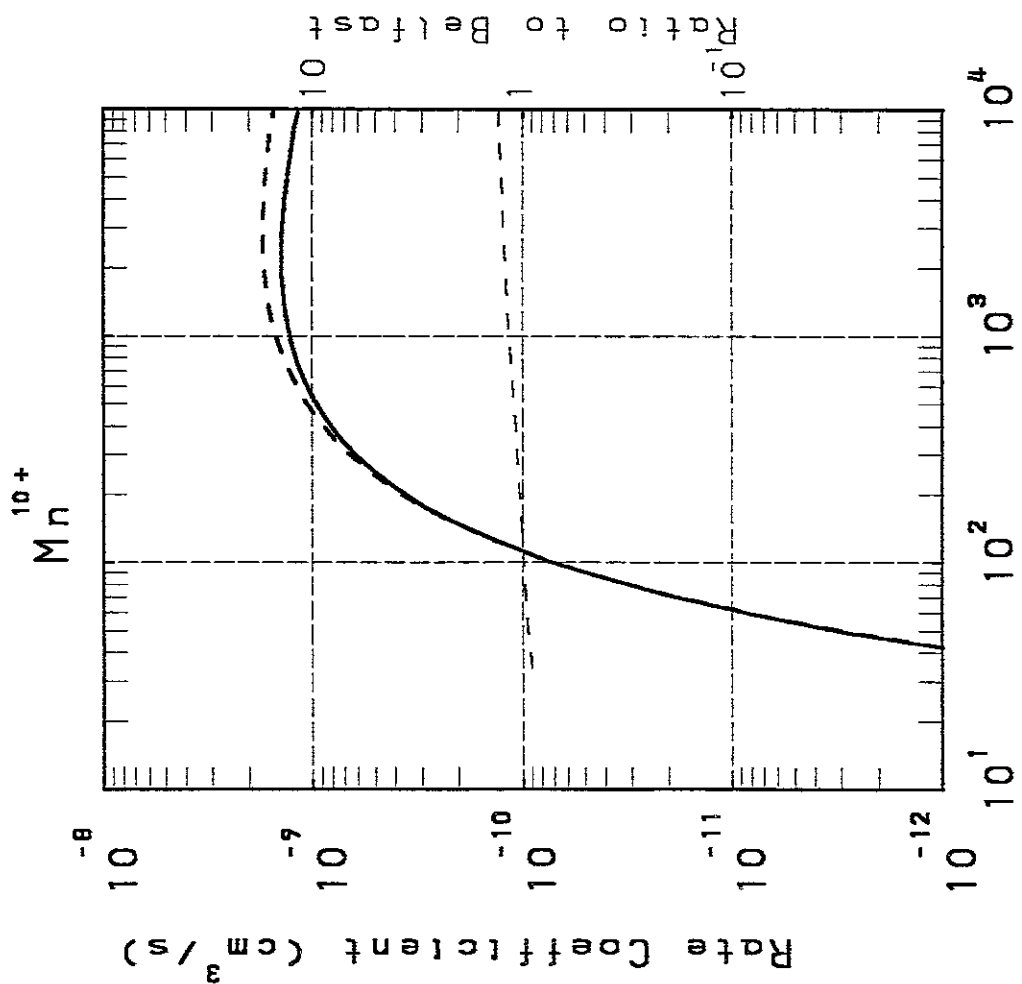
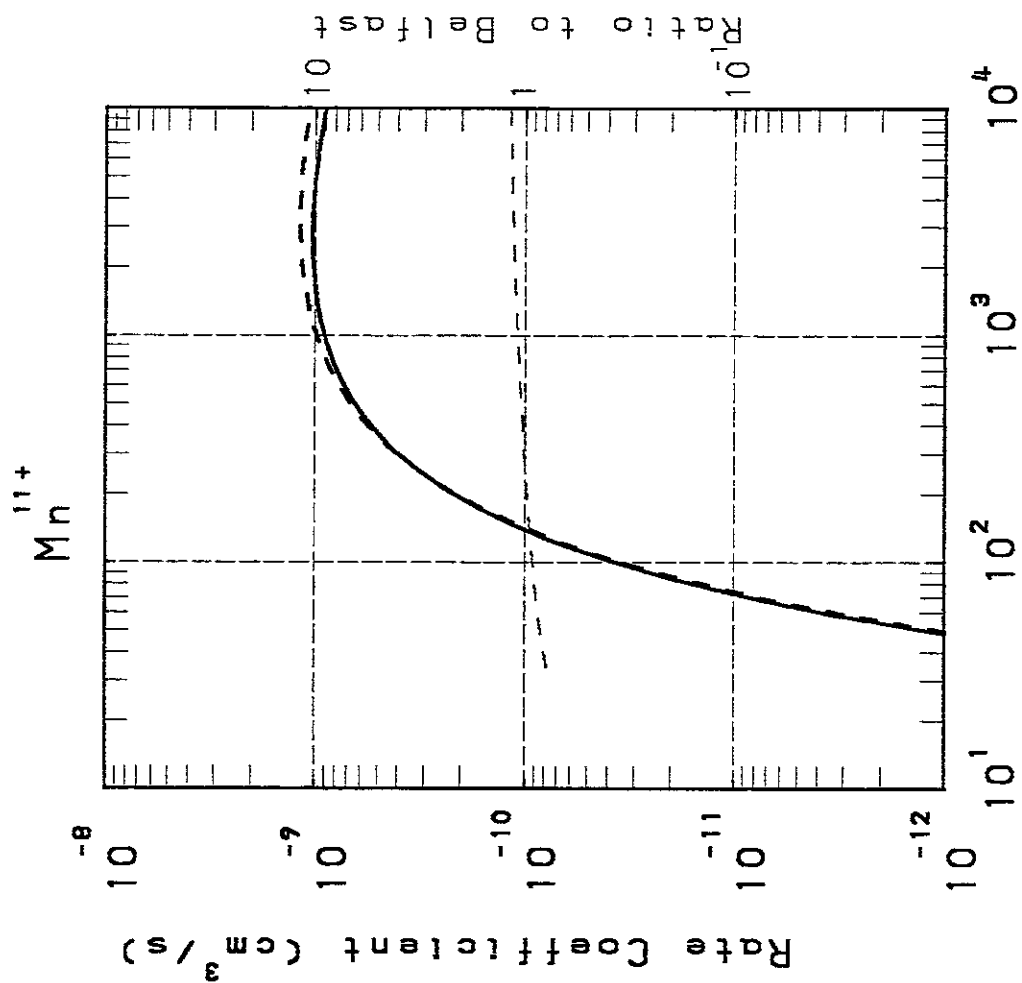


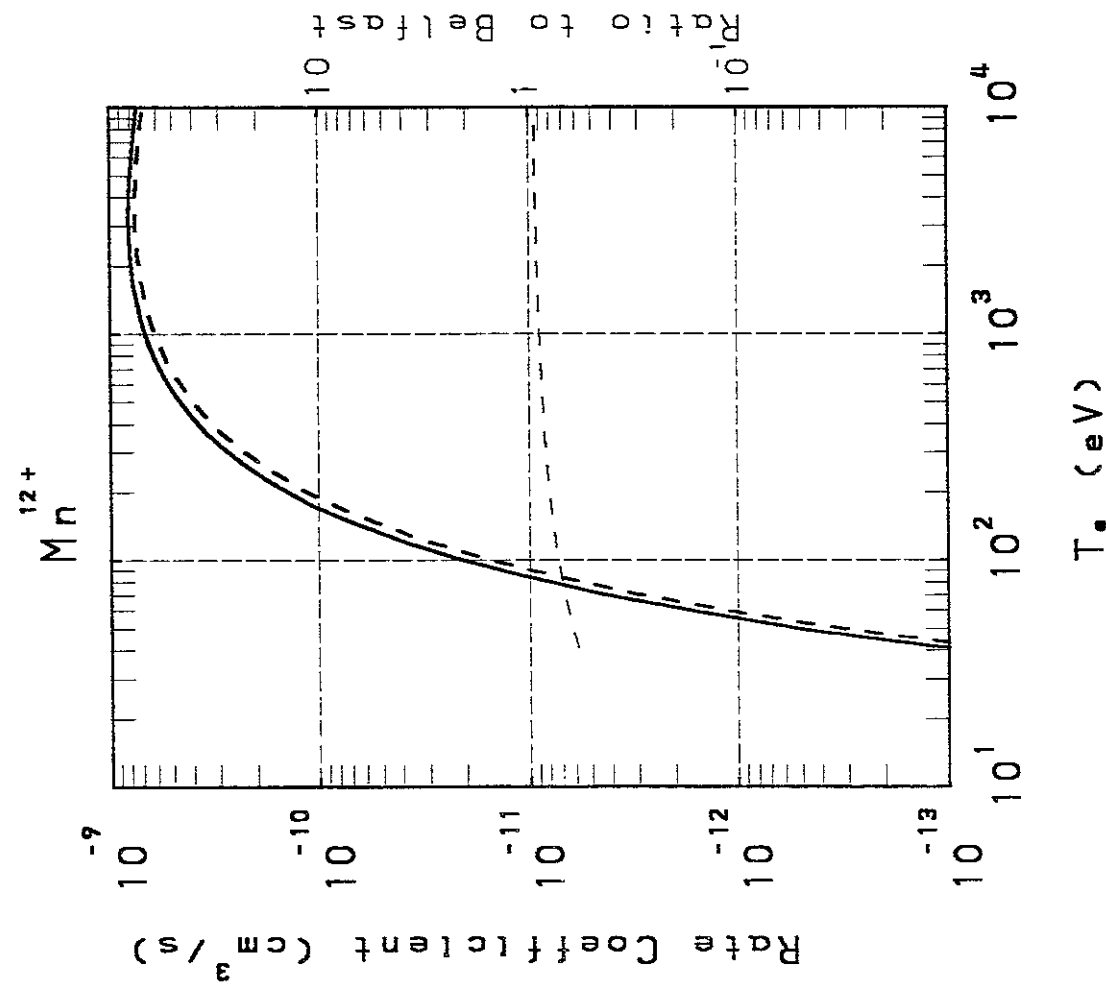
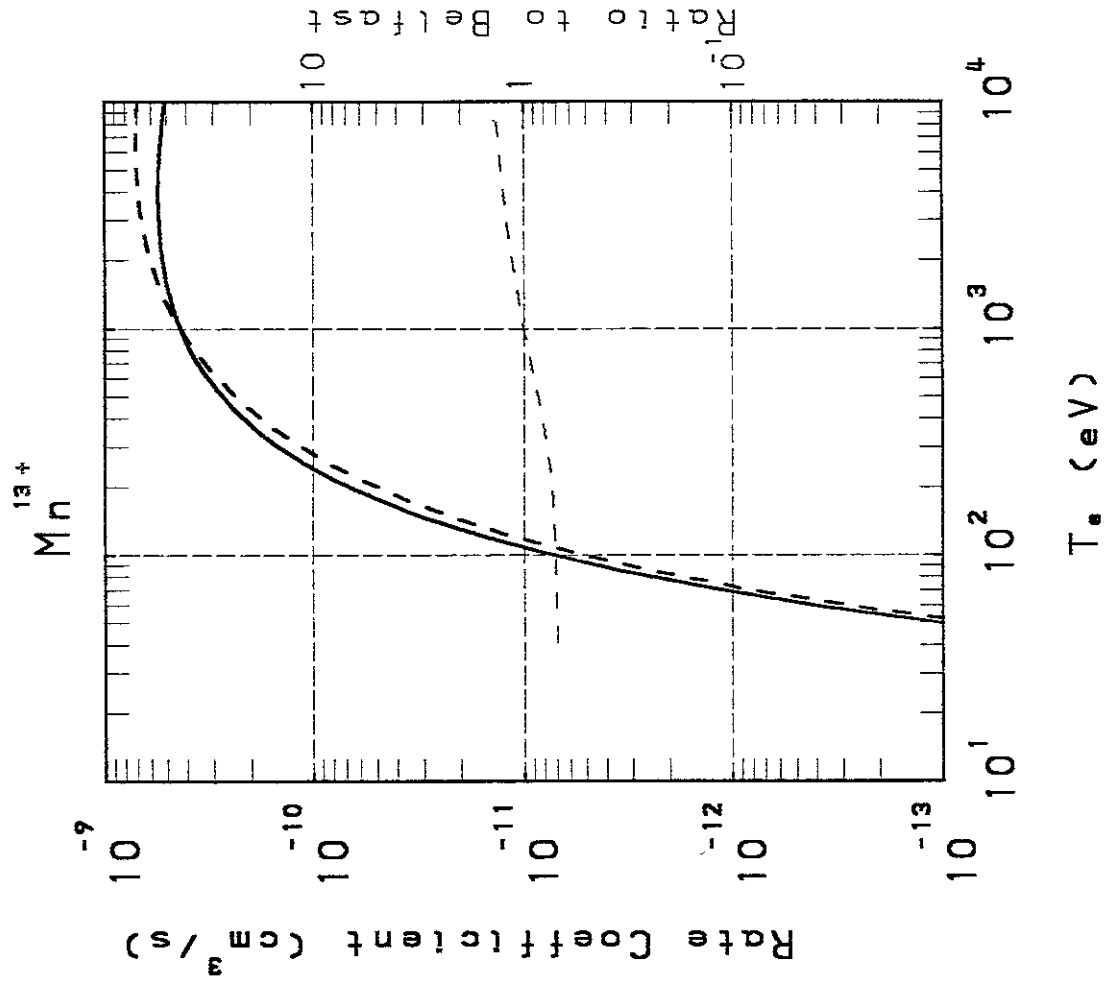


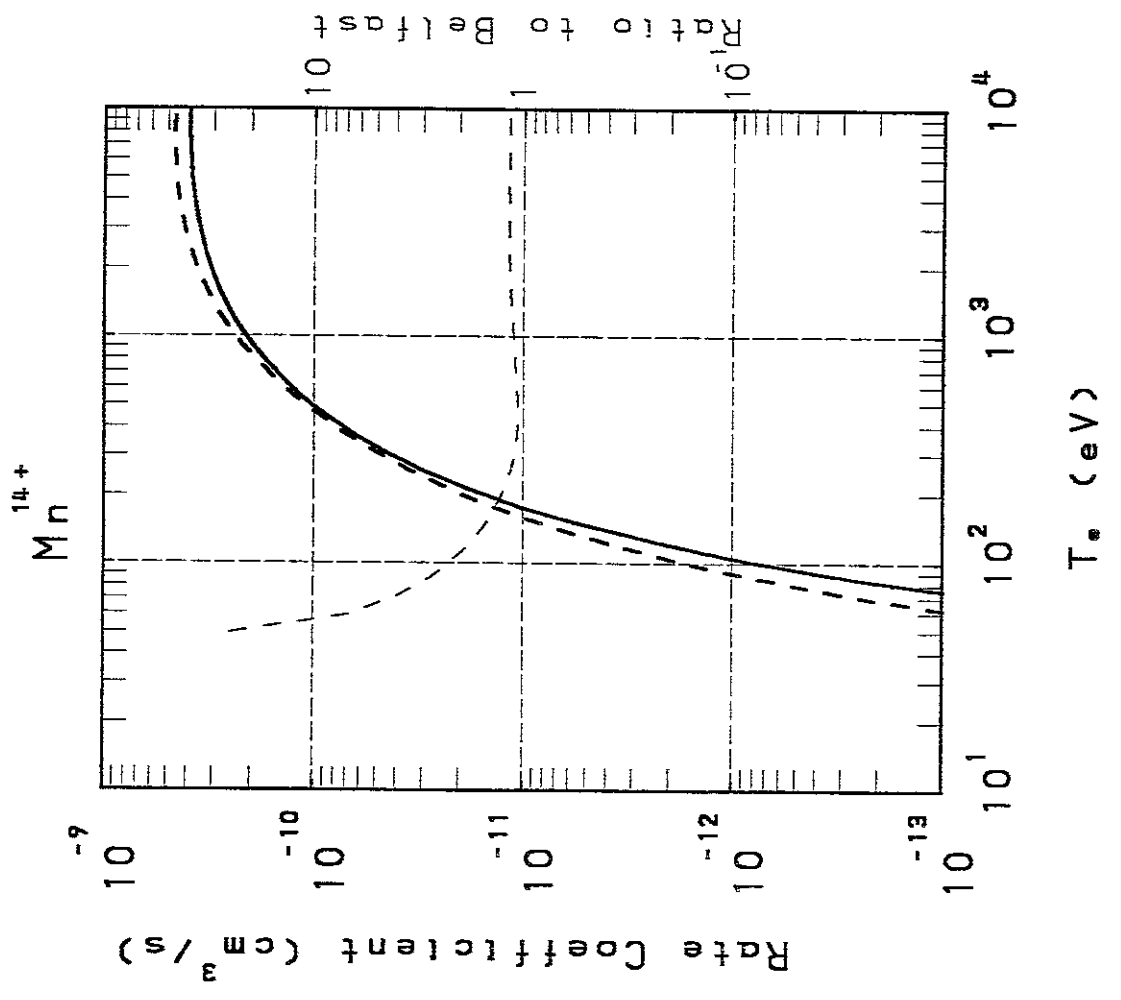
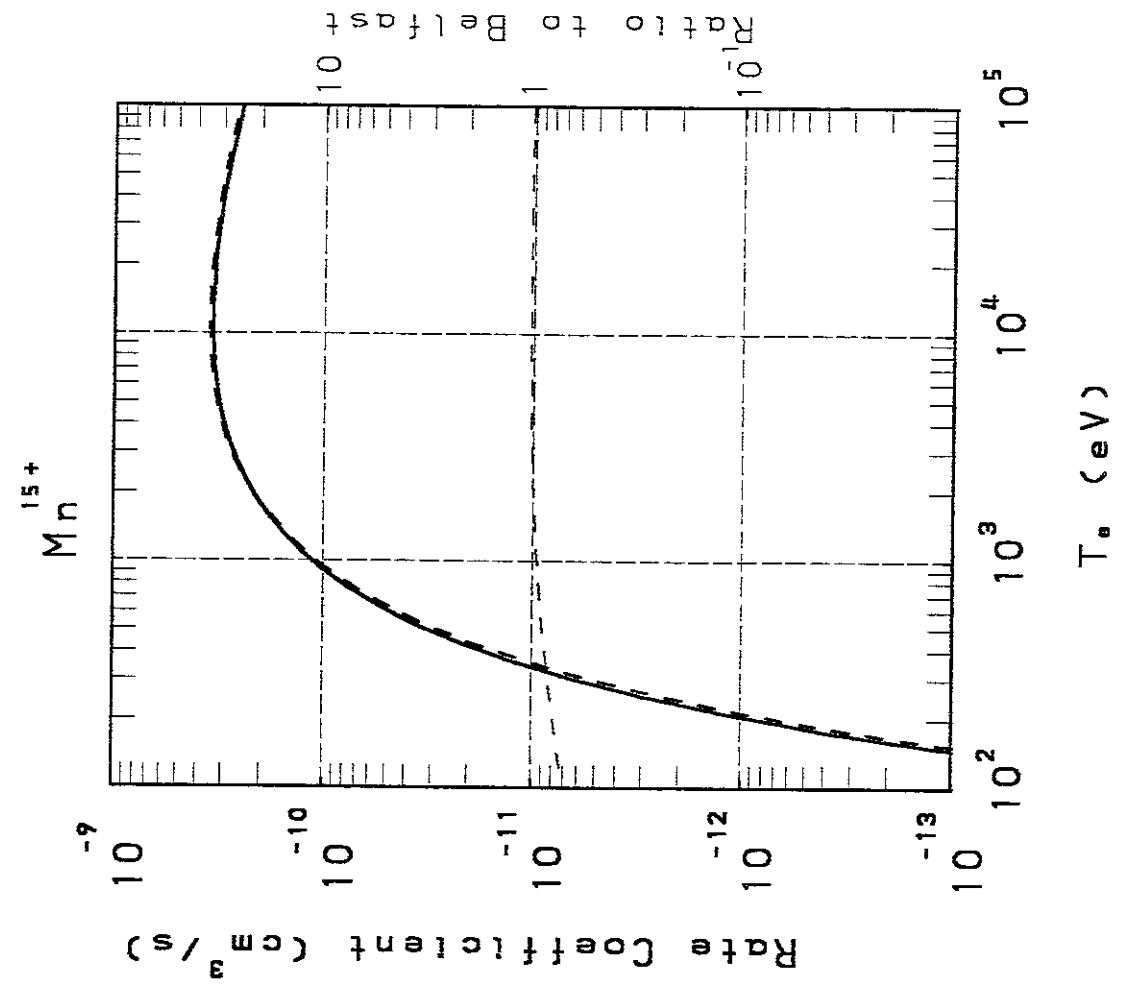


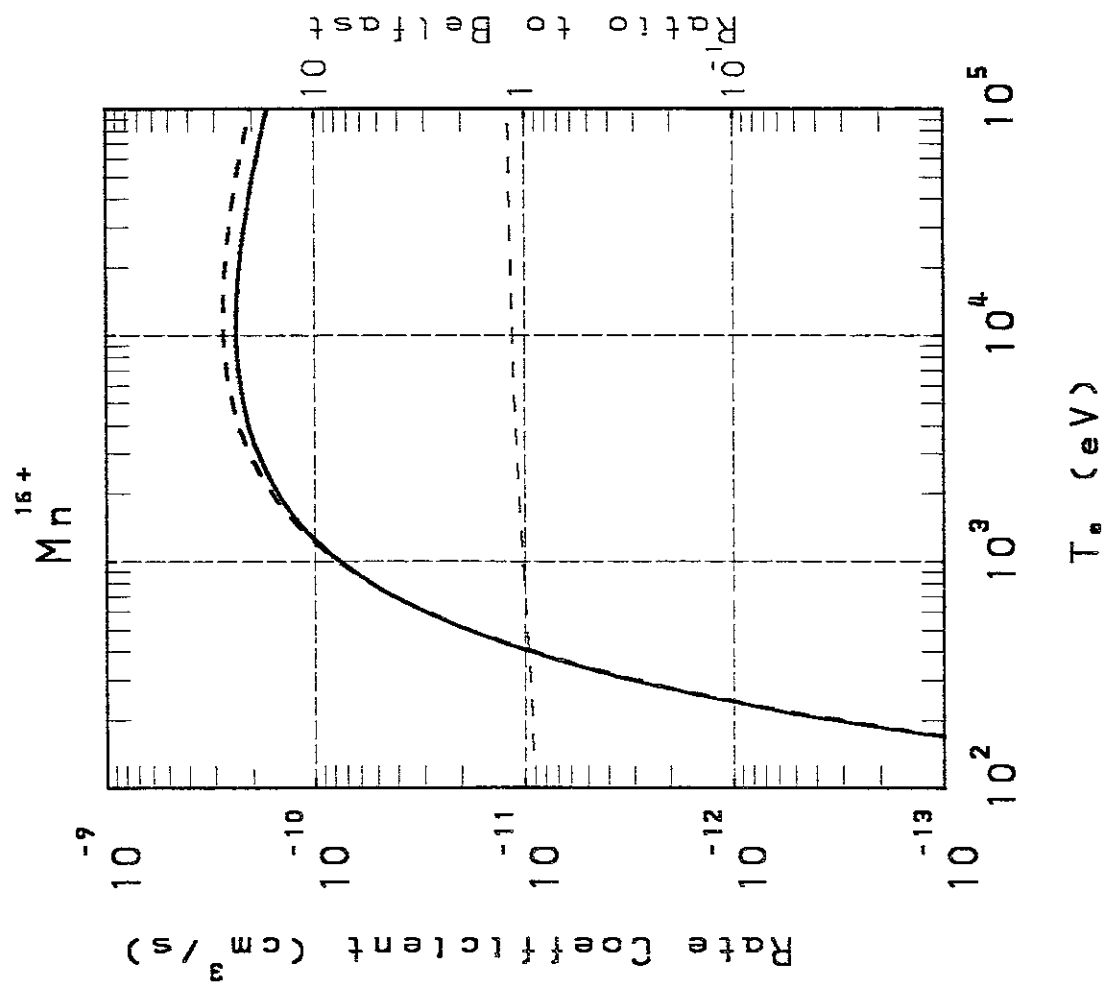
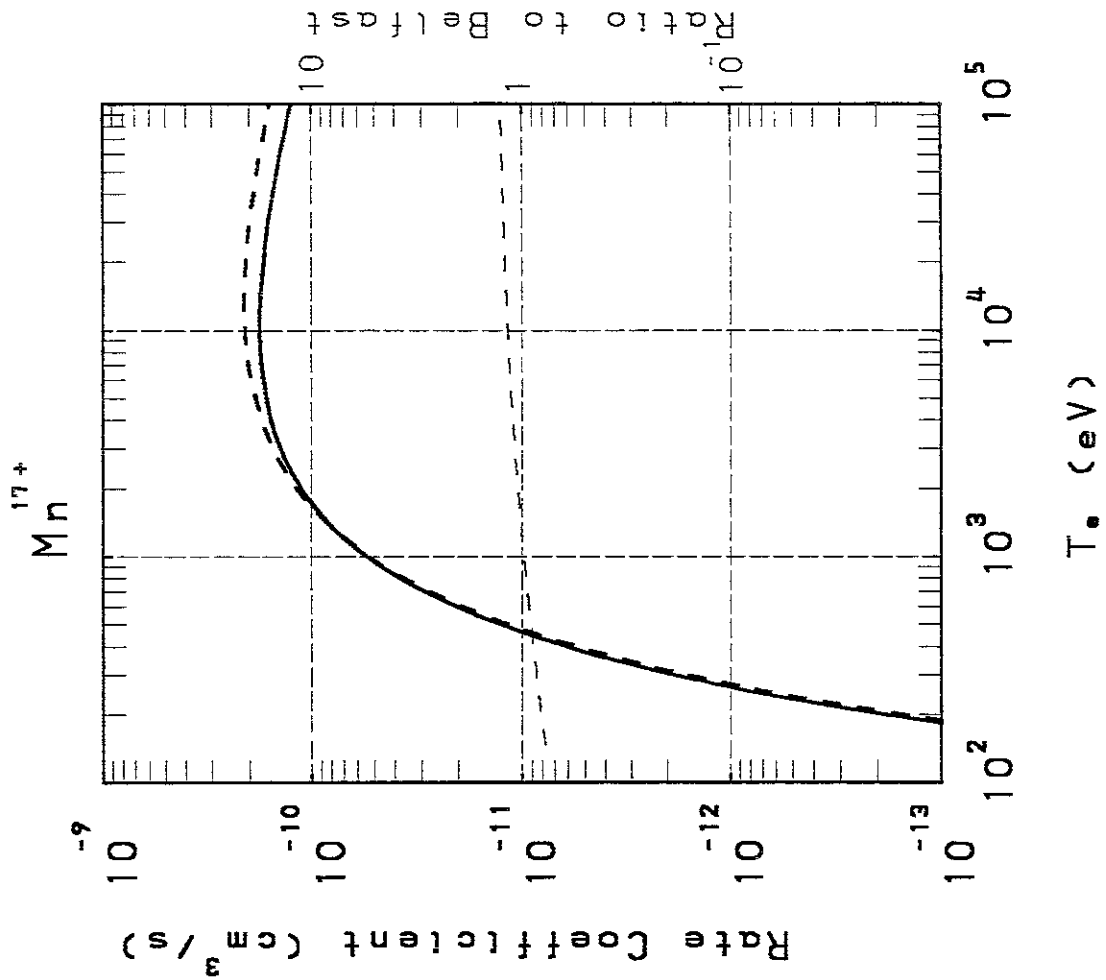


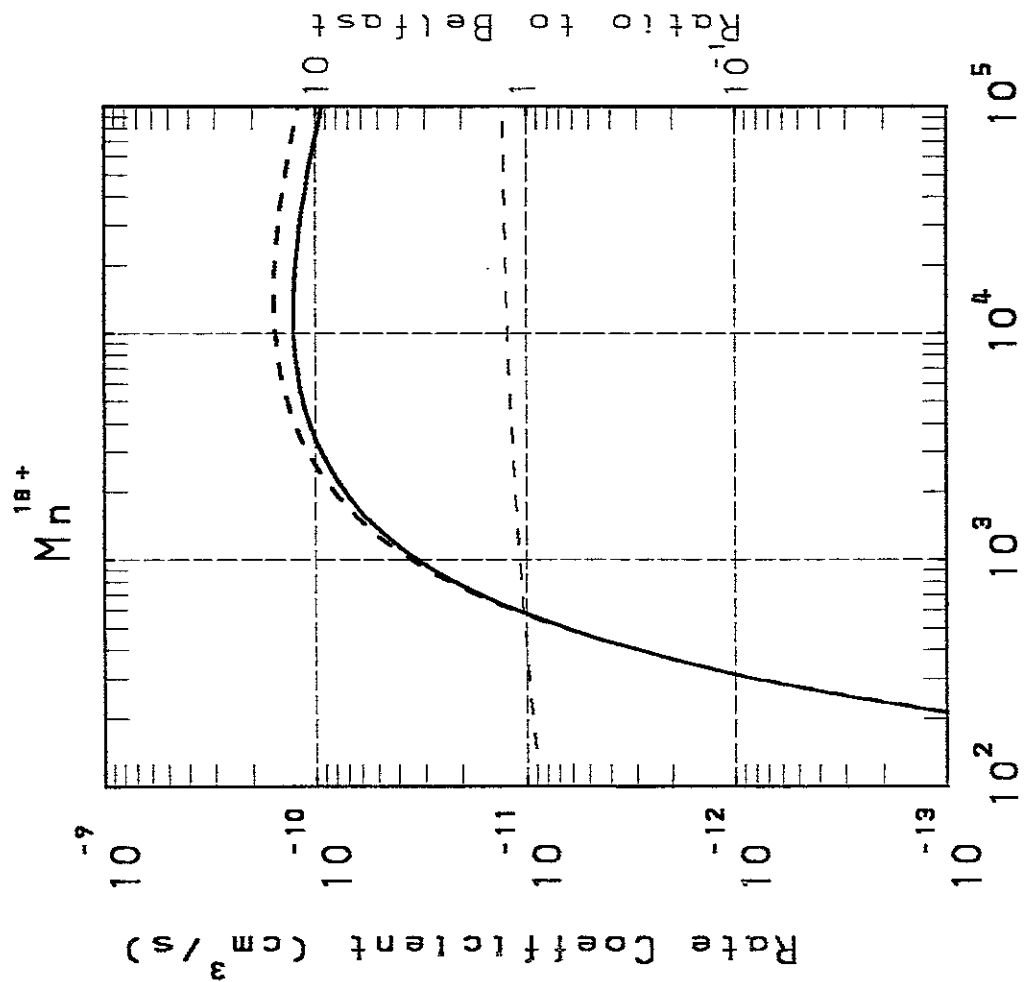
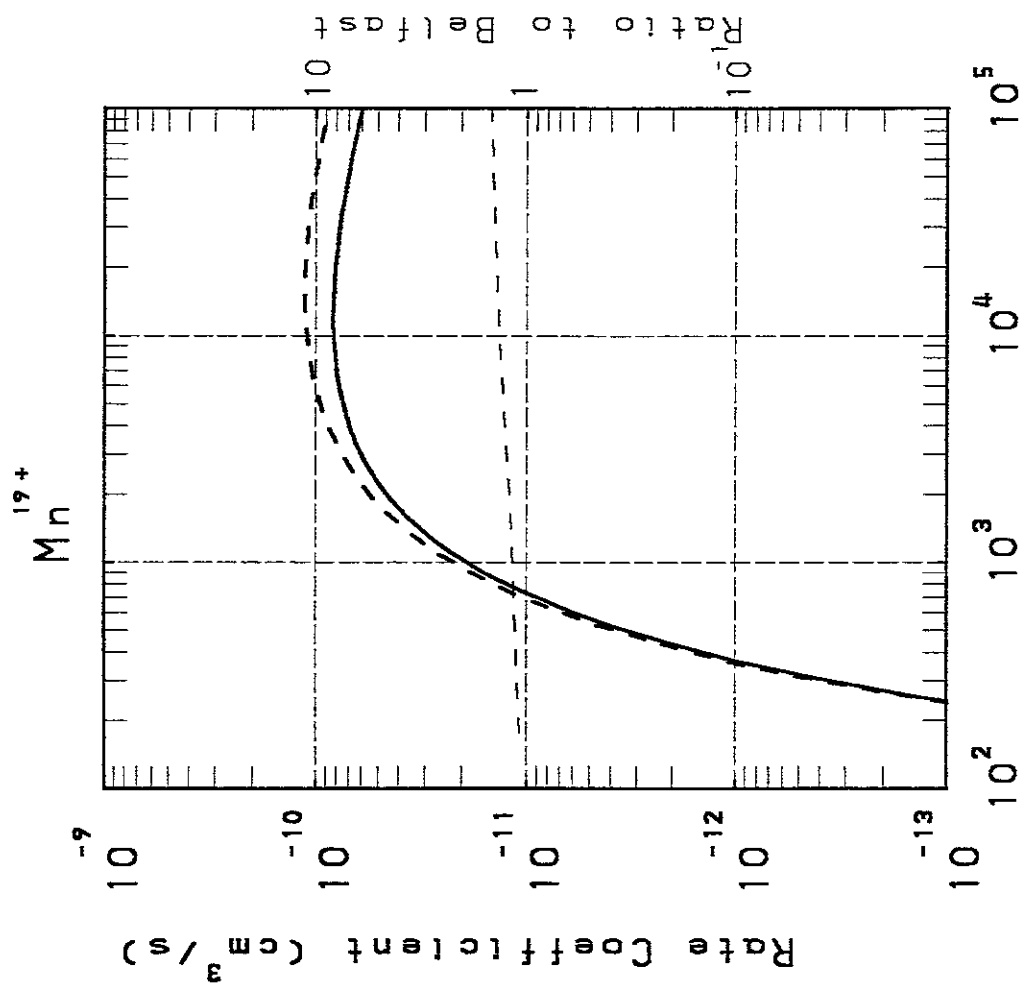


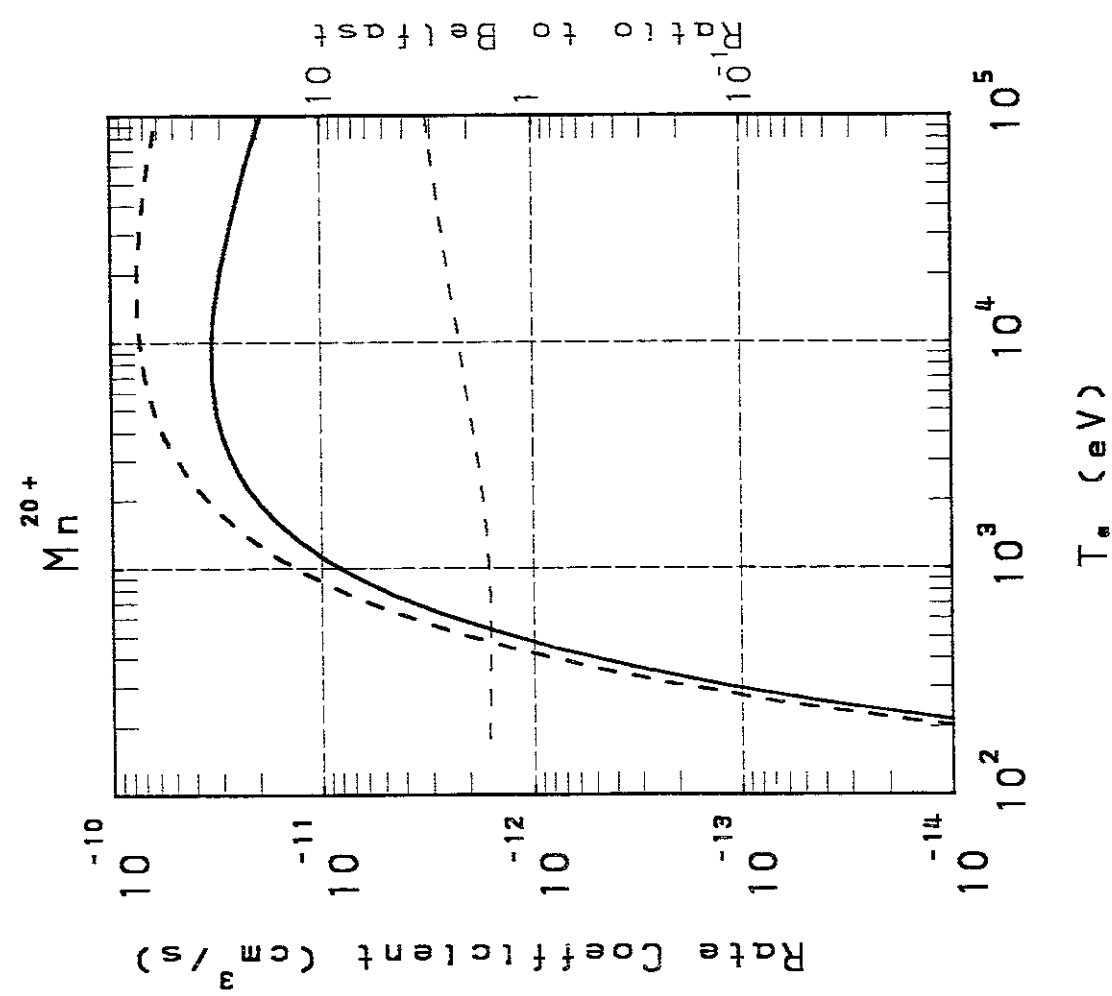
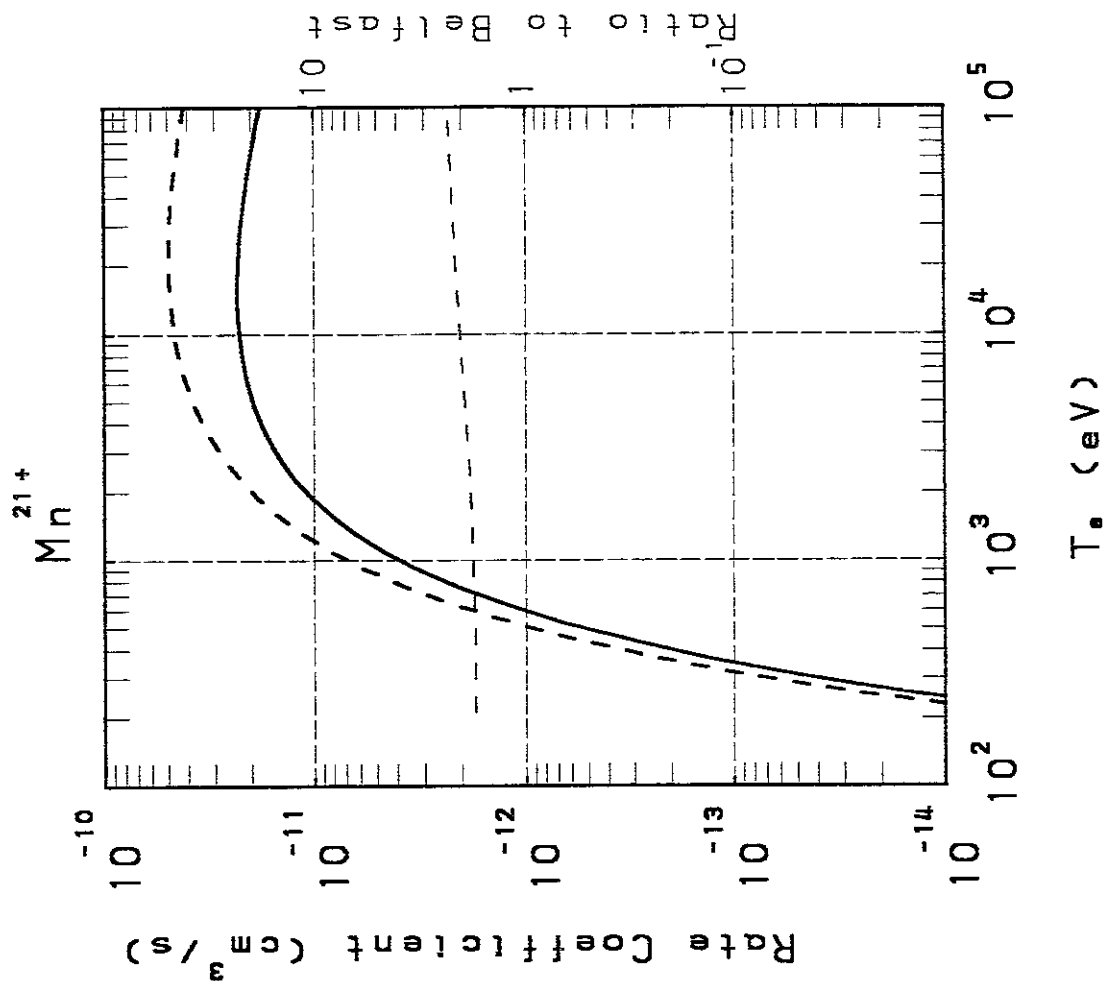


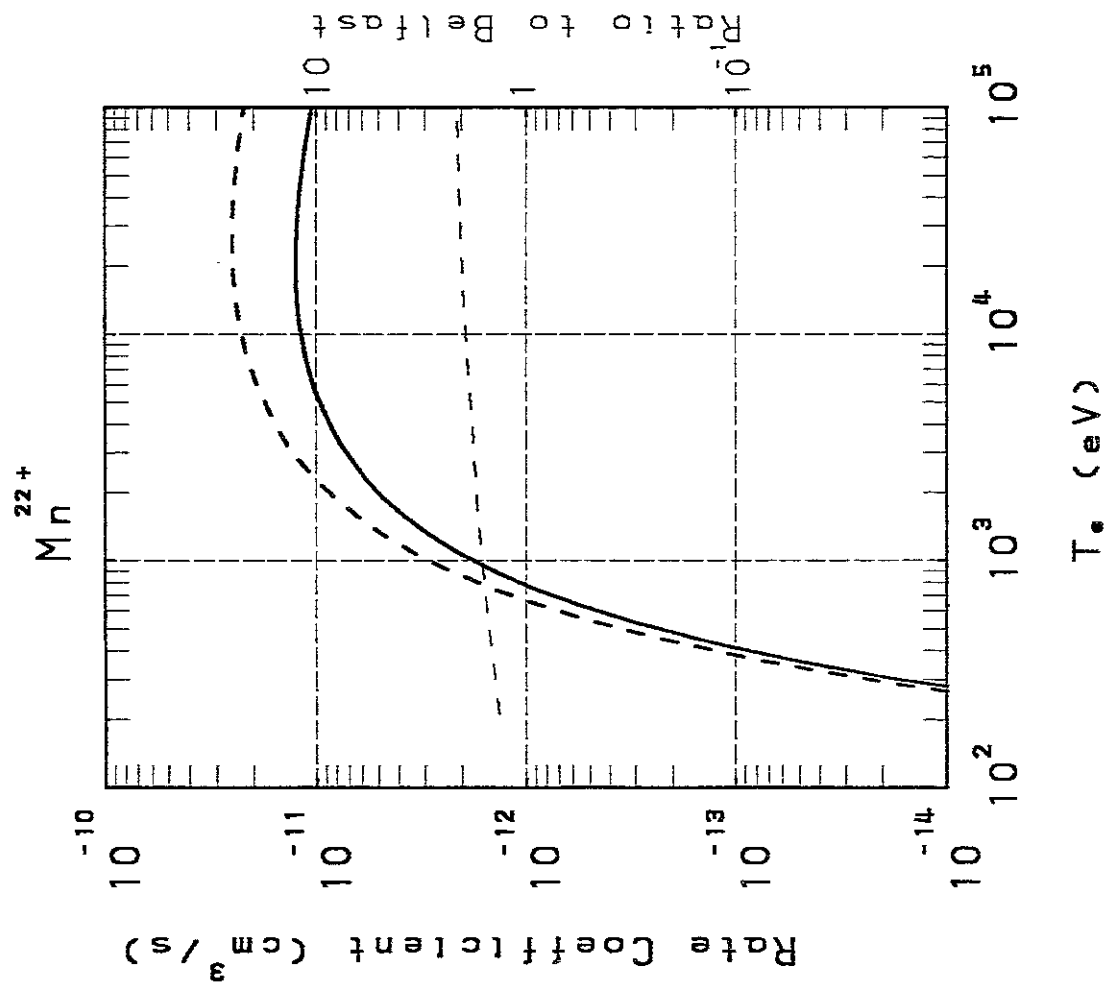
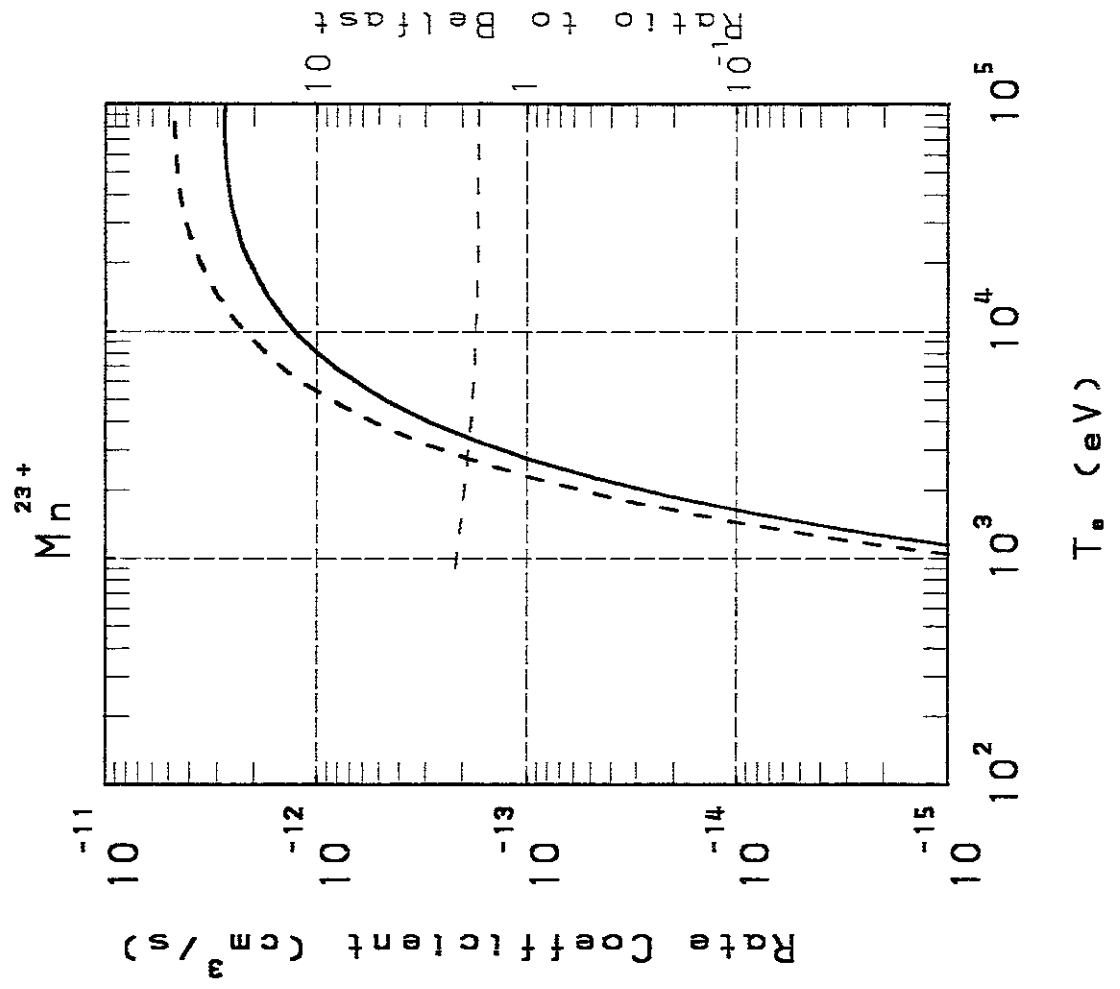


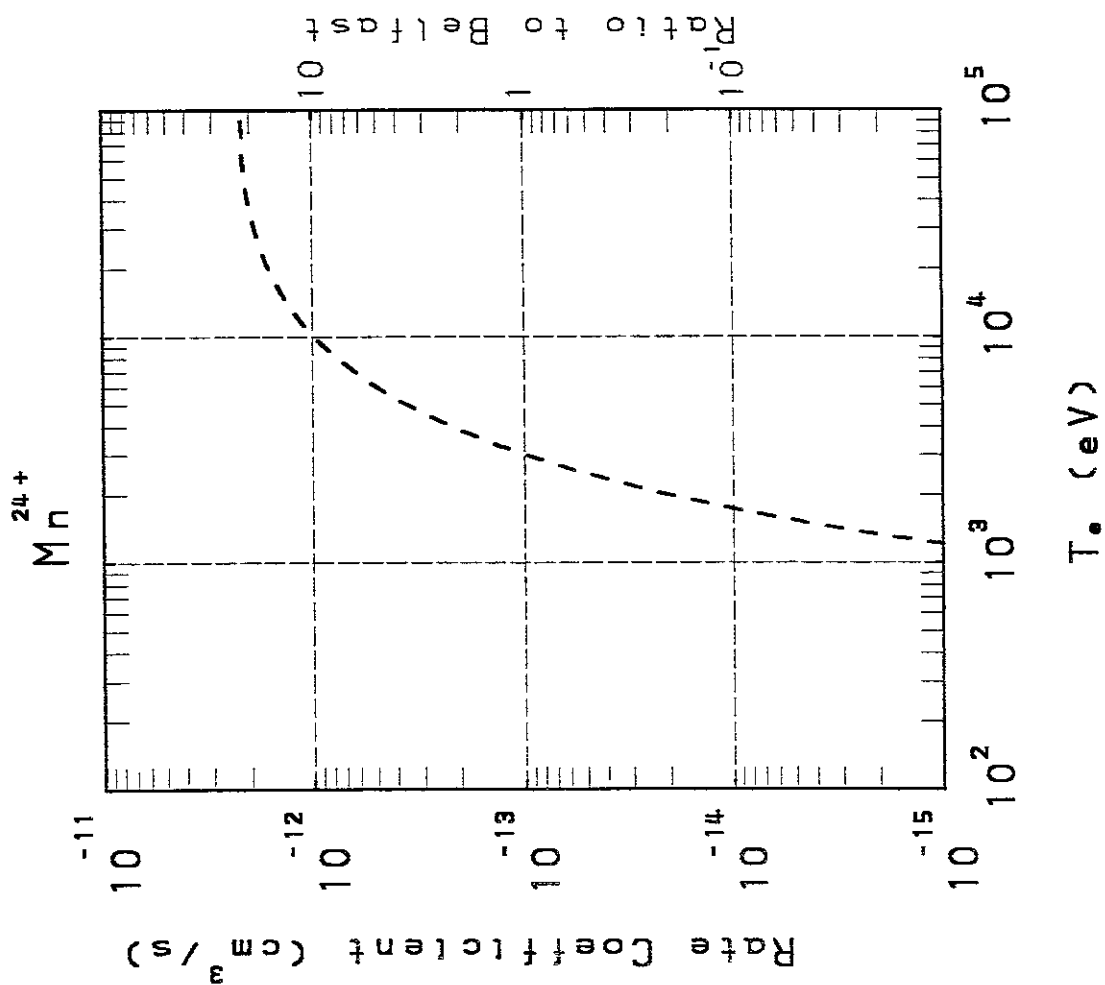


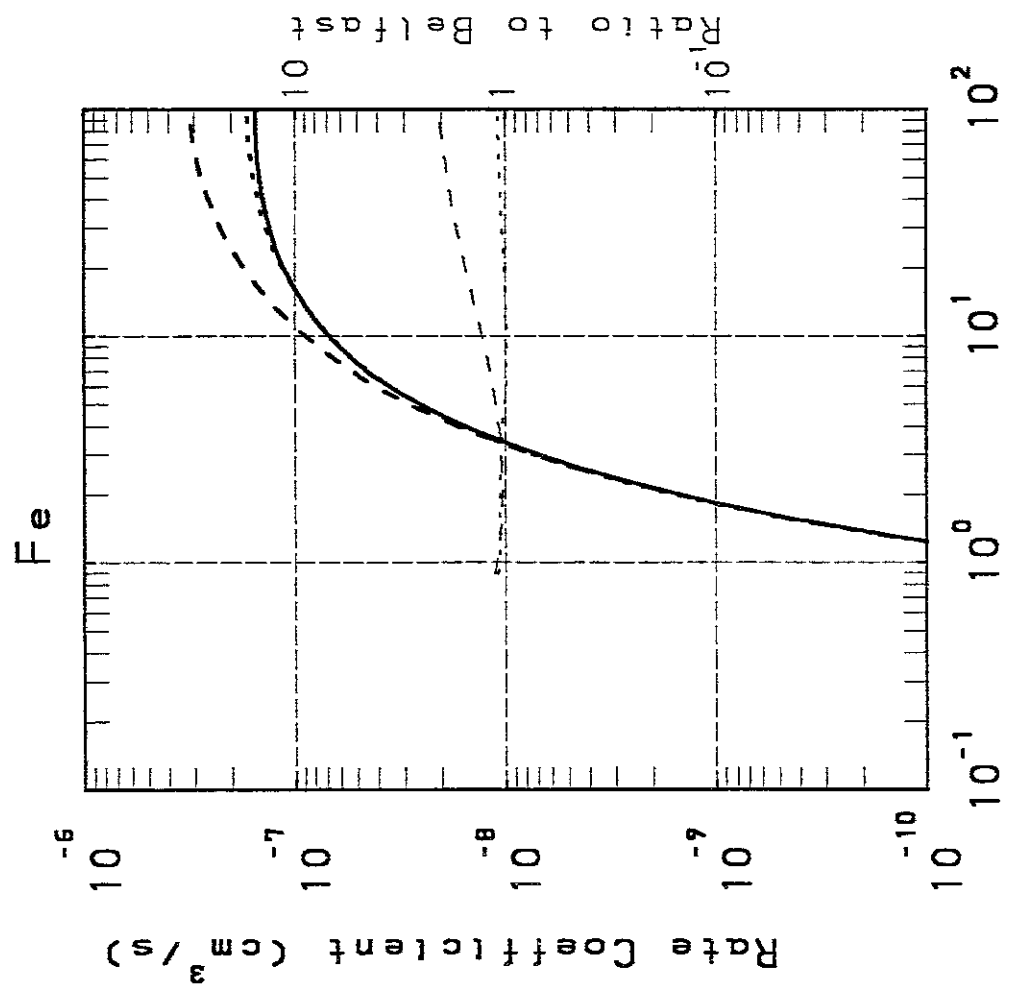
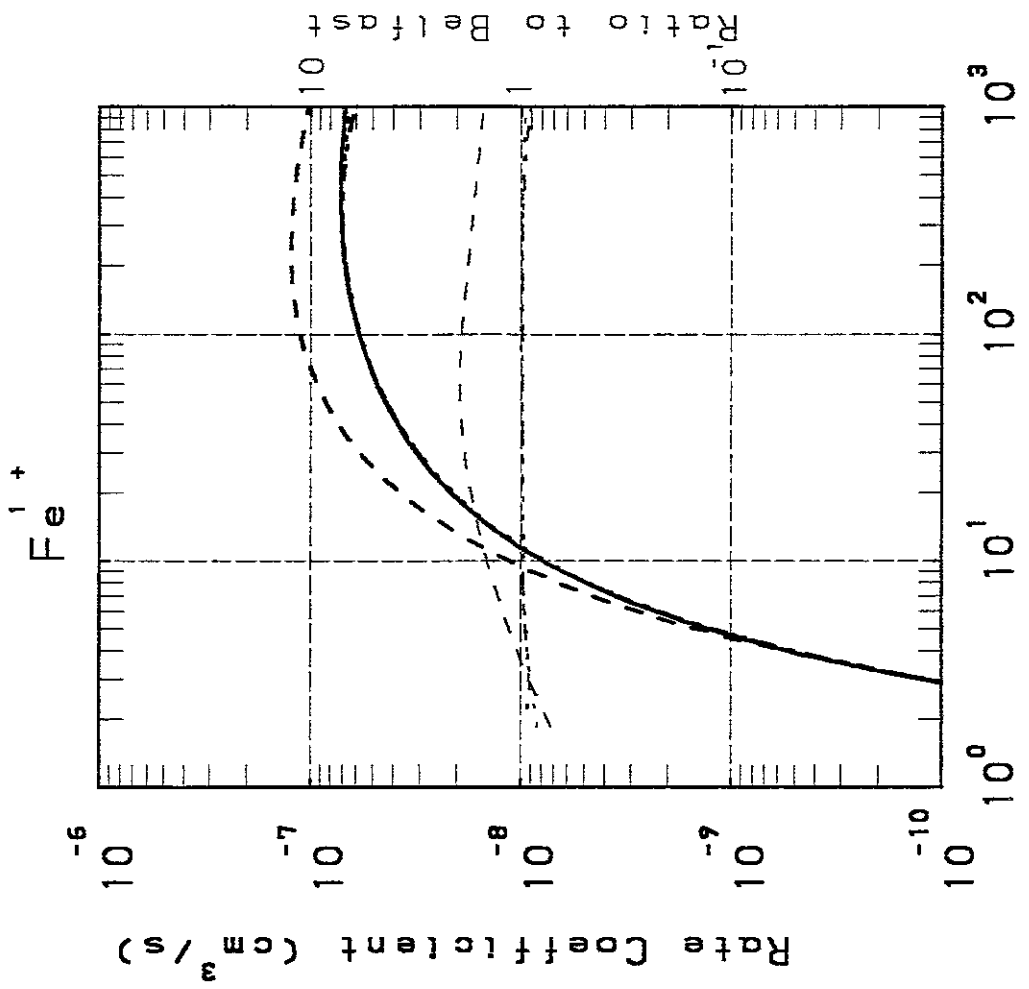


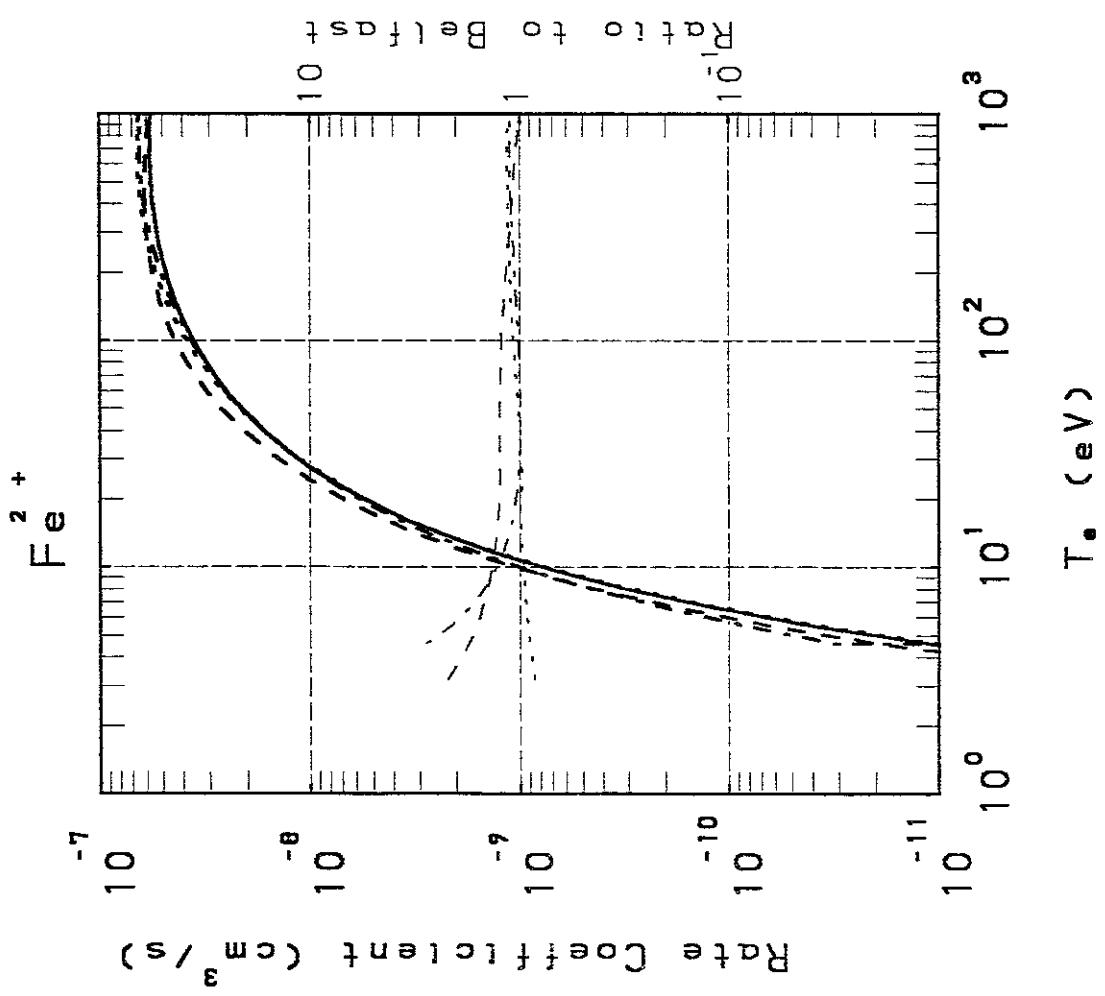
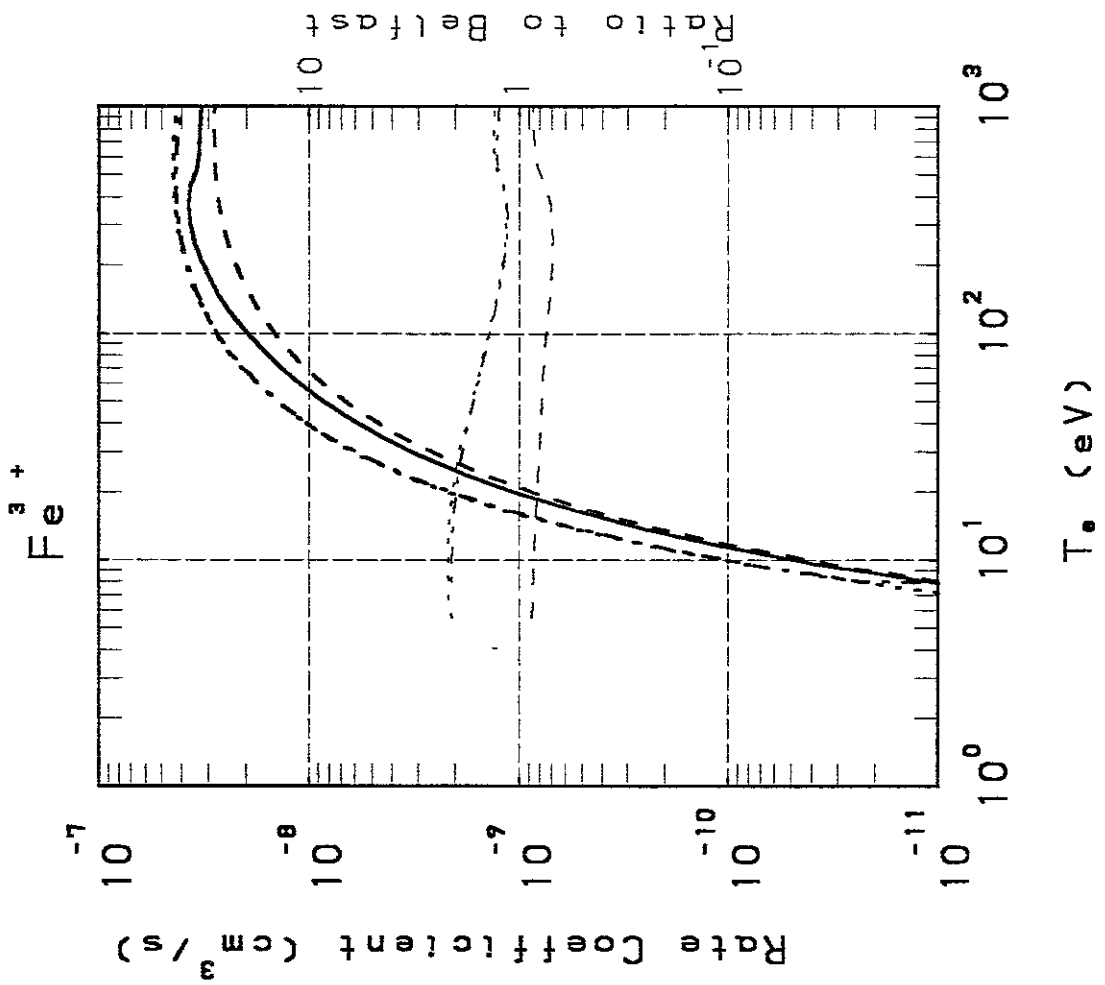


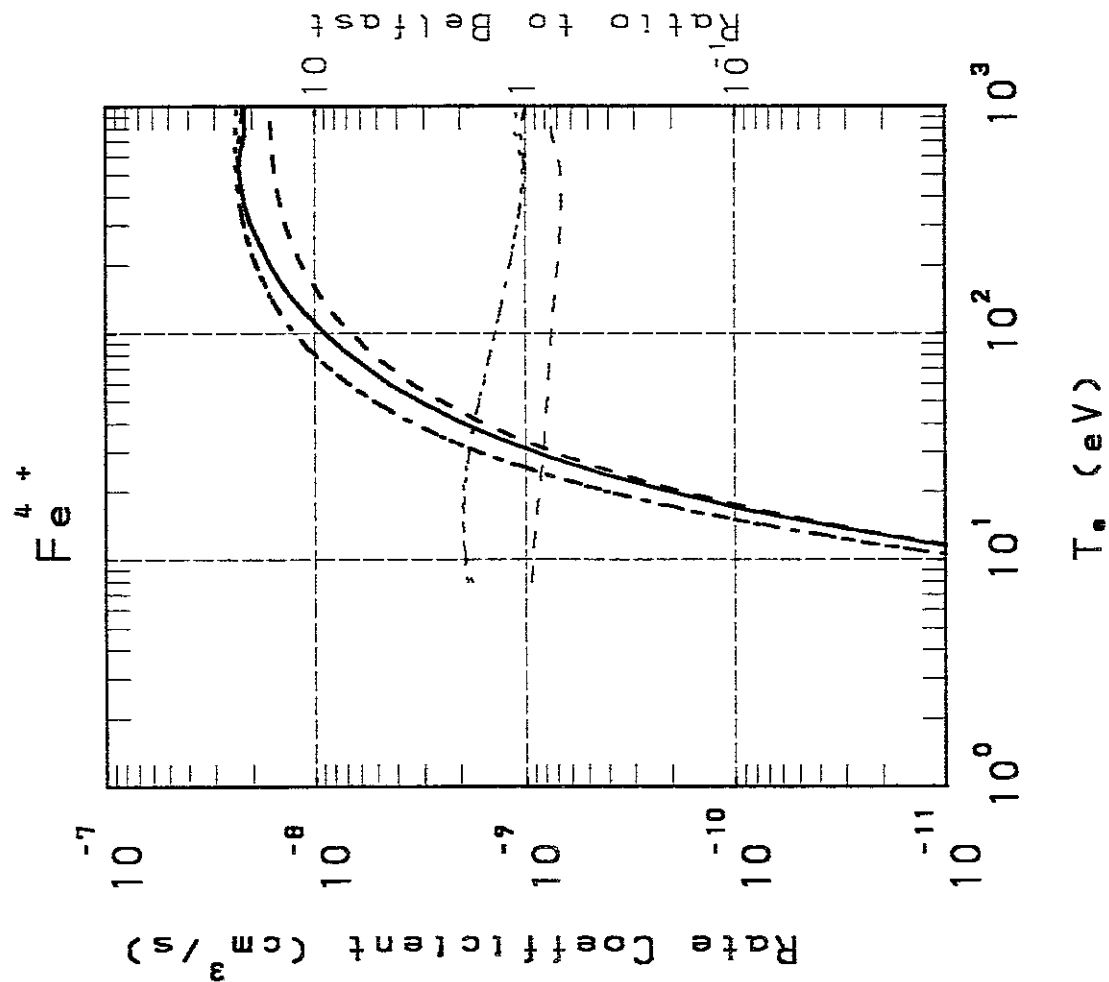
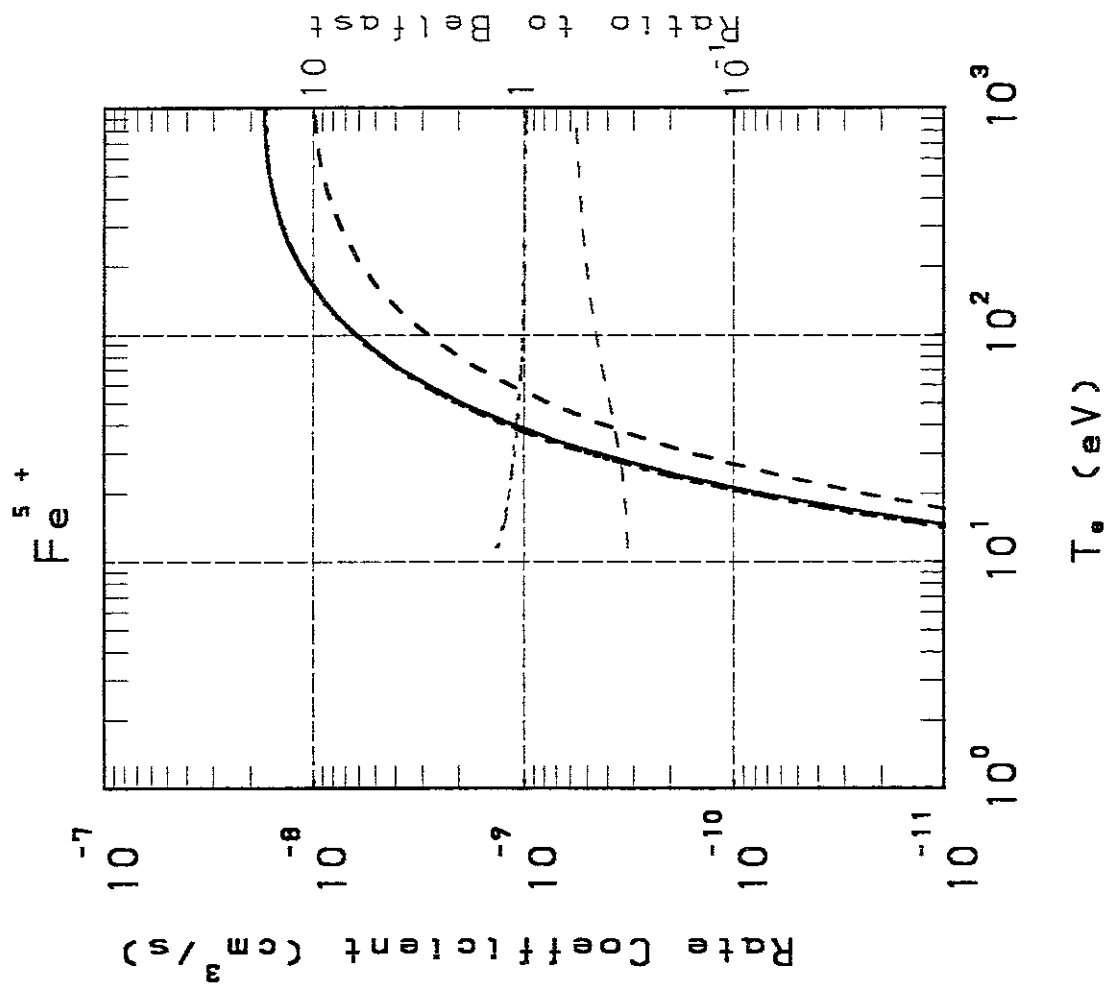


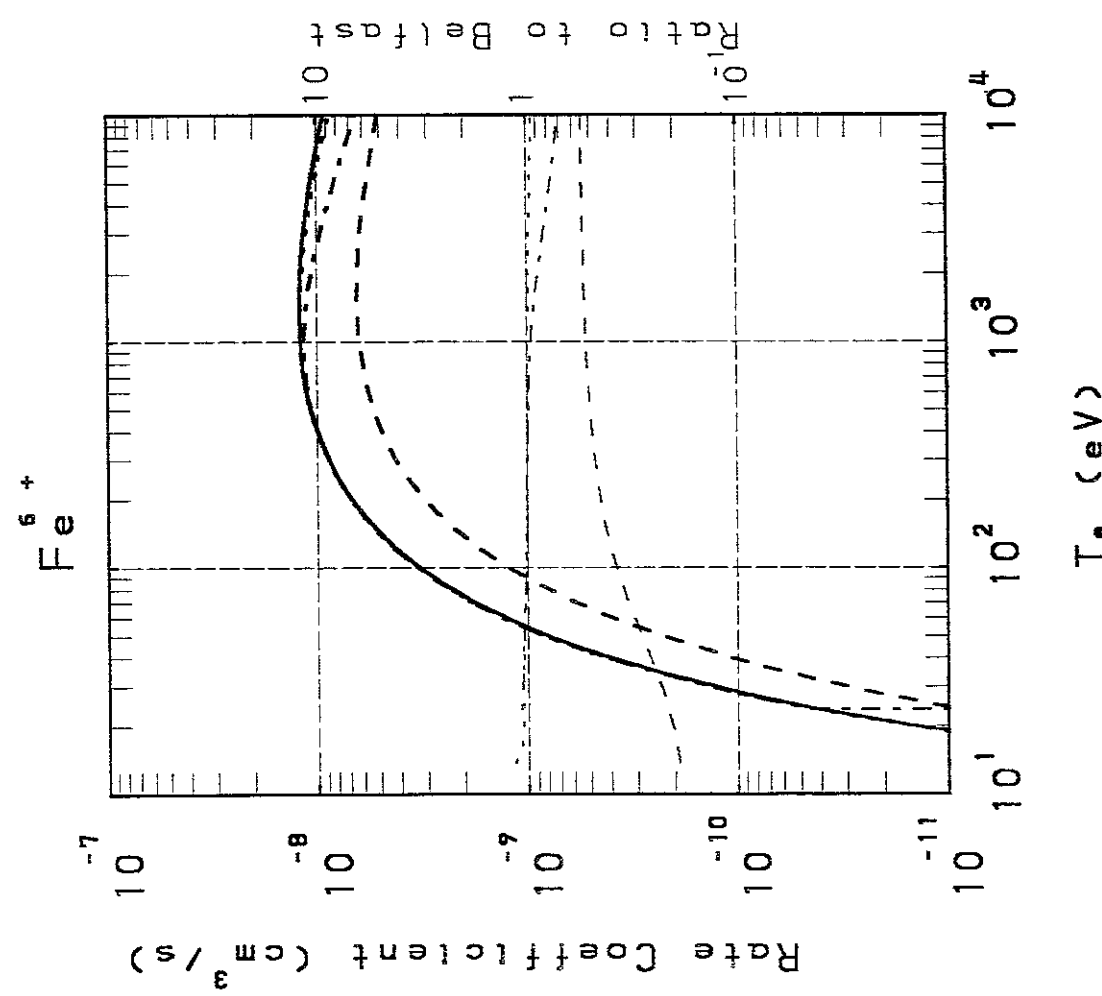
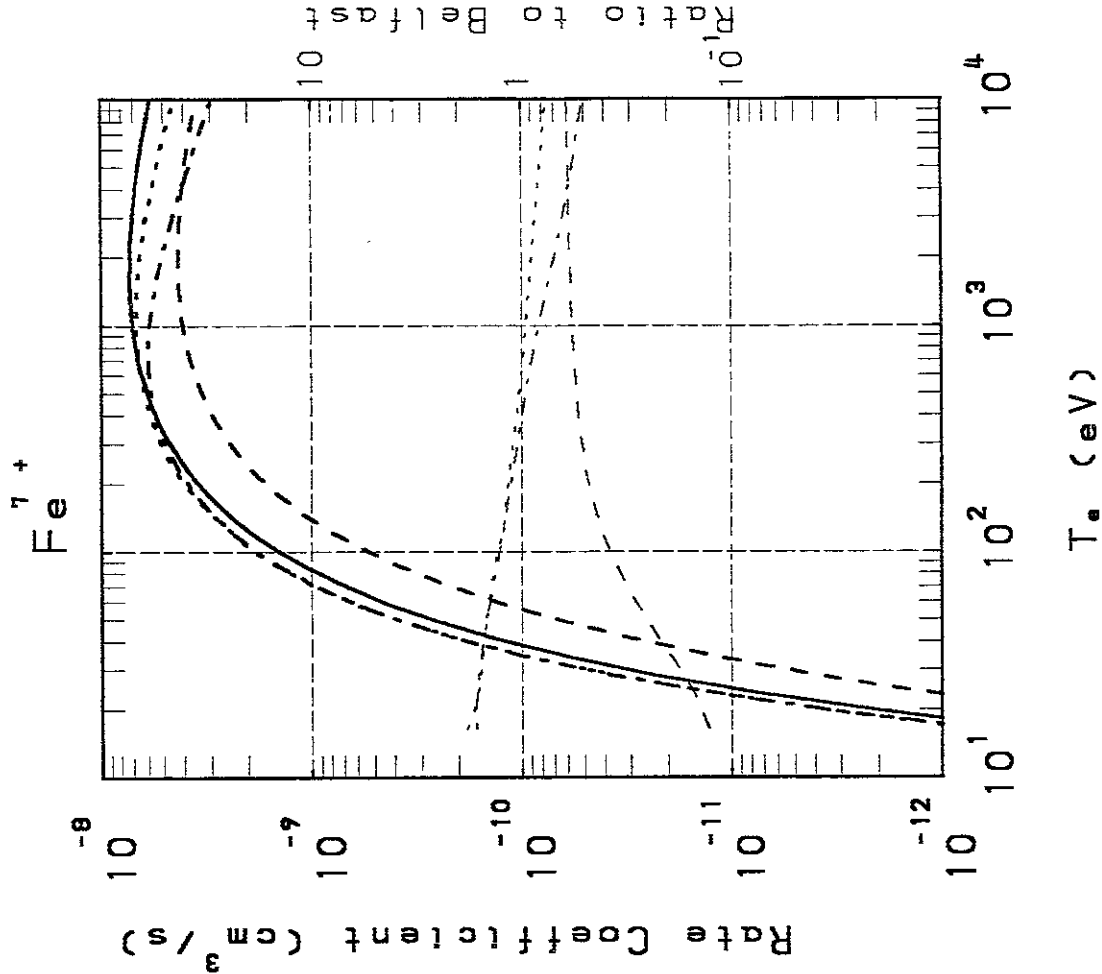


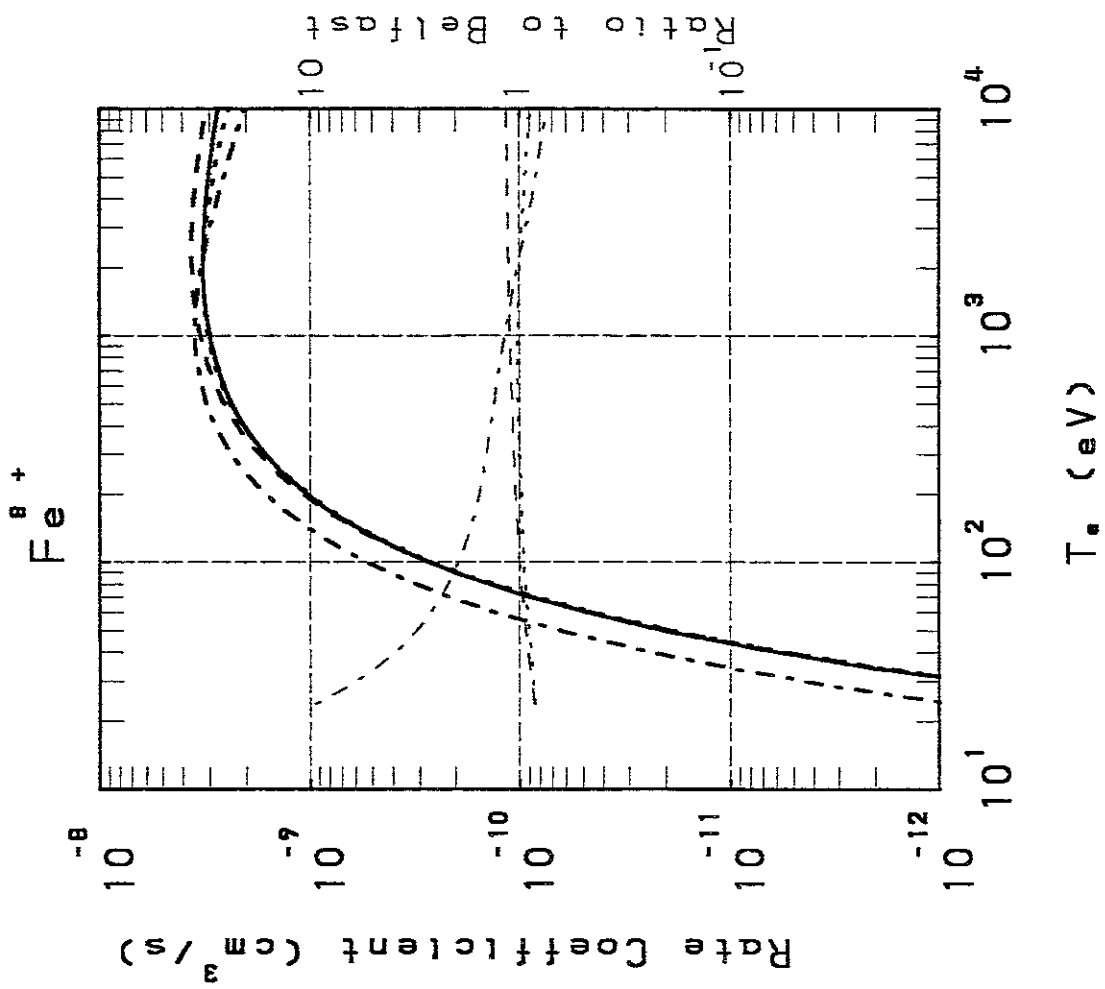
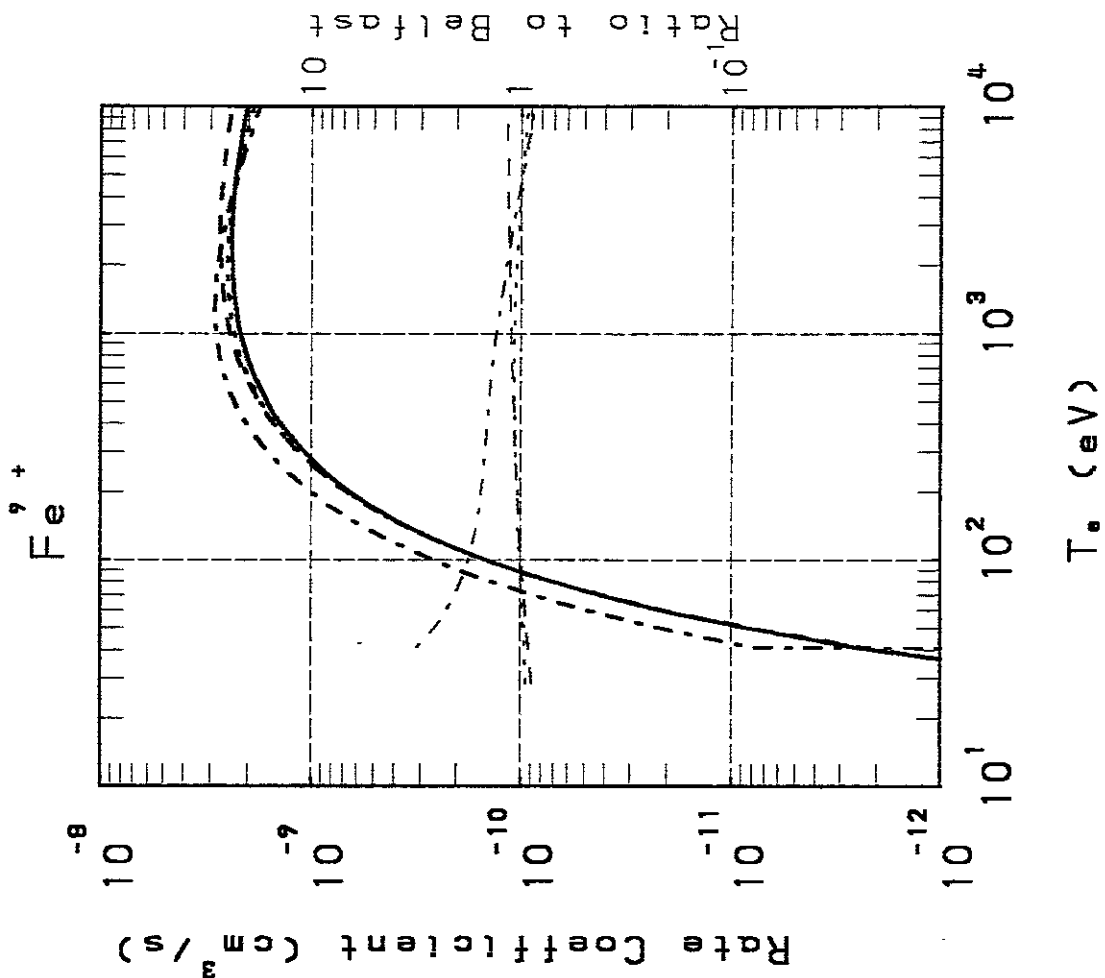


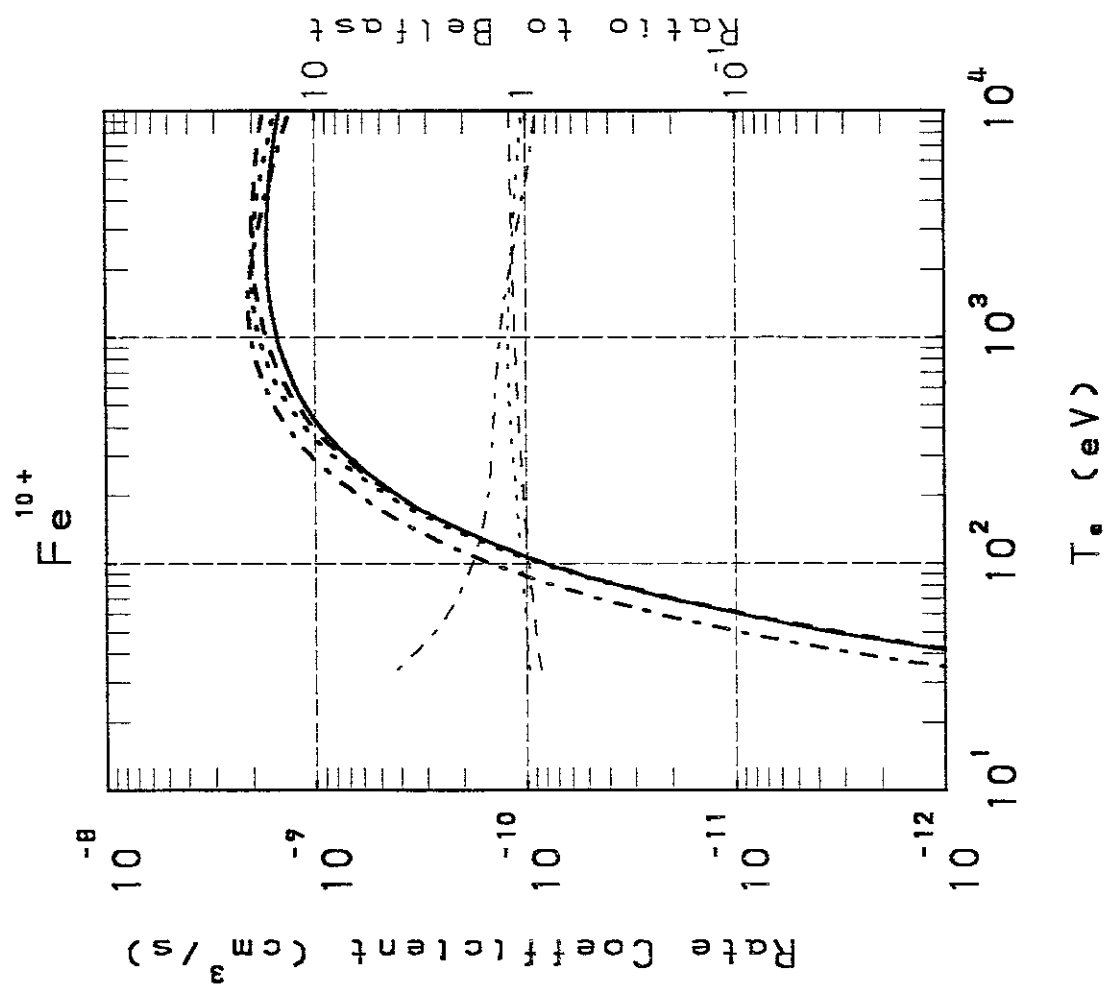
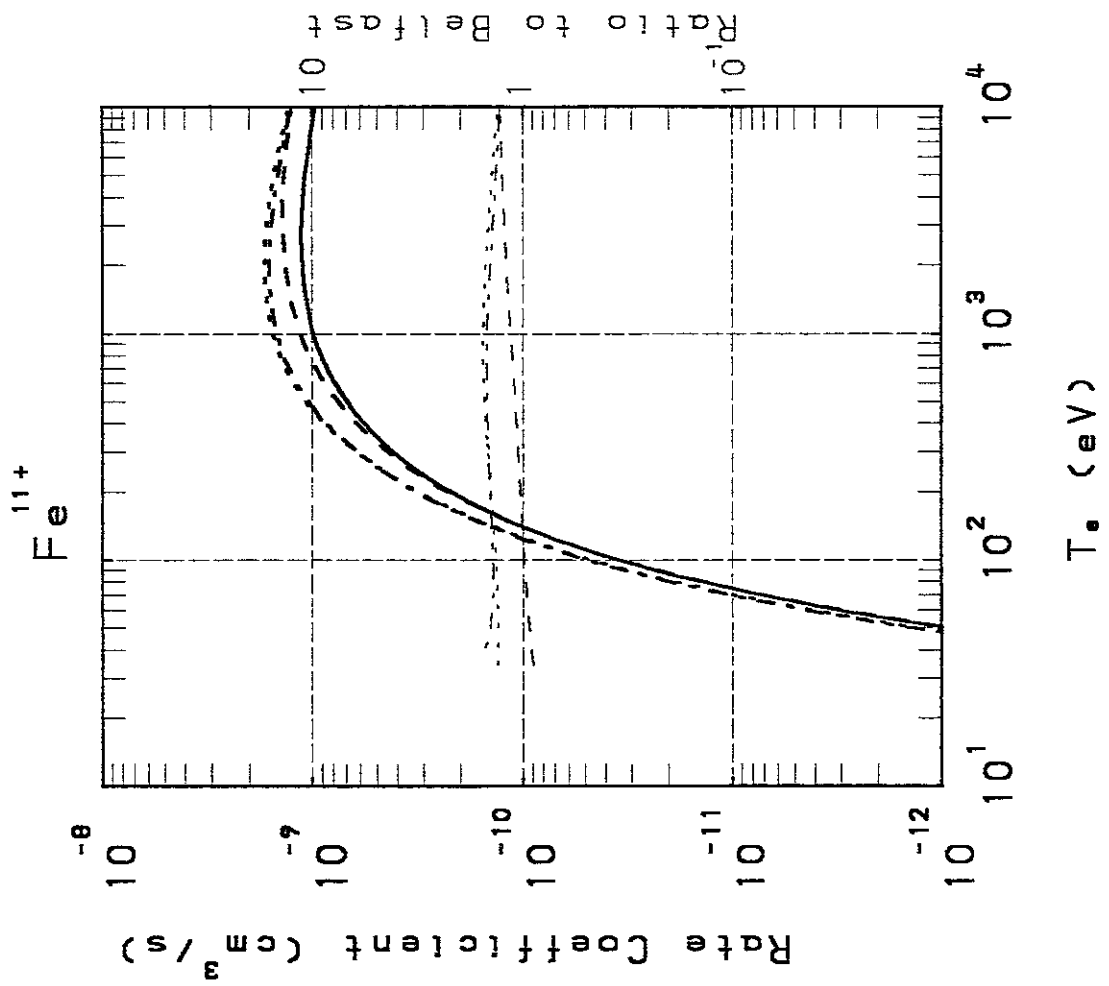


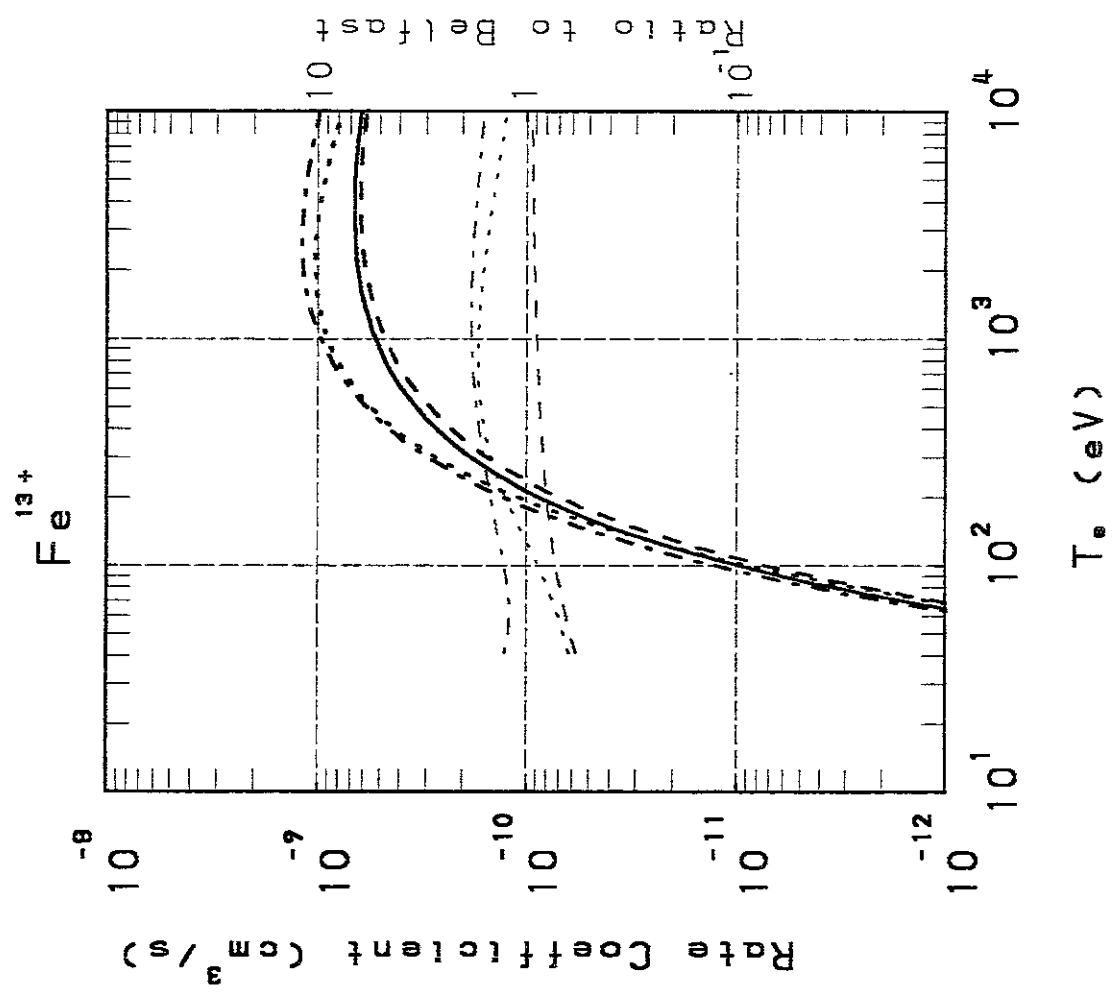
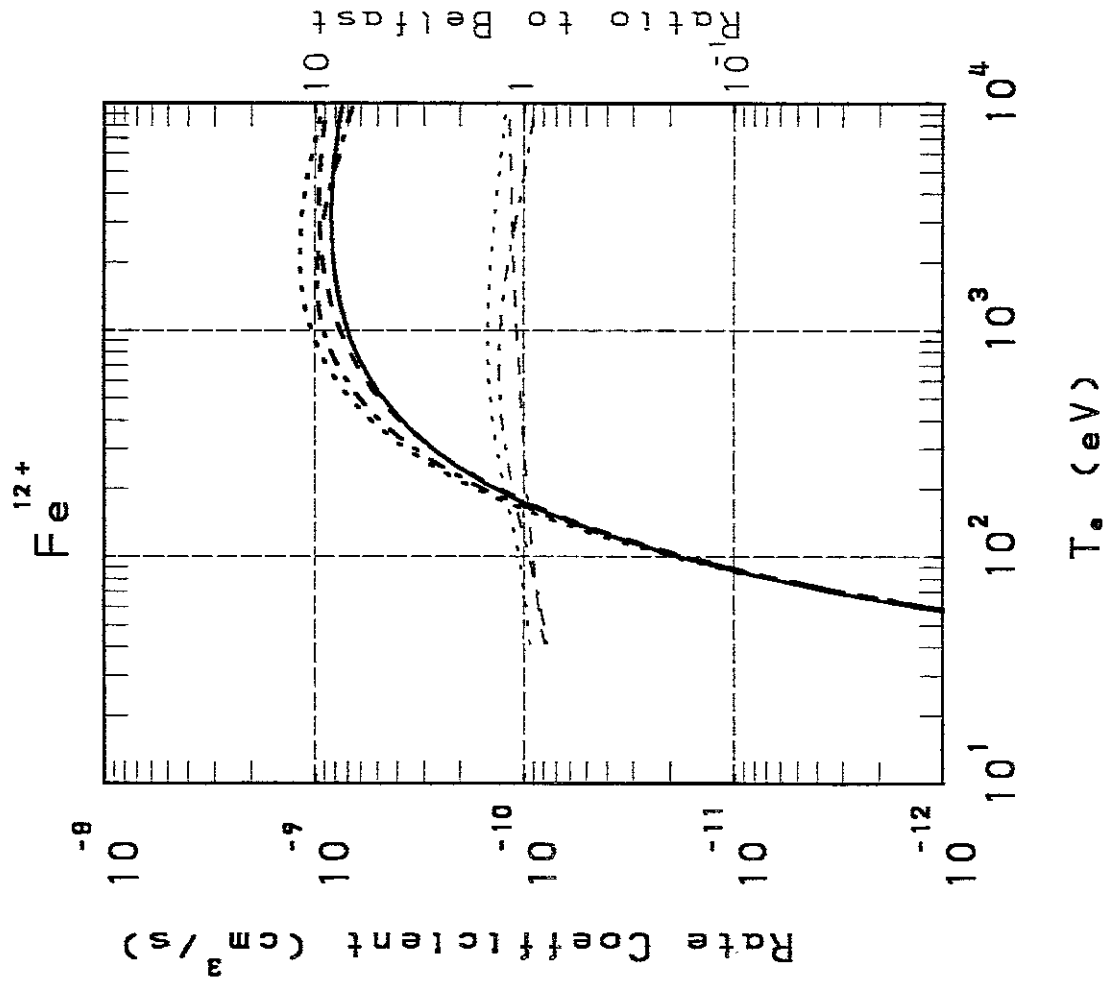


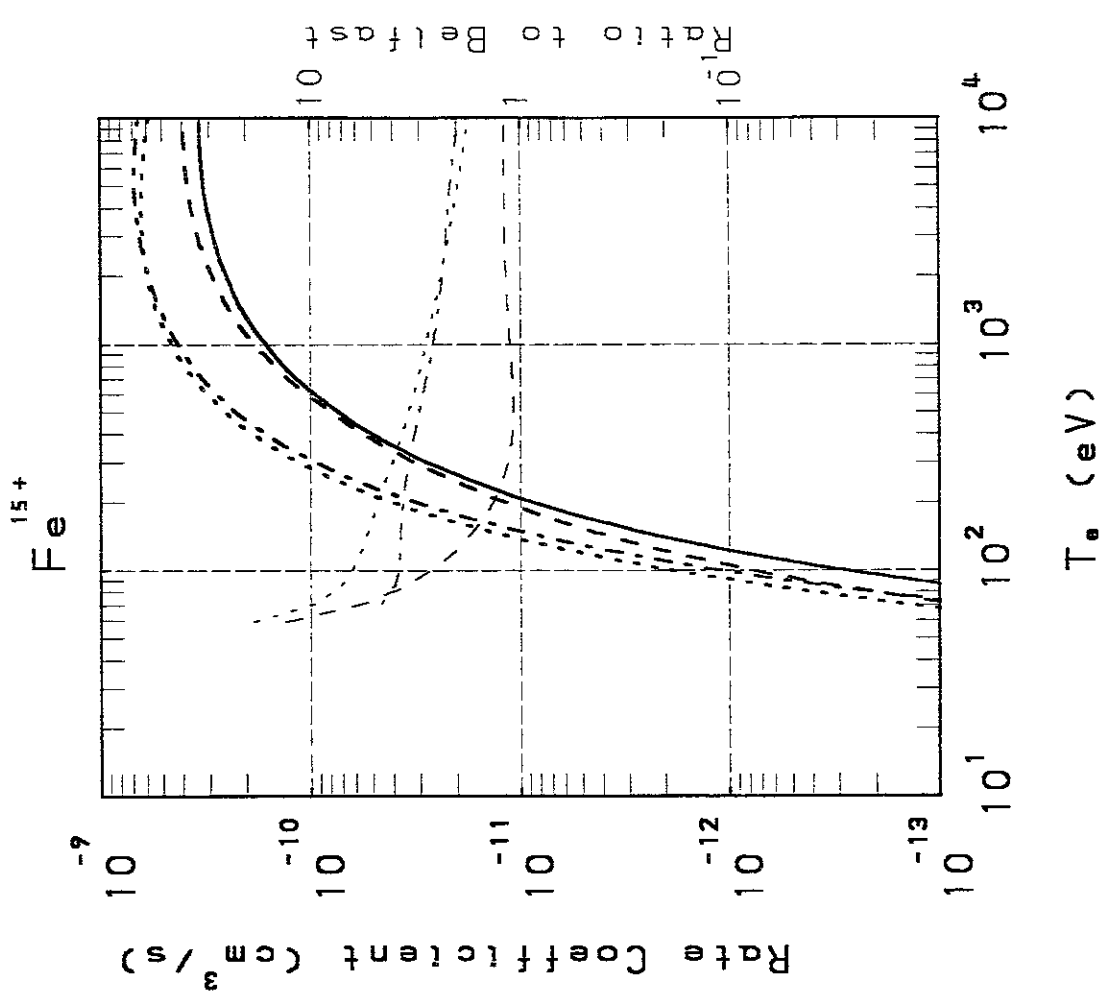
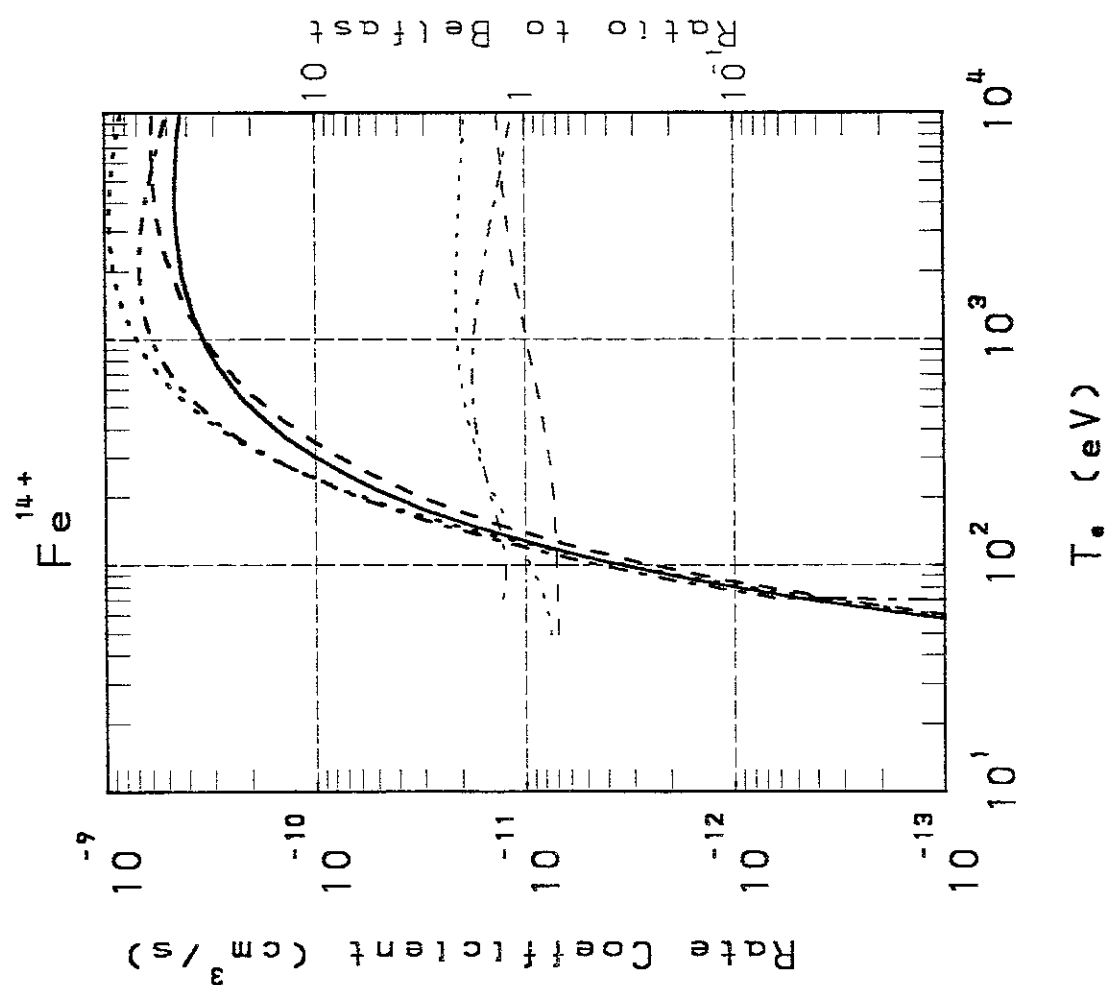


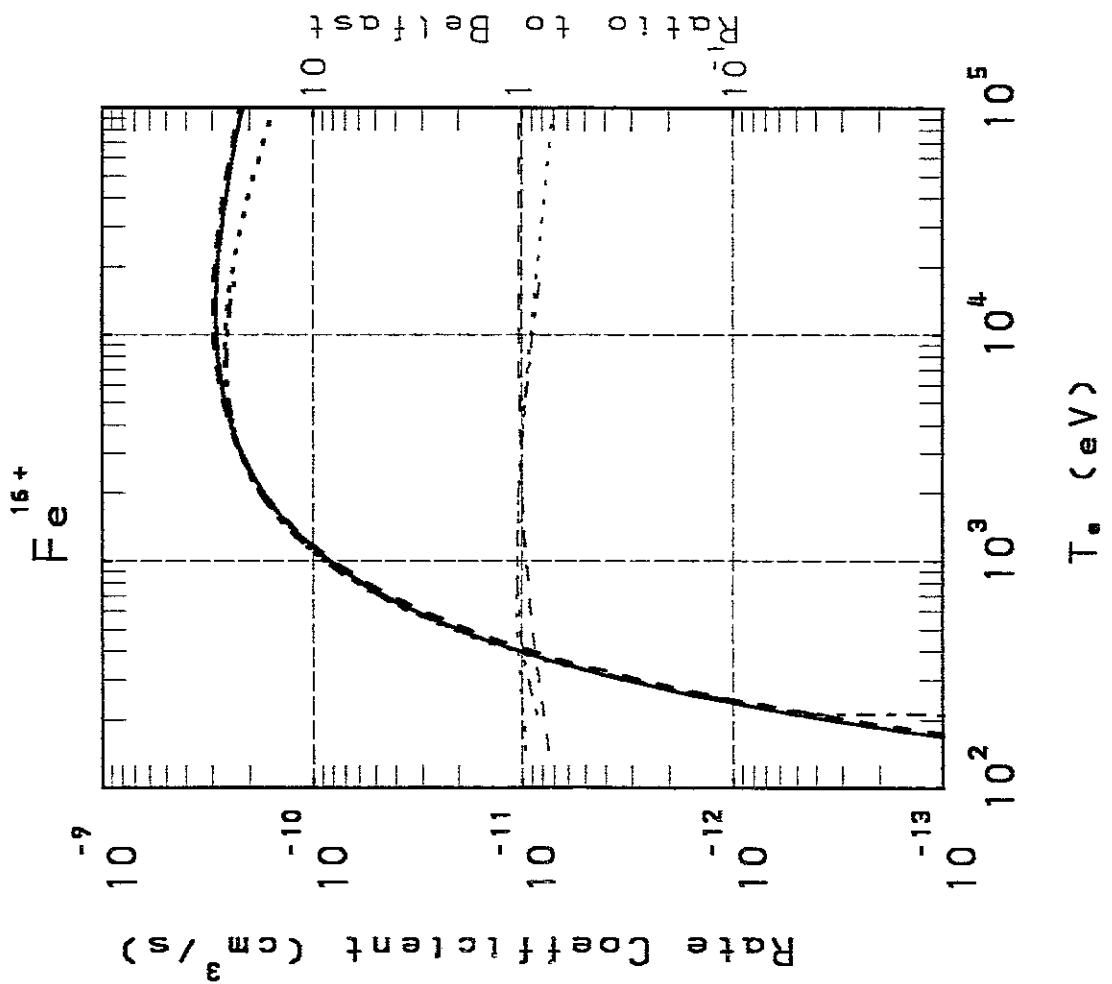
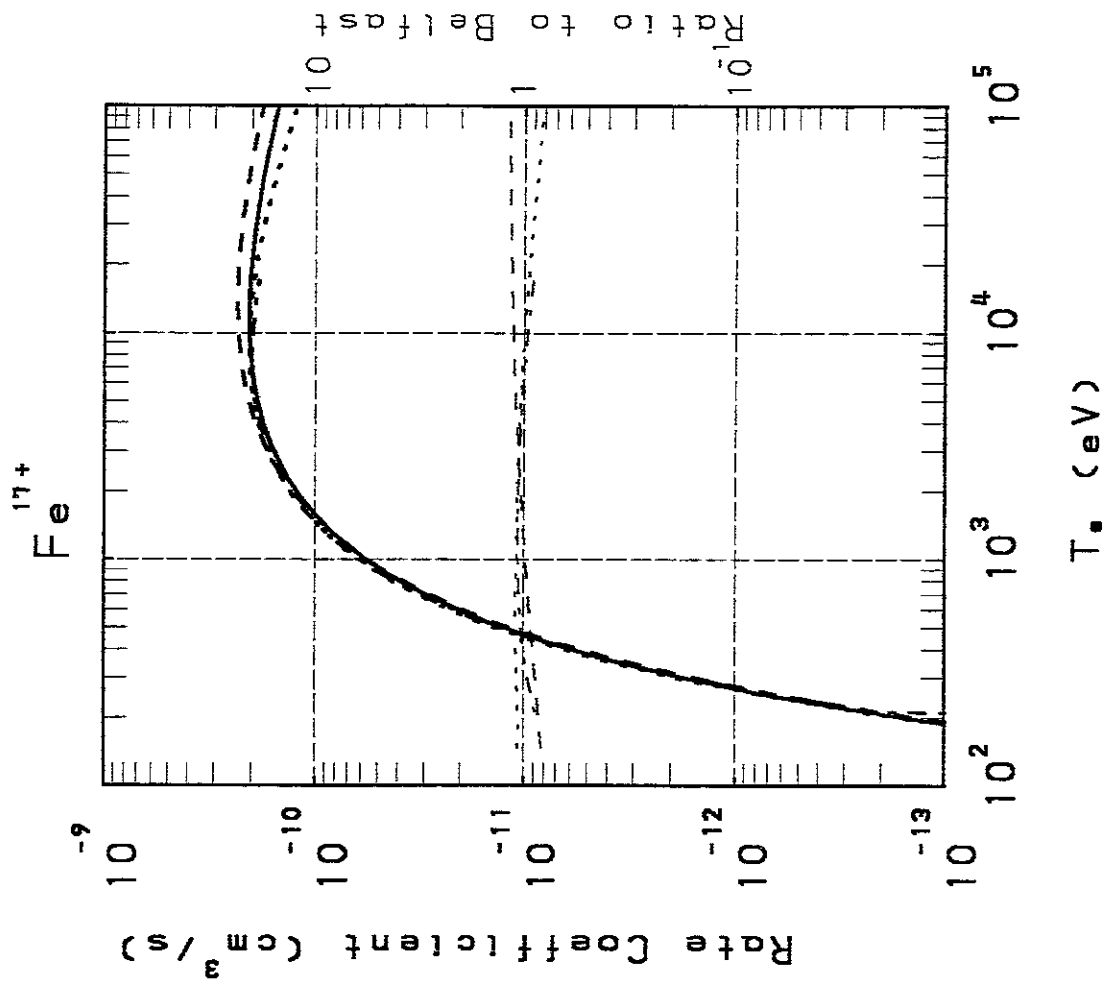


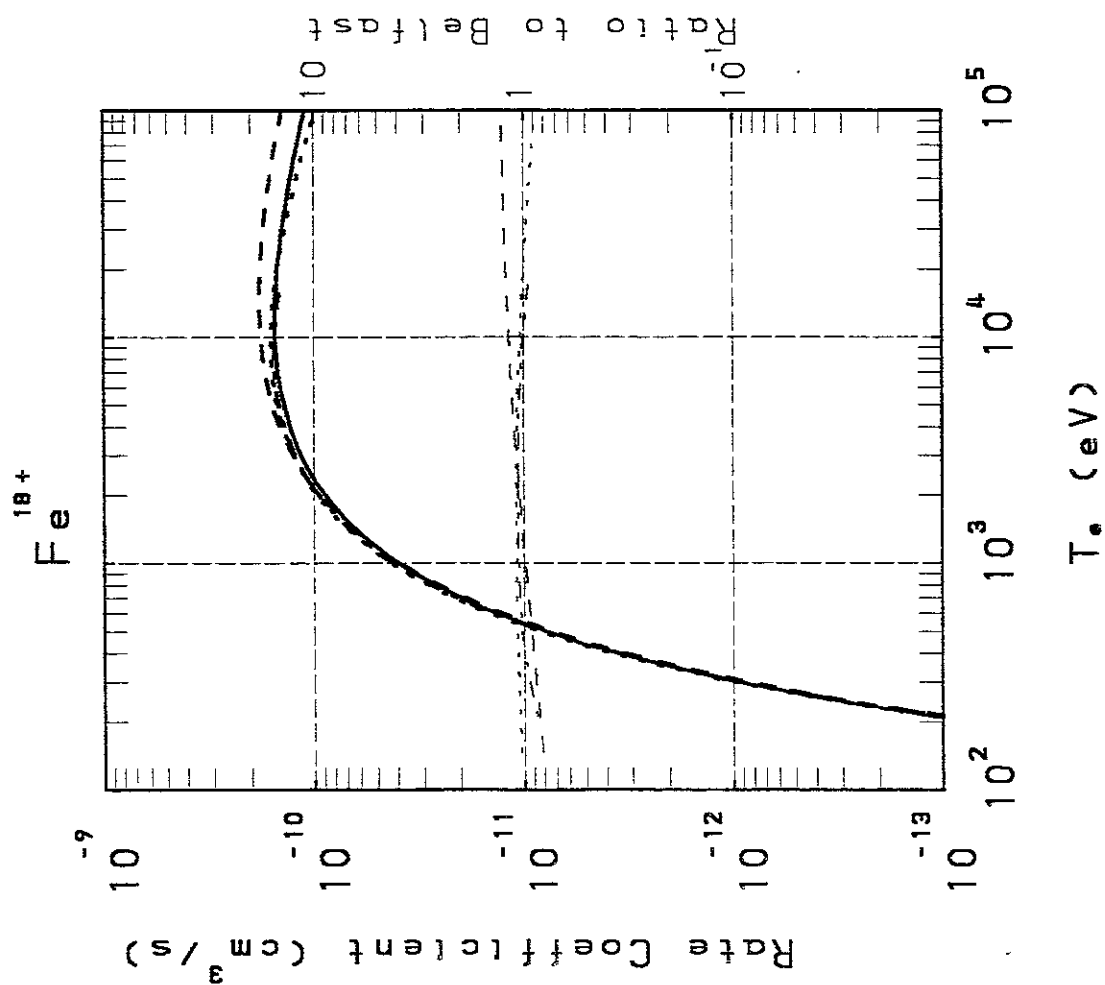
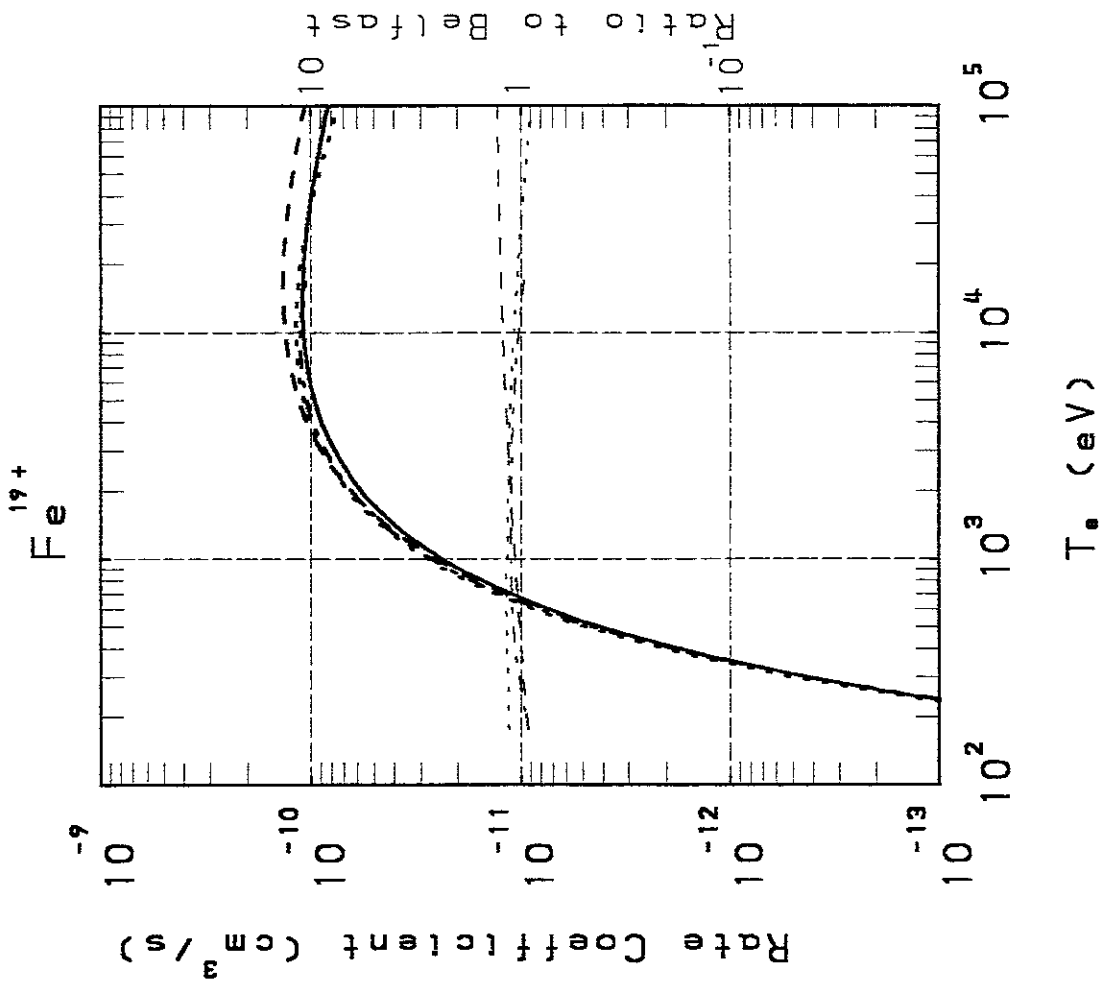


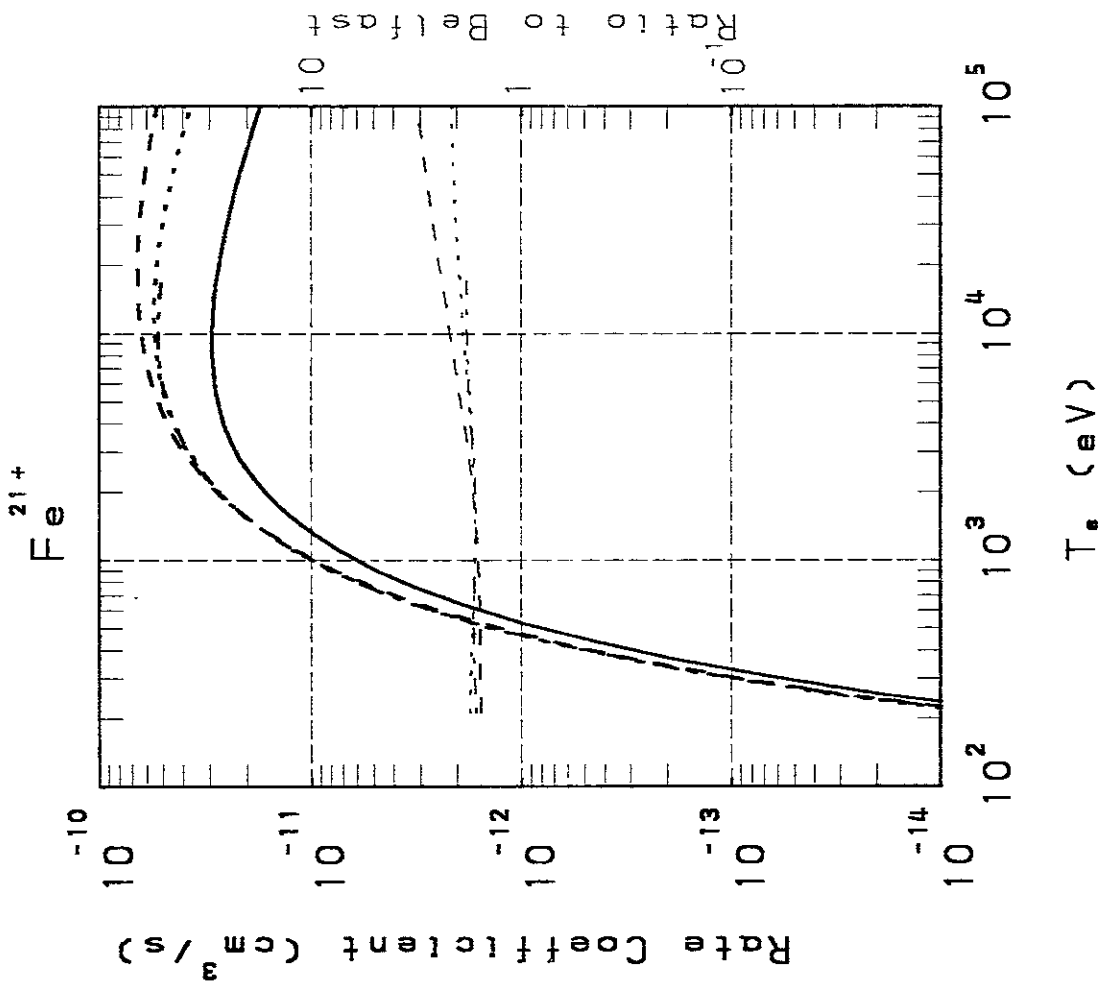
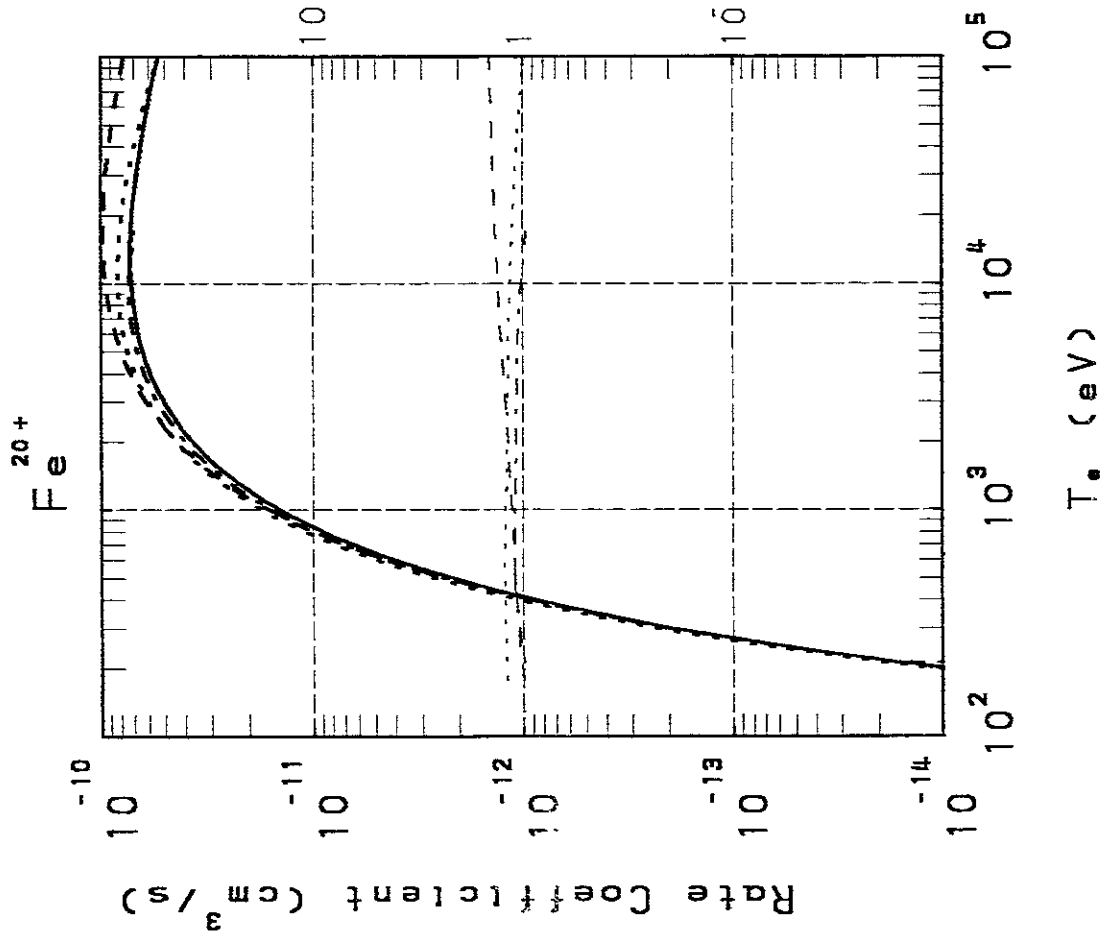


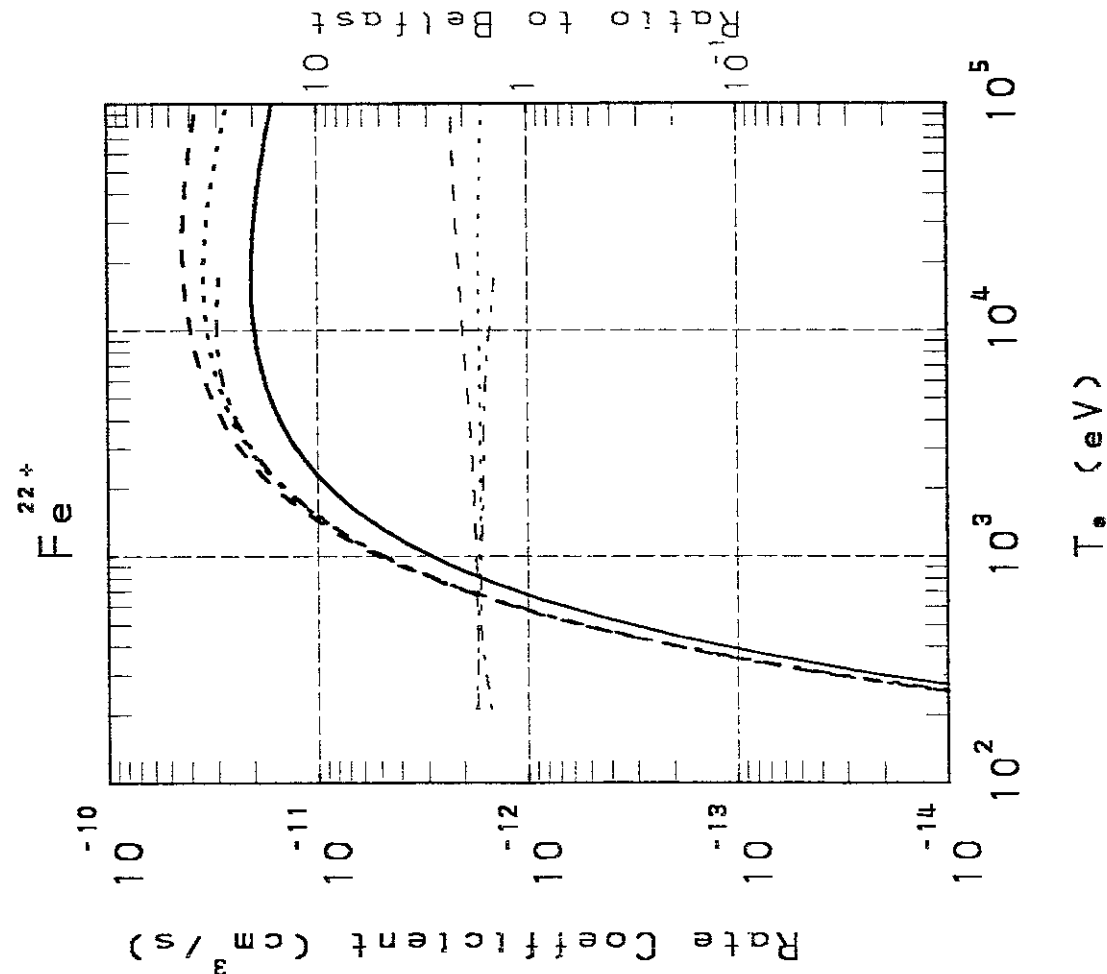
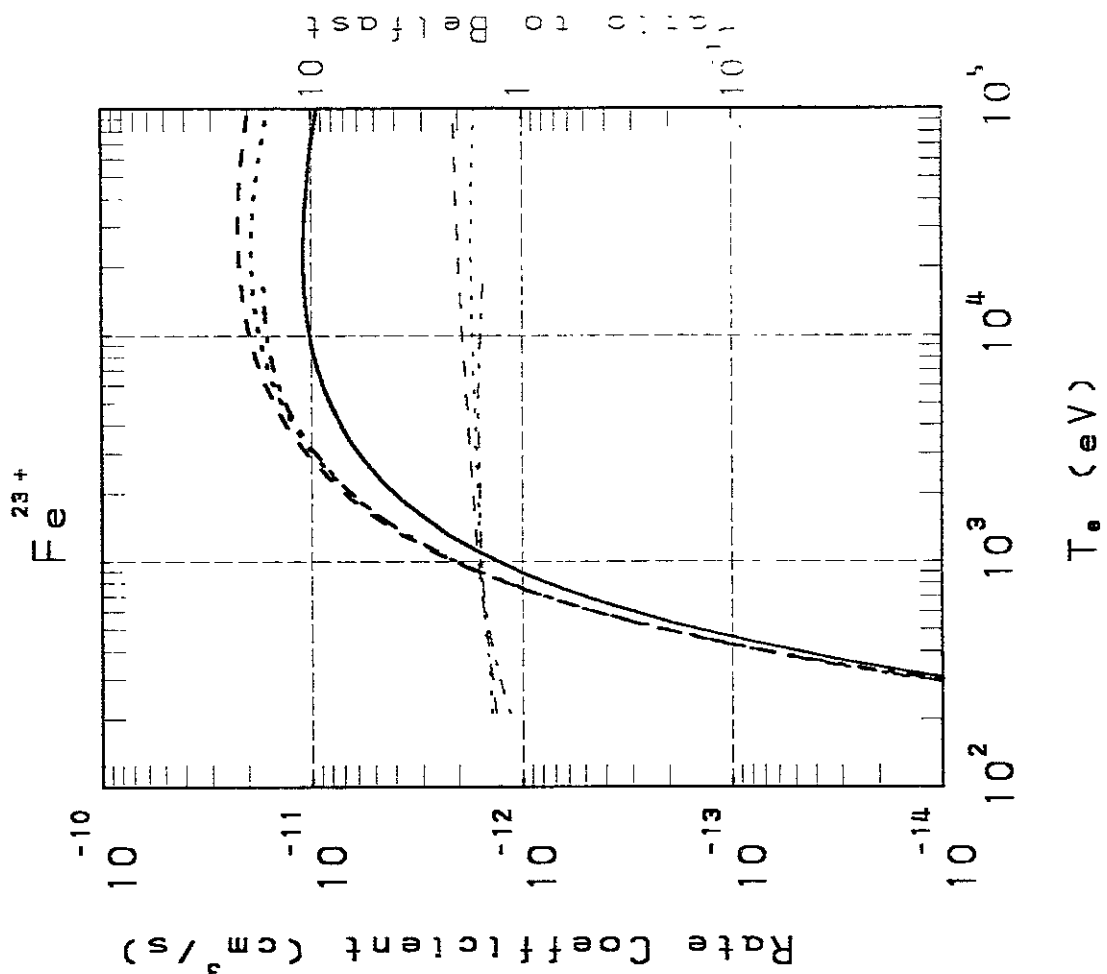


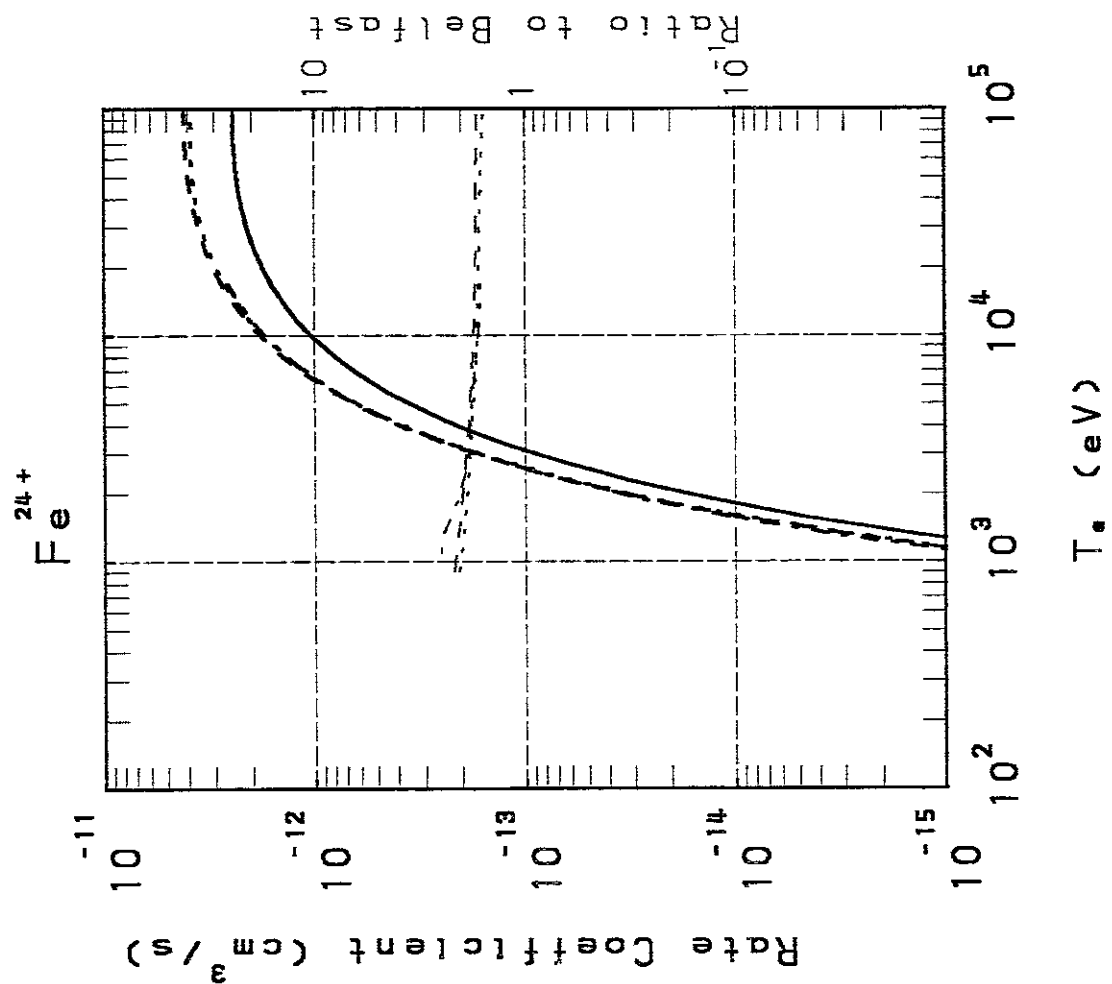
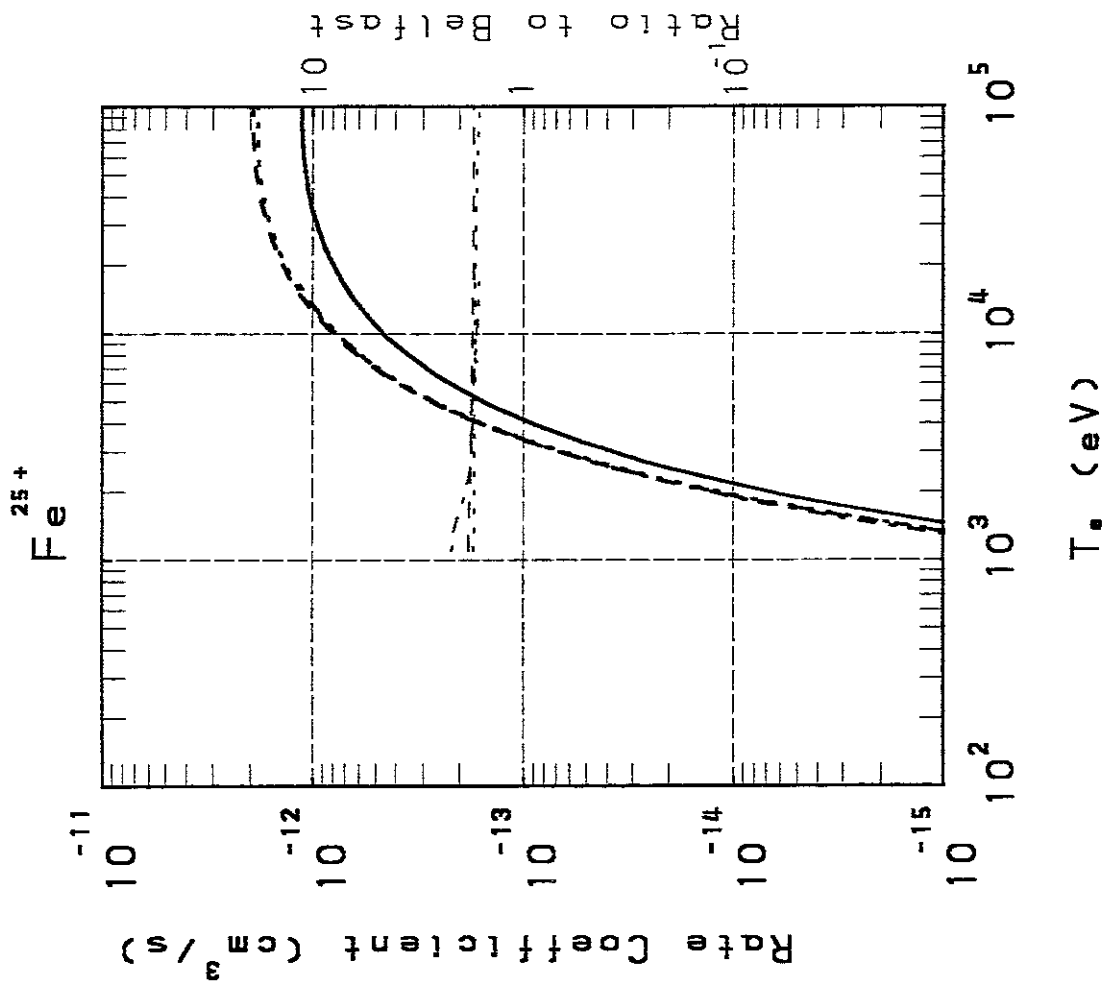


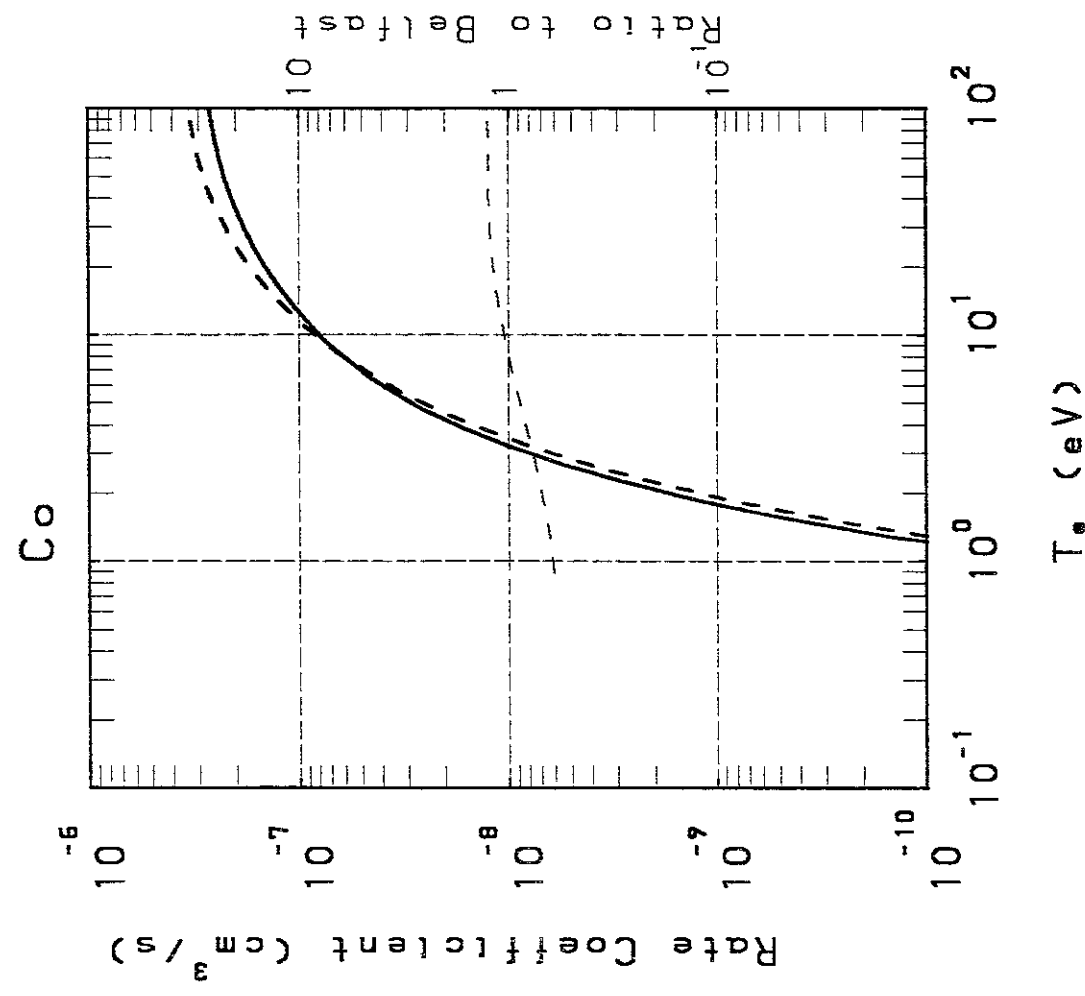
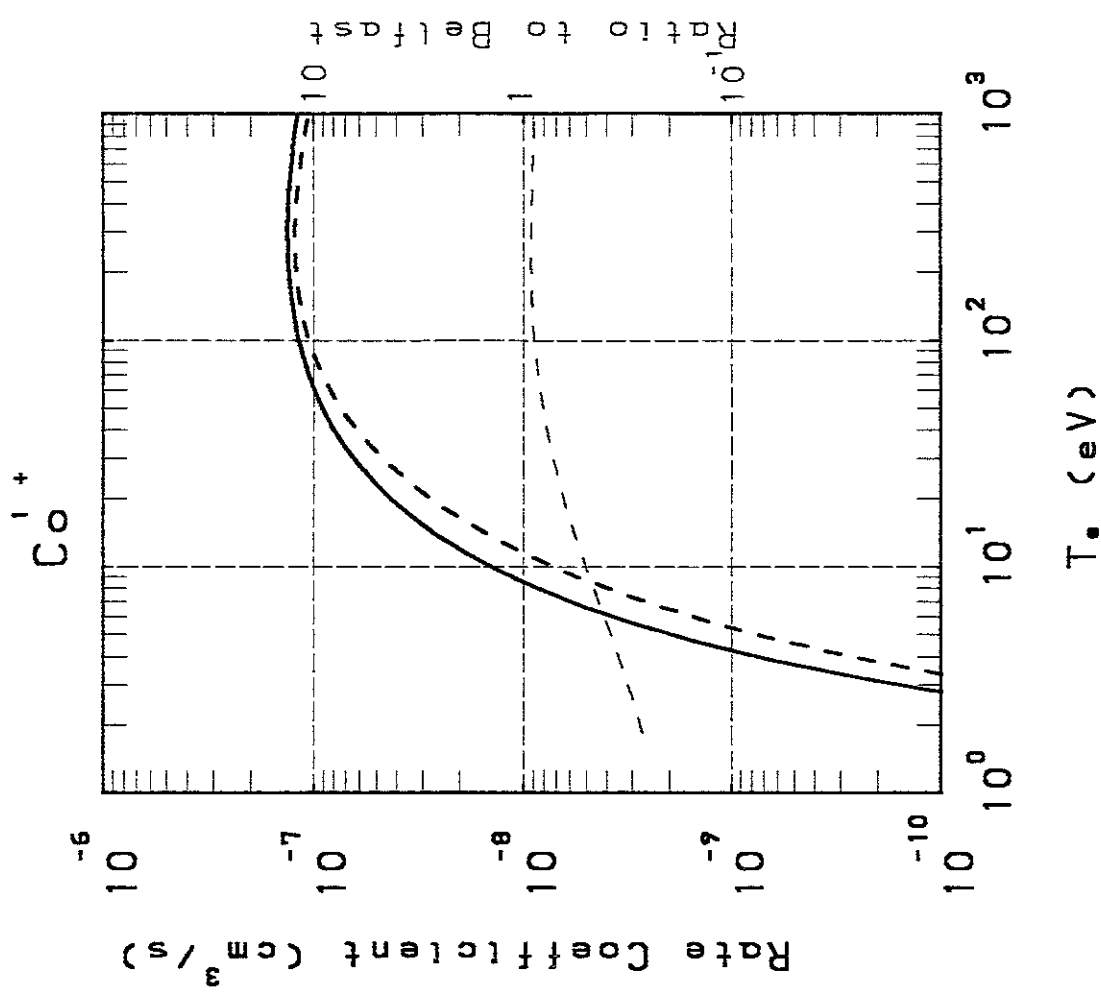


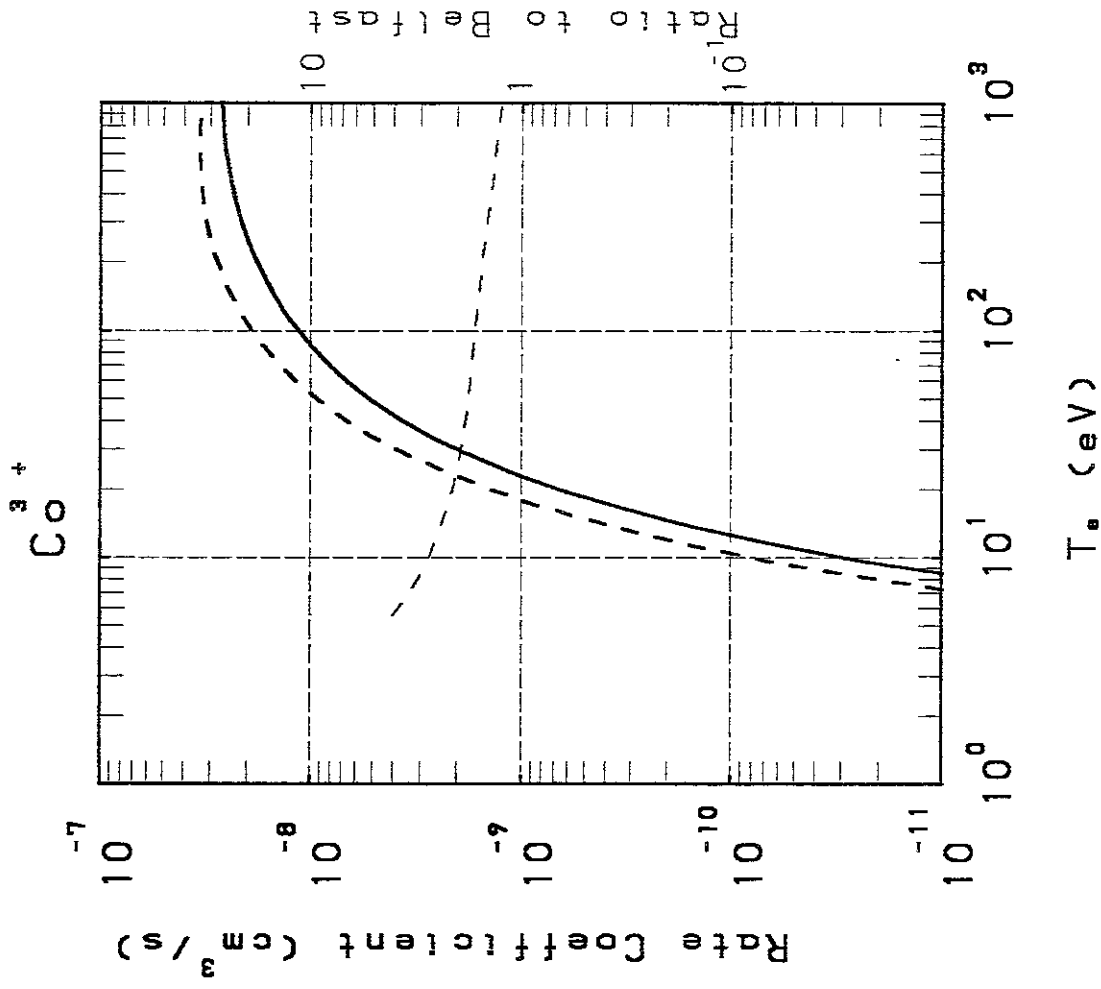
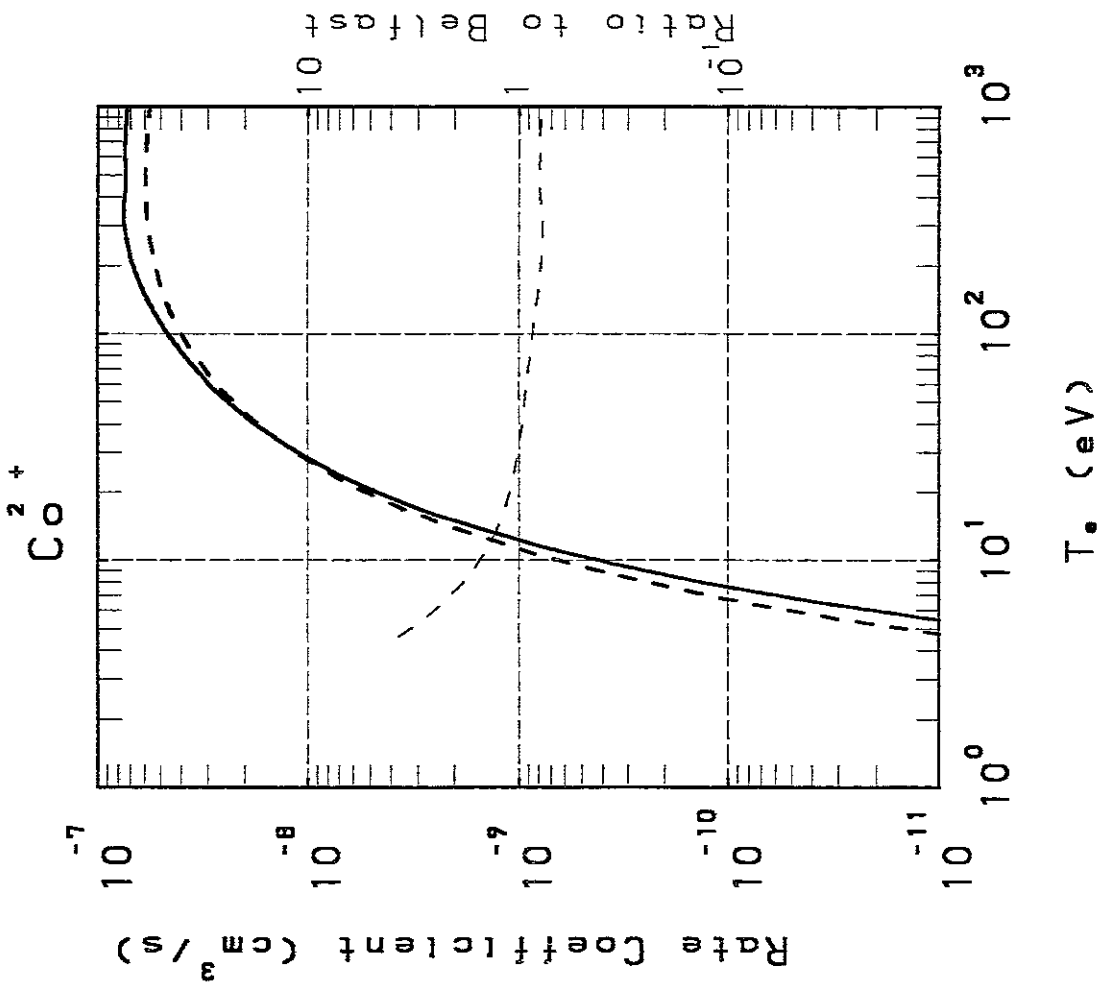


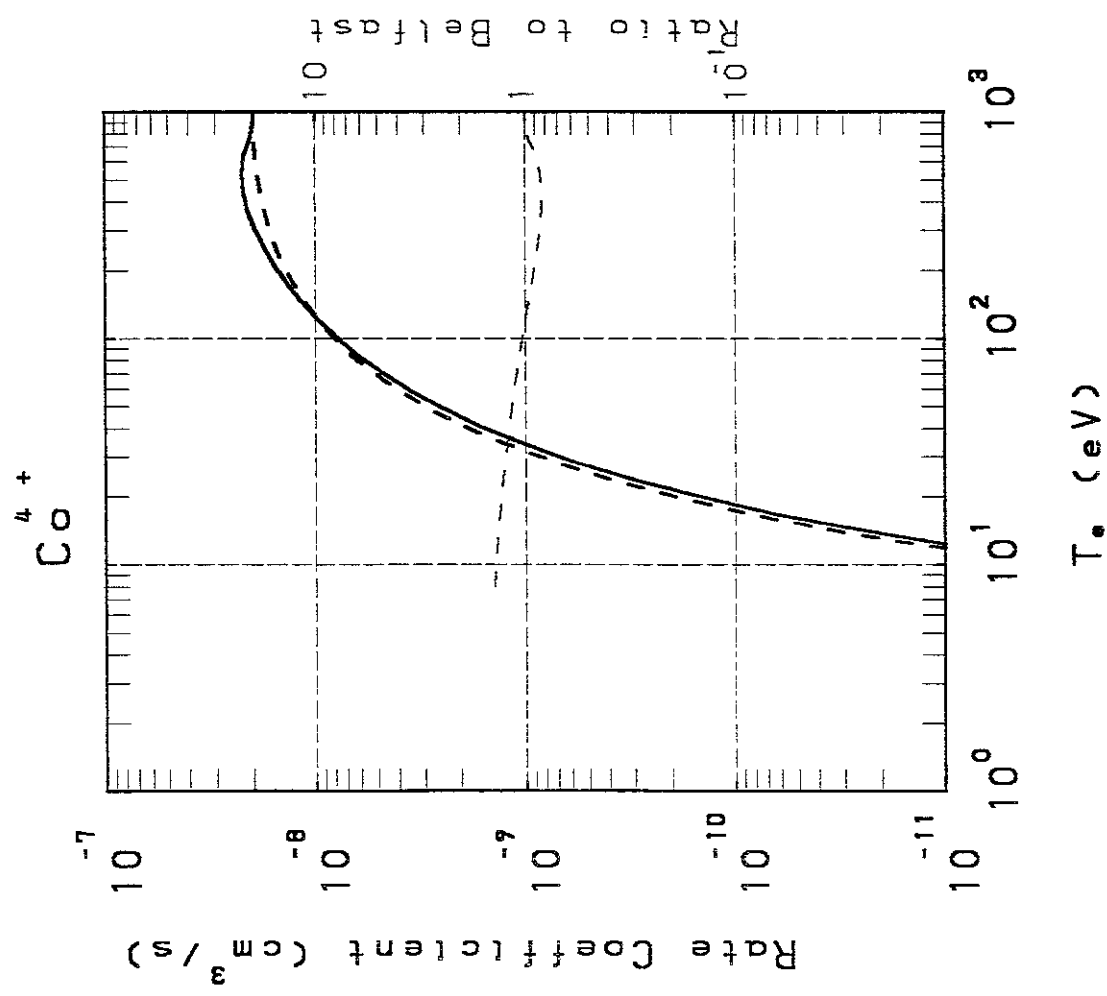
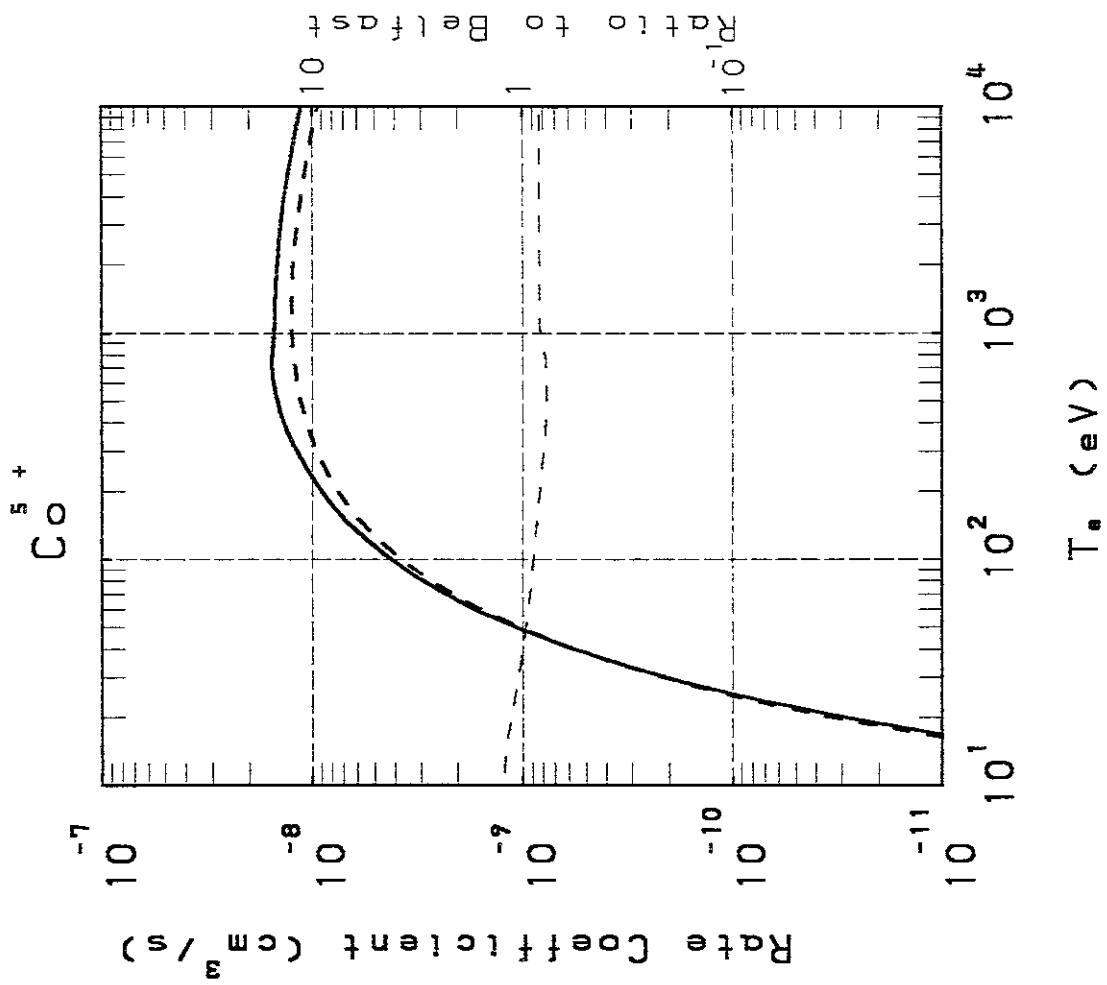


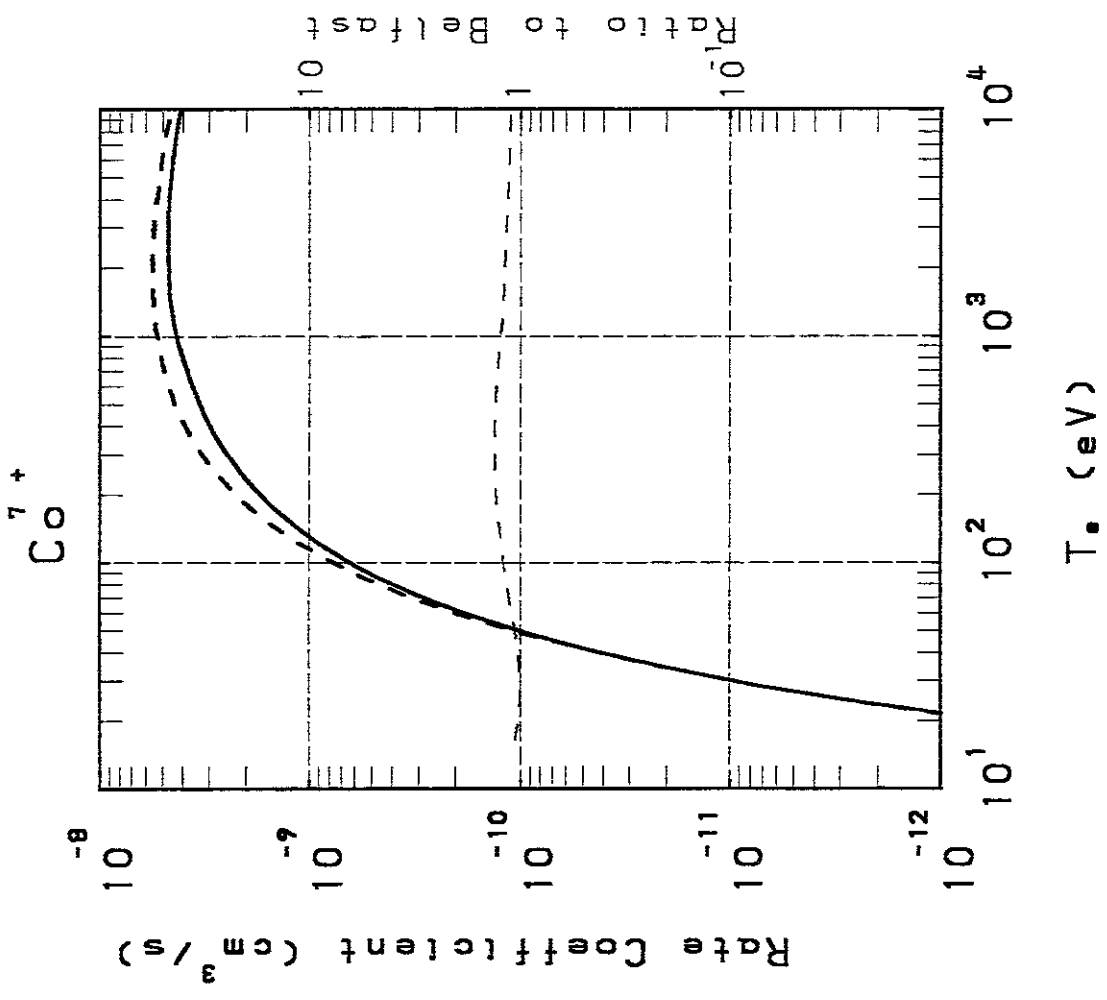
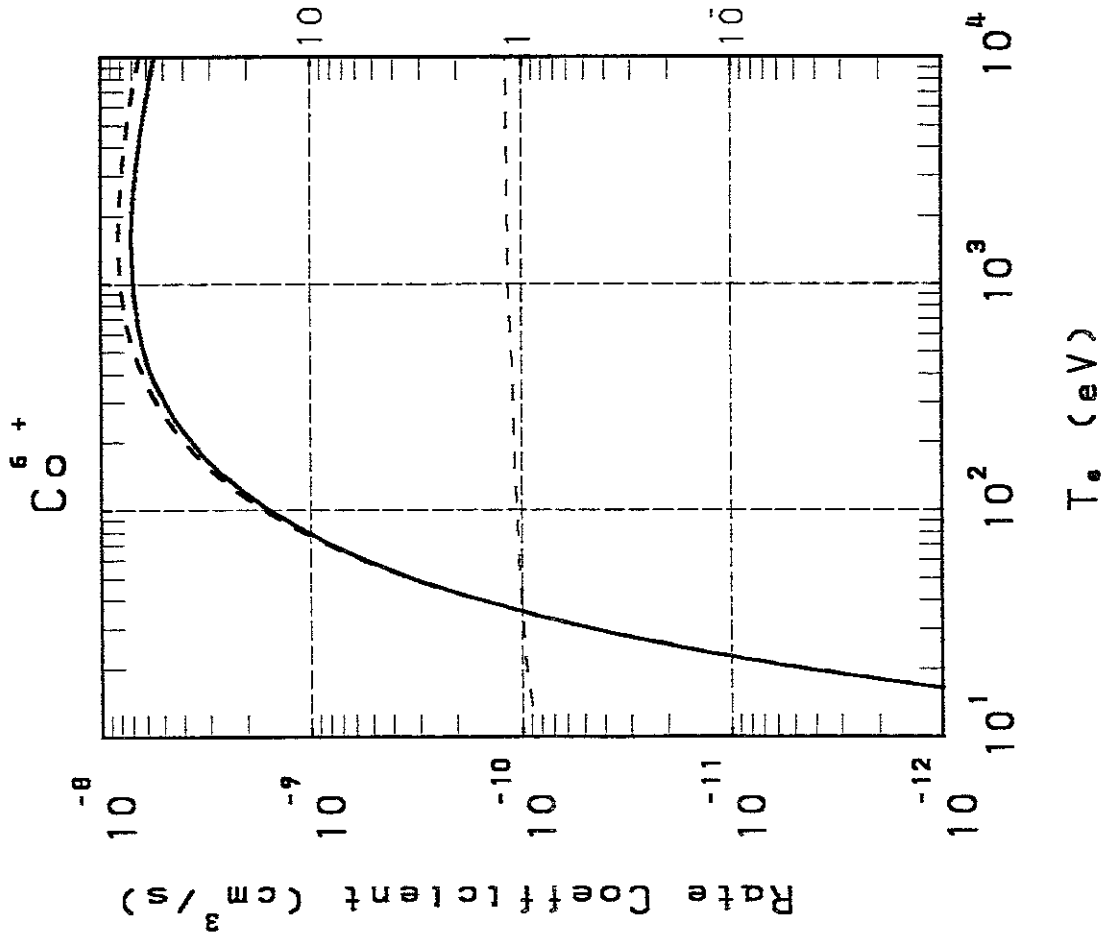


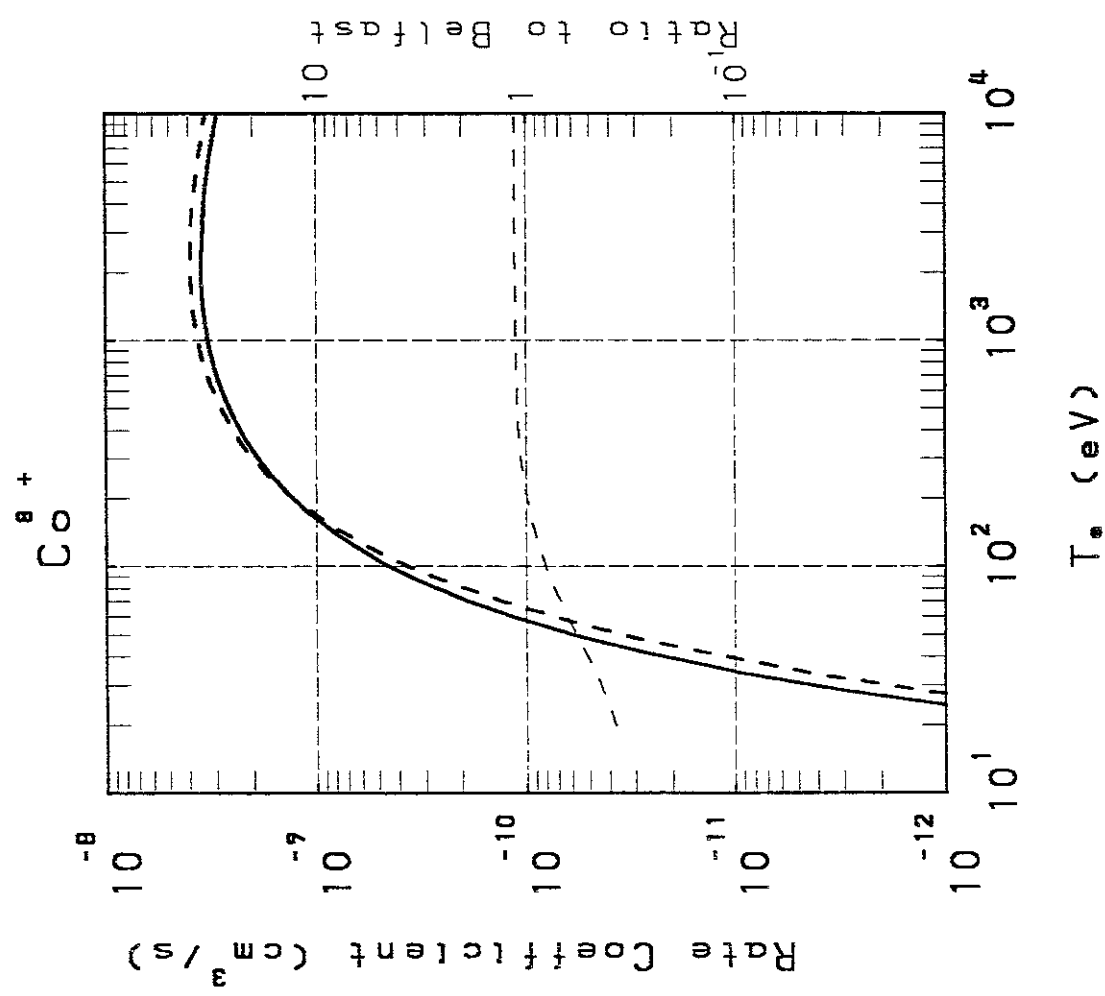
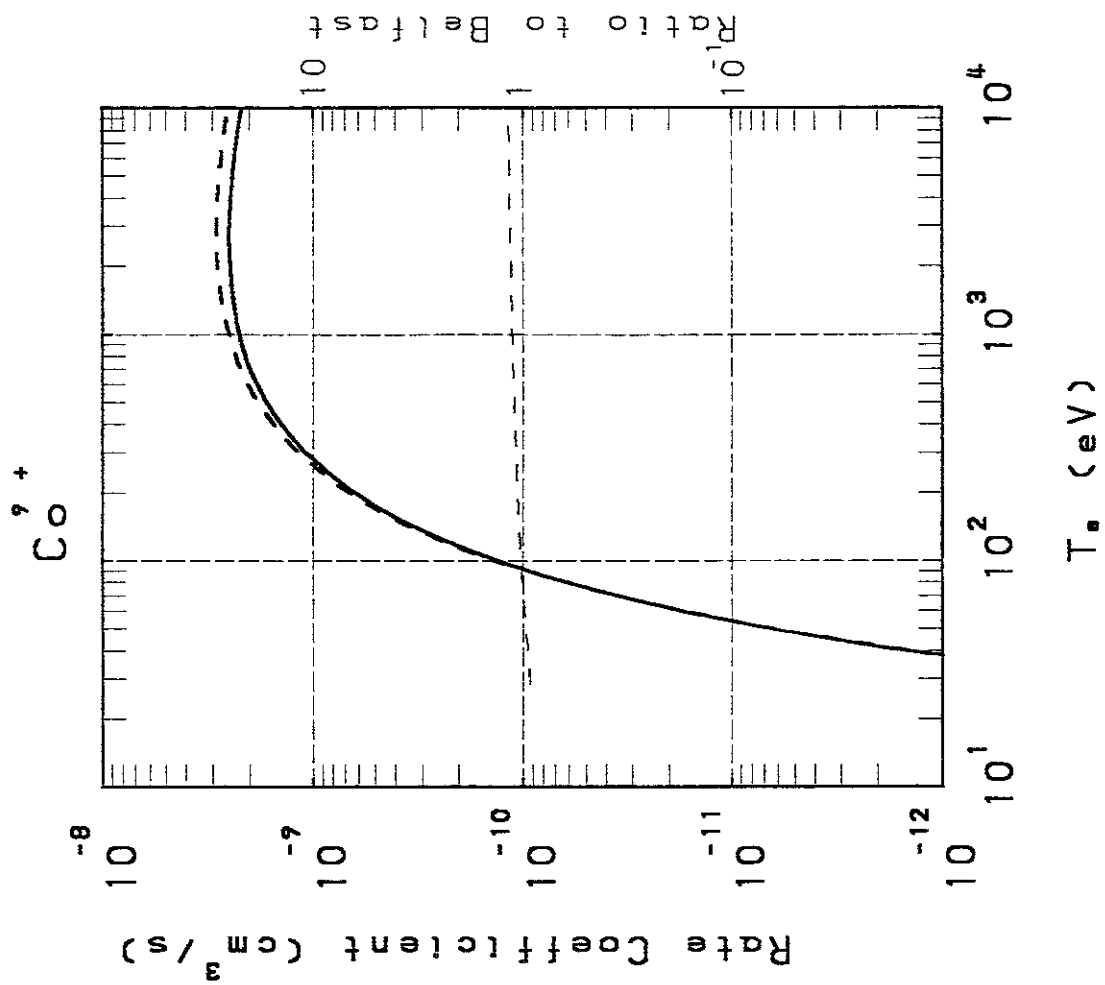


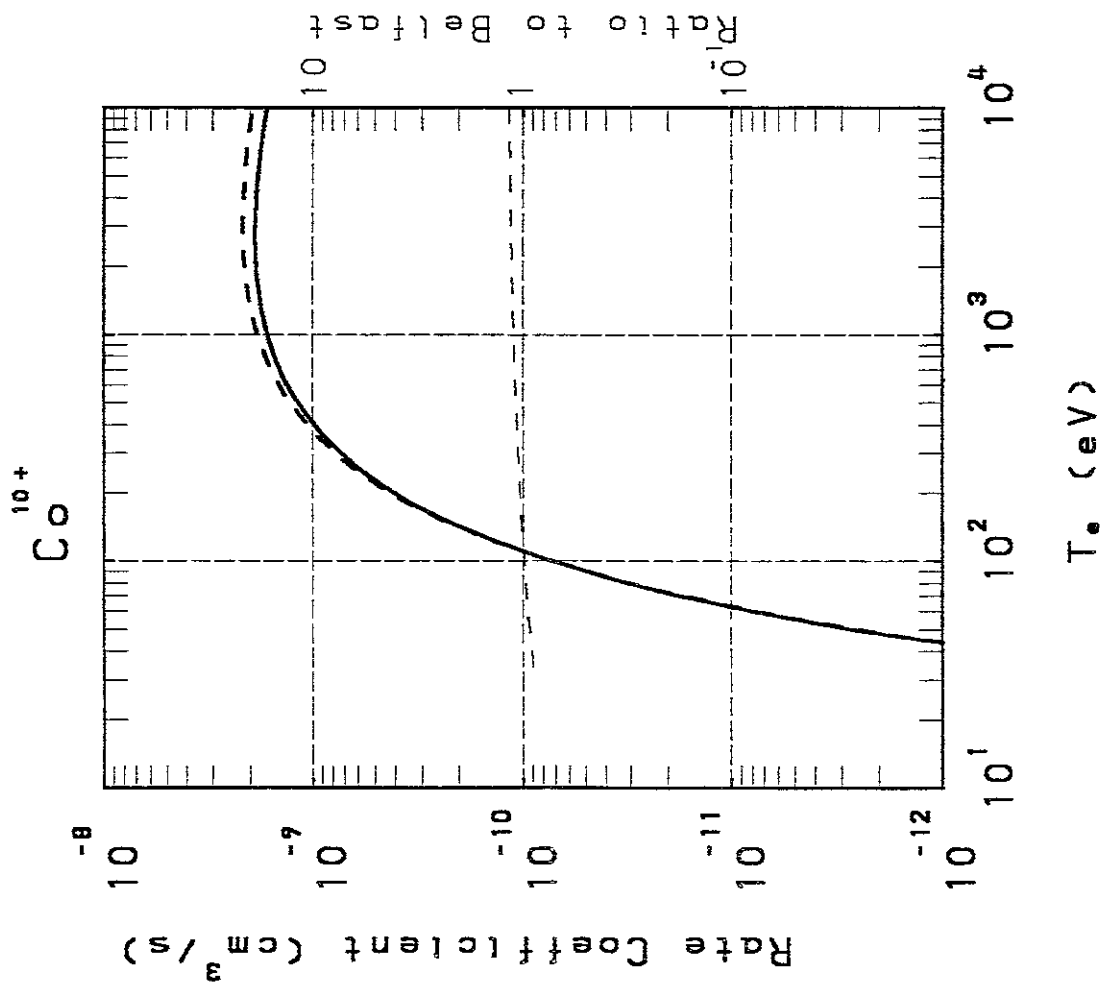
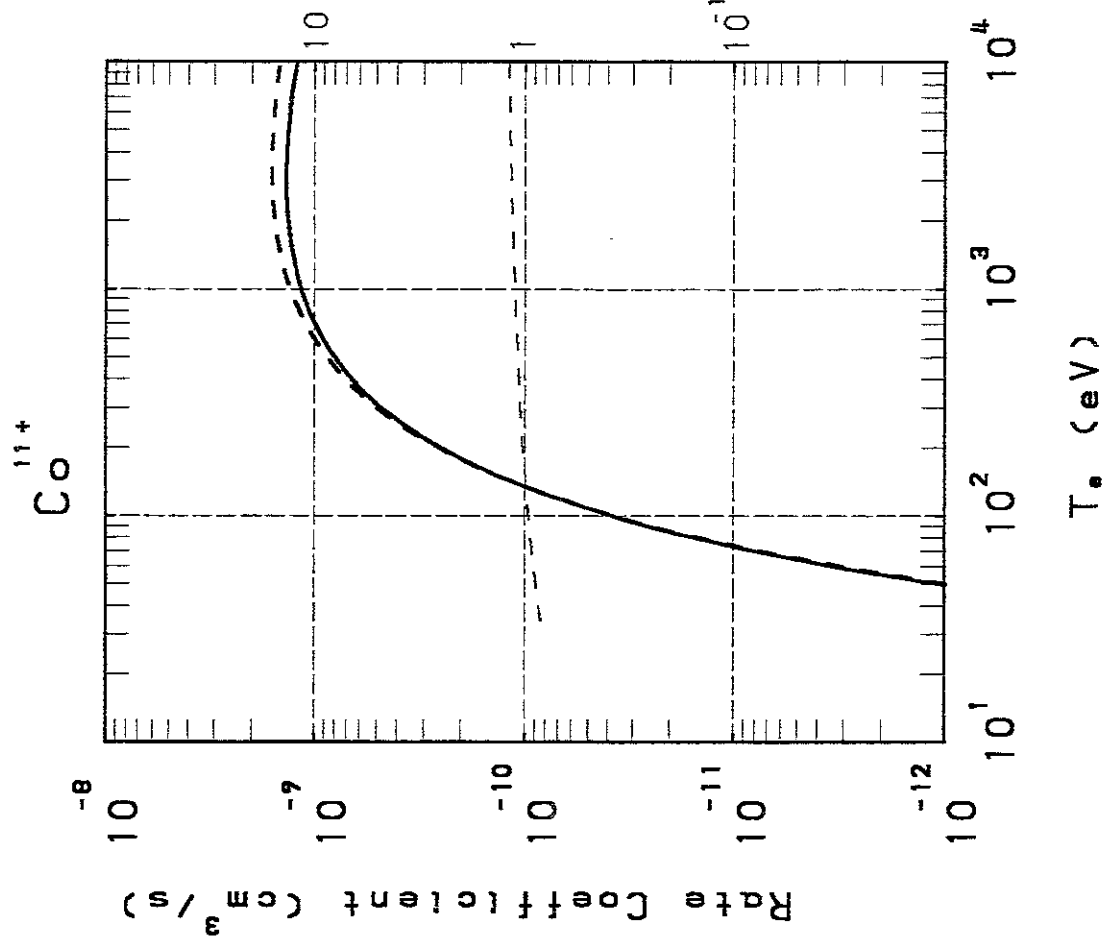


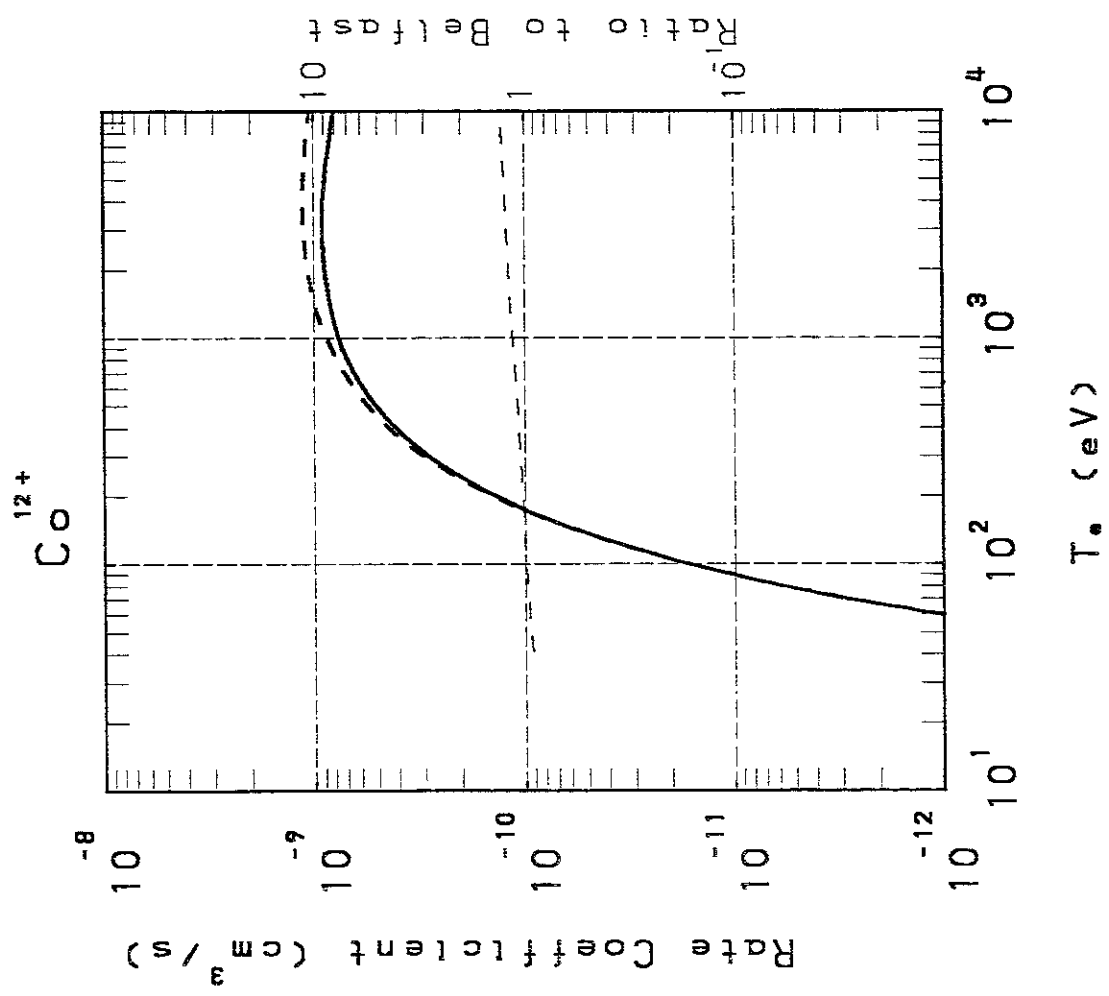
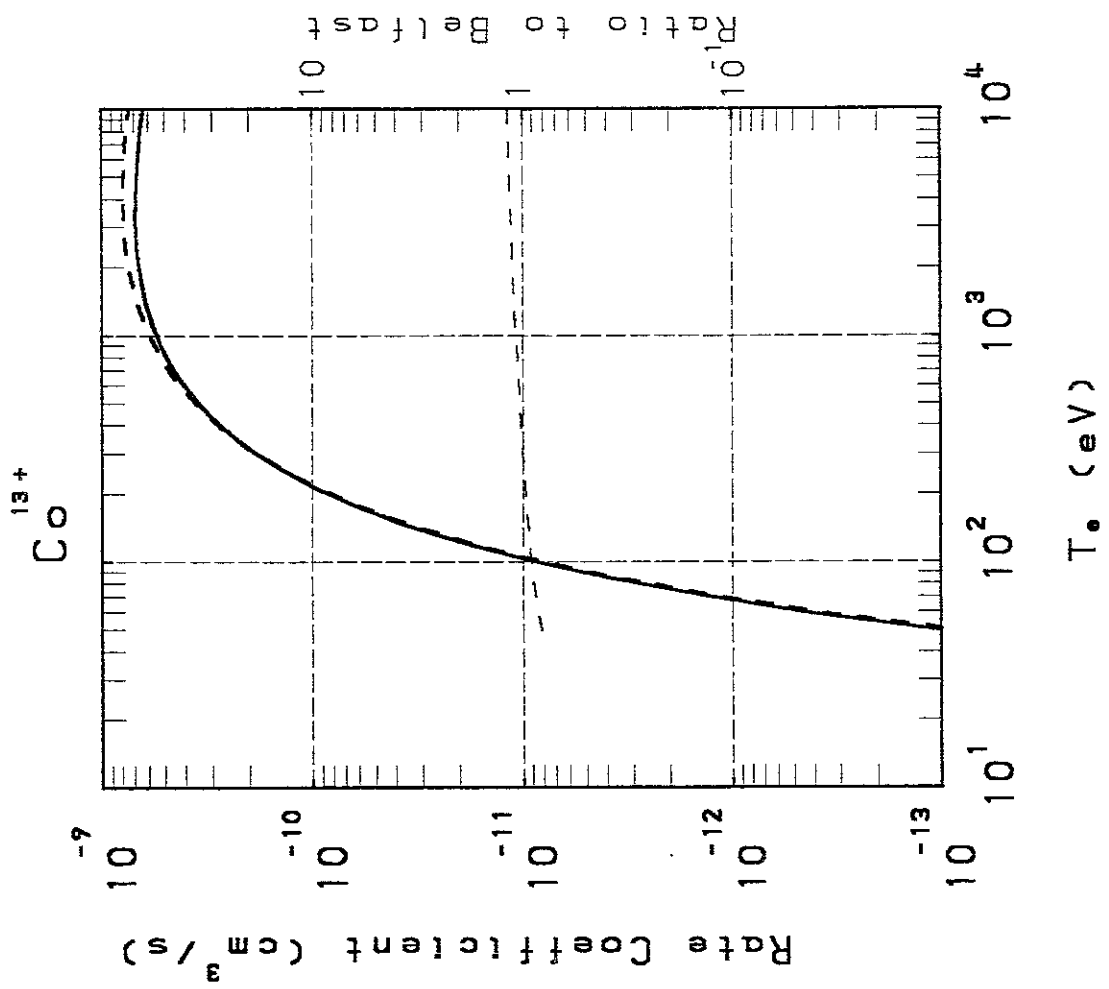


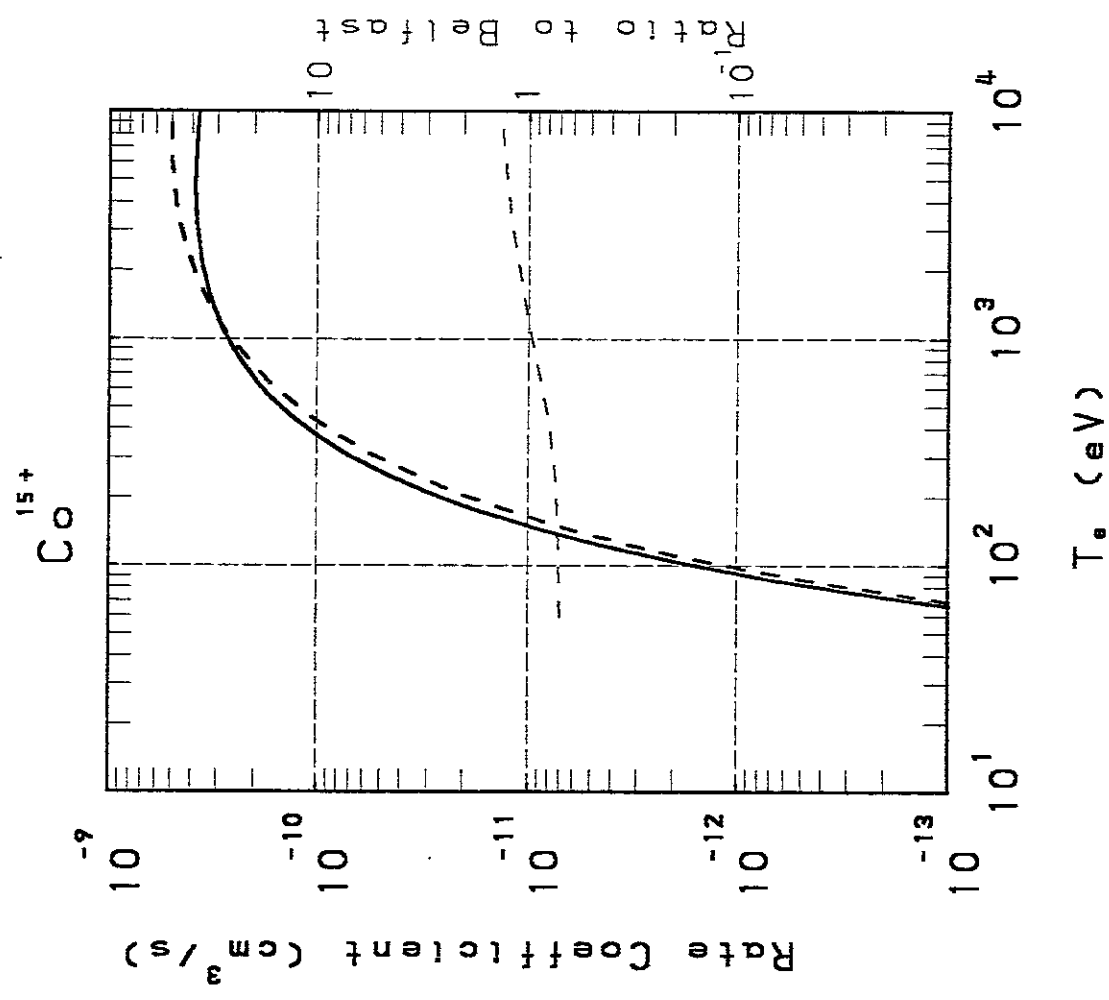
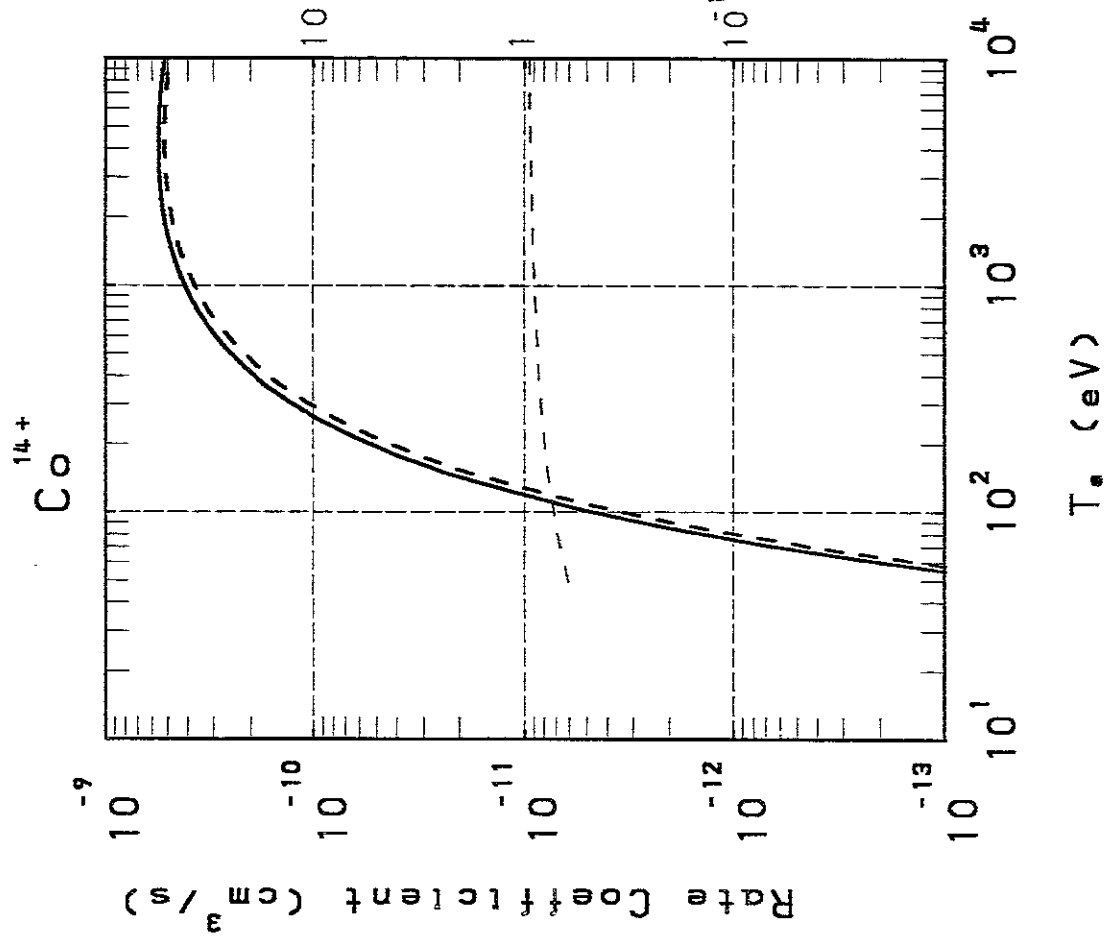


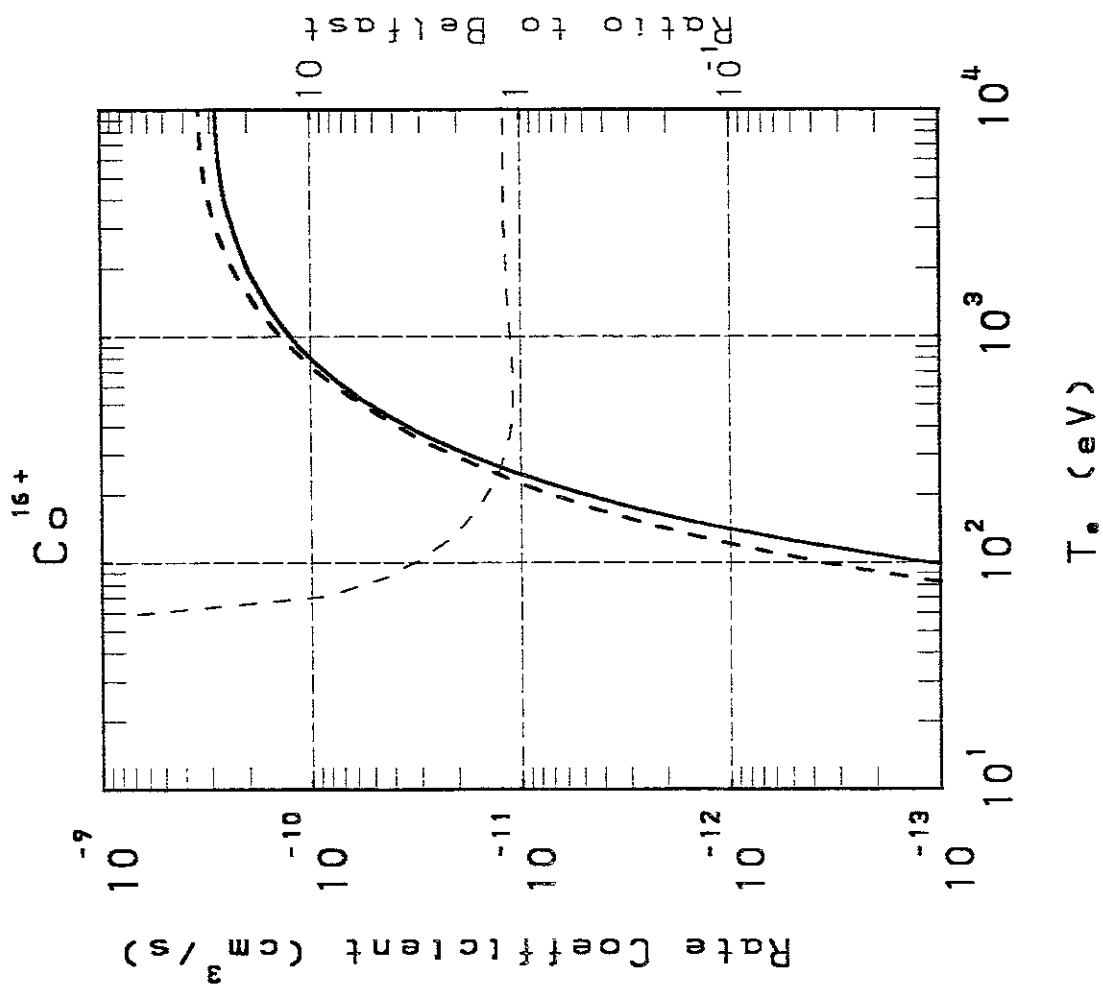
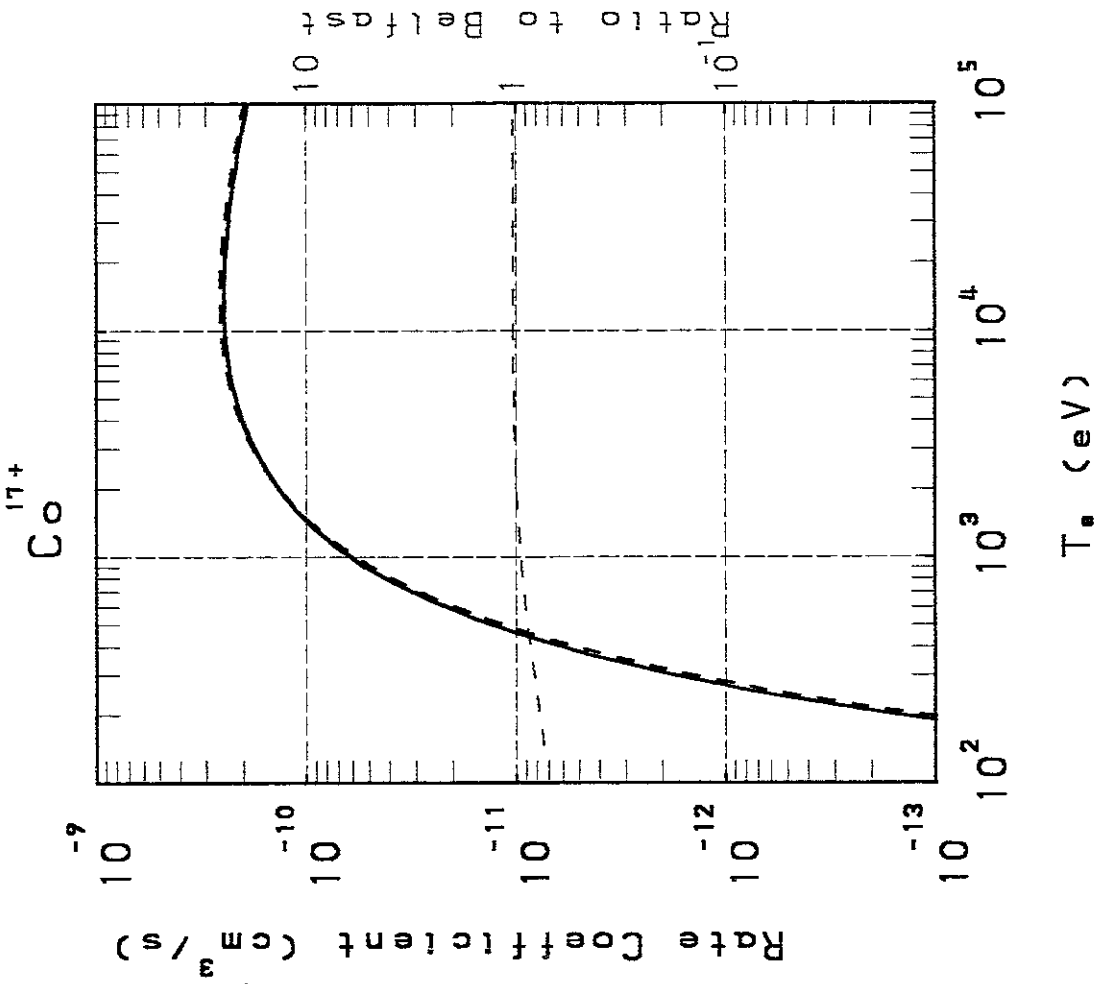


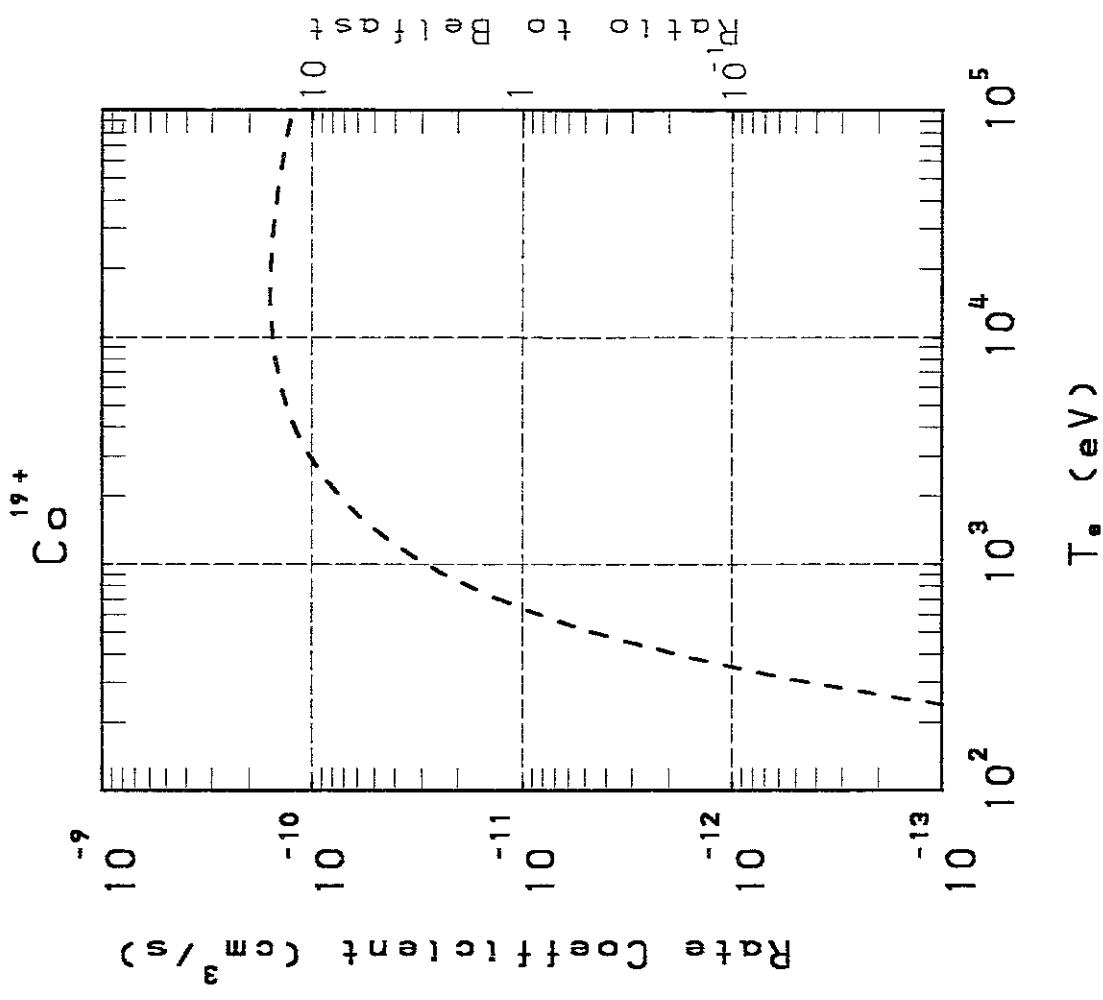
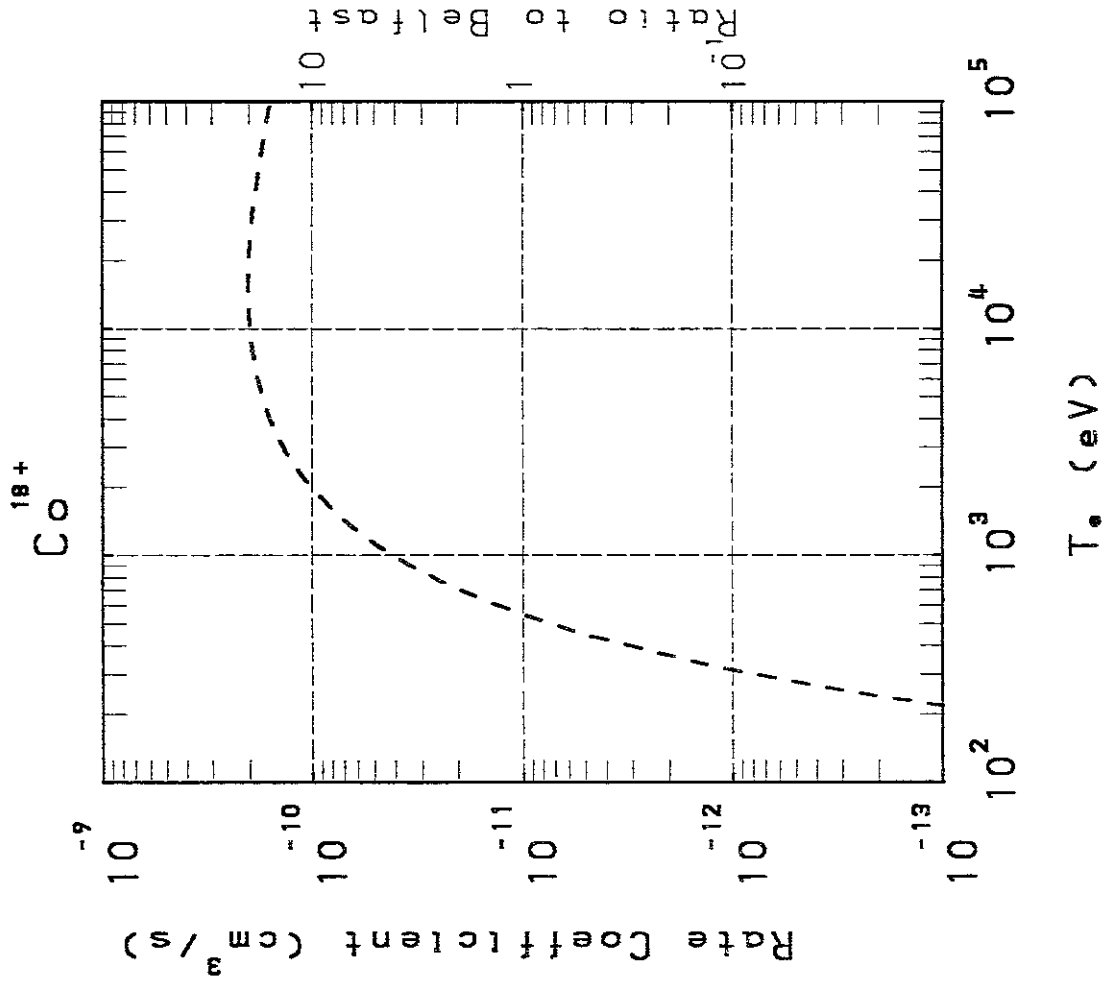


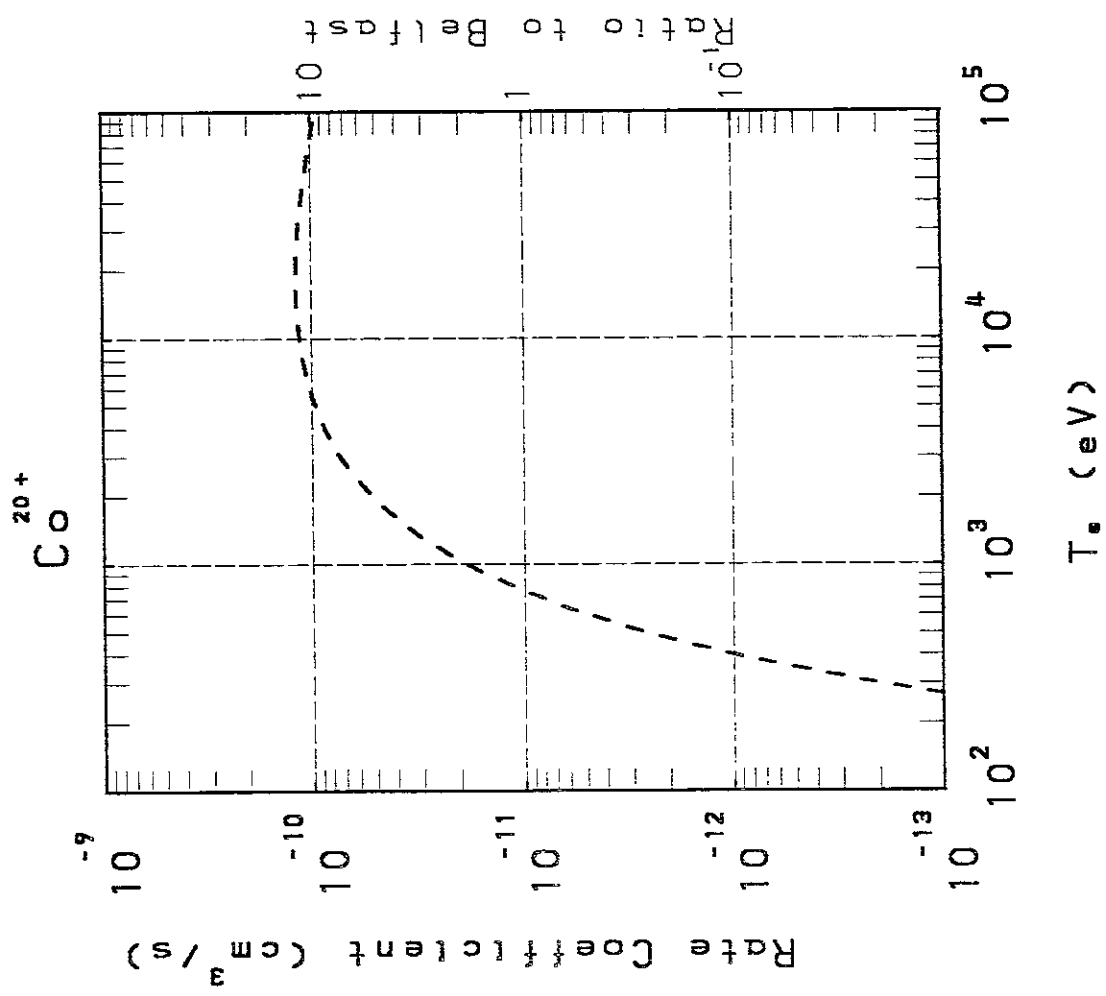
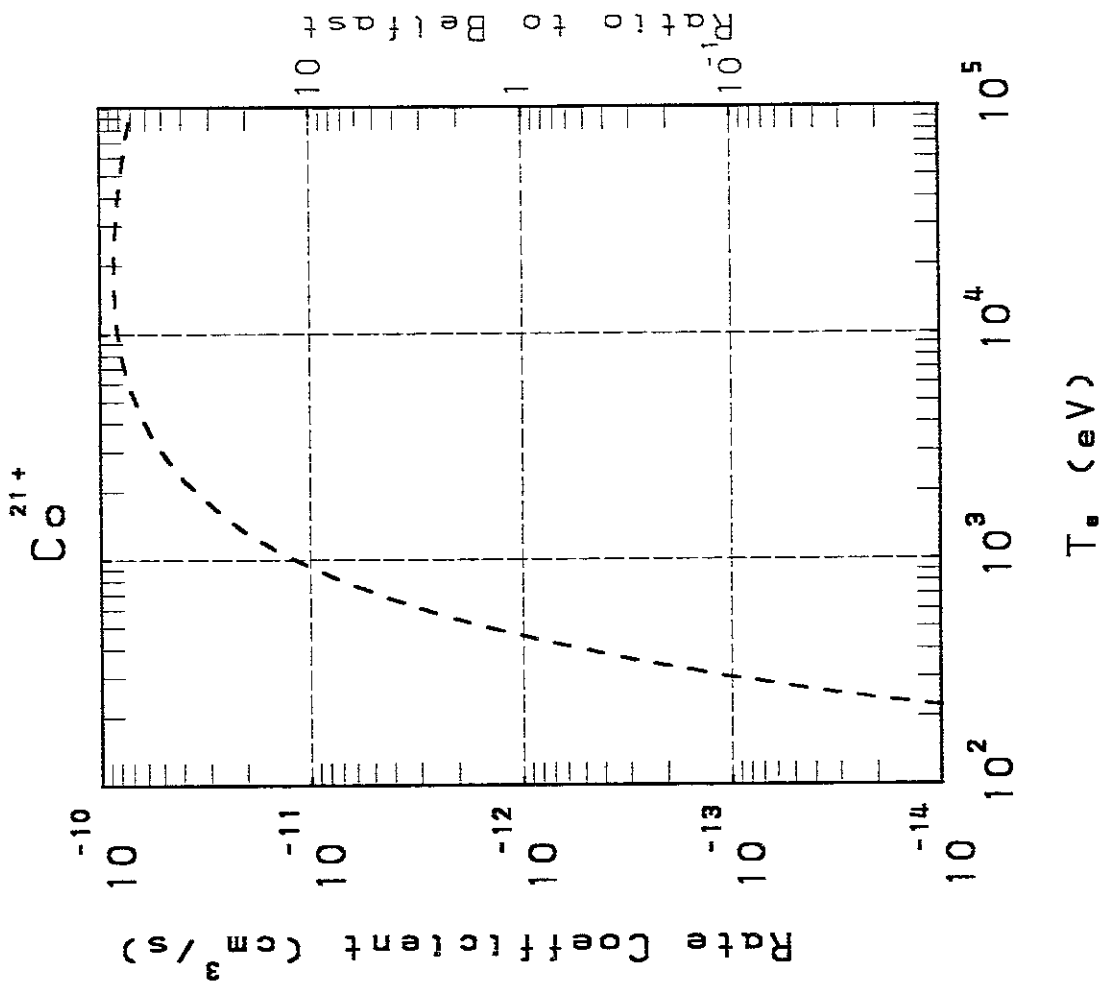


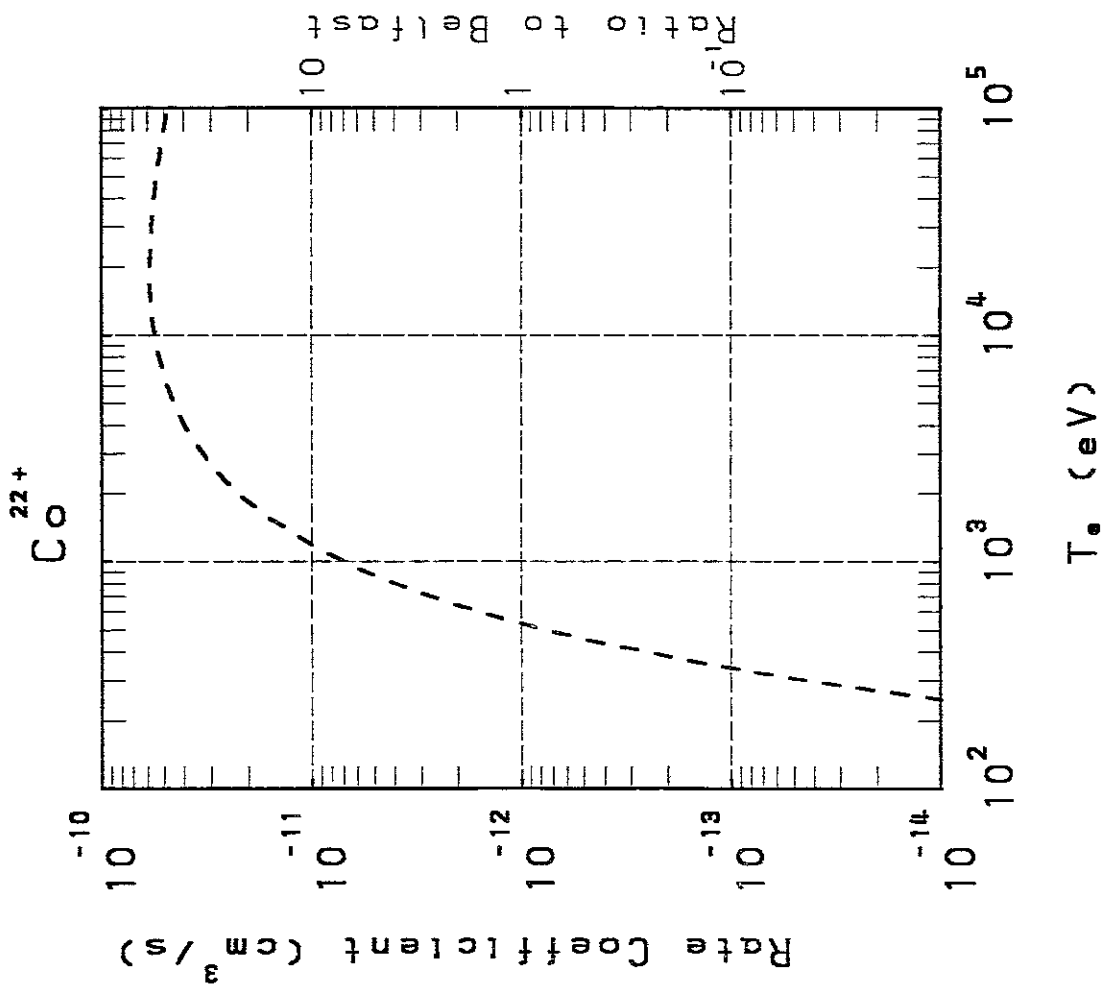
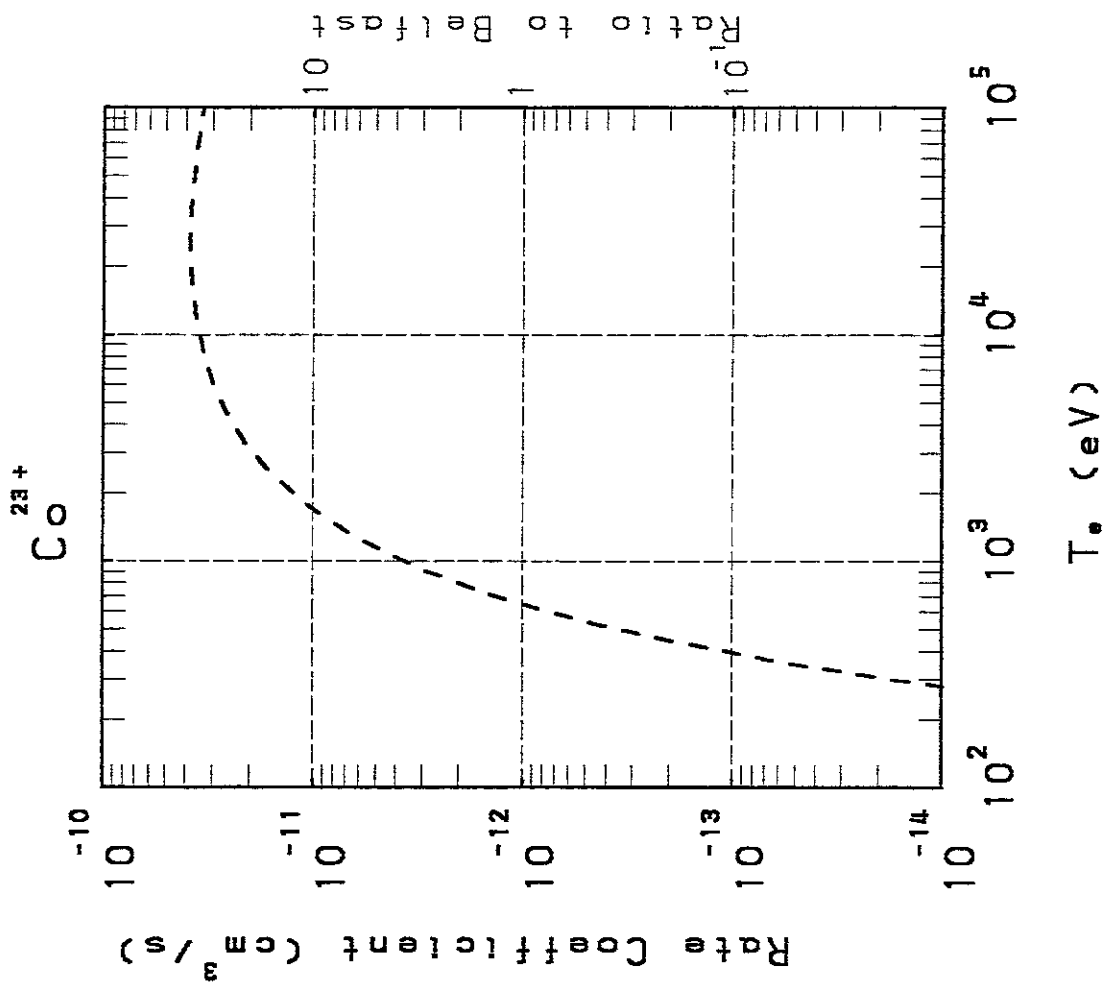


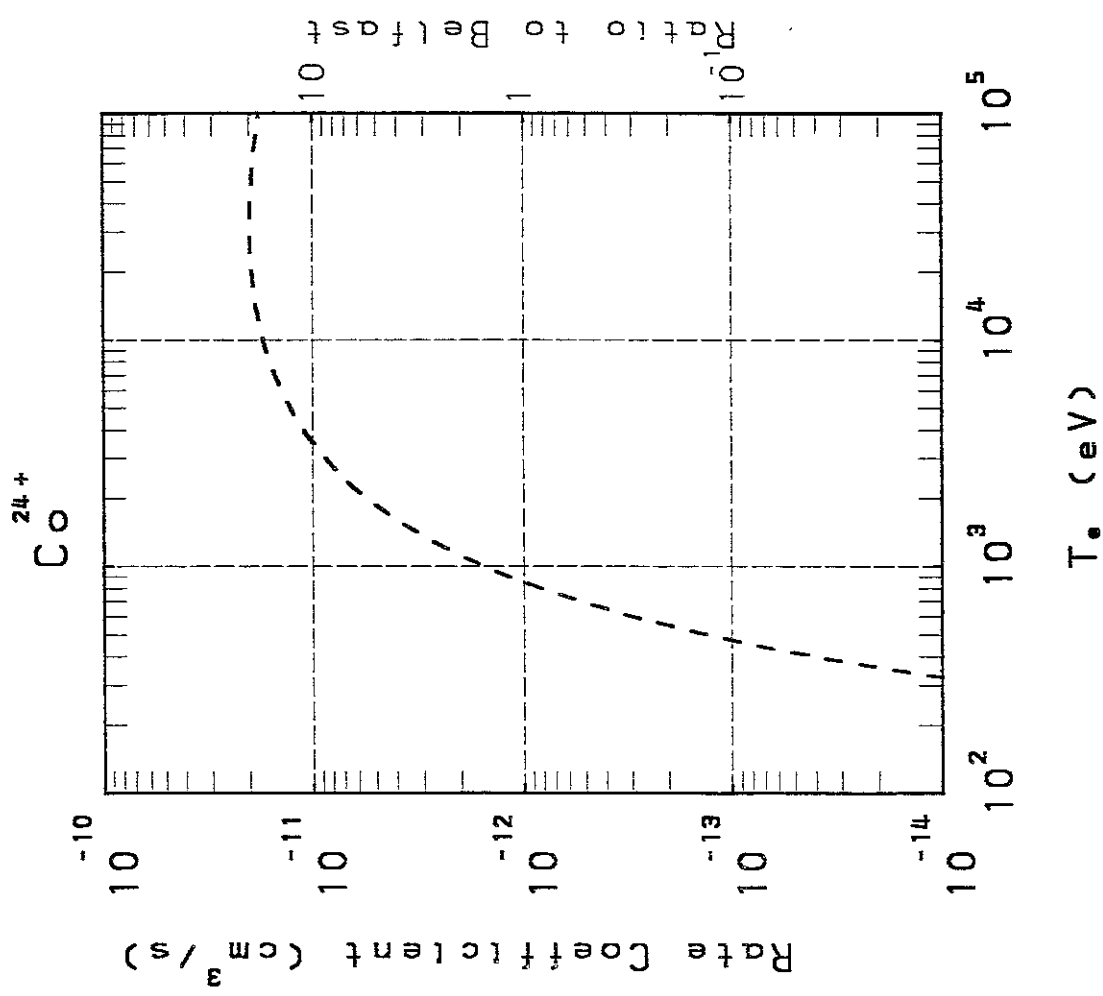
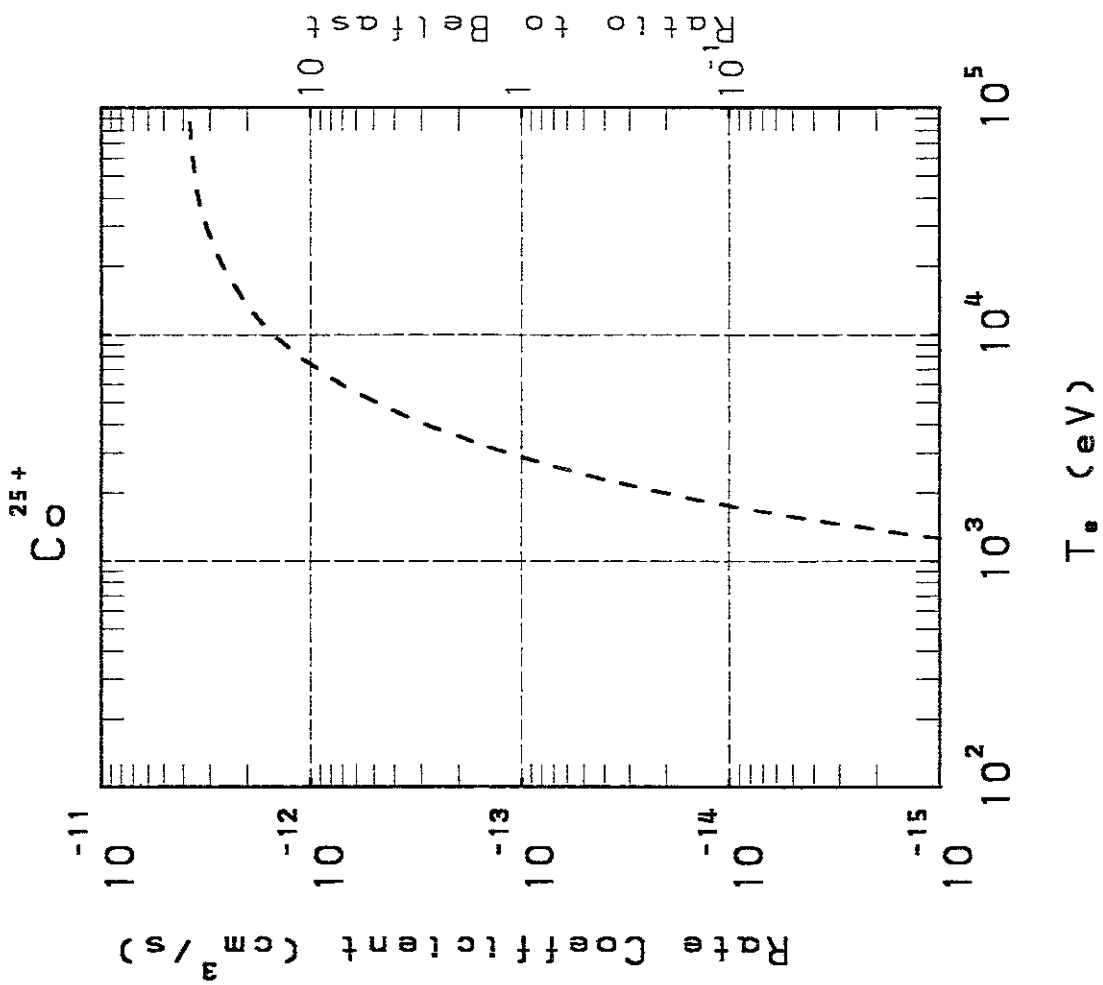


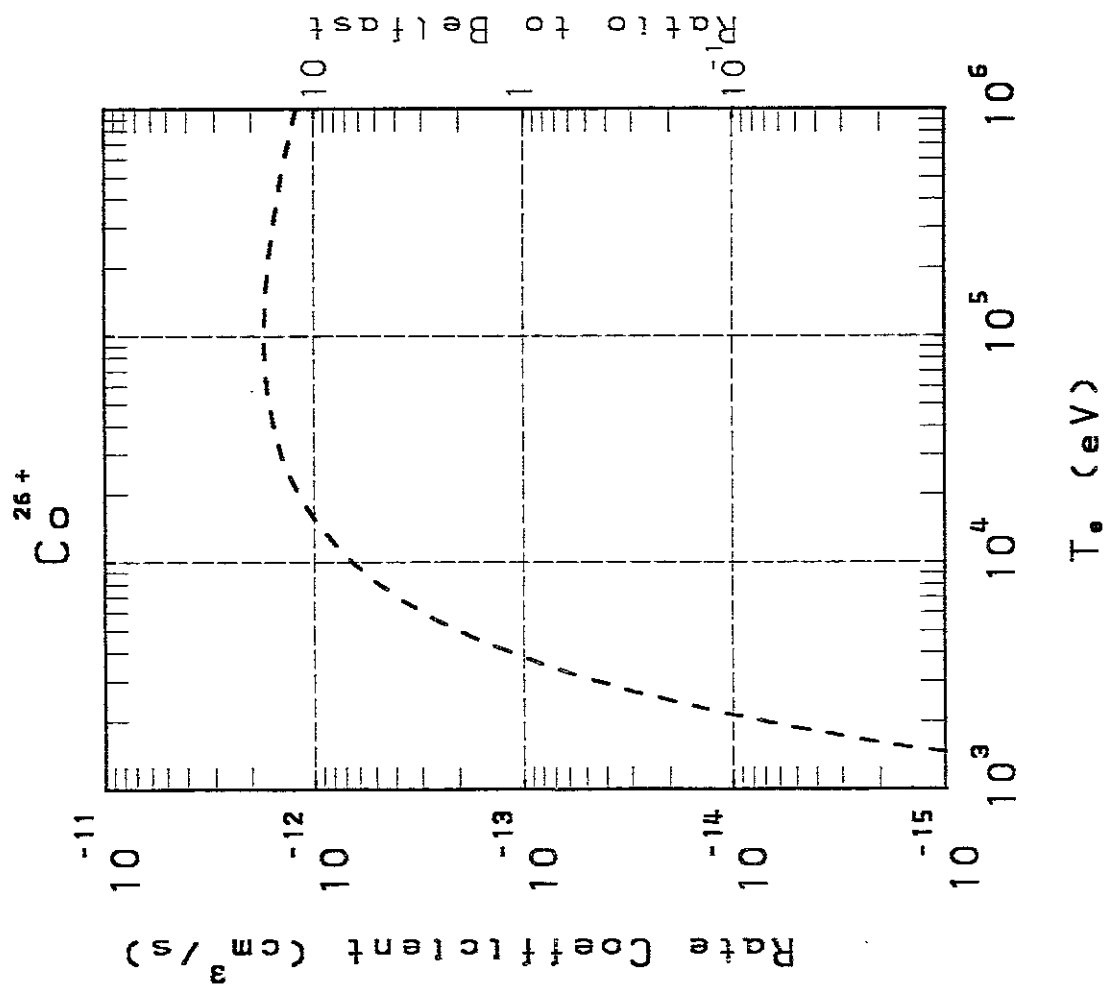


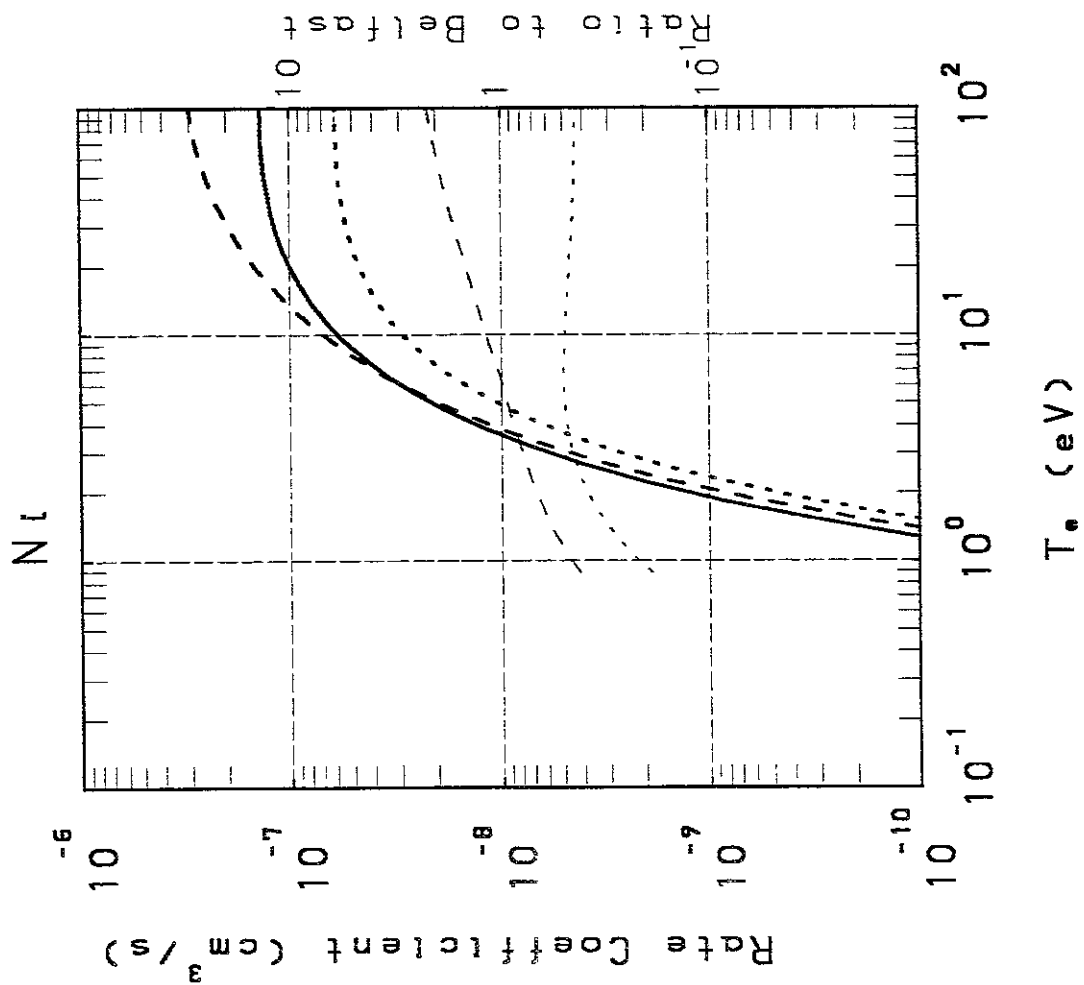
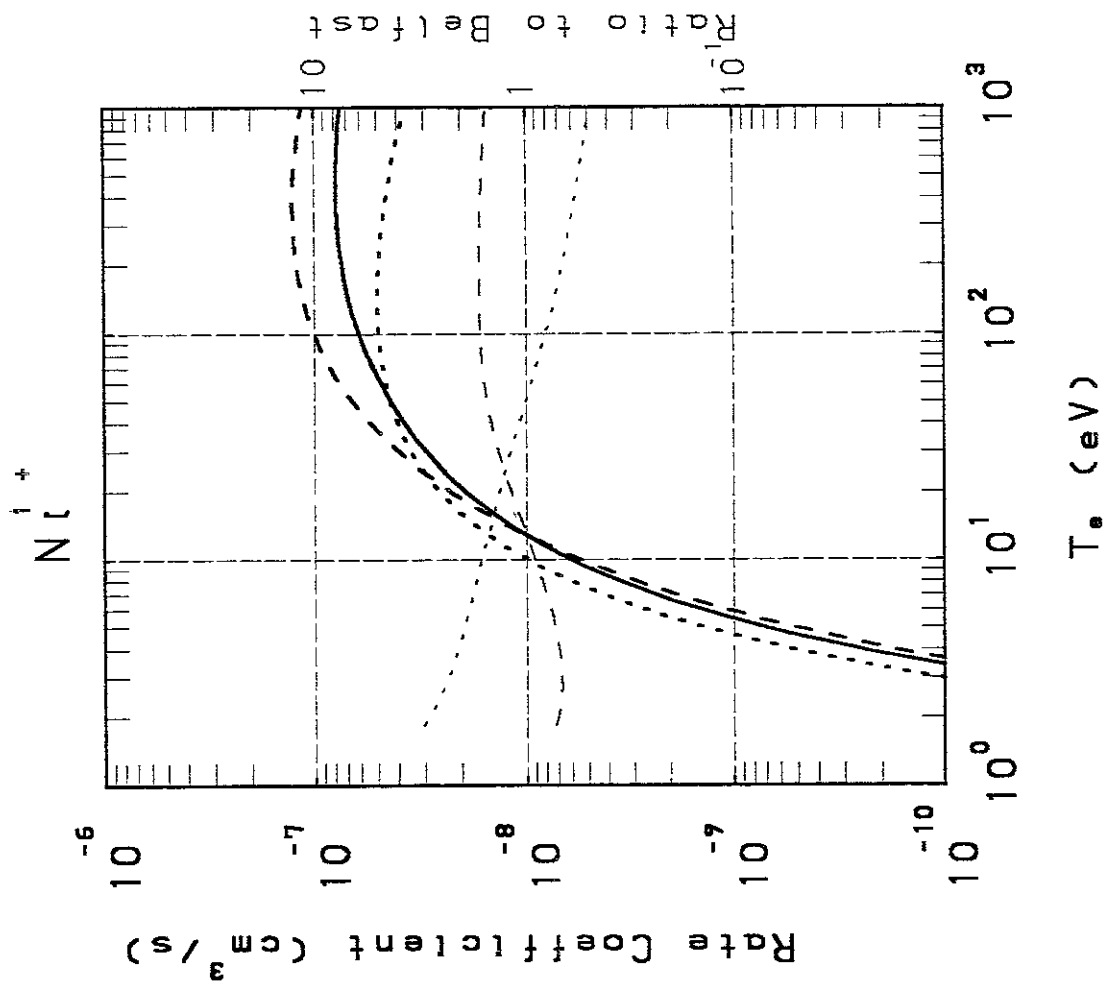


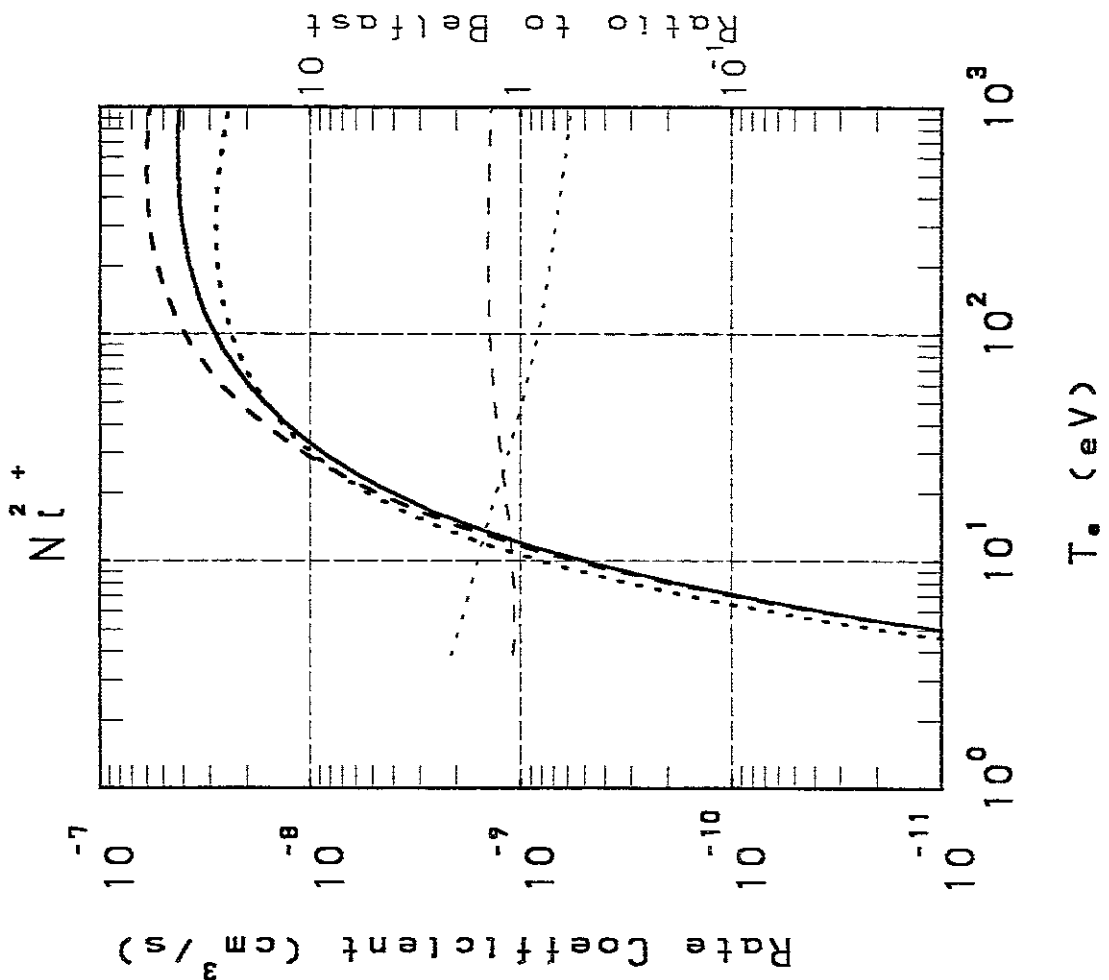
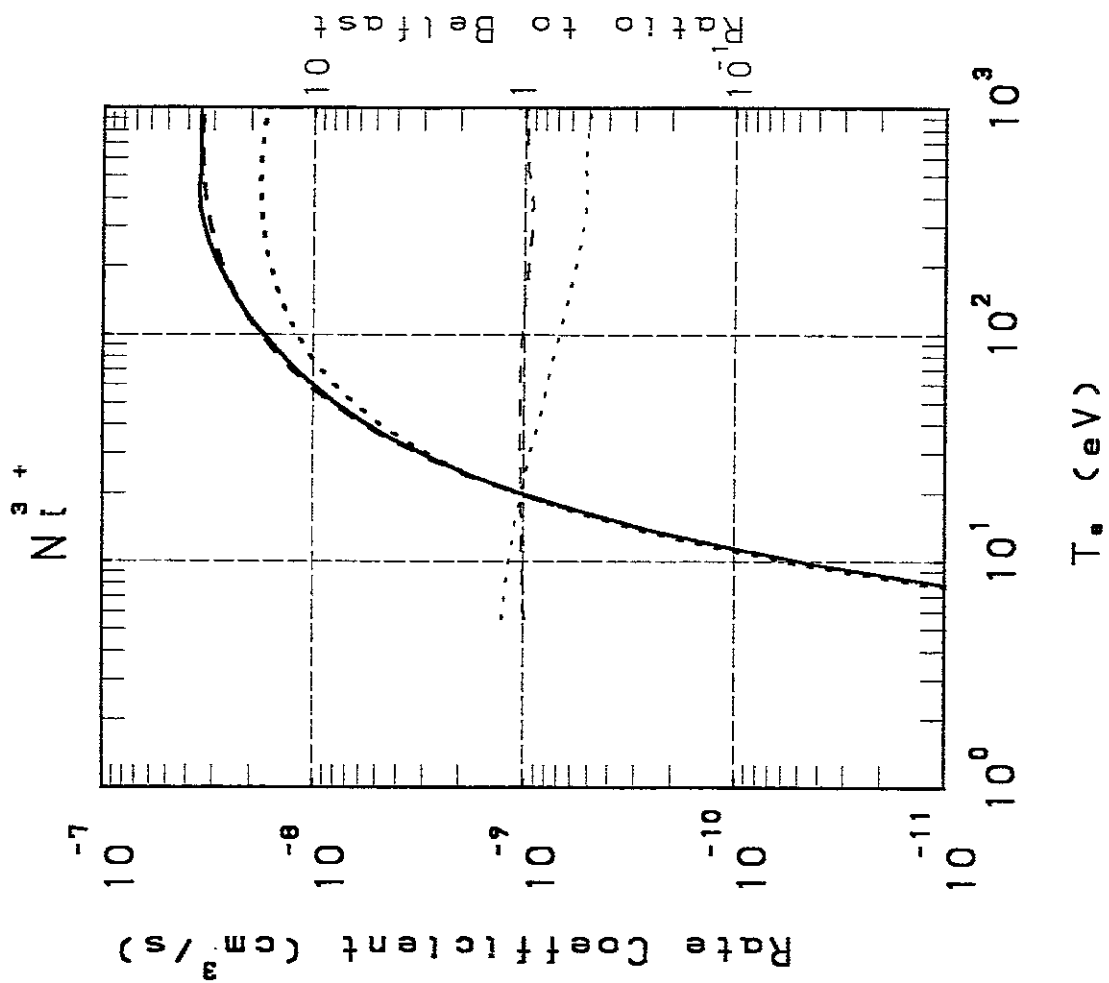


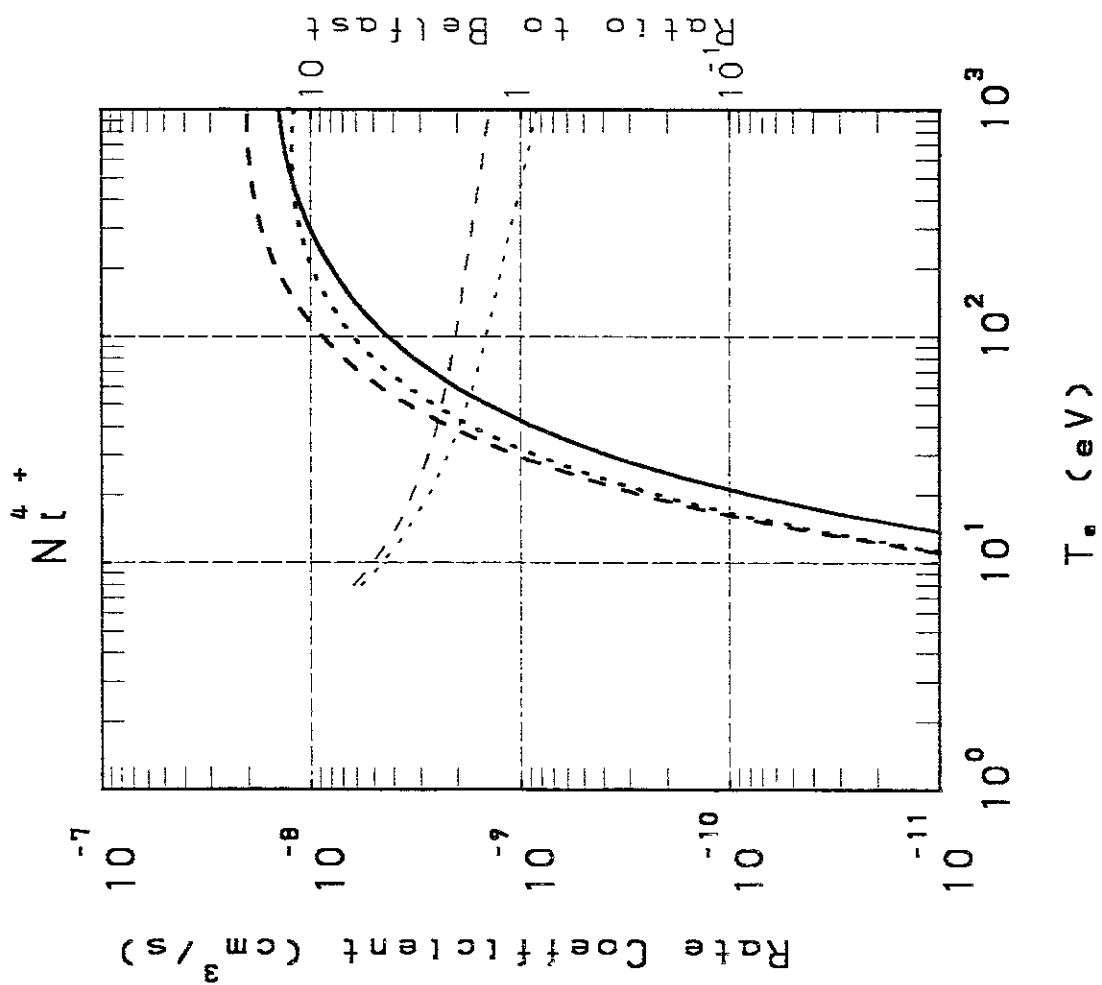
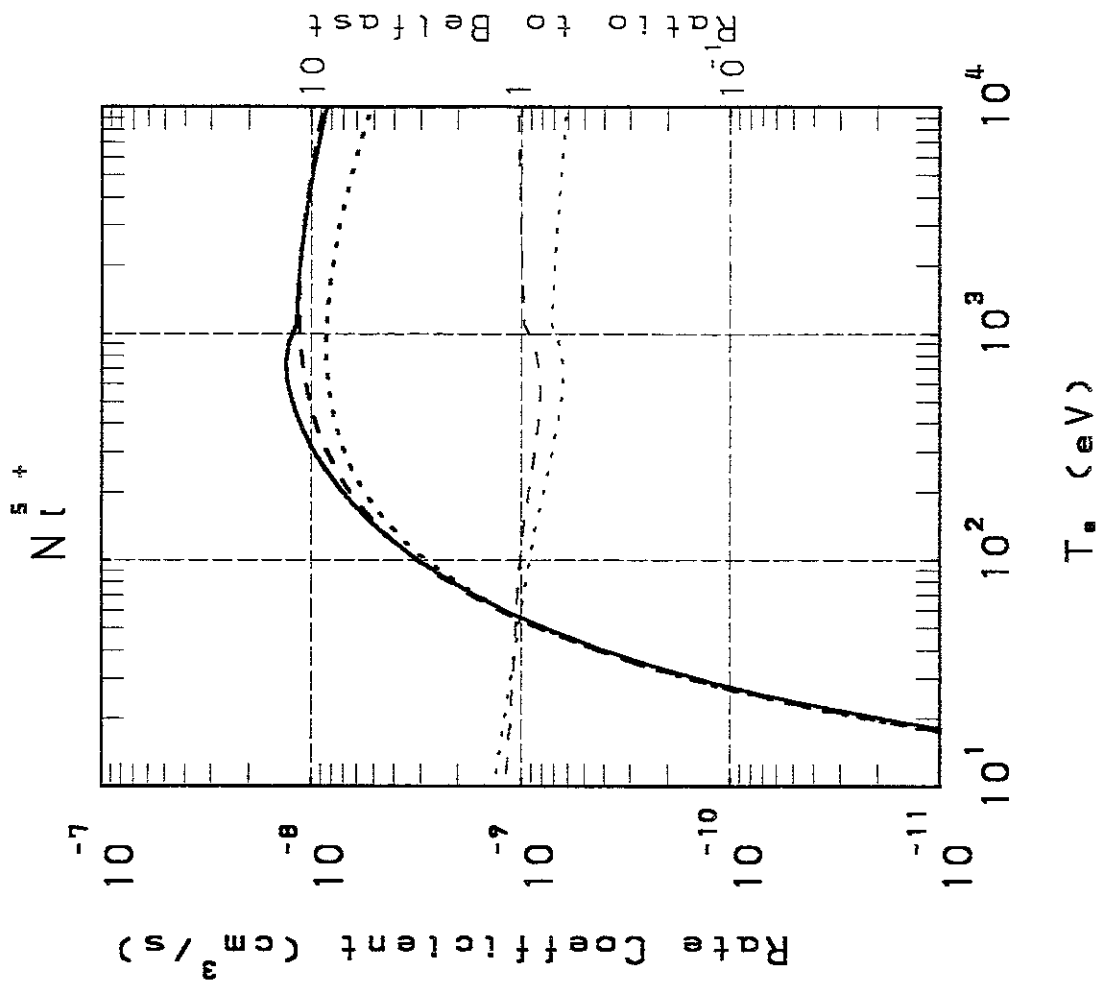


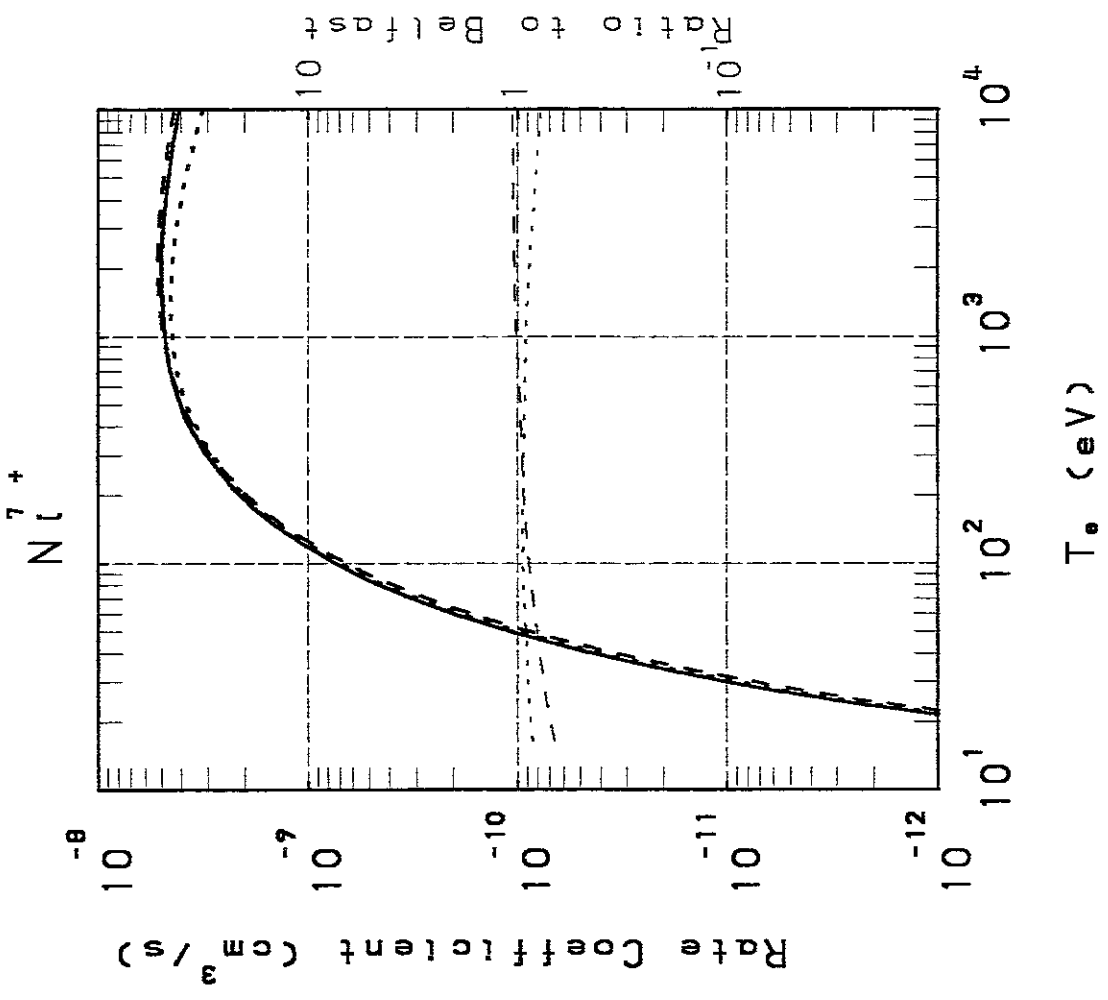
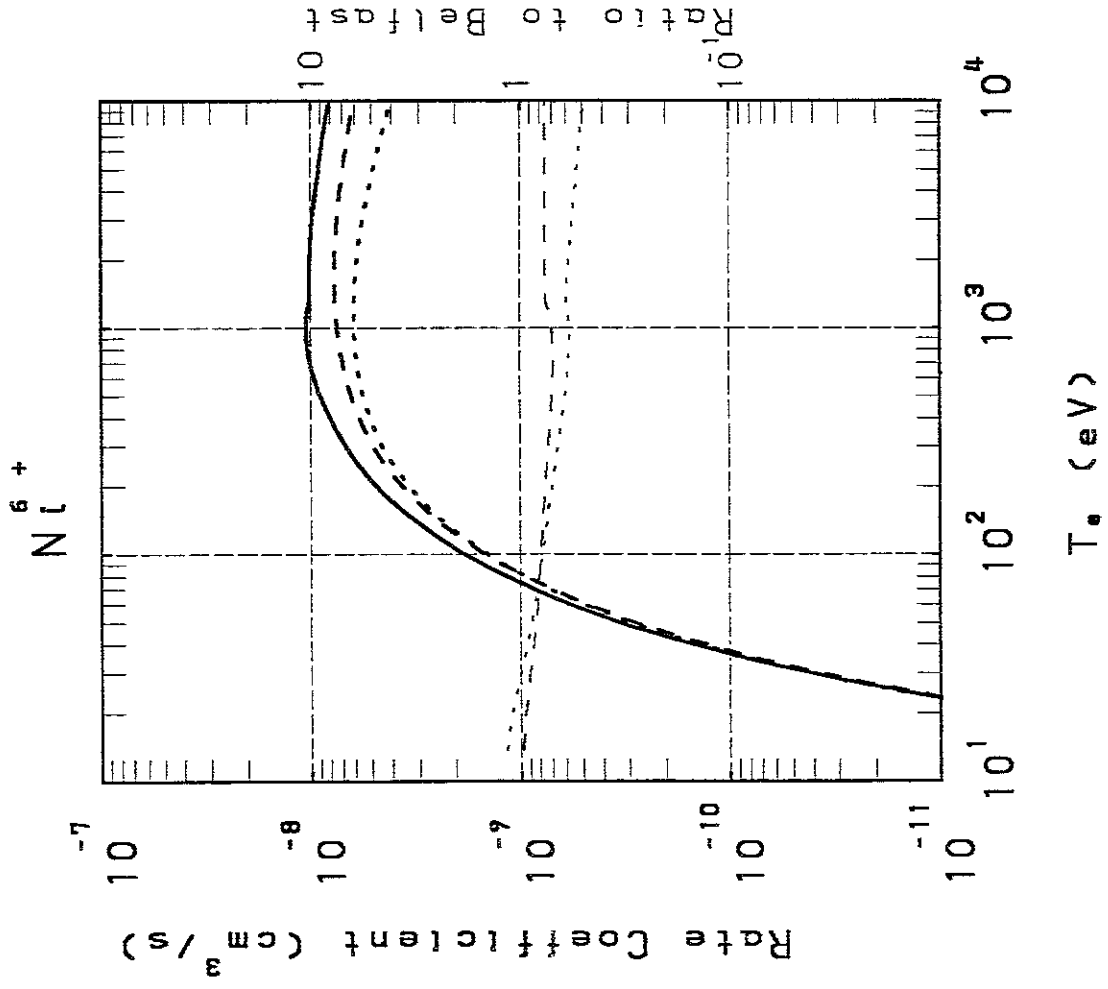


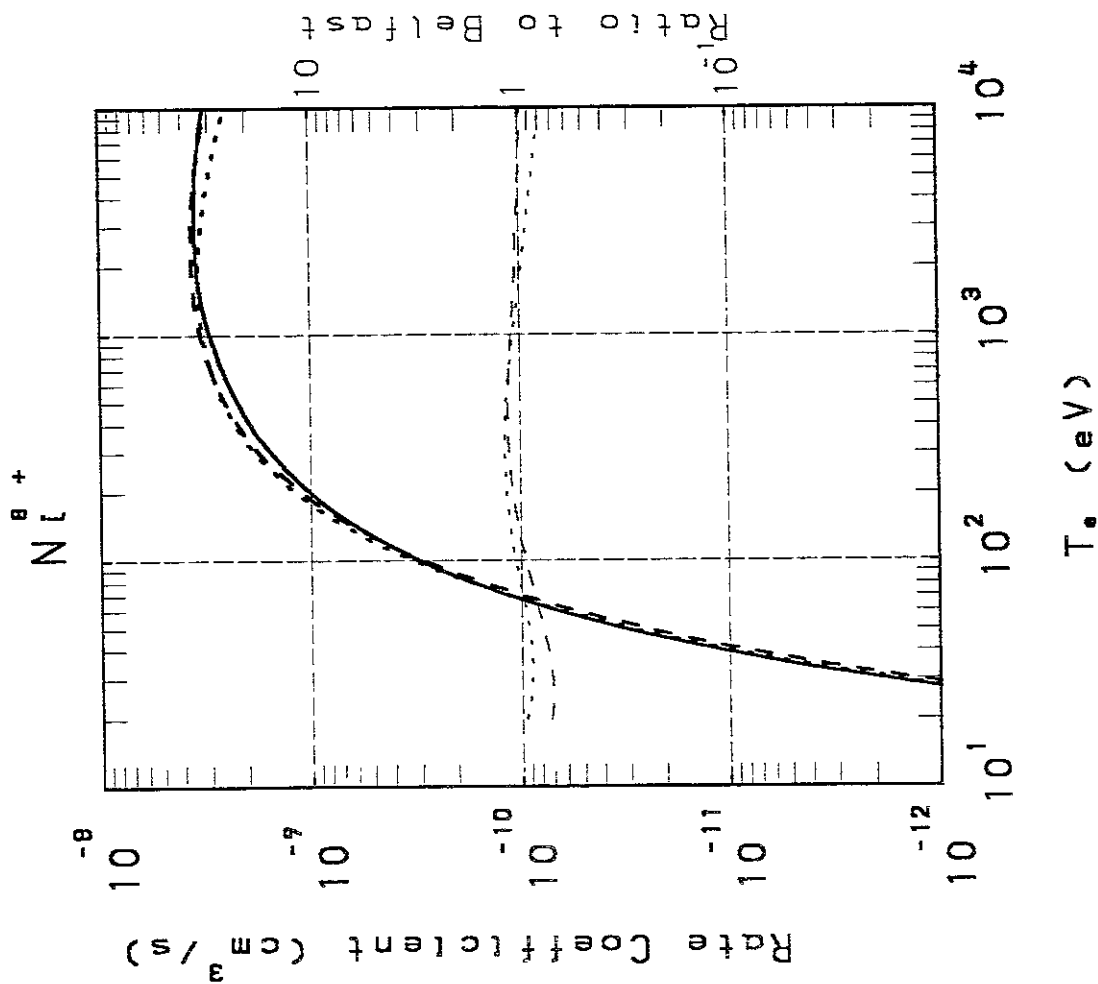
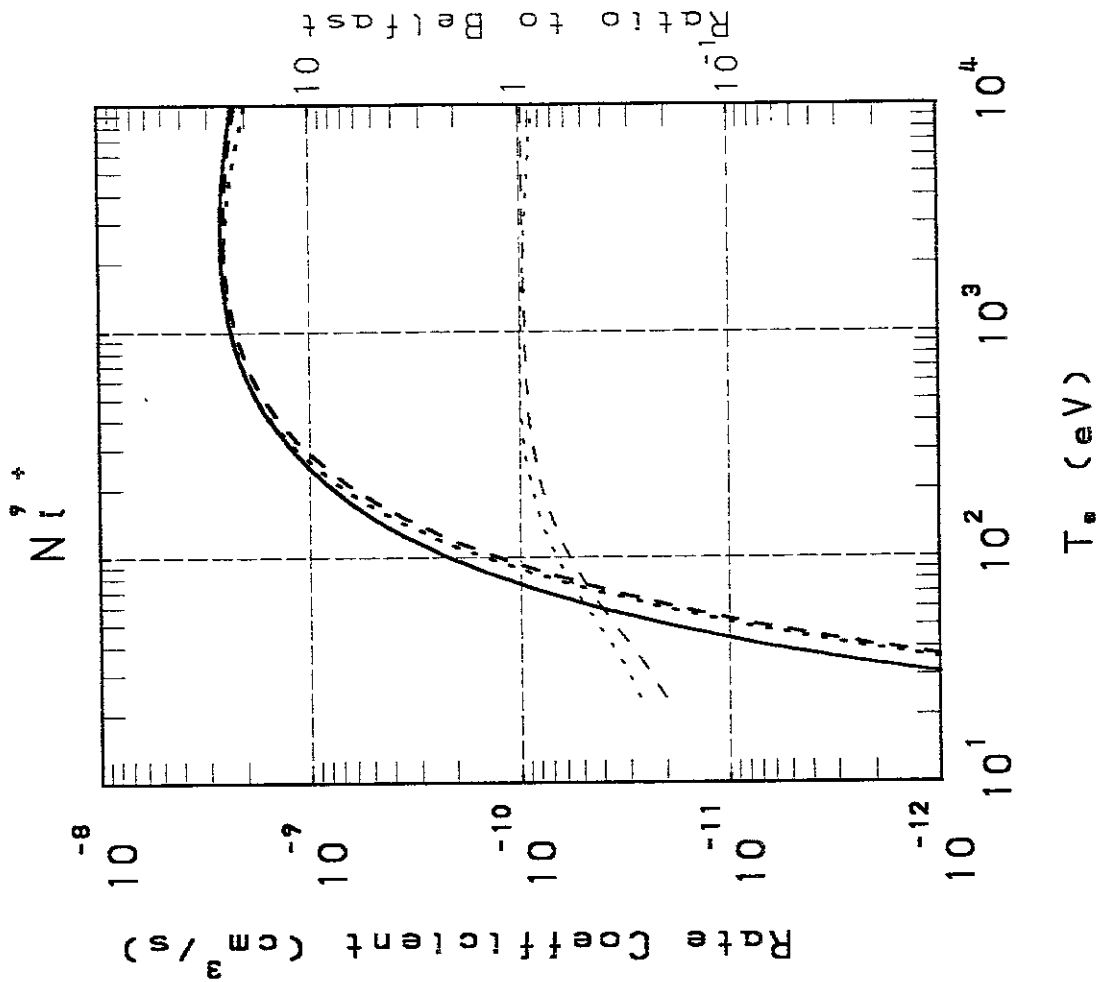


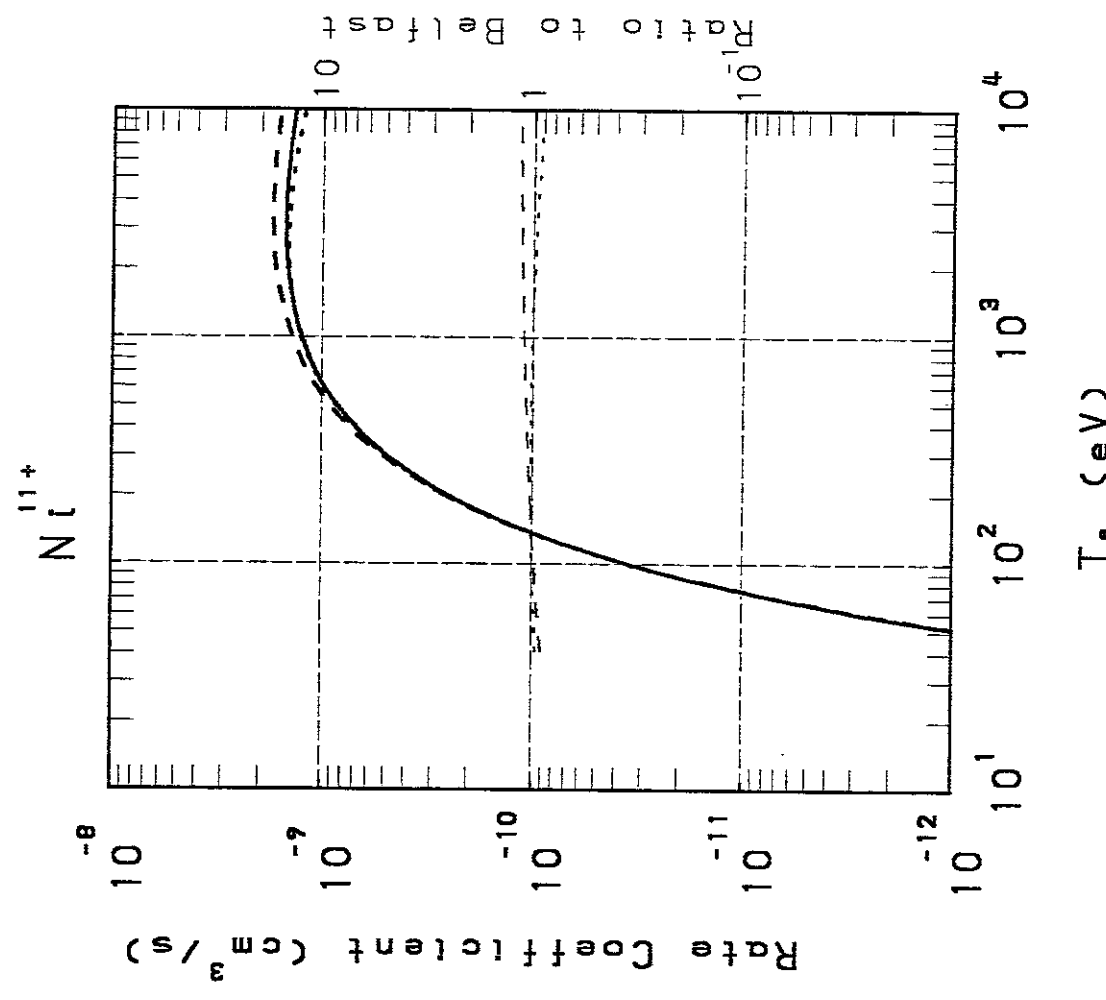
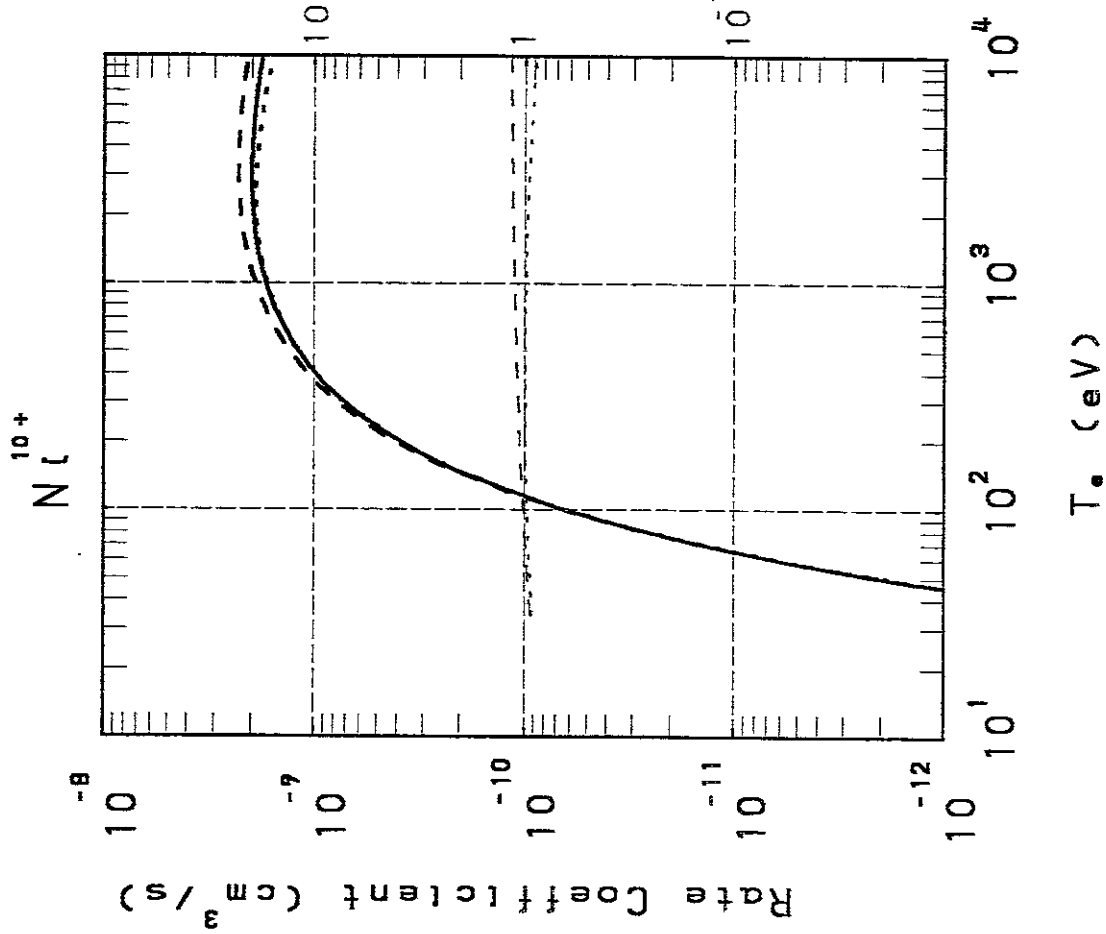


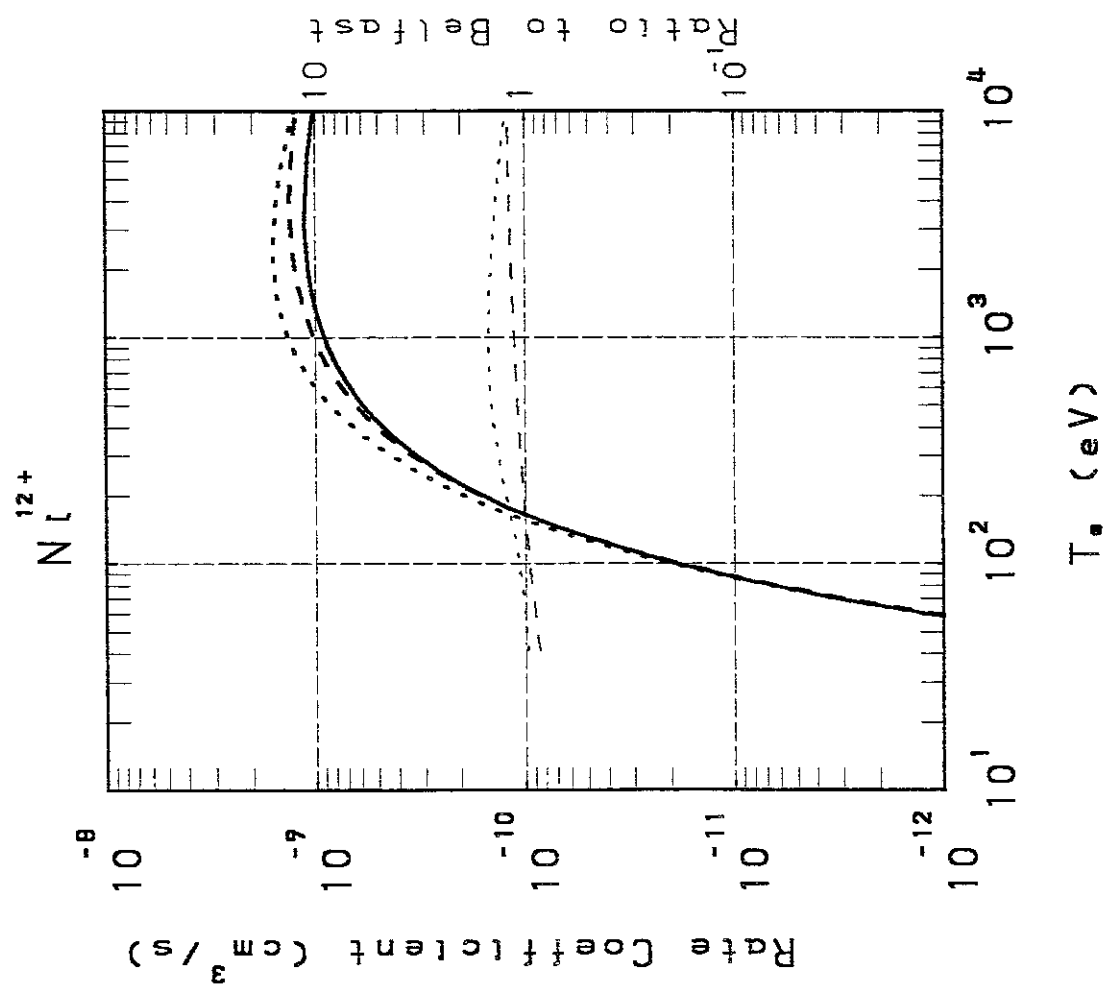
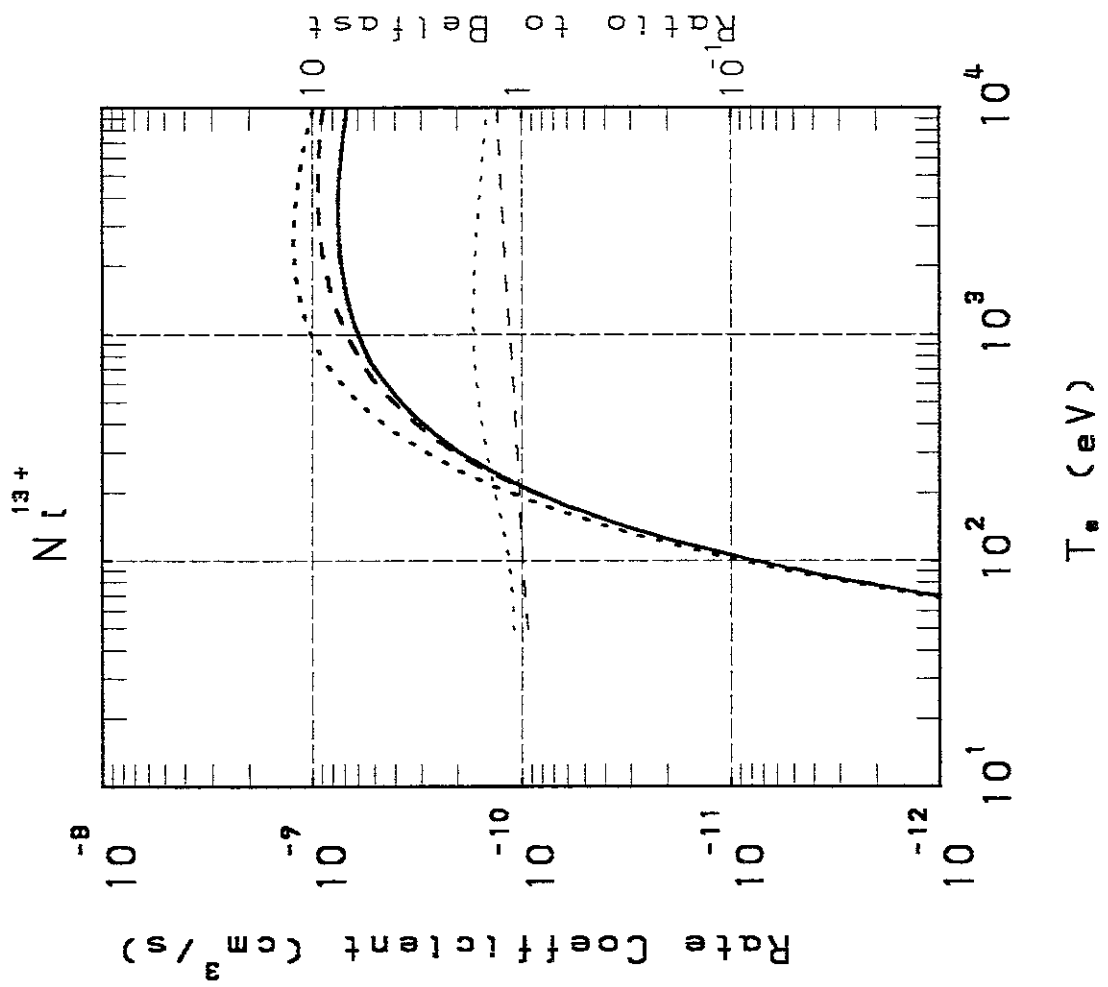


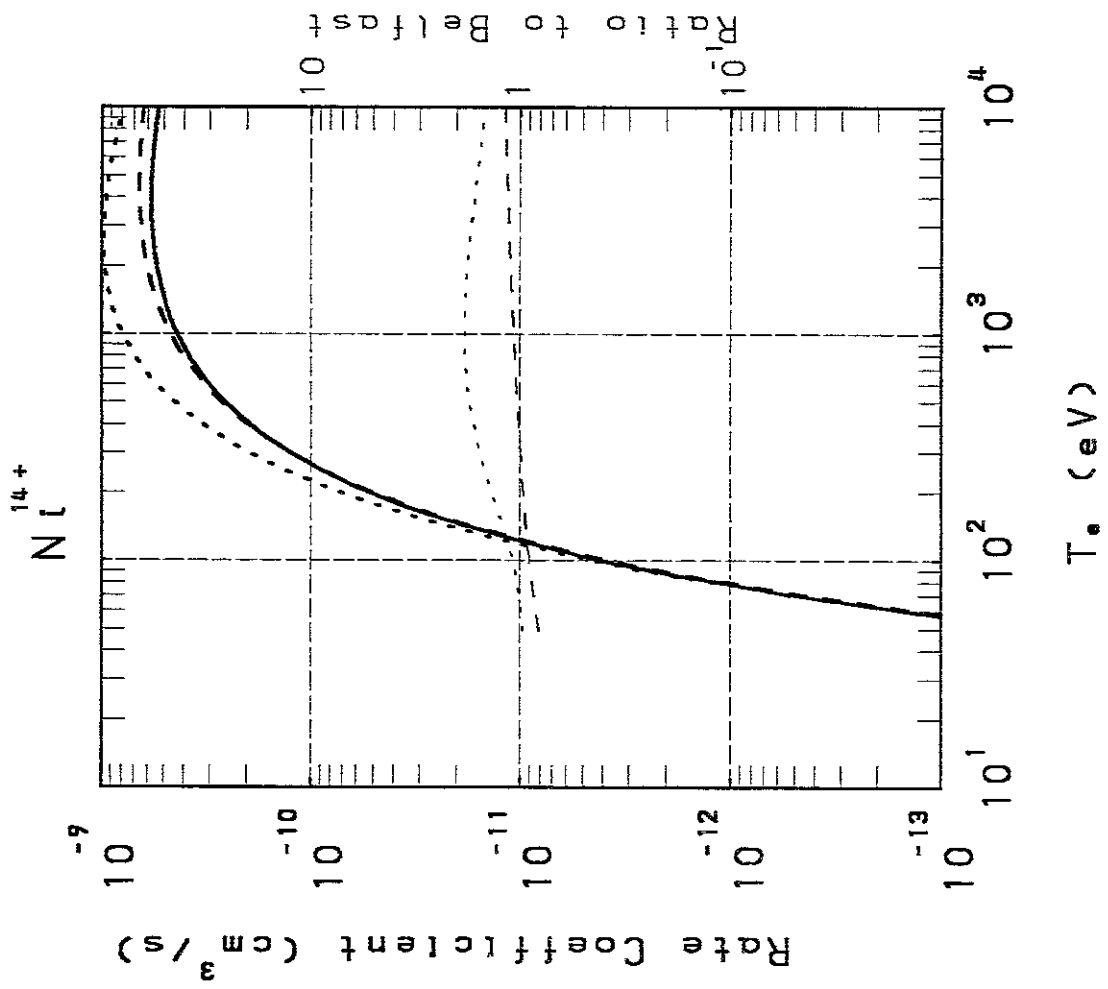
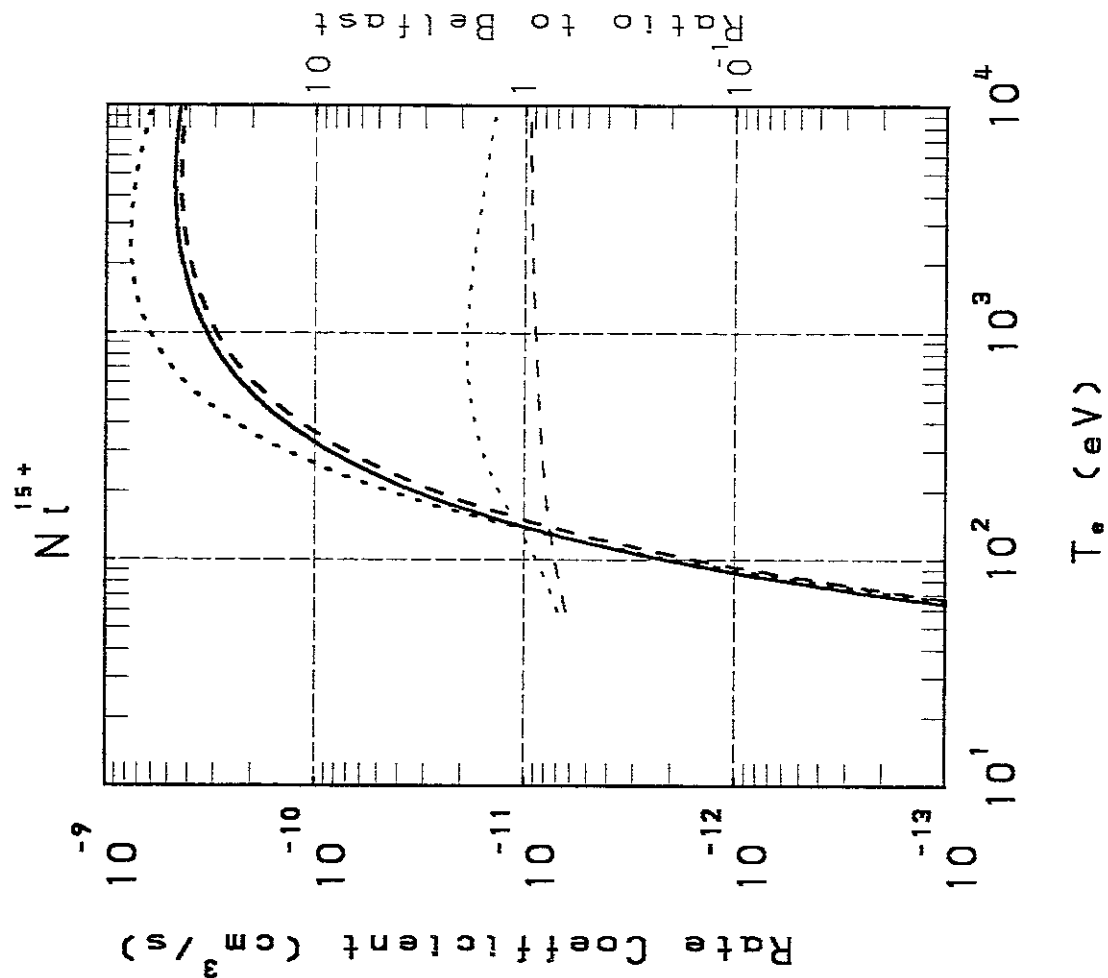


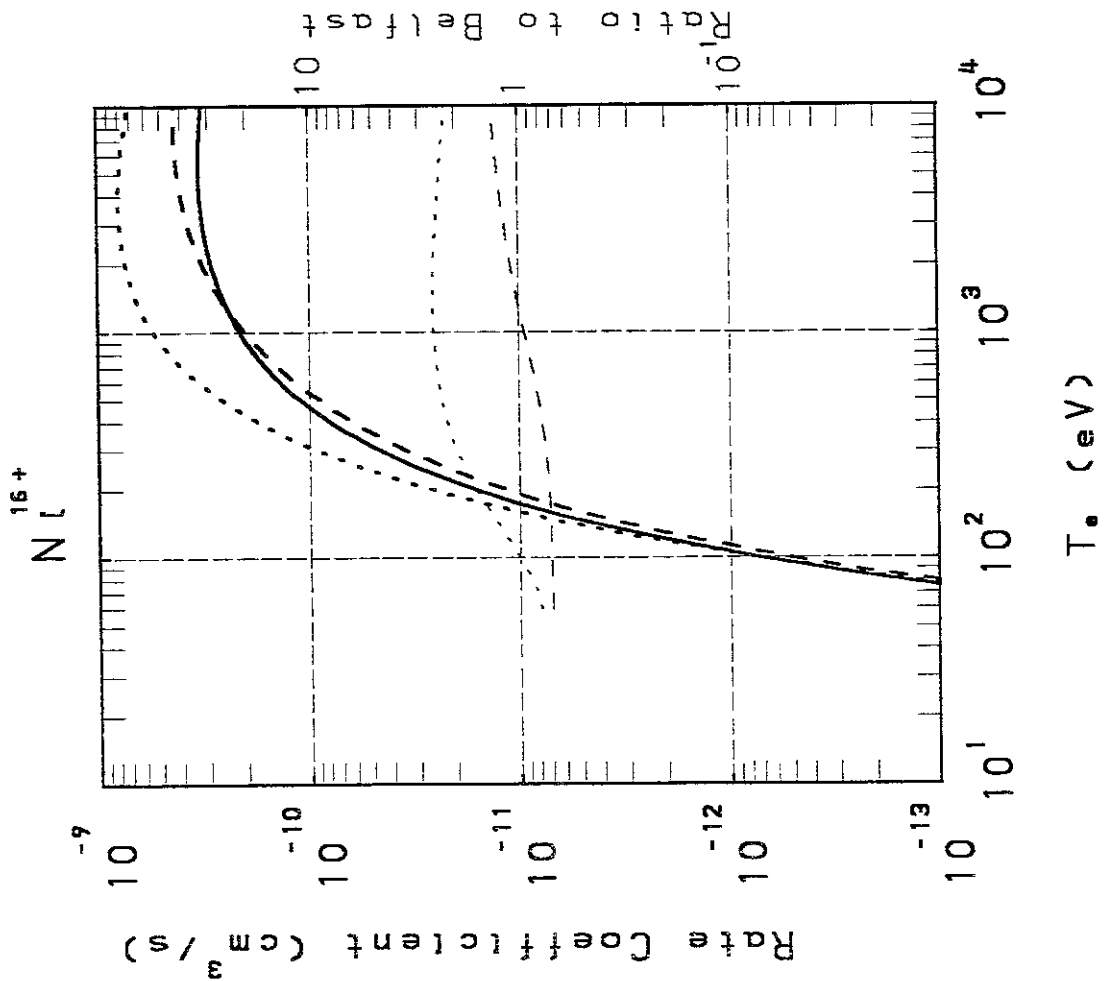
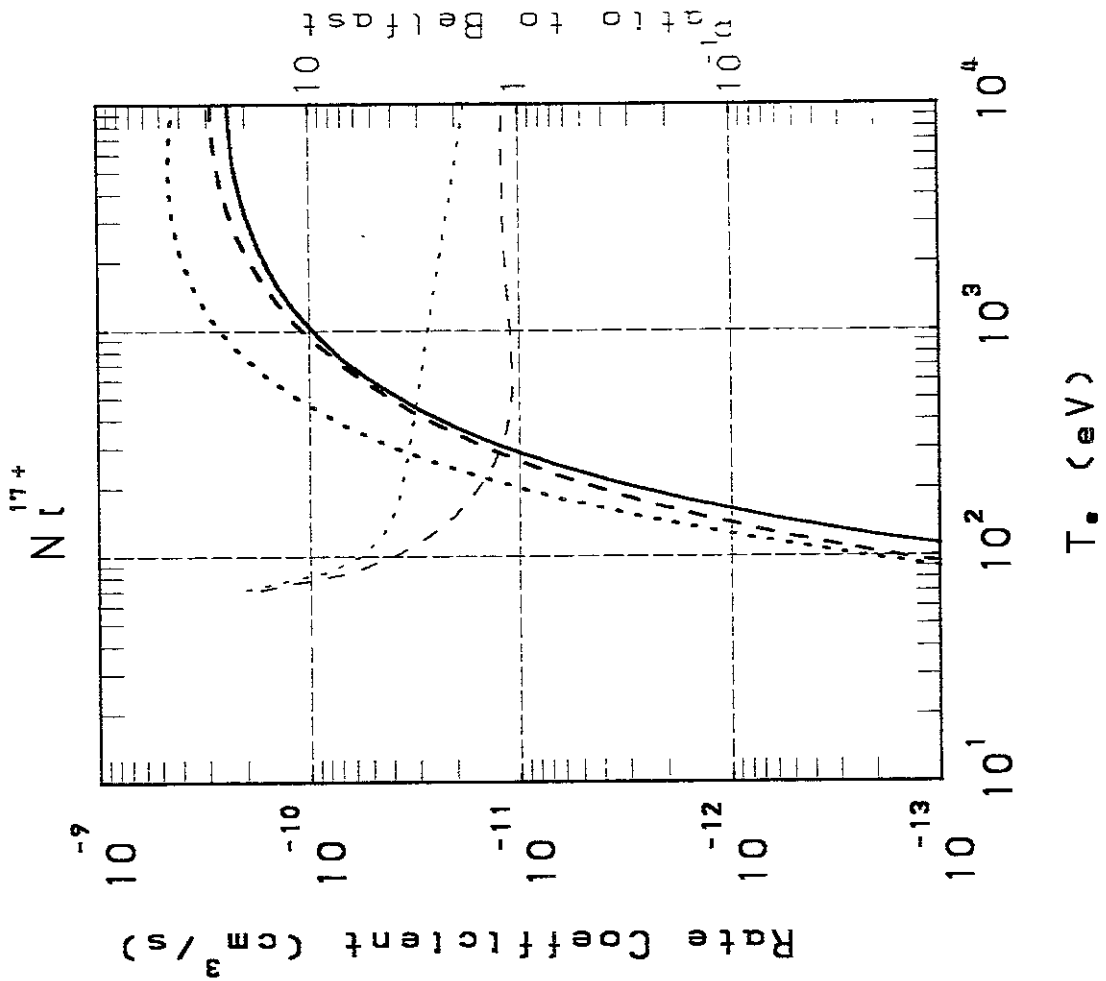


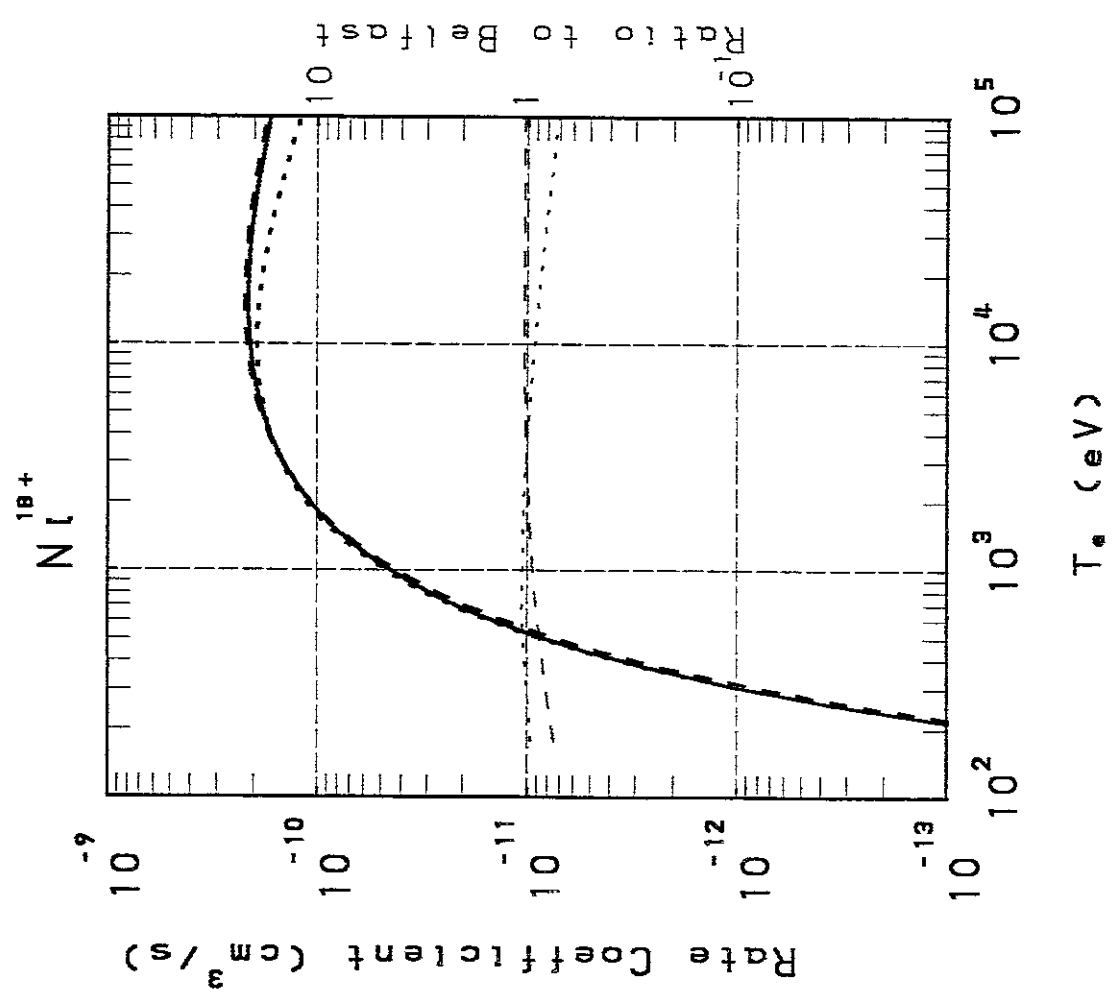
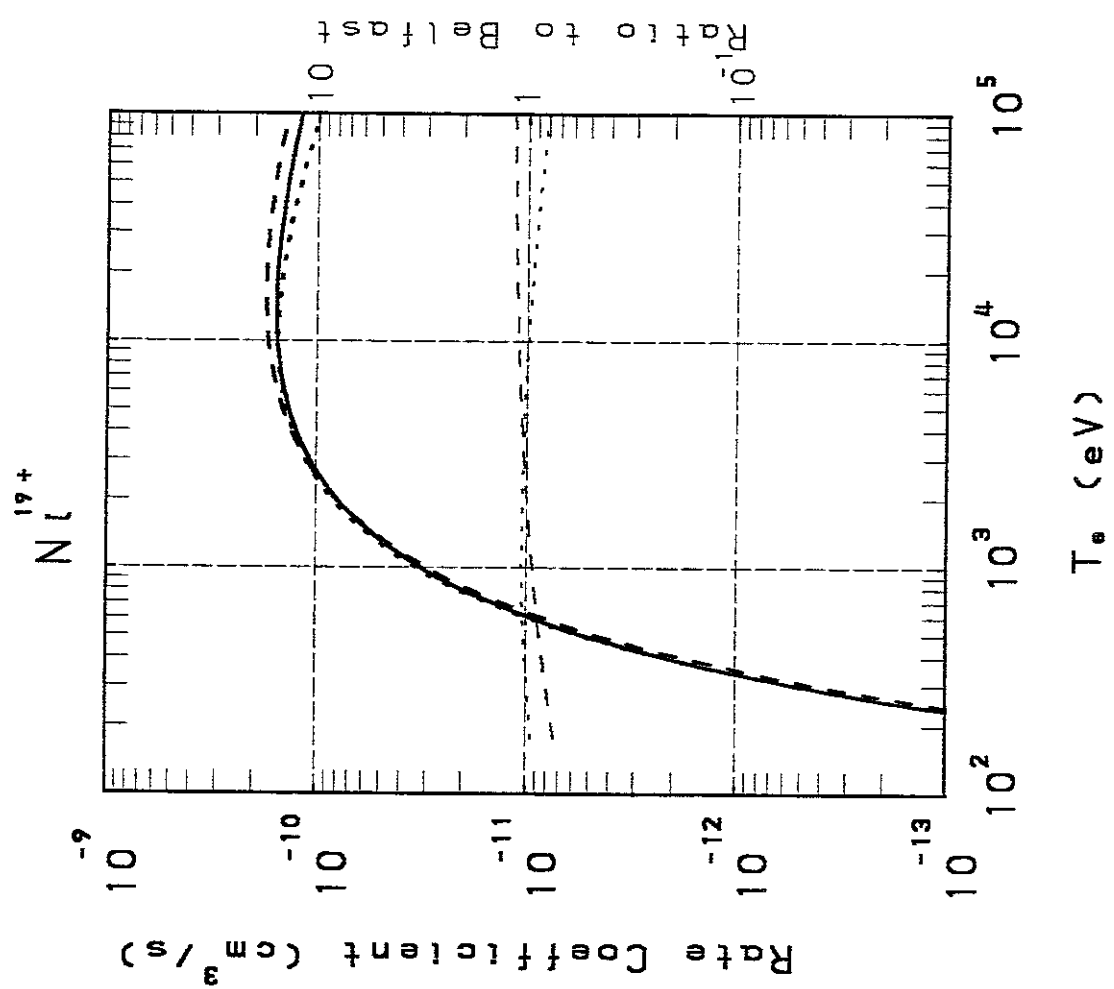


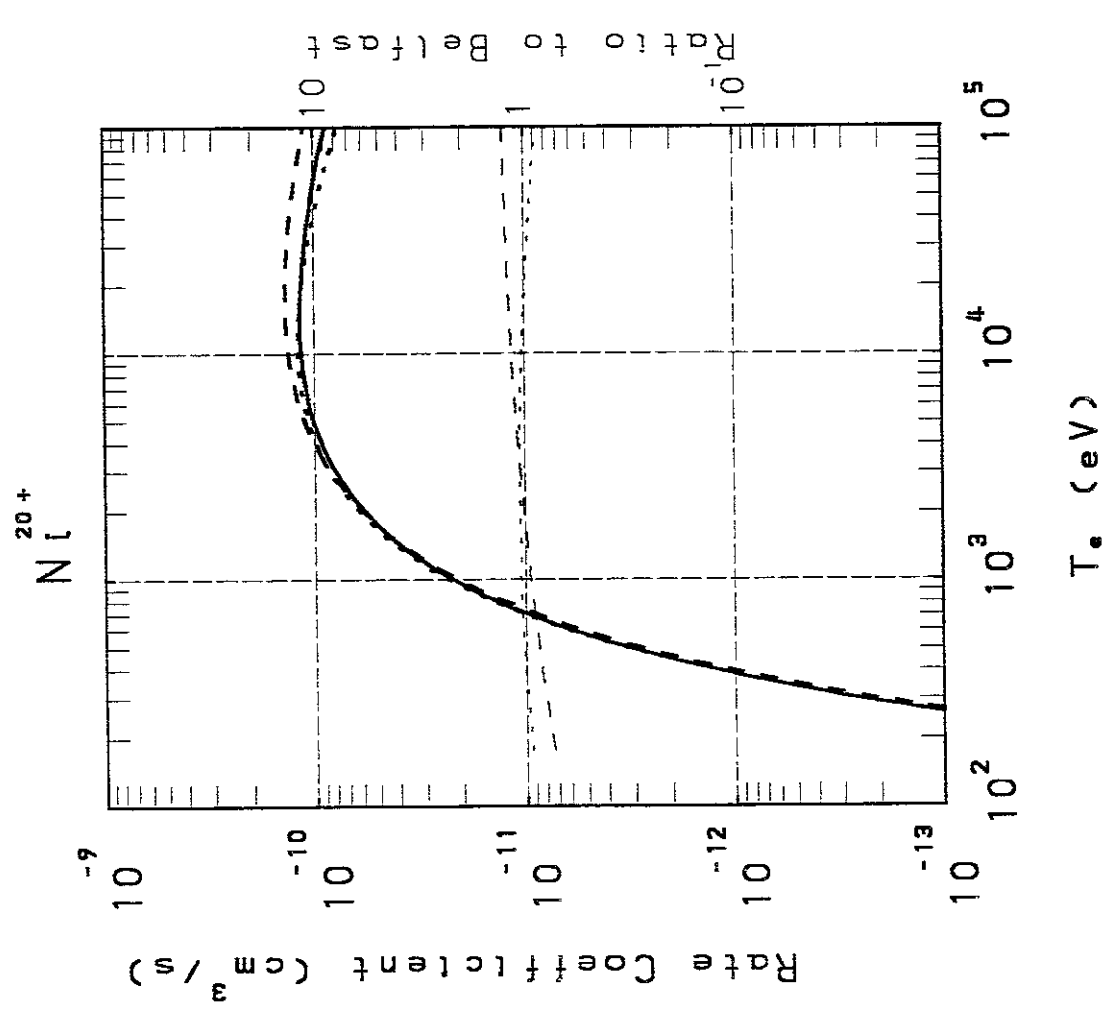
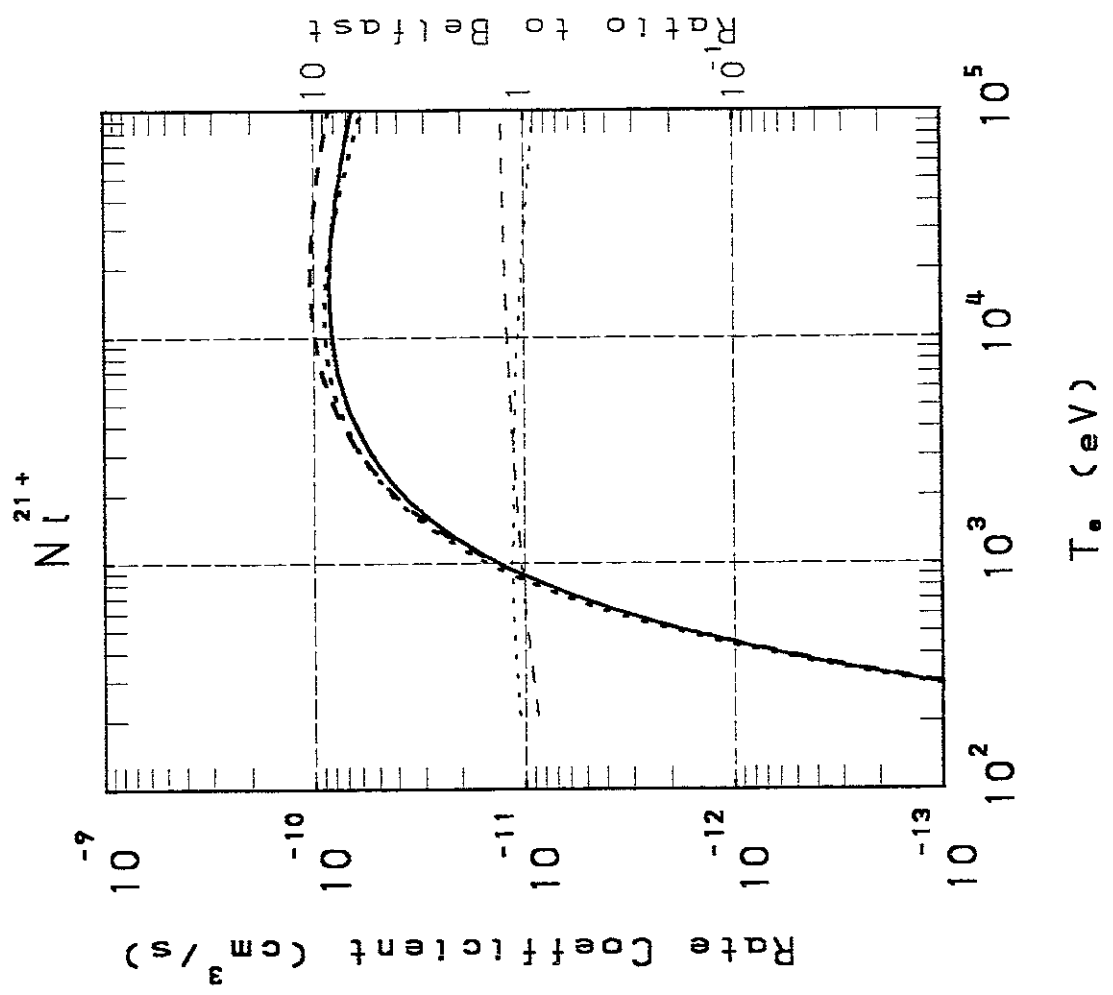


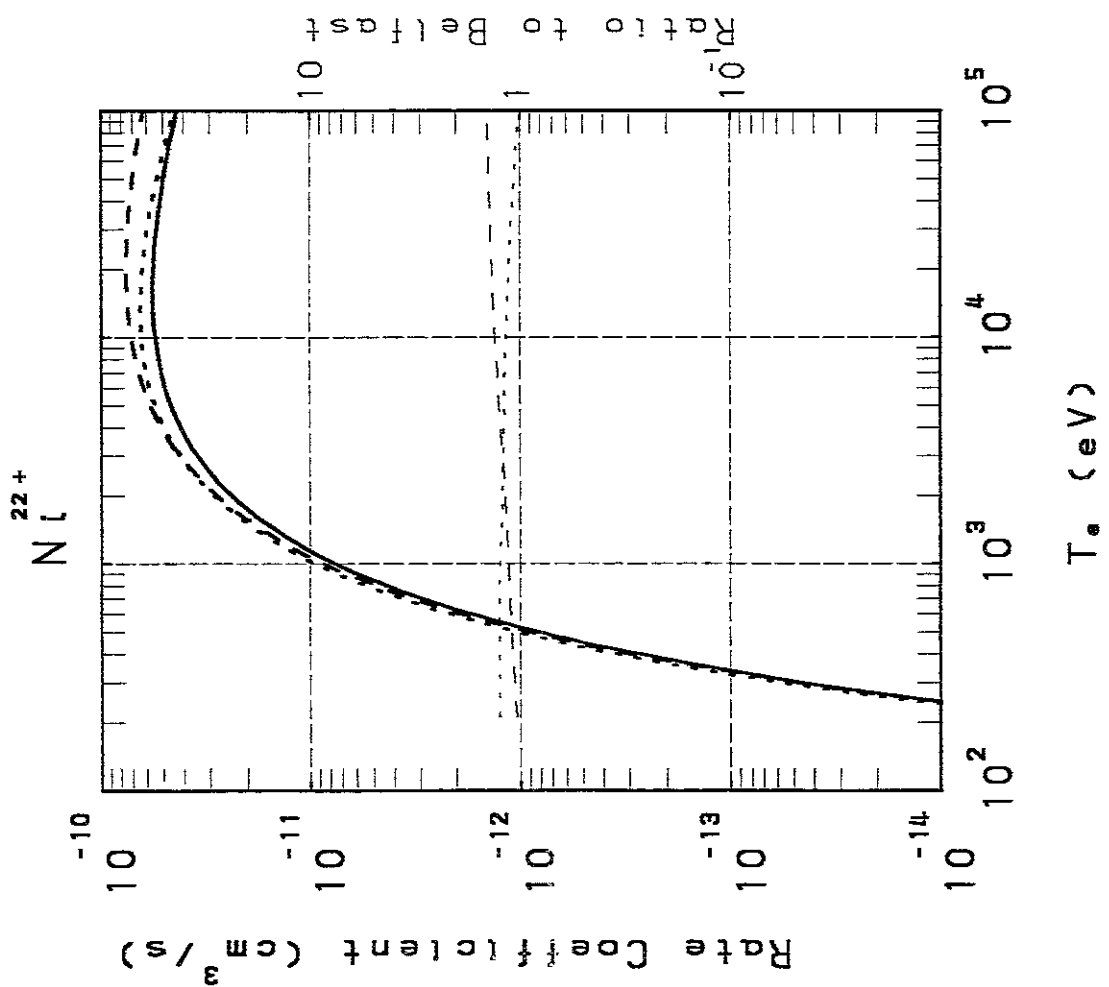
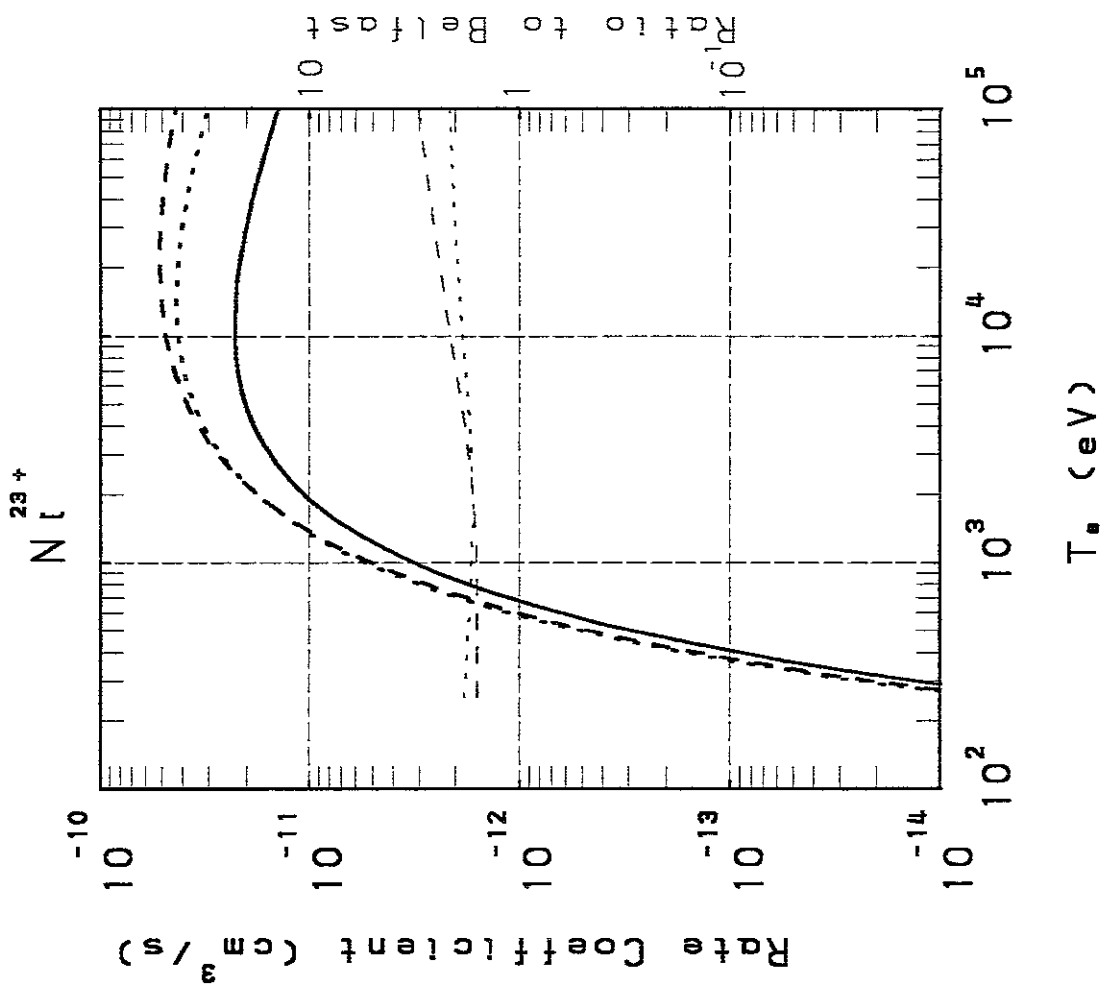


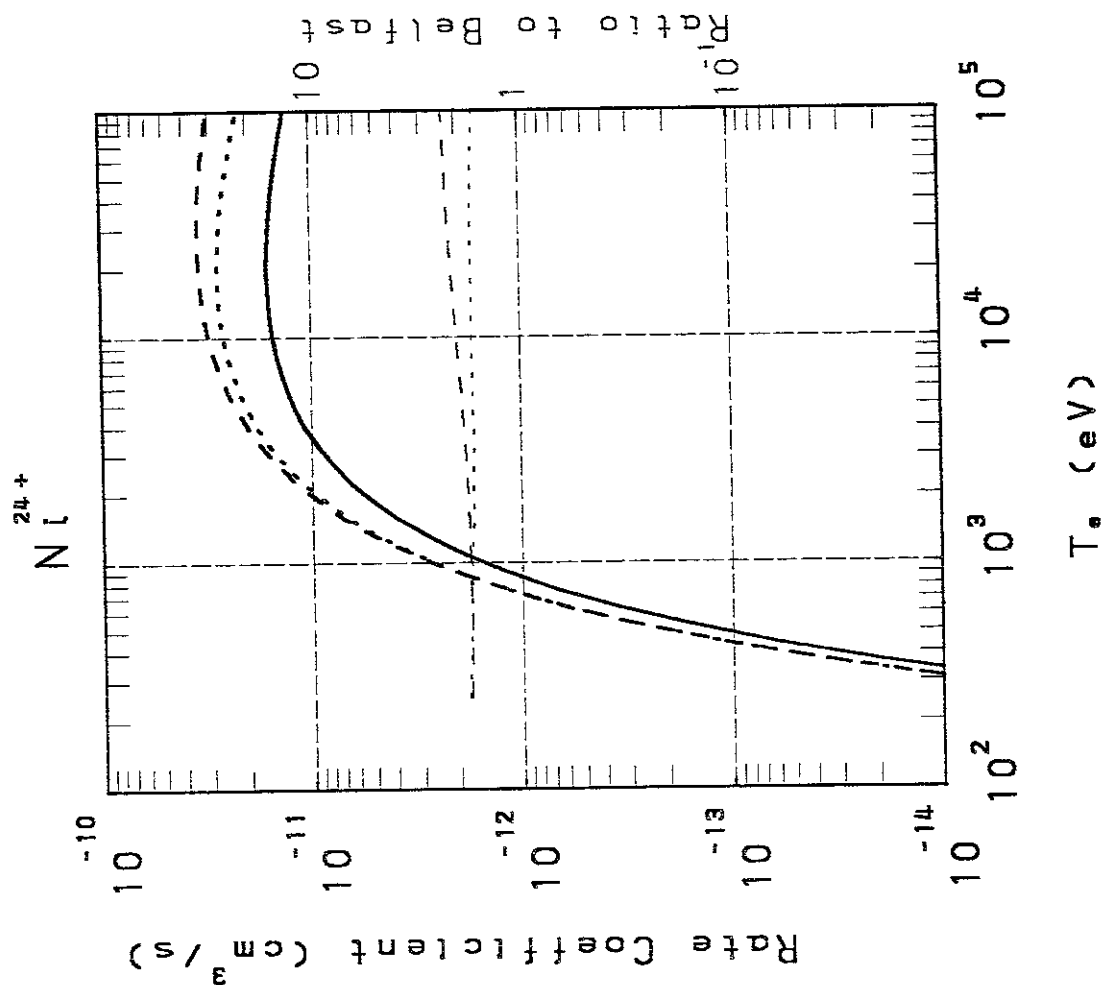
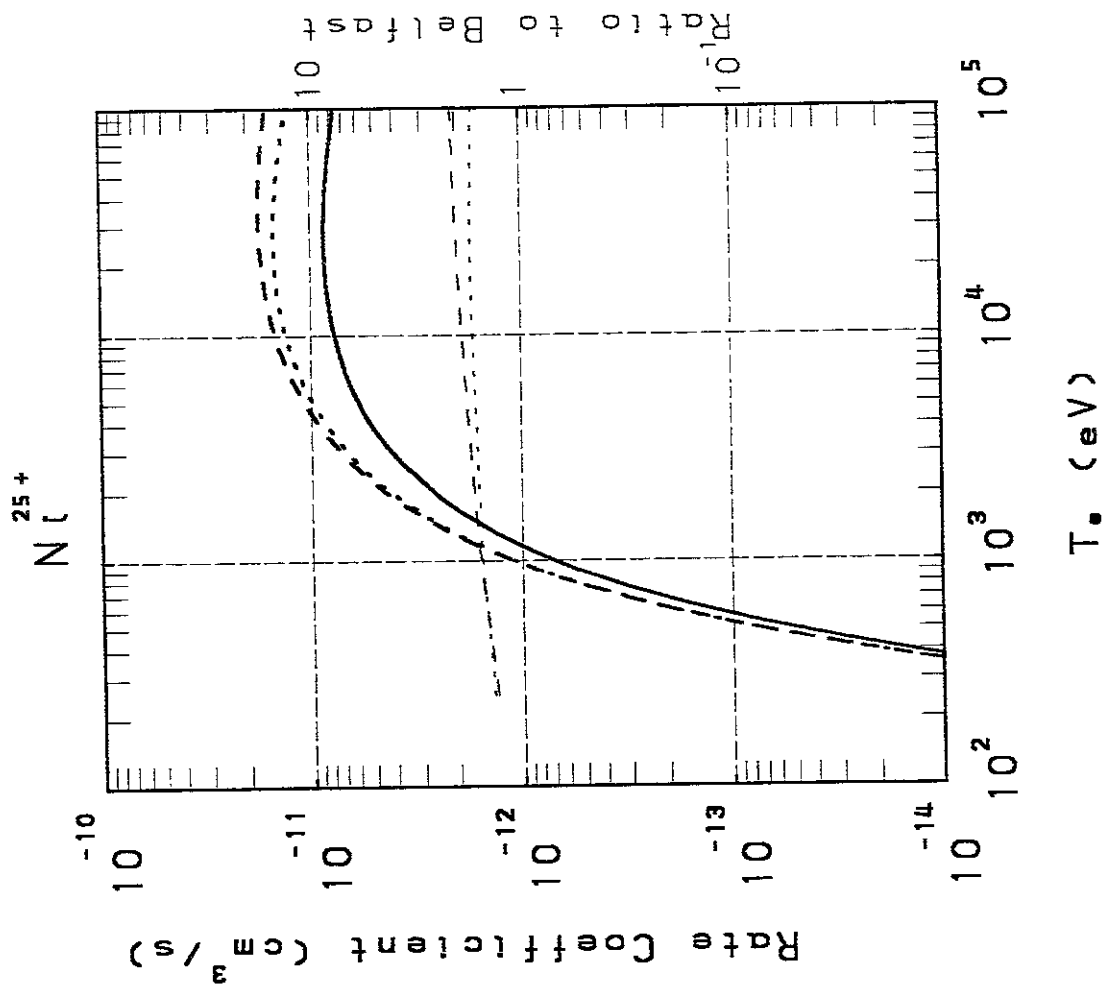


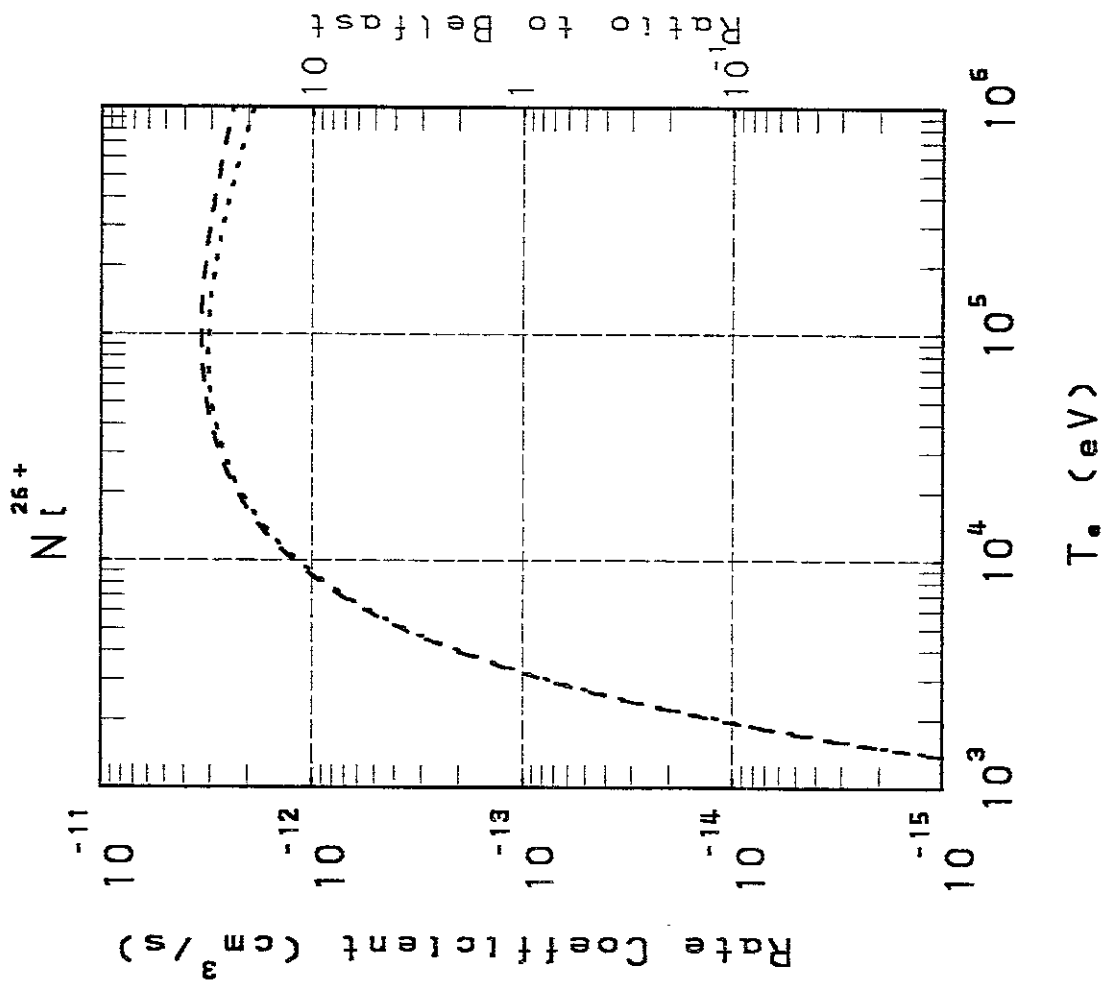
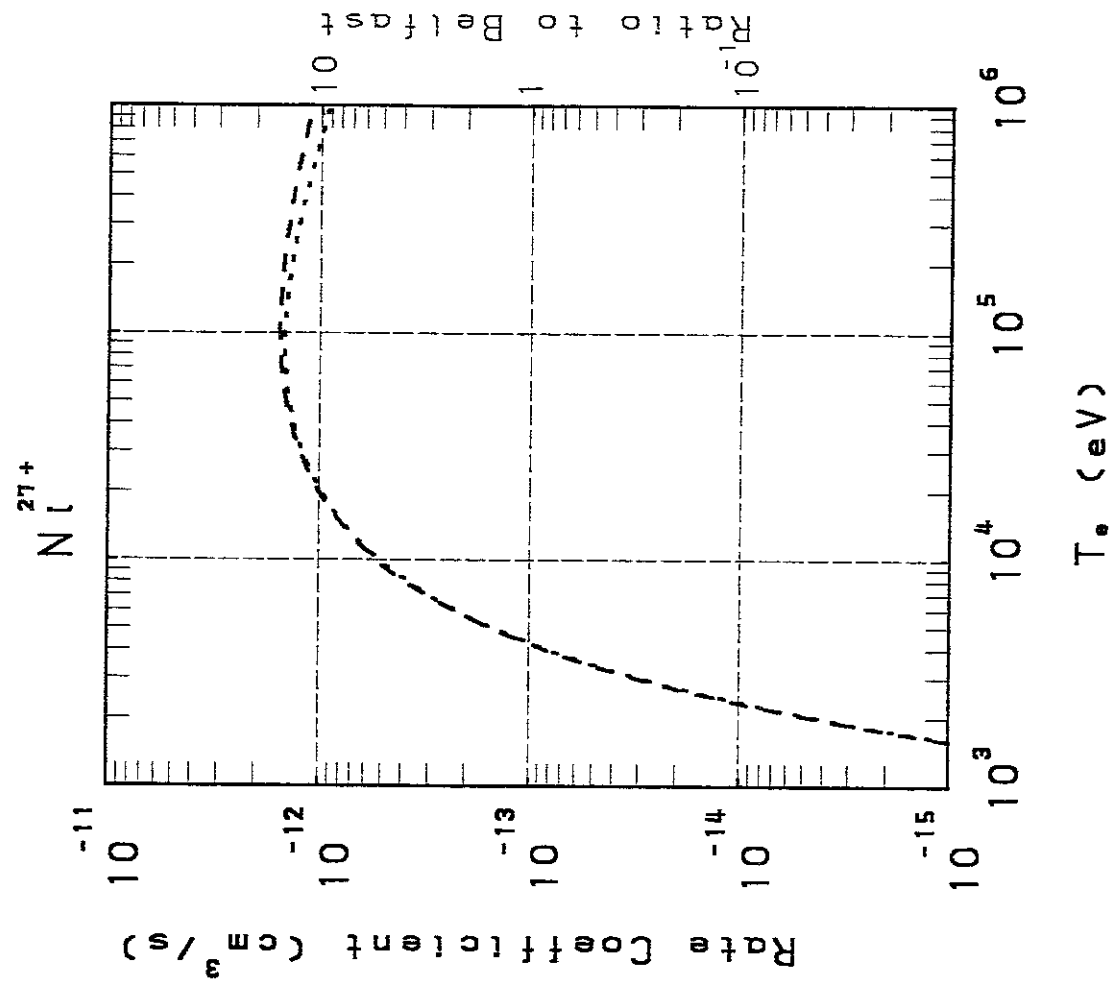












Recent Issues of NIFS Series

- NIFS-DATA-1 Y. Yamamura, T. Takiguchi and H. Tawara, *Data Compilation of Angular Distributions of Sputtered Atoms* ; Jan. 1990
- NIFS-DATA-2 T. Kato, J. Lang and K. E. Berrington, *Intensity Ratios of Emission Lines from OV Ions for Temperature and Density Diagnostics* ; Mar. 1990
- NIFS-DATA-3 T. Kaneko, *Partial Electronic Straggling Cross Sections of Atoms for Protons* ; Mar. 1990
- NIFS-DATA-4 T. Fujimoto, K. Sawada and K. Takahata, *Cross Section for Production of Excited Hydrogen Atoms Following Dissociative Excitation of Molecular Hydrogen by Electron Impact* ; Mar. 1990
- NIFS-DATA-5 H. Tawara, *Some Electron Detachment Data for H- Ions in Collisions with Electrons, Ions, Atoms and Molecules – an Alternative Approach to High Energy Neutral Beam Production for Plasma Heating–* ; Apr. 1990
- NIFS-DATA-6 H. Tawara, Y. Itikawa, H. Nishimura, H. Tanaka and Y. Nakamura, *Collision Data Involving Hydro-Carbon Molecules* ; July 1990
- NIFS-DATA-7 H.Tawara, *Bibliography on Electron Transfer Processes in Ion-Ion/Atom/Molecule Collisions –Updated 1990–*; Oct. 1990
- NIFS-DATA-8 U.I.Safronova, T.Kato, K.Masai, L.A.Vainshtain and A.S.Shlyapzeva, *Excitation Collision Strengths, Cross Sections and Rate Coefficients for OV, SiXI, FeXXIII, MoXXXIX by Electron Impact($1s^22s^2-1s^22s2p-1s^22p^2$ Transitions)* ;Dec.1990
- NIFS-DATA-9 T.Kaneko, *Partial and Total Electronic Stopping Cross Sections of Atoms and Solids for Protons*; Dec 1990
- NIFS-DATA-10 K.Shima, N.Kuno, M.Yamanouchi and H.Tawara, *Equilibrium Charge Fraction of Ions of $Z=4-92$ (0.02-6 MeV/u) and $Z=4-20$ (Up to 40 MeV/u) Emerging from a Carbon Foil*; Jan.1991
- NIFS-DATA-11 T. Kaneko, T. Nishihara, T. Taguchi, K. Nakagawa, M. Murakami, M. Hosono, S. Matsushita, K. Hayase, M.Moriya, Y.Matsukuma, K.Miura and Hiro Tawara; *Partial and Total Electronic Stopping Cross Sections of Atoms for a Singly Charged Helium Ion: Part I*; Mar. 1991
- NIFS-DATA-12 Hiro Tawara, *Total and Partial Cross Sections of Electron Transfer Processes for Be^{q+} and B^{q+} Ions in Collisions with H, H₂ and He Gas Targets -Status in 1991-*; Jun. 1991
- NIFS-DATA-13 T. Kaneko, M. Nishikori, N. Yamato, T. Fukushima, T. Fujikawa, S.Fujita, K. Miki, Y. Mitsunobu, K. Yasuhara, H. Yoshida and Hiro Tawara, *Partial and Total Electronic Stopping Cross Sections of Atoms for a Singly Charged Helium Ion : Part II*; Aug. 1991